Technische Universität München
TUM School of Natural Sciences

Synthesis, Isolation, and Reactivity of NHC-stabilized Aluminum Chalcogenides and Dialumenes

Huihui Xu

Vollständiger Abdruck der von der TUM School of Natural Sciences der

Technischen Universität München zur Erlangung des akademischen Grades einer

Doktorin der Naturwissenschaften (Dr. rer. nat.)

genehmigten Dissertation.

Vorsitz: Prof. Dr. Nicole Strittmatter

Prüfer*innen der Dissertation:

1. Prof. Dr. Shigeyoshi Inoue
2. Prof. Dr. Angela Casini

Die Dissertation wurde am 23.03.2023 bei der Technischen Universität München eingereicht

und durch die TUM School of Natural Sciences am 11.04.2023 angenommen.

Follow your heart but take your brain with you.

Alfred Adler

Folge deinem Herzen. Aber vergiss dabei nicht, dein Hirn mitzunehmen.

Alfred Adler

Dedicated to my father

Zihai Xu

Acknowledgments

Thank You for Being There, I Truly Don’t Know What I Would Have Done Without Flowers, Sun, Rain and, Especially, You!

First, I must thank Prof. Shigeyoshi Inoue. I will never forget where I first met you at ‘Tai Shan’ (Mountain Tai) in my hometown. I am very lucky that you gave me the opportunity to work in your group and led me into the world of aluminum. I enjoyed this topic very much, it gave me a chance to learn many new skills, techniques, and how to be a researcher, writer, and presenter. Your endless ideas, unbounded energy, and inexhaustible patience to discover new things have always affected me a lot. You taught me how to learn English, and discussed my work in seminar, office, lab, kitchen, and online. Your support will continue in future. Thank you, Shige!

I want to thank the committee for accepting to review my work. I am very grateful to Prof. Dr. Angela Casini for acting as the examiner for this thesis, and Prof. Dr. Nicole Strittmatter for being the chairman of the examination committee. Thank you very much for your time and attention!

Next, I would thank my mentor, Dr. Catherine Weetman. I cannot imagine how you could teach a novice who had never used a Schlenk line and especially who cannot speak English. I remember you guided me really a lot, for example, to write experimental notebook, how to do a safety hazard assessment, set up equipment and so on. All these let me finally just sit to finish the important part of my thesis. I have been receiving excellent help from you for my English, my life, my mental health, my manuscript, my every project and this thesis. Thank you again, Cath!

Dr. Amelie Porzelt, I am lucky to meet you and be colleagues and friends with you. Your strict attitude and broad profound theoretical knowledge affected me positively. You encouraged me to do something instead of being cowardly. I learned a lot from you. The bicycle from you allowed me to enjoy a lot of beautiful scenery everywhere in Munich.

Dr. Gizem Dübek Bengi, thank you for letting me share the bench and work alongside with you. You always helped me to deal with the ‘accidents’. I am very thankful for your ‘Morning’, ‘No, no, no’, and ‘Good evening’ almost every day.

Dr. Franziska Hanusch, thank you very much for your time and attention for helping me to check the ‘poor-quality’ crystals although I thought they were perfect. You always spent at least two hours introducing the Lab Rules and Safety for every new member. This makes me never

forget you. Thank you very much for being responsible for many instruments to keep everything going well in our lab and helping me to deal with a lot of problems. Thank you!

Dr. Arseni Kostenko, you impressed me a lot with your intelligence and amazing singing! Thank you for believing me and cooperating with me. Thank you for your suggestions on my projects and thoughtful discussions.

Dr. John Kelly, thank you very much for your time, attention, and comments on revisions of this thesis. Thank you very much for sharing Cockney culture, that sounds very interesting.

Dr. Shiori Fujimori, your quiet operation and hardworking motivated me a lot. Thank you.

Dechuang Niu and Huaiyuan Zhu, you are my friends and partners in the lab. I will never forget every moment we discussed, quarreled and sometimes were speechless about different respective points on Chemistry, Knowledge, Life, Movies, and News. Also, I will never forget every exciting moment whoever got an interesting crystal or acceptance of publications. Thank you.

Simone Hirmer, I am lucky to be colleague with you. You are the funniest girl who I've met before. I like you. I could learn from you to be energetic, sunny, positive, and equal. Thank you very much for your help to translate the abstracts in German. Thank you.

Florian Tschernuth, thank you very much for your incessant help for variable-temperature NMR measurement, and every affirmation ('I like your talk') of my work progress after my talk. I will never forget one time you lied on floor for dealing with projector problem despite dirtying your white T-shirt. That is one of the wonderful things I have seen before.

Fiona Kiefer, thank you for checking my crystals. You are always friendly. I felt very comfortable to work with you. Thank you.

Dr. Daniel Franz, you impressed me very much for your earnestness and sufficient knowledge. Whenever I asked you, you always gave me multidirectional and feasible advices. Thank you.

Dr. Debotra Sarkar, thank you bro. You helped me a lot in the beginning of my Ph.D. and gave me a lot of good ideas for my work.

Dr. Matthew Roy, thank you very much for your humor and clever perspicacity on chemistry. I enjoyed drinking a lot of beer with you.

Sebastian Stigler, thank you very much for organizing a lot of interesting parties. I really enjoyed drinks, BBQ, and every party at Garching Campus. It was you let the life in lab is not so boring!

My time at the Technical University of Munich would not have been as enjoyable without the fantastic members of our group. Thank you again, Teresa Eisner, Moritz Ludwig, Martin Doleschal, Ramona Baierl, Yueer Zhu, Dr. Xuan-Xuan Zhao, Dr. Dominik Reiter, Lisa Groll, Dr. Vitaly Nesterov, Dr. Philipp Frisch, Dr. Richard Holzner, Dr. Xufang Liu, Fengming Rong and Ke Li for helps and doing a lot together.

In addition, I need to say a special thank you to Christian Jandl (for crystallography), Ulrike Ammari (for Elemental Analysis), Maximilian Muhr and Ivan Antsiburov (for LIFDI-Mass and ESI-Mass). I am also grateful to Melanie Lorenz and Anke Wohlketzetter as secretaries as you helped me a lot in Germany.

For financial support I want to acknowledge the TUM as well as china scholarship council (CSC).

Thanks to all my families and friends. Thank you, Ziqi Huo, Kun Dai, Jianguo Hu, Yuxin Duan, Chunhuan Li, Kairui Du, Xiucui Hu, Marc Breaz (Măkè Tóngzhì), John Vico Strauß, Maria Susanne Simon and WG 8 roommates. You accompanied me with happy conversations! All these are essential parts of my life in Germany.

At last but not least, thanks to my parents, Xu Zihai and Lei Xiuqing. You are the best parents. Thanks to my sister, Xu Yingying, you are the best sister. All of you supported and encouraged me to have a chance to pursue Ph.D. in Germany. I love you. 谢谢您们，爸爸妈妈姐姐！

List of Abbreviations and Formulas

$\Delta\chi p$	Pauling electronegativity difference
q	natural population charge
ζ_d	d-polarization function
ε	bond ellipticity
δ	chemical shift [ppm]
λ	wavelength [nm]
[2.2.2]-cryptand	4,7,13,16,21,24-hexaoxa-1,10-diazabicyclo[8.8.8]hexacosane
Ar	aryl
BCP	bond critical point
Bu	butyl (C_4H_9)
Bbp	2,6-$(CH(SiMe_3)_2)_2$-C_6H_3
cAAC	cyclic alkyl-amino carbene
CGMT	Carter-Goddard-Malrieu-Trinquier
Ch	chalcogen (O, S, Se, Te, Po, Lv)
Cp	cyclpentadienyl (C_5H_5)
Cp*	pentamethylcyclopentadienyl (C_5Me_5)
CVD	chemical vapor deposition
d	day(s)
DFT	density functional theory
Dipp	2,6-diisopropylphenyl (2,6-*i*Pr_2-C_6H_3)
E	element
e.g.	latin exempli gratia: “for example”
EPR	electron paramagnetic resonance
Et	ethyl (C_2H_5)
et al.	latin et alii: “and others”
etc.	latin phrase et cetera: ‘and others’
Et_2O	diethylether
h	hour(s)
HOMO	highest occupied molecular orbital
i	iso
i.e.	latin (id est): “that is”
I*i*Pr_2Me_2	1,3-diisopropyl-4,5-dimethylimidazolin-2-ylidene
IMe_4	1,3,4,5-tetramethylimidazolin-2-ylidene
in situ	latin: “on site”
IR	infrared
kcal	kilocalorie
L	substituent (ligand)
LA	Lewis acid
LB	Lewis base
LUMO	lowest unoccupied molecular orbital

M	alkali metal (Li, Na, K, Rb, Cs, Fr; or transition metal)
m	meta
m.p.	melting point
MBO	Mayer bond order
Me	methyl (CH_3)
Mes	mesityl (2,4,6-Me_3-C_6H_2)
Mes*	supermesityl (2,4-6-*t*Bu_3-C_6H_2)
MO	molecular orbital
NAO	natural atomic orbital
Nacnac	β-diketiminato
^{Dipp}Nacnac	$HC[(CMe)N(Dipp)]_2$
$^{Dipp\mathit{t}Bu}$NON	4,5-bis(2,6-diisopropylanilido)-2,7-di-*tert*-butyl-9,9-dimethylxanthene
^{DippSi}NON	$[O(SiMe_2N(2,6\text{-}i\text{Pr}_2C_6H_3)_2)]^{2-}$
^{Mes}Nacnac	$HC[(CMe)N(2,4,6\text{-}\ Me_3C_6H_2)]_2$
NBO	natural bond order
NHC	*N*-heterocyclic carbene
NHI	*N*-heterocyclic imine
NMR	nuclear magnetic resonance
NPA	natural population analysis
o	*ortho*
p	*para*
Ph	phenyl (C_6H_5)
PPh_3	triphenyl phosphine
ppm	parts per million
QTAIM	quantum theory of atoms in molecules
R	substituent (functional group)
r.t.	room temperature
SC-XRD	single-crystal X-ray diffractometry
t	*tert*
Tbb	2,6-$[CH(SiMe_3)_2]_2$-4-*t*BuC_6H_2
*t*Bu	*tert*-butyl
THF	tetrahydrofuran (C_4H_8O)
^{Tipp}Ter	2,6-bis(2,4,6-*i*Pr_3-C_6H_2)C_6H_3
Tipp	triisopropylphenyl (2,4,6-*i*Pr_3-C_6H_2)
TM	transition metal
TMS	trimethylsilyl ($SiMe_3$)
Tol	toluene
UV-vis	ultraviolet-visible
VT	variable temperature
WBI	Wiberg bond index
WCA	weakly coordinating anion
X	halogen atom (F, Cl, Br, I, At)

Publication List

- **Xu, H.**; Kostenko, A.; Weetman, C.; Fujimori, S.; Inoue, S., An Aluminum Telluride with a Terminal Al=Te Bond and its Conversion to an Aluminum Tellurocarbonate by CO_2 Reduction. *Angewandte Chemie International Edition* **2023**, *62* (11), e202216021; *Angew. Chem.* **2023**, *135*(11), e202216021. https://doi.org/10.1002/anie.202216021

- **Xu, H.**; Weetman, C.; Hanusch, F.; Inoue, S., Isolation of Cyclic Aluminium Polysulfides by Stepwise Sulfurization. *Chemistry – A European Journal* **2022**, *28* (8), e202104042. https://doi.org/10.1002/chem.202104042

- **Xu, H.**; Roy, D. M. M.; Kostenko, A.; Fujimori S.; Inoue, S., Dialumene-Mediated Production of Tertiary Phosphines through P_4 Reduction. Draft.

- Weetman, C.; **Xu, H.**; Inoue, S., Recent Developments in Low-Valent Aluminum Chemistry. In *Encyclopedia of Inorganic and Bioinorganic Chemistry*, Scott, R. A., Ed. **2020**; pp 1-20. https://doi.org/10.1002/9781119951438.eibc2753

Conference Contributions

- **Xu, H.**; Kostenko, A.; Inoue, S., Synthesis and Reactivity of Heavier Aluminium Chalcogenides. *29th International Conference on Organometallic Chemistry* **2022**, *Prague*, Czech, **Poster Presentation**

Abstract

Aluminum has attracted a huge amount of attention due to it being one of the most abundant and environmentally friendly elements as such it is widely used in industry. It is most encountered in form of alumina (Al_2O_3), which owing to the strong bonding nature of Al–O results in an inert and robust material. In this context, insights into the bonding nature and aggregation processes for Al–O and the heavier analogues Al–Ch (Ch = S, Se, Te) are essential to develop new materials or catalysts both of which are of interest to academia and industry. Specifically, isolation, characterization and reactivity study of multiply bonded heavier aluminum chalcogenides are vital for understanding the aggregation to bulk materials from atoms. Accordingly, this thesis focuses on isolating both homo- and hetero-multiply bonded aluminum species.

Firstly, we set out to isolate an aluminum sulfide containing a discrete Al=S double bond, using *N*-heterocyclic carbene (NHC) stabilized aryl aluminum dihydrides (R(NHC)AlH_2, R = Tipp (2,4,6-*i*Pr_3-C_6H_2) or ^{Tipp}Ter (2,6-(2,4,6-*i*$Pr_3C_6H_2$)$_2C_6H_3$); NHC = I*i*Pr_2Me_2 (1,3-diisopropyl-4,5-dimethylimidazolin-2-ylidene) or IMe_4 (1,3,4,5-tetramethylimidazolin-2-ylidene)) as the precursors. Treatment of various thiation reagents with R(NHC)AlH_2 did not obtain the desired Al=S double bonds. However, step-by-step sulfurization is achievable and results in the series of hydride hydrogensulfide, bisthiol and five- or six- membered cyclic aluminum sulfides. These compounds feature various Al–S bonding natures, and they give us insights for ligand requirements to prepare new Al–S single bond containing molecules. This motivated us to test further reactions of such compounds and to use aluminum dihydrides in the formation of heavier analogues Al–Ch (Se, or Te) containing complexes.

The second chapter aims to synthesize the aluminum chalcogenide containing an Al=Ch (Se, or Te) double bond. Initially, Tipp(I*i*Pr_2Me_2)AlH_2 was treated with elemental selenium or tellurium yielding dimeric species containing Al–Ch (Se, or Te) single bond. Attempts to cleave the dimeric unit of Al–Ch by use of stoichiometric amounts of IMe_4, a strong NHC donor, resulted in ligand exchange reactions. However, in the presence of excess IMe_4, the cleavage of Al–Te single bond was observed and resulted in the formation of a terminal Al=Te double bond. The spectroscopic, structural, and computational analysis support the discrete Al=Te double bond character. Reactivity studies of Al=Te species towards CO_2 revealed a unique triple CO_2 insertion product, which included a carbonate analogue, tellurocarbonate ($[CO_2Te]^{2-}$)

moiety. In the case of Se, we did not observe monomeric species only stabilized by such NHC and aryl ligands.

Finally, the third chapter puts attention on homoleptic aluminum double bonds, namely dialumenes, and their reactivity towards P_4. Facile access to different P_4 products with *Trans* or *Cis* geometry under mild conditions was achieved. Further reactivity towards various electrophiles resulted in the corresponding phosphines, which avoids elevated temperatures or high pressures which are routinely employed to prepare such phosphines in industry.

Zusammenfassung

Aufgrund seiner Häufigkeit auf der Erde und Umweltfreundlichkeit, erregte Aluminium viel Aufmerksamkeit und wird daher in der Industrie oftmals verwendet. Am häufigsten ist es in Form von Aluminiumoxid (Al_2O_3) anzutreffen, welches aufgrund der starken Bindung von Al–O-Bindungen ein inertes und robustes Material wird. In diesem Zusammenhang sind Erkenntnisse über die Bindungsart und die Aggregationsprozesse von Al–O und der schwereren Analoga Al–Ch (Ch = S, Se, Te) von wesentlicher Bedeutung für die Entwicklung neuer Materialien oder Katalysatoren, die sowohl für die Wissenschaft als auch für die Industrie von Interesse sind. Insbesondere die Isolierung, Charakterisierung und Untersuchung der Reaktivität von mehrfach gebundenen schwereren Aluminium–Chalkogeniden ist für das Verständnis der Aggregation zu Bulkware aus Atomen unerlässlich. Dementsprechend konzentriert sich diese Arbeit auf die Isolierung sowohl homo- als auch hetero-mehrfach gebundener Aluminiumspezies.

Zunächst haben wir versucht, ein Aluminiumsulfid mit einer diskreten Al=S-Doppelbindung zu isolieren, indem wir N-heterozyklische Carbene (NHC) stabilisierte Arylaluminiumdihydride (R(NHC)AlH_2, R = Tipp (2,4,6-*i*Pr_3-C_6H_2) oder ^{Tipp}Ter (2,6-(2,4,6-*i*$Pr_3C_6H_2$)$_2C_6H_3$) verwendeten; NHC = I*i*Pr_2Me_2 (1,3-Diisopropyl-4,5-dimethylimidazolin-2-yliden) oder IMe_4 (1,3,4,5-Tetramethylimidazolin-2-yliden)) als Vorstufen. Die Behandlung verschiedener Thionierungsreagenzien mit R(NHC)AlH_2 führte nicht zu den gewünschten Al=S-Doppelbindungen. Eine schrittweise Sulfurierung ist jedoch möglich und führt zu einer Reihe von Hydridhydrogensulfiden, Bisthiolen und fünf- oder sechsgliedrigen cyclischen Aluminiumsulfiden. Diese Verbindungen weisen verschiedene Al–S-Bindungen auf und geben uns Einblicke über die Anforderungen an die Liganden zur Herstellung neuer Moleküle mit Al–S-Einfachbindungen. Dies hat uns dazu motiviert, weitere Reaktionen mit solchen Verbindungen zu testen und Aluminiumdihydride für die Bildung von schwereren analogen Al–Ch (Se oder Te) enthaltenden Komplexen zu verwenden.

Im zweiten Kapitel geht es um die Synthese von Aluminium–Chalkogeniden mit einer Al=Ch (Se oder Te) Doppelbindung. Zunächst wurde Tipp(I*i*Pr_2Me_2)AlH_2 mit elementarem Selen oder Tellur behandelt, was zu dimeren Spezies führte, die eine Al–Ch (Se oder Te)-Doppelbindung enthalten. Versuche, die dimere Einheit von Al–Ch durch Verwendung stöchiometrischer Mengen von IMe_4, einem starken NHC-Donor, zu spalten, führten zu Ligandenaustauschreaktionen. In Anwesenheit von überschüssigem IMe_4 wurde die Spaltung

der Al–Te-Einfachbindung beobachtet und führte zur Bildung einer endständigen Al=Te-Doppelbindung. Die spektroskopischen, strukturellen und rechnerischen Analysen unterstützen den Charakter der diskreten Al=Te-Doppelbindung. Reaktivitätsstudien von Al=Te-Spezies gegenüber CO_2 ergaben ein einzigartiges dreifaches CO_2-Insertionsprodukt, das ein Carbonat-Analogon, eine Tellurocarbonat-Einheit ($[CO_2Te]^{2-}$), enthält. Im Falle von Se konnten wir keine monomeren Spezies beobachten, die nur durch solche NHC- und Aryl-Liganden stabilisiert wurden.

Das dritte Kapitel befasst sich schließlich mit homoleptischen Aluminium-Doppelbindungen, den Dialumenen, und ihrer Reaktivität gegenüber P_4. Es wurde ein einfacher Zugang zu verschiedenen P_4-Produkten mit trans- oder cis-Geometrie unter milden Bedingungen erreicht. Die weitere Reaktivität gegenüber verschiedenen Elektrophilen führte zu den entsprechenden Phosphinen, wodurch erhöhte Temperaturen oder hoher Druck vermieden wird, die in der Industrie routinemäßig zur Herstellung solcher Phosphine eingesetzt werden.

Diese Arbeit wurde in der Zeit von September 2018 bis März 2023 im Rahmen der Professur für Siliciumchemie der Technischen Universität München unter Betreuung von Herrn Prof. Dr. Shigeyoshi Inoue angefertigt.

Table of Contents

1. Introduction

Aluminum is found in the second row of group 13 with atomic number 13 and the electron configuration [Ne] $3s^2$ $3p^1$. It is the third most abundant element (and the most abundant metal) in earth's crust (8.1%, by weight) only being surpassed by oxygen (46.6 %) and silicon (27.7 %) (Figure 1).[1]

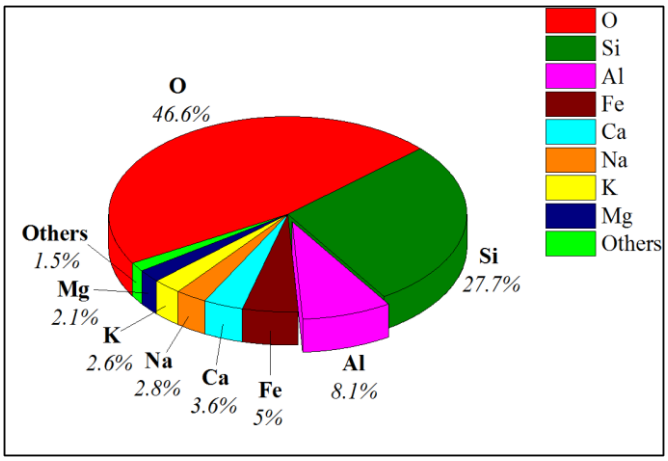

Figure 1. Abundances (Percentages by weight, %) of elements in the Earth's crust.

Aluminum's discovery dates back to the beginning of nineteenth century, as in 1825, Hans Christian Ørsted produced the almost pure metal by the reaction of potassium amalgam on $AlCl_3$.[2] These days, aluminum metal is refined from alumina which is extracted from bauxite ore through a Bayer's process.[3-5] It features a much lower density than those of other commonly encountered metals including iron (Fe), copper (Cu), lead (Pb), silver (Ag), and gold (Au). It is soft (i.e., not as strong as steel), non-magnetic, ductile, and possesses a great affinity towards oxygen, concomitantly forming an oxide layer on the surface when it is exposed to air. Therefore these characteristic features have led to aluminum metal playing a great role in a wide range of applications in daily life, where light weight and relatively high strength are necessary.[6] For instance, aluminum is widely used in transportation such as in aircrafts (e.g., in 1918 in Germany, Hugo Junkers assembled an all-metal airplane made out of aluminum alloy), cars, bicycles, and packaging (e.g., cans and foils). It is also employed in construction industry (e.g., windows, doors, transformers, and capacitors). In more recent time, used aluminum drink cans have been used in the assembly of laptops (Macbook), smartphones and smartwatches, whereby the aluminum can be recycled.

In nature, aluminum is mostly encountered in its oxide form, alumina Al_2O_3. It has an extremely high melting point (2045 °C), a particularly low volatility and it is chemically inert. These features allow it to be effective as electrical insulators, abrasives (e.g., toothpaste), refractory materials, and ceramics.[7] The high stability of alumina stems from not only the high oxygen affinity of Al, but also the large difference in the electronegativity between Al (1.61, Pauling scale) and O (3.44) leading to highly polarized bonds and a tendency towards head-to-tail self-oligomerization.[8-9] If well-defined molecular aluminum oxides, which are stable in the condensed phase at ambient temperatures, and even multiply bonded Al–O moieties could be isolated, this would provide insights of Al–O bonding nature for the comprehension of alumina and the subsequent development of novel materials. However there has been only a few reports so far on low coordinate and multiple bonded Al–O motifs,[10] generally stabilized by employing sterically demanding ancillary ligands and coordination of Lewis acids (LA) or bases (LB). The fundamental studies are imperative to inform future developments in aluminum oxides.[11-13]

In contrast to the aluminum oxides, the chemistry of the heavier aluminum chalcogenides (i.e. Al–S, Al–Se, and Al–Te) still remains in its infancy which poses a challenge to their viability.[8, 14-16] Very recently, they especially multiply-bonded aluminum-chalcogen (Al–Ch) species have attracted significant attention not only because they have proven easier to handle than elusive aluminum oxides, but also due to their unusual transition-metal like reactivity and novel bonding motifs as well as applications in chemical vapor deposition (CVD), catalysis and materials.[17-22]

Despite Al–Ch species, multiple bonds involving aluminum obviously contain the homobimetallic Al=Al bonds, namely dialumenes. The formation, once considered to be impossible according to the so-called double bond rule, has been highly desirable to identify multiple-bond nature and to explore their potential reactivity.[23] This kind of species exhibits interesting bonding nature and good reactivity on unique bond-activation[24] wherein transition metal (TM) compounds were often dominant. It has proven there is legitimate parallels between Al and TM. [8, 15, 17, 23, 25-26] While TM have been studied in academia and employed in industry widely, dialumenes deserve more investigation on a broad range of reactions to access novel Al-based functional material and organoaluminum compounds.

2. Aluminum chemistry

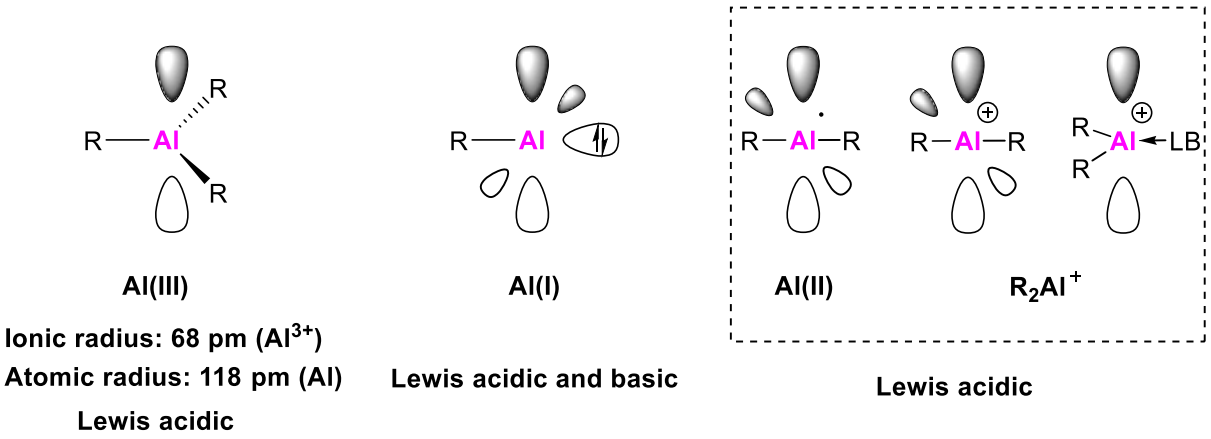

Figure 2. Molecular orbitals for aluminum (I, II, III) species.

Aluminum with three outermost electrons ($3s^1$ $3p^2$) is commonly found in the +3 oxidation state. It is highly polarizing due to its small cation size and features an empty p-orbital making it electron deficient (i.e. Lewis Acidic) in nature (Figure 2, **Al(III)**).[27] Al(III) compounds (e.g. $LiAlH_4$) have been widely used in organic and inorganic transformations due to their oxophilicity and Lewis acidic nature. For example, trialkyl or trihalide Al(III) complexes are remarkable catalysts in Ziegler-Natta and Friedel-Crafts reactions in industry.[28-29]

Compared with Al(III), low oxidation state aluminum species (Figure 2, **Al(I)** and **Al(II)**) are much rarer. It is necessary to supply sufficiently large substituents to kinetically stabilize the highly reactive aluminum center. Otherwise, it is difficult to balance the stability and reactivity against disproportionation. Examples of Al(I) species, e.g. AlH, AlX (Cl, Br, I), or Al_2O were discovered only at low pressures or/and elevated temperatures and trapped in matrices.[30-34] AlR (R = monoanionic substituent) possesses a singlet ground state (Al(I)), in which the HOMO is a non-bonding n_σ-type orbital with sp character. The first monovalent aluminum stable at room temperature is Cp*Al(I) (Cp* = η^5-$C_5(CH_3)_5$)) reported by Schnöckel in 1991.[35] As compounds of this type feature a lone pair of electrons, Lewis basic character is observed in contrast to the Lewis acidic Al(III) compounds.[8] Importantly, the Al(I) center features similar energetically accessible frontier orbitals comparable to those found in transition metals (Figure 3, **i** and **ii**), which enables Al(I) compounds to activate small molecules and are a prime candidate for redox reactions due to accessible Al(III) and Al(I) states.[8, 36-37]

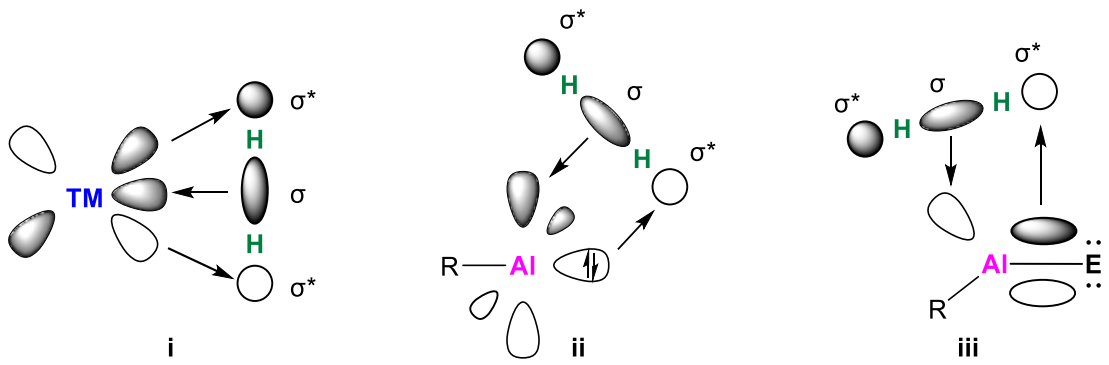

Figure 3. Frontier orbitals involved in the activation of H_2, i) transition metals, ii) singlet alumylene compounds, iii) compounds containing Al–E multiple bonds.

Monomeric Al(II) complexes (Figure 2, **Al(II)**) with an unpaired electron (i.e., radical species) are paramagnetic. However, these are very rarer due to the rule about the main group elements preference for the closed-shell configuration and the inherent instability of mononuclear neutral radical species, which prefers to dimerize forming Al–Al single bonded compounds.[38-49] Compounds of the form $R_2Al–AlR_2$ offer a potential way for stabilizing Al(II) centers. The first example of which was isolated by Uhl and coworkers with bulky $CH(TMS)_2$ ligand.[50-52] As Figure 2, **Al(II)** showed, there is another general formula $\mathbf{R_2Al^+}$, which could be stabilized by using weakly coordinating anions (WCAs),[53] intramolecular π-coordination of sterically demanding m-terphenyl ligands,[54] and the β-silicon effect of silyl group.[55] In addition, Al(II) cations are decent catalysts in the oligomerization or polymerization.[56-58]

Following on from this, main group multiple bonds have attracted much attention in the last few decades as they also have similarly accessible frontier orbitals (Figure 3, **iii**).[14, 36-38, 59-62] In the case of the lighter group 14 element, carbon, its multiple bonds feature planar geometries on the basis of the usual σ plus π model (i.e., the unhybridized carbon p-orbitals overlap to form π-bonds) (Figure 4, **A**). Distinctively, trans-bent geometries are observed among multiple bonds of heavier group 14 element (e.g., Si, Ge, Sn, Pb) in the solid state, not as planar or linear (Figure 4, **B**). It stems from the increased size difference of a valence orbital resulting the less effective hybridization between elements. Thereby the weaker bonding between the heavier elements lead to greatly increased core-core repulsion resulting trans-bending of the geometry.[38, 63-64] In solution, heavier group 14 multiple bonds often dissociate to their monomeric counterparts.[65] The same trends in double dative bond formation are also observed in multiple bonds of group 13 element (i.e., in the case of Al,[24, 66] Figure 4, **C**). As Figure 3 (**ii** and **iii**) and Figure 4 (**C**) shown, similarly to monomeric Al(I) species, polar Al–Ch and

nonpolar Al–Al multiple bonds can mimic transition metals to activate the challenging bonds.[8] In the end, they probably would be the viable takeover in synthesis or catalysis in industry as energy-saving and environment-friendly products.

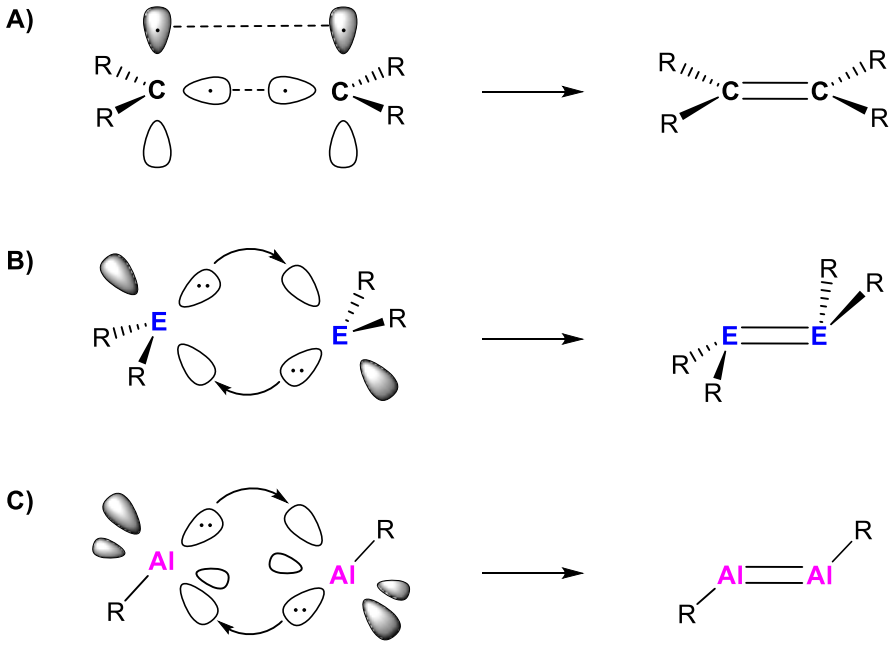

Figure 4. The Carter–Goddard–Malrieu–Trinquier (CGMT) models for differences in observed geometries for triplet, singlet multiple bonds, and dialumenes.

In a short summary, a compelling reason to synthesize and study low-valent aluminum compounds or multiply bonded Al–E compounds stems from their potential reactivity, in particular oxidative addition, and the prospect of offering an alternate to rare and expensive transition metals. Multiply bonded aluminum chemistry remains a subject of ongoing interest given the fundamental interest as well as the numerous and growing applications both in synthetic chemistry or material science.[67] To access to stable multiply bonded aluminum species, steric congestion by use of bulky ligands to allow for kinetic stabilization in combination with strongly electron-donating substituents LB or LA, as well as suitable precursors are required.

2.1. Aluminum dihydrides

Main-group metal hydrides have attracted extensive attention due to their potential application as hydrogen storage materials as well as their use in a diverse range of organometallic and organic synthesis.[68] Aluminum hydrides have been applied widely in chemical synthesis and is of great interest in homogeneous catalysis (e.g. catalyzing the hydroboration of aldehydes, ketones, and terminal alkynes, as well as dehydrocoupling of amine boranes, thiol, and phenol molecules).[69-71]

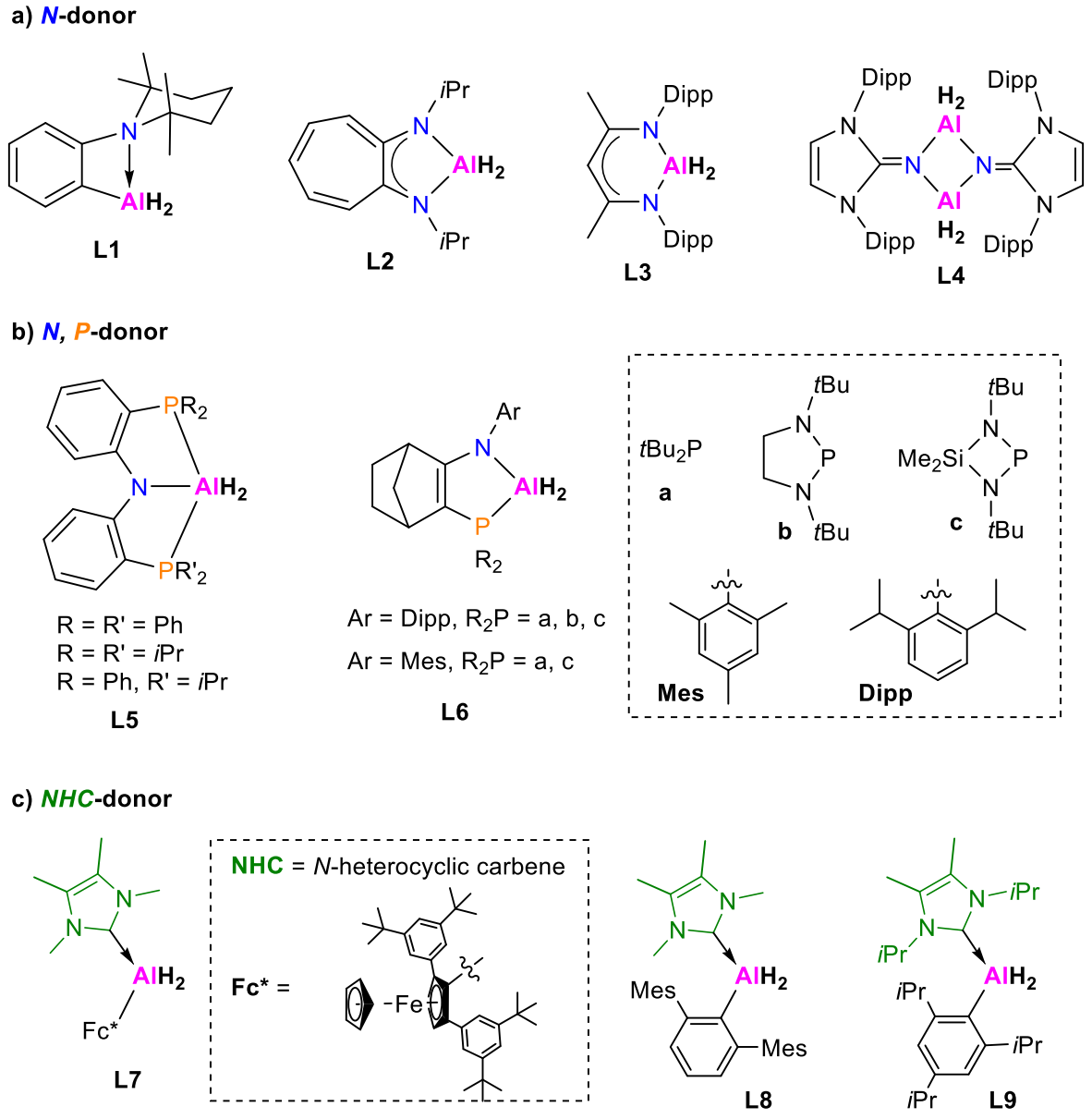

Figure 5. Selected currently reported aluminum dihydrides (**L1**-**L9**).

Aluminum dihydride complexes have been reported for a variety of ligand classes, with those the use of *N*-donor ligands (as intramolecular LB) is the most widely reported.[72-74] For example, the aminophenyl groups supported aluminum dihydrides (Figure 5, **L1**) activate arenes and alkynes and achieve selective catalytic functionalization.[71, 75-77] The various pyrrolyl ligands stabilized species are widely used in polymerization catalysis.[78-82] Bisamino (**L2**) supported species can activate small molecules such as CO_2.[83-87] Among these, β-diketiminato dihydridoaluminum (**L3** [^{Dipp}Nacnac]AlH_2, ^{Dipp}Nacnac = HC[(CMe)N(Dipp)]$_2$, Dipp = 2,6-*i*Pr$_2$C$_6$H$_3$)[88] has been the most widely studied, including many variations on the ligand.[89-105] They have proven good precursors for aluminum chalcogenides.[88, 106] In this regard, our group used a monodentate *N*-heterocyclic imino ligand (NHI) to support a dimeric aluminum dihydride (**L4** [(μ-NHI)AlH_2]$_2$, NHI = bis(2,6-diisopropylphenyl)imidazolin-2-imino)[17, 107-108] for the preparation of aluminum sulfides[107] or aluminum tellurides bearing a terminal Al=Te.[17]

There are few aluminum hydrides supported by the *N, P* (amido-phosphine)-donor ligands.[109-111] **L5** is supported by *o*-phenylene-derived amido diphosphine ligands.[109] **L6** is supported by amido monophosphine ligands[110-111] and can be used to form the corresponding Al(II) compounds.[111]

Only few examples stabilized by *N*-heterocyclic carbenes (NHC) were reported. Braunschweig and coworkers employed ferrocenyl supported **L7** to prepare structurally-diverse dialane species[112] and the bulky terphenyl substituent stabilized **L8** to generate a transient base-stabilized arylalumylene (Al:) and a "masked" dialumene (Al=Al).[24] Our group used phenyl stabilized Tipp(I*i*Pr$_2$Me$_2$)AlH_2 **L9** (Tipp = 2,4,6-*i*Pr$_3$-C$_6$H$_2$, I*i*Pr$_2$Me$_2$ (1,3-diisopropyl-4,5-dimethylimidazolin-2-ylidene)) to isolate the corresponding dialumene.[25]

Aluminum dihydrides have been playing a great role in reduction of various polar functional and unsaturated substrates, catalysis for the formation of compounds with B−E (E = C, N, S, O) bonds, small molecule activation (e.g., alcohols, silanols, phosphorus acids, peroxides).[68] Especially, as mentioned before, they have proven a good precursor for the preparation of low-valent aluminum complexes and aluminum chalcogenides as well as dialumenes.

2.2. Aluminum chalcogenides

2.2.1. Aluminum oxides

Archetypal aluminum chalcogenides (i.e., compounds containing Al–group 16 elements) are mainly encountered as aluminum oxides with either an Al_2O_3 (i.e., alumina) or $(RAlO)_n$ composition (i.e., alumoxanes). The Al–O motif is among the most ubiquitous in nature such as minerals, ores, and gemstones,[113] and can be used as a catalyst in various polymerization reactions (e.g., aldehydes,[114-115] epoxides[116-118] and alkenes[119]) and in various applications in industry.[120-121]

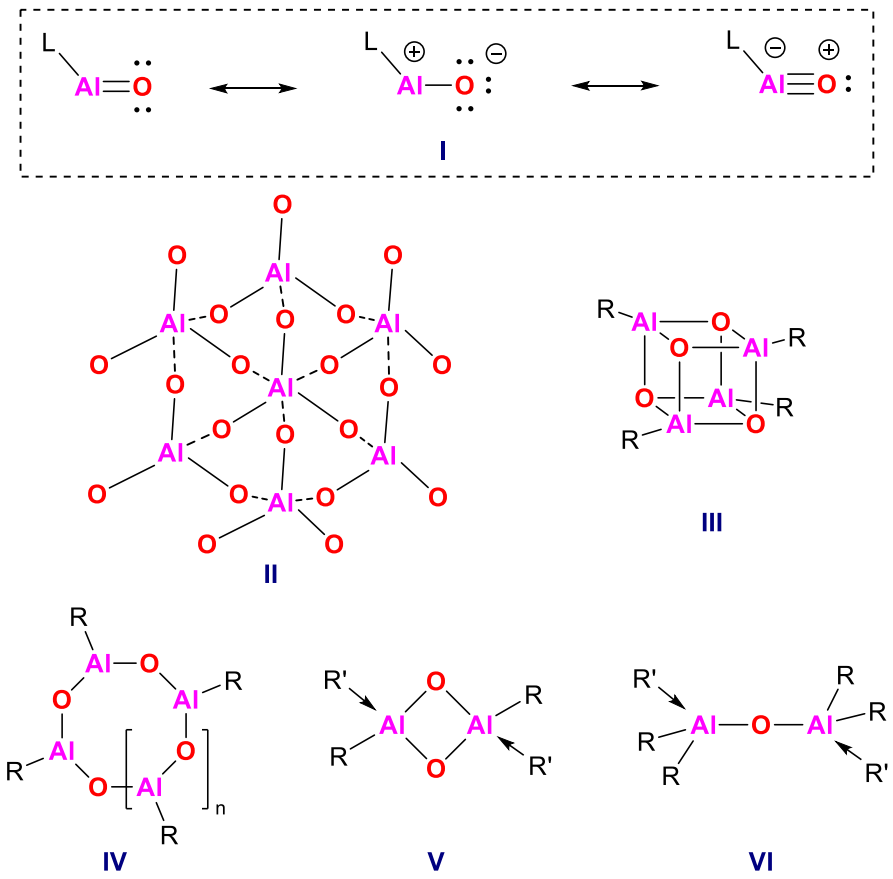

Figure 6. Aluminum–oxygen multiple bonds with an illustrative ionic resonance contribution (**I**). Aggregation of Al–O motifs (**II** - **VI**).

The large difference in electronegativities between Al (1.61) and O (3.44) results in a highly polarized Al=O bond and can be described by the dipolar resonance structure Al^+–O^- (Figure 6, **I**). This facilitates the head-to-tail self-oligomerization through Al–O–Al bridges to form clusters (**II**), tetramers (**III**), trimers (**IV**, n = 0), dimers (**V**) as well as other oligomers (**IV**, n ≥ 1; **VI**). Consequently, the Al–O bond is one of the strongest heteroatom single bonds (ca. 502

- 585 kJ mol^{-1})[122] as such molecular aluminum oxide units are highly thermodynamically stable.[123] To study intermediates of the oligomerization processes in the formation of bulk materials, low-temperature matrix isolation techniques and theoretical studies are required.[124] Insights into these processes are essential for developing advanced materials.

The oxygenation of organo-aluminum compounds is achievable by water, aqueous metal salts, or oxygen-containing species (e.g. $(Me_2SiO)_3$). This results in various alumoxanes of formula $[RAlO]_n$ (e.g., **II**,[125] **IV**,[126-127] **V**,[120] and **VI**[128]). For example, the direct oxygenation (O_2 or N_2O) of $[Cp^*Al]_4$ the Al(I) compound obtained $[Cp^*AlO]_4$ (**III**, R = Cp*). It was further hydrolyzed to form Al–O–Al containing compounds, with structures similar to those found in boehmite or diaspore, i.e., two of the main minerals found in bauxite rocks, used for extracting alumina.[129]

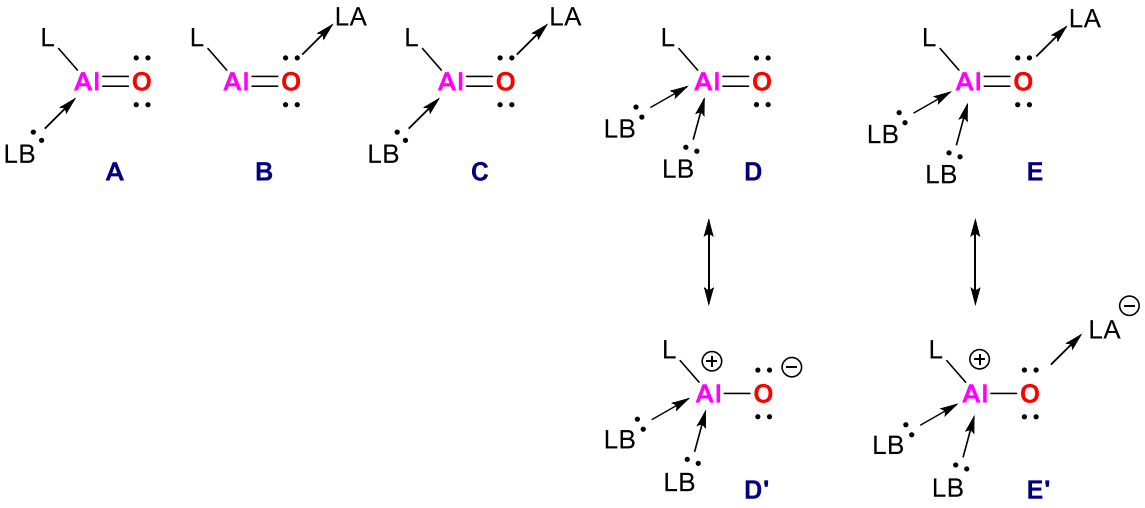

Figure 7. Stabilization of Al–O multiple bonds by Lewis base (**A**, **D**), Lewis acid (**B**) or both (**C**, **E**).

An alternative way for the preparation of elusive species at ambient temperature, avoiding low-temperature matrix isolation techniques, requires intricate ligand systems. For example, with the use of sterically demanding ancillary ligands, Al–O–Al motifs have been isolated successfully.[10, 12] Isolation of the monotopic Al=O fragment, i.e., the parent entity of the aggregates mentioned above, as a well-defined molecule at ambient temperature has been of high interest so far. To achieve this, not only sterically demanding ligands, but also the additional kinetic and/or thermodynamic stabilization by combination with LAs or/and LBs is required to hinder self-oligomerization and subsequent aggregation. As shown in Figure 7, there are various strategies (**A**-**E**) to stabilize the discrete Al–O multiple bonds, which have allowed for the successful isolation of a handful of examples.[10] Herein, the electron-donating LB

coordinates to the electron-poor Al^+ center while the electron-accepting LA attaches to the electron-rich O^- center.

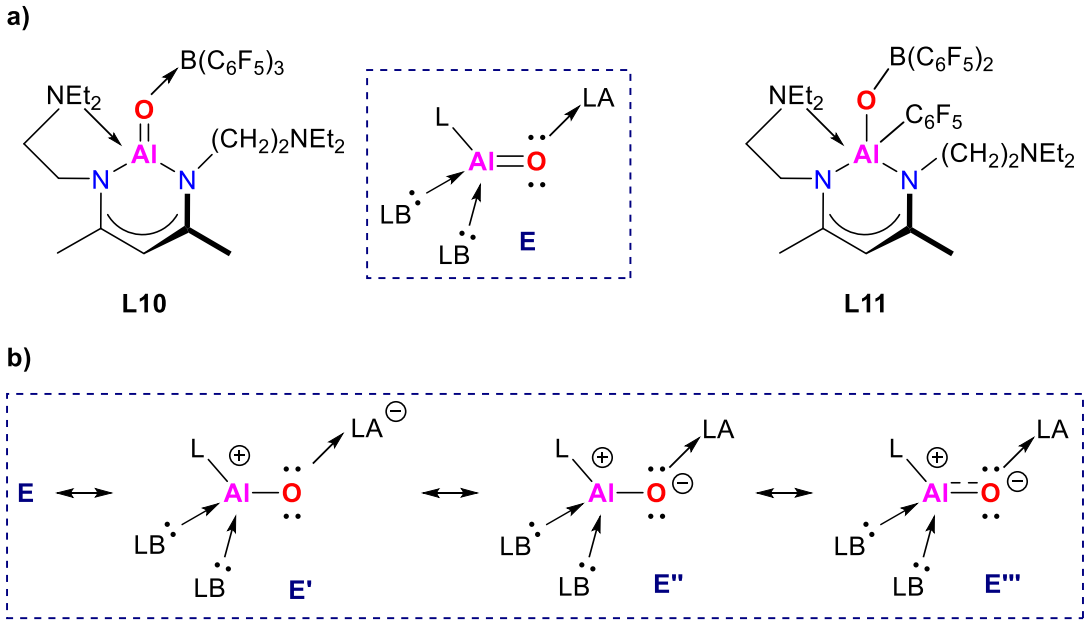

Figure 8. a) The first neutral Al=O double bond containing compound **L10** and a related compound **L11**. b) Proposed resonance structures for **L10**.[11]

The first monoalumoxane featuring an Al=O double bond was of type E, which was stabilized by tris(pentafluorophenyl)borane at the oxygen ([^{Amino}Nacnac]Al=O·B(C_6F_5)$_3$ **L10**, Figure 8, a).[11] The Al–O bond features double bond character stabilized by an amino-tethered β-diketiminato ligand providing additional LB stabilization to the Al center, by combination with the LA stabilization. These can be explained by the nature of bonds and the resonance structures (e.g., **E'''**) given in Figure 8 (b). The LA disperses the negative charge from oxygen and prevents oligomerization. This is also supported by the presence of another product isolated as **L11** (Figure 8, a).

Al–O multiply bonded compounds are limited to a few examples due to their inherent instability. Until now, there has been no example of type **A-D** (Figure 7). The study of molecular aluminum oxide ions with the O center bearing a negative charge are scarce,[11-12, 130-131] owing to the electrostatic drive towards oligomerization. As the first example of anionic species, ([^{Dipp}Nacnac]Al(Me)OLi)$_3$ (**L12**, Figure 9) exists as a tightly-bound trimer in the solid state by deprotonation of an aluminum hydroxide [^{Dipp}Nacnac]Al(Me)OH by using Li[N($SiMe_3$)$_2$].[130]

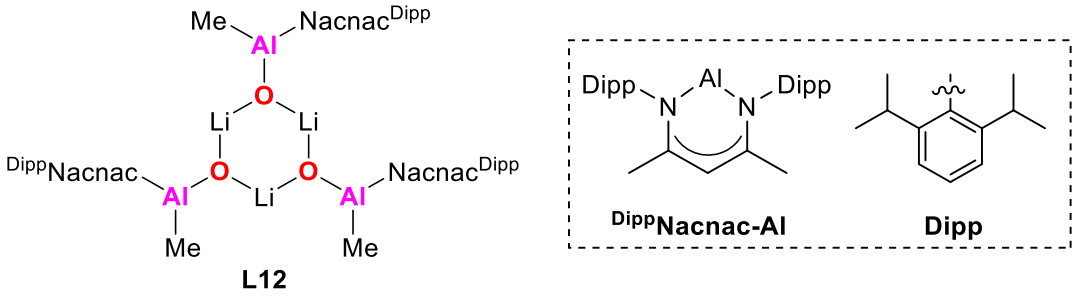

Figure 9. The first example of anionic Al–O species (**L12**)

Aldridge and coworkers pioneered anionic aluminyl chemistry with the first report of the dimethylxanthene stabilized potassium aluminyl anion, $K_2[Al(^{Dipp\textit{t}Bu}NON)]_2$ ($^{Dipp\textit{t}Bu}NON$ = 4,5-bis(2,6-diisopropylanilido)-2,7-di-*tert*-butyl-9,9-dimethylxanthene).[132] This is an unprecedented compound that offers potential as a nucleophilic reagent with the idea of reversing polarity on the Al center. The anionic Al(I) center is balanced by an alkali metal counterpart. This species displays unusual reactivity in the formation of aluminum–element covalent bonds and in the C–H oxidative addition of benzene.[44, 133-141] Meanwhile, Coles and coworkers isolated the alkali metal aluminyl $M_2[Al(^{DippSi}NON)]_2$ ($^{DippSi}NON$ = $[O(SiMe_2NAr)_2]^{2-}$, Ar = 2,6-*i*$Pr_2C_6H_3$). M = K[142], Li, and Na.[143] The anionic nature has been employed for the isolation of discrete Al=O bonds in Figure 10.

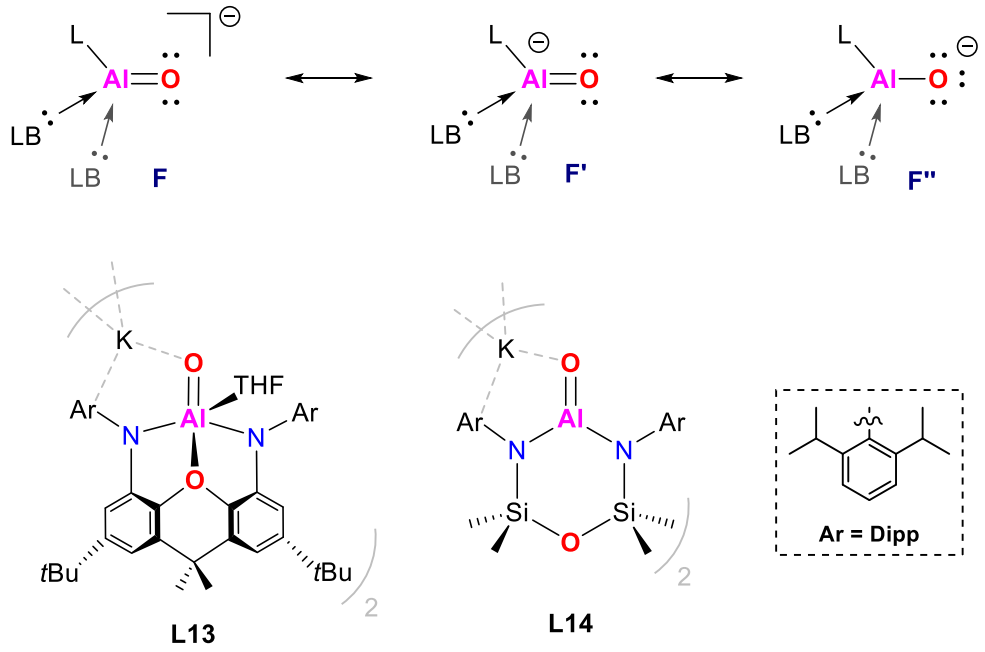

Figure 10. Major resonance forms of the aluminyl anions, and currently reported examples of the aluminyl anion (**L13** and **L14**).

As the example of type F, [(^{Dipp}*t*^{Bu}NON)Al=O(THF)]$^{-}_2$K$^{+}_2$ (**L13**)[12] features the unquenched Lewis basic character at the O center in conjunction with the Lewis acidic aluminum center. As shown in Figure 11, the reactivity towards H_2 showed the extent of the polarization of the Al–O bond which is comparable to that of multiple bonds in transition metal.[144-145] This is also the evidence of the Frontier orbitals described in Figure 3, **iii**. The multiple bond character of Al–O was further supported by cycloaddition reaction of CO_2 yielding **L16**.[12]

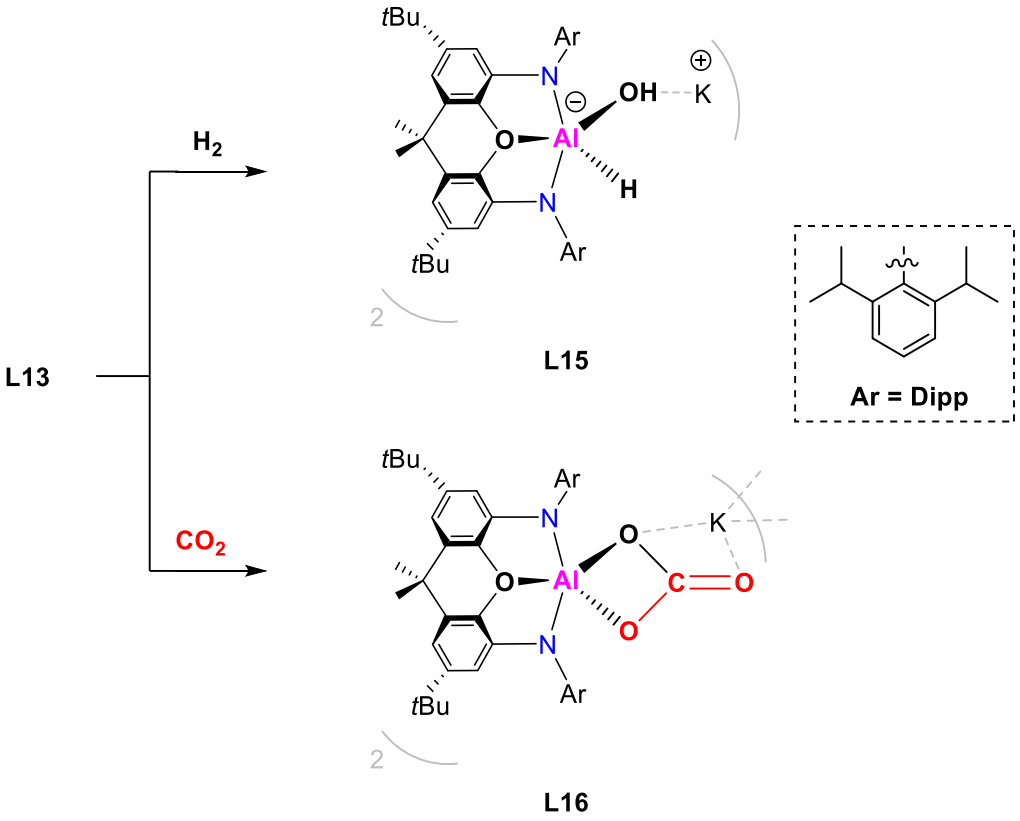

Figure 11. Reactions of the aluminum oxide [(^{Dipp}*t*^{Bu}NON)Al=O(THF)]$^{-}_2$K$^{+}_2$ **L13** with H_2 and CO_2.

[(^{Dipp}Si NON)Al=O]$^{-}_2$K$^{+}_2$ **L14**[13] bears an Al–O bond with multiple bond character which is dominated by the ionic resonance **F''** (Figure 10). Cycloaddition reactions with CO_2 or N_2O were observed. As shown in Figure 12, **L17** was formed through a formal [2+2]-cycloaddition,[13] which is same to the reaction of CO_2 and **L13**. Treatment of CO with **L14** obtained **L18**, through generating the aluminum carbene species.[146] These results proved again **L14** features double bond character of Al=O.

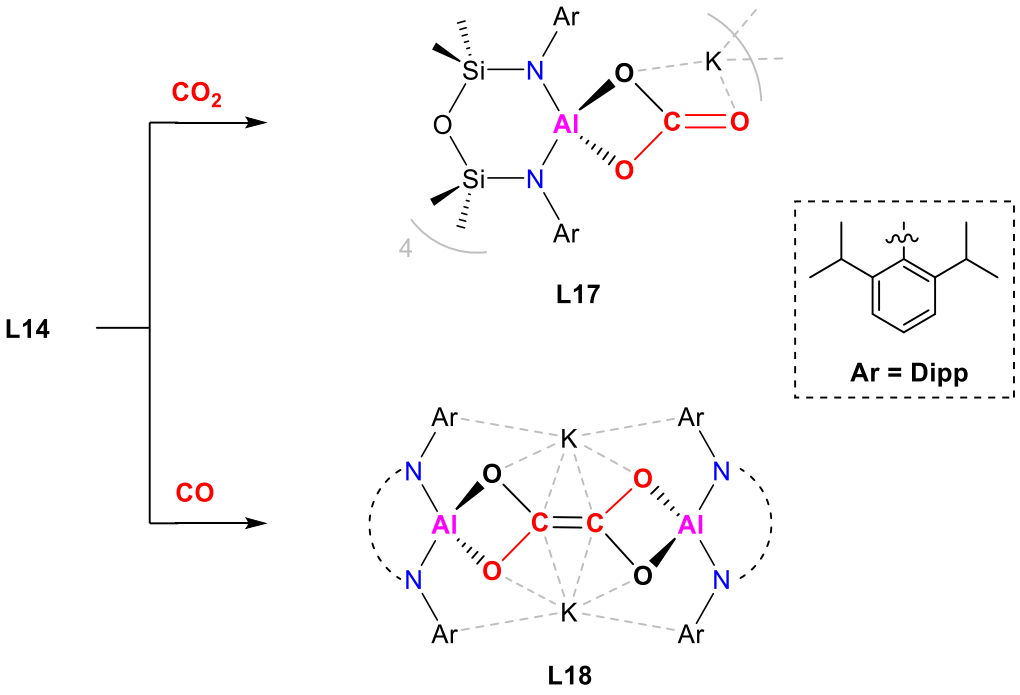

Figure 12. Reactions of the aluminum oxide [(^{DippSi}NON)Al=O]$^{-}_{2}$K$^{+}_{2}$ **L14** with CO_2 and CO.

With the oxygen as the lightest element of group 16, the reported study of Al–O bonds has paved the way for the research of heavier aluminum chalcogenides (Al–S, Al–Se, Al–Te) reported in this thesis.

2.2.2. Heavier aluminum chalcogenides

2.2.2.1. Aluminum sulfides

Aluminum sulfides have attracted great interest as catalysts and intermediates in oxidation or enzymatic activity.[147] They also see use on an industrial scale in catalytic/biological reactions, such as the hydrodesulfurization of fossil fuels/desulfurization processes of crude oil and flue-gas, as well as in chemical vapor deposition (CVD). They also have provided a rational candidate for sulfur transfer and the preparation of new Al–Ch multiple bonds. Despite being known for a long time, the inherent instability (caused by the large angle strain and repulsive interaction between the lone pair electrons) of aluminum sulfides has limited their study and further reactivity.

A promising approach to aluminum sulfides is the sulfurization of aluminum dihydrides (Figure 5) forming Al–SH bonds. These kinds of species are a good candidate for further sulfurization or reduction to obtain new Al–S containing compounds. Roesky and coworkers isolated **L19** (Figure 13) by the reaction of S_8 and the aluminum dihydride **L3** in the presence of $P(NMe_2)_3$ as catalyst.[148] Similarly, $[(^{Mes}Nacnac)Al(SH)]_2(\mu\text{-}S)$ ($^{Mes}Nacnac$ = $HC[(CMe)N(2,4,6\text{-}Me_3C_6H_2)]_2$) was prepared by treatment of S_8 with $(^{Mes}Nacnac)AlH_2$.[106] Our group prepared mono- and bis(hydrogensulfide) aluminum sulfides **L20** and **L21** by employing the aluminum dihydride **L4** as the precursor.[107]

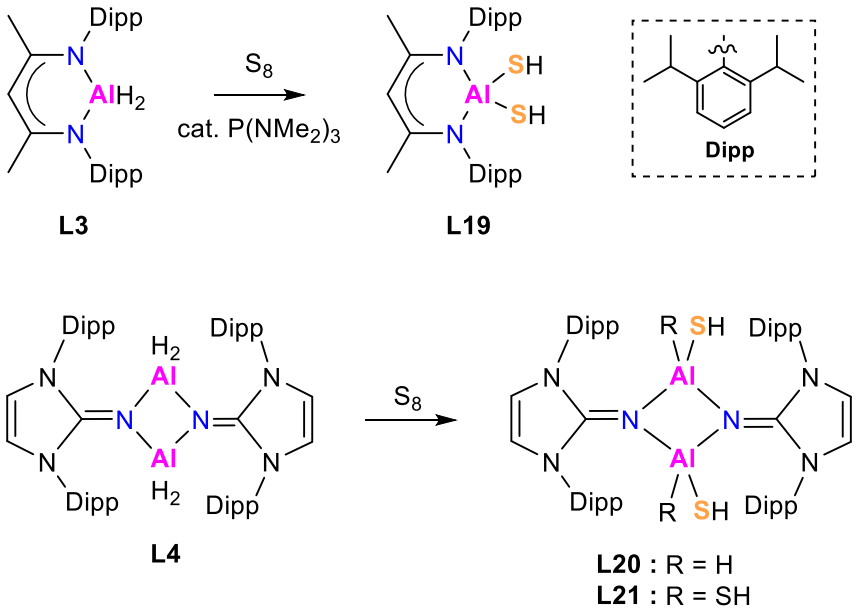

Figure 13. Selected examples of aluminum sulfides containing Al–SH bonds (**L19**-**L21**).

Like Al–O described in Figure 6, analogous clusters containing the Al–S bonds, tetramers, dimers, and other oligomers can be formed (Figure 14). For instance, aluminum polysulfides [^{Dipp}Nacnac]AlS$_6$ **L22** and [^{Dipp}Nacnac]AlS$_4$ **L23** were obtained as side products through the process of the preparation of the heterobimetallic cluster [(^{Dipp}Nacnac)Al-μ-S$_2$Cu$_2$]$_2$ and [(^{Dipp}Nacnac)Al-μ-S$_2$Ag$_2$]$_4$ by using ^{Dipp}NacnacAlH$_2$ **L3** as the precursor.[149] [(^{Dipp}Nacnac)Al]$_2$(μ-S$_3$)$_2$ (**L24**) bearing an eight-membered Al$_2$S$_6$ ring was isolated by using [^{Dipp}Nacnac]Al(I) as the precursor.[150] Other oligomers (e.g., [Al$_4$(μ-S)$_6$-(NMe$_3$)$_4$] and [Al$_4$H$_2$(μ-S)$_5$(NMe$_3$)$_4$][151] were also formed. Similarly to the oxygenated product, tetrameric [Cp*AlS]$_4$ (**L25**, R = Cp*) was obtained by the reaction of S$_8$ and [Cp*Al(I)]$_4$.[129] The tetramer (**L25**, R = C(SiMe$_3$)$_3$) together with [C(SiMe$_3$)$_3$]$_3$(Me)Al$_4$[152] and the tetramer (**L25**, R = Me$_2$EtC) together with the hexamer [(Me$_2$EtC)Al(μ_3-S)]$_6$[153] were obtained.

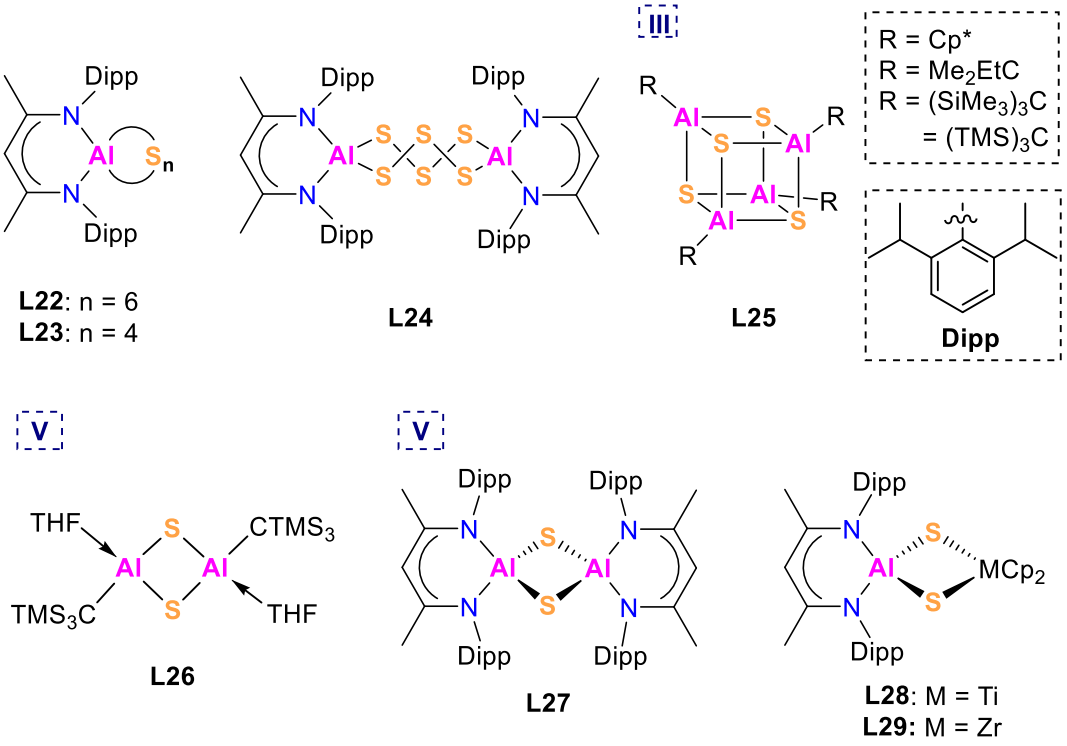

Figure 14. Selected oligomer examples of aluminum sulfides containing Al–S bonds (**L22-L29**) (**III** in the dashed square box: the tetrameric form, **V**: the dimeric form).

Like the dimeric aluminum oxides of type V (Figure 6), dimeric aluminum sulfides were isolated through use of bulky ligands or in combination with donor ligands. For example, one bulky ligand supporting [MesAlS]$_2$ dimer[154] is formed by the reaction of aluminum hydride (Mes*AlH$_2$)$_2$ (Mes* = 2,4,6-*t*Bu$_3$C$_6$H$_2$)[155] with S(SiMe$_3$)$_2$, and in the presence of THF,

[((Me$_3$Si)$_3$C)(THF)Al(μ-S)]$_2$ **L26**[152] was obtained. By using a chelating ligand system, [(^{Dipp}Nacnac)Al-μ-S]$_2$ (**L27**) was prepared by the reaction of [^{Dipp}Nacnac]Al(SH)$_2$ **L19** and [^{Dipp}Nacnac]AlH$_2$ **L3**.[156] In addition, the heterobimetallic aluminum sulfides [^{Dipp}Nacnac]Al(μ-S)$_2$MCp$_2$ (M = Ti (**L28**), M = Zr (**L29**)) were prepared by the lithiation products of **L19**.[157] A similar procedure and precursor, led to the formation of mixed main group compound [^{Dipp}Nacnac]Al(μ-S)$_2$GeR$_2$ (R = Me or Ph).[158] Aggregation can be avoided with very bulky ligands such as chelating *N*-*N* donor ligand (i.e. pyrazolato) used in the isolation of dialuminum sulfide **L30** (Figure 15).[159]

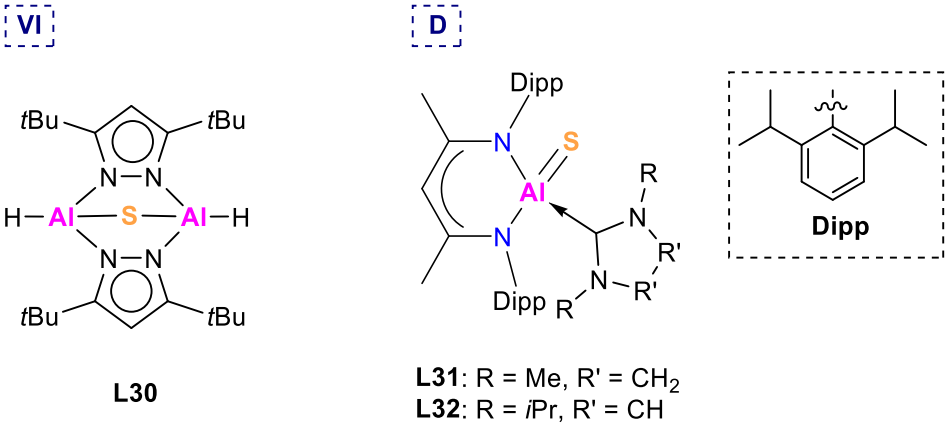

Figure 15. Dialuminum sulfide (**L30**) and aluminum sulfides containing Al=S double bonds (**L31** and **L32**) (**VI** in the dashed square box: the oligomer form, **D**: the Lewis base stabilization type).

The donor stabilized aluminum sulfides consisting of Al=S double bonds **L31** and **L32** were obtained as neutral species by the treatment of [^{Dipp}Nacnac]Al(I) with chelating thioureas. Whereby, the thermally unstable [^{Dipp}Nacnac]Al=S(S=PPh$_3$) was observed by treatment of S=PPh$_3$ with Al(I) species. They present the first monomeric examples bearing a terminal Al=S double bond.[160] The reactivity of the Al=S bond was demonstrated by the facile oxidative chemistry giving new aluminum oxo and imido species.

Figure 16 shows [(^{DippSi}NON)AlS$_4$K]$_n$ **L33** bearing the form of AlS$_4$ is the congener of [^{Dipp}Nacnac]AlS$_4$ **L23** (Figure 14). The treatment of PPh$_3$ with **L33** yielded a tetramer [((^{DippSi}NON)Al=S)$^-$K$^+$]$_4$ **L34** bearing Al=S double bonds with combination of K$^+$. The potassium counterion can be sequestered by [2.2.2]-cryptand, which subsequently afforded the monomeric species [K$^+$(2.2.2-crypt)][(^{DippSi}NON)Al=S]$^-$ **L35**, an aluminum sulfide with an Al=S double bond.[161]

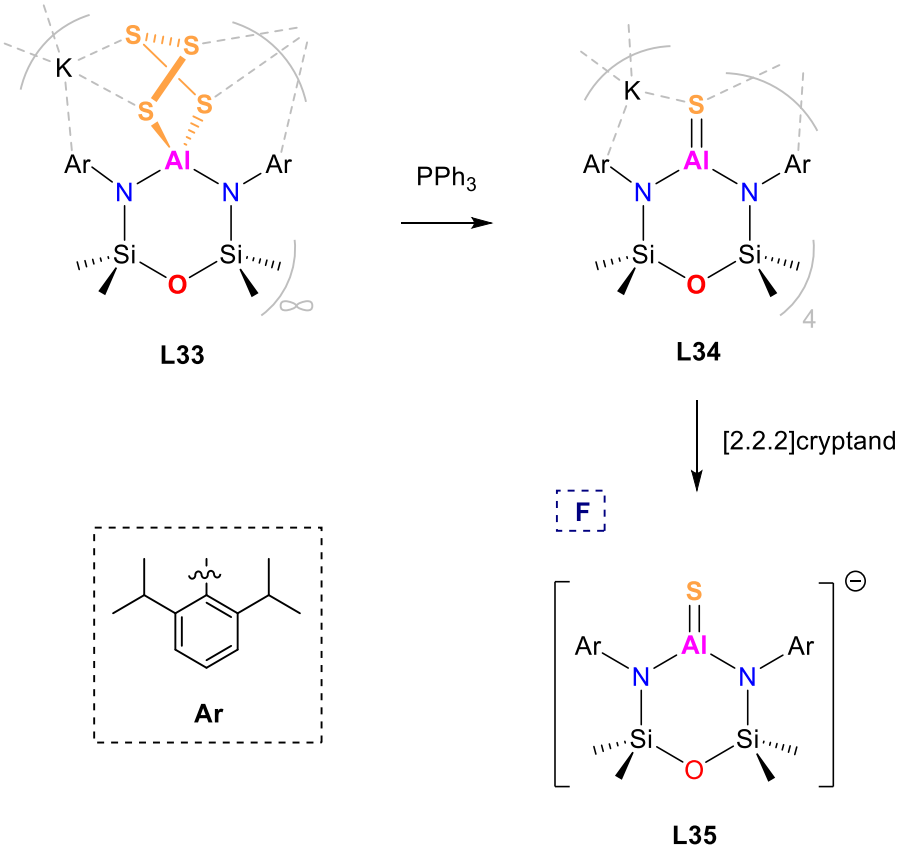

Figure 16. Formation of $[K^+(2.2.2\text{-crypt})][(^{DippSi}NON)Al{=}S]^-$ **L35** from $[(^{DippSi}NON)AlS_4K]_n$ **L33** and $[((^{DippSi}NON)Al{=}S)^-K^+]_4$ **L34** (**F** in the dashed square box: the anionic stabilization type).

As a result, the facile access to Al–Ch multiple bonds derived from aluminyls has facilitated the study of their physical and chemical properties. Multiply bonded Al–S compounds are reactive to activate and functionalize a number of substrates such as unsaturated substances (C=O, C=C, O=N et. al).[147, 161]

2.2.2.2. Aluminum selenides

Roesky and coworkers reported the first structurally characterized Al–SeH compounds **L36** and **L37** supported by the β-diketiminato ligands by using the aluminum dihydride [^{Dipp}Nacnac]AlH$_2$ **L3** as a precursor (Figure 17).[88]

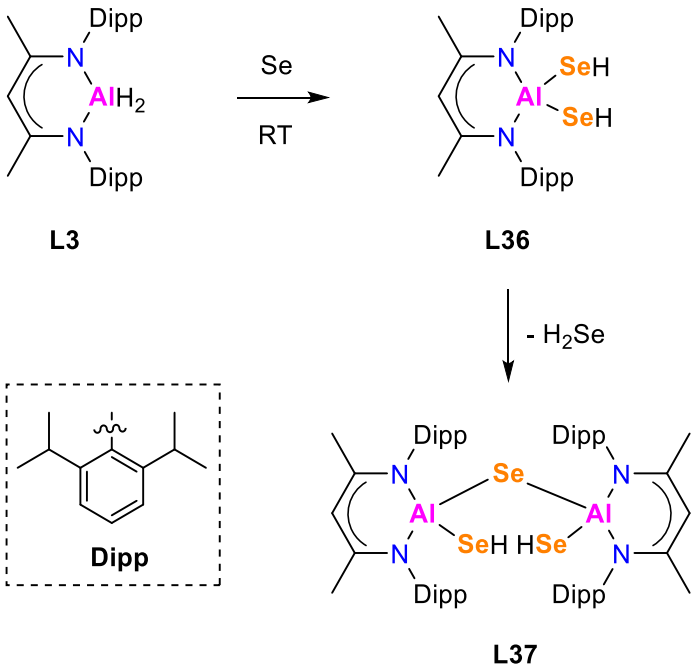

Figure 17. Selected examples of Al–SeH bonds (**L36**, **L37**).

Following the trend of the Al–O polarization (Figure 6), various Al–Se containing tetramers **L38** (R = *t*Bu,[19] Cp*,[162] Me$_2$EtC,[153] (Me$_3$Si)$_3$C[163]) (Figure 18) and the tetranuclear cluster [Al$_4$H$_2$(μ-Se)$_5$(NMe$_3$)$_4$][164] were reported. There are numerous Al–Se dimers **L39** supported by different ligands (R = H, R' = NMe$_3$;[165] R = PhE, R' = NMe$_3$ (E = Te[164], S or Se[166]); R = N(Me$_3$Si)$_2$, R' = NMe$_3$;[166] R = (SiMe$_3$)$_3$C, R' = Me (with Me on Se);[152] R = Mes, R' = Mes (with Me on Se)[167]).

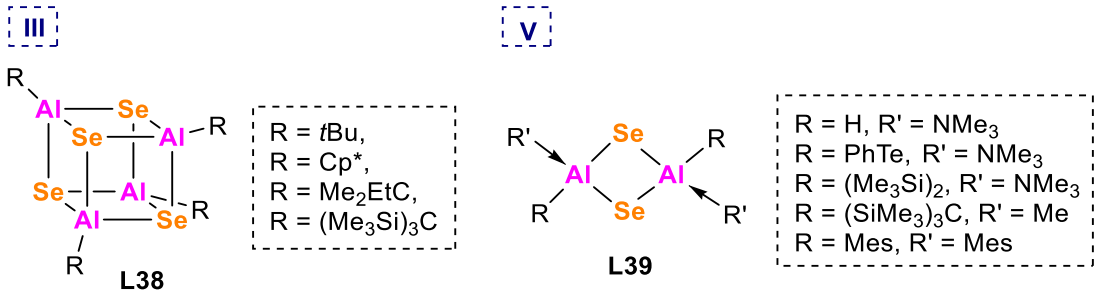

Figure 18. Selected aluminum selenide oligomers containing Al–Se bonds (**L38**, **L39**) (**III** in the dashed square box: the tetrameric form, **V**: the dimeric form).

Chelating ligands have been shown to be effective in isolating dimeric aluminum selenides (Figure 19). For example, Roesky and coworkers prepared **L40**[156] using the β-diketiminato ligand by the reaction of [^{Dipp}Nacnac]AlH$_2$ **L3** and Te=P(NMe$_2$)$_3$, **L41** **[**(^{Dipp}NH(CH$_2$)$_3$N^{Dipp})Al(μ-Se)]$_2$[168], **L42** by using the dimer **L39** (R = H, R' = NMe$_3$) as a precursor,[166] and the dimer **L43**[18] as well as **L44**.[169] Dialuminum selenide **L45** was isolated by treatment of Se with the corresponding aluminum hydrides[159] and [R$_2$Al]$_2$–μ–Se (R = CH(SiMe$_3$)$_2$) **L46** was prepared by [((TMS)$_2$HC)$_2$Al]$_2$ as a precursor.[170] So far, there has been no neutral example bearing an Al=Se double bond, although there are such various stabilization strategies in Figure 7.

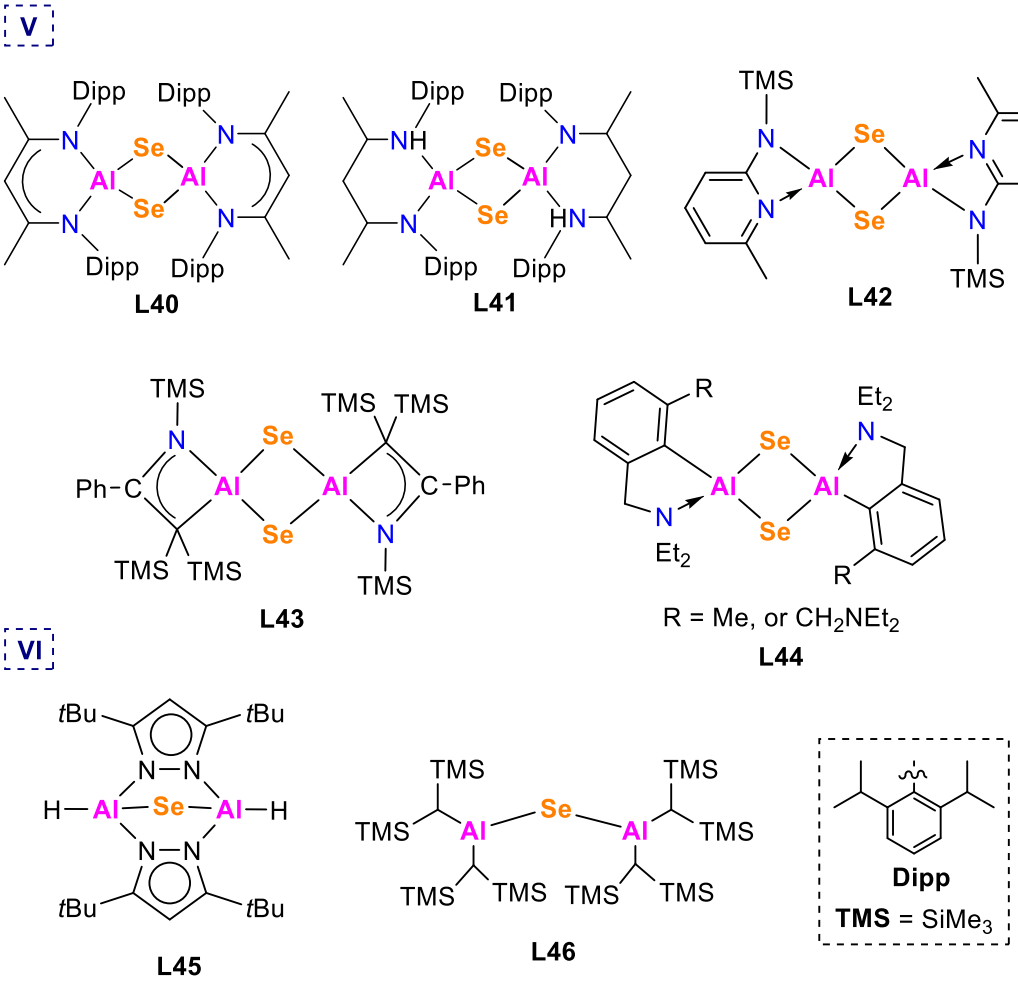

Figure 19. Selected examples of aluminum selenides containing Al–Se bonds (**L40**-**L46**) (**V** in the dashed square box: the dimeric form, **VI**: the oligomer form).

Recently, Coles and Anker reported [K$^+$(2.2.2-crypt)][(^{DippSi}NON)Al=Se]$^-$ **L48** (Figure 20)[171] as the first and only monomeric anion with a terminal Al=Se bond. It was isolated by

using the aluminyl selenide **L47** [((^{DippSi}NON)Al=Se)$^{-}$K^{+}(THF)]$_n$ in the presence of [2.2.2]cryptand. The asymmetric unit of **L47** comprises the [(^{DippSi}NON)Al=Se]$^{-}$ anion, which is linked to a [K(THF)]$^{+}$ cation through Se···K and π-arene interactions. The double bond character of **L48** was further evidenced by the formation of the aluminyl diselenirane ring in **L49** (Figure 20).

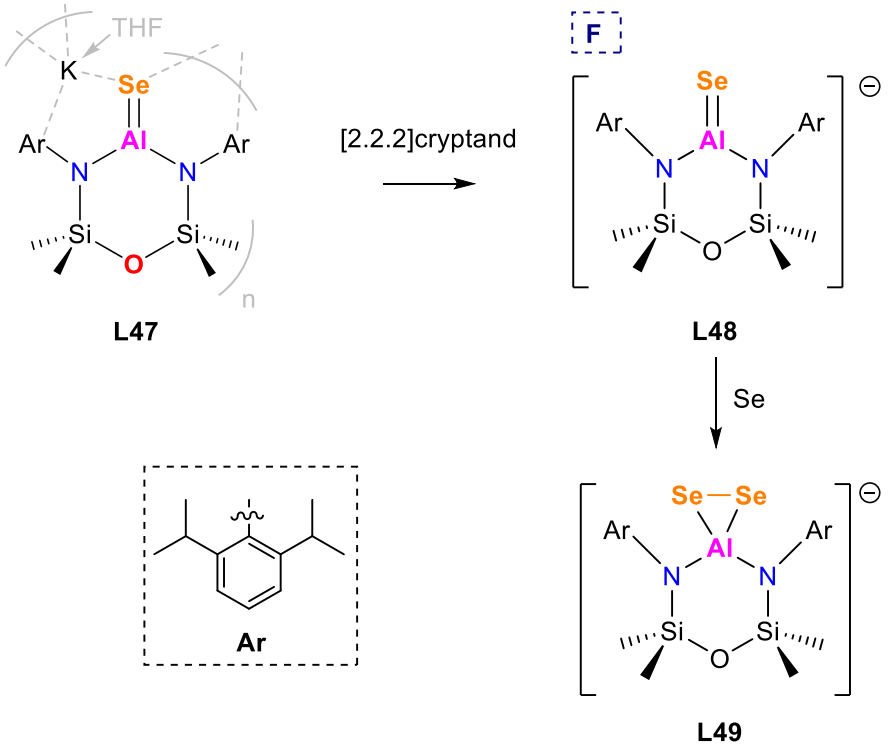

Figure 20. Synthesis of the first monomeric anion bearing Al=Se double bond **L48**, and its reaction with elemental Se (**F** in the dashed square box: the anionic stabilization type).

2.2.2.3. Aluminum tellurides

Aluminum telluride is the heaviest reported aluminum–chalcogen species. Of the Al–Ch series, tellurido species are the least reported presumably due to the synthetic challenges caused by a longer Al–Te bond accelerating aggregation.[16]

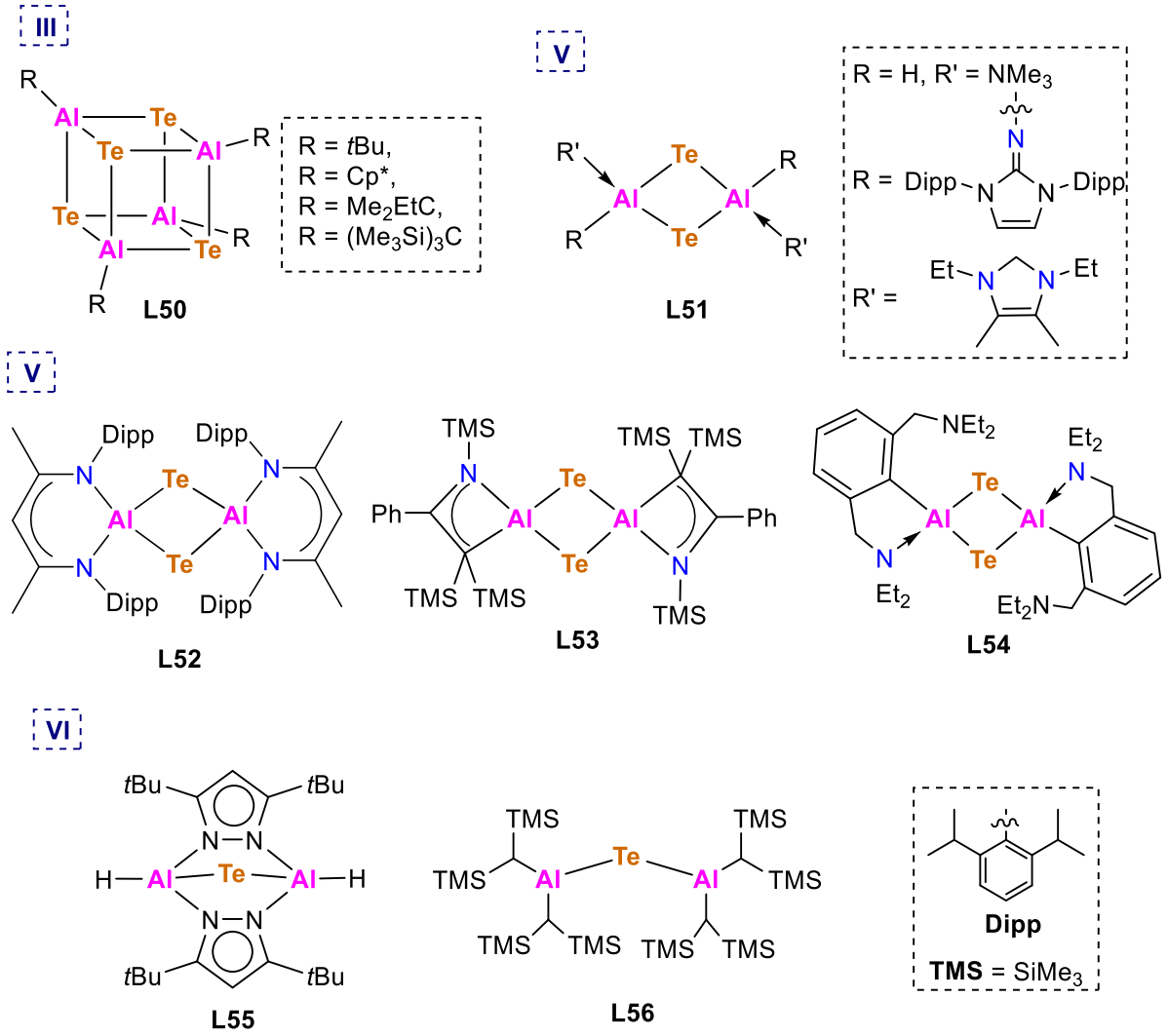

Figure 21. Selected examples of tetramer and dimers containing Al–Te bonds (**L50**-**L56**) (**III** in the dashed square box: the tetrameric form, **V**: the dimeric form, **VI**: the oligomer form).

Figure 21 shows the Al–Te tetramers **L50** (R = *t*Bu,[19] Cp*,[162] Me_2EtC,[153] $(Me_3Si)_3C$[163]), the dimers **L51** stabilized by various ligands (R = H, R' = NMe_3;[165] R = L^{Dip}, R' = IMe_2Et_2;[17] R = *t*Bu, R' = *t*Bu (with *t*Bu on Te)[19]), and the chelating ligands stabilized dimers, such as **L52** supported by β-diketiminato ligand by the reaction of [^{Dipp}Nacnac]AlH_2 **L3** and $Te{=}PMe_3$,[156] the dimers **L53**[18] and **L54**[169]. Very bulky ligands allowed to prepare dialuminum tellurides **L55**[159] and **L56** $[R_2Al]_2$–μ–Te (R = $CH(SiMe_3)_2$).[172]

Our group isolated [NHI(IMe$_2$Et$_2$)$_2$]Al=Te **L57** which is the first monotopic aluminum telluride comprising the electron-precise and discrete Al=Te double bond (Figure 22).[17] It is stabilized by one NHI and two NHCs. Al–Te features a high polarity similarly to the showed ionic resonance contribution in Figure 6 (**I**), which is the evidence for the formation of [NHI(IMe$_2$Et$_2$)Al]$_2$ (**L51**, R = NHI, R' = IEt$_2$Me$_2$) by the dimerization of **L57** at elevated temperature.

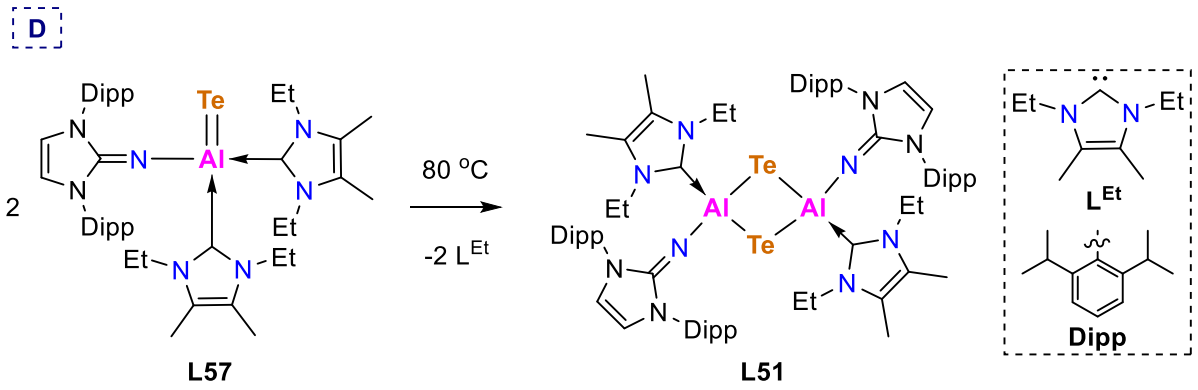

Figure 22. The dimerization of [NHI(IMe$_2$Et$_2$)$_2$]Al=Te **L57** (**D** in the dashed square box: the Lewis base stabilization type).

However, the bidentate supporting ligands were used on the Al center for the family bearing an Al=Ch double bond, the neutral aluminum oxide **L10** bearing Al=O (Figure 8), the neutral aluminum sulfides **L31** and **L32** with Al=S (Figure 15) and the aluminyl anionic species (**L13** and **L14** (Al=O, Figure 10), **L34** and **L35** (Al=S, Figure 16), **L48** (Al=Se, Figure 20)), which resulted in the steric and electronic stabilization on the Al–Ch unit limiting the investigation of their reactivity.

[(^{DippSi}NON)(THF)Al=Te]$^-$ **L58** presents as the second example bearing a terminal Al=Te double bond (Figure 23).[16] It is the final member of the homologous series of [(^{DippSi}NON)Al=Ch]$^-$ aluminyl anions containing Al=Ch double bonds (Ch = O, S, Se, Te). The double bond character of the Al–Te bond in **L58** is confirmed by the cycloaddition reaction with CO_2 yielding the double CO_2 insertion product **L59** .[16] Similarly, as Figure 23 showed the Al=S double bond of **L34** and the Al=Se bond of **L47** show chemical reactivity towards CO_2 obtaining the cycle-oxidation products **L60** and **L61**,[161] which is consistent with the Al=O double bonds of **L13** and **L14** (Figure 11 and 12).

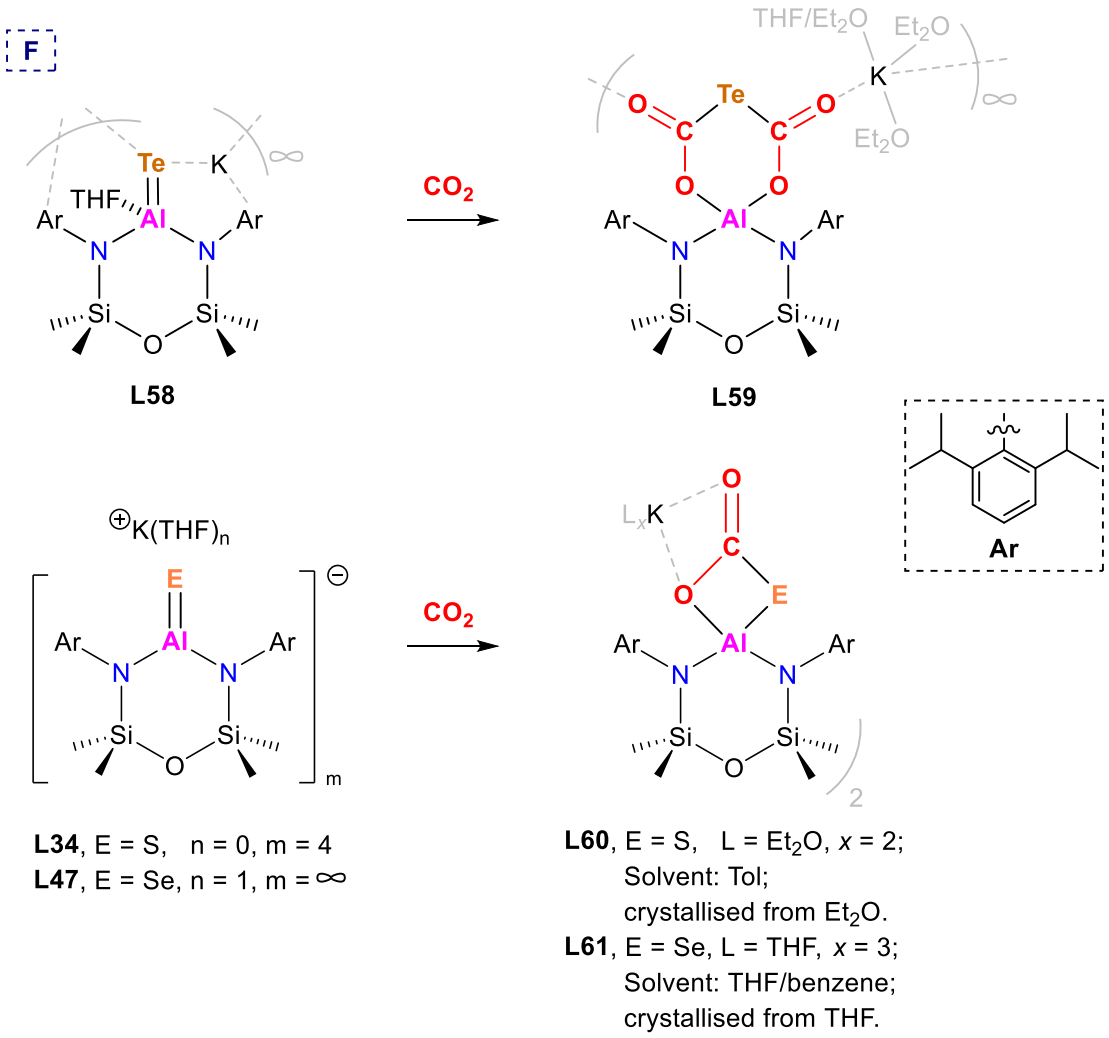

Figure 23. The reactions of CO_2 with compounds containing Al=Te (**L58**), Al=Se (**L47**), and Al=S (**L34**) (**F** in the dashed square box: the anionic stabilization type).

In summary, currently reported heavier Al–Ch (Ch = S, Se, Te) multiple bonds have proven easier to handle than Al=O while there are more emerging isolable examples. The facile access to multiply bonded Al–Ch molecules facilitates the discovery on their bonding natures. The subsequent studies on their reactivity towards various substrates yielded new Al–Ch containing species which are showed above and also summarized in some reviews.[8, 14, 37, 65, 142, 173-174] All studies on these species accordingly offer fundamental theory in aluminum chalcogenides, especially aluminum oxides, whose bond nature and aggregation principle deserve being unveiled and inform future development of new materials.

2.2.3. Molecular structures and theoretical study

The nature of the multiple bonds between aluminum and chalcogen has been investigated by spectroscopic, crystallographic, and computational methods. Table 1 showed the characteristic structural or calculated data of the compounds bearing multiply bonded Al–Ch (O, S, Se, and Te) bonds for rational comparisons.

Among neutral species bearing Al=Ch double bonds (**L10** (Al=O), **L32** (Al=S), **L57** (Al=Te)), the Al=O double bond length in **L10** is 1.659(3) Å, is the shortest Al–O bond compared with other examples in literature, and consistent with multiple-bond character.[11] The Al=S double bond length in **L32** is 2.104(1) Å which is shorter than the predicted sum of the molecular covalent double bond radii, r_2 ($\Sigma(r_2)$=2.111 Å).[160] The Al=Te double bond length in [NHI(IMe$_2$Et$_2$)$_2$]Al=Te **L57** is 2.5130(14) Å,[17] which is shorter than the 2.549(1)Å[170] found for the ditopic [((SiMe$_3$)$_2$CH)$_2$Al]$_2$–μ–Te **L46** and other compounds containing the Al–Te single bonds.

For anionic species bearing Al–Ch multiple bonds, one example supported by ^{Dipp}*t*^{Bu}NON ligand (**L13**, Table 1) consists of a dimer but with two discrete Al=O double bonded moieties, has a mean bond length of 1.676 Å.[12] They are significantly shorter than those found in the lithium aluminum oxide trimer [(^{Dipp}Nacnac)Al(Me)OLi]$_3$ **L12** (1.698(1) Å, Figure 9),[130] but slightly longer than that of the neutral species **L10** (1.659(3) Å). The ^{DippSi}NON ligand has been reported for the full species of Al–Ch (O, S, Se, Te) multiple bonds (Table 1). The terminal Al=O double bond length in **L14** is 1.6362(14) Å,[13] which is shorter than r_2 ($\Sigma(r_2)$=1.66 Å). The Al=S double bonds in **L34** are within the range 2.0857(7)-2.1039(7) Å,[161] which are shorter than the Al–S multiple bond found in **L32** (2.104(1) Å) and the predicted value for the sum of the molecular covalent double bond radii, r_2 ($\Sigma(r_2)$ = 2.13 Å), showing a significant shortening of the bond. The terminal Al=S double bond length in **L35** is 2.0760(11) Å[161] which is shorter than those in **L34**. This data suggests that there is no S···K interaction in **L35** which would cause a decrease of the Al–S distance. This trend was also observed for the Al–Se bond length, that in **L47** (2.2253(11) Å)[171] is slightly longer than the observed bond length in **L48** (2.2032(6) Å)[171] wherein the cation is sequestered. The Al=Te bond length in **L58** is 2.5039(7) Å,[16] which is shorter than that in **L57** (2.5130(14) Å), consistent with multiple-bond character contributing to a shortening of the bond, although longer than $\Sigma(r_2)$, 2.46 Å.

Table 1. Summary of structural and computational results for the current reported neutrals and anions bearing the Al=Ch (O, S, Se, Te) multiple bonds

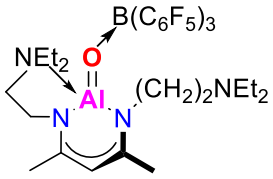

L10

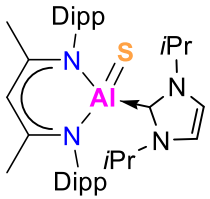

L32

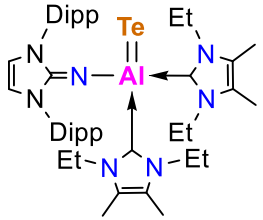

L57

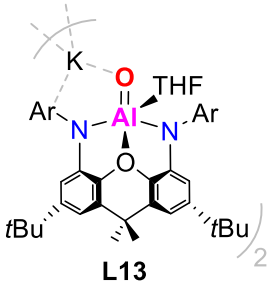

L13

	L10	L32	L57	L13
Al-Ch/Å (X-ray)	1.659(3)	2.104(1)	2.5130(14)	1.6754(12), 1.6772(12)
Al-Ch/Å (Calculated)		2.111		1.66/1.640(without THF)
$\Delta\chi_p$ (Electronegativity difference)	1.83	0.97	0.49	1.83
NPA charges (*q*) (Natural Population Analysis)			*q*(Al) = +1.24, *q*(Te) = -0.95	*q*(Al) = +2.07, *q*(O) = -1.52 *q*(Al) = +1.96, *q*(O) = -1.44 (without THF)
Wiberg bond index (WBI)		1.20	1.20	0.64/0.89(without THF)
Mayer bond order (MBO)		1.49		

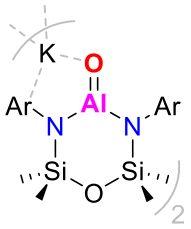

L14

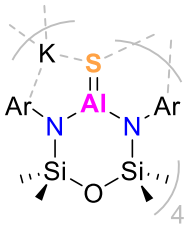

L34

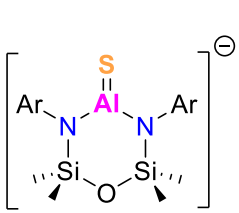

L35

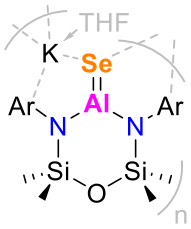

L47

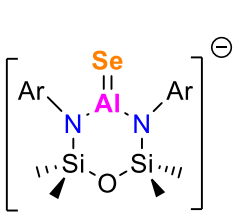

L48

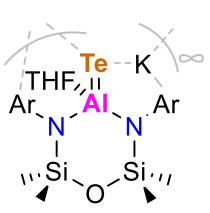

L58

	L14	L34	L35	L47	L48	L58
Al-Ch/Å (X-ray)	1.6362(14)	2.0873(7), 2.0957(7), 2.1039(7), 2.0857(7)	2.0760(11)	2.2253(11)	2.2032(6)	2.5039(7)
Al-Ch/Å (Calculated)	1.66	2.13	2.11	2.27	2.24	2.46
Δd_{AlCh} (%)[a]	6.5[b]	Range: 6.1-6.9[c]	7.4[c]	5.7[d]	6.6[d]	3.4[e]
$\Delta\chi_p$[f]	1.83	0.97	0.97	0.94	0.94	0.49
NPA charges (*q*)	*q*(Al) = +1.93, *q*(O) = -1.23		*q*(Al) = +1.85, *q*(S) = -1.26		*q*(Al) = +1.82, *q*(Se) = -1.23	*q*(Al) = +1.78, *q*(Te) = -1.19
WBI	1.11 (without K^+) 0.91 (with K^+)		1.30 (without K^+) 1.15 (with K^+)		1.38 (without K^+) 1.24 (with K^+)	1.53 (without K^+) 1.44 (with K^+)
Bond critical point (BCP) analysis						
$p(r)/e$ Å^{-3}	0.115		0.076		0.068	0.061
$\nabla^2 p(r)/e$ Å^{-5}	+0.990		+0.290		+0.183	+0.089
Ellipticity, ε	0.033		0.080		0.108	0.139

Note: [a] Δd_{AlCh} (%) = [1-*d*(Al=Ch)/*d*(Al–Ch)]×100% with *d*(Al–Ch) equal to the average value calculated from structurally determined Al–Ch bonds listed in the Cambridge Structural Database (CSD). [b] Calculated using the average value of *d*(Al–O) = 1.74 Å from 35 entries of Al–OH bonds in the CSD. [c] Calculated using the average value of *d*(Al–S) = 2.59 Å from 12 entries of Al–SH bonds in the CSD. [d] Calculated using the average value of *d*(Al–Se) = 2.36 Å from 9 entries of Al–SeH bonds in the CSD. [e] Calculated using the average value of *d*(Al–Te) = 2.59 Å from 4 entries of Al–TePh bonds in the CSD. [f] $\Delta\chi_p = \chi_p(Ch)-\chi_p(Al)$, where χ_p (Al) = 1.61, χ_p(O) = 3.44, χ_p(S) = 2.58, χ_p(Se) = 2.55, χ_p(Te) = 2.1, according to the Pauling electronegativity scale.[161]

To further elucidate the bonding situation in aluminum chalcogenides bearing multiple bonds, density-functional theory (DFT) calculations were performed including Wiberg bond index (WBI), Natural population analysis (NPA), Mayer bond order (MBO) by using the method outlined by Bridgeman et al., Natural resonance theory (NRT), as well as the molecular orbital (MO) analysis together with the frontier Kohn-Sham (KS) orbitals.

For the consistency and to allow accurate comparisons between the different Al–Ch multiple bonds, the terminal Al–Ch in [Al(NON^{SiDipp})(E)]$^-$ (E = O (**L14**), S (**L34**, **L35**), Se (**L47**, **L48**), and Te (**L58**)) have been described by DFT, which was calculated by using the BP86 functional and the SDDALL basis set with additional d-polarization functions to describe Al (ζ_d = 0.190), Si (ζ_d = 0.284), S (ζ_d = 503), Se (ζ_d = 0.364) and Te (ζ_d = 0.252) and 6-31G** for all other atoms.[16, 161]

The major contributions to the highest occupied molecular orbital (HOMO) and HOMO-1 come from the orthogonal lone pairs located on the chalcogen atoms. Antibonding π-interaction among groups is found for the lowest unoccupied molecular orbital (LUMO).[11-13, 16-17, 160-161, 171]

The expected increase in orbital size for Al–Ch bonds involving the chalcogens is observed, with a notable extension of the principal lobes towards the aluminum for the series [Al-Te]$^-$ > [Al-Se]$^-$ > [Al-S]$^-$ > [Al-O]$^-$. This reflects the decrease in the electronegativity of the chalcogenides as the group is descended, presented as Pauling electronegativity difference across the Al–Ch bond ($\Delta\chi_p$). This is supported by NPA charges (*q*) for the aluminum and chalcogen atoms, which show a decrease when presented as the difference. The WBI calculated for the anions reflect this trend, increasing from O (1.11) < S (1.30) < Se (1.38) < Te (1.53) and are consistent with a greater bond order. Although this contradicts the expected greater orbital energy mismatch in orbital energy between Al and the heavier chalcogens, as the greater MO coefficients from the chalcogen atoms to the HOMO and HOMO-1 change from 2p, 3p (for O) to a combination of 3p, 4p and 5p for Te.[16, 161]

Quantum theory of atoms in molecules (QTAIM) analysis have also been performed on the BP86-optimised anionic Al–Ch species. The electron density associated with the Bond Critical Point (BCP), ρ(r), along the Al–Ch bond path decreases as the group 16 elements increase in molecular weight, showing a weaker Al–Ch interaction as the electronegativity of the element decreases. This is accompanied by an increase in the bond ellipticity, ε, from 0.033 in $[Al–O]^-$ to 0.139 in $[Al–Te]^-$, indicating a greater π-character of the Al–Ch bond in the order O < S < Se < Te.[16, 161]

2.3. Dialumenes

Homodinuclear multiple bonds involving heavier main group elements i.e., Si=Si, Sn=Sn, Ge=Ge, *etc.* feature accessible frontier orbitals similarly to TMs which have proven they can activate inert bonds such as H_2 (Figure 3, i).[36-37] As an extension to the aluminum analogues of alkenes, dialumenes (Figure 3, iii, E = Al) have been a notoriously difficult synthetic target over the past several decades due to the synthetic challenges (i.e. the appropriate ligand design).

For the heavier main group multiple bonds, the trans-bent geometries are observed in the solid state, while in hydrocarbon solutions these dissociate to their monomeric units. The Carter-Goddard-Malrieu-Trinquier (CGMT) model intuitively describes the geometries of multiple bonds between main group elements (Figure 4).[175-178] Molecular orbital theory is also used to describe the observed trans-bent geometry, as Jahn-Teller distortions used to describe TM geometric distortions accounts for upon descending down the group, the π–σ* gap becomes lower in energy as there is increased mixing of the π and σ* orbitals (Figure 24). It can be explained as an increasing stability of the singlet ground state resulting more trans-bending and weakening of the multiple bonds.[59, 61-62] The consistent trend is found in the group 13 elements.[14-15, 61-62, 124, 179-181]

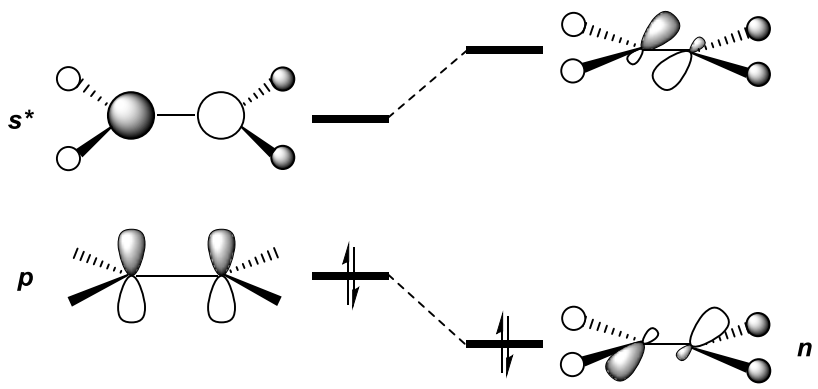

Figure 24. Schematic drawing of the mixing of the π and σ* molecular orbitals in a heavier group 14 species[62]

Due to the increased singlet lone pair character[182] and the high Lewis acidity of the Al center,[15, 60, 180, 183-184] the potential reactivity of aluminum multiple bonds is increased resulting in a very unstable multiple bond. Quantum chemical calculations revealed that the parent dialumene (HAl=AlH) can exist as trans-bent structural motif.[185] The use of more σ-donating and sterically bulky ligands will offer better thermodynamic and kinetic stability to the aluminum center, and in combination with external bases which can alter the potential energy landscape possibly leading to isolable aluminum multiple bonds.[186]

There are few examples containing aluminum multiple-bond character as radical compounds or anionic species (Figure 25). Two structurally characterized examples, tetrakis[bis(trimethylsilyl)methyl] π-radical monoanion **L62** (R = $CH(SiMe_3)$)[187] and an one-electron Al–Al π-bonding complex **L62** (R = 2,4,6-*i*$Pr_3C_6H_2$) were reported.[188] EPR spectra showed one unpaired electron occupies the π-orbital generating multiple bond character of Al–Al bonds with formal bond order >1. The first dianionic "dialuminyne" species **L63** $Na_2(^{Dipp}TerAl)_2$ (^{Dipp}Ter = 2,6-(2,6-*i*$Pr_2C_6H_3)_2C_6H_3$) and the "cyclotrialuminene" **L64** $Na_2(^{Mes}TerAl)_3$ (^{Mes}Ter= 2,6-(2,4,6-$Me_3C_6H_2)_2C_6H_3$) feature multiple-bond character, the latter presents as a trimer due to the usage of a less bulky ligand.[189]

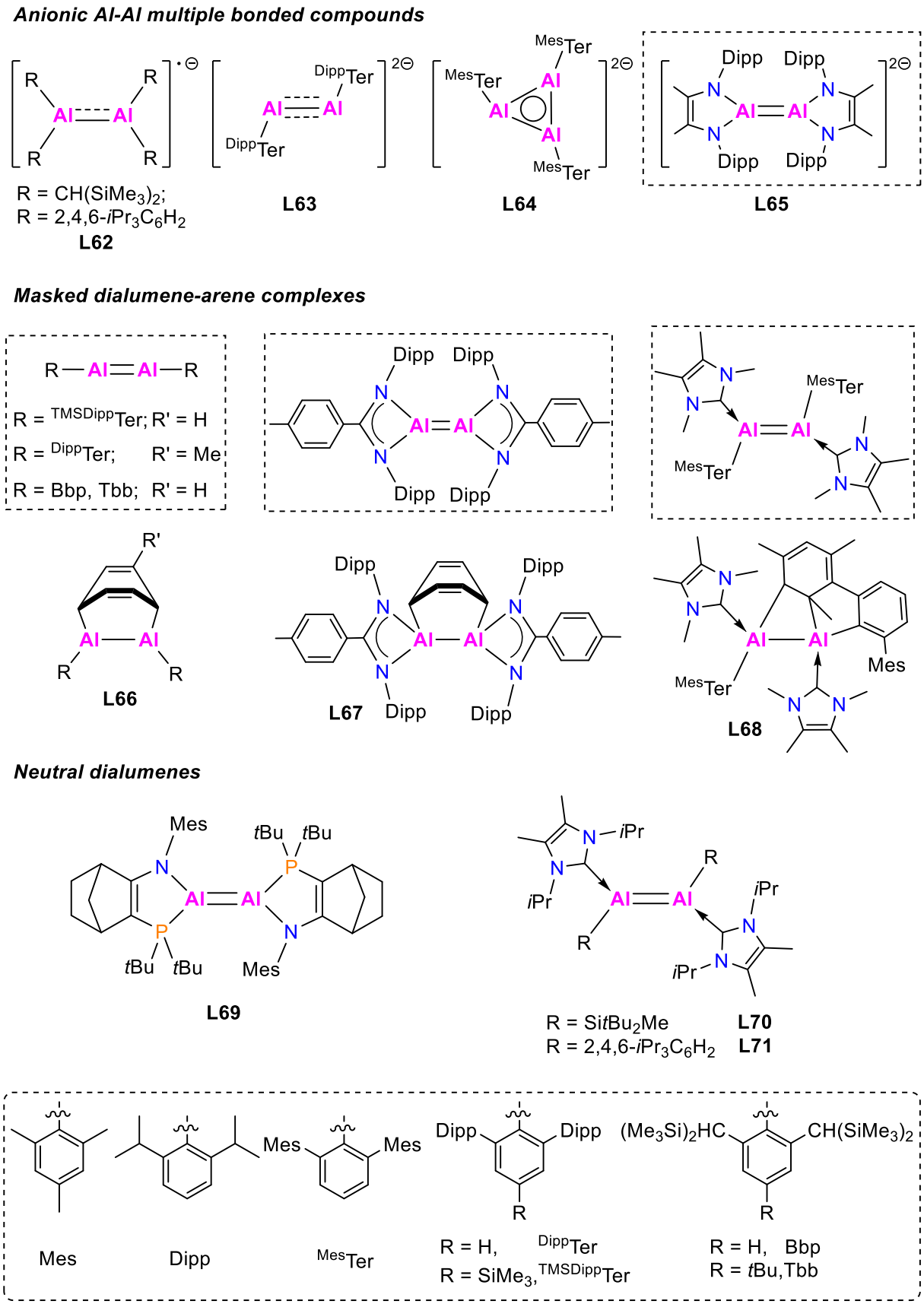

Figure 25. Representative Al–Al multiply-bonded species (Dashed square box: proposed compounds).

Alternative species related to aluminum multiple bonds is the cycloaddition derivatives of masked Al=Al and arene species (Figure 25). The α-diimine-stabilized dianionic "dialumene" **L65** $[RAl=AlR]^{2-}$ (R = $[(2,6\text{-}i\text{Pr}_2\text{C}_6\text{H}_3)\text{NC(Me)}]_2^{2-}$) is proposed to be formed due to the presence of the cycloaddition products by reaction of this "dialumene" and butadienes.[190] Despite the anionic species, there are several neutral examples stabilized by very bulky ligands even combining with LB donor on the Al center. The "dialumenes" **L66** (R = $^{\text{TMSDipp}}$Ter,[26] R = Bbp = $2,6\text{-}[\text{CH}(\text{SiMe}_3)_2]_2\text{C}_6\text{H}_3$,[191] and R = Tbb = $2,6\text{-}[\text{CH}(\text{SiMe}_3)_2]_2\text{-}4\text{-}t\text{BuC}_6\text{H}_2$[192-193]) are trapped as its cycloaddition product with benzene. The "dialumene" **L66** (R = $^{\text{Dipp}}$Ter = $2,6\text{-}[(2,6\text{-}i\text{Pr}_2\text{C}_6\text{H}_3)_2]\text{C}_6\text{H}_3$) is proposed by the addition reaction with toluene[194] or $\text{Me}_3\text{SiCCSiMe}_3$.[195] The amidinato supported **L67** (Am^{Dipp} = $\text{C}[\text{N}(2,6\text{-}i\text{Pr}_2\text{C}_6\text{H}_3)]_2(4\text{-Me}\text{C}_6\text{H}_4)$) reacts with benzene to give the respective cycloaddition product.[196] The NHC supported terphenyl transient dialumene $[\text{IMe}_4(^{\text{Mes}}\text{Ter})\text{Al}]_2$ **L68** is self-stabilized by a peripheral C=C bond of a flanking aryl ring.[24]

The neutral Al=Al double bonds are limited but are highly desirable to understand its true bonding nature as well as to explore their reactivity.[14] In the case of boron, various compounds containing boron−boron multiple bonds have been reported by complexation with NHC.[181, 197-200] In the case of other heavier group 13 (Ga, In, Tl), neutral double-bonded compounds have been isolated and characterized by the usage of sterically bulky terphenyl ligand, e.g. ArM=MAr (M = Ga, In, Tl; Ar = $2,6\text{-}(2,6\text{-}i\text{Pr}_2\text{C}_6\text{H}_3)_2\text{C}_6\text{H}_3$).[14, 201-203] Therefore, neutral multiple-bonded Al compounds can be possibly accessible by complexation of Lewis bases and bulky aryl ligands conferring stability on the reactive Al center. Cowley and coworkers reported an amidophosphine base-coordinated (chelating ligand system) dialumene **L69** which reversibly dissociates to monomers in solution (Al=Al to Al:).[66] Our group reported NHC together with aryl or silyl group stabilized dialumenes **L70** (R = $\text{Si}t\text{Bu}_2\text{Me}$)[23] and **L71** (R = $2,4,6\text{-}i\text{Pr}_3\text{C}_6\text{H}_2$)[25] featuring reactivity towards unsaturated organic molecules while the latter can even activate dihydrogen.

3. Scope of This Work

With the highest abundance among metals in the earth's crust and the environmental-friendly nature, aluminum chemistry has undergone a renaissance, from synthetic curiosity to realized applications. As highlighted before, the transition-metal like properties of low oxidation state Al species have emerged in recent times, gaining tremendous attention in academia. However, aluminum is generally found in the +3 oxidation state, and in nature in the form of polymeric aluminum chalcogenides (e.g., Al_2O_3). The nature of the bulk materials should be investigated by exploring the bonding nature of discrete Al=Ch containing complexes, as this will support the development of novel advanced aluminum materials. In this context, the isolation of new aluminum multiple bonds and their reactivity are highly desired. Prior to this thesis, there were only few neutral homo/hetero multiply bonded aluminum examples (e.g., Al=Ch, Ch = O, Se, Te, and Al=Al)[8, 17, 23, 161] and reactivity towards challenging small molecules is relatively unexplored. Thus, this thesis aims to synthesize multiply bonded Al=Ch and Al=Al molecules and examine their reactivity to further understand the bonding in multiply bonded aluminum compounds and to reveal their true potential and suitability for materials chemistry.

A major goal in contemporary aluminum research is the synthesis of a neutral low-valent aluminum compounds containing a discrete Al=O double bond. This would give direct insights into alumina materials. There are no neutral examples bearing freestanding Al=O double bond. They are all classified as oligomers or polymers, with the only example with oxygen moiety complexed with a Lewis acid. Considering the difference in electronegativities between Al and the chalcogen elements (Al 1.61, O 3.44, S 2.58, Se 2.55, Te 2.1), the heavier chalcogen (S, Se, Te) features less discrepancy than oxygen. Compounds containing Al–Ch (S, Se, Te) multiple bonds have proven easier to handle than aluminum oxides, and there are neutral examples with a terminal Al=S (^{Dipp}Nacnac(NHC)Al=S, **L31** and **L32**) and [NHI(IMe_2Et_2)$_2$]Al=Te **L57** with a terminal Al=Te. Therefore, this thesis started to synthesize Al=S, Al=Se or Al=Te as the priority and subsequently test activation of challenging bonds such as CO_2.

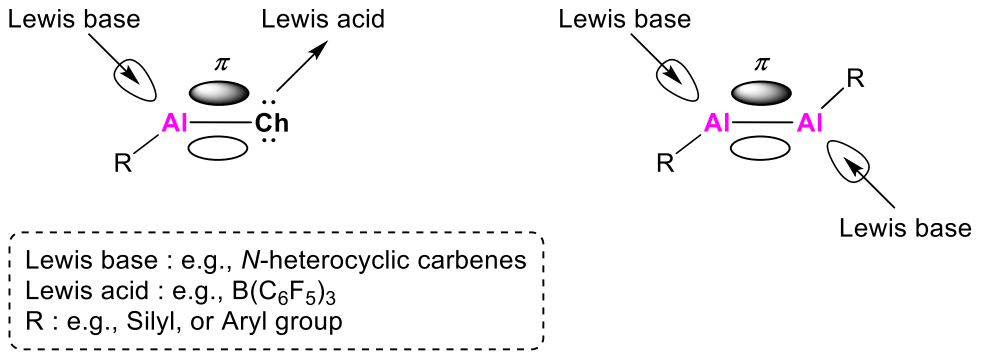

Figure 26. Stabilization strategies for Al–E multiple bonds and their molecular orbitals.

These are challenging targets due to the absence of suitable stabilization to the reactive Al center and the very weak Al–E (E = Ch or Al) multiple bonds. Thus, as shown in Figure 26, a potential approach to gain access to these elusive species will be usage of sterically demanding ligands and complexation with Lewis base or acid to hinder oligomerization. Aryl ligands are sterically tunable by varying the wingtip substituents, and NHCs are strong σ-donors and poor π-acceptors, they are very promising candidates to provide sufficient electronic and kinetic stabilization for the Al–Ch multiple bonds. While three examples ^{Dipp}Nacnac(NHC)Al=S, **L31** and **L32**, [NHI(IMe$_2$Et$_2$)$_2$]Al=Te **L57**, [Si*t*Bu$_2$Me(I*i*Pr$_2$Me$_2$)Al]$_2$ **L70** were isolated owing to the persuasive electron donation from the adjacent NHCs, [Tipp(I*i*Pr$_2$Me$_2$)Al]$_2$ **L71** (Figure 27) has already been observed by usage of the corresponding aluminum dihydride Tipp(I*i*Pr$_2$Me$_2$)AlH$_2$ **L9** as a feasible precursor in our laboratory, but the structure of the product was unpublished at the beginning of this thesis. All these prompted us to use the aryl group tuned by changing the substituents and adjacent to the different NHCs for isolation Al=Ch double bonds. During this project, the very bulky terphenyl ligand has proven that it could even support a monomeric Al(I), which reacted with H$_2$ resulting in the dimeric aluminum hydride (Figure 27). This motivated us to employ Tipp(I*i*Pr$_2$Me$_2$)AlH$_2$ **L9** as a precursor or even attempt to tune the aluminum hydride by utilizing bulkier aryl group. Following the successful synthesis, a detailed reactivity study of Al=Ch will be performed. In addition, a particular emphasis will be to understand the effect of different supporting ligands on the stability and reactivity of the resulting complexes.

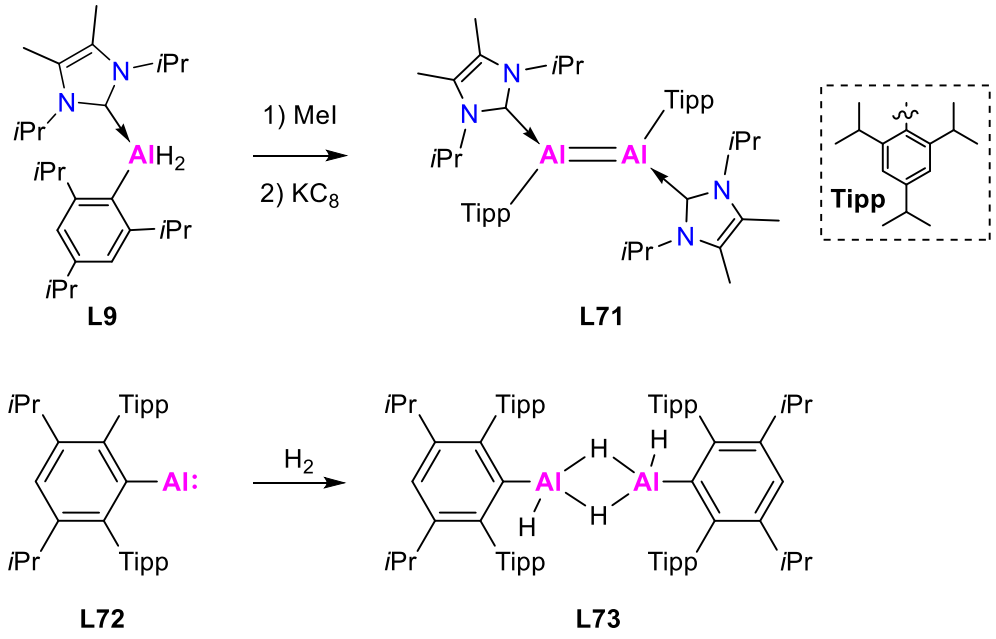

Figure 27. Reported ligands system for low-valent aluminum species (**L71** and **L72**).

This thesis will start with the synthesis of Al=S using aluminum dihydride as a precursor and to study the fundamental differences between the aryl ligands, see chapter 4. Inspired by the Al–S project, this approach is further extended to Al=Se and Al=Te projects in chapter 5. Of particular focus is the activation of small molecules, as this is considered challenging even for TMs due to the high bond strengths found in small molecules such as H_2, CO_2, CO and so on.

The chapter 6 will concern the reactivity of Al=Al double bonds. Our group already reported a comparative reactivity study between silyl- and aryl-substitution towards unsaturated and small molecule including CO_2, N_2O, O_2 (Figure 28).[23, 25] The functionalization of white phosphorus P_4 by a number of TMs has been of paramount significance in phosphorus chemistry over the past decades.[204] Analogously, various main group molecules, especially aluminum, are also known to react with P_4. The reactivity of both dialumenes ([R(NHC)Al]$_2$, R = Tipp or *t*Bu$_2$MeSi) with P_4 is performed and discussed.

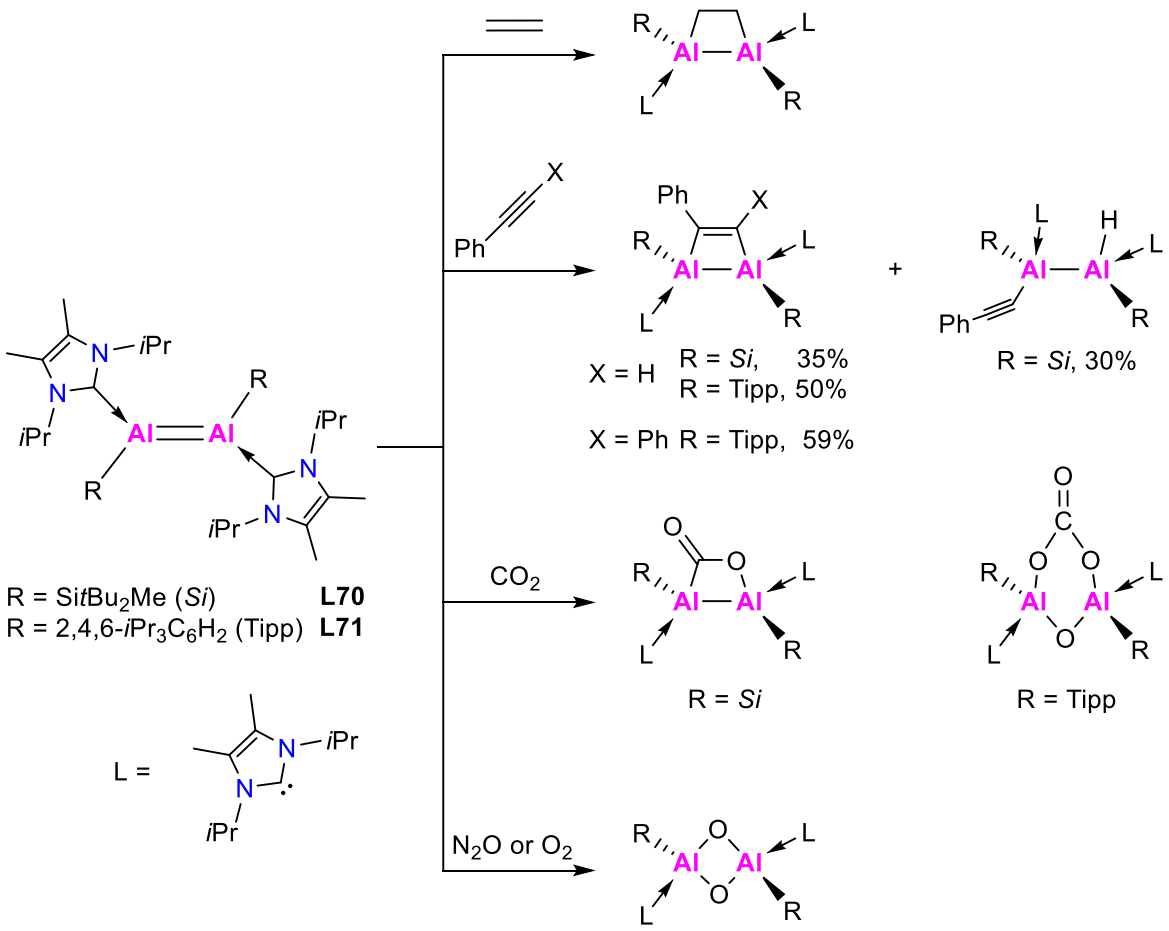

Figure 28. The current reactivity study on dialumenes (**L70** and **L71**).

Overall, this thesis is intended to gain a deeper understanding of the multiply bonded aluminum chemistry. The knowledge obtained in this work will open new avenues, which will underpin future developments in aluminum materials.

4. Isolation of Cyclic Aluminum Polysulfides by Stepwise Sulfurization

Title: Isolation of Cyclic Aluminum Polysulfides by Stepwise Sulfurization

Status: Research Article, published online: 01 December 2021

Journal: *Chemistry - A European Journal* **2022**, *28*, e202104042.

Publisher: Wiley-VCH Verlag GmbH & Co. KGaA, Weinheim.

DOI: 10.1002/chem.202104042

Authors: Huihui Xu, Catherine Weetman, Franziska Hanusch, Shigeyoshi Inoue

Content

The NHC stabilized terphenyl dihydridoaluminum, the first monomeric aluminum hydride hydrogensulfide, the aluminum bis(hydrogensulfide), the six- or five-membered cyclic aluminum polysulfide as well as a rare five-membered heterocyclic aluminum sulfide were synthesized controllably in mild manners. Reactions of the known dihydridoaluminum and the terphenyl dihydridoaluminum with various thiation reagents formed a series of aluminum–sulfur species. This provided insights into the influence of the supporting ligands on the reactivity and stability.

Author Contributions

Huihui Xu planned and executed all experiments. Huihui Xu and Dr. Catherine Weetman co-wrote the manuscript. Dr. Franziska Hanusch conducted all SC-XRD measurements and processed the resulting data. All the work was performed under the supervision of Prof. Shigeyoshi Inoue.

Chemistry–A European Journal | Research Article
doi.org/10.1002/chem.202104042
Chemistry Europe
European Chemical Societies Publishing
www.chemeurj.org

Isolation of Cyclic Aluminium Polysulfides by Stepwise Sulfurization

Huihui Xu,[a] Catherine Weetman,[b] Franziska Hanusch,[a] and Shigeyoshi Inoue*[a]

Abstract: Despite the notable progress in aluminium chalcogenides, their sulfur congeners have rarely been isolated under mild conditions owing to limited synthetic precursors and methods. Herein, facile isolation of diverse molecular aluminium sulfides is achievable, by the reaction of *N*-heterocyclic carbene-stabilized terphenyl dihydridoaluminium (**1**) with various thiation reagents. Different to the known dihydridoaluminium $\mathbf{1}^{Tipp}$, **1** features balanced stability and reactivity at the Al center. It is this balance that enables the first monomeric aluminium hydride hydrogensulfide **2**, the six-membered cyclic aluminium polysulfide **4** and the five-membered cyclic aluminium polysulfide **6** to be isolated, by reaction with various equivalents of elemental sulfur. Moreover, a rare aluminium heterocyclic sulfide with Al–S–P five-membered ring (**7**) was obtained in a controlled manner. All new compounds were fully characterized by multinuclear NMR spectroscopy and elemental analysis. Their structures were confirmed by single-crystal X-ray diffraction studies.

Introduction

Inorganic group 13 element chalcogenides (group 16) are omnipresent in transformations, catalysis and materials. There is ongoing interest in economical and environmentally sustainable aluminium chalcogenides, mostly because of their importance in modern industrial chemistry such as chemical vapor deposition, catalysis and electrolyte materials.[1] To understand aggregation processes that create bulk materials from single atoms, it is necessary to elucidate the bond nature between elements. In this context, synthesis and characterization of stable aluminium chalcogenides is thus an important step towards the comprehension of the basic intramolecular architecture of aluminium chemistry.[2] Among heavier aluminium chalcogenides, their sulfur analogues play a significant role in desulfurization processes of crude oil and flue-gas, which is currently receiving considerable attention.[3] However, to the best of our knowledge, only few examples of molecular aluminium sulfides are known due to synthetic challenges.

Aluminium hydrides have already presented themselves as viable precursors for Al–S bond formation, with β-diketiminato dihydridoaluminium [LAlH$_2$] **A** (L = N(Dipp)C(Me)CHC(Me)N(Dipp), Dipp = 2,6-*i*Pr$_2$C$_6$H$_3$, Figure 1) being the most widely studied.[4] Transformation of compound **A** with elemental sulfur furnished

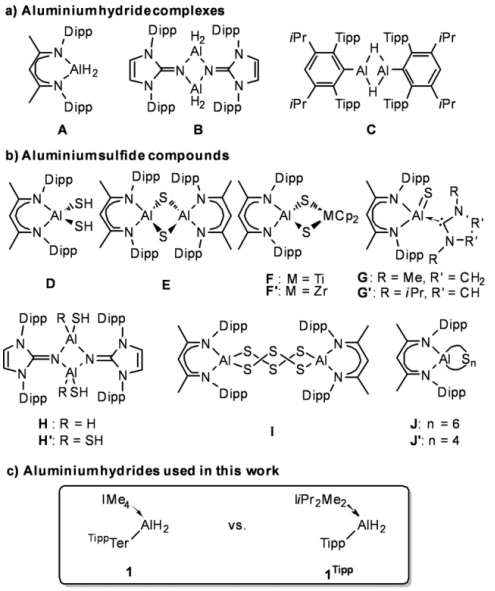

Figure 1. a) Selected aluminium hydride complexes. b) Selected aluminium sulfide compounds. c) Aluminium hydrides used in this work: IMe$_4$Al(^{Tipp}Ter)H$_2$ **1** and *li*Pr$_2$Me$_2$Al(Tipp)H$_2$ $\mathbf{1}^{Tipp}$. Dipp = 2,6-*i*Pr$_2$C$_6$H$_3$; Tipp = 2,4,6-*i*Pr$_3$C$_6$H$_2$; *li*Pr$_2$Me$_2$ = 1,3-diisopropyl-4,5-dimethylimidazol-2-ylidene; Cp = C$_5$H$_5$; IMe$_4$ = 1,3,4,5-tetramethylimidazol-2-ylidene; ^{Tipp}Ter = 2,6-(2,4,6-*i*Pr$_3$C$_6$H$_2$)$_2$C$_6$H$_3$.

[a] *H. Xu, F. Hanusch, Prof. S. Inoue*
Department of Chemistry,
Catalysis Research Center and Institute of Silicon Chemistry
Technische Universität München
Lichtenbergstr. 4, 85748
Garching bei München (Germany)
E-mail: s.inoue@tum.de

[b] *Dr. C. Weetman*
Department of Pure and Applied Chemistry
University of Strathclyde
295 Cathedral St, G1 1XL Glasgow (Scotland)

Supporting information for this article is available on the WWW under https://doi.org/10.1002/chem.202104042

Chemistry–A European Journal | Research Article doi.org/10.1002/chem.202104042 | Chemistry Europe European Chemical Societies Publishing

the first structurally characterized aluminium bis(hydrogensulfide) [LAl(SH)$_2$] **D**.[5] Subsequently, the dimeric aluminium sulfide **E**,[6] heterobimetallic sulfides [LAl(μ–S)$_2$MCp$_2$] (M = Ti, Zr) (**F** and **F′**),[7] and clusters with the Al–S–M (M = Cu and Ag) structural unit were prepared.[8] Deploying the same β-diketiminato ligand, first neutral monomeric terminally bound aluminium sulfides (**G** and **G′**) were isolated through use of an Al$^{(I)}$ compound.[9] Previous work by our group has focused on using a monodentate *N*-heterocyclic imino ligand to support a dimeric aluminium dihydride ({μ-(NHI)AlH$_2$}$_2$ **B**, NHI = bis(2,6-diisopropylphenyl)imidazolin-2-imino).[10] This resulted in the formation of mono- and bis(hydrogensulfide) aluminium complexes ({μ-(NHI)Al(H)SH}$_2$ **H**, {μ-(NHI)Al(SH)$_2$}$_2$ **H′**) on reaction with S_8.[11]

Beyond these aluminium sulfides mentioned, cyclic aluminium polysulfides are of considerable interest, not only because of their structure and reactivity, but also because of their potential applications in oxidation processes and in biological or catalytic systems.[7,12] To date, however, their molecules have been rarely reported due to their elusive generation. For instance, a dimeric polysulfide LAl(μ–S$_3$)$_2$AlL (**I**) with eight-membered ring was obtained by the reaction of an Al$^{(I)}$ compound with S_8.[13] During the synthesis of Al–S–M clusters,[8] an aluminium hexasulfide [LAlS$_6$] **J** was formed as a side product. Whilst in the presence of [MesAg]$_4$, the reaction of **D** with excess of elemental sulfur resulted the more stable aluminium tetrasulfide [LAlS$_4$] **J′**.

Following on from the successful isolation of molecular aluminium sulfides with aluminium hydrides, we focused on expanding the scope with a view to controlling product formation. As an indispensable part of molecular aluminium chemistry, the ligand system is key to balancing stability and reactivity of the Al centre.[14] Very recently, Power and co-workers used an extremely sterically demanding terphenyl ligand Ar^{iPr8} (Ar^{iPr8} = 2,6-(2,4,6-*i*Pr$_3$C$_6$H$_2$)$_2$–3,5-*i*Pr$_2$–C$_6$H) to isolate the monomeric alanediyl: AlAr^{iPr8}, which reacted with H_2, resulting in dimeric aluminium hydride **C**.[15] Our group recently prepared a *N*-heterocyclic carbene (NHC)-stabilized dihydridoaluminium (I*i*Pr$_2$Me$_2$Al(Tipp)H$_2$ **1^{Tipp}**, I*i*Pr$_2$Me$_2$ = 1,3-diisopropyl-4,5-dimethylimidazol-2-ylidene, Tipp = 2,4,6-*i*Pr$_3$C$_6$H$_2$), which was used to isolate the corresponding dialumene.[14] These results prompted us to use the relatively bulky terphenyl ligand and the prime NHC donor to stabilize the aluminium centre for preparing the dihydridoaluminium IMe$_4$Al(^{Tipp}Ter)H$_2$ **1** (IMe$_4$ = 1,3,4,5-tetramethylimidazol-2-ylidene, ^{Tipp}Ter = 2,6-(2,4,6-*i*Pr$_3$C$_6$H$_2$)$_2$C$_6$H$_3$). Treatment of various thiation reagents with **1** and **1^{Tipp}** aims to show the influence of the supporting ligand on the reactivity and stability, in efforts towards isolation of new aluminium sulfides.

Results and Discussion

The dihydridoaluminium **1** was synthesized in good yields (80%) through the reaction of IMe$_4$AlH$_3$ and ^{Tipp}TerLi(THF)$_2$ at ambient temperature, following the reported procedure for preparation of compound **1^{Tipp}**.[14] The identity of compound **1** was confirmed upon inspection of the ^{1}H NMR spectrum wherein two resonances for the *iso*-propyl groups were identified in a 2:1 ratio (*o*-^{Tipp}Ter: *p*-^{Tipp}Ter *iso*-propyl signals) as well as a characteristic broad signal for Al–H protons (^{1}H: br, δ 4.01 ppm). This is more shielded than those observed for amidinato, β-diketiminato, or 1-azaallyl aluminium dihydrides (δ 4.60–4.87 ppm),[1b,16] and the starting material IMe$_4$AlH$_3$ (^{1}H: br, 4.43 ppm), but is more deshielded than dimeric **B** (^{1}H, δ 2.60 ppm).[10] When compared with that of **1^{Tipp}** (^{1}H: br, δ 5.13 ppm) and **A** (^{1}H: br, δ 4.73 ppm),[17] the signal of Al–H protons appears at a lower chemical shift, showing that the electron density of the aluminium centre has increased and thus indicating stronger nucleophilicity. A similar trend was observed in the ^{27}Al spectrum (^{27}Al: δ 112.69 ppm (**1^{Tipp}**) vs. δ 94.72 ppm (**1**)). The solid-state structure of compound **1** was further confirmed by single-crystal X-ray crystallography (SC-XRD, Figure 2), with colourless crystals grown from a saturated pentane solution at −30 °C. The Al centre possesses pseudo-tetrahedral geometry, with the angle C1–Al1–C37 (112.61(7)°) being similar to H1–Al1–H2 (113.7(12)°), the latter being comparable to **A** (H–Al–H: 113.2 (11)°).[5,18] The NHC and terphenyl ligands are located adjacently. Al1–C37 bond length (2.0451(18) Å) indicated the dative nature of the NHC ligand, while Al1–C1 bond length (2.0087(19) Å) is close to the sum of the covalent radii (R_{Al-C} = 2.01 Å).[19]

Sulfurization of **1^{Tipp}** and **1** by treatment with elemental sulfur were studied. **1^{Tipp}** decomposed immediately on reaction with S_8 (Figure S1), however, the treatment of stoichiometric amounts of S_8 with **1** resulted in the step-by-step dehydrogenation reaction, forming a series of molecular aluminium sulfides (Scheme 1). The aluminium hydride hydrogensulfide IMe$_4$Al(^{Tipp}Ter)(SH)H (**2**) was isolated through the mono dehydrogenation reaction of **1** with one equivalent of sulfur (*i.e.*, 1/8 eq. S_8) at ambient temperature (Scheme 1, i). The structure of **2** was determined by spectroscopic and SC-XRD studies. The ^{1}H NMR spectrum of **2** showed a characteristic singlet at δ −1.77 ppm which appears at a higher chemical shift compared to the S–H proton reported for compound **H** (^{1}H: δ −2.05 ppm).[11] The ^{1}H NMR signal of Al–H proton was identified as a broad peak (δ 4.80 ppm), which appears at a higher chemical shift compared with **1** (^{1}H: br, δ 4.01 ppm), this is ascribed to the electron withdrawing capability of the SH group.

Reaction of **1** with two equivalents of sulfur (*i.e.*, 1/4 eq. S_8) yielded the aluminium bis(hydrogensulfide) complex IMe$_4$Al(^{Tipp}Ter)(SH)$_2$ (**3**) in high yields of 90%. This was confirmed on inspection of the ^{1}H NMR spectrum, which revealed a singlet at δ −0.89 ppm that integrates to two protons from SH and is comparable to that of **D** (^{1}H: δ −0.88 ppm).[5] Notably, that is a higher chemical shift compared to the single integral of **2** (^{1}H: δ −1.77 ppm) and bisthiol **H′** (^{1}H: δ −1.86 ppm).[11] SC-XRD studies confirmed the formation of **3** (Figure 2). In addition, it is also possible to obtain **3** in a stepwise manner by addition of sulfur (*i.e.*, 1/8 eq. S_8) to **2** through further dehydrogenation (Figure S2–3 in Supporting Information).

Treatment of excess S_8 with **1** afforded the first six-membered cyclic aluminium polysulfide IMe$_4$Al(^{Tipp}Ter)S$_5$ **4** (Scheme 1, iv) in low yields (13%). This yield could be greatly increased *via* the reaction of bisthiol **3** and excess of S_8 at

Chemistry–A European Journal | Research Article
doi.org/10.1002/chem.202104042
Chemistry Europe
European Chemical Societies Publishing

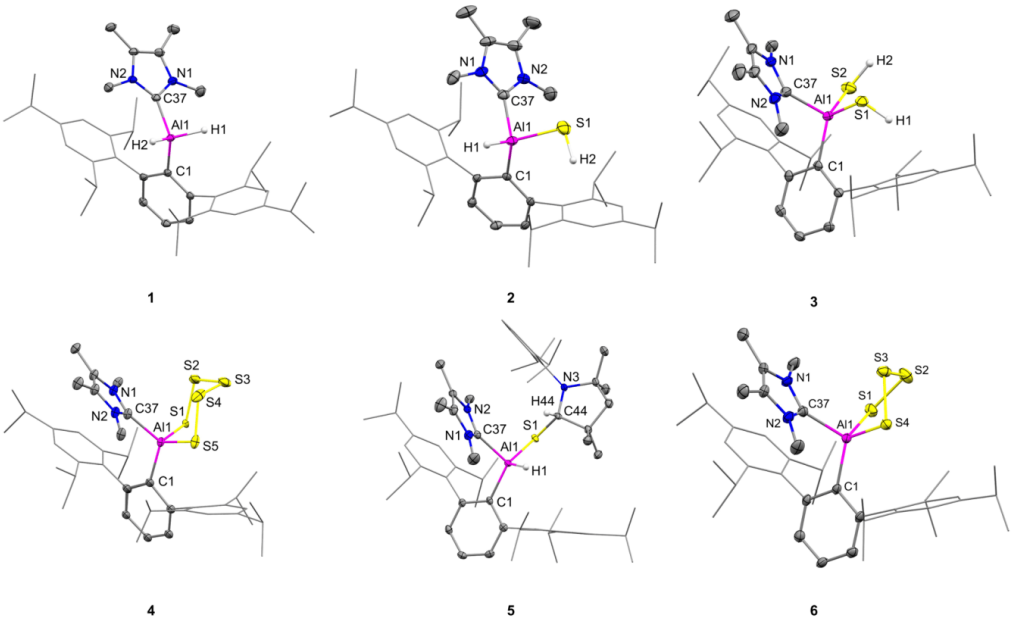

Figure 2. Molecular structures of compound **1**, **2**, **3**, **4**, **5**, **6** in the solid state. Ellipsoids are set at the 50% probability level; hydrogen atoms (except for selected H1 and H2) and co-crystallized solvent molecules are omitted for clarity and parts of the terphenyl ligands and cAAC^{Me} are depicted in wireframe for simplicity.[20] Selected bond lengths (Å) and angles (°): **1**: Al1–C1 2.0087(19), Al1–C37 2.0451(18), Al1–H1 1.53(2), Al1–H2 1.52(2), C1–Al1–C37 112.61(7), H1–Al1–H2 113.7(12); **2**: Al1–C37 2.053(3), Al1–C1 2.000(3), Al1–S1 2.2635(12), Al1–H1 1.61(3), S1–H2 1.42(4), C1–Al1–C37 111.74(11), H1–Al1–S1 111.7(10); **3**: Al1–S1 2.2820(10), Al1–S2 2.2569(11), Al1–C37 2.054(3), Al–C1 2.004(3), S1–H1 1.29(2), S2–H2 1.34(3), C37–Al1–C1 110.59(11), S1–Al1–S2 107.47(4); **4**: Al1–S1 2.273(4), Al1–S5 2.300(4), Al1–C37 2.017(9), Al1–C1 1.950(18), S1–S2 2.082(4), S2–S3 2.041(4), S3–S4 2.058(5), S4–S5 2.049(4), C37–Al1–C1 118.7(6), S1–Al1–S5 106.13(15); **5**: Al1–S1 2.2607(10), Al1–C37 2.069(3), Al–C1 2.013(2), S1–C44 1.882(2), Al1–H1 1.49(3), C37–Al1–C1 111.49(10), S1–Al1–H1 107.4(10), Al1–S1–C44 100.22(8); **6**: Al1–S1 2.300(2), Al1–S4 2.302(2), Al1–C37 2.062(6), Al1–C1 1.987(6), S1–S2 2.093(2), S2–S3 2.048(2), S3–S4 2.086(2), C37–Al1–C1 113.1(2), S1–Al1–S4 101.93(9).

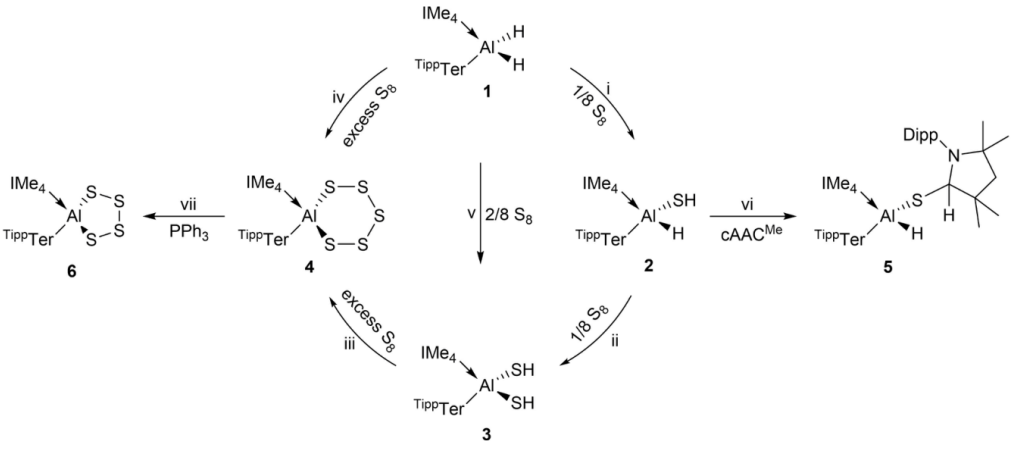

Scheme 1. Formation of aluminium sulfide compounds IMe$_4$Al(^{Tipp}Ter)(SH)H **2**, IMe$_4$Al(^{Tipp}Ter)(SH)$_2$ **3**, IMe$_4$Al(^{Tipp}Ter)S$_5$ **4**, IMe$_4$Al(^{Tipp}Ter)(H)S(H-cAAC^{Me}) **5**, IMe$_4$Al(^{Tipp}Ter)S$_4$ **6**. (i) Pentane, (1) −78 °C, 15 min, (2) rt, 16 h; (ii) C_6D_6, rt, 2 h; (iii) Et_2O, (1) −30 °C, 5 min, (2) rt, 72 h; (iv) Et_2O, (1) −78 °C, 30 min, (2) rt, 16 h; (v) Et_2O, (1) −78 °C, 1 h, (2) rt, 48 h; (vi) Toluene, (1) −30 °C, 5 min, (2) rt, 16 h; (vii) THF, 65 °C, 2 h. ^{Tipp}Ter = 2,6-(2,4,6-*i*Pr$_3$C$_6$H$_2$)$_2$C$_6$H$_3$, IMe$_4$ = 1,3,4,5-tetramethylimidazol-2-ylidene, Dipp = 2,6-*i*Pr$_2$C$_6$H$_3$.

Chemistry–A European Journal | Research Article doi.org/10.1002/chem.202104042 | Chemistry Europe European Chemical Societies Publishing

ambient temperature (85%, Scheme 1, iii). In this instance, **4** was isolated as the sole product, offering a selective and controlled activation of elemental sulfur. Pale yellow single crystals suitable for SC-XRD analysis were grown by slow evaporation of a saturated benzene solution. The single-crystal structure revealed the aluminium centre to have pseudo-tetrahedral geometry (C37–Al1–C1 118.7(6)°, S1–Al1–S5 106.13(15)°), and confirmed the six-membered ring. The S–S bond length (av. 2.058 Å) is longer than in **J** (av. 2.01 Å) and shorter than in **J'** (av. 2.07 Å).[8] The Al1–S1 (2.273(4) Å) and Al1–S5 (2.300(4) Å) bond lengths are longer than in bisthiol **D** (av. 2.22 Å)[5] and dimer **E** (av. 2.24 Å).[6]

When it comes to the reactivity of **2**, **3**, and **4**, dehydrogenation or desulfurization are of considerable interest. Cyclic (alkyl)(amino) carbenes (cAAC^{Me}) have been used in hydrogen or sulfur transfer, due to its relatively strong σ-donating and π-accepting nature.[21] Here, the reaction of **2** with one equivalent of cAAC^{Me} resulted in oxidative addition of the S–H bond at the carbene carbon, yielding compound **5** (Scheme 1, vi). The structure of **5** was determined by ^{1}H and ^{13}C NMR spectroscopy and SC-XRD. The signal for H44 of H–cAAC^{Me} (Figure 2, δ 4.56 ppm) is diagnostic, while the signal for H2 of **2** (δ −1.77 ppm) disappeared. In comparison to that of compound **2** (^{1}H: δ 4.80 ppm) and **1** (^{1}H: δ 4.01 ppm), the Al–H proton signal of **5** (^{1}H: δ 4.25 ppm) resonates in between. The crystal structure of **5** revealed that the Al–S bond length (Al1–S1 2.2607(10) Å) was comparable to **2** (Al1–S1 2.2635(12) Å). The Al1–C37 bond length (2.069(3) Å) and the Al1–C1 bond length (2.013(2) Å) were elongated, compared to other Al compounds (Al1–C37 2.0451(18) Å (**1**), Al1–C37 2.053(3) Å (**2**), Al1–C37 2.054(3) Å (**3**), Al1–C37 2.017(9) Å (**4**); Al1–C1 2.0087(19) Å (**1**), Al1–C1 2.000(3) Å (**2**), Al1–C1 2.004(3) Å (**3**), Al1–C1 1.950(18) Å (**4**)), indicating that the interactions of NHC and terphenyl ligands with the Al center were weakened. Attempts to form analogous products on reaction of **3** or **4** with cAAC^{Me} did not form isolable products.

As the first example of a cyclic six-membered aluminium polysulfide ring, further understanding of the stability and reactivity of **4** is attractive.[12c] As such, the reaction of **4** with triphenylphosphine PPh_3, tris(dimethylamino)phosphine P-$(NMe_2)_3$ and IMe_4 as well as the thermal stability of **4** were studied. Reaction of **4** with $P(NMe_2)_3$, or IMe_4 was unsuccessful, however, treatment of PPh_3 with **4** at 65 °C furnished the five-membered cyclic aluminium polysulfide $IMe_4Al(^{Tipp}Ter)S_4$ **6** within 2 h through desulfurization (Scheme 1, vii). However, it is of note that compound **4** is somewhat unstable in solution, it is slowly converted to **6** at room temperature over 30 days (15% conversion, Figure S5) or at 80 °C over 24 h (30% conversion, Figure S6). These results indicate that the desulfurization of **4** is accelerated significantly by PPh_3. The solid-state structure of compound **6** was confirmed by SC-XRD (Figure 2), with yellow crystals grown from a saturated THF solution. In contrast to **4** (Al1–C37 2.017(9) Å, Al1–C1 1.950(18) Å), the interaction of NHC and aryl ligand with the Al centre in **6** was weakened while the bond lengths were elongated (**6**: Al1–C37 2.062(6) Å, Al1–C1 1.987(6) Å). Whilst the overall ring size decreased from six (**4**) to five (**6**), longer Al–S bonds (**4**: Al1–S1 2.273(4) Å, Al1–S5 2.300(4) Å; **6**: Al1–S1 2.300(2) Å, Al1–S4 2.302(2) Å) and longer S–S bonds (**4**: S–S av. 2.0575 Å; **6**: S–S av. 2.0757 Å) were observed. Further desulfurization attempts with PPh_3 and elevated temperatures, were unsuccessful.

In addition to elemental sulfur, Lawesson's reagent (2,4-bis-(4-methoxyphenyl)-1,3-dithia-2,4-diphosphetane 2,4-disulfide, LR) has received attention in reactions with group 13 compounds. It is an effective thiation reagent, for example in the transformation of aldehydes and ketones to their thio derivatives. Reported by Cowley and co-workers in 1998, unusual reactions of LR with germylenes and stannylenes were described, affording unusual Ge–S and Sn–S compounds.[22] Here, the reaction of **1**^{Tipp} with LR occurred, but the product decomposed immediately. However, the treatment of **1** with 1.5 equivalents of LR gave the first example of a five-membered Al–S–P–P–S ring containing complex **7** (Scheme 2, i). According to the single-crystal structure (Figure 3), the geometry of the Al centre is pseudo-tetrahedral, with an S1–Al1–S2 angle of 99.60(6)°. The distances of Al1–C1 (1.997(3) Å), Al1–C37 (2.032(3) Å) and Al1–S1 (2.2904(18) Å) and Al1–S2 (2.2848(13) Å) were located within the range of all Al compounds mentioned above. In contrast to the afore mentioned Ge–S compound ($[Ge(S–P–C_6H_4OMe)_4]$, P–P: 2.220(2) Å),[22] the P1–P2 bond length of **7** (2.2694(11) Å) was slightly longer, indicating covalent bond character. Moreover, compared with the mentioned Sn–S compound ($[(Me_3Si)_2Sn–(S–S)–P(=S)C_6H_4OMe)]$, P=S 1.9315(9) Å), the P1=S3 (1.9495(14) Å) and P2=S4 (1.9580(16) Å) bond lengths of **7** were slightly longer, which showed double bond features. Compound **7** shows an interesting puckered heterocyclic five-membered Al–S–P ring. It is thermally stable at 75 °C for at least 24 h.

Compared with the effective S_8 and LR thiation reagents, bis(trimethylsilyl) sulfide $S(TMS)_2$ is considered a modest thiation reagent. Whereas no reaction between compound **1** and $S(TMS)_2$ occurred, the treatment of $S(TMS)_2$ with **1**^{Tipp} at high temperature yielded the I*i*Pr$_2$Me$_2$Al(Tipp)(H)STMS complex **8** (Scheme 2, ii) *via* a mono dehydrogenation reaction. This finding is consistent with previous results that **1** features less reactive than **1**^{Tipp}. The ^{1}H NMR spectrum revealed the Al–H

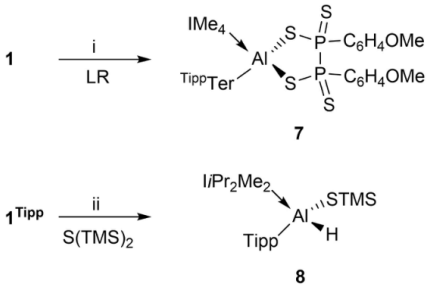

Scheme 2. Formation of compounds **7** and **8**. (i) Toluene, (1) 0 °C, 15 min, (2) rt, 16 h. (ii) Toluene, (1) −78 °C, 15 min, (2) 75 °C, 48 h. LR = Lawesson's reagent; ^{Tipp}Ter = 2,6-(2,4,6-*i*Pr$_3$C$_6$H$_2$)$_2$C$_6$H$_3$; IMe_4 = 1,3,4,5-tetramethylimidazol-2-ylidene; TMS = trimethylsilyl; I*i*Pr$_2$Me$_2$ = 1,3-diisopropyl-4,5-dimethylimidazolin-2-ylidene.

Chemistry–A European Journal | Research Article doi.org/10.1002/chem.202104042 | Chemistry Europe European Chemical Societies Publishing

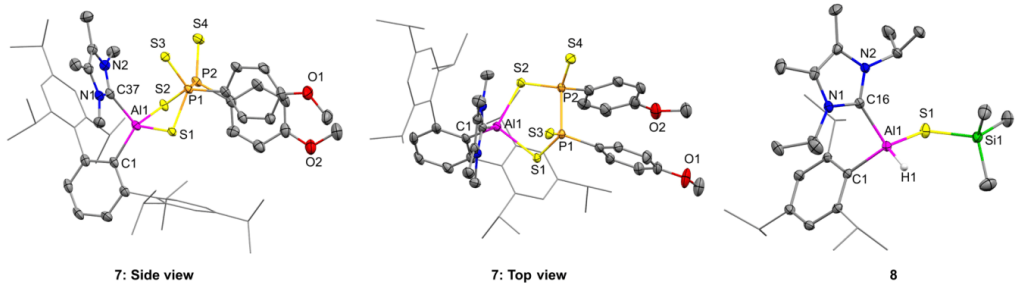

Figure 3. Molecular structure of compound **7** and **8** in the solid state. Ellipsoids are set at the 50 % probability level; hydrogen atoms (except for selected H1) and co-crystallized solvent molecules are omitted for clarity and parts of the terphenyl ligands are depicted in wireframe for simplicity.[20] Selected bond lengths (Å) and angles (°): **7** Al1–C37 2.032(3), Al1–C1 1.997(3), Al1–S2 2.2848(13), Al1–S1 2.2904(18), S1–P1 2.0584(18), S2–P2 2.0712(14), P1–P2 2.2694(11), P1–S3 1.9495(14), P2–S4 1.9580(16), C37–Al1–C1 112.85(12), S1–Al1–S2 99.60(6). **8** Al1–H1 1.4499(12), Al1–C16 2.086(3), Al1–C1 2.013(3), Al1–S1 2.2738(11), S1–Si1 2.1236(11), C1–Al1–C16 102.09(11), Si1–S1–Al1 107.71(5), S1–Al1–H1 111.35(6).

proton as a broad peak (δ 5.43 ppm), which appears at a slightly higher chemical shift compared to $\mathbf{1}^{Tipp}$ (^{1}H: br, δ 5.13 ppm). The singlet at δ 0.72 ppm is assigned to TMS methyl protons. The SC-XRD revealed (Figure 3) that the Al centre is in a pseudo-tetrahedral coordination environment with C1–Al1–C16 (102.09(11)°) and H1–Al1–S1 (111.35(6)°) angles. Compound **8** is thermally stable, as attempts to force the elimination of TMSH at high temperatures was unsuccessful.

Conclusion

Herein, the monomeric dihydridoaluminium **1**, stabilized by NHC and sterically demanding terphenyl ligand has been isolated. **1** shows comparatively more balanced stability and reactivity at the Al centre in contrast to the known dihydridoaluminium $\mathbf{1}^{Tipp}$. It is implicated that **1** could react with conventional thiation reagents such as elemental sulfur and Lawesson's reagent under mild reaction conditions, while elevated temperature only initiated the reaction of modest thiation reagent $S(TMS)_2$ with $\mathbf{1}^{Tipp}$. In this regard, the first aluminium hydride hydrogensulfide **2**, an aluminium bis(hydrogensulfide) complex **3**, the first six-membered cyclic aluminium polysulfide **4** and a five-membered cyclic aluminium polysulfide **6** as well as the first five-membered heterocyclic Al–S–P complex **8** were isolated in a controlled manner. These results offer experimental insight into the nature of Al–S containing compounds, which is significant for molecular aluminium chemistry. The relatively increased stability and reactivity enables commendable prospect on bimetallic catalytic reactions and in addition is able to access novel aluminium species through organic transformations. Especially, the further reactivity and the application in preparation of bimetallic aluminium-sulfur clusters as well as biological or catalytic systems of compound **2**–**8** will be studied in the future.

Experimental Section

Experimental details are discussed in the Supporting Information.

Acknowledgements

We are exceptionally grateful to the European Research Council (ALLOWE 101001591) for financial support. H. X. gratefully acknowledges financial support from the China Scholarship Council. C.W. is thankful to the University of Strathclyde for the award of a Chancellor's Fellowship. Open Access funding enabled and organized by Projekt DEAL.

Conflict of Interest

The authors declare no conflict of interest.

Data Availability Statement

The data that support the findings of this study are available in the supplementary material of this article.

Keywords: aluminium hydride · chalcogenide · controllable · desulfurization · polysulfide

[1] a) D. Franz, T. Szilvasi, E. Irran, S. Inoue, *Nat. Commun.* **2015**, *6*, 10037; b) C. Cui, H. W. Roesky, M. Noltemeyer, H.-G. Schmidt, *Organometallics* **1999**, *18*, 5120–5123; c) A. H. Cowley, R. A. Jones, P. R. Harris, D. A. Atwood, L. Contreras, C. J. Burek, *Angew. Chem. Int. Ed. Engl.* **1991**, *30*, 1143–1145; d) N. Kambe, K. Kondo, N. Sonoda, *Angew. Chem. Int. Ed. Engl.* **1980**, *19*, 1009–1010; e) W. Lee, S.-J. Park, *Chem. Rev.* **2014**, *114*, 7487–7556; f) Y. Ding, X. Ma, Y. Liu, W. Liu, C. Ni, B. Yan, L. Yan, Z. Yang, *Inorg. Chim. Acta* **2019**, *497*, 119091; g) H. Senoh, T. Takeuchi, H. Kageyama, H. Sakaebe, M. Yao, K. Nakanishi, T. Ohta, T. Sakai, K. Yasuda, *J. Power Sources* **2010**, *195*, 8327–8330.

[2] a) C. Weetman, H. Xu, S. Inoue, in *Encyclopedia of Inorganic and Bioinorganic Chemistry* (Ed.: R. A. Scott), **2020**, pp. 1–20; b) P. Bag, C. Weetman, S. Inoue, *Angew. Chem. Int. Ed.* **2018**, *57*, 14394–14413;

Chemistry–A European Journal | Research Article doi.org/10.1002/chem.202104042 | Chemistry Europe European Chemical Societies Publishing

Angew. Chem. **2018**, *130*, 14594–14613; c) D. Franz, S. Inoue, *Dalton Trans.* **2016**, *45*, 9385–9397.
[3] a) C. Schnitter, A. Klemp, H. W. Roesky, H.-G. Schmidt, C. Röpken, R. Herbst-Irmer, M. Noltemeyer, *Eur. J. Inorg. Chem.* **1998**, *1998*, 2033–2039; b) R. J. Wehmschulte, P. P. Power, *Chem. Commun.* **1998**, 335–336; c) R. J. Wehmschulte, P. P. Power, *J. Am. Chem. Soc.* **1997**, *119*, 9566–9567; d) M. Taghiof, M. J. Heeg, M. Bailey, D. G. Dick, R. Kumar, D. G. Hendershot, H. Rahbarnoohi, J. P. Oliver, *Organometallics* **1995**, *14*, 2903–2917; e) W. Uhl, A. Vester, W. Hiller, *J. Organomet. Chem.* **1993**, *443*, 9–17.
[4] C. Cui, H. W. Roesky, H. Hao, H.-G. Schmidt, M. Noltemeyer, *Angew. Chem. Int. Ed.* **2000**, *39*, 1815–1817; *Angew. Chem.* **2000**, *112*, 1885–1887.
[5] V. Jancik, Y. Peng, H. W. Roesky, J. Li, D. Neculai, A. M. Neculai, R. Herbst-Irmer, *J. Am. Chem. Soc.* **2003**, *125*, 1452–1453.
[6] V. Jancik, M. M. Moya Cabrera, H. W. Roesky, R. Herbst-Irmer, D. Neculai, Ana M. Neculai, M. Noltemeyer, H.-G. Schmidt, *Eur. J. Inorg. Chem.* **2004**, *2004*, 3508–3512.
[7] V. Jancik, H. W. Roesky, D. Neculai, A. M. Neculai, R. Herbst-Irmer, *Angew. Chem. Int. Ed.* **2004**, *43*, 6192–6196; *Angew. Chem.* **2004**, *116*, 6318–6322.
[8] B. Li, J. Li, H. W. Roesky, H. Zhu, *J. Am. Chem. Soc.* **2015**, *137*, 162–164.
[9] T. Chu, S. F. Vyboishchikov, B. Gabidullin, G. I. Nikonov, *Angew. Chem. Int. Ed.* **2016**, *55*, 13306–13311; *Angew. Chem.* **2016**, *128*, 13500–13505.
[10] D. Franz, E. Irran, S. Inoue, *Dalton Trans.* **2014**, *43*, 4451–4461.
[11] D. Franz, S. Inoue, *Chem. Eur. J.* **2014**, *20*, 10645–10649.
[12] a) N. Takeda, N. Tokitoh, R. Okazaki, in *Elemental Sulfur und Sulfur-Rich Compounds II* (Ed.: R. Steudel), Springer Berlin Heidelberg, Berlin, Heidelberg, **2003**, pp. 153–202; b) R. Okazaki, *Phosphorus Sulfur Silicon Relat. Elem.* **2001**, *168*, 41–50; c) P. Chen, C. Cui, *Chemistry* **2016**, *22*, 2902–2905.
[13] Y. Peng, H. Fan, V. Jancik, H. W. Roesky, R. Herbst-Irmer, *Angew. Chem. Int. Ed.* **2004**, *43*, 6190–6192; *Angew. Chem.* **2004**, *116*, 6316–6318.
[14] C. Weetman, A. Porzelt, P. Bag, F. Hanusch, S. Inoue, *Chem. Sci.* **2020**, *11*, 4817–4827.
[15] J. D. Queen, A. Lehmann, J. C. Fettinger, H. M. Tuononen, P. P. Power, *J. Am. Chem. Soc.* **2020**, *142*, 20554–20559.
[16] a) M. L. Cole, C. Jones, P. C. Junk, M. Kloth, A. Stasch, *Chem. Eur. J.* **2005**, *11*, 4482–4491; b) N. Kuhn, S. Fuchs, M. Steimann, *Z. Anorg. Allg. Chem.* **2000**, *626*, 1387–1392.
[17] S. Ito, K. Tanaka, Y. Chujo, *Inorganics* **2019**, *7*, 100.
[18] B. Twamley, N. J. Hardman, P. P. Power, *Acta Crystallogr. Sect. E* **2001**, *57*, m227–m228.
[19] P. Pyykkö, M. Atsumi, *Chem. Eur. J.* **2009**, *15*, 186–197.
[20] Deposition Numbers 2118428–2118435 (Compound **1**–**8**) contain the supplementary crystallographic data for this paper. These data are provided free of charge by the joint Cambridge Crystallographic Data Centre and Fachinformationszentrum Karlsruhe Access Structures service.
[21] V. Lavallo, Y. Canac, C. Präsang, B. Donnadieu, G. Bertrand, *Angew. Chem. Int. Ed.* **2005**, *44*, 5705–5709; *Angew. Chem.* **2005**, *117*, 5851–5855.
[22] C. J. Claire, J. A. C. Clyburne, A. H. Cowley, V. Lomeli, B. G. McBurnett, *Chem. Commun.* **1998**, 243–244.

Manuscript received: November 9, 2021
Accepted manuscript online: December 1, 2021
Version of record online: December 21, 2021

5. An Aluminum Telluride with a Terminal Al=Te Bond and its Conversion to an Aluminum Tellurocarbonate by CO_2 Reduction

Title: An Aluminum Telluride with a Terminal Al=Te Bond and its Conversion to an Aluminum Tellurocarbonate by CO_2 Reduction

Status: Research Article, published online: 12 January 2023

Journal: *Angewandte Chemie International Edition* **2023**, *62*, e202216021; *Angew. Chem.* **2023**, *135*, e202216021.

Publisher: Wiley-VCH Verlag GmbH & Co. KGaA, Weinheim.

DOI: 10.1002/anie.202216021

Authors: Huihui Xu, Arseni Kostenko, Catherine Weetman, Shiori Fujimori, Shigeyoshi Inoue

Content

Facile isolation of various dimeric aluminum selenides and tellurides, as well as an aluminum–telluride monomer featuring a terminal Al=Te bond, is reported. The aluminum–telluride monomer exhibits high thermal stability and reacts with three equivalents of CO_2 to form an unprecedented tellurocarbonate $[CO_2Te]^{2-}$ substituted aluminum complex, which is the first example of tellurium analogue of the carbonate $[CO_3]^{2-}$.

Author Contributions

Huihui Xu planned and executed all experiments. Huihui Xu and Dr. Catherine Weetman co-wrote the manuscript. Dr. Arseni Kostenko designed and performed the theoretical investigations. Dr. Shiori Fujimori contributed with significantly important discussions, conducted all SC-XRD measurements and processed the resulting data. All work was performed under the supervision of Prof. Shigeyoshi Inoue.

GDCh Research Articles Angewandte International Edition Chemie www.angewandte.org

Check for updates

Coordination Chemistry

How to cite: *Angew. Chem. Int. Ed.* **2023,** *62,* e202216021
International Edition: doi.org/10.1002/anie.202216021
German Edition: doi.org/10.1002/ange.202216021

An Aluminum Telluride with a Terminal Al=Te Bond and its Conversion to an Aluminum Tellurocarbonate by CO_2 Reduction

*Huihui Xu, Arseni Kostenko, Catherine Weetman, Shiori Fujimori, and Shigeyoshi Inoue**

Abstract: Facile access to dimeric heavier aluminum chalcogenides [(NHC)Al(Tipp)-μ-Ch]$_2$ (NHC = I*i*Pr (1,3-diisopropyl-4,5-dimethylimidazol-2-ylidene, IMe$_4$ (1,3,4,5-tetramethylimidazol-2-ylidene); Tipp = 2,4,6-*i*Pr$_3$C$_6$H$_2$; Ch = Se, Te) by treatment of NHC-stabilized aluminum dihydrides with elemental Se and Te is reported. The higher affinity of IMe$_4$ in comparison with I*i*Pr toward the Al center in [(NHC)Al(Tipp)-μ-Ch]$_2$ can be used for ligand exchange. Additionally, the presence of excess IMe$_4$ allows for cleavage of the dimers to form a rare example of a neutral multiply bonded heavier aluminum chalcogenide in the form of a tetracoordinate aluminum complex, (IMe$_4$)$_2$(Tipp)Al=Te. This species reacts with three equivalents of CO_2 across two Al–C^{NHC} and the Al=Te bond affording a pentacoordinate aluminum complex containing a dianionic tellurocarbonate ligand [CO_2Te]$^{2-}$, which is the first example of tellurium analogue of a carbonate [CO_3]$^{2-}$.

Introduction

Main group complexes with compositions ECh and E$_2$Ch$_3$ (E = Group 13, Ch = Group 16) are of high interest due to their electronic and optoelectronic properties, and their potential applications in innovative technologies.[1] It is, therefore, of high importance to understand their bonding motifs, electronic structure and aggregation processes to aid the development of advanced materials.[2] Aluminum chalcogenides are predominantly encountered in the form of alumina (Al$_2$O$_3$) which are used widely in ceramics, abrasives, refractory materials, and nonconductors.[3] Heavier aluminum chalcogenides (aluminum sulfides, selenides, and tellurides) have also attracted increasing attention, due to their applications in chemical vapor deposition (CVD), catalysis and materials.[4] Neutral multiply bonded heavier aluminum chalcogenides have been notoriously difficult synthetic targets.[5] Structural evidence of discrete molecular aluminum chalcogenides has been limited due to the polarized nature of terminal Al–Ch bonds (Figure 1, **I**) which makes them prone to head-to-tail self oligomerization, resulting in the corresponding tetramers (e.g. **II**) and dimers (e.g. **III**).

Only a few fully characterized tetramers, i.e. group 13 cubic chalcogenides of the composition [RECh]$_4$ (**II**), which have shown potential as precursors in the metal organic CVD,[6] have been reported (e.g. **IIa-c**).[7] As intermediates for the preparation of tetramers, dimers of the composition

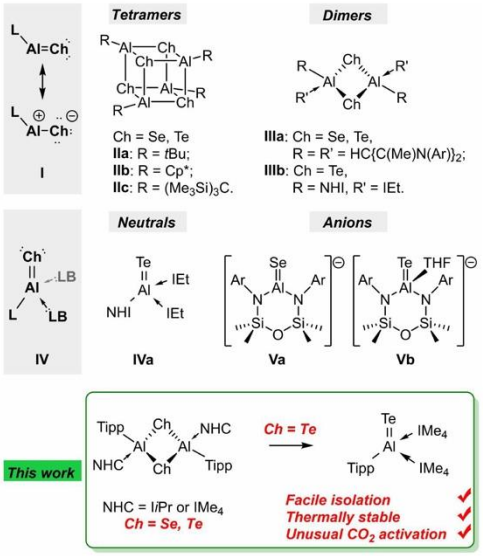

Figure 1. Selected heavier aluminum chalcogenides including tetramers, dimers, monomers (neutrals, anions) and this work. Ar = 2,6-*i*Pr$_2$C$_6$H$_3$; Cp* = C$_5$Me$_5$; NHI = 1,3-(2,6-diisopropylphenyl)-imidazol-2-imine; IEt = 1,3-diethyl-4,5-dimethylimidazol-2-ylidene; I*i*Pr = 1,3-diisopropyl-4,5-dimethylimidazol-2-ylidene; IMe$_4$ = 1,3,4,5-tetramethylimidazol-2-ylidene; Tipp = 2,4,6-*i*Pr$_3$C$_6$H$_2$.

[*] H. Xu, Dr. A. Kostenko, Dr. S. Fujimori, Prof. S. Inoue
School of Natural Sciences, Department of Chemistry, Catalysis Research Center and Institute of Silicon Chemistry, Technische Universität München
Lichtenbergstr. 4, 85748 Garching bei München (Germany)
E-mail: s.inoue@tum.de
Dr. C. Weetman
Department of Pure and Applied Chemistry
University of Strathclyde
295 Cathedral St, Glasgow G1 1XL Scotland (UK)

$[RR'ECh]_2$ (**III**),[1b,8] bearing ligands with increased steric demands in comparison to tetramers, have also been investigated.[9] In the case of the monomeric species, multiply bonded aluminum chalcogenides have been scarcely reported due to the lack of general synthetic routes and their inherent instability.[8d,9a,10] In those that have been isolated, Lewis acids or bases have been employed for kinetic and/or thermodynamic stabilization (e.g. **IV**).[2d,11] This was exemplified by our group in the case of the isolation of the first monomeric aluminum telluride $(IEt)_2Al(NHI)=Te$ **IVa** (IEt = 1,3-diethyl-4,5-dimethylimidazol-2-ylidene; NHI = 1,3-(2,6-diisopropylphenyl)-imidazol-2-imine), which contains a terminal Al=Te double bond.[9b] With the development of anionic aluminyl chemistry, wherein additional stabilization is achieved through interaction with alkali metals, this strategy has been employed for the isolation of discrete Al=Ch bonds.[12] For example, Coles and co-workers isolated $[Al=Se]^-$ (**Va**)[12e,13] and $[Al=Te]^-$ (**Vb**).[12c] With increased anionic character and nucleophilicity, both species showed remarkably nucleophilic reactivity towards Se and CO_2.[12c,13]

In light of our recent report on the stepwise isolation of aluminum sulfides,[11b] we sought to extend the aluminum chalcogenide chemistry to heavier analogues. Here, we present molecular heavier aluminum chalcogenides (Se, Te). Treatment of dimeric tellurides with NHC results in the isolation of a neutral aluminum telluride, $(IMe_4)_2Al(Tipp)=Te$ **5-Te**, containing a discrete Al=Te double bond. Interestingly, **5-Te** shows an unusual reactivity towards CO_2 forming a pentacoordinate aluminum complex **6-Te**, which contains an unprecedented tellurocarbonate $[CO_2Te]^{2-}$ moiety.

Results and Discussion

The synthesis of dimeric aluminum tellurides, $[IiPrAl(Tipp)-\mu-Te]_2$ **2-Te** and $[IMe_4Al(Tipp)-\mu-Te]_2$ **3-Te**, can be achieved by using the recently reported NHC-stabilized aluminum dihydrides $IiPrAl(Tipp)H_2$ **1-IiPr**[10a,11b] and $IMe_4Al(Tipp)H_2$ **1-IMe$_4$**. Unlike $(IEt)_2Al(NHI)=Te$ **IVa**, preparation of which was accomplished by using nBu_3PTe as Te source,[9b] nBu_3PTe was unreactive towards both aluminum dihydrides (even at 100 °C for 72 hours). Instead, reactions of **1-IiPr** or **1-IMe$_4$** with elemental tellurium at room temperature afforded the desired **2-Te** and **3-Te** in 60 % and 70 % yields, respectively (Scheme 1, path a and b). Using an analogous methodology, i.e. reactions of Se with **1-IiPr** or **1-IMe$_4$**, we were able to isolate **2-Se** and **3-Se** in high yields.

Single-crystal X-ray (SC-XRD) structures of **2-Te** and **3-Te** (Figure 2, Top and Middle) show aluminum centers possessing pseudo-tetrahedral geometry with the common chalcogen-bridged connectivity pattern of a four-membered Al_2Te_2 cycle, and the NHC ligands in a *trans* geometry. Al–Te bond lengths, 2.6051(5), 2.6363(5) Å in **2-Te** and 2.5974(9), 2.626(1) Å in **3-Te**, are very similar and closely resemble those of **IIIb** (2.6143(14), 2.6211(15) Å),[9b] but are somewhat longer than those observed in **IIIa** (2.575(3), 2.581(2) Å)[9a] as well as in related compounds reported by Roesky and co-workers (2.54–2.59 Å).[8a,c–e,14] The distances

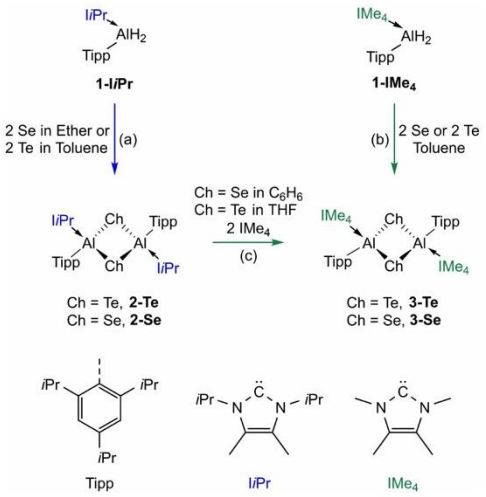

Scheme 1. Formation of **2-Te**, **2-Se**, **3-Te**, and **3-Se**.

of Al–C^{IMe4} (Al1–C16 2.062(3) Å) and Al–C^{Tipp} (Al1–C1 2.014(3) Å) in **3-Te** are noticeably shorter than those measured in **2-Te** (Al1–C16 2.099(2) Å; Al1–C1 2.022(1) Å), respectively. ^{125}Te NMR of **3-Te** exhibits a chemical shift at −954.2 ppm, which is in a higher field than that of **2-Te** (−898.0 ppm).

Although crystals of **2-Se** suitable for SC-XRD crystallography could not be obtained, its structure was confirmed by multinuclear NMR spectroscopy, elemental analysis (EA) and liquid injection field desorption ionization mass spectrometry (LIFDI-MS). The solid-state structure of **3-Se** (Figure 2, Bottom) exhibits a geometry similar to **3-Te** (Middle) featuring an $Al_2(\mu\text{-}Se)_2$ core with the NHC and Tipp substituents bound to Al centers oriented in a *trans* fashion. Al1–Se1 bond length (2.386(1), 2.402(2) Å) is within the range of the typical Al–Se single bond length (2.34–2.54 Å) of reported aluminum selenides,[1b,2a,7a,b,d,8e,9a,15] but notably longer than the Al=Se double bond length (2.2032 (6) Å) of **Va**.[12e] ^{77}Se NMR of the IMe_4-substituted **3-Se** exhibits a chemical shift at −460.5 ppm, which is in a higher field than that of the IiPr-substituted **2-Se** (−355.7 ppm). Similar trend is observed for **2-Te** and **3-Te**. These observations imply a higher electron density at the chalcogen centers in the IMe_4-substituted complexes and may point to a preferential donicity of IMe_4 to the dimeric aluminum chalcogenides in comparison with IiPr. The electronic structures of the dimeric $[NHCAl(Tipp)-\mu-Ch]_2$ complexes were elucidated by density functional theory (DFT) calculations. The results and details of the computational methods are presented in the Supporting Information (Figures S73–S75, Tables S4 and S5).

Reactions of **2-Te** or **2-Se** with two equivalents of IMe_4 resulted in the NHC exchange reaction forming the respective complexes **3-Te** and **3-Se** (Scheme 1, path c). The

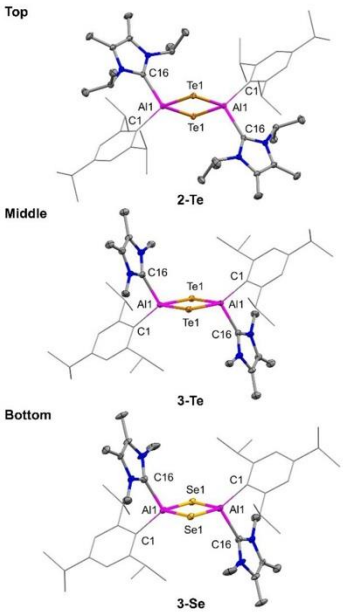

Figure 2. Molecular structures of **2-Te** (Top), **3-Te** (Middle), and **3-Se** (Bottom).[16] Ellipsoids are set at the 50% probability level; hydrogen atoms and co-crystallized solvent molecules are omitted for clarity and Tipp (2,4,6-*i*Pr$_3$C$_6$H$_2$) ligands are depicted in wireframe for simplicity. Selected bond lengths [Å] and angles [°]: **2-Te** Al1–Te1 2.6051(5), 2.6363(5), Al1–C1 2.022(1), Al1–C16 2.099(2), Al1–Te1–Al1 81.62(1). **3-Te** Al1–Te1 2.5974(9), 2.626(1), Al1–C1 2.014(3), Al1–C16 2.062(3), Al1–Te1–Al1 82.31(3). **3-Se** Al1–Se1 2.386(1), 2.402(2), Al1–C1 2.019(9), Al1–C16 2.078(5), Al1–Se1–Al1 80.56(5).

facile exchange of I*i*Pr by IMe$_4$ ligands indicates a higher affinity of IMe$_4$ toward the aluminum centers in the dimeric aluminum chalcogenide complexes. Indeed, the calculated free energy for IMe$_4$ dissociation from **3-Te** is by 8.0 kcal mol^{-1} higher than that of I*i*Pr dissociation from **2-Te** (23.0 vs. 15.0 kcal mol^{-1}). Similar values are calculated for **3-Se** and **2-Se** (24.5 and 13.7 kcal mol^{-1}). Contrary to this are the calculated gas phase proton affinities of I*i*Pr (280.3 kcal mol^{-1}) and IMe$_4$ (275.4 kcal mol^{-1}), which point to I*i*Pr being a better donor, due to the presence of the additional electron-donating alkyl groups. The relatively higher affinity of IMe$_4$ to the dimeric aluminum tellurides can be attributed to the steric effect - the repulsion is higher in the case of the bulkier I*i*Pr, as confirmed by natural steric analysis (Figure S76 in the Supporting Information). The lower steric repulsion results in higher affinity of IMe$_4$ toward the Al center in the dimeric complexes and enables the ligand exchange reaction. The steric effects of the differently substituted NHCs are also evident from the calculated energies of dissociation of **2-Te** and **3-Te** to the corresponding monomers with the respective Gibbs energies of 21.1 and 26.1 kcal mol^{-1} (27.3 kcal mol^{-1} for **2-Se** and 36.4 kcal mol^{-1} for **3-Se**).

Taking into account the above mentioned higher affinity of IMe$_4$ toward aluminum chalcogenides in comparison with I*i*Pr, we wanted to utilize this feature for preparation of the corresponding monomeric complexes featuring a terminal aluminum-tellurium bond. Interestingly, upon monitoring the above mentioned reaction of **2-Te** with IMe$_4$, that ultimately gives **3-Te** (Scheme 1, path c), the monomeric aluminum telluride I*i*Pr(IMe$_4$)Al(Tipp)=Te **4-Te** could be observed (Scheme 2, path a). Its formation was confirmed by multinuclear NMR spectroscopy and its composition was validated by LIFDI-MS (Figures S1–S6 in the Supporting Information). The ^{125}Te NMR signal appears at δ −924.7 ppm, which shifted upfield in comparison to the precursor (**2-Te**, δ −898.0 ppm). Calculations predict the formation of **4-Te** from **2-Te** to be exergonic by full 6.0 kcal mol^{-1} (Scheme 3, path b). Isolation of **4-Te** could not be accomplished since it subsequently and quantitatively converts to **3-Te** (Scheme 2, path b). Calculations predict this step to be exergonic by additional 2.8 kcal mol^{-1} (Scheme 3, path c).

Unlike **2-Te**, which in the presence of IMe$_4$ forms the detectible intermediate I*i*Pr(IMe$_4$)Al(Tipp)=Te **4-Te**, treatment of **2-Se** with IMe$_4$ only affords **3-Se**, and the corresponding intermediate **4-Se** could not be observed. This divergence can be explained by the relative energies of the intermediates involved in these reactions. Although the formation of **3-Te** and **3-Se** from **2-Te** and **2-Se** in the presence of IMe$_4$ is exergonic in both cases, by 8.8 and 11.6 kcal mol^{-1} respectively (Scheme 3 path a), the formation of intermediate **4** is only exergonic in the case of Te (−6.0 kcal mol^{-1} vs. 1.8 kcal mol^{-1} in the case of Se) (Scheme 3, path b). These calculations provide a plausible

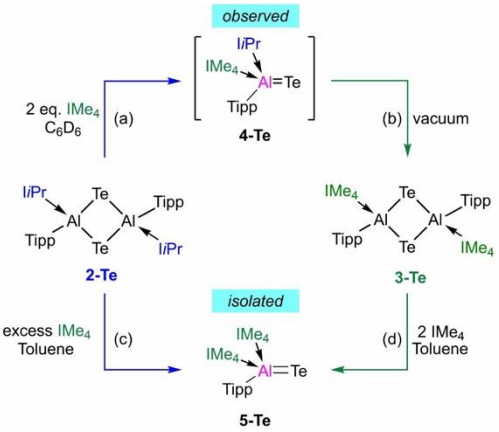

Scheme 2. Formation of **4-Te** and **5-Te**. I*i*Pr = 1,3-diisopropyl-4,5-dimethylimidazol-2-ylidene; IMe$_4$ = 1,3,4,5-tetramethylimidazol-2-ylidene; Tipp = 2,4,6-*i*Pr$_3$C$_6$H$_2$.

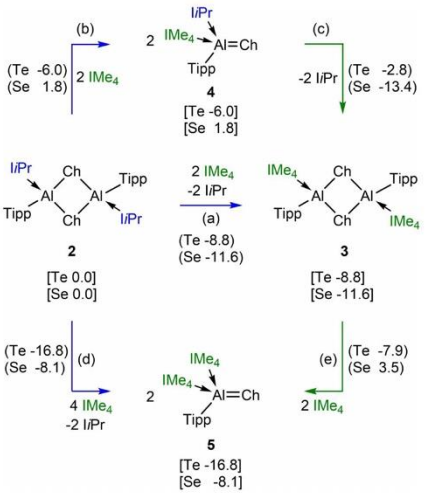

Scheme 3. Calculated energies (kcal mol^{-1}) for the reactions of **2**, **3**, **4** and **5**. Relative Gibbs energies of compounds are shown in square brackets. ΔG of reactions are shown in round brackets.

explanation of why intermediate **4-Se** could not be observed.

In attempt to actually isolate a monomeric aluminum telluride, we introduced IMe_4 in excess to **2-Te** (Scheme 2, path c), which furnished the aluminum telluride $(IMe_4)_2Al(Tipp)=Te$ **5-Te**, containing a tetracoordinate aluminum center and a terminal Al=Te bond, in a 45 % yield. **5-Te** could also be obtained in 63 % yield by introduction of two equivalents of IMe_4 to **3-Te** (Scheme 2, path d). To understand the formation of **5-Te**, Gibbs energy for the reaction of **2-Te** with four equivalents of IMe_4 to give two equivalents of **5-Te** and two equivalents of *i*Pr was calculated giving $\Delta G = -16.8$ kcal mol^{-1} (Scheme 3, path d). Calculations indicate that **5-Te** is the most energetically favored species as its formation from **3-Te** and two equivalents of IMe_4 is also exergonic by 7.9 kcal mol^{-1} (Scheme 3, path e). However, preparation for the selenide analogue of **5-Te** by introduction of stoichiometric or excess amounts of IMe_4 to compound **2-Se** and **3-Se** did not yield the corresponding $(IMe_4)_2Al(Tipp)=Se$ **5-Se**. Unlike the formation of **5-Te** from **3-Te** in the presence of IMe_4, which was calculated to be exergonic by 7.9 kcal mol^{-1} (Scheme 3, path e), analogous formation of the hypothetical **5-Se** from **3-Se** is calculated to be endergonic by 3.5 kcal mol^{-1}. Although the formation of **5-Se** from **2-Se** is predicted to be exergonic by 8.1 kcal mol^{-1} (Scheme 3, path d), dissociation of IMe_4 and dimerization to **3-Se** energetically preferred by 3.5 kcal mol^{-1}. Thus, in the case of Te the most energetically favored compound is **5-Te**, while in the case of Se it is **3-Se**. This tendency could be explained by the higher proclivity for dimerization of Al–Se vs. Al–Te. This is evident from the dissociation energies of **3-Se** (36.4 kcal mol^{-1}) and **3-Te** (26.1 kcal mol^{-1}) to the corresponding monomers.

The single-crystal structure of **5-Te** (Figure 3) shows the Al center bound to the aryl substituent, two geminal IMe_4 ligands and a tellurium atom in a distorted tetrahedral manner. The Al1–Te1 distance of 2.534(1) Å is longer than those in **IVa** (2.5130 (14) Å),[9b] **Vb** (2.5039(7) Å)[12c] as well as the sum of covalent double bond radii ($\Sigma(r_2)=2.41$ Å),[17] although is shorter than the Al–Te single bond lengths in **2-Te** (2.605(5), 2.6363(5) Å) or **3-Te** (2.5974(9), 2.626(1) Å) and other dimeric aluminum tellurides (2.541–2.588 Å).[8d,9] The ^{125}Te NMR displays a signal at −1368.6 ppm, which is more shielded than that of dimeric **2-Te** (δ −898.0 ppm) and **3-Te** (δ −954.2 ppm) as well as monomeric **4-Te** (δ −924.7 ppm).

Selected frontier molecular orbitals of **5-Te** are presented in Figure 4. The HOMO-2 corresponds to the σ-type

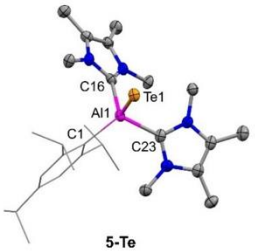

Figure 3. Molecular structure of **5-Te**.[16] Ellipsoids are set at the 50 % probability level; hydrogen atoms and co-crystallized solvent molecules are omitted for clarity and Tipp (2,4,6-$iPr_3C_6H_2$) ligands are depicted in wireframe for simplicity. Selected bond lengths [Å] and angles [°]: Al1–Te1 2.534(1), Al1–C1 2.047(4), Al1–C16 2.082(5), Al1–C23 2.061(5), Te1–Al1–C1 127.2(1), Te1–Al1–C16 108.2(1), Te1–Al1–C23 99.9(1).

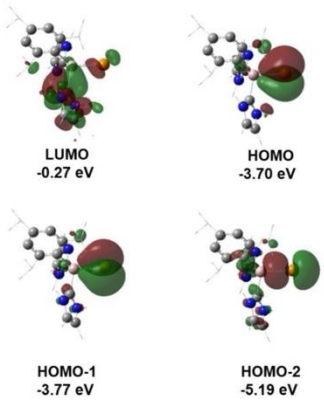

Figure 4. Selected molecular orbitals of **5-Te**. For clarity, hydrogens are omitted, and methyl and isopropyl substituents are shown as wireframes.

lone pair of Te and the σ-bond of Te–Al. The HOMO-1 and HOMO show π-type lone pairs extending toward Al center pointing to a higher bond order between Al and Te. The natural bond orbital (NBO) analysis shows a polarized Te–Al bonding interaction (68.7 % Te ($sp^{3.4}$), 31.3 % Al ($sp^{1.5}$)) with natural charges of −0.92 el. and +1.13 el. on Te and Al, respectively. Both Mayer bond order (MBO, 1.74) and Wiberg bond index (WBI, 1.17) indicate a double bond character of the Te–Al interaction. Second order perturbation theory analysis reveals donor-acceptor interactions (DAI) between one of the π-type lone pairs of Te and a lone vacancy p orbital of Al with occupancy of 0.36 el. (25.3 kcal mol^{-1}) and between the second π-type lone pair of Te and a lone-vacancy $sp^{4.0}$ orbital of Al with occupancy of 0.40 el. (13.0 kcal mol^{-1}). These interactions result in the double bond character of the Al–Te fragment. Additional details regarding the electronic structure of **5-Te** are presented in the Supporting Information (Figure S77).

Unlike **IVa**, for which the reactivity studies could not be carried out due to its instability, **5-Te** is thermally stable as there was no detectable change (^{1}H NMR) in THF-d_8 at 80 °C for at least 72 hours. Reaction of **5-Te** with BPh_3 resulted in elimination of the NHC ligand and formation of **3-Te** dimer (Scheme 4, path a). As chalcogen exchange have been shown to provide a route to isolation of terminal multiple chalcogen bonds,[18] we treated **5-Te** with lighter chalcogens. Reaction of **5-Te** with Se yielded the dimeric **3-Se** (Scheme 4, path b). This transformation presumably proceeds via the initial exchange of Te with Se, forming the transient intermediate **5-Se**, which cannot be isolated, due to its above described tendency to release IMe_4 and dimerize to **3-Se**. The reaction of **5-Te** with S_8 resulted in immediate decomposition with formation of metallic tellurium precipitate and ^{1}H NMR showing signals which correspond to TippH and IMe_4=S (Figure S9 in the Supporting Information).

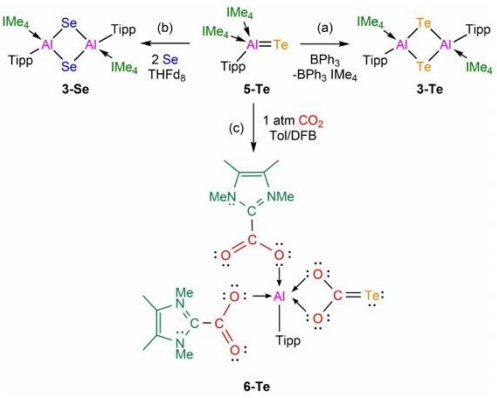

Scheme 4. Reactivity of **5-Te** towards BPh_3, Se and CO_2. IMe_4=1,3,4,5-tetramethylimidazol-2-ylidene; Tipp=2,4,6-$iPr_3C_6H_2$.

Attempts to study the reactivity of **5-Te** towards H_2, N_2O, CO, IMe_4-CO_2, tBu_3PSe, PPh_3, IMe_4-CuMes (Mes=2,4,6-$Me_3C_6H_2$), Diphenylacetylene, 2,6-Dimethylphenyl isocyanide, Phenylacetylene, Ph_2CO, Ni(COD)$_2$ (COD=1,5-cyclooctadiene), MesCu, Benzophenone, NMO (4-Methylmorpholine *N*-oxide), Me_2S-AuCl and Mes_2Fe were unsuccessful (Figure S11 in the Supporting Information). As mentioned in the introduction, the reaction of CO_2 with [Al=Se]$^-$ **Va** and [Al=Te]$^-$ **Vb** resulted in a single CO_2 insertion product, [Al(NON^{Dipp})(SeC{O}O)]$^-$ (NON^{Dipp}=[O(SiMe$_2$NDipp)$_2$]$^{2-}$, Dipp=2,6-$iPr_2C_6H_3$),[13] and a double CO_2 insertion product, [Al(NON^{Dipp})({OC(O)}$_2$Te)]$^-$,[12c] respectively. Here, however, exposure of **5-Te** to CO_2 results in the formation of a triple CO_2 insertion product (Scheme 4, path c), which was identified as (IMe_4CO_2)$_2$Al-(Tipp)-μ-O_2C=Te (**6-Te**). Formally, three equivalents of CO_2 reacted with **5-Te** across two Al–C^{NHC} bonds and the terminal Al=Te bond. We note here that there was no observed reactivity between CO_2 and the dimeric species **2-Te**, **2-Se**, **3-Te**, or **3-Se** even at 80 °C.

The solid-state structure of **6-Te** (Figure 5A) shows that the pentacoordinate Al center, bound to the Tipp substituent, two CO_2–NHC (η^1-κ*O*) moieties and CO_2Te (η^2-κ*O*,*O*′), adopts a distorted trigonal bipyramidal geometry. The

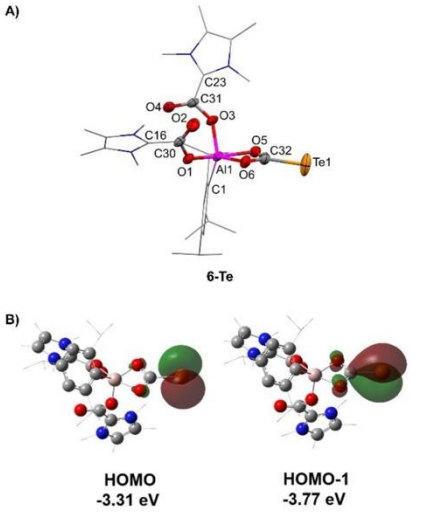

Figure 5. A) Molecular structure of **6-Te**.[16] Ellipsoids are set at the 50 % probability level; hydrogen atoms and co-crystallized solvent molecules are omitted for clarity and the Tipp (2,4,6-$iPr_3C_6H_2$) ligand is depicted in wireframe for simplicity. Selected bond lengths [Å] and angles [°]: C32–Te1 2.088(5), Al1–O1 1.865(4), Al1–O3 1.824(3), Al1–O5 2.028(4), Al1–O6 1.871(4), Al1–C1 1.992(5), C30–O1 1.288(6), C30–O2 1.221(7), C32–O5 1.268(7), C32–O6 1.317(7), C31–O3 1.294(6), C31–O4 1.211(6), C23–C31 1.474(7), C16–C30 1.546(16), O5–C32–O6 113.4(4), O5–Al1–O6 67.16(15). B) Selected Molecular orbitals of **6-Te**. For clarity, hydrogens are omitted, and methyl and isopropyl substituents are shown as wireframes.

corresponding structural parameters in a μ-CO_2-$\kappa^2O,O':\kappa C$ fashion[19] are comparable to previous examples[20] involving Al^{I}[21] and Al^{III}[22] bimetallic precursors. Bond lengths of Al1–O1 (1.865(4) Å), Al1–O3 (1.824(3) Å), Al1–O6 (1.871 (4) Å) are within the range of typical Al–O single bond (ca. 1.87 Å),[23] whereas Al1–O5 (2.028(4) Å) is notably longer than this single bond length. C–O bond lengths for the Al–μ–O_2C–Te unit (C32–O5 1.268(7) Å, C32–O6 1.317 (7) Å) fall between the typical ranges for C–O single and double bonds,[24] supporting the idea of a formal two-electron reduction of CO_2 and being consistent with delocalization of the π-electron density over the entirety of the CO_2 fragment. The C32–Te1 distance of 2.088(5) Å is slightly longer than the average C=Te length (ca. 1.93 Å)[25] and still shorter than an average of typical C–Te single bond (ca. 2.158 Å).[26] In ^{13}C NMR, the carbon of the terminal C=Te bond appears at δ 226.56 ppm, which is more shielded than those of typical telluroketones with terminal C=Te double bond (^{13}C NMR: δ 284.00–351.00 ppm),[27] but more deshielded than measured in NHC supported telluroketones (δ 126.00–187.00 ppm).[25,28] The ^{125}Te NMR signal appears at a higher chemical shift (δ −187.6 ppm) than that of **5-Te** (δ −1368.6 ppm), but it is more shielded than the resonance measured for [Al(NON^{Dipp})({OC(O)}$_2$Te)]$^-$ (CO_2 activation product of **Vb**, δ −17.80 ppm)[12c] and significantly more deshielded for the complex containing terminal Si=Te (δ −1010.4 or −982.5 ppm).[29]

The DFT calculated Gibbs energy for reaction of **5-Te** with three molecules of CO_2 to give **6-Te** is −23.4 kcal mol^{-1}. Calculated energies of the possible intermediates (Figure S78 in the Supporting Information) indicate that the reaction most likely proceeds via two initial CO_2 insertions into the Al–C^{NHC} bond with the third addition across the Al=Te bond taking place at the last step. WBI and MBO of 1.19 and 1.39 indicate a multiple bond character of the C–Te interaction.

The NBO analysis shows a polarized Te1 (34.8 %)–C (65.2 %) bonding interaction. Additionally, the Te center contains one σ-type and two π-type lone pairs. The π-type lone pairs correspond to HOMO-1 and HOMO (Figure 5B), with the former extending toward the carbon center. The second order perturbation analysis shows a significant DAI between the Te lone pair and the p-orbital of the carbon of 223.4 kcal mol^{-1}, which is of higher magnitude than the DAIs between the lone pair of the oxygens and the empty p orbital of the carbon (191.6 and 153.1 kcal mol^{-1}), resulting in Te–C with multiple bond character. Inquiry into the bonding situation around the Al center reveals essentially dative interactions between Al and the κ^2-coordinated CO_2Te and the κ^1-coordinated NHC–CO_2 moieties. The calculated WBIs and MBOs show rather weak bonding between Al and the oxygen atoms of the CO_2Te and NHC–CO_2 substituent, with Al1–O1 (0.24, 0.60), Al1–O3 (0.28, 0.70), Al1–O5 (0.26, 0.69), Al1–O6 (0.30, 0.79) (Figure 6a). Each of the oxygen atoms bonded to Al (O1, O3, O5 and O6) contains three lone pairs that are donated into the lone-vacancy orbitals of Al. Detailed NBO analysis and additional features of the electronic structure of **6-Te** are presented in the Supporting Information (Figures S79–81,

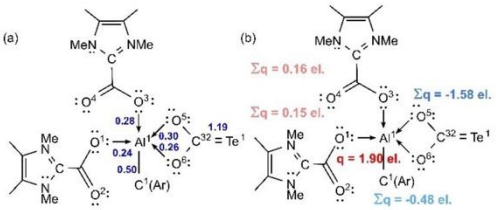

Figure 6. a) Selected WBI in **6-Te**; b) Distribution of natural charge in **6-Te**.

Table S6). Most of the positive natural charge resides on Al (+1.90 el.), while the NHC-CO_2 moieties are almost neutral (Σq = +0.16 and +0.15 el.). Most of the negative charge is concentrated on the CO_2Te moiety with Σq = −1.58 el. and remaining −0.48 el. reside on the aryl substituent.

Thus the DFT calculations suggest that the CO_2Te moiety in **6-Te** can be described as tellurocarbonate $[CO_2Te]^{2-}$, which is the first example of a tellurium analogue of a carbonate $[CO_3]^{2-}$. Carbonate is a ubiquitous ligand in transition metal chemistry. A few examples of alkali metal, alkaline earth metal and main-group-element complexes coordinated by carbonates also have been reported.[30] However, to the best of our knowledge, there are no examples of complexes substituted by heavy carbonate analogues. The preferred mode of coordination of the tellurocarbonate to aluminum center is via the two oxygen atoms, as calculations show that the isolated (tellurocarbonate-κ^2 O,O′)Al isomer is by 5.2 kcal mol^{-1} more energetically favored than the hypothetical (tellurocarbonate-κ^2 O,Te)Al isomer. In general, contrary to carbonyl (C=O) and thiocarbonyl compounds (C=S), compounds with heavier terminal C=Ch bonds[25,27c,31] have been much less explored because of their high reactivity. In the case of tellurium it can be ascribed to the unfavorable C_{2p}–Te_{5p} orbital overlap,[32] and strong tendency for oligomerization, isomerization into singly bonded molecules, or decomposition into simpler entities.[33] But, while C=O and C=S are ubiquitous building blocks in nature and have been explored for their uses from the chemical industry to bioscience,[34] the potential of heavier C=Ch in the context of biological functionalities is yet to be unveiled. In terms of the reactivity exploration of **6-Te**, this compound features poor solubility in benzene, toluene, acetonitrile, THF and pyridine, but is soluble in 1,2-difluorobenzene. **6-Te** is thermally unstable, and decomposes even at −30 °C to IMe_4=Te, IMe_4-CO_2 and unidentified species (Figure S12–S16, in the Supporting Information). Due to the poor solubility and inherent thermal instability of **6-Te**, our attempts to study its reactivity towards a variety of reagents (i.e. IMe_4, $cAAC^{Me}$ (1-(2,6-*i*$Pr_2C_6H_3$)-3,3,5,5-tetramethylpyrrolidin-2-ylidene), $Na_2Fe(CO)_4$, BPh_3, PPh_3, KOTf, KC_8, diphenylacetylene, styrene, ethylene, hydrogen) have been unsuccessful so far. (Figure S17–19, in the Supporting Information).

Conclusion

In summary, we have isolated a series of dimeric aluminum tellurides and selenides and a monomeric aluminum telluride **5-Te**, which bears a terminal Al=Te double bond. Attempts to isolate the analogous monomeric aluminum selenide containing an Al=Se double bond were unsuccessful due to its preference to form thermodynamically more favorable dimeric species, as confirmed by DFT calculations. In contrast to our previously reported aluminum telluride (**IVa**), **5-Te** features better stability that enables its reactivity studies towards small molecules. Reaction of elemental Se results in the lighter dimeric species via an inferred transient aluminum selenide with a terminal Al–Se bond. Most interestingly, the reactivity of **5-Te** towards CO_2 results a triple CO_2 insertion product **6-Te** with an unusual pentacoordinate aluminum center. It possesses a tellurocarbonate moiety with a terminal C=Te double bond, representing a unique case of tellurium analogue of a carbonate ligand. Numerous attempts to study further reactivity of the dimeric species, **5-Te** or **6-Te**, towards unsaturated substrates and transition metals have been unsuccessful thus far, however the research of synthetic capabilities of these and similar systems is ongoing in our group.

Acknowledgements

We are grateful to the European Research Council (ALLOWE 101001591) for financial support. H.X. gratefully acknowledges financial support from the China Scholarship Council (CSC). C.W. is thankful to the University of Strathclyde for the award of a Chancellor's Fellowship. We thank Dr. Franziska Hanusch for the SC-XRD measurements, Ivan Antsiburov and Maximilian Muhr for the LIFDI-MS measurements. The authors gratefully acknowledge the Leibniz Supercomputing Centre for funding this project by providing computing time on its Linux-Cluster. Open Access funding enabled and organized by Projekt DEAL.

Conflict of Interest

The authors declare no conflict of interest.

Data Availability Statement

The data that support the findings of this study are available in the Supporting Information of this article.

Keywords: Aluminum Selenide · Aluminum Telluride · CO_2 Activation · Chalcogen · Tellurocarbonate

[1] a) G. Bai, H. W. Roesky, J. Li, M. Noltemeyer, H.-G. Schmidt, *Angew. Chem. Int. Ed.* **2003**, *42*, 5502–5506; *Angew. Chem.* **2003**, *115*, 5660–5664; b) C. Schnitter, A. Klemp, H. W. Roesky, H.-G. Schmidt, C. Röpken, R. Herbst-Irmer, M. Noltemeyer, *Eur. J. Inorg. Chem.* **1998**, 2033–2039; c) K. A. Evans in *The Chemistry of Aluminium, Indium and Gallium* (Ed.: A. J. Downs), Blackie Academic & Professional, Glasgow, **1993**, p. 248.

[2] a) C. Cui, H. W. Roesky, H. Hao, H.-G. Schmidt, M. Noltemeyer, *Angew. Chem. Int. Ed.* **2000**, *39*, 1815–1817; *Angew. Chem.* **2000**, *112*, 1885–1887; b) J. Hicks, A. Heilmann, P. Vasko, J. M. Goicoechea, S. Aldridge, *Angew. Chem. Int. Ed.* **2019**, *58*, 17265–17268; *Angew. Chem.* **2019**, *131*, 17425–17428; c) M. D. Anker, M. P. Coles, *Angew. Chem. Int. Ed.* **2019**, *58*, 18261–18265; *Angew. Chem.* **2019**, *131*, 18429–18433; d) C. Weetman, H. Xu, S. Inoue in *Encyclopedia of Inorganic and Bioinorganic Chemistry* (Ed.: R. A. Scott), Wiley, Hoboken, **2020**, pp. 1–20.

[3] a) D. Neculai, H. W. Roesky, A. M. Neculai, J. Magull, B. Walfort, D. Stalke, *Angew. Chem. Int. Ed.* **2002**, *41*, 4294–4296; *Angew. Chem.* **2002**, *114*, 4470–4472; b) M. R. Mason, J. M. Smith, S. G. Bott, A. R. Barron, *J. Am. Chem. Soc.* **1993**, *115*, 4971–4984; c) R. J. Wehmschulte, P. P. Power, *J. Am. Chem. Soc.* **1997**, *119*, 8387–8388.

[4] A. R. Barron, *Adv. Mater. Opt. Electron.* **1995**, *5*, 245–258.

[5] P. Bag, C. Weetman, S. Inoue, *Angew. Chem. Int. Ed.* **2018**, *57*, 14394–14413; *Angew. Chem.* **2018**, *130*, 14594–14613.

[6] a) M. G. Simmonds, W. L. Gladfelter, *The Chemistry of Metal CVD*, Wiley, New York, **1994**, pp. 45–103; b) M. B. Power, A. R. Barron, D. Hnyk, H. E. Robertson, D. W. H. Rankin, *Adv. Mater. Opt. Electron.* **1995**, *5*, 177–185.

[7] a) A. H. Cowley, R. A. Jones, P. R. Harris, D. A. Atwood, L. Contreras, C. J. Burek, *Angew. Chem. Int. Ed. Engl.* **1991**, *30*, 1143–1145; *Angew. Chem.* **1991**, *103*, 1164–1166; b) S. Schulz, H. W. Roesky, H. J. Koch, G. M. Sheldrick, D. Stalke, A. Kuhn, *Angew. Chem. Int. Ed. Engl.* **1993**, *32*, 1729–1731; *Angew. Chem.* **1993**, *105*, 1828–1830; c) K. S. Klimek, J. Prust, H. W. Roesky, M. Noltemeyer, H.-G. Schmidt, *Organometallics* **2001**, *20*, 2047–2051; d) C. J. Harlan, E. G. Gillan, S. G. Bott, A. R. Barron, *Organometallics* **1996**, *15*, 5479–5488.

[8] a) M. G. Gardiner, C. L. Raston, V.-A. Tolhurst, *J. Chem. Soc. Chem. Commun.* **1995**, 2501–2502; b) W. J. Grigsby, C. L. Raston, V.-A. Tolhurst, B. W. Skelton, A. H. White, *J. Chem. Soc. Dalton Trans.* **1998**, 2547–2556; c) H. Zhu, J. Chai, H. W. Roesky, M. Noltemeyer, H.-G. Schmidt, D. Vidovic, J. Magull, *Eur. J. Inorg. Chem.* **2003**, 3113–3119; d) C. Cui, H. W. Roesky, M. Noltemeyer, H.-G. Schmidt, *Inorg. Chem.* **2000**, *39*, 3678–3681; e) C. Cui, H. W. Roesky, M. Noltemeyer, H.-G. Schmidt, *Organometallics* **1999**, *18*, 5120–5123.

[9] a) V. Jancik, M. M. Moya Cabrera, H. W. Roesky, R. Herbst-Irmer, D. Neculai, A. M. Neculai, M. Noltemeyer, H.-G. Schmidt, *Eur. J. Inorg. Chem.* **2004**, 3508–3512; b) D. Franz, T. Szilvasi, E. Irran, S. Inoue, *Nat. Commun.* **2015**, *6*, 10037.

[10] a) C. Weetman, A. Porzelt, P. Bag, F. Hanusch, S. Inoue, *Chem. Sci.* **2020**, *11*, 4817–4827; b) P. Bag, A. Porzelt, P. J. Altmann, S. Inoue, *J. Am. Chem. Soc.* **2017**, *139*, 14384–14387; c) R. L. Falconer, K. M. Byrne, G. S. Nichol, T. Krämer, M. J. Cowley, *Angew. Chem. Int. Ed.* **2021**, *60*, 24702–24708; *Angew. Chem.* **2021**, *133*, 24907–24913; d) C. Bakewell, K. Hobson, C. J. Carmalt, *Angew. Chem. Int. Ed.* **2022**, *61*, e202205901; *Angew. Chem.* **2022**, *134*, e202205901.

[11] a) D. Franz, S. Inoue, *Dalton Trans.* **2016**, *45*, 9385–9397; b) H. Xu, C. Weetman, F. Hanusch, S. Inoue, *Chem. Eur. J.* **2022**, *28*, e202104042.

[12] a) J. Hicks, P. Vasko, J. M. Goicoechea, S. Aldridge, *Nature* **2018**, *557*, 92–95; b) R. J. Schwamm, M. D. Anker, M. Lein, M. P. Coles, *Angew. Chem. Int. Ed.* **2019**, *58*, 1489–1493; *Angew. Chem.* **2019**, *131*, 1503–1507; c) M. J. Evans, M. D. Anker, C. L. McMullin, N. A. Rajabi, M. P. Coles, *Chem. Commun.* **2021**, *57*, 2673–2676; d) T. X. Gentner, R. E. Mulvey,

Angew. Chem. Int. Ed. **2021**, *60*, 9247–9262; *Angew. Chem.* **2021**, *133*, 9331–9348; e) M. D. Anker, M. P. Coles, *Angew. Chem. Int. Ed.* **2019**, *58*, 13452–13455; *Angew. Chem.* **2019**, *131*, 13586–13589.
[13] M. J. Evans, M. D. Anker, C. L. McMullin, S. E. Neale, N. A. Rajabi, M. P. Coles, *Chem. Sci.* **2022**, *13*, 4635–4646.
[14] W. Uhl, U. Schütz, *Z. Naturforsch. B* **1994**, *49*, 931–934.
[15] W. Uhl, R. Gerding, I. Hahn, S. Pohl, W. Saak, H. Reuter, *Polyhedron* **1996**, *15*, 3987–3992.
[16] Deposition Numbers 2215503 (for **2-Te**), 2215504 (for **3-Se**), and 2215505 (for **3-Te**), 2215506 (for **5-Te**), 2215507 (for **6-Te**) contain the supplementary crystallographic data for this paper. These data are provided free of charge by the joint Cambridge Crystallographic Data Centre and Fachinformationszentrum Karlsruhe Access Structures service.
[17] P. Pyykkö, M. Atsumi, *Chem. Eur. J.* **2009**, *15*, 12770–12779.
[18] D. Sarkar, D. Wendel, S. U. Ahmad, T. Szilvasi, A. Pothig, S. Inoue, *Dalton Trans.* **2017**, *46*, 16014–16018.
[19] C. Yoo, Y. Lee, *Chem. Sci.* **2017**, *8*, 600–605.
[20] H. Corona, M. Pérez-Jiménez, F. de la Cruz-Martínez, I. Fernández, J. Campos, *Angew. Chem. Int. Ed.* **2022**, *61*, e202207581; *Angew. Chem.* **2022**, *134*, e202207581.
[21] a) J. Hicks, A. Mansikkamaki, P. Vasko, J. M. Goicoechea, S. Aldridge, *Nat. Chem.* **2019**, *11*, 237–241; b) C. McManus, J. Hicks, X. Cui, L. Zhao, G. Frenking, J. M. Goicoechea, S. Aldridge, *Chem. Sci.* **2021**, *12*, 13458–13468; c) H.-Y. Liu, R. J. Schwamm, M. S. Hill, M. F. Mahon, C. L. McMullin, N. A. Rajabi, *Angew. Chem. Int. Ed.* **2021**, *60*, 14390–14393; *Angew. Chem.* **2021**, *133*, 14511–14514; d) D. Sorbelli, L. Belpassi, P. Belanzoni, *J. Am. Chem. Soc.* **2021**, *143*, 14433–14437; e) M. M. D. Roy, J. Hicks, P. Vasko, A. Heilmann, A.-M. Baston, J. M. Goicoechea, S. Aldridge, *Angew. Chem. Int. Ed.* **2021**, *60*, 22301–22306; *Angew. Chem.* **2021**, *133*, 22475–22480.
[22] S. Sinhababu, M. R. Radzhabov, J. Telser, N. P. Mankad, *J. Am. Chem. Soc.* **2022**, *144*, 3210–3221.
[23] a) G. I. Shcherbakova, M. K. Shaukhin, A. D. Kirilin, P. A. Storozhenko, *Russ. Chem. Bull.* **2021**, *70*, 1275–1280; b) Z. Sun, H. Wang, Y. Zhang, J. Li, Y. Zhao, W. Jiang, L. Wang, *Dalton Trans.* **2013**, *42*, 12956–12964.
[24] a) N. T. Thuy Tran, S.-Y. Lin, O. E. Glukhova, M.-F. Lin, *RSC Adv.* **2016**, *6*, 24458–24463; b) A. Walsh, *Trans. Faraday Soc.* **1946**, *42*, 56–62.
[25] N. Kuhn, G. Henkel, T. Kratz, *Chem. Ber.* **1993**, *126*, 2047–2049.
[26] F. H. Allen, O. Kennard, D. G. Watson, L. Brammer, A. G. Orpen, R. Taylor, *J. Chem. Soc. Perkin Trans. 2* **1987**, S1–S19.
[27] a) M. Minoura, T. Kawashima, N. Tokitoh, R. Okazaki, *Chem. Commun.* **1996**, 123–124; b) Y. Mutoh, N. Kozono, K. Ikenaga, Y. Ishii, *Coord. Chem. Rev.* **2012**, *256*, 589–605; c) M. Minoura, T. Kawashima, R. Okazaki, *J. Am. Chem. Soc.* **1993**, *115*, 7019–7020.
[28] a) S. T. Manjare, S. Sharma, H. B. Singh, R. J. Butcher, *J. Organomet. Chem.* **2012**, *717*, 61–74; b) D. Rottschäfer, D. E. Fuhs, B. Neumann, H.-G. Stammler, R. S. Ghadwal, *Z. Anorg. Allg. Chem.* **2020**, *646*, 574–579.
[29] a) S. Yao, Y. Xiong, M. Brym, M. Driess, *Chem. Asian J.* **2008**, *3*, 113–118; b) S. Yao, Y. Xiong, M. Driess, *Chem. Eur. J.* **2010**, *16*, 1281–1288.
[30] a) S. E. Wolf, L. Müller, R. Barrea, C. J. Kampf, J. Leiterer, U. Panne, T. Hoffmann, F. Emmerling, W. Tremel, *Nanoscale* **2011**, *3*, 1158–1165; b) C. Sanloup, J. M. Hudspeth, V. Afonina, B. Cochain, Z. Konôpková, G. Lelong, L. Cormier, C. Cavallari, *Front. Earth Sci.* **2019**, *7, 72*.
[31] M. Minoura, T. Kawashima, R. Okazaki, *Tetrahedron Lett.* **1997**, *38*, 2501–2504.
[32] M. Minoura, T. Kawashima, N. Tokitoh, R. Okazaki, *Phosphorus Sulfur Silicon Relat. Elem.* **1998**, *136*, 549–552.
[33] N. B. Jaufeerally, H. H. Abdallah, P. Ramasami, H. F. Schaefer, *J. Phys. Chem. A* **2013**, *117*, 5567–5577.
[34] a) N. Kuhn, G. Verani, *Handbook of Chalcogen Chemistry: New Perspectives in Sulfur, Selenium and Tellurium*, The Royal Society of Chemistry, London, **2007**, pp. 107–144; b) N. B. Jaufeerally, P. Ramasami, P. Jerabek, G. Frenking, *J. Mol. Model.* **2014**, *20*, 2433; c) E. R. T. Tiekink, *Dalton Trans.* **2012**, *41*, 6390–6395.

Manuscript received: October 31, 2022
Accepted manuscript online: January 12, 2023
Version of record online: February 6, 2023

6. Dialumene-Mediated Production of Tertiary Phosphines through P_4 Reduction

Title: Dialumene-Mediated Production of Tertiary Phosphines through P_4 Reduction

Status: Draft

Authors: Huihui Xu, Matthew M. D. Roy, Arseni Kostenko, Shiori Fujimori, Shigeyoshi Inoue

Content

The controlled formation of phosphorus-rich aryl dialumene featuring different geometries, and chemically reversible inter-conversion between them were achieved. The two-electron reduction product of P_4 feature a unique P_4^{2-} structure and extremely reactivity, acting as a source of P^{3-}. Treatments of different electrophiles including various halides to them under mild conditions obtained different phosphines which avoid the requirements of elevated temperature and high pressure are necessary in industry.

Author Contributions

Huihui Xu planned and executed all experiments (in parts together with Dr. Matthew M. D. Roy). Huihui Xu and Dr. Matthew M. D. Roy co-wrote the manuscript. Dr. Arseni Kostenko designed and performed the theoretical analyses. Dr. Shiori Fujimori conducted all SC-XRD measurements and processed the resulting data. All the work was performed under the supervision of Prof. Shigeyoshi Inoue.

COMMUNICATION WILEY-VCH

Dialumene-Mediated Production of Tertiary Phosphines through P_4 Reduction

Huihui Xu,[a] Matthew M. D. Roy,[a] Arseni Kostenko,[a] Shiori Fujimori,[a] and Shigeyoshi Inoue*[a]

[a] H. Xu, Dr. M. M. D. Roy, Dr. S. Fujimori, Dr. A. Kostenko, Prof. Dr. S. Inoue
Department of Chemistry
Catalysis Research Center, Technische Universität München
Lichtenbergstraße 4, 85748 Garching (Germany)
E-mail: s.inoue@tum.de

Supporting information for this article is given via a link at the end of the document.

Abstract: The functionalization of white phosphorus P_4 by main group complexes has been of paramount significance in phosphorus chemistry. Herein, we reported the controlled formation of phosphorus-rich aryl dialumene featuring different geometries, and chemically reversible inter-conversion between them. The two-electron reduction product of P_4 feature a unique P_4^{2-} structure and extremely reactivity, acting as a source of P^{3-}. Treatments of different electrophiles including various halides to them under mild conditions obtained different phosphines which avoid the requirements of elevated temperature and high pressure are necessary in industry.

The chemistry of multiple bonded p-block complexes has been the subject of intense research since the seminal isolation of West's disilene and Yoshifuji's diphosphene in 1981.[1] Both the reduced nature of the main group element in these complexes and the relatively low electronegativity of inorganic p-block elements render such species highly reactive. Harnessing this reactivity can sometimes lead to the observation of transition metal-like reactivity, such as the activation/functionalization of relatively inert substrates and catalysis.[2] This reactivity is particularly intriguing when observed for highly abundant, low-toxicity elements such as silicon and aluminum, as they present potential alternatives to generally more costly and toxic transition metal systems which are currently in place. As a result, both the search for new π-bonded main group complexes and reactivity investigations thereof present a fruitful avenue to new abundant element-mediated synthesis approaches.

The industrial production of useful monophosphorus (P1) products typically relies on the use of white phosphorus as a chemical feedstock, most commonly via oxidation by elemental chlorine to PCl_3 or PCl_5 and subsequent functionalization.[3] To mitigate the use of hazardous chlorine gas and improve the atom economy of such chemistry, the direct functionalization of P_4 to phosphorus-based products is highly desirable.[4] As such, the stoichiometric reactivity of both main group[5] and transition metal-based organometallic complexes[6] towards P_4 has been well-explored. While P–P bond cleavage and the formation of new element-phosphorus compounds is now well known for many elements of the periodic table, the subsequent release of P1 products is far more rare.[4]

The controlled activation of P_4 by main group compounds is most commonly observed for carbene-like complexes bearing lone electron pairs at the main group element. For example, both neutral and anionic aluminum(I) reagents have been shown to react with P_4, yielding various formal reduction products such as the P_4 insertion isomers **I**[7] and **III**[8] (Figure 1) and the P_4 fragmentation compounds **II**[9] and **IV**.[10] Meanwhile, unsaturated

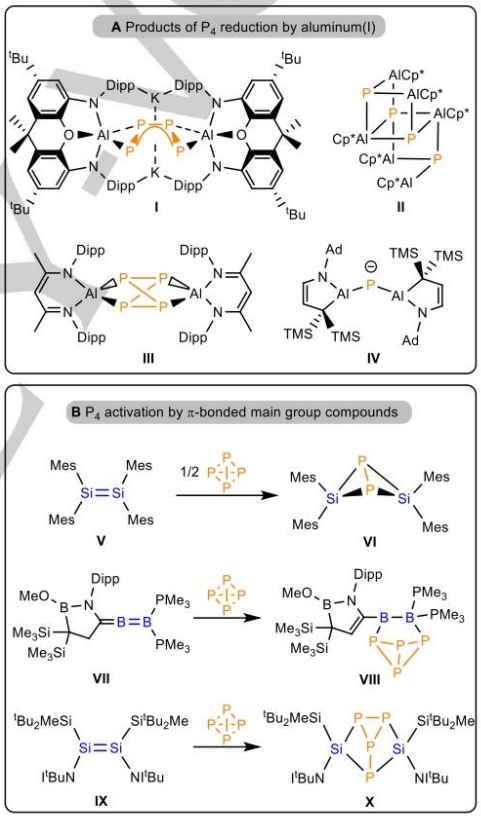

Figure 1. Selected products of P_4 activation as mediated by Al(I) reagents (A) and known examples of P_4 activation by π-bonded main group complexes (B).

main group complex reactivity towards white phosphorus is limited to three examples: that of two disilenes[11] and a diboraallene.[12] Since our 2018 report of a dialumene bearing an Al=Al double bond[13] we and others have been exploring the reactivity of this class of compound towards various substrates

such as alkenes, alkynes, CO_2, and H_2.[14] In this contribution, we disclose our efforts to extend this reactivity to white phosphorus. We demonstrate that both aryl- and silyl-substituted dialumenes selectively afford novel P_4 activation products which are amenable to further functionalization on exposure to electrophiles, affording silyl-, aryl-substituted tertiary phosphines as well as PH_3.

Silyl or Tipp stabilized dialumenes **1** and **2** were synthesized in good yields following the reported procedures.[13-14] Treatment of one equivalent of **1** with white phosphorus in toluene at room temperature after 2 hours obtained brown solids in a 65% (Scheme 1, path a). ^{1}H and ^{13}C{^{1}H} spectroscopy showed two NHC and two Tipp ligands are all asymmetric (Figure S1 and S5, in the supporting information). In addition, ^{31}P{^{1}H} NMR data showed signals of P_2 and P_3 appeared at -128.78 ppm and -138.74 ppm respectively, which represented somewhat NHC and Tipp feature *trans* manners.

All attempts to crystallize this product were failed but obtained another one species, the pale brown crystals. SC-XRD data confirms the solid structure (Figure 2), which showing that it crystallizes in the monoclinic space group C 2/c. It features butterfly geometry with adjacent I*i*Pr and Tipp ligands on Al centers in a *Cis* manner. It possesses the moiety of the insertion of P_4 tetrahedron into Al=Al bond. Thus we preliminarily named it as **3-Cis**. To best our knowledge, this is a new strategy of P_4 insertion to aluminum center. This was only reported recently by our group about the insertion of the P_4 tetrahedron into the Si=Si bond (Figure 1, **IX** and **X**).[11c] The P-P bond lengths (av. 2.2357 Å) vary in the range from 2.1934 Å to 2.2844 Å, which fall in the range of typical P-P single bond (*cf.* 2.1891(7)-2.2937(7) Å in **X**),[11c] and are slightly shorter than the observed in **III** (av. 2.29 Å).[8] But they are definitely longer than the measured in **I** (ca. 2.13 Å) with the presence of a delocalized π-bond within the P_4^{4-} unit.[7] The Al-P bond lengths (2.3515 or 2.3539 Å) of **3-Cis** are in the range of those in **II** (2.31–2.42 Å),[9] but shorter than those of **III** (av. 2.37 Å)[11c] and **I** (av. 2.54 Å).[7] But they are longer than that in **IV** (2.246(1) Å) bearing highly polarized Al(δ+) and P(δ−).[10] The average P-Al-P bond angle is 93.98°.

Subsequently, ^{1}H and ^{31}P{^{1}H} NMR spectroscopy of the pale brown crystals (**3-Cis**) were checked. The ^{31}P{^{1}H} NMR spectrum showed three signals at -55.06 ppm (d, P1), -138.25 ppm (d, P2 and P3) and -159.36 ppm (ddd, P4), which shifted downfield than the observed in **X** (106.6 ppm (dt), -44.0 ppm (dd), -217.6 ppm (dt))[11c] and **IV** (-295.4 ppm)[10]. They appeared at higher chemical shifts than that of **III** (78.6 ppm)[8] and **I** (374.2 ppm (br), 54.3 ppm (br)).[7] These data show P2 and P3 of **3-Cis** are chemically inequivalent to be functionalized by the Al center. The ^{1}H NMR spectrum exhibits sets of resonance signals for two chemically asymmetric Tipp ligands with 1.24 ppm (12 H) and 1.30 ppm (12 H) assigned to the isopropyl protons from NHC, as well as 1.54 ppm (6H), 1.33 ppm (6H) and 1.02-1.06 (12 H) assigned to the isopropyl protons from Tipp in *o*-positions. Similar to ^{13}C{^{1}H} NMR 21.76 ppm and 21.92 ppm assigned to carbon of CH_3 from the isopropyl groups of NHC. Signals of 35.99 ppm and 35.73 ppm were assigned to carbon of $CHMe_2$ from the isopropyl groups of Tipp in *o*-positions. In addition, the composition is confirmed by LIFDI-MS. **3-Cis** is highly thermostable without any change in C_6D_6 at 80 °C with 72 hours, based on the results of ^{1}H and ^{31}P{^{1}H} NMR spectra.

What is the brown product? Together with analysis of the geometry of start material with NHC and Tipp ligands in a *trans* manner and compared with ^{1}H and ^{31}P{^{1}H} NMR spectroscopy of **3-Cis**, nuclear NMR data showed NHC and Tipp ligands feature *trans* positions as an intermediate, resulting **3-Trans**. The ^{31}P{^{1}H} NMR data showed four signals at -52.69 ppm (d, P1), -128.78 ppm (dd, P2), -138.74 ppm (dd, P3), and -147.82 (td, P4), which shifted slightly downfield than the observed in **3-Cis**. P2 and P3 featuring quartet peaks at different shifts showed both located in the asymmetric chemical environment. In order to support the formation of **3-Trans** for which single crystals could not be obtained we calculated its ^{31}P{^{1}H} NMR chemical shifts and coupling constants and compared the results to the experimental ^{31}P{^{1}H} NMR spectrum. The simulated spectrum of the proposed **3-Trans** reproduces the experimentally observed pattern (Figure S45 in the supporting information). These all results showed **3-Trans** features *trans* geometry.

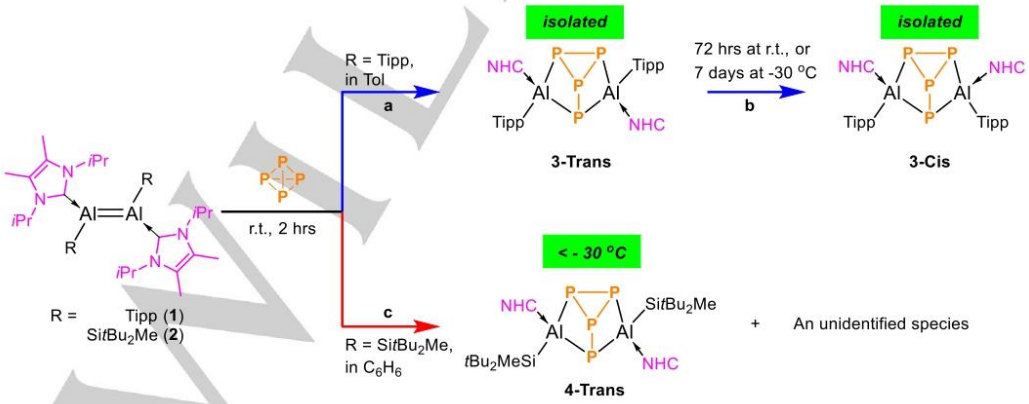

Scheme 1. Reactions of P_4 and dialumenes (**1** and **2**).

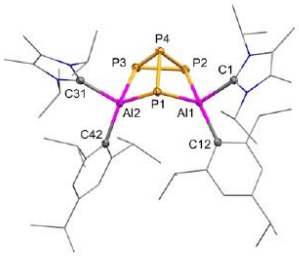

Figure 2. Molecular structures of **3-Cis** in the solid state. Ellipsoids are set at the 50% probability level; hydrogen atoms and co-crystallized solvent molecules are omitted for clarity and NHC, Tipp, and silyl ligands are depicted in wireframe for simplicity. Selected bond lengths (Å) and angles (°): **3-Cis**: Al1-C1 (NHC) 2.1288, Al2-C31 (NHC) 2.0781, Al1-C12 (Tipp) 2.0187, Al2-C42 (Tipp) 2.0116, Al1-P1 2.3515, Al2-P1 2.3539, Al1-P2 2.3998, Al2-P3 2.3842, P1-P4 2.2844, P2-P4 2.2462, P3-P4 2.2189, P2-P3 2.1934, Al1-P1-Al2 79.86, P1-Al2-P3 93.84, P1-Al1-P2 94.12, Al1-P1-P4 78.56, P1-P4-P3 100.43.

Accordingly, **3-Trans** can transform to **3-Cis** at -30 °C after 7 days or at r.t. after 72 hours (Scheme 1, path b), while heating accelerates the conversion rate (Figure 3). These data showed **3-Trans** is more thermally unstable, compared with **3-Cis**.

Quantum chemical calculations on the proposed mechanism of the reaction of compound **1** with P_4 to form the **3-Trans** and **3-Cis** is presented in Figure S42 in the Supporting Information. The formation of **3-Cis** is expected to be exergonic by 84.5 kcal mol^{-1}. We proposed that the formation of **3-Cis** takes place via the initial formation of **3-Trans** that was observed by NMR spectroscopy, which later isomerized to the energetically more favoured isomer **3-Cis**. Relaxed surface scans show that the NHC dissociation from **3-Trans** and **3-Cis**, which are barrier less, results in the essentially similar intermediates **3'** and **3''**. We proposed that the **3-Trans** to **3-Cis** isomerization proceeds via the NHC dissociation from **3-Trans** to form **3'**, which is only endergonic by 14.6 kcal mol^{-1}. **3'** isomerizes to **3''** at 13.9 kcal mol^{-1}, followed by re-association of the NHC at Al1. **3-Cis** is calculated to be by 4.3 kcal mol^{-1} energetically more favourable,

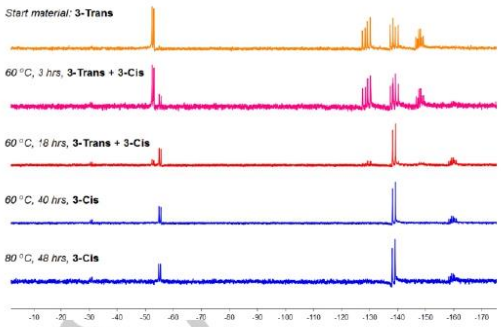

Figure 3. Stacked $^{31}P\{^1H\}$ NMR (162 MHz) spectra for **3-Trans** or **3-Cis** (in different conditions) in C_6D_6 at 300 K.

therefore although the low NHC dissociation energies are expected to allow **3-Trans** and **3-Cis** to exist in thermodynamic equilibrium in ambient conditions, only **3-Cis** can be observed when the equilibrium is reached.

Alongside with compound **2**, we attempted to study on the reactivity towards P_4. Treatment of one equivalent amount of white phosphorus with the freshly prepared **2** in benzene at room temperature after 2 hours obtained pale orange powders in a 40% yield (Scheme 1, path c). Signals of ^1H and $^{31}P\{^1H\}$ NMR featuring asymmetric shapes showed there was two products. (Figure S18-21 in the supporting information).

All attempts to crystallize **4** only obtained the crystal of **4-Trans**, named accordingly to **3-Trans**. SC-XRD data showed it features the aluminum center with NHC and Silyl group adjacently in a *Trans* manner (Figure 4). This result confirmed the structure of the product featuring *Trans* geometry. **4-Trans** features butterfly geometry, which is definitely similar to **3-Cis** (Figure 2). The distances between Al centers and NHC as well as P-P bond lengths were slightly longer than those of **3-Cis**.

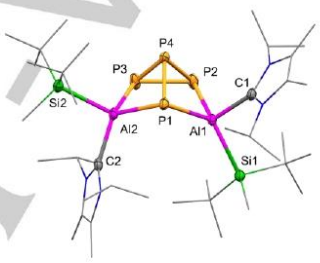

Figure 4. Molecular structures of **4-Trans** in the solid state. Ellipsoids are set at the 50% probability level; hydrogen atoms and co-crystallized solvent molecules are omitted for clarity and NHC, Tipp, and silyl ligands are depicted in wireframe for simplicity. Selected bond lengths (Å) and angles (°): **4-Trans**: Al1-C1 (NHC) 2.103(3), Al2-C2 (NHC) 2.066(3), Al1-Si1 2.520(1), Al2-Si2 2.500(1), Al1-P1 2.366(1), Al2-P1 2.342(1), Al1-P2 2.401(1), Al2-P3 2.391(1), P1-P4 2.291(1), P2-P4 2.226(1), P3-P4 2.232(1), P2-P3 2.198(1), Al1-P1-Al2 105.08(4), P1-Al2-P3 93.84(4), P1-Al1-P2 92.83(4), Al1-P1-P4 79.79(4), P1-P4-P3 99.70(4).

When we selected the crystals of **4-Trans** for NMR technologies at room temperature, the data showed there are mixtures, **4**. Therefore, we checked the variable-temperature NMR of **4-Trans** crystals in deuterated toluene from -70 °C to 50 °C (Figure 5). At -70 °C, -50 °C and 0 °C, low-temperature NMR showed there is only **4-Trans**. The spectrum is definitely similar to the observed pattern in **3-Trans** and also is consistent with the simulated spectrum by calculations (Figure S45 in the Supporting Information). The $^{31}P\{^1H\}$ NMR showed multiple peaks of P4 in around -118.5 ppm which significantly shifted to downfield compared with the signal of P4 in **3-Trans** (-147.82 ppm) and **3-Cis** (-159.36 ppm). As a result, we confirmed the one of mixture **4** is **4-Trans**.

While at r.t. or even at 50 °C, NMR data showed **4-Trans** would partially transform to another unidentified species resulting the spectrum of the mixture **4**. On the contrary, we checked the NMR from 50 °C to –70 °C (Figure S26-27 in the Supporting Information), the consistent trend was observed. In summary, we proposed that there is an equilibrium between **4-**

Trans and the unidentified species at room temperature, and the unidentified species could transform to **4-Trans** at low temperature (< 0 °C). Quantum chemical calculations show that the formation of **4-Trans** from the reaction of **2** and P_4 is exergonic by 73.8 kcal mol^{-1}. Actually the **4-Trans** isomer is more favoured by 4.1 kcal mol^{-1} than the proposed **4-Cis**.

When **4** was heated at 80 °C over 2 hours, unidentified decomposed compounds were observed by ^1H and $^{31}P\{^1H\}$ NMR spectra, while all compounds decomposed over 24 hours (Figure S22 in the Supporting Information).

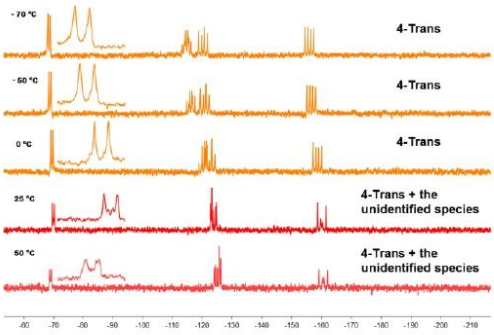

Figure 5. Stacked $^{31}P\{^1H\}$ NMR (162 MHz) spectra for the freshly-prepared **4-Trans** in Toluene-d_8 at variable temperatures.

The functionalization of **3** and **4** was studied with various electrophiles including Me_3SiCl, Me_3SiI, HCl (4M in dioxane) and CH_3COCl. (Table 1) The treatment of excess Me_3SiCl to **3-Trans** in C_6D_6 at 80 °C obtained Compound **5a** and $P(SiMe_3)_3$ after 2 hours, which is confirmed by *situ* ^1H and $^{31}P\{^1H\}$ NMR. While $P(TMS)_3$ could also be obtained at room temperature by the reaction of TMSI and **3-Trans** within 12 hours. PH_3 and $P(OCCH_3)_3$ were obtained by reactions of **3-Trans** and 4M HCl in dioxane and CH_3COCl, respectively, at room temperature. Similar reactions occurred to **3-Cis** resulting various tertiary phosphines.

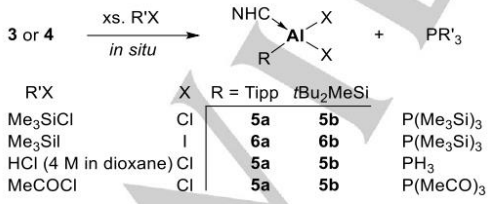

R'X	X	R = Tipp	tBu_2MeSi	
Me_3SiCl	Cl	**5a**	**5b**	$P(Me_3Si)_3$
Me_3SiI	I	**6a**	**6b**	$P(Me_3Si)_3$
HCl (4 M in dioxane)	Cl	**5a**	**5b**	PH_3
MeCOCl	Cl	**5a**	**5b**	$P(MeCO)_3$

Scheme 2. Formation of tertiary phosphines.

The excess of the electrophile was added by drop to the solution of freshly prepared **4** in C_6D_6. The results tracked by *situ* ^1H and $^{31}P\{^1H\}$ NMR, showed **4** reacted with Me_3SiCl at r.t. resulting $PTMS_3$ and **5b** after 12 hours. The similar results showed **4** reacted with Me_3SiI or HCl (4M in dioxane) at r.t. resulting $PTMS_3$ or PH_3, respectively. **4** reacted with CH_3COCl at r.t. after 0.25 hours, resulting $P(OCCH_3)_3$.

Table 1. Reactions of different electrophiles with **4** and **3**.

Electrophile	Entry	*t* [h]	T [°C]	Yield vs. P [%][a]	Product
Me_3SiCl	**4**	9	r.t.	3.5	$P(SiMe_3)_3$
	3-Trans	2	50	2	
	3-Cis	2	65	5	
Me_3SiI	**4**	4	r.t.	6.0	$P(SiMe_3)_3$
	3-Trans	12	r.t.	1	
	3-Cis	12	50	2	
4M HCl in dioxane	**4**	1	r.t.	quantitative[b]	PH_3
	3-Trans	0.25	r.t.	8	
	3-Cis	0.25	r.t.	12	
CH_3COCl	**4**	0.25	r.t.	quantitative	$P(OCCH_3)_3$
	3-Trans	0.25	r.t.	quantitative	
	3-Cis	0.25	r.t.	quantitative	

[a] One equivalent amount of PPh_3 as a reference. [b] Complete conversion

As a conclusion, we isolated silyl and aryl dialumene. Their reactivity towards white phosphorus showed a P_4 reduction to P_4^{2-} of Al centers. During this procedure, we managed to isolate the P-rich aryl dialumene with different geometries. It is the first example to elucidate the mechanism of the reaction of P_4 with π-bond together with DFT calculations. In addition, the further reactivity towards electrophiles were studied while **3** or **4** acted as the P^{3-} source. Finally, various phosphines were obtained under mild conditions.

Acknowledgements

We are grateful to the European Research Council (ALLOWE 101001591) for financial support. H.X. gratefully acknowledges financial support from the China Scholarship Council (CSC). We thank Dr. Franziska Hanusch for the SC-XRD measurements, Dr. John Kelly for SC-XRD refine and Florian Tschernuth for VT-NMR, Ivan Antsiburov for LIFDI-Mass, Dr. Catherine Weetman for comments, Dr. Debotra Sarkar for ideas on this project.

Keywords: Dialumene • P_4 • phosphines • aluminum dihalide

[1] a) M. Yoshifuji, I. Shima, N. Inamoto, K. Hirotsu, T. Higuchi, *J. Am. Chem. Soc.* **1981**, *103*, 4587-4589; b) R. WEST, M. J. FINK, J. MICHL, *Science* **1981**, *214*, 1343-1344.

[2] a) P. P. Power, *Nature* **2010**, *463*, 171-177; b) S. Yadav, S. Saha, S. S. Sen, *ChemCatChem* **2016**, *8*, 486-501; c) C. Weetman, S. Inoue, *ChemCatChem* **2018**, *10*, 4213-4228; d) P. Bag, C. Weetman, S. Inoue, *Angewandte Chemie International Edition* **2018**, *57*, 14394-14413; e) R. L. Melen, *Science* **2019**, *363*, 479-484; f) J. Hicks, P. Vasko, J. M. Goicoechea, S. Aldridge, *Angewandte Chemie International Edition* **2021**, *60*, 1702-1713; g)

C. Weetman, *Chemistry – A European Journal* **2021**, *27*, 1941-1954; h) F. Dankert, C. Hering-Junghans, *Chem. Commun.* **2022**, *58*, 1242-1262.
[3] G. Bettermann, W. Krause, G. Riess, T. Hofmann, in *Ullmann's Encyclopedia of Industrial Chemistry, Vol. 27*, Wiley-VCH, Weinheim, **2000**, pp. 6-13.
[4] D. J. Scott, *Angew. Chem. Int. Ed.* **2022**, *61*, e202205019.
[5] a) M. Scheer, G. Balázs, A. Seitz, *Chem. Rev.* **2010**, *110*, 4236-4256; b) N. A. Giffin, J. D. Masuda, *Coord. Chem. Rev.* **2011**, *255*, 1342-1359; c) S. Khan, S. S. Sen, H. W. Roesky, *Chem. Commun.* **2012**, *48*, 2169-2179.
[6] a) B. M. Cossairt, N. A. Piro, C. C. Cummins, *Chem. Rev.* **2010**, *110*, 4164-4177; b) M. Caporali, L. Gonsalvi, A. Rossin, M. Peruzzini, *Chemical Reviews* **2010**, *110*, 4178-4235; c) J. E. Borger, A. W. Ehlers, J. C. Slootweg, K. Lammertsma, *Chem. Eur. J.* **2017**, *23*, 11738-11746.
[7] M. M. D. Roy, A. Heilmann, M. A. Ellwanger, S. Aldridge, *Angewandte Chemie International Edition* **2021**, *60*, 26550-26554.
[8] Y. Peng, H. Fan, H. Zhu, H. W. Roesky, J. Magull, C. E. Hughes, *Angewandte Chemie International Edition* **2004**, *43*, 3443-3445.
[9] C. Dohmeier, H. Schnöckel, C. Robl, U. Schneider, R. Ahlrichs, *Angewandte Chemie International Edition in English* **1994**, *33*, 199-200.
[10] K. Koshino, R. Kinjo, *Organometallics* **2020**, *39*, 4183-4186.
[11] a) M. Driess, A. D. Fanta, D. R. Powell, R. West, *Angewandte Chemie International Edition in English* **1989**, *28*, 1038-1040; b) A. D. Fanta, R. P. Tan, N. M. Comerlato, M. Driess, D. R. Powell, R. West, *Inorganica Chimica Acta* **1992**, *198-200*, 733-739; c) R. Holzner, A. Porzelt, U. S. Karaca, F. Kiefer, P. Frisch, D. Wendel, M. C. Holthausen, S. Inoue, *Dalton Transactions* **2021**, *50*, 8785-8793.
[12] W. Lu, K. Xu, Y. Li, H. Hirao, R. Kinjo, *Angewandte Chemie International Edition* **2018**, *57*, 15691-15695.
[13] P. Bag, A. Porzelt, P. J. Altmann, S. Inoue, *J Am Chem Soc* **2017**, *139*, 14384-14387.
[14] a) C. Weetman, A. Porzelt, P. Bag, F. Hanusch, S. Inoue, *Chemical Science* **2020**, *11*, 4817-4827; b) C. Weetman, P. Bag, T. Szilvási, C. Jandl, S. Inoue, *Angewandte Chemie International Edition* **2019**, *58*, 10961-10965; c) R. L. Falconer, K. M. Byrne, G. S. Nichol, T. Krämer, M. J. Cowley, *Angewandte Chemie International Edition* **2021**, *60*, 24702-24708.

Entry for the Table of Contents

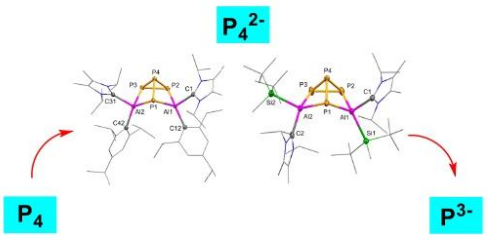

The controlled formation of phosphorus-rich aryl dialumene featuring different geometries, and chemically reversible inter-conversion between them were achieved. The two-electron reduction product of P_4 feature a unique P_4^{2-} structure and extremely reactivity, acting as a source of P^{3-}. Treatments of different electrophiles including various halides to them under mild conditions obtained different phosphines which avoid the requirements of elevated temperature and high pressure are necessary in industry.

Institute and/or researcher Twitter usernames: @InoueGroupTUM

7. Summary and Outlook

7.1 Aluminum sulfides

With the aim to prepare aluminum sulfides bearing an Al=S double bond, aluminum hydride (Tipp(I*i*Pr$_2$Me$_2$)AlH$_2$, **L9**) was chosen as a suitable precursor, as it was used in the preparation of the corresponding dialumene.[25] However, the treatment of the thiation reagent, S_8, with **L9** was unsuccessful in forming the desired Al=S bond, only resulting in the immediate decomposition to several unidentified species. Therefore, we attempted to use the bulkier aryl ligand, ^{Tipp}Ter (2,6-(2,4,6-*i*Pr$_3$C$_6$H$_2$)$_2$C$_6$H$_3$) instead of Tipp to prepare new aluminum dihydride (^{Tipp}Ter(IMe$_4$)AlH$_2$ **1**) for possible reaction with S_8. We also chose Lawesson reagent (2,4-bis-(4-methoxyphenyl)-1,3-dithia-2,4-diphosphetane 2,4-disulfide) and bis(trimethylsilyl) sulfide (S(TMS)$_2$) as additional thiation agents. The first project focused on the isolation, characterization, and bonding nature study of novel aluminum sulfides, especially targeting Al=S double bonds, as well as the study on differences of aryl ligands on reactivity of obtained species.

According to experimental data, ^{Tipp}Ter(IMe$_4$)AlH$_2$ **1** appears to be more stable than Tipp(I*i*Pr$_2$Me$_2$)AlH$_2$ **L9** because bulkier terphenyl ligand offers better kinetic protection to the Al center. When decomposition occurred in the case of **L9**, the treatment of S_8 with **1** under mild conditions resulted in the stepwise products including the first monomeric aluminum hydride hydrogensulfide **2**, an aluminum dihydrogensulfide **3**, and a cyclic six-membered aluminum polysulfide **4** (Figure 29). With targeting Al=S bond in mind, dehydrogenation or desulfurization of all available compounds was of high interest. As a result, the cyclic five-membered aluminum polysulfide **5** was obtained by reduction of **4** in presence of PPh$_3$ and the compound **6**, dehydrogenation product of SH in the compound **2** by the cyclic(alkyl)(amino) carbene (cAAC^{Me}), was isolated. Full characterization by multinuclear NMR spectroscopy and elemental analysis (EA), single-crystal X-ray diffraction (SC-XRD) studies gave experimental insights on the bonding nature of Al–S.

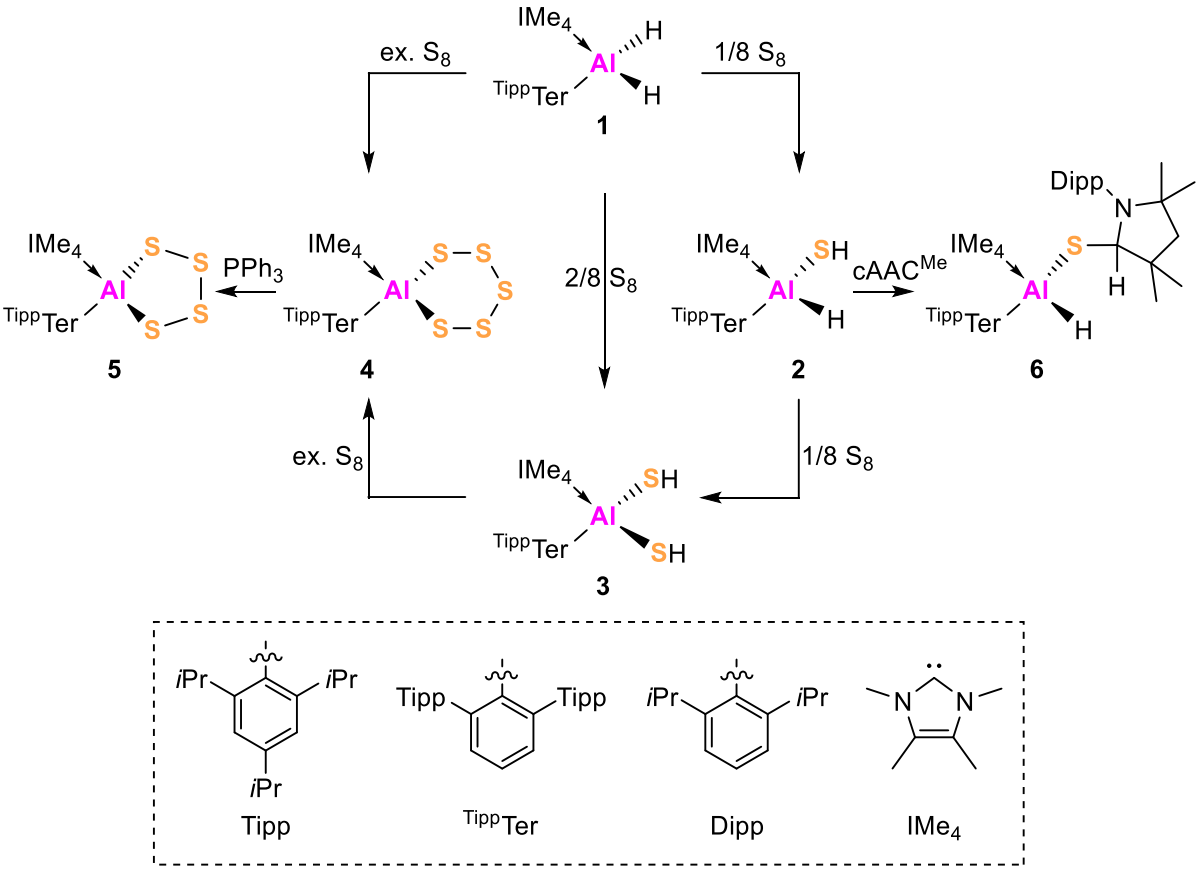

Figure 29. Various aluminum sulfides obtained from Al–S project.

The reaction of Lawesson reagent with Tipp(I*i*Pr$_2$Me$_2$)AlH$_2$ **L9** formed an intractable mixture of products (Figure 30). In the case of ^{Tipp}Ter(IMe$_4$)AlH$_2$ **1**, compound **7** was isolated as the first example of a five-membered Al–S–P–P–S ring containing complex. The reaction of S(TMS)$_2$, a milder thiation reagent, with **L9** resulted in the dehydrogenation product by S(TMS) group (the compound **8**), whereas no reaction occurred in the case of **1**.

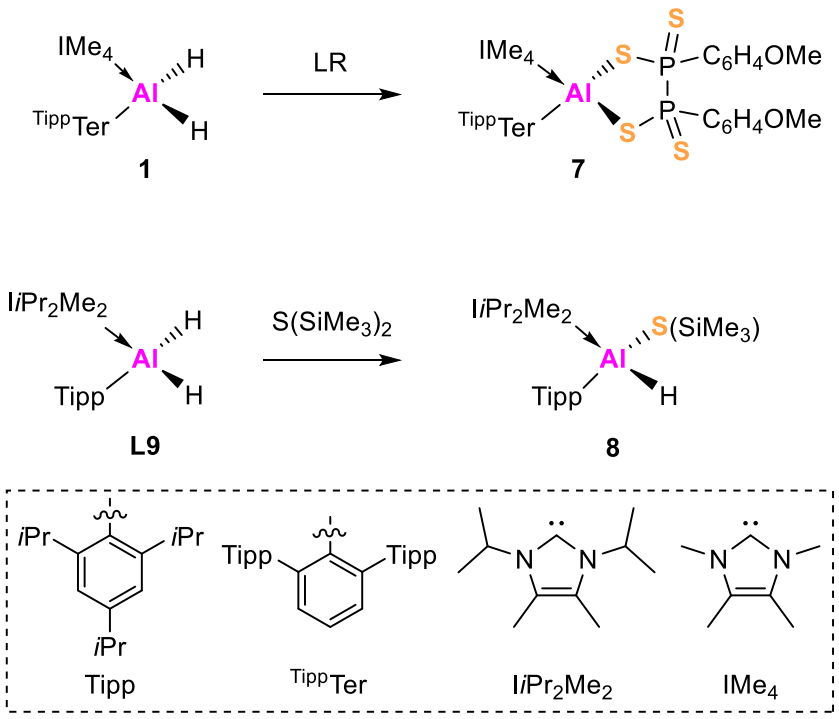

Figure 30. The reactions of compound **1** and **L9** with LR and $S(TMS)_2$.

This is the first report on the controlled stepwise preparation of various aluminum sulfides through dehydrogenation and subsequent sulfurization reactions. Although not obtaining the Al=S double bond moiety, these novel aluminum sulfides feature various bonding nature and deserve attention, especially, on the further reactivity and the application in the synthesis of new heterometallic Al–S–TM clusters as well as biological or catalytic systems in future.

7.2 Aluminum selenides and aluminum tellurides

In light of the previous work on Al–S, we attempted to synthesize heavier analogues with Al=Se or Al=Te double bonds by reactions of Tipp(I*i*Pr$_2$Me$_2$)AlH$_2$ **L9** with elemental Se and Te, respectively (Figure 31).

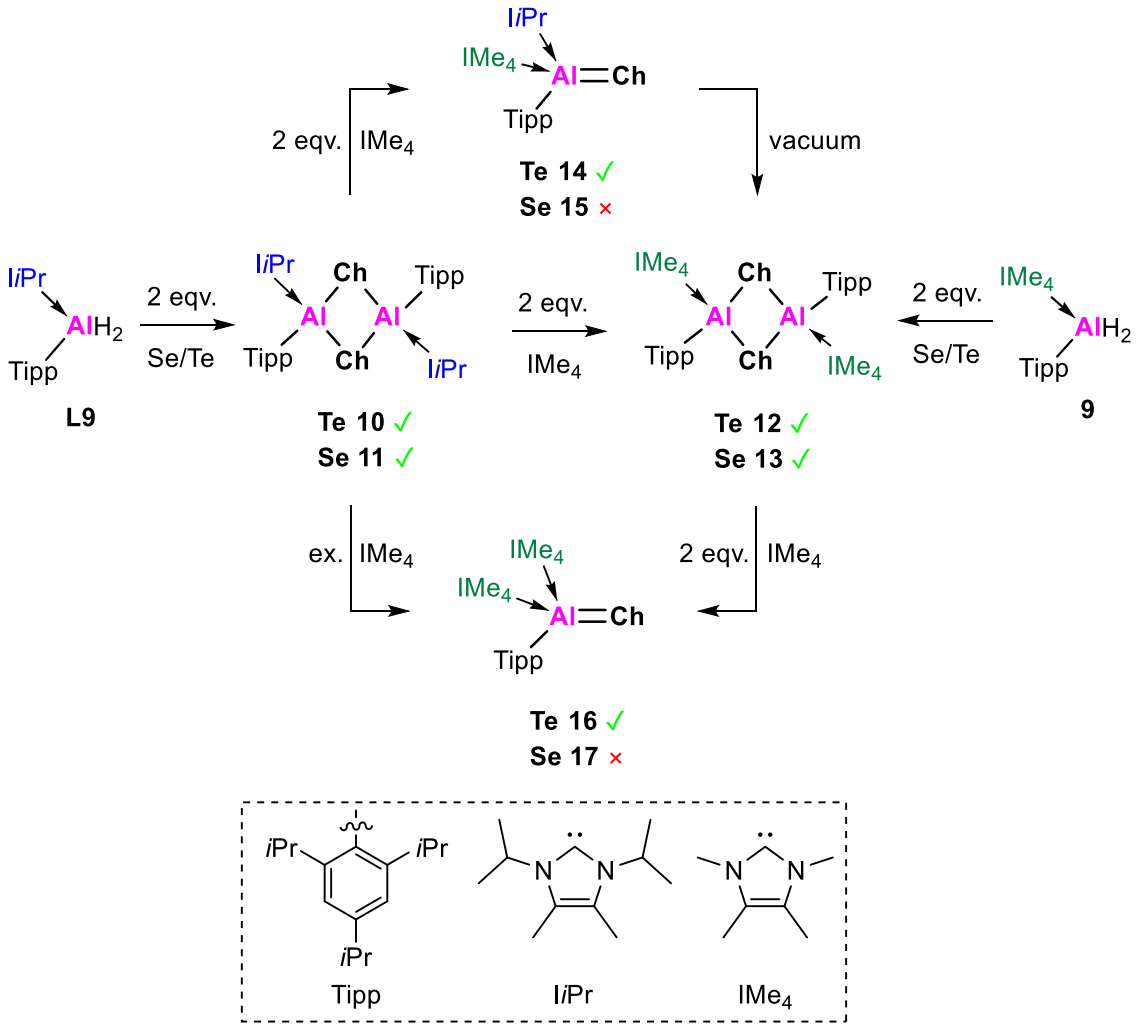

Figure 31. Various aluminum chalcogenides (Al–Se/Te) obtained from Al–Se/Te project.

In the case of Te, we obtained not only dimers [Tipp(I*i*Pr$_2$Me$_2$)Al-μ-Te]$_2$ **10**, [Tipp(IMe$_4$)Al-μ-Te]$_2$ **12**, but also monomers [Tipp(I*i*Pr$_2$Me$_2$)(IMe$_4$)]Al=Te **14**, Tipp(IMe$_4$)$_2$Al=Te **16**. Whereas, in the case of Se, only dimeric species were obtained ([Tipp(I*i*Pr$_2$Me$_2$)Al-μ-Se]$_2$ **11**, [Tipp(IMe$_4$)Al-μ-Se]$_2$ **13**). The monomeric aluminum telluride (I*i*Pr$_2$Me$_2$)(IMe$_4$)Al(Tipp)=Te **14** was observed by multinuclear NMR and Mass spectroscopy. It quantitatively converts to **12** through I*i*Pr$_2$Me$_2$ release and subsequent dimerization by vacuum at room temperature. Calculations predict this step to be exergonic only in the case of Te. This tendency could be

explained by the higher proclivity for dimerization of Al–Se vs. Al–Te, and the higher dissociation energies of [IMe_4Al(Tipp)-μ-Se]$_2$ **13** (36.4 kcal mol^{-1}) vs. [IMe_4Al(Tipp)-μ-Te]$_2$ **12** (26.1 kcal mol^{-1}) to the corresponding monomers. It also can be explained by more difference of the electronegativity of between Al–Se (0.94) vs. Al–Te (0.49), which against the formation of multiply bonded Al–Se.

Reactions of [(I*i*Pr$_2$Me$_2$)Al(Tipp)-μ-Ch]$_2$, Ch = Se (**11**) or Te (**10**) with two equivalents of IMe_4 resulted in the NHC exchange reaction forming the respective complexes ([IMe_4Al(Tipp)-μ-Ch]$_2$, Ch = Se (**13**) or Te (**12**). The facile exchange of I*i*Pr$_2$Me$_2$ by IMe_4 ligands indicates a higher affinity of IMe_4 toward the aluminum centers. It can be attributed to the steric effect thereof the repulsion is lower in the case of IMe_4 which was confirmed by natural steric analysis and the calculated Gibbs energies of dissociation of dimers to the corresponding monomers. This was also reflected on the formation of Tipp(IMe_4)$_2$Al=Te **16** by cleavage of the dimers to form monomer in the presence of IMe_4.

Alongside the neutral Al=Te double bonds in Tipp(IMe_4)$_2$Al=Te **16** and [NHI(IMe_2Et_2)$_2$]Al=Te **L57** in our group, we focused on comparative study on the thermal stability and reactivity towards numerous reagents. We found **16** could be isolated under mild conditions and from different ways (e.g., using new aluminum dihydride Tipp(IMe_4)AlH_2 **9** as a precursor), feature better thermal stability than **L57** which enabled the reactivity studies towards small molecules.

Acting in concert with the first project targeting the Al=S bond formation, we attempted to achieve it by reaction of S_8 with Tipp(IMe_4)$_2$Al=Te **16** expecting that Te is replaced by S, unfortunately, this resulted in immediate decomposition. This data showed Tipp and NHC is not sufficient for stabilizing multiply bonded Al–S bond.

The further reactivity towards CO_2 of **16** was performed and discussed (Figure 32). **16** reacts with three equivalents of CO_2 across two Al–C^{NHC} and the Al=Te bond affording the pentacoordinate aluminum complex (IMe_4CO_2)$_2$Al(Tipp)-μ-O_2C=Te **18**. It features a dianionic tellurocarbonate moiety [CO_2Te]$^{2-}$, which is an unprecedented tellurido analogue of the carbonate anion [CO_3]$^{2-}$. The C–Te bond features a polarized multiple bond character supported by WBI (1.19), MBO (1.39), and NBO (Te (34.8%)–C(65.2%)) analysis as well as the second order perturbation analysis (a significant donor-acceptor interactions (DAI) between the Te lone pair and the p-orbital of the carbon of 223.4 kcal mol^{-1}, which is of higher magnitude than the DAIs between the lone pair of the oxygens and the empty p orbital of the carbon (191.6 and 153.1 kcal mol^{-1}).

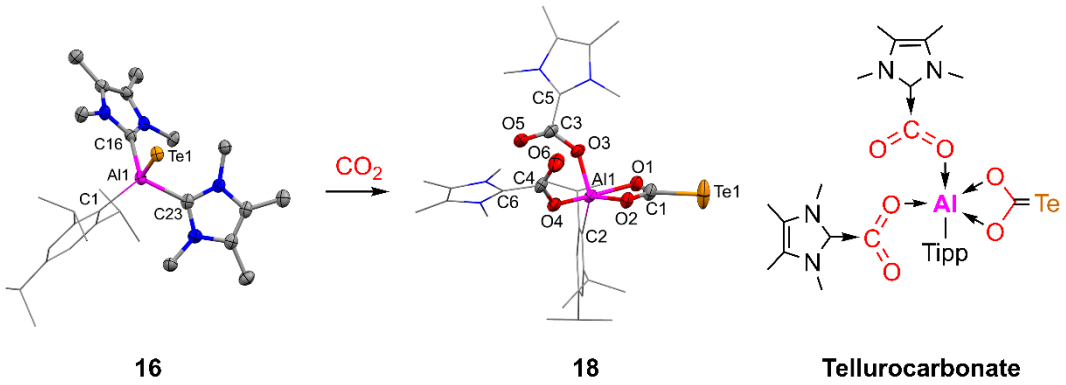

Figure 32. Formation of the first tellurido analogue of carbonate, compound **18**.

In conclusion, Tipp and IMe_4 can stabilize a monomeric compound bearing a terminal Al=Te double bond (Tipp(IMe_4)$_2$Al=Te **16**), whilst only dimers were formed in the case of Se. **16** features good thermal stability that enables further study on its reactivity towards CO_2 resulting in the interesting carbonate analogue (IMe_4CO_2)$_2$Al(Tipp)-μ-O_2C=Te **18**.

7.3 P_4 activation of dialumenes

With two dialumenes [Si*t*Bu$_2$Me(I*i*Pr$_2$Me$_2$)Al]$_2$ **L70**, [Tipp(I*i*Pr$_2$Me$_2$)Al]$_2$ **L71** readily available within our laboratory, and ones that have shown varying reactivity based on differences in supporting ligands (Figure 28), we focused on P_4 activation. By comparison, we isolated different compounds with *trans* or *cis* geometries (Figure 33).

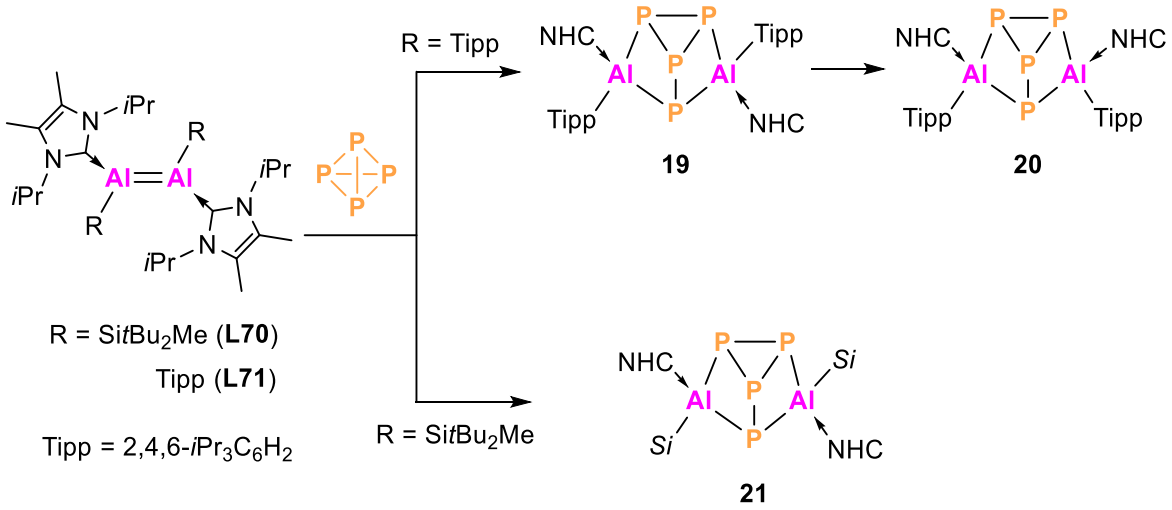

Figure 33. Aluminum phosphides with different geometries obtained from P_4 activation by **L70** and **L71**.

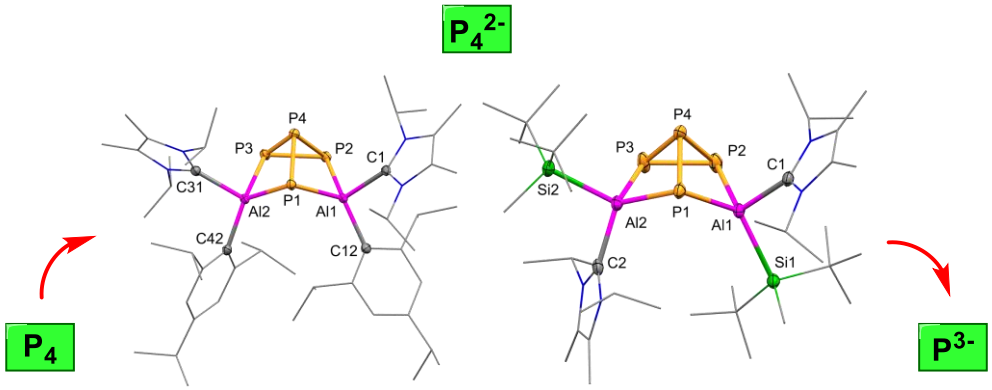

Figure 34. Formation of tertiary phosphines from P_4.

In industry, the preparation of phosphine requires elevated temperature or high pressure. Here P_4 products of dialumenes could act as P transfer reagents to synthesize various phosphines under mild conditions from P_4^{2-} to P^{3-} (Figure 34).

As a conclusion, this thesis showed a systematic and detailed research on synthesis, characterization, and reactivity of multiply bonded aluminum compounds through experiments and calculations. New cyclic aluminum sulfides, dimeric aluminum selenides, a monomer with a discrete Al=Te double bond as well as P_4 products of dialumenes will discover more bonding nature and offer new possibility on aluminum chemistry.

8. Bibliography

[1] Lutgens Frederick K, Tarbuck Edward J., *Essentials of Geology*, 7th ed., Prentice Hall, **2000**.

[2] H. Kvande, *JOM* **2008**, *60*, 23-24.

[3] F. Habashi, *Bull. Hist. Chem.* **1995**, *17/18*, 15-19.

[4] L. Torró, J. A. Proenza, T. Aiglsperger, T. Bover-Arnal, C. Villanova-de-Benavent, D. Rodríguez-García, A. Ramírez, J. Rodríguez, L. A. Mosquea, R. Salas, *Ore Geology Reviews* **2017**, *89*, 114-131.

[5] A. S. Verma, N. M. Suri, S. Kant, *Waste Management & Research* **2017**, *35*, 999-1012.

[6] J. R. Davis, *Aluminum and aluminum alloys*, ASM international, **1993**.

[7] K. A. Evans, in *The Chemistry of Aluminium, Indium and Gallium* (Ed.: A. J. Downs), Blackie Academic & Professional, Glasgow, **1993**, p. 248.

[8] C. Weetman, H. Xu, S. Inoue, in *Encyclopedia of Inorganic and Bioinorganic Chemistry* (Ed.: R. A. Scott), **2020**, pp. 1-20.

[9] A. Paparo, C. D. Smith, C. Jones, *Angew. Chem. Int. Ed.* **2019**, *58*, 11459-11463.

[10] S. Grams, J. Maurer, N. Patel, J. Langer, S. Harder, *Z. Anorg. Allg. Chem.* **2022**, *648*, e202200035.

[11] D. Neculai, H. W. Roesky, A. M. Neculai, J. Magull, B. Walfort, D. Stalke, *Angew. Chem. Int. Ed.* **2002**, *41*, 4294-4296.

[12] J. Hicks, A. Heilmann, P. Vasko, J. M. Goicoechea, S. Aldridge, *Angew. Chem. Int. Ed.* **2019**, *58*, 17265-17268.

[13] M. D. Anker, M. P. Coles, *Angew. Chem. Int. Ed.* **2019**, *58*, 18261-18265.

[14] C. Weetman, *Chem. Eur. J.* **2021**, *27*, 1941-1954.

[15] P. Bag, C. Weetman, S. Inoue, *Angew. Chem. Int. Ed.* **2018**, *57*, 14394-14413.

[16] M. J. Evans, M. D. Anker, C. L. McMullin, N. A. Rajabi, M. P. Coles, *Chem. Commun.* **2021**, *57*, 2673-2676.

[17] D. Franz, T. Szilvasi, E. Irran, S. Inoue, *Nat Commun* **2015**, *6*, 10037.

[18] C. Cui, H. W. Roesky, M. Noltemeyer, H.-G. Schmidt, *Organometallics* **1999**, *18*, 5120-5123.

[19] A. H. Cowley, R. A. Jones, P. R. Harris, D. A. Atwood, L. Contreras, C. J. Burek, *Angew. Chem. Int. Ed. Engl.* **1991**, *30*, 1143-1145.

[20] N. Kambe, K. Kondo, N. Sonoda, *Angew. Chem. Int. Ed. Engl.* **1980**, *19*, 1009-1010.

[21] Y. Ding, X. Ma, Y. Liu, W. Liu, C. Ni, B. Yan, L. Yan, Z. Yang, *Inorg. Chim. Acta* **2019**, *497*, 119091.

[22] H. Senoh, T. Takeuchi, H. Kageyama, H. Sakaebe, M. Yao, K. Nakanishi, T. Ohta, T. Sakai, K. Yasuda, *J. Power Sources* **2010**, *195*, 8327-8330.

[23] P. Bag, A. Porzelt, P. J. Altmann, S. Inoue, *J. Am. Chem. Soc.* **2017**, *139*, 14384-14387.

[24] D. Dhara, A. Jayaraman, M. Härterich, R. D. Dewhurst, H. Braunschweig, *Chem. Sci.* **2022**, *13*, 5631-5638.

[25] C. Weetman, A. Porzelt, P. Bag, F. Hanusch, S. Inoue, *Chem. Sci.* **2020**, *11*, 4817-4827.

[26] J. D. Queen, P. P. Power, *Chem. Commun.* **2023**, *59*, 43-46.

[27] R. Shannon, *Acta Crystallographica Section A* **1976**, *32*, 751-767.

[28] J. Boor, in *Ziegler–Natta Catalysts Polymerizations* (Ed.: J. Boor), Academic Press, **1979**, pp. 19-31.

[29] G. A. Olah, *Friedel-Crafts and Related Reactions: Acylation and related reactions. 2 v, Vol. 3*, Interscience Publishers, **1963**.

[30] W. Klemm, E. Voss, K. Geiersberger, *Z. Anorg. Chem.* **1948**, *256*, 15-24.

[31] M. Mocker, C. Robl, H. Schnöckel, *Angew. Chem. Int. Ed. Engl.* **1994**, *33*, 1754-1755.

[32] A. Ecker, H. Schnöckel, *Z. Anorg. Allg. Chem.* **1996**, *622*, 149-152.

[33] H.-J. Himmel, J. Bahlo, M. Haussmann, F. Kurth, G. Stösser, H. Schnöckel, *Inorg. Chem.* **2002**, *41*, 4952-4960.

[34] M. Tacke, H. Schnoeckel, *Inorg. Chem.* **1989**, *28*, 2895-2896.

[35] C. R. Carsten Dohmeier, Matthias Tacke, Hansgeorg Schnockel, *Angew. Chem. Int. Ed. Engl.* **1991**, *30*, 564-565.

[36] P. P. Power, *Nature* **2010**, *463*, 171-177.

[37] C. Weetman, S. Inoue, *ChemCatChem* **2018**, *10*, 4213-4228.

[38] W. Kutzelnigg, *Angew. Chem. Int. Ed. Engl.* **1984**, *23*, 272-295.

[39] D. Mandal, T. I. Demirer, T. Sergeieva, B. Morgenstern, H. T. A. Wiedemann, C. W. M. Kay, D. M. Andrada, *Angew. Chem. Int. Ed.* **2023**, *62*, e202217184.

[40] B. Li, B. L. Geoghegan, H. M. Weinert, C. Wölper, G. E. Cutsail, S. Schulz, *Chem. Commun.* **2022**, *58*, 4372-4375.

[41] M. M. Siddiqui, S. Banerjee, S. Bose, S. K. Sarkar, S. K. Gupta, J. Kretsch, N. Graw, R. Herbst-Irmer, D. Stalke, S. Dutta, D. Koley, H. W. Roesky, *Inorg. Chem.* **2020**, *59*, 11253-11258.

[42] B. Li, S. Kundu, A. C. Stückl, H. Zhu, H. Keil, R. Herbst-Irmer, D. Stalke, B. Schwederski, W. Kaim, D. M. Andrada, G. Frenking, H. W. Roesky, *Angew. Chem. Int. Ed.* **2017**, *56*, 397-400.

[43] S. Kundu, S. Sinhababu, S. Dutta, T. Mondal, D. Koley, B. Dittrich, B. Schwederski, W. Kaim, A. C. Stückl, H. W. Roesky, *Chem. Commun.* **2017**, *53*, 10516-10519.

[44] K. Koshino, R. Kinjo, *J. Am. Chem. Soc.* **2020**, *142*, 9057-9062.

[45] I. L. Fedushkin, M. V. Moskalev, A. N. Lukoyanov, A. N. Tishkina, E. V. Baranov, G. A. Abakumov, *Chem. Eur. J.* **2012**, *18*, 11264-11276.

[46] P. Henke, T. Pankewitz, W. Klopper, F. Breher, H. Schnöckel, *Angew. Chem. Int. Ed.* **2009**, *48*, 8141-8145.

[47] V. A. Dodonov, W. Chen, L. Liu, V. G. Sokolov, E. V. Baranov, A. A. Skatova, Y. Zhao, B. Wu, X.-J. Yang, I. L. Fedushkin, *Inorg. Chem.* **2021**, *60*, 14602-14612.

[48] W. Uhl, *Z. Naturforsch. B* **1988**, *43*, 1113-1118.

[49] Y. Zhao, Y. Liu, L. Yang, J.-G. Yu, S. Li, B. Wu, X.-J. Yang, *Chem. Eur. J.* **2012**, *18*, 6022-6030.

[50] W. Uhl, A. Vester, *Chem. Ber.* **1993**, *126*, 941-945.

[51] H. Hoberg, S. Krause, *Angew. Chem. Int. Ed. Engl.* **1976**, *15*, 694-694.

[52] H. Hoberg, S. Krause, *Angew. Chem. Int. Ed. Engl.* **1978**, *17*, 949-950.

[53] K.-C. Kim, C. A. Reed, G. S. Long, A. Sen, *J. Am. Chem. Soc.* **2002**, *124*, 7662-7663.

[54] J. D. Young, M. A. Khan, R. J. Wehmschulte, *Organometallics* **2004**, *23*, 1965-1967.

[55] M. Nakamoto, K. Shimizu, A. Sekiguchi, *Chem. Lett.* **2007**, *36*, 984-985.

[56] W. Gu, M. R. Haneline, C. Douvris, O. V. Ozerov, *J. Am. Chem. Soc.* **2009**, *131*, 11203-11212.

[57] M. Khandelwal, R. J. Wehmschulte, *Angew. Chem. Int. Ed.* **2012**, *51*, 7323-7326.

[58] M. Saleh, D. R. Powell, R. J. Wehmschulte, *Organometallics* **2017**, *36*, 4810-4815.

[59] R. C. Fischer, P. P. Power, *Chem. Rev.* **2010**, *110*, 3877-3923.

[60] Y. Wang, G. H. Robinson, *Chem. Commun.* **2009**, 5201-5213.

[61] P. P. Power, *Chem. Rev.* **1999**, *99*, 3463-3504.

[62] P. P. Power, *J. Chem. Soc., Dalton Trans.* **1998**, 2939-2951.

[63] M. Lein, A. Krapp, G. Frenking, *J. Am. Chem. Soc.* **2005**, *127*, 6290-6299.

[64] P. P. Power, *Organometallics* **2007**, *26*, 4362-4372.

[65] P. P. Power, *Organometallics* **2020**, *39*, 4127-4138.

[66] R. L. Falconer, K. M. Byrne, G. S. Nichol, T. Krämer, M. J. Cowley, *Angew. Chem. Int. Ed.* **2021**, *60*, 24702-24708.

[67] C. Fliedel, G. Schnee, T. Avilés, S. Dagorne, *Coord. Chem. Rev.* **2014**, *275*, 63-86.

[68] M. M. D. Roy, A. A. Omaña, A. S. S. Wilson, M. S. Hill, S. Aldridge, E. Rivard, *Chem. Rev.* **2021**, *121*, 12784-12965.

[69] D. Franz, E. Irran, S. Inoue, *Dalton Trans.* **2014**, *43*, 4451-4461.

[70] S. Ito, K. Tanaka, Y. Chujo, *Inorganics* **2019**, *7*, 100.

[71] S. Chen, B. Li, X. Wang, Y. Huang, J. Li, H. Zhu, L. Zhao, G. Frenking, H. W. Roesky, *Chem. Eur. J.* **2017**, *23*, 13633-13637.

[72] B. Luo, B. E. Kucera, W. L. Gladfelter, *Dalton Trans.* **2006**, 4491-4498.

[73] J. L. Atwood, K. D. Robinson, C. Jones, C. L. Raston, *J. Chem. Soc., Chem. Commun.* **1991**, 1697-1699.

[74] A. E. Nako, S. J. Gates, A. J. P. White, M. R. Crimmin, *Dalton Trans.* **2013**, *42*, 15199-15206.

[75] Y. Chen, W. Jiang, B. Li, G. Fu, S. Chen, H. Zhu, *Dalton Trans.* **2019**, *48*, 9152-9160.

[76] D. R. Willcox, D. M. De Rosa, J. Howley, A. Levy, A. Steven, G. S. Nichol, C. A. Morrison, M. J. Cowley, S. P. Thomas, *Angew. Chem. Int. Ed.* **2021**, *60*, 20672-20677.

[77] A. Bodach, J. Ortmeyer, B. Herrmann, M. Felderhoff, *Eur. J. Inorg. Chem.* **2021**, *2021*, 2248-2256.

[78] J.-C. Chang, C.-H. Hung, J.-H. Huang, *Organometallics* **2001**, *20*, 4445-4447.

[79] Y.-L. Lien, Y.-C. Chang, N.-T. Chuang, A. Datta, S.-J. Chen, C.-H. Hu, W.-Y. Huang, C.-H. Lin, J.-H. Huang, *Inorg. Chem.* **2010**, *49*, 136-143.

[80] J.-C. Chang, Y.-C. Chen, A. Datta, C.-H. Lin, C.-S. Hsiao, J.-H. Huang, *J. Organomet. Chem.* **2011**, *696*, 3673-3680.

[81] W.-Y. Huang, S.-J. Chuang, N.-T. Chunag, C.-S. Hsiao, A. Datta, S.-J. Chen, C.-H. Hu, J.-H. Huang, T.-Y. Lee, C.-H. Lin, *Dalton Trans.* **2011**, *40*, 7423-7433.

[82] I. C. Chen, S.-M. Ho, Y.-C. Chen, C.-Y. Lin, C.-H. Hu, C.-Y. Tu, A. Datta, J.-H. Huang, C.-H. Lin, *Dalton Trans.* **2009**, 8631-8643.

[83] T. S. Koptseva, M. V. Moskalev, A. A. Skatova, R. V. Rumyantcev, I. L. Fedushkin, *Inorg. Chem.* **2022**, *61*, 206-213.

[84] M. V. Moskalev, D. A. Razborov, A. A. Bazanov, V. G. Sokolov, T. S. Koptseva, E. V. Baranov, I. L. Fedushkin, *Mendeleev Commun.* **2020**, *30*, 94-96.

[85] L. Contreras, A. H. Cowley, F. P. Gabbaï, R. A. Jones, C. J. Carrano, M. R. Bond, *J. Organomet. Chem.* **1995**, *489*, C1-C3.

[86] H. V. R. Dias, W. Jin, R. E. Ratcliff, *Inorg. Chem.* **1995**, *34*, 6100-6105.

[87] K. Hobson, C. J. Carmalt, C. Bakewell, *Inorg. Chem.* **2021**, *60*, 10958-10969.

[88] C. Cui, H. W. Roesky, H. Hao, H.-G. Schmidt, M. Noltemeyer, *Angew. Chem. Int. Ed.* **2000**, *39*, 1815-1817.

[89] B. Twamley, N. J. Hardman, P. P. Power, *Acta Crystallographica Section E* **2001**, *57*, m227-m228.

[90] W. Uhl, B. Jana, *Chem. Eur. J.* **2008**, *14*, 3067-3071.

[91] Y. Yang, H. Li, C. Wang, H. W. Roesky, *Inorg. Chem.* **2012**, *51*, 2204-2211.

[92] T. N. Hooper, M. Garcon, A. J. P. White, M. R. Crimmin, *Chem Sci* **2018**, *9*, 5435-5440.

[93] Z. Yang, M. Zhong, X. Ma, K. Nijesh, S. De, P. Parameswaran, H. W. Roesky, *J. Am. Chem. Soc.* **2016**, *138*, 2548-2551.

[94] S.-C. Huo, Y. Li, P.-F. Ji, D.-X. Zhang, Z.-J. Zhang, Y. Yang, H. W. Roesky, *Z. Anorg. Allg. Chem.* **2022**, *649*, e202200279.

[95] I. M. Riddlestone, S. Edmonds, P. A. Kaufman, J. Urbano, J. I. Bates, M. J. Kelly, A. L. Thompson, R. Taylor, S. Aldridge, *J. Am. Chem. Soc.* **2012**, *134*, 2551-2554.

[96] Z. Yang, M. Zhong, X. Ma, S. De, C. Anusha, P. Parameswaran, H. W. Roesky, *Angew. Chem. Int. Ed. Engl.* **2015**, *54*, 10225-10229.

[97] X. Ma, P. Hao, J. Li, H. W. Roesky, Z. Yang, *Z. Anorg. Allg. Chem.* **2013**, *639*, 493-496.

[98] P. Hao, Z. Yang, X. Ma, X. Wang, Z. Liu, H. W. Roesky, K. Sun, J. Li, M. Zhong, *Dalton Trans.* **2012**, *41*, 13520-13524.

[99] P. Hao, Z. Yang, W. Li, X. Ma, H. W. Roesky, Y. Yang, J. Li, *Organometallics* **2015**, *34*, 105-108.

[100] Z. Yang, P. Hao, Z. Liu, X. Ma, H. W. Roesky, K. Sun, J. Li, *Organometallics* **2012**, *31*, 6500-6503.

[101] S. S. Kumar, S. Singh, F. Hongjun, H. W. Roesky, D. Vidović, J. Magull, *Organometallics* **2004**, *23*, 6327-6329.

[102] L. K. Keyes, A. D. K. Todd, N. A. Giffin, A. J. Veinot, A. D. Hendsbee, K. N. Robertson, S. J. Geier, J. D. Masuda, *RSC Advances* **2017**, *7*, 37315-37323.

[103] X. Ma, Z. Yang, X. Wang, H. W. Roesky, F. Wu, H. Zhu, *Inorg. Chem.* **2011**, *50*, 2010-2014.

[104] Z. Yang, X. Ma, R. B. Oswald, H. W. Roesky, M. Noltemeyer, *J. Am. Chem. Soc.* **2006**, *128*, 12406-12407.

[105] Z. Yang, Y. Yi, M. Zhong, S. De, T. Mondal, D. Koley, X. Ma, D. Zhang, H. W. Roesky, *Chem. Eur. J.* **2016**, *22*, 6932-6938.

[106] S. Gonzalez-Gallardo, V. Jancik, R. Cea-Olivares, R. A. Toscano, M. Moya-Cabrera, *Angew. Chem. Int. Ed. Engl.* **2007**, *46*, 2895-2898.

[107] D. Franz, S. Inoue, *Chem. Eur. J.* **2014**, *20*, 10645-10649.

[108] D. Franz, L. Sirtl, A. Pöthig, S. Inoue, *Z. Anorg. Allg. Chem.* **2016**, *642*, 1245-1250.

[109] P.-Y. Lee, L.-C. Liang, *Inorg. Chem.* **2009**, *48*, 5480-5487.

[110] R. L. Falconer, G. S. Nichol, M. J. Cowley, *Inorg. Chem.* **2019**, *58*, 11439-11448.

[111] R. L. Falconer, G. S. Nichol, I. V. Smolyar, S. L. Cockroft, M. J. Cowley, *Angew. Chem. Int. Ed.* **2021**, *60*, 2047-2052.

[112] D. Dhara, F. Fantuzzi, M. Härterich, R. D. Dewhurst, I. Krummenacher, M. Arrowsmith, C. Pranckevicius, H. Braunschweig, *Chem. Sci.* **2022**, *13*, 9693-9700.

[113] A. S. Marfunin, *Advanced Mineralogy*, 1 ed., Springer Berlin, Heidelberg, **1994**.

[114] T. Saegusa, Y. Fujii, H. Fujii, J. Furukawa, *Die Makromolekulare Chemie* **1962**, *55*, 232-235.

[115] S.-I. Ishida, *J. Polym. Sci.* **1962**, *62*, 1-14.

[116] E. J. Vandenberg, *J. Polym. Sci. A-1 Polym. Chem.* **1969**, *7*, 525-567.

[117] E. J. Vandenberg, in *Polymerization of Heterocycles (Ring Opening)* (Ed.: S. Penczek), Pergamon, **1977**, pp. 295-306.

[118] Z. Florjańczyk, A. Plichta, M. Sobczak, *Polymer* **2006**, *47*, 1081-1090.

[119] H. S. Zijlstra, S. Harder, *Eur. J. Inorg. Chem.* **2015**, *2015*, 19-43.

[120] H. Zhu, J. Chai, V. Jancik, H. W. Roesky, W. A. Merrill, P. P. Power, *J. Am. Chem. Soc.* **2005**, *127*, 10170-10171.

[121] James H. Gary, James H. Handwerk, Mark J. Kaiser, D. Geddes, *Petroleum Refining Technology and Economics*, 5th Edition ed., CRC Press, Boca Raton, **2007**.

[122] S. Aldridge, A. J. Downs, *The Group 13 Metals Aluminium, Gallium, Indium and Thallium; Chemical Patterns and Peculiarities*, John Wiley & Sons, **2011**.

[123] W. J. Borer, H. H. Günthard, *Helv. Chim. Acta* **1970**, *53*, 1043-1050.

[124] D. Franz, S. Inoue, *Dalton Trans.* **2016**, *45*, 9385-9397.

[125] C. J. Harlan, M. R. Mason, A. R. Barron, *Organometallics* **1994**, *13*, 2957-2969.

[126] R. J. Wehmschulte, P. P. Power, *J. Am. Chem. Soc.* **1997**, *119*, 8387-8388.

[127] G. Bai, H. W. Roesky, J. Li, M. Noltemeyer, H.-G. Schmidt, *Angew. Chem. Int. Ed.* **2003**, *42*, 5502-5506.

[128] M. R. Mason, J. M. Smith, S. G. Bott, A. R. Barron, *J. Am. Chem. Soc.* **1993**, *115*, 4971-4984.

[129] A. C. Stelzer, P. Hrobárik, T. Braun, M. Kaupp, B. Braun-Cula, *Inorg. Chem.* **2016**, *55*, 4915-4923.

[130] S. Singh, J. Chai, A. Pal, V. Jancik, H. W. Roesky, R. Herbst-Irmer, *Chem. Commun.* **2007**, 4934-4936.

[131] M. D. Anker, M. P. Coles, *Angewandte Chemie* **2019**, *131*, 18429-18433.

[132] J. Hicks, P. Vasko, J. M. Goicoechea, S. Aldridge, *Nature* **2018**, *557*, 92-95.

[133] R. J. Schwamm, M. S. Hill, H.-Y. Liu, M. F. Mahon, C. L. McMullin, N. A. Rajabi, *Chem. Eur. J.* **2021**, *27*, 14971-14980.

[134] R. J. Schwamm, M. P. Coles, M. S. Hill, M. F. Mahon, C. L. McMullin, N. A. Rajabi, A. S. S. Wilson, *Angew. Chem. Int. Ed.* **2020**, *59*, 3928-3932.

[135] S. Grams, J. Eyselein, J. Langer, C. Färber, S. Harder, *Angew. Chem. Int. Ed.* **2020**, *59*, 15982-15986.

[136] S. Grams, J. Mai, J. Langer, S. Harder, *Organometallics* **2022**, *41*, 2862-2867.

[137] J. Hicks, P. Vasko, J. M. Goicoechea, S. Aldridge, *Angew. Chem. Int. Ed.* **2021**, *60*, 1702-1713.

[138] C. Yan, R. Kinjo, *Angew. Chem. Int. Ed.* **2022**, *61*, e202211800.

[139] J. Hicks, P. Vasko, J. M. Goicoechea, S. Aldridge, *J. Am. Chem. Soc.* **2019**, *141*, 11000-11003.

[140] R. J. Schwamm, M. D. Anker, M. Lein, M. P. Coles, *Angew. Chem. Int. Ed.* **2019**, *58*, 1489-1493.

[141] S. Kurumada, S. Takamori, M. Yamashita, *Nat. Chem.* **2020**, *12*, 36-39.

[142] M. P. Coles, M. J. Evans, *Chem. Commun.* **2023**, *59*, 503-519.

[143] M. J. Evans, M. D. Anker, C. L. McMullin, S. E. Neale, M. P. Coles, *Angew. Chem. Int. Ed.* **2021**, *60*, 22289-22292.

[144] A. M. Geer, C. Tejel, J. A. López, M. A. Ciriano, *Angew. Chem. Int. Ed.* **2014**, *53*, 5614-5618.

[145] H. S. La Pierre, J. Arnold, F. D. Toste, *Angew. Chem. Int. Ed.* **2011**, *50*, 3900-3903.

[146] M. D. Anker, C. L. McMullin, N. A. Rajabi, M. P. Coles, *Angew. Chem. Int. Ed.* **2020**, *59*, 12806-12810.

[147] M. Á. Baeza Cinco, T. W. Hayton, *Eur. J. Inorg. Chem.* **2020**, *2020*, 3613-3626.

[148] V. Jancik, Y. Peng, H. W. Roesky, J. Li, D. Neculai, A. M. Neculai, R. Herbst-Irmer, *J. Am. Chem. Soc.* **2003**, *125*, 1452-1453.

[149] B. Li, J. Li, H. W. Roesky, H. Zhu, *J. Am. Chem. Soc.* **2015**, *137*, 162-164.

[150] Y. Peng, H. Fan, V. Jancik, H. W. Roesky, R. Herbst-Irmer, *Angew. Chem. Int. Ed.* **2004**, *43*, 6190-6192.

[151] R. J. Wehmschulte, P. P. Power, *J. Am. Chem. Soc.* **1997**, *119*, 9566-9567.

[152] C. Schnitter, A. Klemp, H. W. Roesky, H.-G. Schmidt, C. Röpken, R. Herbst-Irmer, M. Noltemeyer, *Eur. J. Inorg. Chem.* **1998**, *1998*, 2033-2039.

[153] C. J. Harlan, E. G. Gillan, S. G. Bott, A. R. Barron, *Organometallics* **1996**, *15*, 5479-5488.

[154] R. J. Wehmschulte, P. P. Power, *Chem. Commun.* **1998**, 335-336.

[155] R. J. Wehmschulte, P. P. Power, *Inorg. Chem.* **1994**, *33*, 5611-5612.

[156] V. Jancik, Monica M. Moya Cabrera, Herbert W. Roesky, R. Herbst-Irmer, D. Neculai, Ana M. Neculai, M. Noltemeyer, H.-G. Schmidt, *Eur. J. Inorg. Chem.* **2004**, *2004*, 3508-3512.

[157] V. Jancik, H. W. Roesky, D. Neculai, A. M. Neculai, R. Herbst-Irmer, *Angew. Chem. Int. Ed.* **2004**, *43*, 6192-6196.

[158] Z. Yang, X. Ma, Z. Zhang, H. W. Roesky, J. Magull, A. Ringe, *Z. Anorg. Allg. Chem.* **2008**, *634*, 2740-2742.

[159] W. Zheng, N. C. Mösch-Zanetti, H. W. Roesky, M. Noltemeyer, M. Hewitt, H.-G. Schmidt, T. R. Schneider, *Angew. Chem. Int. Ed.* **2000**, *39*, 4276-4279.

[160] T. Chu, S. F. Vyboishchikov, B. Gabidullin, G. I. Nikonov, *Angew. Chem. Int. Ed.* **2016**, *55*, 13306-13311.

[161] M. J. Evans, M. D. Anker, C. L. McMullin, S. E. Neale, N. A. Rajabi, M. P. Coles, *Chem. Sci.* **2022**, *13*, 4635-4646.

[162] S. Schulz, H. W. Roesky, H. J. Koch, G. M. Sheldrick, D. Stalke, A. Kuhn, *Angew. Chem. Int. Ed. Engl.* **1993**, *32*, 1729-1731.

[163] K. S. Klimek, J. Prust, H. W. Roesky, M. Noltemeyer, H.-G. Schmidt, *Organometallics* **2001**, *20*, 2047-2051.

[164] P. D. Godfrey, C. L. Raston, V.-A. Tolhurst, P. D. Godfrey, B. W. Skelton, A. H. White, *Chem. Commun.* **1997**, 2235-2236.

[165] M. G. Gardiner, C. L. Raston, V.-A. Tolhurst, *J. Chem. Soc., Chem. Commun.* **1995**, 2501-2502.

[166] W. J. Grigsby, C. L. Raston, V.-A. Tolhurst, B. W. Skelton, A. H. White, *J. Chem. Soc., Dalton Trans.* **1998**, 2547-2556.

[167] R. Kumar, D. G. Dick, S. U. Ghazi, M. Taghiof, M. J. Heeg, J. P. Oliver, *Organometallics* **1995**, *14*, 1601-1607.

[168] H. Zhu, J. Chai, Herbert W. Roesky, M. Noltemeyer, H.-G. Schmidt, D. Vidovic, J. Magull, *Eur. J. Inorg. Chem.* **2003**, *2003*, 3113-3119.

[169] C. Cui, H. W. Roesky, M. Noltemeyer, H.-G. Schmidt, *Inorg. Chem.* **2000**, *39*, 3678-3681.

[170] W. Uhl, R. Gerding, I. Hahn, S. Pohl, W. Saak, H. Reuter, *Polyhedron* **1996**, *15*, 3987-3992.

[171] M. D. Anker, M. P. Coles, *Angew. Chem. Int. Ed.* **2019**, *58*, 13452-13455.

[172] W. Uhl, U. Schütz, *Z. Naturforsch. B* **1994**, *49*, 931-934.

[173] K. Hobson, C. J. Carmalt, C. Bakewell, *Chem. Sci.* **2020**, *11*, 6942-6956.

[174] M.-C. Yang, M.-D. Su, *New J. Chem.* **2019**, *43*, 9364-9375.

[175] E. A. Carter, W. A. Goddard, *J. Phys. Chem.* **1986**, *90*, 998-1001.

[176] G. Trinquier, J. P. Malrieu, P. Riviere, *J. Am. Chem. Soc.* **1982**, *104*, 4529-4533.

[177] G. Trinquier, J. P. Malrieu, *J. Am. Chem. Soc.* **1987**, *109*, 5303-5315.

[178] J. P. Malrieu, G. Trinquier, *J. Am. Chem. Soc.* **1989**, *111*, 5916-5921.

[179] A. J. Bridgeman, N. A. Nielsen, *Inorg. Chim. Acta* **2000**, *303*, 107-115.

[180] G. H. Robinson, in *Adv. Organomet. Chem., Vol. 47*, Academic Press, **2001**, pp. 283-294.

[181] D. E. Trujillo-González, G. González-García, T. A. Hamlin, F. M. Bickelhaupt, H. Braunschweig, J. O. C. Jiménez-Halla, M. Solà, *Eur. J. Inorg. Chem.* **2023**, e202200767.

[182] J. Moilanen, P. P. Power, H. M. Tuononen, *Inorg. Chem.* **2010**, *49*, 10992-11000.

[183] A. J. Downs, *Coord. Chem. Rev.* **1999**, *189*, 59-100.

[184] Y. Wang, G. H. Robinson, *Organometallics* **2007**, *26*, 2-11.

[185] Z. Palagyi, R. S. Grev, H. F. Schaefer, III, *J. Am. Chem. Soc.* **1993**, *115*, 1936-1943.

[186] N. Holzmann, A. Stasch, C. Jones, G. Frenking, *Chem. Eur. J.* **2011**, *17*, 13517-13525.

[187] W. Uhl, A. Vester, W. Kaim, J. Poppe, *J. Organomet. Chem.* **1993**, *454*, 9-13.

[188] R. J. Wehmschulte, K. Ruhlandt-Senge, M. M. Olmstead, H. Hope, B. E. Sturgeon, P. P. Power, *Inorg. Chem.* **1993**, *32*, 2983-2984.

[189] R. J. Wright, M. Brynda, P. P. Power, *Angew. Chem. Int. Ed.* **2006**, *45*, 5953-5956.

[190] Y. Zhao, Y. Lei, Q. Dong, B. Wu, X.-J. Yang, *Chem. Eur. J.* **2013**, *19*, 12059-12066.

[191] T. Agou, K. Nagata, N. Tokitoh, *Angew. Chem. Int. Ed.* **2013**, *52*, 10818-10821.

[192] K. Nagata, T. Agou, T. Sasamori, N. Tokitoh, *Chem. Lett.* **2015**, *44*, 1610-1612.

[193] T. M. Koichi Nagata, Tomohiro Agou, Takahiro Sasamori, Tsukasa Matsuo, Norihiro Tokitoh, *Angew. Chem. Int. Ed.* **2016**, *55*, 12877-12880.

[194] R. J. Wright, A. D. Phillips, P. P. Power, *J. Am. Chem. Soc.* **2003**, *125*, 10784-10785.

[195] C. Cui, X. Li, C. Wang, J. Zhang, J. Cheng, X. Zhu, *Angew. Chem. Int. Ed.* **2006**, *45*, 2245-2247.

[196] C. Bakewell, K. Hobson, C. J. Carmalt, *Angew. Chem. Int. Ed.* **2022**, *61*, e202205901.

[197] Y. Wang, B. Quillian, P. Wei, Y. Xie, C. S. Wannere, R. B. King, H. F. Schaefer, P. v. R. Schleyer, G. H. Robinson, *J. Am. Chem. Soc.* **2008**, *130*, 3298-3299.

[198] Y. Wang, B. Quillian, P. Wei, C. S. Wannere, Y. Xie, R. B. King, H. F. Schaefer, P. v. R. Schleyer, G. H. Robinson, *J. Am. Chem. Soc.* **2007**, *129*, 12412-12413.

[199] H. Braunschweig, R. D. Dewhurst, K. Hammond, J. Mies, K. Radacki, A. Vargas, *Science* **2012**, *336*, 1420-1422.

[200] M. Arrowsmith, H. Braunschweig, T. E. Stennett, *Angew. Chem. Int. Ed. Engl.* **2017**, *56*, 96-115.

[201] N. J. Hardman, R. J. Wright, A. D. Phillips, P. P. Power, *Angew. Chem. Int. Ed.* **2002**, *41*, 2842-2844.

[202] R. J. Wright, A. D. Phillips, N. J. Hardman, P. P. Power, *J. Am. Chem. Soc.* **2002**, *124*, 8538-8539.

[203] R. J. Wright, A. D. Phillips, S. Hino, P. P. Power, *J. Am. Chem. Soc.* **2005**, *127*, 4794-4799.

[204] M. Caporali, L. Gonsalvi, A. Rossin, M. Peruzzini, *Chem. Rev.* **2010**, *110*, 4178-4235.

9. Appendix

9.1. Supporting Information for Chapter 4

Chemistry–A European Journal

Supporting Information

Isolation of Cyclic Aluminium Polysulfides by Stepwise Sulfurization

Huihui Xu, Catherine Weetman, Franziska Hanusch, and Shigeyoshi Inoue*

Contents

1 Experimental Section

1.1 General Methods and Instrumentation

All manipulations of air- and water-sensitive reactions were carried out under rigorous exclusion of water and oxygen under an atmosphere of argon 4.6 (≥99.996%; Westfalen AG) using the dual manifold Schlenk techniques or in an argon-filled LABstar glovebox from MBraun Inertgas-Systeme GmbH with water and oxygen levels below 0.5 ppm.

The glassware used was heat-dried under high vacuum prior to use with Triboflon III grease (mixture of polytetrafluoroethylene (PTFE) and perfluoropolyether (PFPE)) from Freudenberg & Co. KG as sealant.

All Solvents were dried by using a solvent purification system (SPS), freshly distilled under argon and deoxygenated before use. Deuterated benzene (C_6D_6) was obtained from Sigma-Aldrich Chemie GmbH, stored over 4 Å molecular sieves in the glovebox.

NMR samples were prepared under argon in NMR tubes. The NMR spectra were recorded on Bruker AV300US (^{1}H: 300.13 MHz, ^{27}Al: 78 MHz), Avance Neo 400 (^{1}H: 400.23 MHz, ^{13}C: 100.65 MHz, ^{31}P: 162.01 MHz, ^{29}Si: 79 MHz), spectrometers at ambient temperature (300 K). The ^{1}H, ^{13}C{^{1}H} and ^{29}Si{^{1}H} NMR spectroscopic chemical shifts δ are reported in ppm relative to tetramethylsilane. ^{1}H and ^{13}C{^{1}H} NMR spectra are calibrated against the residual proton and natural abundance carbon resonances of the deuterated solvent as internal standard (C_6D_6: $\delta(^1H)$ = 7.16 ppm and $\delta(^{13}C)$ = 128.1 ppm). The following abbreviations are used to describe signal multiplicities: s = singlet, d = doublet, t = triplet, sept = septet, m = multiplet, br = broad and combinations thereof (e.g. dd = doublet of doublets). Some NMR spectra include resonances for silicone grease (C_6D_6: $\delta(^1H)$ = 0.29 ppm, $\delta(^{13}C)$ = 1.4 ppm) derived from B. Braun Melsungen AG Sterican® cannulas.

Quantitative elemental analyses (EA) were carried out using a EURO EA (HEKA tech) instrument equipped with a CHNS combustion analyzer at the Laboratory for Microanalysis at the TUM Catalysis Research Center.

Melting Points (m.p.) were determined in sealed glass capillaries under inert gas by a Büchi M-565 melting point apparatus.

Lawesson's reagent (LR) and bis(trimethylsilyl) sulfide {S(TMS)$_2$} were obtained from Sigma-Aldrich Chemie GmbH. The compounds I*i*Pr$_2$Me$_2$Al(Tipp)H$_2$,[S1] IMe$_4$·AlH$_3$,[S2] 2,6-(2,4,6-*i*Pr$_3$C$_6$H$_2$)$_2$C$_6$H$_3$Li(THF)$_2$ (^{Tipp}TerLi(THF)$_2$),[S3] the cyclic (alkyl)(amino)carbene (cAAC^{Me}),[S4] 1,3,4,5-tetramethylimidazolin-2-ylidene (IMe$_4$)[S5] and 1,3-diisopropyl-4,5-dimethylimidazolin-2-ylidene (I*i*Pr$_2$Me$_2$),[S5] Me$_3$N·AlH$_3$,[S6] I*i*Pr$_2$Me$_2$·AlH$_3$,[S2] LiTipp·OEt$_2$[S7] were prepared according to the corresponding literature procedures.

1.2 Synthesis and Characterization

1.2.1 Synthesis of IMe$_4$Al (^{Tipp}Ter)H$_2$ (Compound 1)

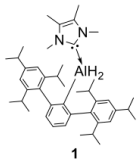

1
$C_{43}H_{63}AlN_2$
634.97 g/mol

^{Tipp}TerLi(THF)$_2$ (4.63g, 7.32 mmol) in 60 mL of Et$_2$O was added via dropping funnel over a period of 30 minutes to a Et$_2$O solution of IMe$_4$AlH$_3$ (1.20g, 7.75 mmol, 1.06 eqv.) at -78 °C. The reaction was kept at -78 °C for 15 minutes and then slowly warmed to room temperature with 16 hours. Volatiles were removed under reduced pressure and crude product was extracted with pentane (3 x 60 mL). Colourless crystalline material was obtained from the concentrated pentane solution at -30 °C. Yield = 3.94 g, 84%.

m.p.: 186.0 °C (decomposition; colour change from colourless to brown).

^{1}H NMR (400 MHz, Benzene-d_6) δ 7.29 (dd, *J* = 8.4, 6.5 Hz, 1H, Ph-H(*p*)), 7.21 (d, *J* = 6.8 Hz, 2H, Ph-H(*m*)), 7.18 (s, 4H, Tipp-H), 4.01 (br, 2H, Al-H), 3.29 (hept, *J* = 6.9 Hz, 4H, Tipp-CH(*o*)), 2.95 (s, 6H, N-CH$_3$), 2.89 (h, *J* = 6.9 Hz, 2H, Tipp-CH(*p*)), 1.37 (d, *J* = 6.8 Hz, 12H, Tipp-CH-CH$_3$(*o*)), 1.30 (d, *J* = 7.0 Hz, 12H, Tipp-CH-CH$_3$(*p*)), 1.24 (d, *J* = 6.7 Hz, 12H, Tipp-CH-CH$_3$(*o*)), 1.16 (s, 6H, N-C-CH$_3$).

^{13}C{^{1}H} NMR (101 MHz, Benzene-d_6) δ 169.70(N-C-N), 152.35(Al-C), 149.81, 146.77, 146.57, 142.63, 128.28, 125.22, 124.20(N-C-C-N), 119.95, 34.44, 33.32(N-C), 30.57, 26.11, 24.25, 22.65, 7.43 (N-C-C).

^{27}Al{^{1}H} NMR (78 MHz, Benzene-d_6) δ 94.72.

Anal. Calcd. [%] for $C_{43}H_{63}AlN_2$: C, 81.34; H, 10.00; N, 4.41. Found [%]: C, 81.25; H, 10.13; N, 4.46.

1.2.2 Synthesis of IMe$_4$Al (^{Tipp}Ter)(SH)H (Compound 2)

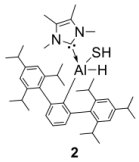

2
$C_{43}H_{63}AlN_2S$
667.03 g/mol

A pentane solution (30 mL) of elemental sulfur, S_8 (20 mg, 0.077 mmol, 0.16 eqv.) was added dropwise to a pentane solution (30 mL) of IMe$_4$Al (^{Tipp}Ter)H$_2$ (306 mg, 0.482 mmol) at -78 ºC. The solution was kept at -78 ºC for 15 minutes then warmed to room temperature with 16 hours, during this time the solution changed from an opaque off-white to a clear pale yellow solution. Volatiles were removed under reduced pressure and the crude product was extracted with Et_2O (3 x 15 mL). The Et_2O solution was concentrated to the point of crystallization and then placed in a -30 ºC freezer. Pale yellow crystals were obtained (181 mg, 56%).

^{1}H NMR (400 MHz, Benzene-d_6) δ 7.28 (d, J = 1.9 Hz, 2H, Tipp-*m*-H), 7.27 – 7.24 (m, 1H, ^{Tipp}Ter-H), 7.21 (s, 1H, ^{Tipp}Ter-H), 7.19 (t, J = 2.1 Hz, 1H, ^{Tipp}Ter-H), 7.06 (d, J = 1.9 Hz, 2H, Tipp-*m*-H), 4.80 (br, 1H, Al-H), 3.42 (hept, J = 6.8 Hz, 2H, Tipp-*o*-iso-*C*H), 3.07 (s, 6H), 2.87 (dq, J = 14.1, 7.0 Hz, 2H, Tipp-*p*-iso-*C*H), 1.68 (d, J = 6.8 Hz, 6H, Tipp-*o*-iso-C-*C*H$_3$), 1.28 (dp, J = 8.5, 2.8 Hz, 18H, Tipp-*o* or *p*-iso-C-*C*H$_3$), 1.19 – 1.10 (m, 18H, Tipp-*o* or *p*-iso-C-*C*H$_3$), -1.77 (s, 1H, SH).

^{13}C{^{1}H} NMR (101 MHz, Benzene-d_6) δ 167.72 (IMe-*C*:), 149.24 (^{Tipp}Ter-*o*-C), 147.38 (Tipp-*o*-C), 147.25 (Tipp-*p*-C), 147.15 (Tipp-*1-C*-^{Tipp}Ter), 141.34 (Tipp-*o*-C), 129.10 (^{Tipp}Ter-*m*-C), 125.57(^{Tipp}Ter-*p*-C), 124.62(IMe-*C*-CH$_3$), 120.70 (Tipp-*m*-C), 119.78 (Tipp-*m*-C), 34.46 (Tipp-*p*-iso-*C*), 33.75 (Tipp-*p*-iso-*C*), 30.96 (Tipp-*o*-iso-*C*-CH$_3$), 30.46 (Tipp-*o*-iso-*C*-CH$_3$), 26.30, 26.05 (Tipp-*o*-iso-C-*C*H$_3$), 25.47 (IMe-N-C), 24.35 (Tipp-*p*-iso-C-*C*H$_3$), 24.08 (Tipp-*p*-iso-C-*C*H$_3$), 22.23(Tipp-*o*-iso-C-*C*H$_3$), 7.40 (IMe-C-*C*H$_3$).

Anal. Calcd. [%] for $C_{43}H_{63}AlN_2S$: C, 77.43; H, 9.52; N, 4.20; S, 4.81. Found [%]: C, 76.25; H, 9.30; N, 4.18; S, 4.90.

1.2.3 Synthesis of IMe$_4$Al (^{Tipp}Ter)(SH)$_2$ (Compound 3)

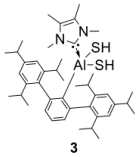

3
$C_{43}H_{63}AlN_2S_2$
699.09 g/mol

Method A: IMe$_4$Al (^{Tipp}Ter)H$_2$ (1.00 g, 1.57 mmol) and S_8 (106 mg, 0.41 mmol, 0.26 eqv.) was mixed in Glove Box. Subsequently, Et_2O (100 ml) was transferred by drop slowly to the mixture at -78 ºC. The solution was kept at -78 ºC for 1 hour then warmed to room temperature and stirred for two nights. Volatiles were removed under reduced pressure to afford a colorless powder, which was subsequently washed with pentane (3 x 50 mL). The product was extracted with Et_2O (3 x 50 mL), concentrated and then placed in a -30 ºC freezer with 16 hours. A pale yellow powder was isolated after filtration and drying under reduced pressure. Yield: 1.00 g, 91%.

^{1}H NMR (400 MHz, Benzene-d_6) δ 7.24 (s, 3H, ^{Tipp}Ter-*H*), 7.19 (s, 4H, Tipp-H), 3.26 (p, J = 6.8 Hz, 4H, Tipp-*o*-iso-H), 3.18 (s, 6H, IMe-N-CH), 2.88 (p, J = 6.9 Hz, 2H, Tipp-*p*-iso-H), 1.42 (d, J = 6.8 Hz, 12H, Tipp-*o*-iso-CH-C*H*), 1.29 (d, J = 6.9 Hz, 12H, Tipp-*p*-iso-CH-C*H*), 1.19 (d, J = 6.6 Hz, 12H, Tipp-*o*-iso-CH-C*H*), 1.11 (s, 6H, IMe-C-CH), -0.89 (s, 2H, S-H).

^{13}C{^{1}H} NMR (101 MHz, Benzene-d_6) δ 165.03 (IMe-*C*:), 148.62 (^{Tipp}Ter-*o*-*C*), 147.56 (Tipp-*p*-*C*), 147.38 (Tipp-*o*-*C*), 141.56 (Tipp-*1-C*), 130.39 (^{Tipp}Ter-*m*-*C*), 125.27(^{Tipp}Ter-*p*-*C*), 125.08(IMe-*C*-CH$_3$), 120.31 (Tipp-*m*-*C*), 34.50 (Tipp-*p*-iso-C), 30.71 (IMe-N-*C*), 26.28 (Tipp-*o*-iso-*C*), 24.20 (Tipp-*p*-iso-C-*C*H$_3$), 22.70 (Tipp-*o*-iso-C-*C*H$_3$), 7.50 (IMe-C-*C*H$_3$).

Anal. Calcd. [%] for $C_{43}H_{63}AlN_2S_2$ with 0.15 eqv. S_8: C, 69.83; H, 8.86; N, 3.79; S 13.87. Found [%]: C, 69.08; H, 8.57; N, 3.98; S, 13.79. This result was affected by excess S_8 (approximately 0.15 eqv).

1.2.4 Synthesis of IMe$_4$Al (^{Tipp}Ter)S$_5$ (Compound 4)

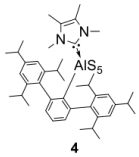

4
$C_{43}H_{61}AlN_2S_5$
793.26 g/mol

Method A: A Et_2O (30 mL) solution of S_8 (250 mg, 1.00mmol, 0.56 eqv.) was added dropwise to a Et_2O solution (50 mL) of IMe$_4$Al (^{Tipp}Ter)H$_2$ (1.12 g, 1.76 mmol) at -78 ºC. The solution was kept at -78 ºC for half an hour before warming to room temperature and stirring with 16 hours. Volatiles were removed under reduced pressure, whilst being kept in a cool water bath. The crude products were extracted by pentane (3 x 25 mL and concentrated to the point of crystallization before being placed in a -30 ºC freezer with 16 hours. Pale yellow solids were isolated via canula filtration and dried under vacuum (Yield: 183 mg, 13%).

Method B: IMe$_4$Al (^{Tipp}Ter)(SH)$_2$ (150 mg, 0.215 mmol) and S_8 (55 mg, 0.215 mmol, 1 eqv.) were mixed in cold Et_2O (10 mL) which was at -30 ºC with 5 min, inside the glove box. The reaction was stirred for 3 days at room temperature. Volatiles were removed under reduced pressure and the crude product was washed with cold pentane (10 mL), followed by extraction with THF (8 ml). The solution was concentrated to the point of crystallization and then put in the freezer (-30 ºC). Pale yellow powder was isolated after filtration and drying under vacuum. Yield: 150 mg, 88%.

^{1}H NMR (300 MHz, Benzene-d_6) δ 7.22 – 7.18 (m, 1H, ^{Tipp}Ter-*m*-H), 7.17 (s, 4H,Tipp-H), 7.13 (d, *J* = 1.9 Hz, 1H, ^{Tipp}Ter-*p*-H), 7.03 (d, *J* = 1.5 Hz, 1H, ^{Tipp}Ter-*m*-H), 3.30 (s, 6H, IMe-N-C*H*), 3.15 (p, *J* = 13.4, 7.4 Hz, 4H, Tipp-iso-CH), 2.89 (p, *J* = 6.9 Hz, 2H, ^{Tipp}Ter-*p*-iso-CH), 1.42 (d, *J* = 6.7 Hz, 12H, Tipp-*o*-iso-C-CH$_3$), 1.33 (s, 6H, Tipp-*p*-iso-C-CH$_3$), 1.30 (d, *J* = 2.6 Hz, 12H, IMe-C-CH$_3$), 1.10 (d, *J* = 6.7 Hz, 12H, Tipp-*o*-iso-C-CH$_3$).

^{13}C{^{1}H NMR (101 MHz, Benzene-d_6) δ 161.44 (IMe-C:), 148.58 (^{Tipp}Ter-*o*-C), 147.92 (Tipp-*p*-C), 147.41 (Tipp-*o*-C), 140.67 (Tipp-*1*-C-Ter^{Tipp}), 130.53 (^{Tipp}Ter-*p*-C), 128.96 (^{Tipp}Ter-*m*-C), 128.19 (^{Tipp}Ter-*m*-C), 126.10 (IMe-*C*-CH$_3$), 120.66 (Tipp-*m*-C), 34.49 (Tipp-*p*-iso-*C*), 34.20 (IMe-N-C), 30.73 (Tipp-*o*-iso-C-*C*H$_3$), 25.94 (Tipp-*o*-iso-*C*), 24.21 (Tipp-*p*-iso-C-*C*H$_3$), 22.81 (Tipp-*o*-iso-C-*C*H$_3$), 7.79(IMe-C-*C*H$_3$).

Anal. Calcd. [%] for $C_{43}H_{61}AlN_2S_5$: C, 65.11; H, 7.75; N, 3.53; S, 20.21. Found [%]: C, 65.13; H, 7.56; N, 3.72; S, 19.39.

1.2.5 Synthesis of [IMe$_4$Al (^{Tipp}Ter)(S-cAAC^{Me})H] (Compound 5)

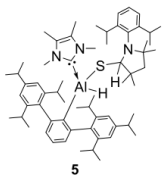

5
$C_{63}H_{94}AlN_3S$
952.51 g/mol

IMe$_4$Al (^{Tipp}Ter)(SH)H (50 mg, 0.075 mmol) and the cyclic (alkyl)(amino)carbene (cAAC^{Me}) (24 mg, 0.0825 mmol, 1.1 eqv.) were weighed into a Schlenk flask in the glove box and cold toluene which was at -30 °C with 5 min, was added dropwise. The solution was stirred at room temperature with 16 hours, and then volatiles were removed under reduced pressure. The crude product was extracted by pentane (3 x 5 mL) and then concentrated to the point of crystallization before being placed in the 30 ºC freezer with 16 hours. Colorless crystalline material was isolated after filtration and drying under vacuum (35 mg, 49%).

^{1}H NMR (400 MHz, Benzene-d_6) δ 7.26 (d, *J* = 1.6 Hz, 2H, C-H, ^{Tipp}Ter), 7.18 (t, 1H) 7.13 (s, 1H, C-H, ^{Tipp}Ter), 7.09 (d, *J* = 1.6 Hz, 2H), 7.06 (dd, *J* = 7.7, 1.6 Hz, 1H, Dipp), 6.94 (t, *J* = 7.6 Hz, 1H, Dipp), 6.68 (dd, *J* = 7.5, 1.7 Hz, 1H, Dipp), 4.56 (s, 1H, S-*H*-cAAC), 4.25 (br, 4.25, Al-H), 4.08 (dt, *J* = 13.4, 6.7 Hz, 1H, iso-Dipp), 3.40 (p, *J* = 6.6 Hz, 2H,), 3.01 (dd, *J* = 13.6, 6.8 Hz, 1H, iso-Dipp), 2.99 – 2.90 (m, 2H), 2.85 (hept, *J* = 6.8, 6.3 Hz, 2H, iso-^{Tipp}Ter), 2.68 (s, 6H), 1.95 (d, *J* = 12.0 Hz, 1H, cAAC-H), 1.86 (d, *J* = 12.0 Hz, 1H, cAAC-H), 1.66 (d, *J* = 6.8 Hz, 6H, iso-^{Tipp}Ter), 1.58 (s, 3H, IMe$_4$), 1.44 (d, *J* = 6.7 Hz, 3H), 1.42 – 1.36 (m, 12H), 1.35 (s, 6H), 1.27 – 1.14 (m, 15H, iso-^{Tipp}Ter), 1.11 (d, *J* = 6.9 Hz, 6H), 1.04 (d, *J* = 6.8 Hz, 3H), 0.78 (s, 3H, cAAC), 0.26 (d, *J* = 6.7 Hz, 3H, cAAC).

^{13}C{^{1}H} NMR (101 MHz, Benzene-d_6) δ 166.50 (*C*:, IMe$_4$), 152.79 (Ar-C), 150.01 (Ar-H), 149.82 (Ar-C), 147.01 (Ar-C), 146.85 (Ar-C), 146.58 (Ar-C), 142.30 (Ar-C), 142.18 (Ar-H), 129.06 (Ar-H), 125.49 (Ar-C), 125.24 (Ar-C), 124.74 (Ar-C), 123.90 (Ar-C), 123.74 (Ar-C), 120.24 (Ar-C), 120.17 (Ar-C), 82.94 (S-*C*-cAAC), 61.64 (*C*H$_2$, cAAC), 60.20, 43.52, 34.48, 32.84, 32.59 (C-iso-Ar), 31.54 (C-iso-Ar), 31.22 (C-iso-Ar), 30.93 (C-iso-Ar), 30.50 (C-iso-Ar), 28.59 (*C*Me$_2$), 27.70 (C-iso-Ar), 27.30 (C-iso-Ar), 26.79 (C-iso-Ar), 26.10 (C-iso-Ar), 25.97 (C-iso-Ar), 25.75 (C-iso-Ar), 24.53 (C-iso-Ar), 24.36 (C-iso-Ar), 24.22 (C-iso-Ar), 22.96 (C-iso-Ar), 22.90 (*C*Me$_2$), 21.94 (C-iso-Ar), 7.58 (N-C-*C*, IMe$_4$).

Anal. Calcd. [%] for $C_{63}H_{94}AlN_3S$: C, 79.44; H, 9.95; N, 4.41; S, 3.37. Found [%]: C, 78.95; H, 9.38; N, 4.57; S,3.16.

1.2.6 Synthesis of IMe$_4$Al (^{Tipp}Ter)S$_4$ (Compound 6)

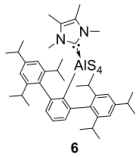

6
$C_{43}H_{61}AlN_2S_4$
761.20 g/mol

Compound **4** (50 mg, 0.063 mmol) and PPh_3 (68 mg, 0.259 mmol, 4.1 eqv.) were mixed in THF (10 mL) inside the glove box. The reaction was stirred for 2 hrs at 65 ºC. Volatiles were removed under reduced pressure, followed by extraction with THF (5 ml). The solution was concentrated to the point of crystallization and then put in the freezer (-30 ºC). The pale yellow powders were obtained after filtration and drying under vacuum. The yield of products was 85% (40 mg), as yellow crystals from recrystallization of saturated THF solution. However, the byproducts such as S=PPh_3 and PPh_3 could not be removed by washing, extraction or recrystallization methods, with being the colorless crystals (PPh_3 or S=PPh_3) together with the yellow crystals (targets). Compound **6** was unstable, which decomposed at 80 ºC within few minutes.

^{1}H NMR (300 MHz, Benzene-d_6) ^{1}H NMR (400 MHz, Benzene-d_6) δ 7.28 (m, *J* = 3.2 Hz, 1H, ^{Tipp}Ter-CH), 7.22 (d, *J* = 1.5 Hz, 2H, ^{Tipp}Ter-CH), 7.20 (s, 4H, Tipp-*m*-C*H*), 3.20 (dt, *J* = 13.4, 6.2 Hz, 4H, Tipp-*o*-iso-C*H*-CH$_3$), 3.19 (s, 6H, NHC-N-CH$_3$), 2.89 (p, *J* = 6.9 Hz, 2H, Tipp-*p*-iso-C*H*-CH$_3$), 1.38 (d, *J* = 6.4 Hz, 12H, ^{Tipp}Ter-CH$_3$), 1.31 (d, *J* = 6.9 Hz, 12H, ^{Tipp}Ter-CH$_3$), 1.18 (d, *J* = 6.7 Hz, 12H, ^{Tipp}Ter-CH$_3$), 1.13 (s, 6H, NHC-C-CH$_3$).

^{1}H NMR (400 MHz, THF-d_8) δ 7.12 (d, J = 7.5 Hz, 2H), 7.01 (s, 4H, Tipp-*m*-C*H*), 3.36 (d, J = 29.8 Hz, 6H, NHC-N-CH$_3$), 2.94 (dt, J = 11.4, 6.9 Hz, 6H, Tipp-iso-C*H*), 2.01 (d, J = 26.6 Hz, 6H, NHC-C-CH$_3$), 1.30 (d, J = 6.9 Hz, 12H, ^{Tipp}Ter-CH$_3$), 1.17 (d, J = 6.8 Hz, 12H, ^{Tipp}Ter-CH$_3$), 0.96 (d, J = 6.6 Hz, 12H, ^{Tipp}Ter-CH$_3$).

^{13}C{^{1}H} NMR (126 MHz, Benzene-d_6) δ 163.92 (*C*:, IMe$_4$), 149.37 (Ar-C), 147.87 (Tipp-C), 147.10 (Tipp-C), 141.11 (Ar-C), 130.06 (Ar-C), 125.13 (IMe-*C*-CH$_3$), 120.63 (Tipp-C), 34.53 (IMe-N-C), 30.86 (iso-*C*-(CH$_3$)$_2$), 26.51(iso-*C*H$_3$), 24.22(iso-*C*H$_3$), 22.59 (iso-*C*H$_3$), 7.45 (N-C-*C*, IMe$_4$).

Anal. Calcd. [%] for $C_{43}H_{61}AlN_2S_4$ C, 67.67; H, 8.32; N, 3.67; S, 16.80 Found [%]: C, 67.54; H, 7.93; N, 3.11; S, 16.36. (after drying of only selected yellow crystals)

1.2.7 Synthesis of [IMe$_4$Al (^{Tipp}Ter){SP(=S)C$_6$H$_4$OMe}$_2$] (Compound 7)

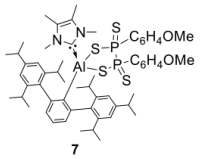

7
$C_{57}H_{75}AlN_2O_2P_2S_4$
1037.41 g/mol

A toluene solution (20 mL) of Lawesson's reagent (190 mg, 0.471 mmol, 1.5 eqv.) was transferred dropwise to a solution of IMe$_4$Al (^{Tipp}Ter)H$_2$ (200 mg, 0.314 mmol) dissolved in toluene (15 mL) over 15 minutes at 0 °C. The reaction mixture was stirred with 16 hours at room temperature, followed by removal of volatiles under reduced pressure. The crude products were extracted by toluene (3 x 20 mL), concentrated to the point of crystallization and then placed in the freezer (-30 °C). A colourless powder was isolated via filtration and drying under vacuum (Yield: 148 mg, 46%).

^{1}H NMR (400 MHz, Benzene-d_6) δ 7.89 (dt, *J* = 8.6, 6.3 Hz, 4H, LR-Ph-H), 7.26 (q, *J* = 3.4, 2.5 Hz, 6H), 7.04 – 6.98 (m, 1H, ^{Tipp}Ter-*p*-H), 6.48 (d, *J* = 8.7 Hz, 4H, LR-Ph-H), 3.37 (s, 6H, IMe-N-CH$_3$), 3.12 – 3.04 (m, 10H), 3.07 (s, 6H, LR-CH$_3$), 2.95 (dt, *J* = 13.8, 6.8 Hz, 2H, Tipp-*p*-iso-CH), 1.47 (s, 6H, IMe-C-CH$_3$), 1.34 (d, *J* = 6.9 Hz, 24H, Tipp-*o*-iso-C-CH$_3$), 1.14 (d, *J* = 6.6 Hz, 12H).

^{13}C{^{1}H} NMR (101 MHz, Benzene-d_6) δ 161.77 (O-*C*-Ph), 149.74 (Ar-C), 148.23 (Ar-C), 147.34 (Ar-C), 140.83 (Ar-C), 134.50 (O-Ph-C), 126.94 (NHC-*C*-C), 120.80 (Ar-C), 112.48 (O-Ph-C), 54.23 (O-*C*), 35.26 (NHC-N-*C*), 34.60 (Ar-iso-*C*), 30.98(Ar-iso-*C*), 26.71(Ar-iso-*C*), 24.21(Ar-iso-*C*), 22.31(Ar-iso-*C*), 7.88 (NHC-C-*C*).

^{31}P{^{1}H} NMR (162 MHz, Benzene-d_6) δ 76.67.

Anal. Calcd. [%] for $C_{57}H_{75}AlN_2O_2P_2S_4$: C, 65.99; H, 7.29; N, 2.70; S, 12.36. Found [%]: C, 66.42; H, 7.29; N, 2.67; S, 11.63.

1.2.8 Synthesis of I*i*Pr$_2$Me$_2$Al(Tipp)(H)STMS (Compound 8)

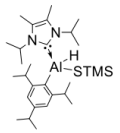

8
$C_{29}H_{53}AlN_2SSi$
516.88 g/mol

A toluene solution (10 mL) of bis(trimethylsilyl) sulfide (S(TMS)$_2$) (216 mg, 1.21 mmol, 2.5 eq) was added dropwise to the toluene solution (20 mL) of I*i*Pr$_2$Me$_2$Al(Tipp)H$_2$ (200 mg, 0.48 mmol.) at -78 °C. The reaction mixture was kept at -78 ºC for 15 minutes, before warming to room temperature and subsequently heating at 75 ºC for two nights. Volatiles were removed under reduced pressure, and the crude products were extracted by pentane (3 x 5 mL) and concentrated to the point of crystallisation. After storage in the freezer (-30 °C) with 16 hours, the colorless crystalline material was isolated via filtration and dried under vacuum. (59 mg, 23%)

^{1}H NMR (400 MHz, Benzene-d_6) δ 7.17 (s, 2H, Tipp-*m*-H), 5.78 (hept, *J* = 7.1 Hz, 2H, Tipp-*o*-iso-CH), 5.43 (br, 1H, Al-H), 4.04 (hept, *J* = 6.8 Hz, 2H, I*i*Pr-N-CH), 2.92 (dt, *J* = 13.8, 6.9 Hz, 1H, Tipp-*p*-iso-CH), 1.47 (s, 6H, I*i*Pr-C-CH$_3$), 1.40 (d, *J* = 6.8 Hz, 6H, Tipp-*o*-iso-CH$_3$), 1.35 (d, *J* = 6.9 Hz, 12H, I*i*Pr-N-C-CH$_3$), 1.06 (d, *J* = 7.0 Hz, 6H, Tipp-*p*-iso-CH$_3$), 1.03 (d, *J* = 7.0 Hz, 6H, Tipp-*o*-iso-CH$_3$), 0.72 (s, 9H, Si-CH).

^{13}C{^{1}H}1K NMR (101 MHz, Benzene-d_6) δ 168.73 (NHC-*C*:), 157.09 (Ar-C), 147.86(Ar-C), 125.31 (NHC-*C*-C), 119.87(Ar-C), 51.68, 35.75 (NHC-N-*C*-C), 34.59, 25.16 (NHC-N-C-*C*), 24.20, 20.76, 9.47 (NHC-C-*C*), 5.02 (TMS-*C*).

^{29}Si{^{1}H} NMR (79 MHz, Benzene-d_6) δ 11.35.

Anal. Calcd. [%] for $C_{29}H_{53}AlN_2SSi$: C, 67.39; H, 10.34; N, 5.42; S, 6.20. Found [%]: C, 67.05; H, 10.45; N, 5.25; S, 5.66.

1.3 NMR Experiments

1.3.1 The reaction of I*i*Pr$_2$Me$_2$Al(Tipp)H$_2$ (Compound 1^{Tipp}) with S$_8$

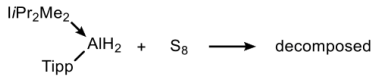

I*i*Pr$_2$Me$_2$Al(Tipp)H$_2$ (25 mg, 0.061 mmol) and S$_8$ (2 mg, 0.0076 mmol, 0.125 eqv.; or 4 mg, 0.0157 mmol, 0.25 eqv.; or excess) were mixed and precooled C_6D_6 was added to the mixture in a J-Young NMR tube. After 15 minutes, the solution became slurry from clear solution (pale yellow). After 24 hours, there was oily precipitate in the bottom of the tube. The reaction showed decomposition. (Tipp:[S8] ^{1}H NMR (300 MHz, C_6D_6, 300 K): δ 7.00 (s, 3H), 2.82 (sept, 3H), 1.24 (18H) ppm; Pronated NHC (NHC-H): The singlet (Me) and the doublet (iso-CH$_3$) are overlapped in around 1.48 ppm.)

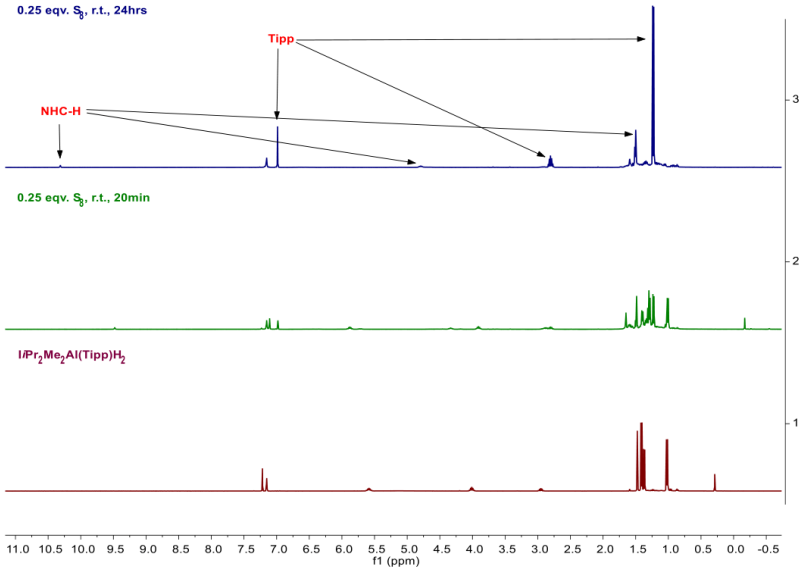

Figure S1: Stacked ^{1}H NMR (400 MHz) spectra for the mixture of compound **1**^{Tipp} with excess S$_8$ in C_6D_6 at 300 K.

1.3.2 Synthesis of IMe$_4$Al (^{Tipp}Ter)(SH)$_2$ (Compound 3) from IMe$_4$Al (^{Tipp}Ter)(SH)H (Compound 2)

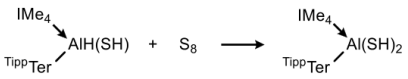

Method B: Compound **2** (25 mg, 0.037 mmol) and S$_8$ (1.20 mg, 0.0047 mmol, 0.125 eqv.; or 2.40 mg, 0.0094 mmol, 0.25 eqv.; or excess) were mixed and precooled C_6D_6 was added to the mixture in a J-Young NMR tube.

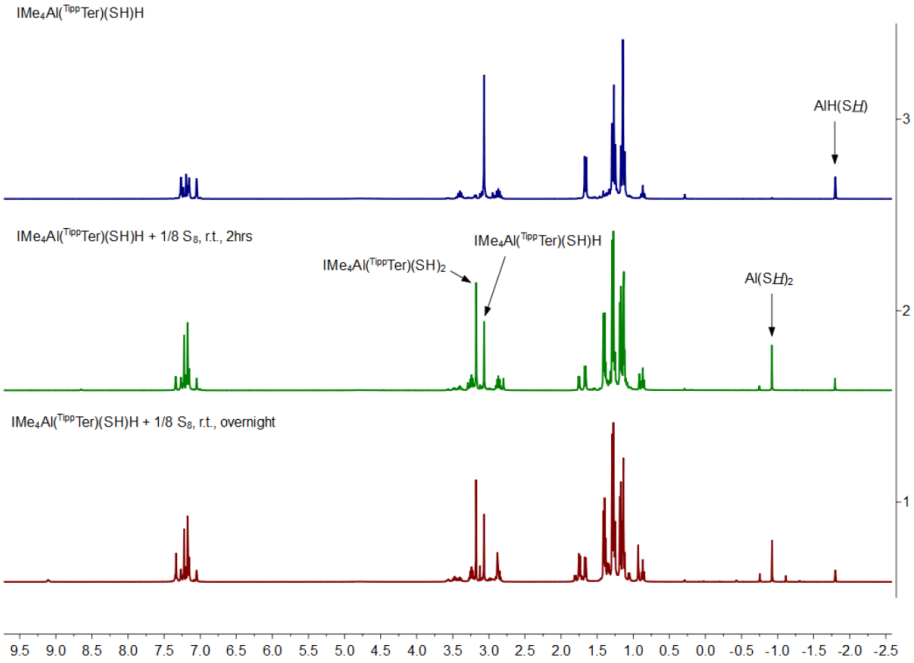

Figure S2: Stacked ^{1}H NMR (400 MHz) spectra for the mixture of compound **2** with 1/8 eqv. S_8 in C_6D_6 at 300 K.

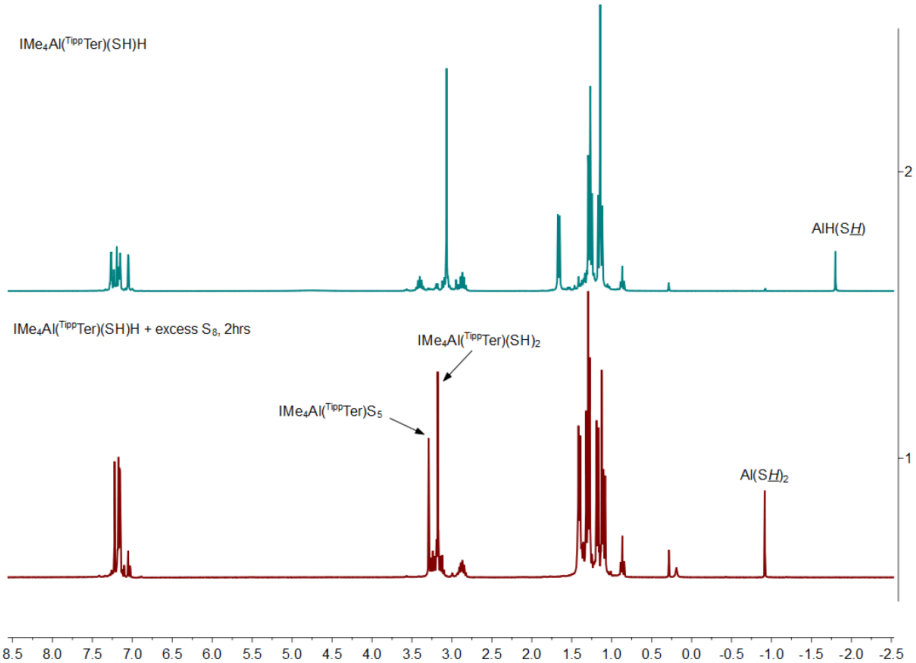

Figure S3: Stacked ^{1}H NMR (400 MHz) spectra for the mixture of compound **2** with excess S_8 in C_6D_6 at 300 K. [δ (silicone grease) = 0.29 ppm]

1.3.3 The thermal stability of $IMe_4Al(^{Tipp}Ter)S_5$ (compound 4)

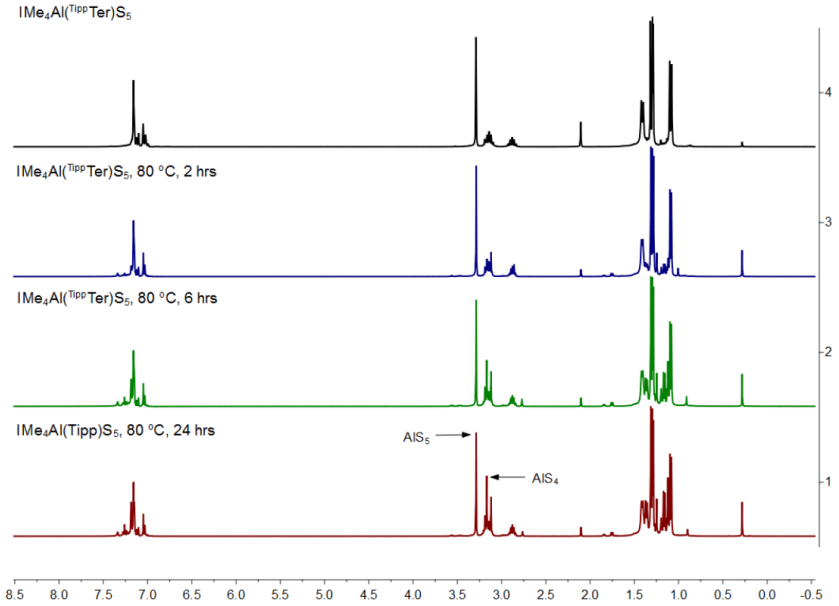

Figure S4: Stacked ^1H NMR (400 MHz) spectra for compound **4** (in different conditions) in C_6D_6 at 300 K. [δ (silicone grease) = 0.29 ppm]

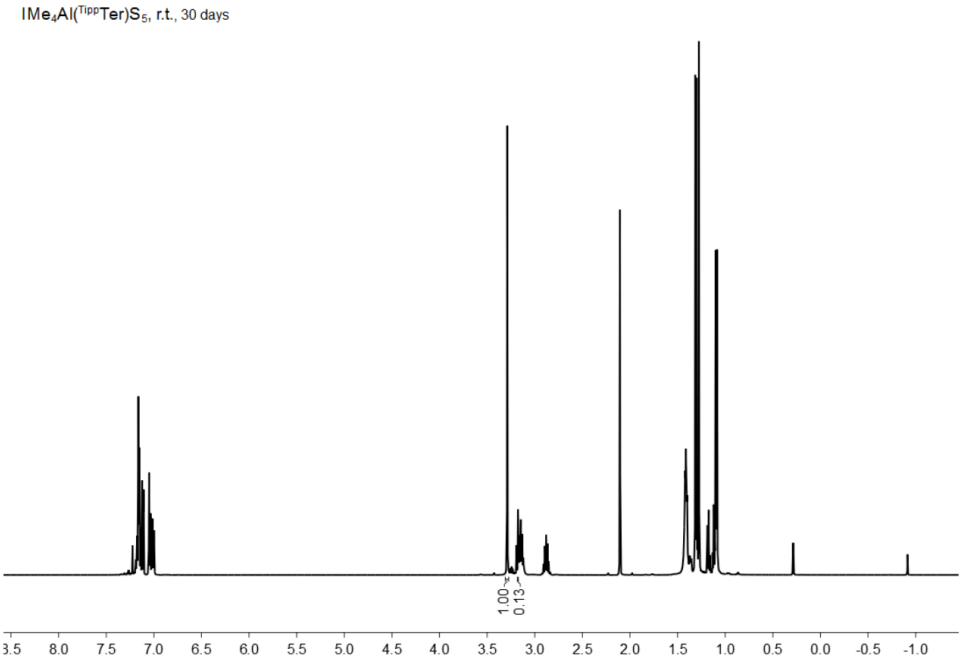

Figure S5: ^1H NMR spectrum (400 MHz) of compound **4** (in r.t. after 30 days) in C_6D_6 at 300 K. [δ (silicone grease) = 0.29 ppm]

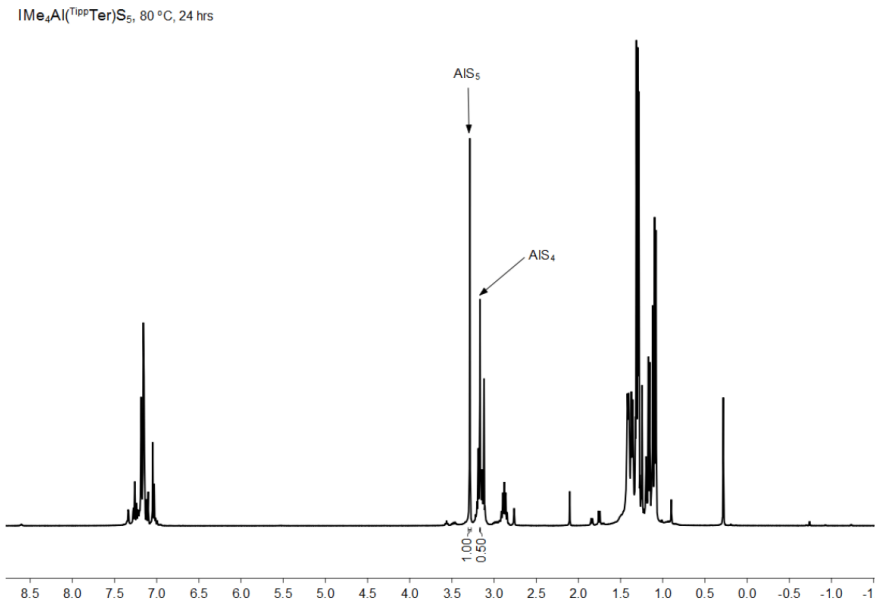

Figure S6: ^{1}H NMR spectrum (400 MHz) of compound **4** (in 80 °C after 24 hours) in C_6D_6 at 300 K. [δ (silicone grease) = 0.29 ppm]

2 Crystallographic Data

2.1 General considerations

The X-ray intensity data were collected on an X-ray single crystal diffractometer Bruker Photon CMOS system, with a rotating anode (Bruker TXS) with MoKα radiation (λ = 0.71073 Å) and a Helios mirror optic by using the APEX III software package or an IMS microsource with MoKα radiation (λ = 0.71073 Å) and a Helios mirror optic by using the APEX III software package.[S9] The measurement was performed on single crystals coated with perfluorinated ether. The crystal was fixed on the top of a microsampler, transferred to the diffractometer and frozen under a stream of cold nitrogen (100K). A matrix scan was used to determine the initial lattice parameters. Reflections were merged and corrected for Lorenz and polarization effects, scan speed, and background using SAINT.[S10] Absorption corrections, including odd and even ordered spherical harmonics were performed using SADABS.[S10] Space group assignments were based upon systematic absences, E statistics, and successful refinement of the structures. Structures were solved by direct methods with the aid of successive difference Fourier maps, and were refined against all data using the APEX III software[S9] in conjunction with SHELXL-2014[S11] and SHELXLE.[S12] Following hydrogen atoms could be found in the difference fourier maps and were allowed to refine freely: compound **1** H1, H2 and compound **5** H1. The following hydrogen atoms could be found in the difference fourier maps but needed to be fixed in ideal position for successful refinement: compound **2** H1, H2; compound **3** H1, H2; compound **8**, H1, H2. Methyl hydrogen atoms were refined as part of rigid rotating groups, with a C–H distance of 0.98 Å and Uiso(H) = 1.5·Ueq(C). Other H atoms were placed in calculated positions and refined using a riding model, with methylene and aromatic C–H distances of 0.99 and 0.95 Å, respectively, and Uiso(H) = 1.2·Ueq(C). If not mentioned otherwise, non-hydrogen atoms were refined with anisotropic displacement parameters. Full-matrix least-squares refinements were carried out by minimizing $\Delta w(Fo^2-Fc^2)^2$ with SHELXL-97[S13] weighting scheme. Neutral atom scattering factors for all atoms and anomalous dispersion corrections for the non-hydrogen atoms were taken from International Tables for Crystallography.[S14] Images of the crystal structures were generated by Platon and Mercury.[S15] The CCDC numbers CCDC-2118428 to CCDC-2118435 contain the supplementary crystallographic data for the structures **1** to **8**. These data can be obtained free of charge from the Cambridge Crystallographic Data Centre via https://www.ccdc.cam.ac.uk/structures/.

2.2 SC-XRD Analysis

2.2.1 Crystal Structure of $IMe_4Al(^{Tipp}Ter)H_2$ (Compound 1)

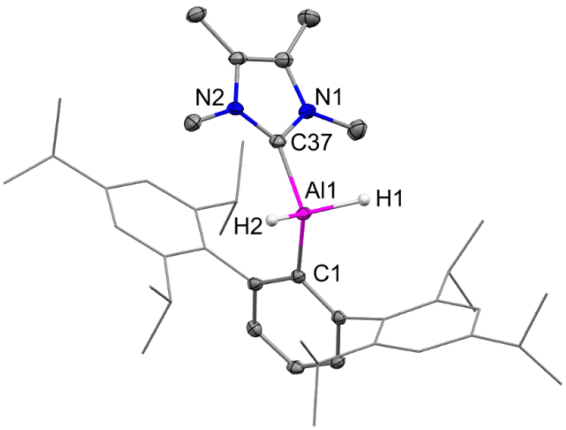

Figure S7: Molecular structures of compound **1** in the solid state. Ellipsoids are set at the 50% probability level; hydrogen atoms (except for selected H1 and H2) and co-crystallized solvent molecules are omitted for clarity. Selected bond lengths (Å) and angles (°): Al1-C1 2.0087(19), Al1-C37 2.0451(18), Al1-H1 1.53(2), Al1-H2 1.52(2), C1-Al1-C37 112.61(7), H1-Al1-H2 113.7(12).

2.2.2 Crystal Structure of IMe$_4$Al (^{Tipp}Ter)(SH)H (Compound 2)

Positional disorder of one Tipp substituent is addressed by refinement as two-component 60/40 disorder. The unit cell contains one disordered molecule of benzene which was treated as a diffuse contribution to the overall scattering without specific atom positions by SQUEEZE/PLATON.

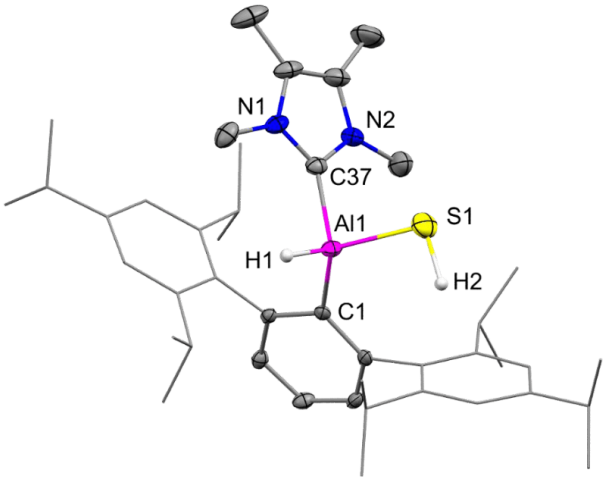

Figure S8: Molecular structures of compound **2** in the solid state. Ellipsoids are set at the 50% probability level; hydrogen atoms (except for selected H1 and H2) and co-crystallized solvent molecules are omitted for clarity. Selected bond lengths (Å) and angles (°): Al1-C37 2.053(3), Al1-C1 2.000(3), Al1-S1 2.2635(12), Al1-H1 1.61(3), S1-H2 1.42(4), C1-Al1-C37 111.74(11), H1-Al1-S1 111.7(10).

2.2.3 Crystal Structure of IMe$_4$Al (^{Tipp}Ter)(SH)$_2$ (Compound 3)

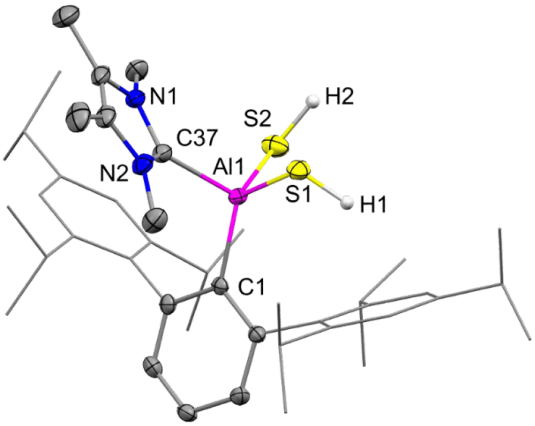

Figure S9: Molecular structures of compound **3** in the solid state. Ellipsoids are set at the 50% probability level; hydrogen atoms (except for selected H1 and H2) and co-crystallized solvent molecules are omitted for clarity. Selected bond lengths (Å) and angles (°): Al1-S1 2.2820(10), Al1-S2 2.2569(11), Al1-C37 2.054(3), Al-C1 2.004(3), S1-H1 1.29(2), S2-H2 1.34(3), C37-Al1-C1 110.59(11), S1-Al1-S2 107.47(4).

2.2.4 Crystal Structure of IMe_4Al ($^{Tipp}Ter)S_5$ (Compound 4)

The structure suffered from severe positional disorder in ligand framework and twinning. Disorder was addressed by expanded two-component disorder routine and the structure is refined as 4 component racemic twin, resulting in ambiguous Flack parameter. The unit cell contains 4 disordered molecules of THF which were treated as a diffuse contribution to the overall scattering without specific atom positions by SQUEEZE/PLATON.

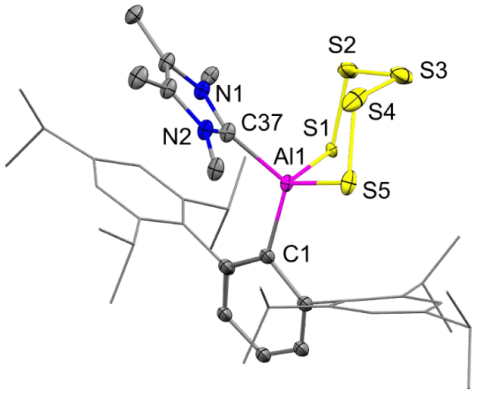

Figure S10: Molecular structures of compound **4** in the solid state. Ellipsoids are set at the 50% probability level; hydrogen atoms and co-crystallized solvent molecules are omitted for clarity. Selected bond lengths (Å) and angles (°): Al1-S1 2.273(4), Al1-S5 2.300(4), Al1-C37 2.017(9), Al1-C1 1.950(18), S1-S2 2.082(4), S2-S3 2.041(4), S3-S4 2.058(5), S4-S5 2.049(4), C37-Al1-C1 118.7(6), S1-Al1-S5 106.13(15).

2.2.5 Crystal Structure of [IMe_4Al ($^{Tipp}Ter)(S\text{-}cAAC^{Me}$)H] (Compound 5)

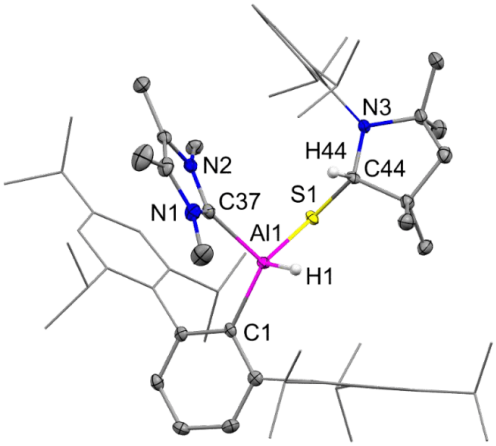

Figure S11: Molecular structures of compound **5** in the solid state. Ellipsoids are set at the 50% probability level; hydrogen atoms (except for selected H1 and H44) and co-crystallized solvent molecules are omitted for clarity. Selected bond lengths (Å) and angles (°): Al1-S1 2.2607(10), Al1-C37 2.069(3), Al-C1 2.013(2), S1-C44 1.882(2), Al1-H1 1.49(3), C37-Al1-C1 111.49(10), S1-Al1-H1 107.4(10), Al1-S1-C44 100.22(8).

2.2.6 Crystal Structure of IMe_4Al ($^{Tipp}Ter)S_4$ (Compound 6)

The structure is refined as 4 component racemic twin. The unit cell contains 4 disordered molecules of THF, which were treated as a diffuse contribution to the overall scattering without specific atom positions by SQUEEZE/PLATON.

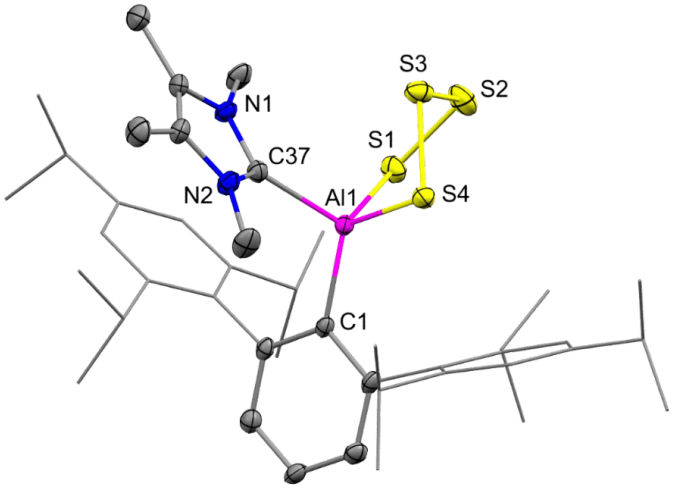

Figure S12: Molecular structures of compound **6** in the solid state. Ellipsoids are set at the 50% probability level; hydrogen atoms and co-crystallized solvent molecules are omitted for clarity. Selected bond lengths (Å) and angles (°): Al1-S1 2.300(2), Al1-S4 2.302(2), Al1-C37 2.062(6), Al1-C1 1.987(6), S1-S2 2.093(2), S2-S3 2.048(2), S3-S4 2.086(2), C37-Al1-C1 113.1(2), S1-Al1-S4 101.93(9).

2.2.7 Crystal Structure of [IMe$_4$Al (^{Tipp}Ter){SP(=S)C$_6$H$_4$OMe}$_2$] (Compound 7)

Positional disorder of lattice solvent (80/20), ligand frame work (80/20) and the S4P4-unti (94/6) is addressed by refinement as two-component disorder.

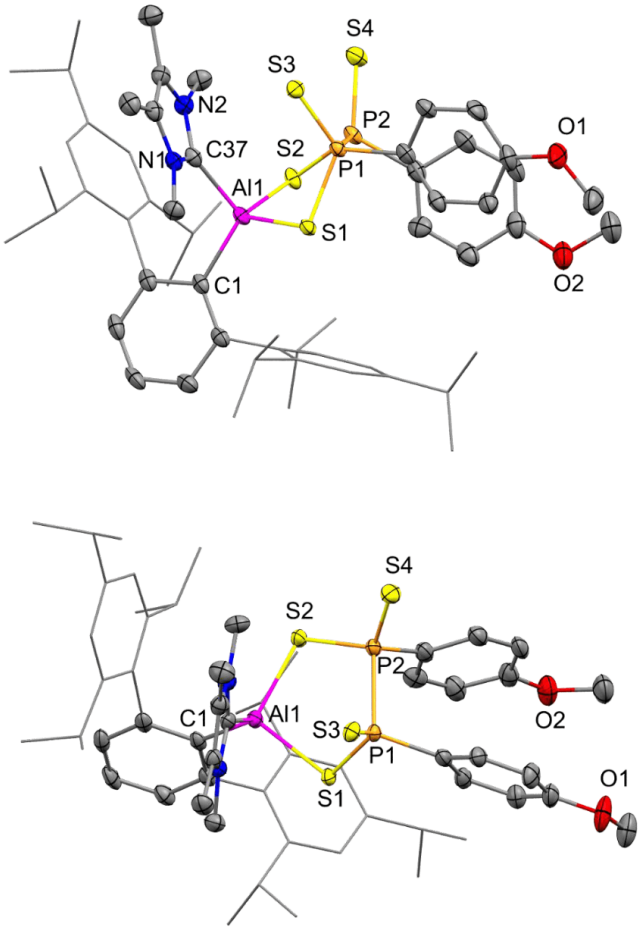

Figure S13: Molecular structure of compound **7** in the solid state (Side view and Top view). Ellipsoids are set at the 50% probability level; hydrogen atoms (except for selected H1) and co-crystallized solvent molecules are omitted for clarity. Selected bond lengths (Å) and angles (°): Al1-C37 2.032(3), Al1-C1 1.997(3), Al1-S2 2.2848(13), Al1-S1 2.2904(18), S1-P1 2.0584(18), S2-P2 2.0712(14), P1-P2 2.2694(11), P1-S3 1.9495(14), P2-S4 1.9580(16), C37-Al1-C1 112.85(12), S1-Al1-S2 99.60(6).

2.2.8 Crystal Structure of I*i*Pr$_2$Me$_2$Al(Tipp)(H)STMS (Compound 8)

The structure is refined as 2 component racemic twin.

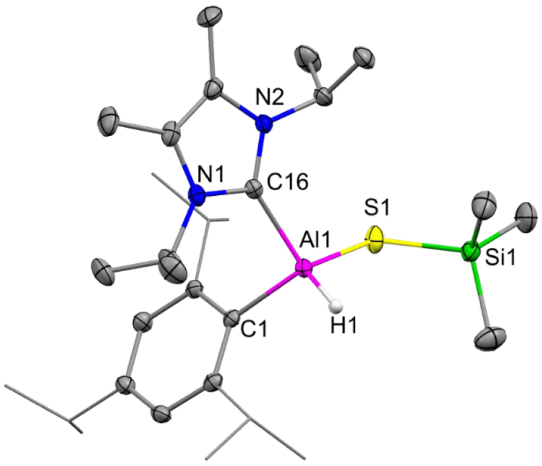

Figure S14: Molecular structure of compound 8 in the solid state. Ellipsoids are set at the 50% probability level; hydrogen atoms and co-crystallized solvent molecules are omitted for clarity. Selected bond lengths (Å) and angles (°): Al1-H1 1.4499(12), Al1-C16 2.086(3), Al1-C1 2.013(3), Al1-S1 2.2738(11), S1-Si1 2.1236(11), C1-Al1-C16 102.09(11), Si1-S1-Al1 107.71(5), S1-Al1-H1 111.35(6).

2.3 Crystal data and structure refinement for compound 1 - 8

Table S1. Crystal data and structure refinement for compound 1 - 8.

Compound #	1	2	3	4
CCDC-Number	2118428	2118429	2118430	2118431
Chemical formula	C43 H63 Al N2 (C5 H12)	C43 H63 Al N2 S	C43 H63 Al N2 S2	C43 H61 Al N2 S5
Formula weight	707.08 g/mol	666.99 g/mol	699.05 g/mol	793.262 g/mol
Temperature	100 K	100 K	100 K	100 K
Wavelength	0.71073 Å	0.71073 Å	0.71073 Å	0.71073 Å
Crystal size	0.282 x 0.250 x 0.133 mm	0.253 x 0.161 x 0.146 mm	0.231 x 0.155 x 0.131 mm	0.179 x 0.172 x 0.125 mm
Crystal habit	clear colorless fragment	clear colorless fragment	clear colorless fragment	clear colorless fragment
Crystal system	triclinic	monoclinic	tetragonal	monoclinic
Space group	P -1	P 21/n	P -4 21 c	P c
Unit cell dimensions	a = 11.1969(6) Å; α = 106.464(3)° b = 14.2845(8) Å; β = 103.258(2)° c = 15.4908(9) Å; γ = 98.382(2)°	a = 12.5633(9) Å; α = 90° b = 16.2067(11) Å; β = 100.932(3)° c = 21.7104(14) Å; γ = 90°	a = 23.8686(13) Å; α = 90° b = 23.8686(13) Å; β = 90° c = 14.9681(10) Å; γ = 90°	a = 19.110(3) Å; α = 90° b = 14.8919(19) Å; β = 92.292(4)° c = 18.479(2) Å; γ = 90°
Volume	2253.0(2) Å³	4340.2(5) Å³	8527.5(11) Å³	5254.6(12) Å³
Z	2	4	8	4
Density (calculated)	1.042 g/cm³	1.021 g/cm³	1.089 g/cm³	1.003 g/cm³
Radiation source	IMS microsource	IMS microsource	IMS microsource	IMS microsource
Theta range for data collection	2.04 to 25.35°	2.06 to 25.35°	2.18 to 25.35°	2.03 to 25.35°
Index ranges	-13<=h<=13, -17<=k<=17, -18<=l<=18	-15<=h<=15, -19<=k<=19, -26<=l<=26	-28<=h<=28, -28<=k<=28, -18<=l<=18	-23<=h<=23, -17<=k<=17, -22<=l<=22
Reflections collected	66983	168677	341330	191634
Independent reflections	8237	7943	7793	19225
Completeness	0.997	1.000	0.998	0.999
Absorption correction	Multi-Scan	Multi-Scan	Multi-Scan	Multi-Scan
Max. and min. transmission	0.7452 and 0.6878	0.7452 and 0.6991	0.7448 and 0.7153	0.7087 and 0.6512
Refinement method	Full-matrix least-squares on F^2	Full-matrix least-squares on F^2	Full-matrix least-squares on F^2	Full-matrix least-squares on F^2
Function minimized	$\Sigma w(F_o^2 - F_c^2)^2$	$\Sigma w(F_o^2 - F_c^2)^2$	$\Sigma w(F_o^2 - F_c^2)^2$	$\Sigma w(F_o^2 - F_c^2)^2$
Data / restraints / parameters	7943 / 569 / 590	16712 / 658 / 1151	7793 / 2 / 457	19225 / 3194 / 1711
Goodness-of-fit on F^2	1.093	1.147	1.115	1.031
Final R indices [I>2sigma(I)]	R1 = 0.0497, wR2 = 0.1078	R1 = 0.0743, wR2 = 0.1617	R1 = 0.0344, wR2 = 0.0950	R1 = 0.0885, wR2 = 0.2211
R indices (all data)	R1 = 0.0609, wR2 = 0.1132	R1 = 0.0809, wR2 = 0.1660	R1 = 0.0355, wR2 = 0.0957	R1 = 0.1009, wR2 = 0.2312
Largest diff. peak and hole	0.466 and -0.318 eÅ^{-3}	0.781 and -0.945 eÅ^{-3}	0.701 and -0.401 eÅ^{-3}	0.662 and -1.005 eÅ^{-3}

16

Compound #	5	6	7	8
CCDC-Number	2118432	2118433	2118434	2118435
Chemical formula	C63 H94 Al N3 S	C43 H61 Al N2 S4	C57 H75 Al N2 O2 P2 S4 $(C7 H8)_3$	C29 H53 Al N2 S Si
Formula weight	952.45 g/mol	761.16 g/mol	1313.75 g/mol	516.86 g/mol
Temperature	100 K	100 K	150.00(10) K	100 K
Wavelength	0.71073 Å	0.71073 Å	0.71073 Å	0.71073 Å
Crystal size	0.196 x 0.193 x 0.070 mm	0.293 x 0.256 x 0.162 mm	0.436 x 0.230 x 0.087 mm	0.315 x 0.279 x 0.144 mm
Crystal habit	clear colorless fragment	clear yellow block	clear colorless block	clear colorless fragment
Crystal system	monoclinic	monoclinic	triclinic	orthorhombic
Space group	P 21/c	P 21/c	P -1	P c a 21
Unit cell dimensions	a = 17.0758(11) Å; α = 90° b = 13.5333(8) Å; β = 102.715(2)° c = 25.9950(15) Å; γ = 90°	a = 14.881(2) Å; α = 90° b = 18.635(3) Å; β = 97.491(4)° c = 37.232(5) Å; γ = 90°	a = 16.6769(8) Å; α = 104.580(2)° b = 16.6832(8) Å; β = 102.386(2)° c = 16.7584(8) Å; γ = 118.979(2)°	a = 18.4096(10) Å; α = 90° b = 17.3121(8) Å; β = 90° c = 20.3593(11) Å; γ = 90°
Volume	5859.9(6) Å³	10237(3) Å³	3622.4(3) Å³	6488.7(6) Å³
Z	4	8	2	8
Density (calculated)	1.080 g/cm³	0.988 g/cm³	1.204 g/cm³	1.058 g/cm³
Radiation source	IMS microsource	TXS rotating anode	IMS microsource	TXS rotating anode
Theta range for data collection	1.94 to 25.35°	1.90 to 25.20°	2.41 to 25.38°	2.21 to 25.35°
Index ranges	-20<=h<=20, -16<=k<=16, -31<=l<=31	-17<=h<=17, -16<=k<=22, -44<=l<=44	-20<=h<=20, -20<=k<=20, -20<=l<=20	-22<=h<=22, -20<=k<=20, -24<=l<=24
Reflections collected	122785	159362	102400	154669
Independent reflections	10738	18352	13287	11890
Completeness	1.000	0.979	0.998	0.999
Absorption correction	Multi-Scan	Multi-Scan	Multi-Scan	Multi-Scan
Max. and min. transmission	0.7452 and 0.7158	0.7452 and 0.6404	0.7452 and 0.7032	0.7452 and 0.7132
Refinement method	Full-matrix least-squares on F^2	Full-matrix least-squares on F^2	Full-matrix least-squares on F^2	Full-matrix least-squares on F^2
Function minimized	$\Sigma w(F_o^2 - F_c^2)^2$	$\Sigma w(F_o^2 - F_c^2)^2$	$\Sigma w(F_o^2 - F_c^2)^2$	$\Sigma w(F_o^2 - F_c^2)^2$
Data / restraints / parameters	10738 / 0 / 641	18352 / 576 / 932	13287 / 795 / 1085	11890 / 3 / 648
Goodness-of-fit on F^2	1.205	1.039	1.064	1.010
Final R indices [I>2sigma(I)]	R1 = 0.0670, wR2 = 0.1218	R1 = 0.0966, wR2 = 0.2482	R1 = 0.0516, wR2 = 0.1223	R1 = 0.0356, wR2 = 0.0992
R indices (all data)	R1 = 0.0776, wR2 = 0.1258	R1 = 0.1058, wR2 = 0.2558	R1 = 0.0632, wR2 = 0.1284	R1 = 0.0369, wR2 = 0.1006
Largest diff. peak and hole	0.294 and -0.294 eÅ^{-3}	1.559 and -0.586 eÅ^{-3}	0.732 and -0.429 eÅ^{-3}	0.996 and -0.519 eÅ^{-3}

17

3 NMR Spectra

3.1 NMR spectra of IMe_4Al ($^{Tipp}Ter)H_2$ (Compound 1)

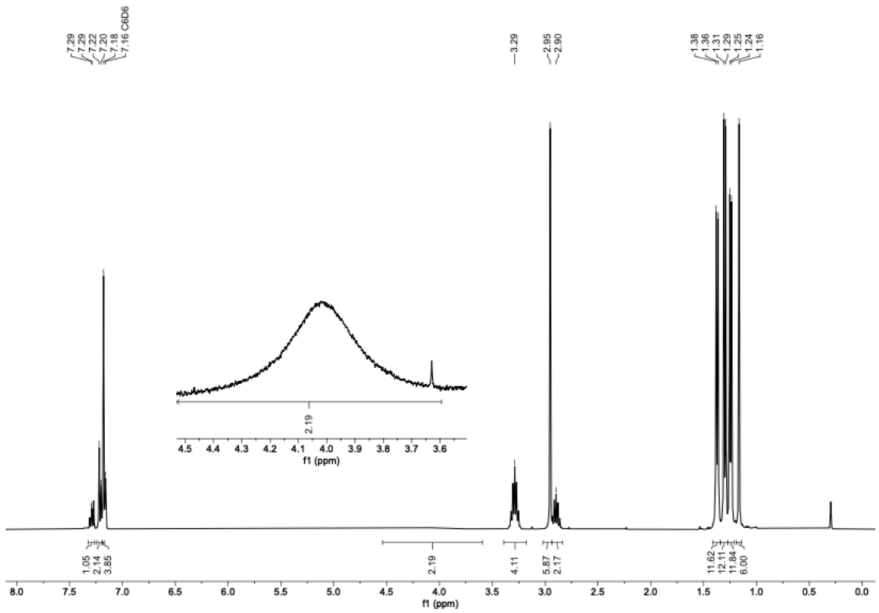

Figure S15: ^{1}H NMR spectrum (400 MHz) of compound **1** in C_6D_6 at 300 K. [δ (silicone grease) = 0.29 ppm]

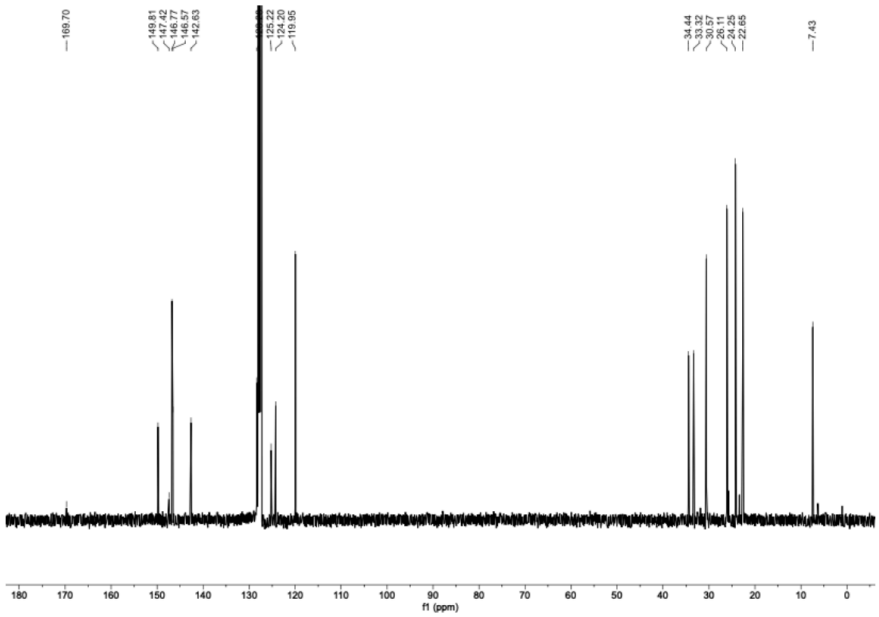

Figure S16: $^{13}C\{^{1}H\}$ NMR spectrum (101 MHz) of compound **1** in C_6D_6 at 300 K.

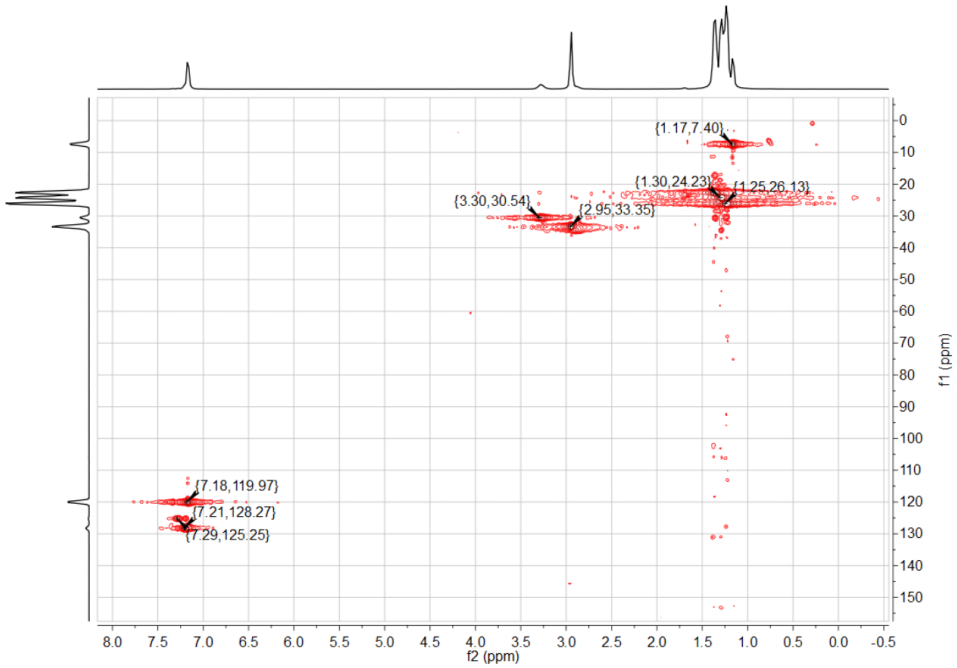

Figure S17: $^{1}H/^{13}C$ HSQC spectrum of compound **1** in C_6D_6 at 300 K.

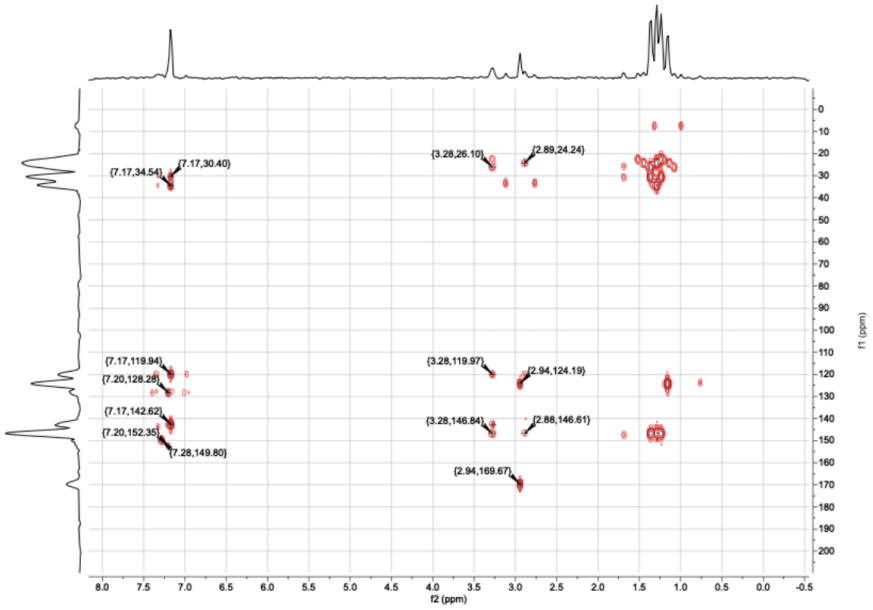

Figure S18: $^{1}H/^{13}C$ HMBC spectrum of compound **1** in C_6D_6 at 300 K.

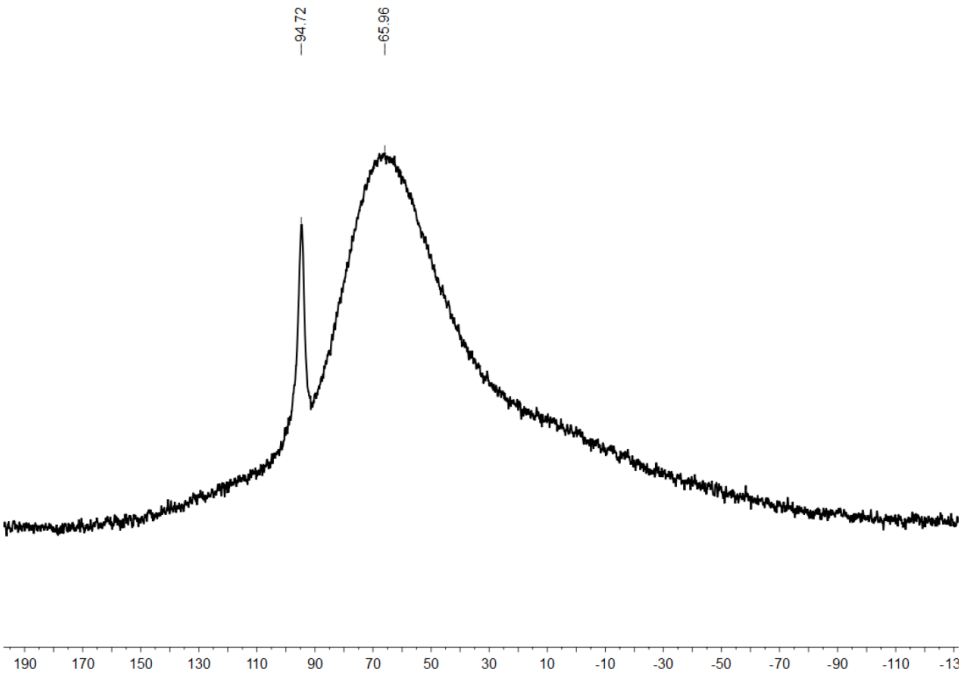

Figure S19: $^{27}Al\{^{1}H\}$ NMR spectrum (78 MHz) of compound **1** in C_6D_6 at 300 K.

3.2 NMR spectra of $IMe_4Al(^{Tipp}Ter)(SH)H$ (Compound 2)

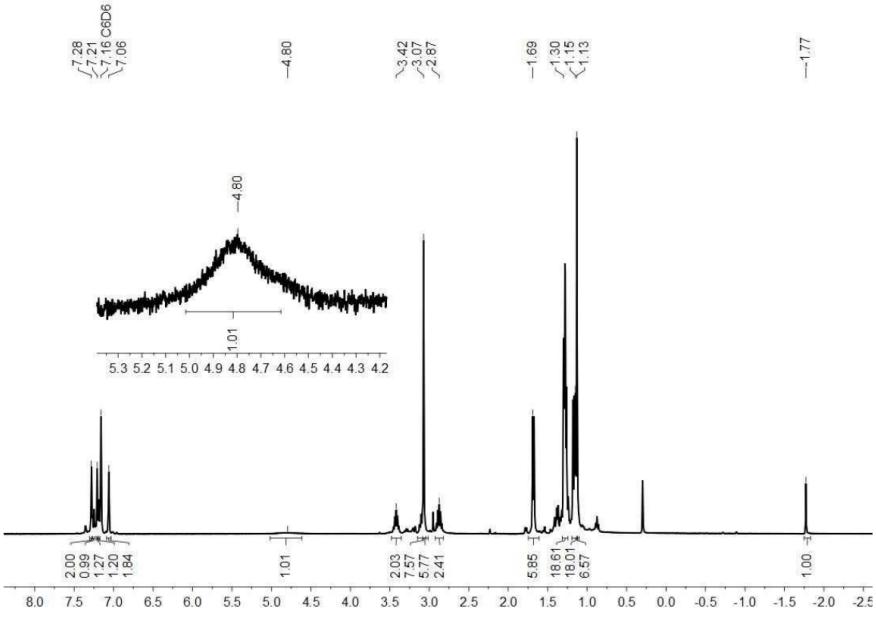

Figure S20: ^{1}H NMR spectrum (400 MHz) of compound **2** in C_6D_6 at 300 K. [δ (silicone grease) = 0.29 ppm]

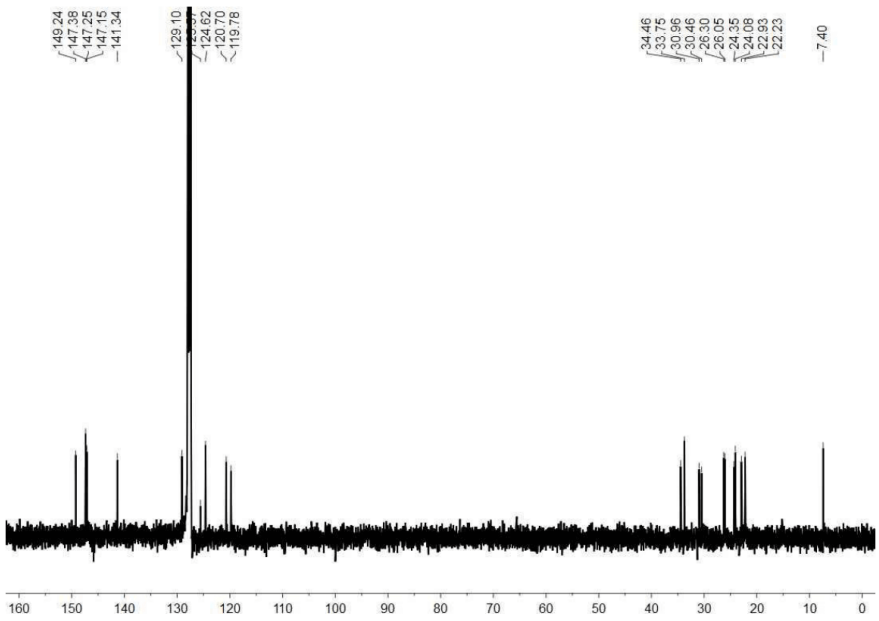

Figure S21: $^{13}C\{^{1}H\}$ NMR spectrum (101 MHz) of compound **2** in C_6D_6 at 300 K.

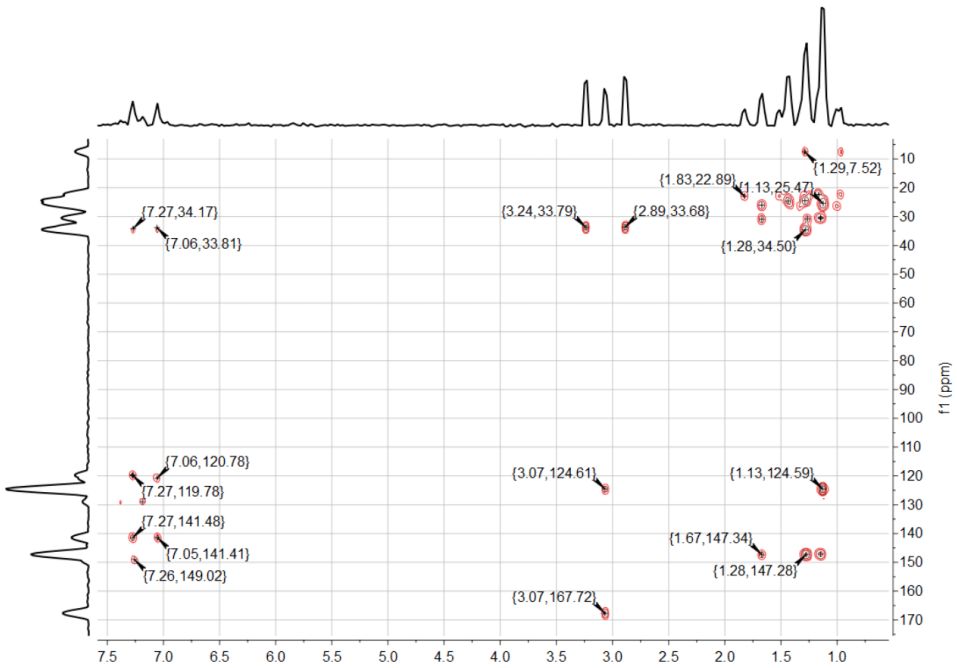

Figure S22: $^{1}H/^{13}C$ HMBC spectrum of compound **2** in C_6D_6 at 300 K.

3.3 NMR Spectra of $IMe_4Al(^{Tipp}Ter)(SH)_2$ (Compound 3)

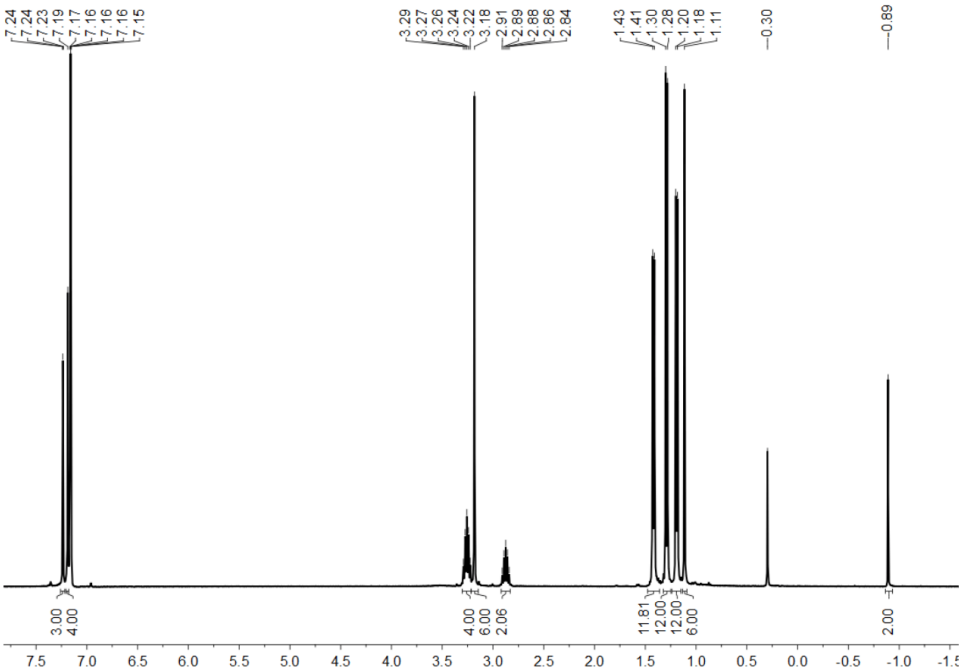

Figure S23: ^{1}H NMR spectrum (400 MHz) of compound **3** in C_6D_6 at 300 K. [δ (silicone grease) = 0.30 ppm]

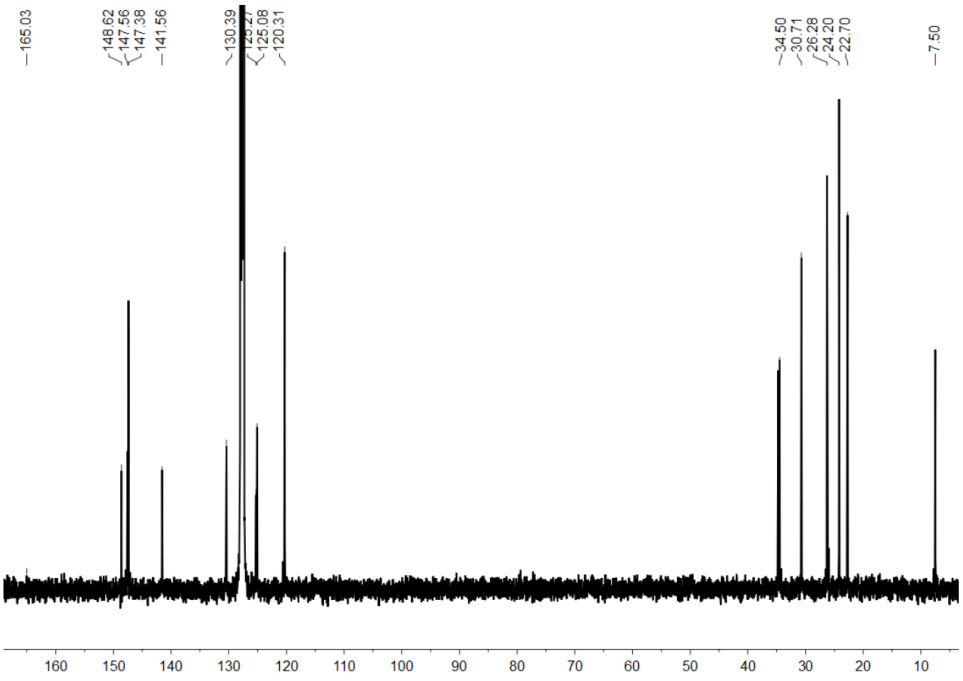

Figure S24: $^{13}C\{^{1}H\}$ NMR spectrum (101 MHz) of compound **3** in C_6D_6 at 300 K.

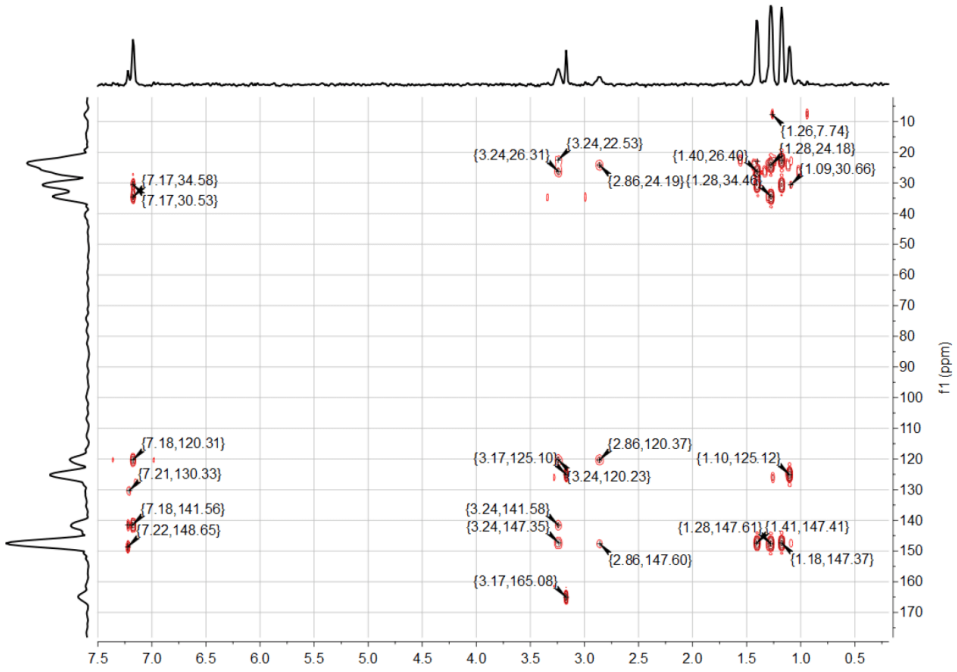

Figure S25: $^{1}H/^{13}C$ HMBC spectrum of compound **3** in C_6D_6 at 300 K.

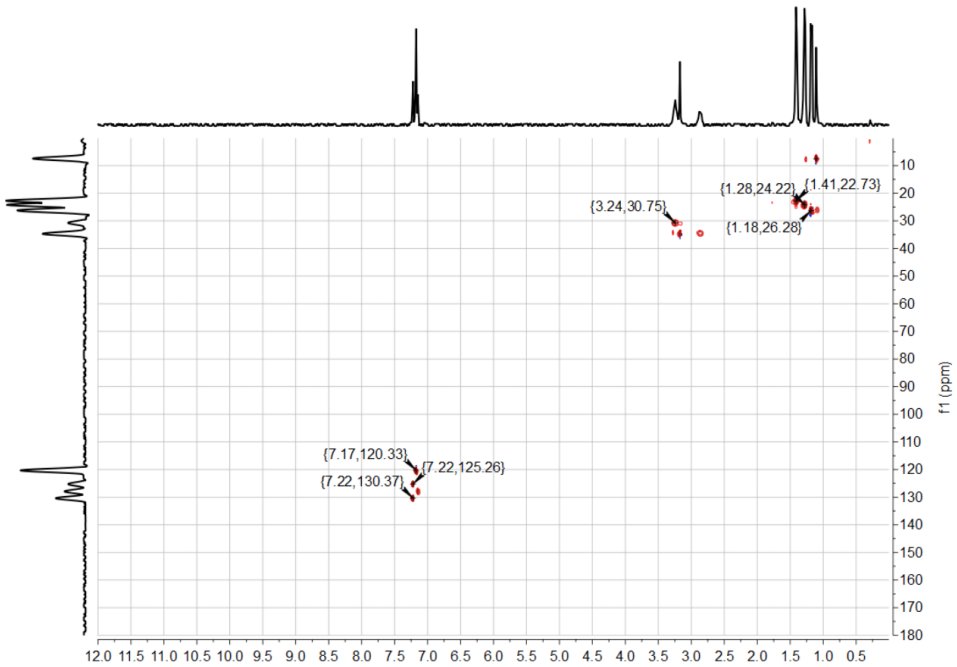

Figure S26: $^{1}H/^{13}C$ HSQC spectrum of compound **3** in C_6D_6 at 300 K.

3.4 NMR Spectra of $IMe_4Al(^{Tipp}Ter)S_5$ (Compound 4)

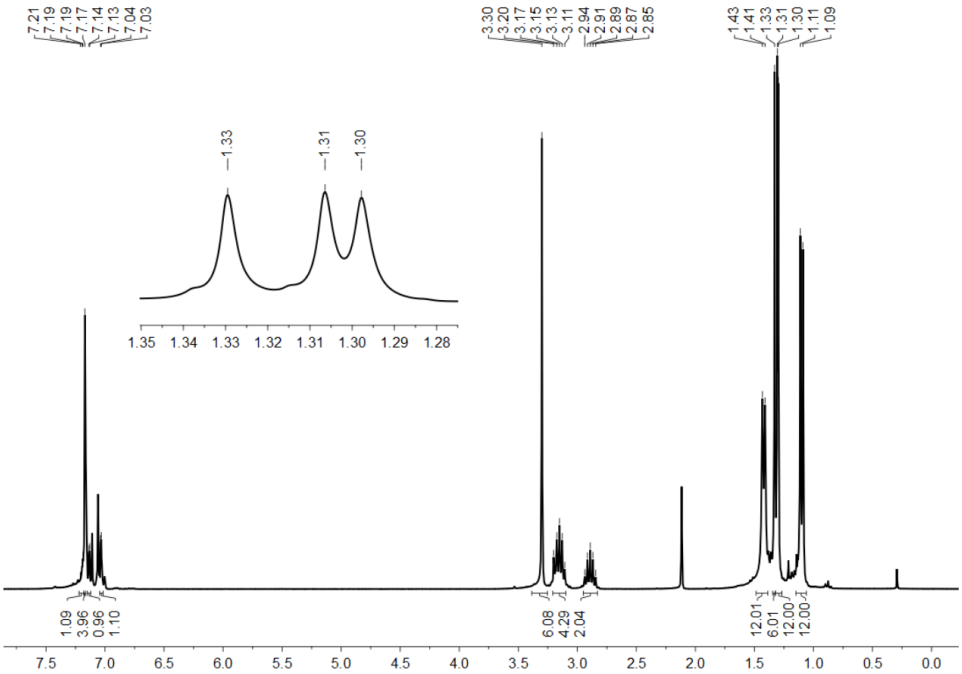

Figure S27: ^{1}H NMR spectrum (400 MHz) of compound **4** in C_6D_6 at 300 K. [δ (silicone grease) = 0.29 ppm]

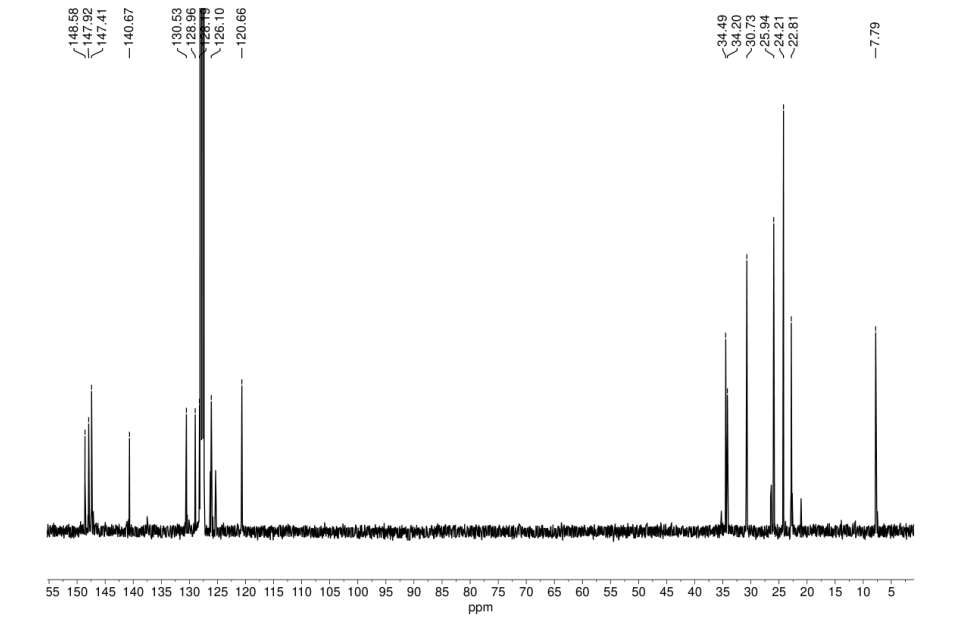

Figure S28: $^{13}C\{^{1}H\}$ NMR spectrum (101 MHz) of compound **4** in C_6D_6 at 300 K.

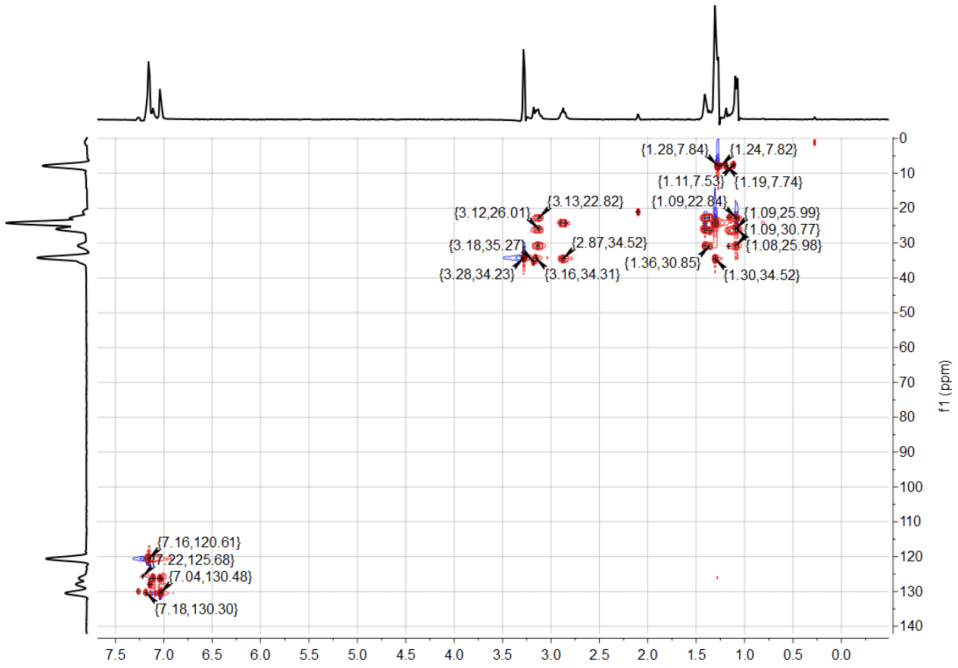

Figure S29: $^{1}H/^{13}C$ HSQC spectrum of compound **4** in C_6D_6 at 300 K.

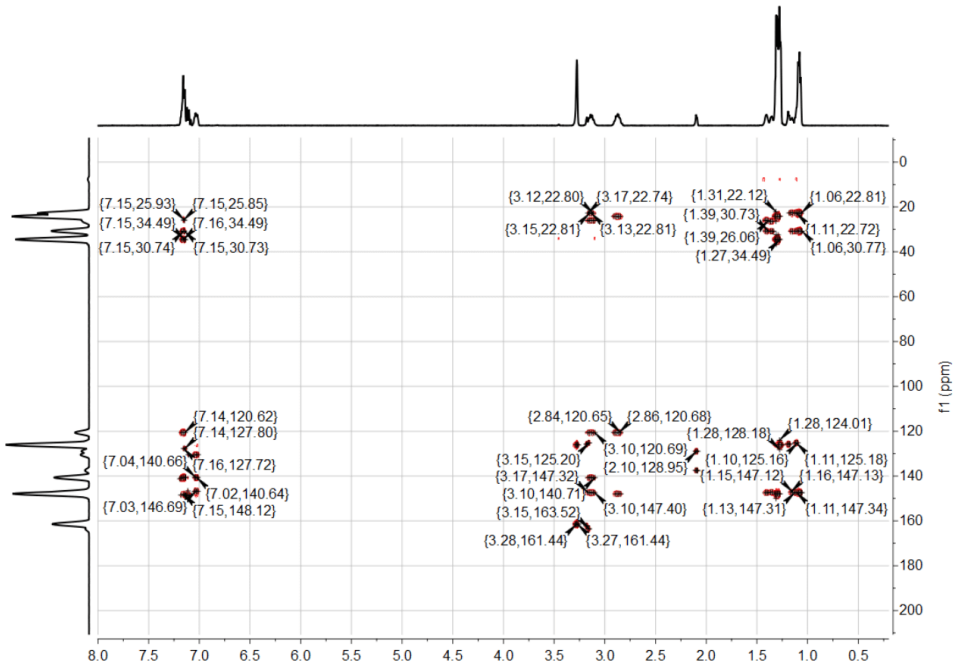

Figure S30: $^{1}H/^{13}C$ HMBC spectrum of compound **4** in C_6D_6 at 300 K.

3.5 NMR Spectra of [IMe$_4$Al (^{Tipp}Ter)(S-cAAC^{Me})H] (Compound 5)

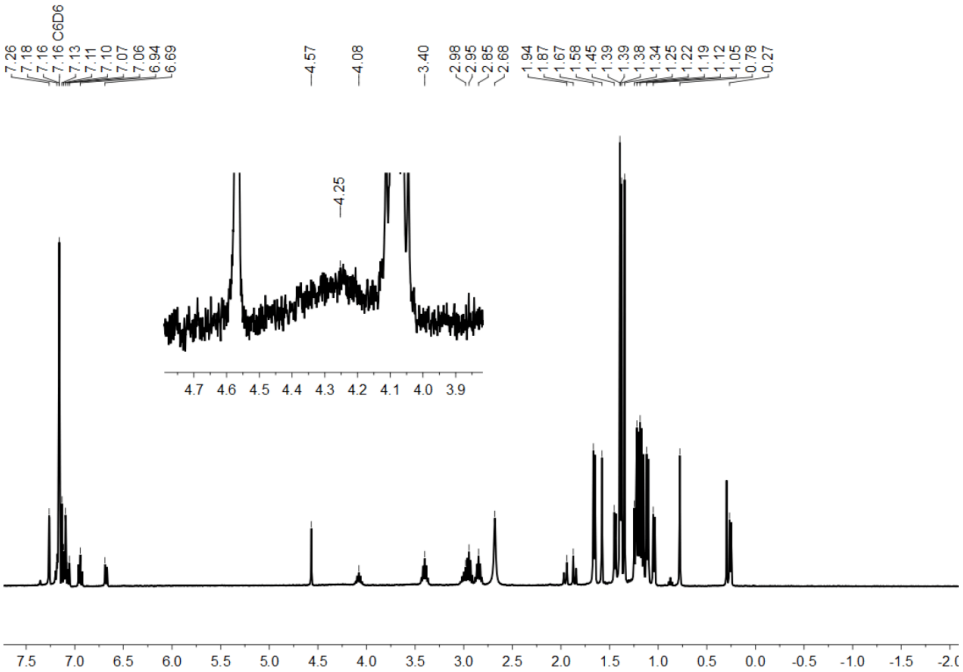

Figure S31: ^{1}H NMR spectrum (400 MHz) of compound **5** in C_6D_6 at 300 K. [δ (silicone grease) = 0.29 ppm]

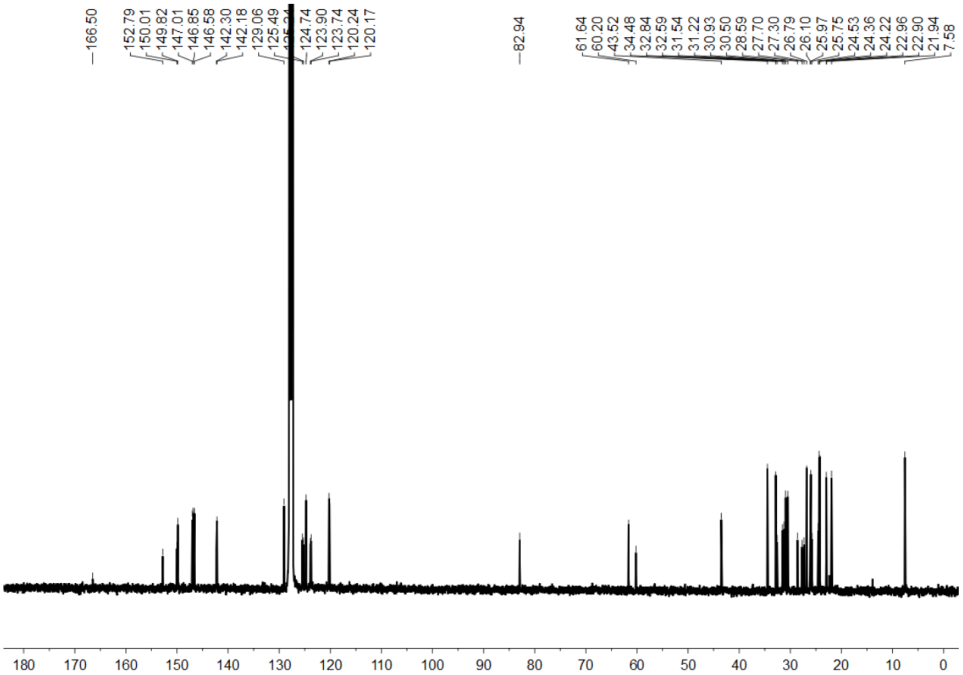

Figure S32: $^{13}C\{^1H\}$ NMR spectrum (101 MHz) of compound **5** in C_6D_6 at 300 K.

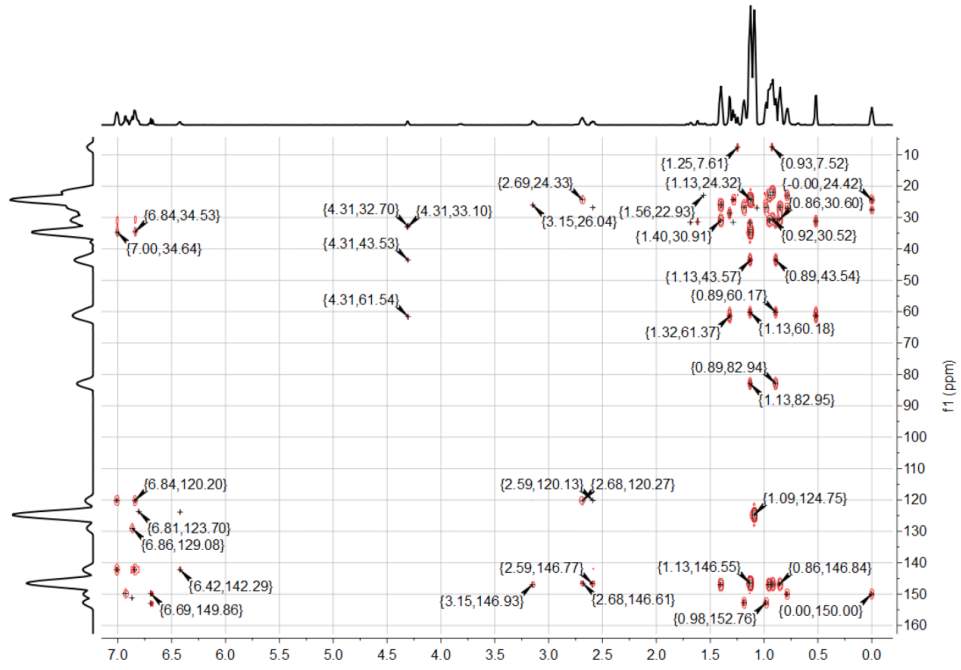

Figure S33: $^{1}H/^{13}C$ HMBC spectrum of compound **5** in C_6D_6 at 300 K.

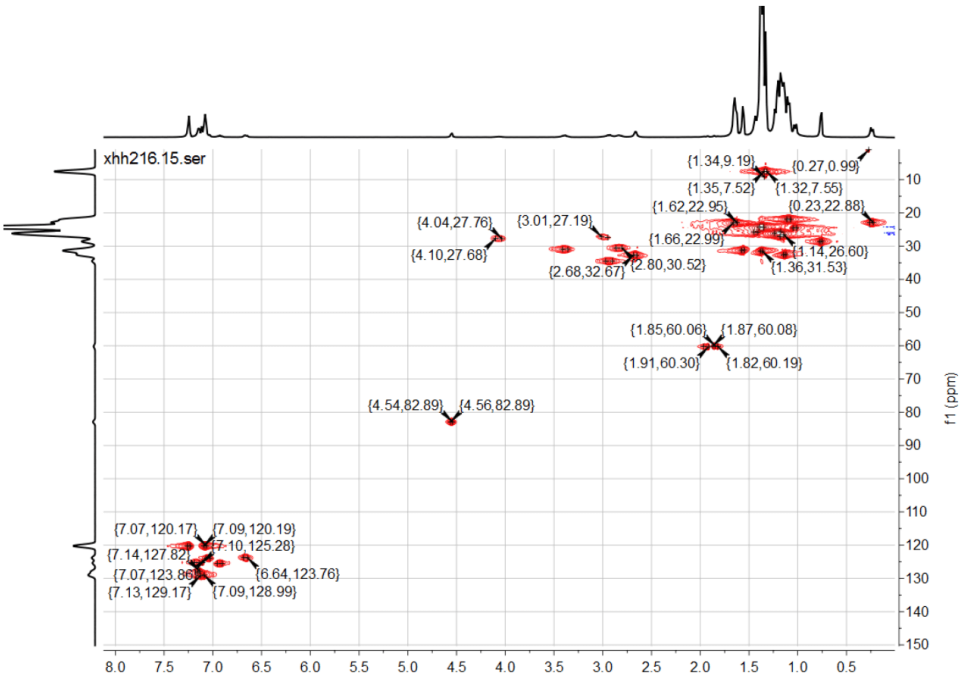

Figure S34: $^{1}H/^{13}C$ HSQC spectrum of compound **5** in C_6D_6 at 300 K.

3.6 NMR Spectra of IMe_4Al ($^{Tipp}Ter)S_4$ (Compound 6)

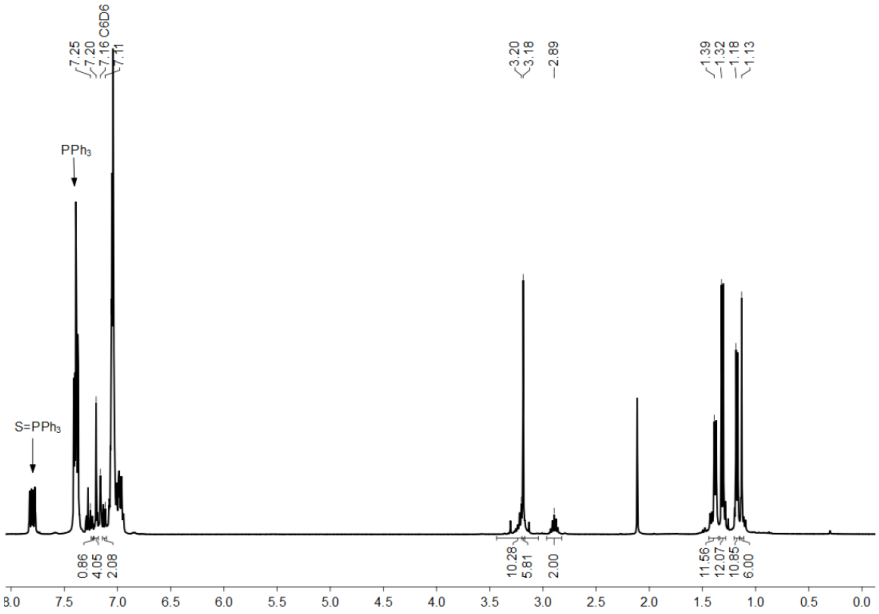

Figure S35: ^{1}H NMR spectrum (400 MHz) of compound **6** in C_6D_6 at 300 K. [δ (silicone grease) = 0.29 ppm]. Impurities such as PPh_3 and $S{=}PPh_3$ are marked.

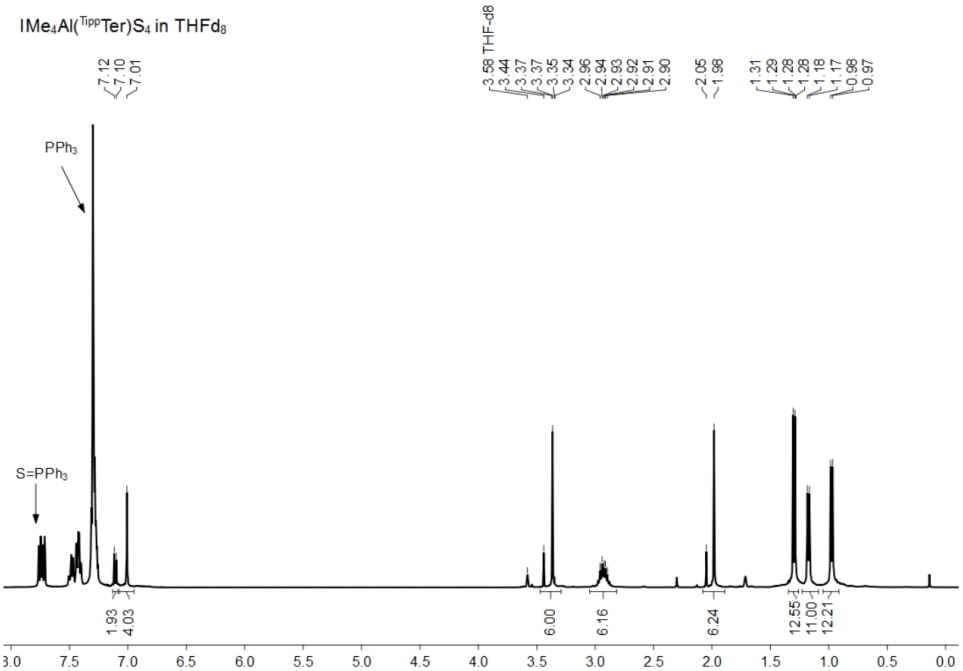

Figure S36: ^{1}H NMR spectrum (400 MHz) of compound **6** in $THFd_8$ at 300 K. [δ (silicone grease) = 0.11 ppm]. Impurities such as PPh_3 and $S{=}PPh_3$ are marked.

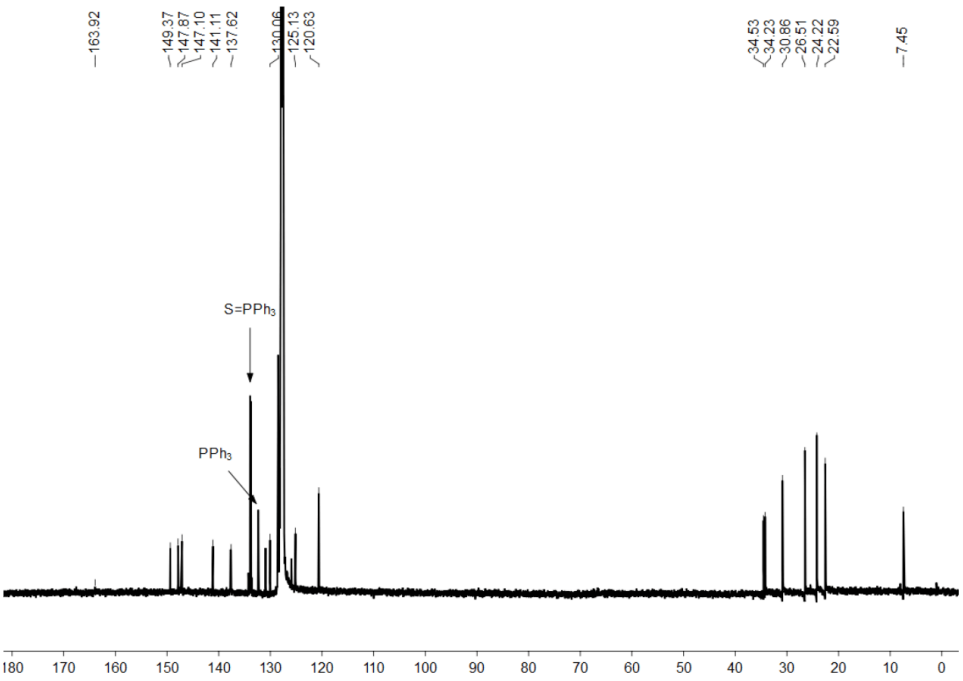

Figure S37: $^{13}C\{^{1}H\}$ NMR spectrum (126 MHz) of compound **6** in C_6D_6 at 300 K.

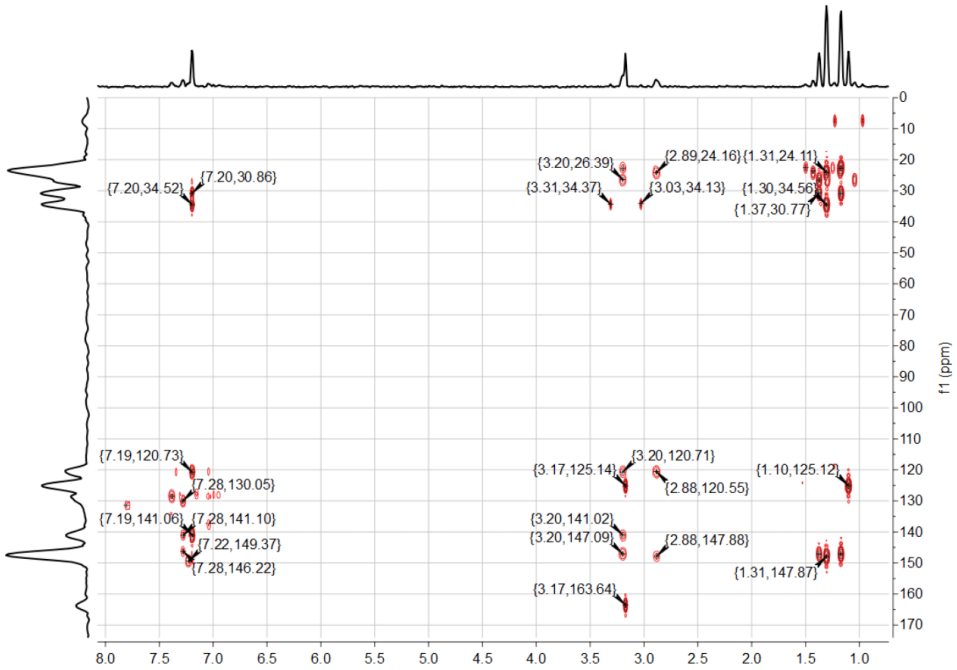

Figure S38: $^{1}H/^{13}C$ HMBC spectrum of compound **6** in C_6D_6 at 300 K.

3.7 NMR Spectra of [IMe$_4$Al (^{Tipp}Ter){SP(=S)C$_6$H$_4$OMe}$_2$] (Compound 7)

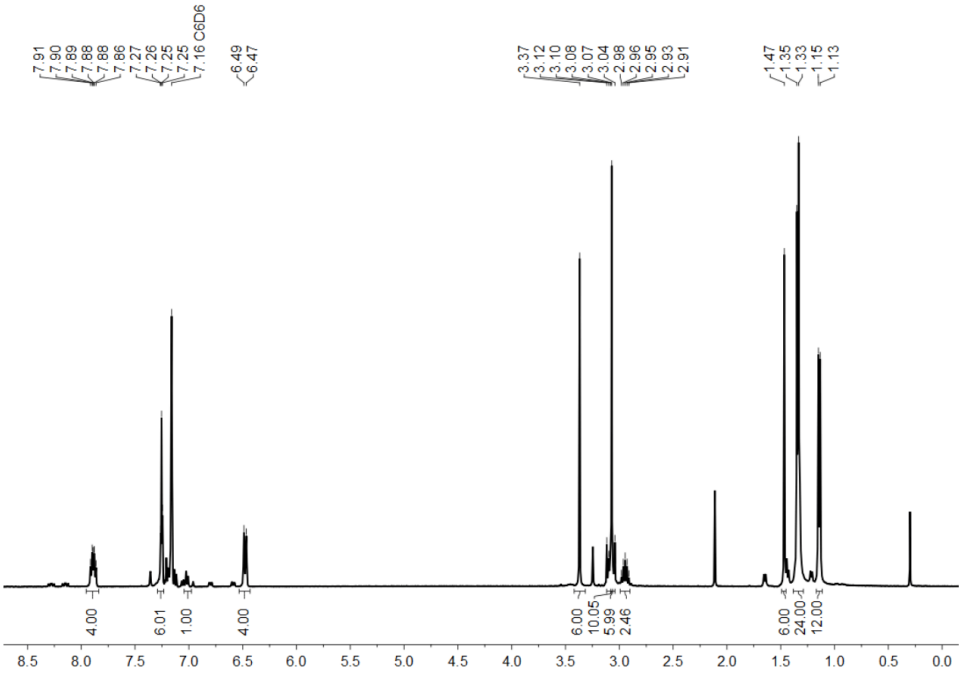

Figure S39: ^{1}H NMR spectrum (400 MHz) of compound **7** in C_6D_6 at 300 K. [δ (silicone grease) = 0.29 ppm]

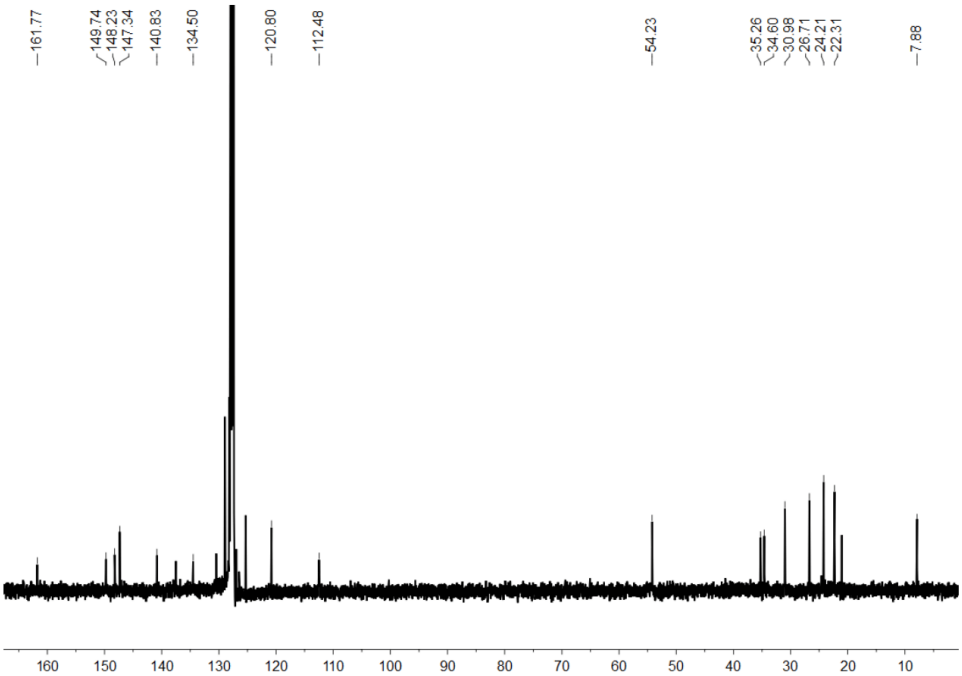

Figure S40: ^{13}C{^{1}H}NMR spectrum (101 MHz) of compound **7** in C_6D_6 at 300 K.

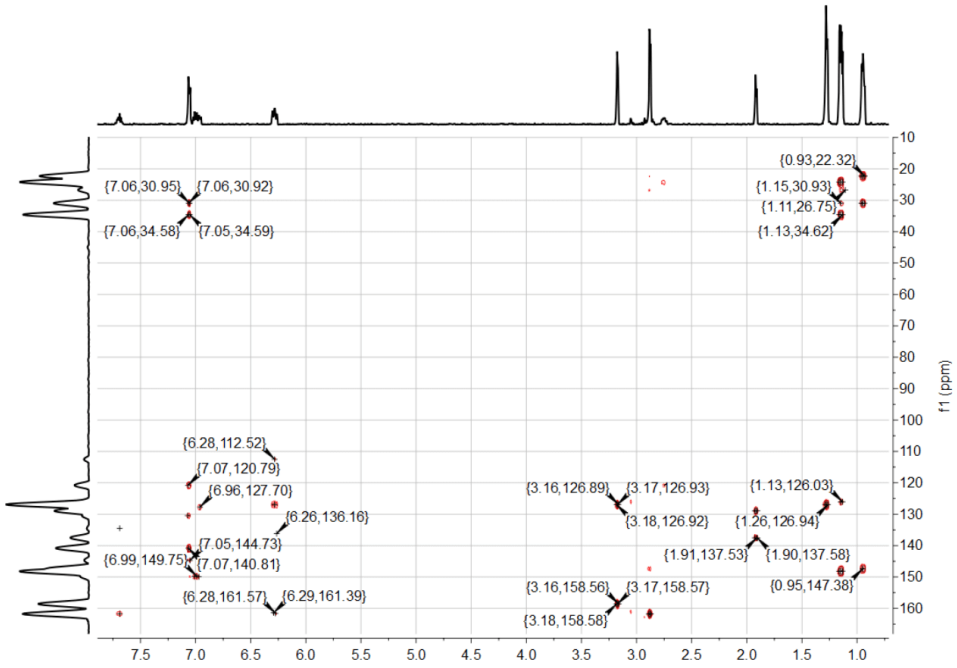

Figure S41: $^{1}H/^{13}C$ HMBC spectrum of compound **7** in C_6D_6 at 300 K.

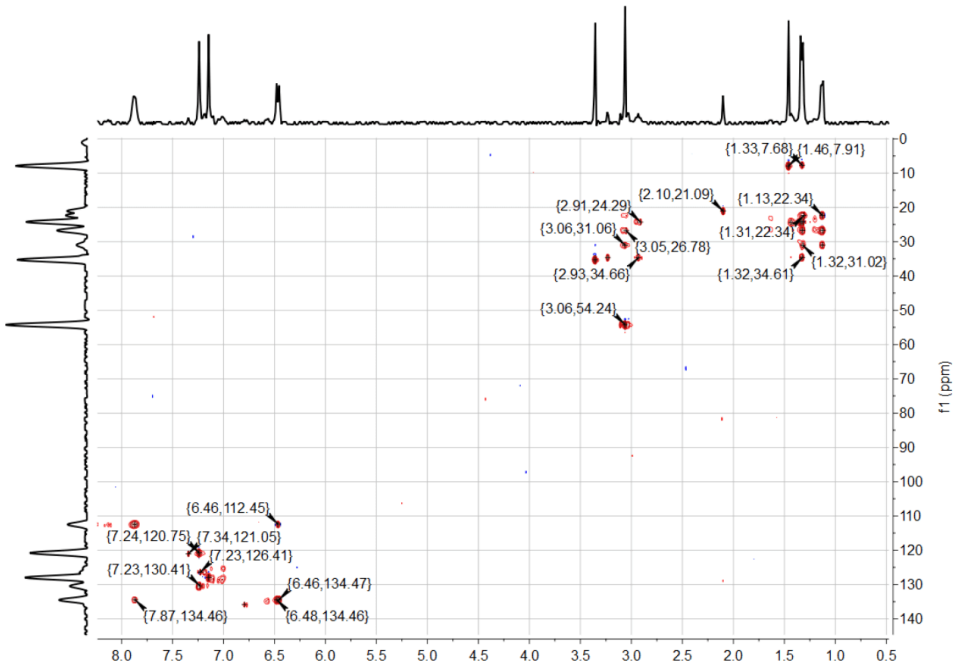

Figure S42: $^{1}H/^{13}C$ HSQC spectrum of compound **7** in C_6D_6 at 300 K.

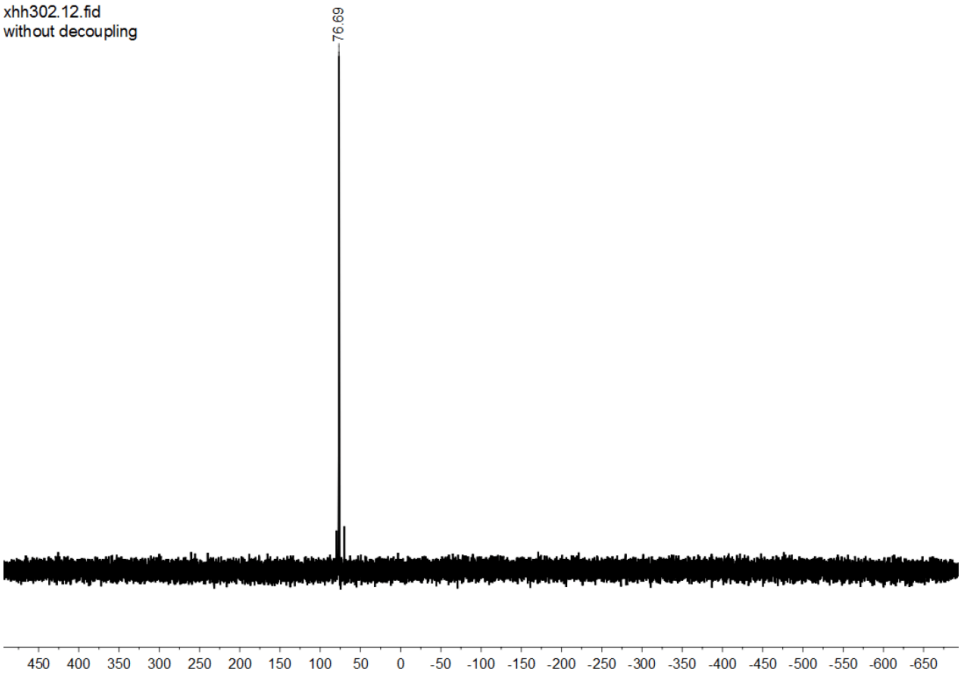

Figure S43: $^{31}P\{^{1}H\}$ NMR spectrum (162 MHz) of compound **7** in C_6D_6 at 300 K.

3.8 NMR Spectra of *i*Pr_2Me_2Al(Tipp)(H)STMS (Compound 8)

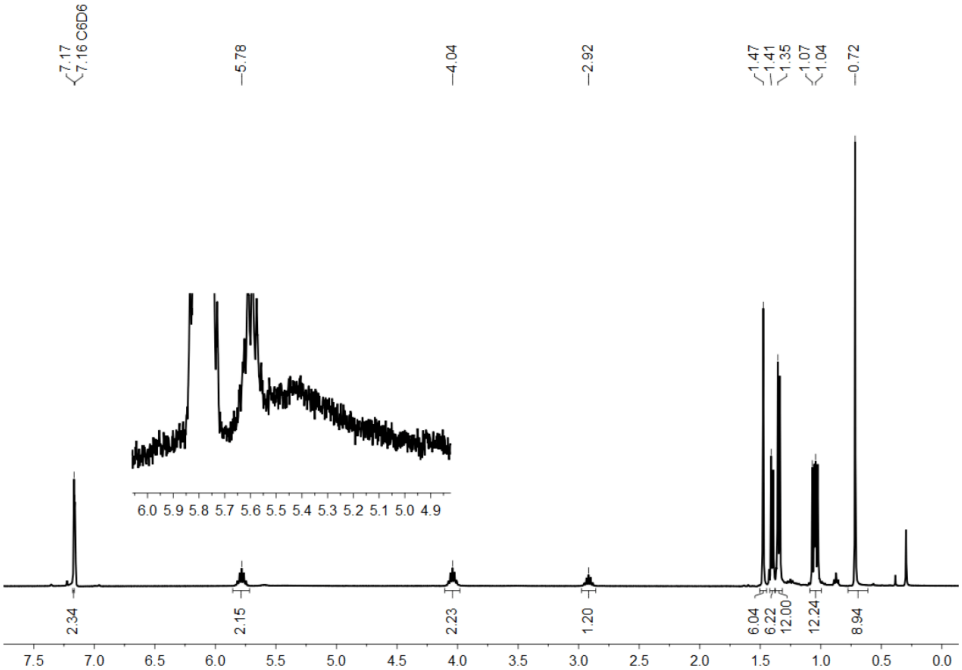

Figure S44: ^{1}H NMR spectrum (400 MHz) of compound **8** in C_6D_6 at 300 K. [δ (silicone grease) = 0.29 ppm]

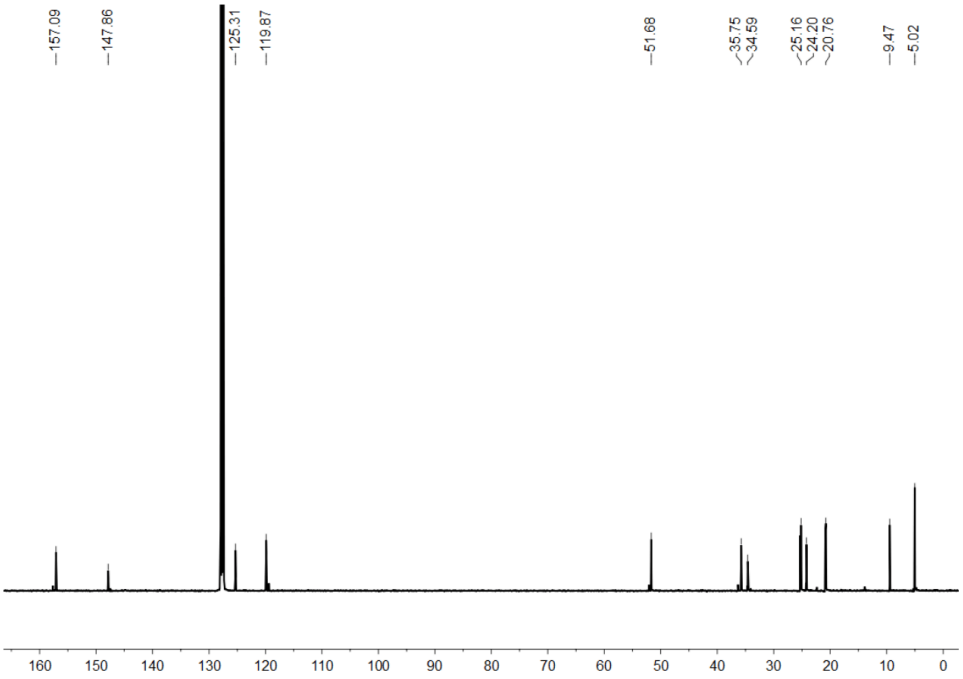

Figure S45: $^{13}C\{^{1}H\}$ NMR spectrum (101 MHz) of compound **8** in C_6D_6 at 300 K.

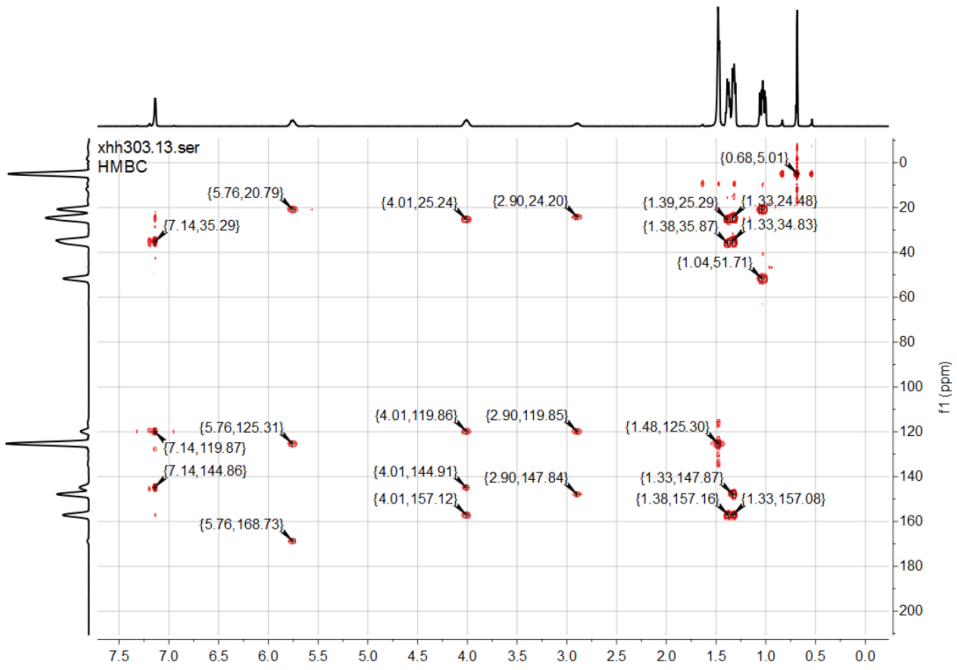

Figure S46: $^{1}H/^{13}C$ HMBC spectrum of compound **8** in C_6D_6 at 300 K.

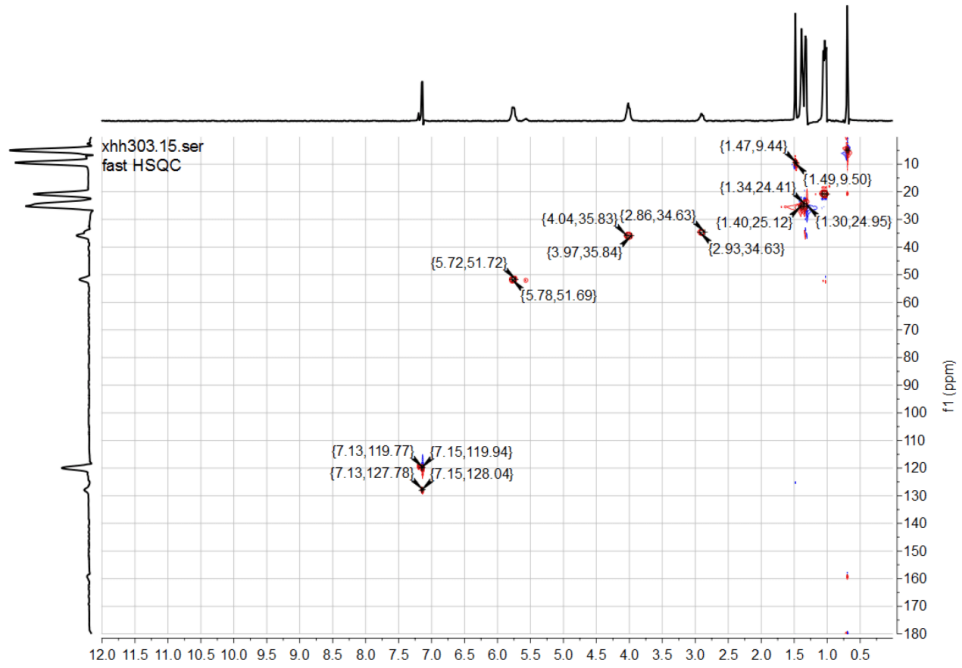

Figure S47: $^{1}H/^{13}C$ HSQC spectrum of compound **8** in C_6D_6 at 300 K.

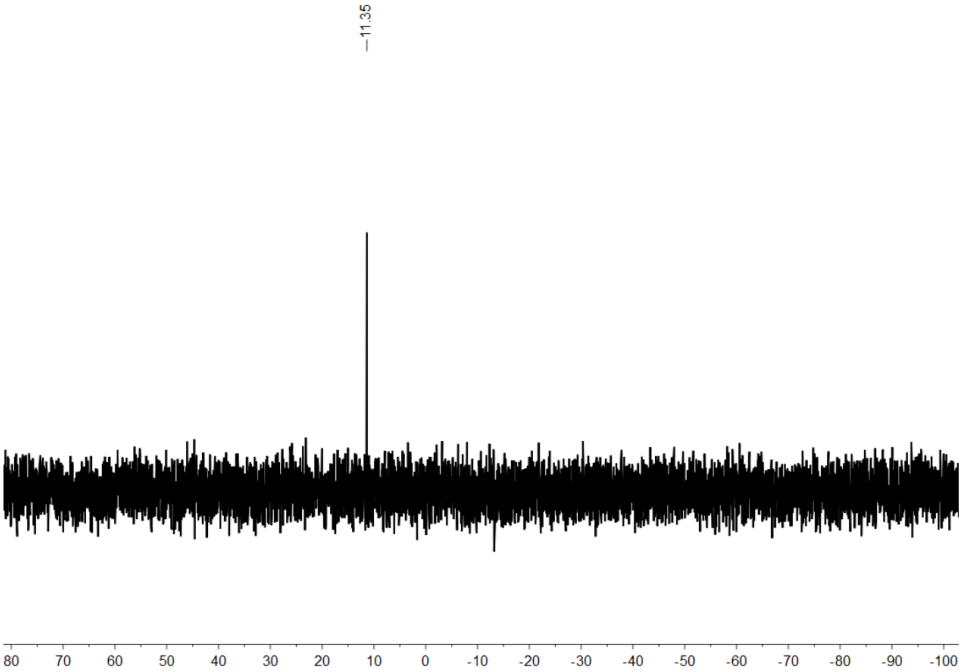

Figure S48: $^{29}Si\{^{1}H\}$ INEPT NMR spectrum (79 MHz) of compound **8** in C_6D_6 at 300 K.

4 Reference

[S1] C. Weetman, A. Porzelt, P. Bag, F. Hanusch, S. Inoue, *Chem. Sci.* **2020**, *11*, 4817-4827.

[S2] M. D. Francis, D. E. Hibbs, M. B. Hursthouse, C. Jones, N. A. Smithies, *J. Chem. Soc., Dalton Trans.* **1998**, 3249-3254.

[S3] C. Gerdes, W. Saak, D. Haase, T. Muller, *J. Am. Chem. Soc.* **2013**, *135*, 10353-10361.

[S4] V. Lavallo, Y. Canac, C. Präsang, B. Donnadieu, G. Bertrand, *Angew. Chem. Int. Ed.* **2005**, *44*, 5705-5709.

[S5] N. Kuhn, T. Kratz, *Synthesis*, **1993**, 561-562.

[S6] J. K. Ruff, M. F. Hawthorne, *J. Am. Chem. Soc.* **1960**, *82*, 2141-2144.

[S7] R. A. Bartlett, H. V. R. Dias, P. P. Power, *J. Organomet. Chem.* **1988**, *341*, 1-9.

[S8] D. Nieder, L. Klemmer, Y. Kaiser, V. Huch, D. Scheschkewitz, *Organometallics* **2018**, *37*, 632-635.

[S9] APEX suite of crystallographic software, APEX 3 version 2015.5-2; Bruker AXS Inc.: Madison, Wisconsin, USA, **2015.**

[S10] SAINT, Version 7.56a and SADABS Version 2008/1; Bruker AXS Inc.: Madison, Wisconsin, USA, **2008**.

[S11] G. M. Sheldrick, SHELXL-2014, University of Göttingen, Göttingen, Germany, **2014**.

[S12] C. B. Hübschle, G. M. Sheldrick, B. Dittrich, *J. Appl. Cryst.* **2011**, *44*, 1281-1284.

[S13] G. M. Sheldrick, SHELXL-97, University of Göttingen, Göttingen, Germany, **1998**.

[S14] Wilson, A. J. C. International Tables for Crystallography, Vol. C, Tables 6.1.1.4 (pp. 500-502), 4.2.6.8 (pp. 219-222), and 4.2.4.2 (pp. 193-199); Kluwer Academic Publishers: Dordrecht, The Netherlands, **1992**.

[S15] C. F. Macrae, I. J. Bruno, J. A. Chisholm, P. R. Edgington, P. McCabe, E. Pidcock, L. Rodriguez-Monge, R. Taylor, J. van de Streek, P. A. Wood, *J. Appl. Cryst.* **2008**, *41*, 466-470.

9.2. Supporting Information for Chapter 5

Angewandte Chemie
Eine Zeitschrift der Gesellschaft Deutscher Chemiker

Supporting Information

An Aluminum Telluride with a Terminal Al=Te Bond and its Conversion to an Aluminum Tellurocarbonate by CO_2 Reduction

*H. Xu, A. Kostenko, C. Weetman, S. Fujimori, S. Inoue**

Contents

1 Experimental Section

1.1 General Methods and Instrumentation

All manipulations of air- and water-sensitive reactions were carried out under rigorous exclusion of water and oxygen under an atmosphere of argon 4.6 (≥99.996%; Westfalen AG) using the dual manifold Schlenk techniques or in an argon-filled LABstar glovebox from MBraun Inertgas-Systeme GmbH with water and oxygen levels below 0.5 ppm. The glassware used was heat-dried under high vacuum prior to use with Triboflon III grease (mixture of polytetrafluoroethylene (PTFE) and perfluoropolyether (PFPE)) from Freudenberg & Co. KG as sealant. All Solvents were dried by using a solvent purification system (SPS), freshly distilled under argon and deoxygenated before use. Deuterated benzene (C_6D_6), deuterated toluene (Toluene-d_8) and deuterated tetrahydrofuran (THF-d_8) was obtained from Sigma-Aldrich Chemie GmbH, stored over 4 Å molecular sieves in the glovebox. NMR samples were prepared under argon in NMR tubes. The NMR spectra were recorded on Bruker AV300US (^{1}H: 300.13 MHz, ^{13}C: 75 MHz), Avance Neo 400 (^{1}H: 400.23 MHz, ^{13}C: 100.65 MHz, ^{125}Te: 126 HMz, ^{77}Se: 76 HMz), AV500 (^{1}H: 500.13 MHz) spectrometers at ambient temperature (300 K). The ^{1}H, ^{13}C{^{1}H} spectroscopic chemical shifts δ are reported in ppm relative to tetramethylsilane. ^{1}H and ^{13}C{^{1}H} NMR spectra are calibrated against the residual proton and natural abundance carbon resonances of the deuterated solvent as internal standard (C_6D_6: $\delta(^1H)$ = 7.16 ppm and $\delta(^{13}C)$ = 128.1 ppm; THF-d_8: $\delta(^1H)$ = 3.58 ppm, 1.72 ppm and $\delta(^{13}C)$ = 67.21 ppm, 25.31 ppm; Toluene-d_8: $\delta(^1H)$ = 2.08, 6.97, 7.01, 7.09 ppm, $\delta(^{13}C)$ = 137.48, 128.87, 127.96, 125.13, 20.43 ppm). The following abbreviations are used to describe signal multiplicities: s = singlet, d = doublet, t = triplet, sept = septet, m = multiplet, br = broad and combinations thereof (e.g. dd = doublet of doublets). Some NMR spectra include resonances for silicone grease (C_6D_6: $\delta(^1H)$ = 0.29 ppm, $\delta(^{13}C)$ = 1.4 ppm; THF-d_8: $\delta(^1H)$ = 0.11 ppm, $\delta(^{13}C)$ = 1.2 ppm) derived from B. Braun Melsungen AG Sterican® cannulas.

Quantitative elemental analyses (EA) were carried out using a EURO EA (HEKA tech) instrument equipped with a CHNS combustion analyzer at the Laboratory for Microanalysis at the TUM Catalysis Research Center. Liquid Injection Field Desorption Ionization Mass Spectrometry (LIFDI-MS) was measured directly from an inert atmosphere glovebox with a Thermo Fisher Scientific Exactive Plus Orbitrap equipped with an ion source from Linden CMS.[S1] Melting Points (m.p.) were determined in sealed glass capillaries under inert gas by a Büchi M-565 melting point apparatus.

Elemental sulfur, elemental selenium, elemental tellurium, BPh_3, and nBu$_3$PTe were obtained from Sigma-Aldrich Chemie GmbH. The compounds [NHI(L^{Et})$_2$Al=Te] (NHI = 1,3-(2,6-diisopropylphenyl)-imidazolin-2-imine, L^{Et} = 1,3-diethyl-4,5-dimethyl-imidazolin-2-ylidene)[S2] 1,3,4,5-tetramethylimidazolin-2-ylidene (IMe_4)[S3] and 1,3-diisopropyl-4,5-dimethylimidazolin-2-ylidene (IiPr),[S3] IiPrAl(Tipp)H$_2$,[S4] the cyclic (alkyl)(amino)carbene (cAAC^{Me}),[S5] 1,3-(2,6-diisopropylphenyl)-imidazolin-2-ylidene (IDipp)[S6] were prepared according to the corresponding literature procedures.

Table S1. Acquisition parameters for ^{77}Se and ^{125}Te NMR

	2-Te	3-Te	5-Te	2-Se	3-Se	6-Te	4-Te
Solvent	C_6D_6	C_6D_6	THF-d_8 (+DFB)	Tol-d_8	THF-d_8 (+DFB)	THF-d_8 (+DFB)	C_6D_6
	^{125}Te	^{125}Te	^{125}Te	^{77}Se	^{77}Se	^{125}Te	^{125}Te
SFO1 (MHz)	126.13	126.18	126.06	76.32	76.31	126.20	126.14

O1P (ppm)	-900.00	-500.00	-1400.00	100.00	0.00	-300.00	-800.00
SW (Spectral width) (ppm)	1000.00	2000.00	1050.00	3800.00	2000.00	2600.00	2250.00
NS (The number of scans)	6400	6400	6400	2048	6400	9600	6400
P1 (pulses) (µs)	60	16	16	16	16	16	16
Dummy scans	2	2	2	4	4	2	2
D1 (delays) (µs)	0.5						1
D8	0.5						1
Software	TOPSPIN 3.2						
Probe	5 mm PABBO BB/19F-1H/D Z-GRD Z108618/0777						
TD	65536						
Chemical Shift (ppm)	-898.0	-954.2	-1368.6	-355.7	-460.5	-187.6	-924.7

DFB: 1,2-Difluorobenzene

1.2 Synthesis and Characterization

1.2.1 Synthesis of IMe$_4$Al(Tipp)H$_2$ (1-IMe$_4$)

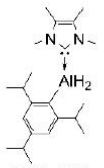

$C_{22}H_{37}AlN_2$
356.53 g/mol

Following a similar procedure for the reported synthesis of *i*PrAl(Tipp)H$_2$ (**1-*i*Pr**),[S4] TippLi(OEt$_2$) (0.92 g, 3.24 mmol) in 100 mL of Et$_2$O was added via dropping funnel over a period of 30 minutes to a Et$_2$O (100 mL) solution of IMe$_4$AlH$_3$ (0.5 g, 3.24 mmol, 1.0 eqv.) at -78 °C. The reaction was kept at -78 °C for 15 minutes and then slowly warmed to room temperature overnight. Volatiles were removed under reduced pressure and crude product was washed with pentane (3 x 60 mL). After that, white solid was obtained. Yield = 0.70 g, 60%.

^{1}H NMR (400 MHz, C_6D_6) δ 7.27 (s, 2H, Tipp-H), 5.07 (br. s, 2H, Al-H), 4.04 (hept, *J* = 6.9 Hz, 2H, Tipp-*o*-iso-CH$_2$-CH$_3$), 3.16 (s, 6H, IMe$_4$-N-CH), 2.97 (p, *J* = 6.9 Hz, 1H, Tipp-*p*-iso-CH$_2$-CH$_3$), 1.45 (d, *J* = 6.8 Hz, 12H, Tipp-*o*-iso-CH$_3$), 1.39 (d, *J* = 6.9 Hz, 6H, Tipp-*p*-iso-CH$_2$-CH$_3$), 1.14 (s, 6H, IMe$_4$-C-CH$_3$).

^{13}C{^{1}H} NMR (101 MHz, C_6D_6) δ 170.1 (IMe$_4$-C:, according to HSQC/HMBC), 158.39 (Tipp-C), 148.08 (Tipp-C), 144.99 (Tipp-C-Al, according to HSQC/HMBC), 125.07 (IMe$_4$-C-CH$_3$), 119.84 (Tipp-C), 36.79 (Tipp-*o*-iPr-CH$_2$-CH$_3$), 35.14 (Tipp-*p*-iPr-CH$_2$-CH$_3$), 33.48 IMe$_4$-N-CH$_3$, 25.47 (Tipp-*o*-iPr-CH$_2$-CH$_3$), 24.70 (Tipp-*p*-iPr-CH$_2$-CH$_3$), 7.74 (IMe$_4$-C-CH$_3$).

1.2.2 Synthesis of [*i*PrAl(Tipp)-*µ*-Te]$_2$ (2-Te)

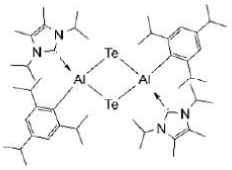

$C_{52}H_{86}Al_2N_4Te_2$
1076.45 g/mol

The solution of *i*PrAl(Tipp)H$_2$ (200 mg, 0.485 mmol) in 25 mL toluene was added via dropping funnel over a period of 15 minutes to a toluene (25 mL) suspension of tellurium (124 mg, 0.970 mmol, 2 eqv.) at -78 °C. The reaction was kept at -78 °C for 15 minutes and then slowly warmed to room temperature over 16 hours. After stirring at room temperature for 3 days, black precipitate formed and was removed by filtration. To ensure all product was transferred, the black precipitate was washed with toluene (3 X 10 mL). Solvent was removed from the combined toluene solutions resulting a colorless gel product. The crude products was extracted by pentane (3 x 50 mL) and then concentrated to the point of crystallization and then put in the freezer (-30 °C). The white solids were isolated via filtration and dried under vacuum (156 mg, 60 %).

m.p.: 261.9 °C.

^{1}H NMR (400 MHz, C_6D_6) δ 7.14 (s, 4H, Tipp-H), 6.58 (dt, J = 12.8, 6.1 Hz, 4H, *i*Pr-N-CH), 4.63 (p, J = 6.5 Hz, 4H, Tipp-*o*-iso-CH$_2$-CH$_3$), 2.90 (p, J = 6.8 Hz, 2H, Tipp-*p*-iso-CH$_2$-CH$_3$), 1.54 (s, 12H, *i*Pr-C-CH$_3$), 1.33-1.35 (d, J = 6.9 Hz, 36H, *i*Pr-N-CH-CH$_3$ and Tipp-*p*-iso-CH$_3$), 1.14 (d, J = 7.0 Hz, 24H, Tipp-*o*-iso-CH$_3$).

^{13}C{^{1}H} NMR (75 MHz, C_6D_6) δ 156.98 (Tipp-C-Al), 147.81 (Tipp-C), 142.55 (Tipp-C, according to HSQC/HMBC), 125.35 (*i*Pr-C-CH$_3$), 120.85 (Tipp-C), 52.33 (*i*Pr-N-C), 35.94 (Tipp-*o*-iPr-CH$_2$-CH$_3$), 34.91 (Tipp-*p*-iPr-CH$_2$-CH$_3$), 24.60 (*i*Pr-N-CH$_2$-CH$_3$), 21.72 (Tipp-*p*-iPr-CH$_2$-CH$_3$, according to HSQC/HMBC), 21.21 (Tipp-*o*-iPr-CH$_2$-CH$_3$), 9.85 (*i*Pr-C-CH$_3$).

^{125}Te NMR (126 MHz, C_6D_6) δ -898.0.

MS (ESI$^+$) *m/z* calcd: 1076.46; m/z found: 1076.46.

Anal. Calcd. [%] for $C_{52}H_{86}Al_2N_4Te_2$: C, 58.02; H, 8.05; N, 5.20. Found [%]: C, 57.07; H, 8.02; N, 5.20.

1.2.3 Synthesis of [IMe$_4$Al(Tipp)-μ-Te]$_2$ (3-Te)

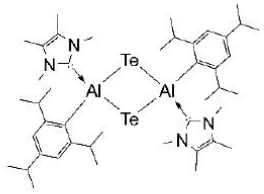

$C_{44}H_{70}Al_2N_4Te_2$
964.24 g/mol

Method A:

A solution of IMe$_4$ (49 mg, 0.39 mmol, 2.0 eqv.) in 20 mL THF was added dropwise to a THF (20 mL) solution of [*i*PrAl(Tipp)-µ-Te]$_2$ (200 mg, 0.186 mmol) at -78 °C, over a period of 20 minutes. The reaction was kept at -78 °C for half an hour and then slowly warmed to room temperature and stirred for 16 hours. Volatiles were removed under reduced pressure. The crude products were extracted by toluene (3 x 40 mL) and THF (40 mL). The solution was concentrated to the point of crystallization, a few drops of pentane was added to aid precipitation and placed in the freezer (- 30 °C). The white solids were isolated via filtration and dried under reduced pressure (110 mg, 61 %).

Method B:

A toluene (50 mL) suspension of metallic tellurium (144 mg, 1.12 mmol, 2 eqv.) was added to IMe$_4$Al(Tipp)H$_2$ (200 mg, 0.56 mmol) in toluene (50 mL) at -78 °C. The reaction was then slowly warmed to room temperature over 16 hours. After stirring at room temperature for a further 48 hours, volatiles were removed under reduced pressure. The crude products were washed with pentane (150 mL) and extracted with toluene (3 x 150 mL). The solution was concentrated to the point of crystallization, a few drops of pentane were added, then placed in the freezer (- 30 °C). The white solids were isolated via filtration and dried under reduced pressure (185 mg, 70 %).

m.p.: 289.9 °C.

^{1}H NMR (400 MHz, THF-d$_8$) δ 6.77 (s, 4H, Tipp-H), 4.26 (p, *J* = 6.6 Hz, 4H, Tipp-*o*-iso-CH), 3.89 (s, 12H, IMe-N-CH$_3$), 2.75 (p, *J* = 6.8 Hz, 2H, Tipp-*p*-iso-CH), 2.10 (s, 12H, IMe-C-CH$_3$), 1.20 (d, *J* = 6.9 Hz, 12H, Tipp-*p*-iso-C-CH$_3$), 1.01 (d, *J* = 6.6 Hz, 24H, Tipp-*o*-iso-C-CH$_3$).

^{13}C{^{1}H} NMR (101 MHz, THF-d$_8$) δ 162.52 (IMe$_4$-C:, according to HSQC/HMBC), 156.12 (Tipp-C-Al), 146.74 (Tipp-C, according to HSQC/HMBC), 142.19 (Tipp-C, according to HSQC/HMBC), 124.58 (IMe$_4$-C-CH$_3$, according to HSQC/HMBC), 119.51(Tipp-C), 35.24 (Tipp-*o*-iPr-CHCH$_3$), 34.19 (Tipp-*p*-iPr-CHCH$_3$, according to HSQC/HMBC), 34.05 (IMe$_4$-N-CH$_3$), 24.41 (Tipp-*o*-iPr-CHCH$_3$, according to HSQC/HMBC), 23.52 (Tipp-*p*-iPr-CHCH$_3$, according to HSQC/HMBC), 7.28 (IMe$_4$-C-CH$_3$).

^{125}Te NMR (126 MHz, C$_6$D$_6$) δ -954.2.

MS (ESI$^+$) *m/z* calcd: 964.33; m/z found: 964.33.

Anal. Calcd. [%] for C$_{44}$H$_{70}$Al$_2$N$_4$Te$_2$: C, 54.81; H, 7.32; N, 5.81. Found [%]: C, 56.11; H, 7.36; N, 5.20.

1.2.4 Synthesis of (IMe$_4$)$_2$Al(Tipp)=Te (5-Te)

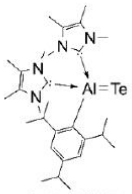

$C_{29}H_{47}AlN_4Te$
606.30 g/mol

Method A:

The solution of [*i*PrAl(Tipp)-µ-Te]$_2$ (200 mg, 0.186 mmol) in 25 mL toluene was added dropwise to a toluene (25 mL) solution of IMe$_4$ (104 mg, 0.84 mmol, 4.5 eqv.) at -78 °C, over a period of 20 minutes. The reaction was kept at -78 °C for half an hour and then slowly warmed to room temperature over 16 hours during which time white precipitate formed. Solids were removed by filtration and further extracted with toluene (3 X 10 mL). All toluene solutions were combined and solvent removed under reduced pressure to leave a sticky yellow solid. The crude product was extracted with THF (3 x 10 mL) and concentrated to the point of crystallization and then put in the freezer (-30 °C). The yellow crystalline solids were isolated via filtration and dried under reduced pressure (100 mg, 45 %).

Method B:

The solution of [IMe$_4$Al(Tipp)-μ-Te]$_2$ (200 mg, 0.21 mmol) in 25 mL toluene was added dropwise to a toluene (25 mL) solution of IMe$_4$ (54 mg, 0.44 mmol, 2.1 eqv.) at -78 °C, over a period of 20 minutes. The reaction was kept at -78 °C for half an hour and then slowly warmed to room temperature over 2 hours during which time white precipitate formed. Solids were removed after filtration and further extracted with toluene (3 X 10 mL). All toluene solutions were combined and solvent removed under reduced pressure to yield a sticky yellow solid. The crude product was extracted by THF (3 x 15 mL) and was concentrated to the point of crystallization and then put in the freezer (-30 °C). The yellow crystalline solids were isolated via filtration and dried under reduced pressure (160 mg, 63 %).

m.p.: 145.4 °C (decomposition; color change from yellow to black).

^{1}H NMR (400 MHz, THF-d$_8$) δ 6.83 (s, 2H, Tipp-H), 4.49 (p, *J* = 6.8 Hz, 2H, Tipp-*o*-iso-CH), 3.76 (s, 12H, IMe$_4$-N-CH$_3$), 2.75 (dt, *J* = 13.5, 6.9 Hz, 1H, Tipp-*p*-iso-CH), 2.13 (s, 12H, IMe$_4$-C-CH$_3$), 1.20 (d, *J* = 6.9 Hz, 6H, Tipp-*p*-iso-CH-CH$_3$), 0.93 (d, *J* = 6.7 Hz, 12H, Tipp-*o*-iso-CH-CH$_3$).

^{13}C{^{1}H} NMR (101 MHz, THF-d$_8$) δ 166.59 (IMe$_4$-C:, according to HSQC/HMBC), 156.13 (Tipp-C), 146.72 (Tipp-C, according to HSQC/HMBC), 144.20 (Tipp-C, according to HSQC/HMBC), 125.51 (IMe$_4$-C-CH$_3$), 119.51 (Tipp-*m*-C), 35.24

(Tipp-*o*-iPr-CHCH$_3$), 35.15 (IMe$_4$-N-CH$_3$), 34.05 (Tipp-*p*-iPr-CHCH$_3$), 24.86 (Tipp-*o*-iPr-CHCH$_3$), 23.61 (Tipp-*p*-iPr-CHCH$_3$), 7.29 (IMe$_4$-C-CH$_3$).

^{125}Te NMR (126 MHz, THF-d$_8$) δ -1368.6.

IR (solid) $\tilde{\nu}$ [cm^{-1}] = 423.32 (Al=Te).

MS (ESI$^+$) *m/z* calcd: 608.27; m/z found: 608.27.

Anal. Calcd. [%] for C$_{29}$H$_{47}$AlN$_4$Te with 0.2 eqv 4-Te: C, 56.81; H, 7.69; N, 8.41. Found [%]: C, 56.89; H, 7.44; N, 8.31. This result was affected by the dimeric **4-Te** (approximately 0.2 eqv).

1.2.5 Synthesis of [I*i*PrAl(Tipp)-*μ*-Se]$_2$ (2-Se)

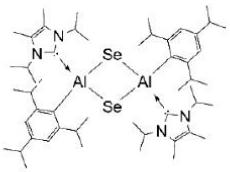

C$_{52}$H$_{86}$Al$_2$N$_4$Se$_2$
979.19 g/mol

A solution of I*i*PrAl(Tipp)H$_2$ (200 mg, 0.49 mmol) in 25 mL diethylether was added dropwise to a diethylether (25 mL) suspension of selenium (79 mg, 0.99 mmol, 2.0 eqv.) at -78 °C, over a period of 30 minutes. The reaction was kept at -78 °C for half an hour and then slowly warmed to room temperature over 16 hours. The reaction was stirred for further 24 hours at room temperature, which resulted in the formation of a grey precipitate. Volatiles were removed under reduced pressure, and the crude product was extracted with pentane (3 x 50 mL). The pentane solution was concentrated to the point of crystallization and then put in the freezer (-30 °C). The white solids were isolated via filtration and dried under reduced pressure (120 mg, 50 %).

m.p.: 219.4 °C

^{1}H NMR (400 MHz, C$_6$D$_6$) δ 7.17 (s, 4H, Tipp-H), 6.64 (br, 4H, I*i*Pr-N-CH), 4.65 (br, 4H, Tipp-*o*-iso-CH), 2.92 (p, *J* = 6.9 Hz, 2H, Tipp-*p*-iso-CH), 1.56 (s, 12H, I*i*Pr-C-CH$_3$), 1.52 (d, *J* = 5.1 Hz, 12H, I*i*Pr-N-CH-CH$_3$), 1.36 (d, *J* = 6.9 Hz, 12H, Tipp-*p*-iso-C-CH$_3$), 1.26 (d, *J* = 6.1 Hz, 12H, I*i*Pr-N-CH-CH$_3$), 1.14 (d, *J* = 6.9 Hz, 24H, Tipp-*o*-iso-C-CH$_3$).

^{13}C{^{1}H} NMR (101 MHz, C$_6$D$_6$) δ 167.49 (I*i*Pr-C:), 157.41 (Tipp-C-Al), 147.72 (Tipp-C), 146.03 (Tipp-C), 125.24 (I*i*Pr-C-CH$_3$), 120.46 (Tipp-*m*-C) , 51.66 (I*i*Pr-N-C), 35.40 (Tipp-*o*-iPr-CH$_2$-CH$_3$), 34.94 (Tipp-*p*-iPr-CH$_2$-CH$_3$), 26.55 (I*i*Pr-N-CH$_2$-CH$_3$), 25.46, 24.63 (Tipp-*p*-iPr-CH$_2$-CH$_3$), 21.27 (Tipp-*o*-iPr-CH$_2$-CH$_3$), 9.95 (I*i*Pr-C-CH$_3$).

^{77}Se NMR (76 MHz, Toluene-d$_8$) δ -355.7.

MS (ESI$^+$) *m/z* calcd: 980.48; m/z found: 980.48.

Anal. Calcd. [%] for C$_{52}$H$_{86}$Al$_2$N$_4$Se$_2$: C, 63.78; H, 8.85; N, 5.72. Found [%]: C, 61.04; H, 8.76; N, 5.64.

1.2.6 Synthesis of [IMe$_4$Al(Tipp)-*μ*-Se]$_2$ (3-Se)

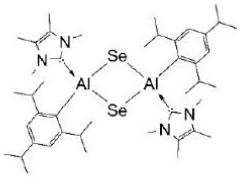

C$_{44}$H$_{70}$Al$_2$N$_4$Se$_2$
866.98 g/mol

Method A:

The solution of IMe$_4$ (53 mg, 0.43 mmol, 2.1 eqv.) in 10 mL C$_6$H$_6$ was added dropwise to a C$_6$H$_6$ (20 mL) solution of [I*i*PrAl(Tipp)-*μ*-Se]$_2$ (200 mg, 0.204 mmol) at -78 °C over half an hour. The reaction was kept at -78 °C for half an hour and then slowly warmed to room temperature over 16 hours. Volatiles were removed under reduced pressure. The crude product was extracted by THF (3 x 30 mL) and concentrated to the point of crystallization. After adding a few drops of pentane, the solution was put in the freezer (- 30 °C). The white crystalline solids were isolated via filtration and dried under reduced pressure (130 mg, 73 %).

Method B:

A toluene (50 mL) suspension of metallic selenium (90 mg, 1.12 mmol, 2 eqv.) was added to IMe$_4$Al(Tipp)H$_2$ (200 mg, 0.56 mmol) in toluene (50 mL) at -78 °C. The reaction was then slowly warmed to room temperature over 16 hours. After stirring for 60 hours, volatiles were removed under reduced pressure. The crude product was washed with pentane (150 mL) and extracted by toluene (3 x 150 mL). The solution was concentrated to the point of crystallization. After adding a few drops of pentane, the solution was put in the freezer (- 30 °C). The white solids were isolated via filtration and dried under reduced pressure (195 mg, 80 %).

m.p.: 285.9 °C

^{1}H NMR (400 MHz, C$_6$D$_6$) δ 7.24 (s, 4H, Tipp-H), 4.75 – 4.67 (m, 4H, Tipp-*o*-iso-CH), 3.66 (s, 12H, IMe$_4$-N-CH$_3$), 2.98 – 2.88 (m, 2H, Tipp-*p*-iso-CH), 1.40 (d, *J* = 6.7 Hz, 24H, Tipp-*o*-iso-CH-CH$_3$), 1.35 (d, *J* = 6.9 Hz, 12H, Tipp-*p*-iso-CH-CH$_3$), 1.16 (s, 12H, IMe$_4$-C-CH$_3$).

^{1}H NMR (400 MHz, THF-d$_8$) δ 6.77 (s, 4H, Tipp-H), 4.23 (hept, *J* = 5.8 Hz, 4H, Tipp-*o*-iso-CH), 3.89 (s, 12H, IMe$_4$-N-CH$_3$), 2.74 (hept, *J* = 6.4 Hz, 2H, Tipp-*p*-iso-CH), 2.07 (s, 12H, IMe$_4$-C-CH$_3$), 1.19 (d, *J* = 6.9 Hz, 12H, Tipp-*p*-iso-CH-CH$_3$), 1.00 (d, *J* = 6.7 Hz, 24H, Tipp-*o*-iso-CH-CH$_3$).

$^{13}C\{^1H\}$ NMR (101 MHz, C_6D_6) δ 166.55 (IMe_4-C:, according to HSQC/HMBC), 157.19 (Tipp-C), 147.51 (Tipp-C), 145.37 (Tipp-C, according to HSQC/HMBC), 123.90 (IMe_4-C-CH_3), 120.02 (Tipp-*m*-C), 35.23 (Tipp-*o*-iPr-$CHCH_3$), 34.62 (Tipp-*p*-iPr-$CHCH_3$), 33.70 (IMe_4-N-CH_3), 25.29 (Tipp-*p*-iPr-$CHCH_3$), 24.27 (Tipp-*o*-iPr-$CHCH_3$), 7.35 (IMe_4-C-CH_3).

$^{13}C\{^1H\}$ NMR (101 MHz, THF-d_8) δ 166.30 (IMe_4-C:, according to HSQC/HMBC), 156.59 (Tipp-C), 146.48 (Tipp-C), 145.21 (Tipp-C, according to HSQC/HMBC),124.53 (IMe_4-C-CH_3), 119.23 (Tipp-*m*-C), 34.59 (Tipp-*o*-iPr-$CHCH_3$), 34.28 (Tipp-*p*-iPr-$CHCH_3$), 24.57 (Tipp-*o*-iPr-$CHCH_3$, according to HSQC/HMBC), 23.72 (Tipp-*p*-iPr-$CHCH_3$, according to HSQC/HMBC), 7.29 (IMe_4-C-CH_3).

^{77}Se NMR (76 MHz, THF-d_8) δ -460.5.

MS (ESI$^+$) *m/z* calcd: 868.36; m/z found: 868.35.

Anal. Calcd. [%] for $C_{44}H_{70}Al_2N_4Se_2$: C, 60.96; H, 8.14; N, 6.46. Found [%]: C, 60.93; H, 8.51; N, 6.25.

1.2.7 Synthesis of $(IMe_4CO_2)_2Al(Tipp)$-μ-O_2C=Te (6-Te)

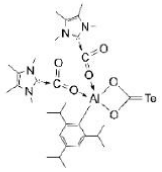

A yellow solution of $(IMe_4)_2Al(Tipp)$=Te (**5-Te**) (100 mg, 0.49 mmol) in 15 mL toluene and 3 mL 1,2-difluorobenzene in a Schlenk flask was freeze-pump-thaw-degassed, and cooled to -50 °C resulting a frozen solution. The flask was backfilled with CO_2 (1 bar), which was added to a frozen solution, and then cooled to -30 °C. A yellow frozen solution became to a red solution immediately after defrosting and subsequently stirring. After few seconds, the flask was put back to the cooling bath (-50 °C) with at least 15 min. More CO_2 (1 bar) was added to a frozen solution. After stirring for 15 min at -30 °C, the red solution was degassed at -50 °C (three times), then placed in the freezer at -30 °C. After 18 hours, red crystalline material was isolated via filtration and dried under reduced pressure (85 mg, 70%).

It is important to note **6-Te** is thermally instable even at -30 °C. It features poor solubility in normal commercial solvents, except 1,2-difluorobenzene. It is recommended that characterization purposes samples should be freshly-prepared.

^1H NMR (500 MHz, Toluene-d_8) δ 7.12 (s, 2H, Tipp-H), 4.09 (dt, *J* = 12.9, 6.4 Hz, 2H, Tipp-*o*-iso-CH), 3.98 (s, 3H, IMe_4-N-CH), 3.46 (s, 9H, IMe_4-N-CH), 2.85 (hept, *J* = 7.0 Hz, 1H, Tipp-*p*-iso-CH), 2.16 (s, 3H, IMe_4-C-CH), 1.53 – 1.40 (m, 22H, IMe_4-C-CH and Tipp-*o*-isopropyl-H), 1.27 (d, *J* = 6.9 Hz, 6H, Tipp-*p*-isopropyl-H). (1.47 ppm, 3.28 ppm, which are assigned to diagnostic signals of IMe_4=Te (13%). The solvent is the mixed solvent of Tol-d_8 and 1,2-difluorobenzene (5:1).

$^{13}C\{^1H\}$ NMR (101 MHz, Toluene-d_8) δ 226.56 (Al-O_2C-Te), 151.18 (Tipp-C), 150.77 (Tipp-C), 131.45 (IMe_4-CO_2-Al), 124.49 (IMe_4-C-CH_3), 122.42 (Tipp-C), 100.48 (IMe_4-CO_2-Al), 37.23 (IMe_4-N-C), 26.42 (Tipp-isopropyl-C-C), 24.40(Tipp-isopropyl-C-C), 9.08 (IMe_4-C-CH_3). (The solvent is the mixed solvent of Tol-d_8 and 1,2-difluorobenzene (5:1))

^{125}Te NMR (126 MHz, THF-d_8) δ -187.6. (The solvent is the mixed solvent of THF-d_8 and 1,2-difluorobenzene (5:1))

IR (solid) $\tilde{\nu}$ [cm^{-1}] = 1698.86, 1668.35, 1312.32, 1260.63, 1032.58, 540.36 (CO_2); 820.98 (C=Te). The latter remarkably hypsochromically shifted compared with the wave number of **5-Te** (423 cm^{-1}) and the characteristic frequency of Si=Te (588 cm^{-1}).[S7]

MS (ESI$^+$) *m/z* calcd: 740.24; m/z found: 652.25. **([6-Te – 2(CO_2)], *m/z* calcd: 652.24)**

Anal. Calcd. [%] for $C_{32}H_{47}AlN_4O_6Te$ (A freshly-prepared sample was constantly stored at -30 °C and directly loaded to EA instrument): C, 52.06; H, 6.42; N, 7.59. Found [%]: C, 51.41; H, 6.79; N, 7.77.

1.3 NMR Experiments

1.3.1 Synthesis of I*i*Pr(IMe_4)Al(Tipp)=Te (4-Te)

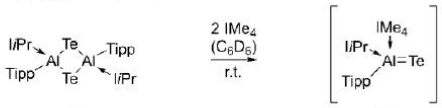

2-Te **4-Te**

[I*i*PrAl(Tipp)-μ-Te]$_2$ (Compound **2-Te**) (20 mg, 0.019 mmol) and IMe_4 (5 mg, 0.04 mmol, 2.2 eqv.) were weighed into the same vial, C_6D_6 which was cooled for 5-10minutes in the glovebox freezer, was then added to the vial and then transferred to a J-Young NMR tube. After two hours at room temperature, the solution became yellow from colorless. After 24 hours, a colorless precipitate was observed to have formed at the bottom of the tube.

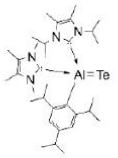

$C_{93}H_{86}AlN_4Te$
662.41 g/mol

^{1}H NMR (400 MHz, C_6D_6) δ 7.26 (s, 2H, Tipp-H), 4.91 (dt, *J* = 13.1, 6.5 Hz, 2H, Tipp-*o*-iso-CH), 3.95 (dt, *J* = 13.2, 6.6 Hz, 2H, I*i*Pr-N-CH), 3.75 (s, 6H, IMe_4-N-CH_3), 2.91 (dt, *J* = 13.7, 6.9 Hz, 1H, Tipp-*p*-iso-CH), 1.74 (s, 6H, IMe_4-C-CH_3), 1.53 (s, 6H, I*i*Pr-C-CH_3), 1.50 (d, *J* = 6.6 Hz, 12H, I*i*Pr-N-C-CH_3), 1.33 (d, *J* = 6.9 Hz, 6H, Tipp-*p*-iso-C-CH_3), 1.30 (d, *J* = 6.7 Hz, 12H, Tipp-*o*-iso-C-CH_3).

^{125}Te NMR (126 MHz, THF-d_8) δ -924.7.

MS (ESI$^+$) *m/z* calcd: 664.33; m/z found: 664.33.

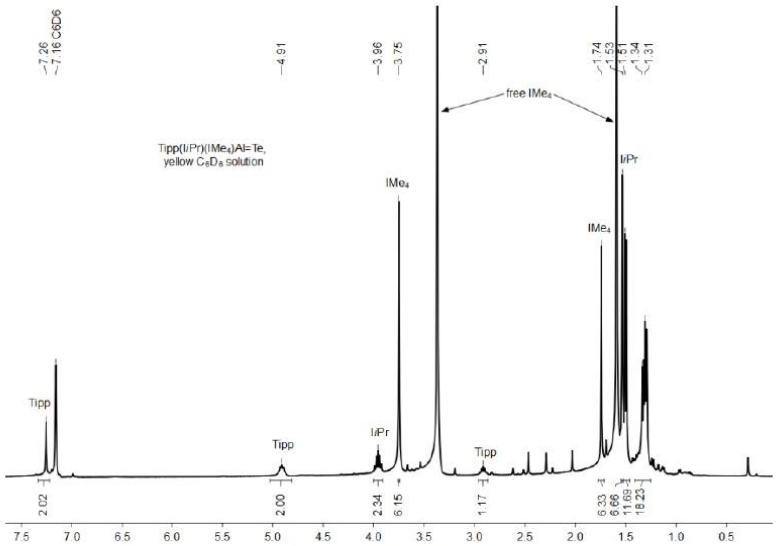

Figure S1. ^{1}H NMR spectrum (400 MHz) of the mixture of compound **4-Te** and IMe_4 in C_6D_6 at 300 K. [δ (silicone grease) = 0.29 ppm]

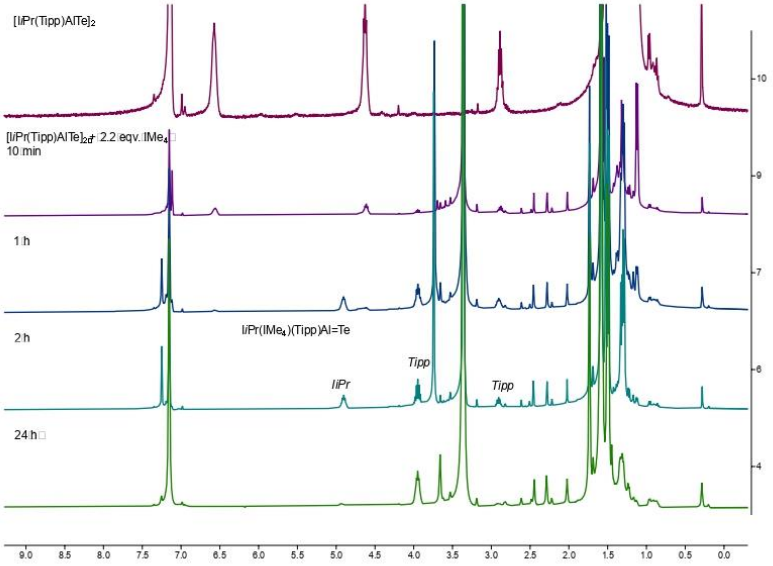

Figure S2: Stacked ^{1}H NMR (400 MHz) spectra for the mixture of compound **2-Te** with 2.2 eqv. IMe_4 in C_6D_6 at 300 K. [δ (silicone grease) = 0.29 ppm]

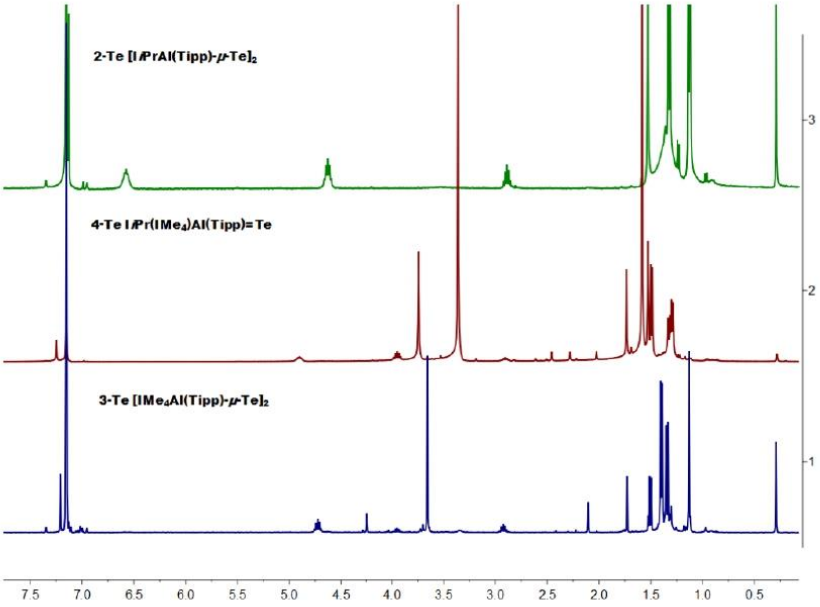

Figure S3. Stacked ^{1}H NMR (400 MHz) spectra for **2-Te**, **4-Te** and **3-Te** in C_6D_6 at 300 K. [δ (silicone grease) = 0.29 ppm]

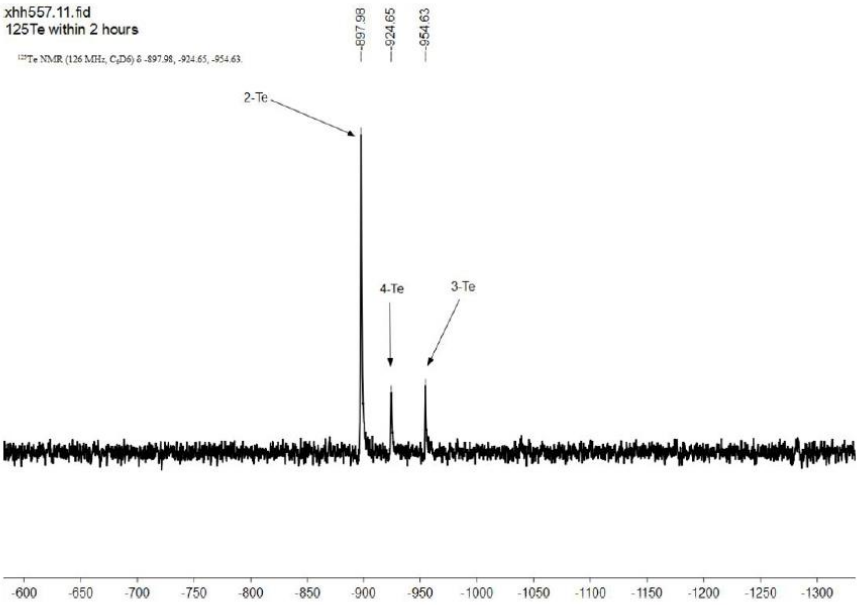

Figure S4. ^{125}Te NMR (126 MHz) spectrum for **2-Te**, **4-Te** and **3-Te** in C_6D_6 at 300 K.

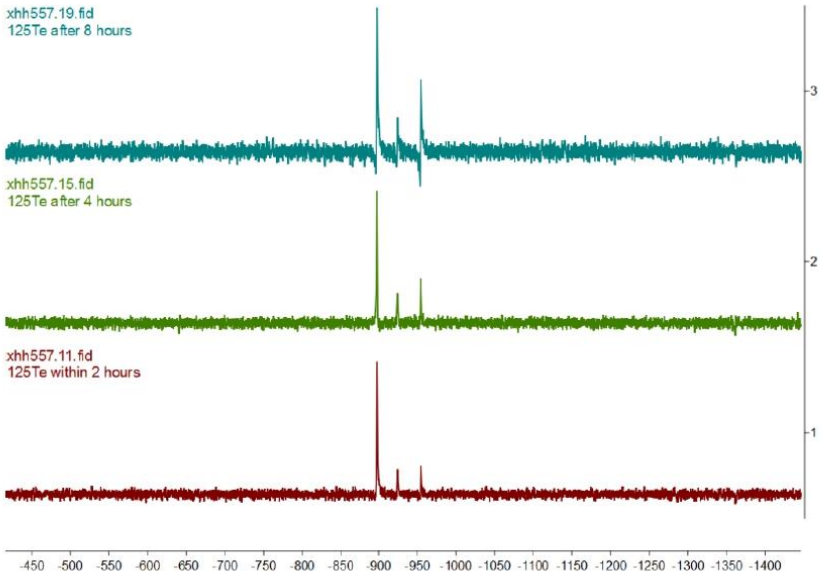

Figure S5. Stacked ^{125}Te NMR (126 MHz) spectra for **2-Te** with 2 eqv. IMe_4 (in different conditions) in C_6D_6 at 300 K.

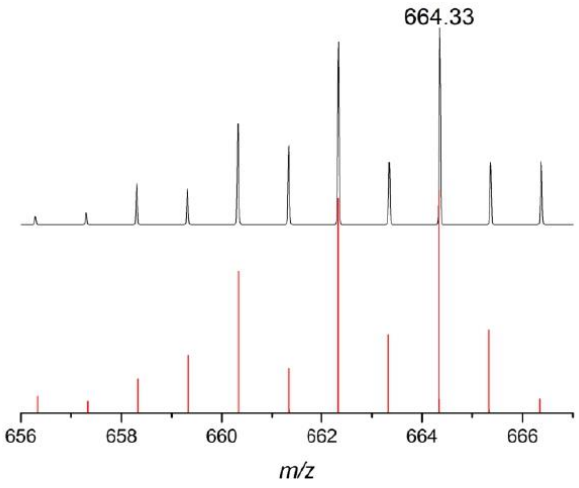

Figure S6. LIFDI-MS spectrometry (detail view with isotope pattern) of I*i*Pr(IMe_4)Al(Tipp)=Te (**4-Te**) (the mixture of compound **2-Te** with 2.2 eqv. IMe_4 in Toluene after 2 hours) (Measured spectrum: top; Simulated spectrum: bottom).

1.3.2 The reaction of 5-Te with Se

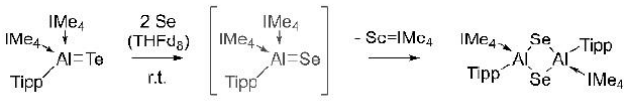

5-Te **5-Se** **3-Se**

$(IMe_4)_2Al(Tipp)=Te$ (25 mg, 0.041 mmol) and Se (7 mg, 0.083 mmol, 2 eqv.) were mixed and precooled THF-d_8 was added to the mixture in a J-Young NMR tube. After 15 minutes, the solution became nearly colorless from yellow. After 24 hours, there was precipitate in the bottom of the tube.

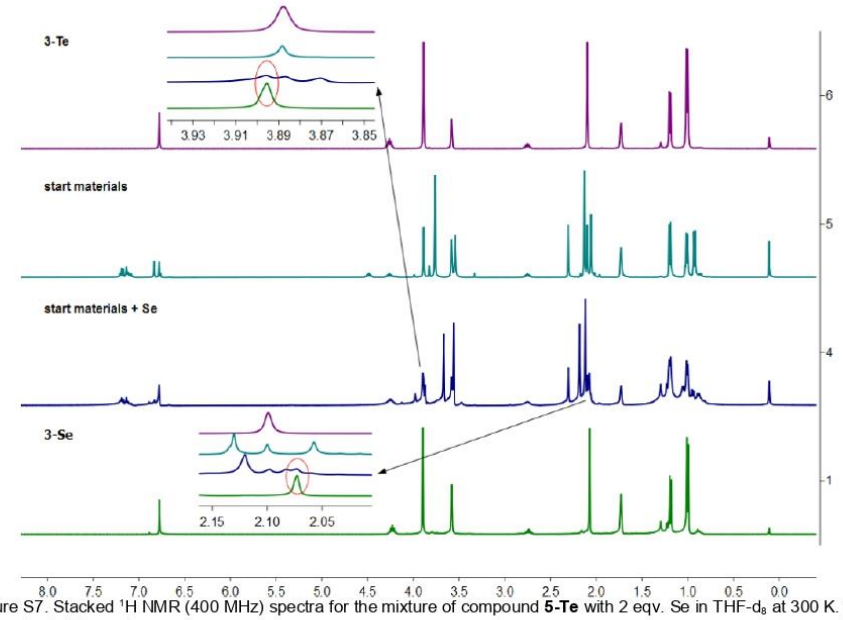

Figure S7. Stacked ^1H NMR (400 MHz) spectra for the mixture of compound **5-Te** with 2 eqv. Se in THF-d_8 at 300 K. [δ (silicone grease) = 0.108 ppm]

1.3.3 The reaction of 5-Te with BPh_3

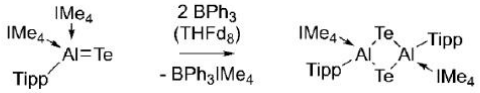

5-Te **3-Te**

$(IMe_4)_2Al(Tipp)=Te$ (25 mg, 0.041 mmol) and BPh_3 (20 mg, 0.083 mmol, 2 eqv.) were mixed and precooled THF-d_8 was added to the mixture in a J-Young NMR tube. After 15 minutes, the solution became colorless from yellow. After 24 hours, there was a little white precipitate in the bottom of the tube.

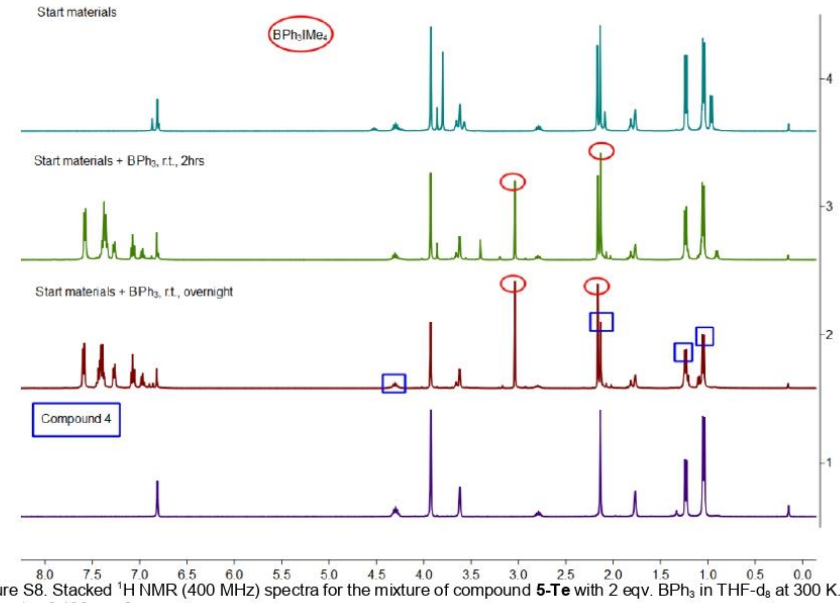

Figure S8. Stacked ^{1}H NMR (400 MHz) spectra for the mixture of compound **5-Te** with 2 eqv. BPh_3 in THF-d_8 at 300 K. [δ (silicone grease) = 0.108 ppm]

1.3.4 The reaction of 5-Te with S_8

$(IMe_4)_2Al(Tipp)$=Te (30 mg, 0.05 mmol) and S_8 (1.6 mg, 0.006 mmol, 1/8 eqv.) were mixed and precooled THF-d_8 was added to the mixture in a J-Young NMR tube. The solution became pale blue from yellow directly, after few seconds it became to brown finally. After several seconds, there was black precipitate in the bottom of the tube.

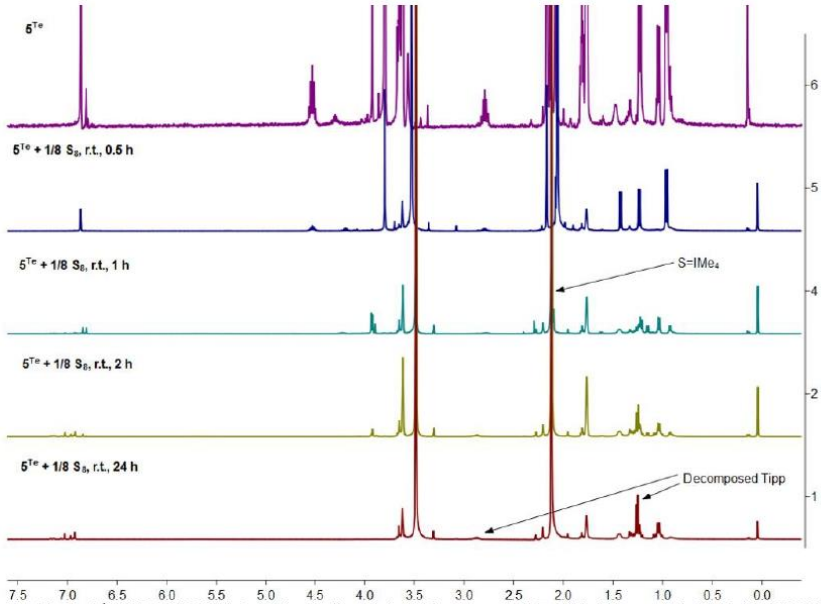

Figure S9. Stacked ^{1}H NMR (400 MHz) spectra for the mixture of compound **5-Te** with 1/8 eqv. S_8 in THF-d_8 at 300 K. [δ (silicone grease) = 0.108 ppm]

1.3.5 The reaction of $(IEt)_2Al(NHI)$=Te IVa with Se, S, or IEt=S

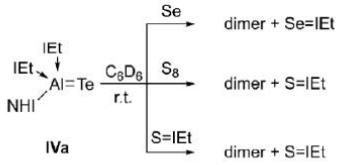

$(IEt)_2Al(NHI)$=Te (20 mg, 0.023 mmol) and Se (6.3 mg, 0.079 mmol, 3.4 eqv.) were mixed and precooled C_6D_6 was added to the mixture in a J-Young NMR tube. After 15 minutes, the solution became reddish brown from yellow. After 24 hours, there was black precipitate in the bottom of the tube.

$(IEt)_2Al(NHI)$=Te (30 mg, 0.035 mmol) and S_8 (1.12 mg, 0.0044 mmol, 1/8 eqv.) were mixed and precooled C_6D_6 was added to the mixture in a J-Young NMR tube. The solution became brown from yellow and there was gray precipitate in the bottom of the tube immediately.

$(IEt)_2Al(NHI)$=Te (20 mg, 0.023 mmol) and S=IEt (4.28 mg, 0.023 mmol, 1 eqv.) were mixed and precooled C_6D_6 was added to the mixture in a J-Young NMR tube. After 24 hours, there was black precipitate in the bottom of the tube.

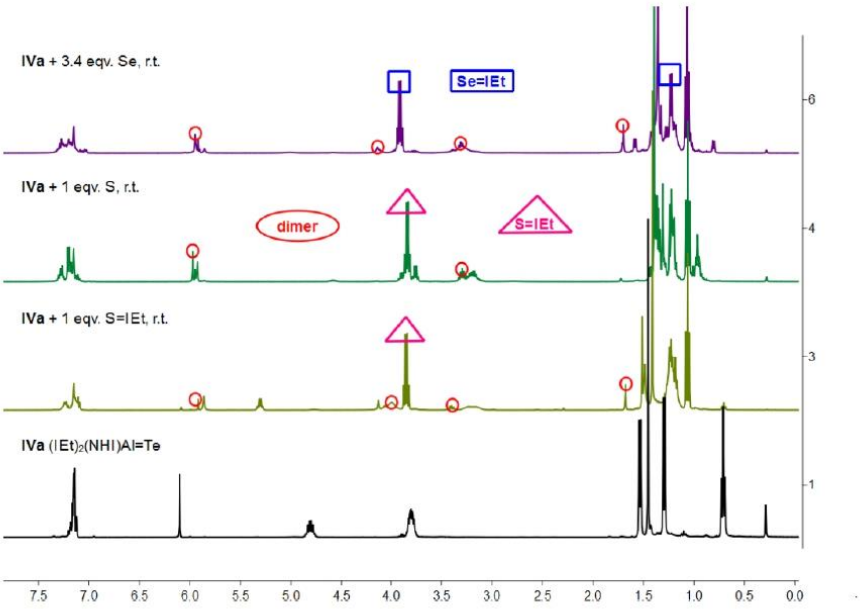

Figure S10. Stacked ^{1}H NMR (400 MHz) spectra for the mixture of $(IEt)_2Al(NHI)$=Te **IVa** with 3.4 eqv. Se, 1/8 eqv. S_8 and 1 eqv. S=IEt, respectively, in C_6D_6 at 300 K. [δ (silicone grease) = 0.108 ppm]

1.3.6 The reactivity study of 5-Te

We made numerous attempts to study the reactivity of **5-Te**. There are no reaction of **5-Te** with excess of $Se=P(tBu)_3$, IMe_4-CO_2, S=IEt, PPh_3, IMe_4-CuMes, even at 80 °C with 72 hours. When we did the reactions of **5-Te** with the stoichiometric amount of Diphenylacetylene, 2,6-Dimethylphenyl isocyanide, Phenylacetylene, Ph_2CO, $Ni(COD)_2$, MesCu, at -30 °C to r.t., respectively, the dimeric **3-Te** was captured by ^{1}H NMR (Figure S11). The products from the reaction of **5-Te** and stoichiometric Benzophenone, NMO, Me_2SAuCl, Mes_2Fe, at -30 °C to r.t., respectively, the decomposed species which cannot be identified due to mass ^{1}H NMR data.

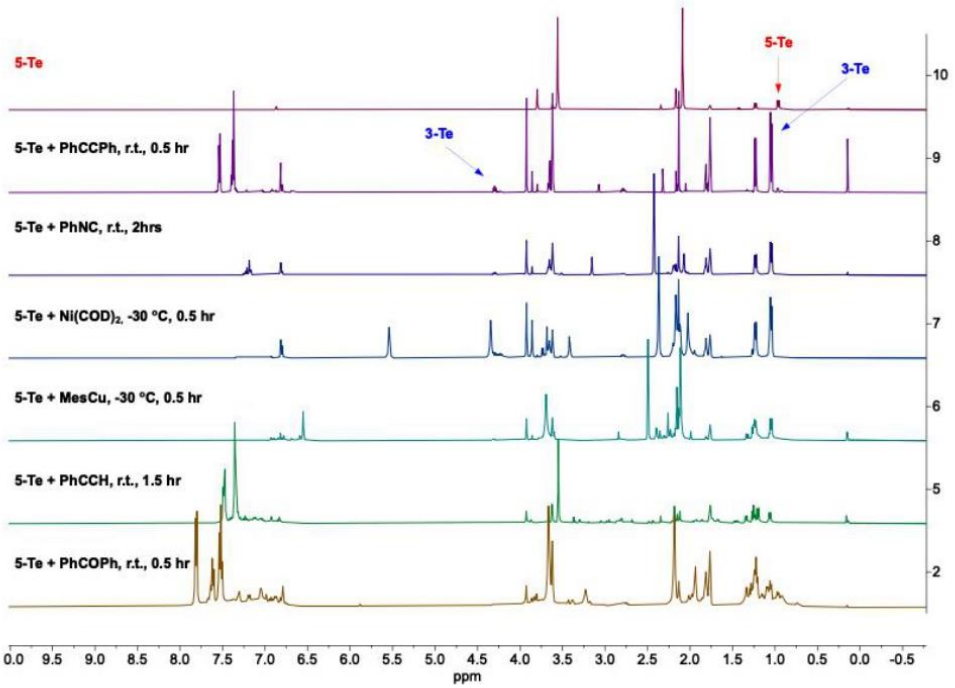

Figure S11: ^{1}H NMR spectra of **5-Te** and Diphenylacetylene, 2,6-Dimethylphenyl isocyanide, $Ni(COD)_2$, MesCu, Phenylacetylene, Ph_2CO, respectively, in different conditions, in $THFd_8$ at 300 K. [δ (silicone grease) = 0.11 ppm].

1.3.7 The thermal stability of 6-Te

The reaction of CO_2 and **5-Te** at -50 °C occurred immediately giving **6-Te**. When raising the temperature of **6-Te** in toluene/1,2-difluorobenzene (5:1) solution to -30 °C, white precipitate formed immediately (Figure S12-13). This white solid is defined as IMe_4-CO_2 by ^{1}H NMR and IR (Figure S14-16). These data are consistent with the reported IMe_4-CO_2 (^{1}H NMR (300 MHz, CD_2Cl_2): δ 3.89 (**s**, 6H, N-CH_3), 2.16 (**s**, 6H, H_3C-C=C-CH_3). IR (KBr): 1669, 1510, 1440, 1423, 1315, 1230 cm^{-1}).[S8] In addition, Figure S12 show that **6-Te** in Tol-d_8/1,2-difluorobenzene (5:1) decomposes to IMe_4=Te, and other unidentified species at -30 °C. Figure S13 shows **6-Te** decomposes gradually at r.t. and completely after 12 hours. Besides, the formation of IMe_4=Te was also confirmed by LIFDI-MS of the fresh-prepared **6-Te** (Figure S16). Therefore, these data showed **6-Te** is extremely thermally unstable, while it decomposed to IMe_4=Te, IMe_4-CO_2 and other unidentified species even at -30 °C.

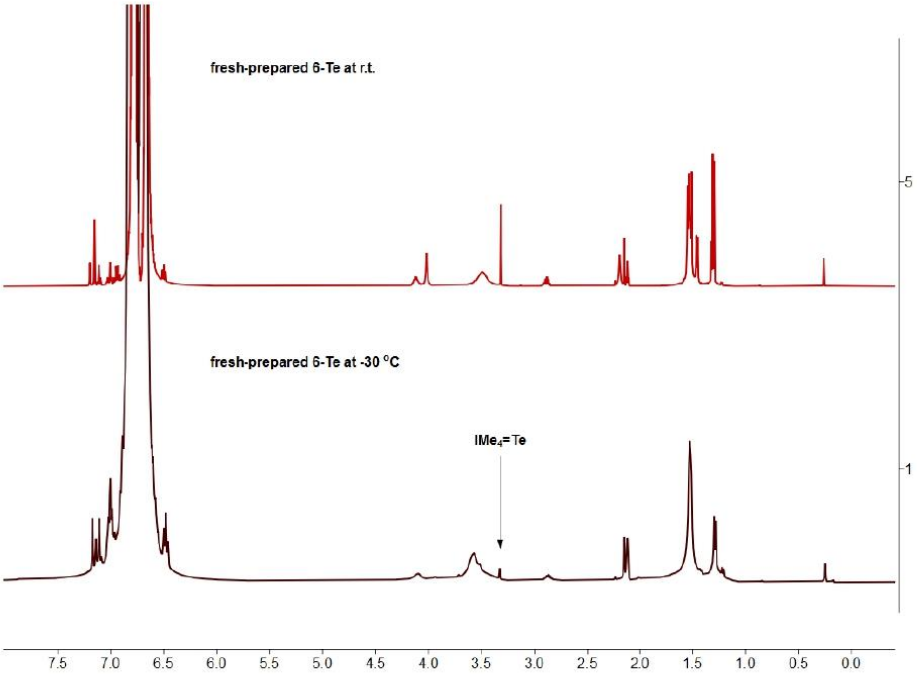

Figure S12: Stacked ^{1}H NMR (500 MHz) spectra for 'the fresh-prepared **6-Te**' at 300 K, and 'the fresh-prepared **6-Te**' at -30 °C, respectively, in Told_8/1,2-difluorobenzene (5:1). [δ (silicone grease) = 0.227 ppm]

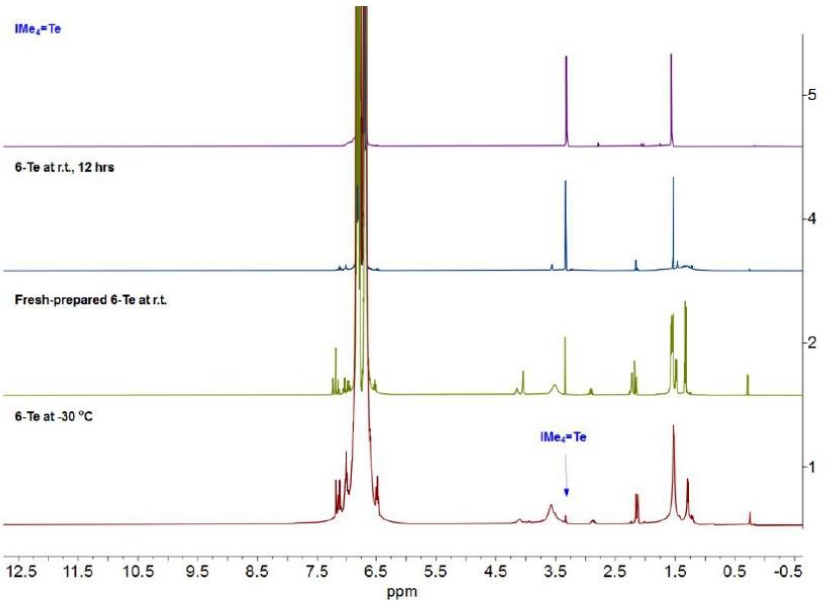

Figure S13. Stacked ^{1}H NMR (500 MHz) spectra for IMe_4=Te (at 300 K), '**6-Te** at r.t. after 12 hours' (at 300 K), 'fresh-prepared 6-Te' (at 300 K) and 'fresh-prepared **6-Te**' at -30 °C, in Tol-d_8/1,2-difluorobenzene (5:1). [δ (silicone grease) = 0.227 ppm]

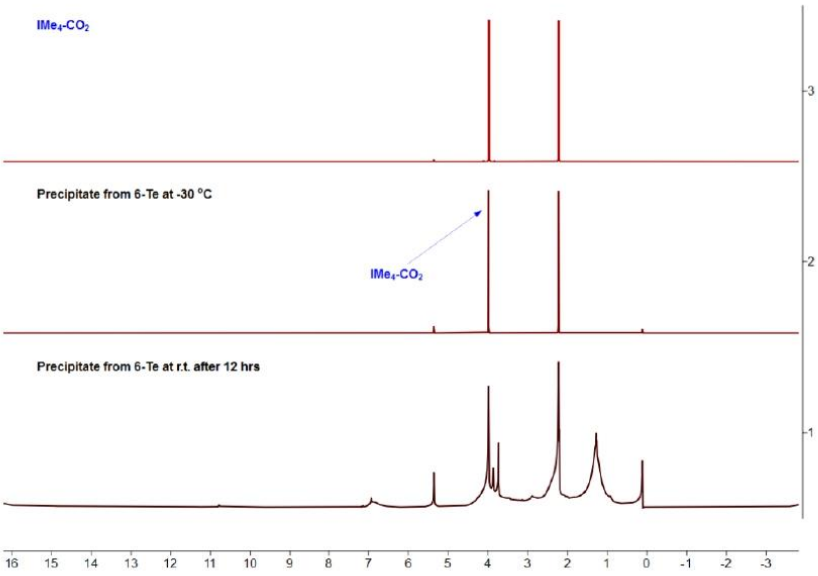

Figure S14. Stacked ^{1}H NMR (500 MHz) spectra for IMe_4-CO_2 at 300 K, the precipitate from '**6-Te** at -30 °C' (at 300 K), and the precipitate from '**6-Te** at r.t. after 12 hours' (at 300 K), respectively, in CD_2Cl_2. [δ (silicone grease) = 0.09 ppm]

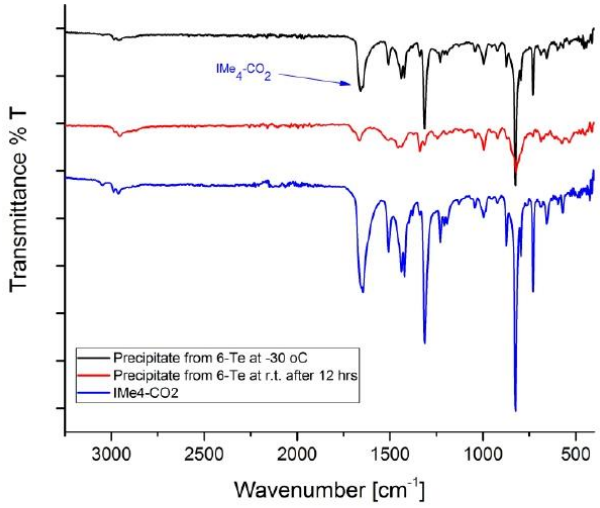

Figure S15. Stacked solid-state FT-IR spectra of for IMe_4-CO_2, the precipitate from '**6-Te** at -30 °C', and the precipitate from '**6-Te** at r.t. after 12 hours'.

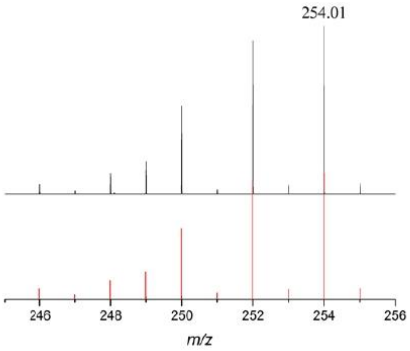

Figure S16. LIFDI-MS spectrometry (detail view with isotope pattern) of IMe_4=Te from 'the fresh-prepared **6-Te**' (Measured spectrum: top; Simulated spectrum: bottom).

1.3.8 The reactivity study of 6-Te

Here for clarifying the subsequent reactions of **6-Te**, we have tried some further reactivity of **6-Te** towards IMe_4 or $cAAC^{Me}$, $Na_2Fe(CO)_4$, BPh_3, PPh_3, KOTf, KC_8, diphenylacetylene, styrene, ethylene and hydrogen from -30 °C to r.t.. All data showed only NHC=Te (Figure S17), NHC=CO_2 (Figure S18-19), TippH (Figure S17) and other unidentified species were captured as the decomposed compounds. All attempts to capture new reactivity products were failed due to **6-Te** is thermal unstable even at -30 °C.

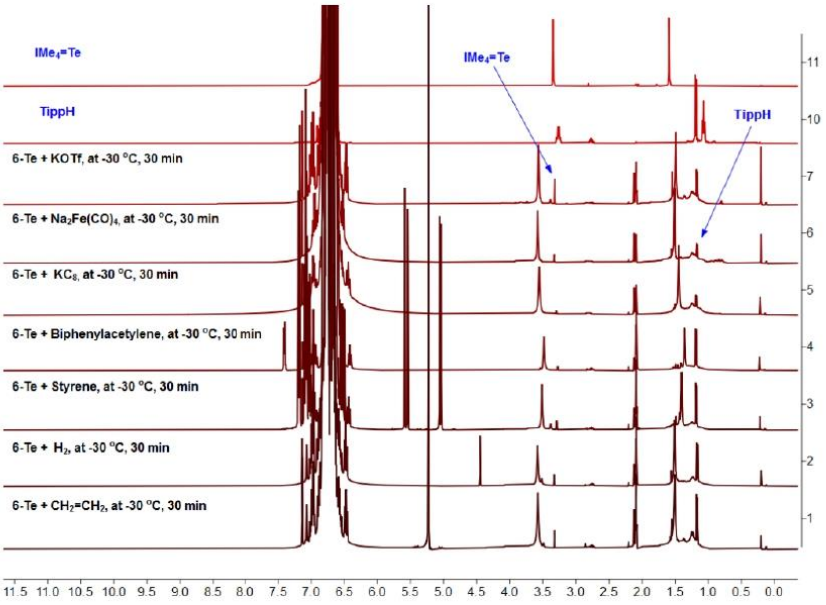

Figure S17. Stacked ^{1}H NMR (500 MHz) spectra for reaction of **6-Te** and excess KOTf, $Na_2Fe(CO)_4$, KC_8, biphenylacetylene, styrene, H_2 and CH_2=CH_2, at -30 °C, respectively, in Tol_{d8} and 1,2-difluorobenzene (5:1) at 300 K. [δ (silicone grease) = 0.227 ppm]

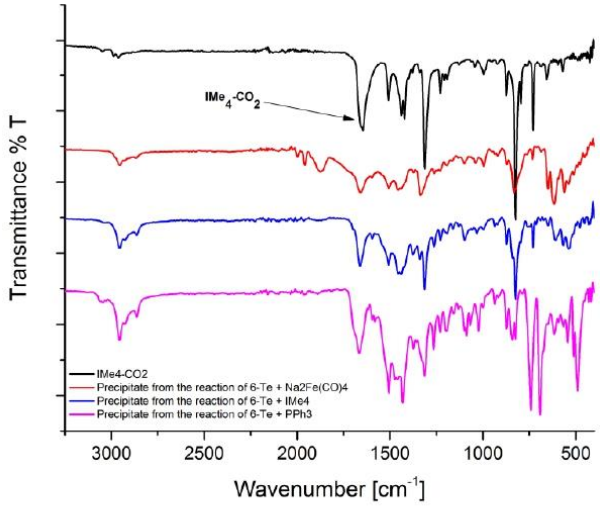

Figure S18. Stacked solid-state FT-IR spectra of for IMe_4-CO_2, the precipitate from reactions of **6-Te** and excess $Na_2Fe(CO)_4$, IMe_4 and PPh_3, respectively.

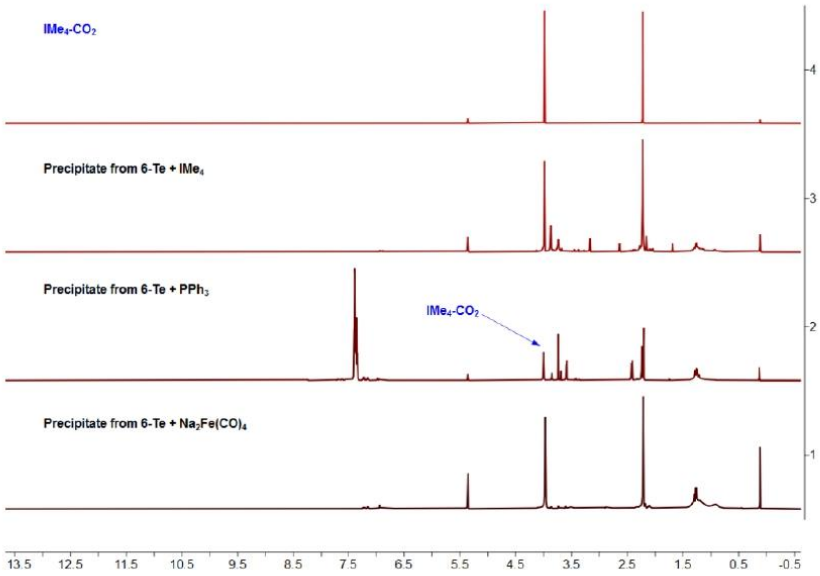

Figure S19. Stacked ^1H NMR (500 MHz) spectra for IMe_4-CO_2, the precipitate from reactions of **6-Te** and excess of $Na_2Fe(CO)_4$, IMe_4 and PPh_3, respectively, in CD_2Cl_2 at 300 K. [δ (silicone grease) = 0.09 ppm]

2 Crystallographic Data

2.1 General considerations

The X-ray intensity data were collected on an X-ray single crystal diffractometer Bruker Photon CMOS system, with a rotating anode (Bruker TXS) with MoKα radiation (λ = 0.71073 Å) or CuKα radiation (λ = 1.54184 Å) and a Helios mirror optic by using the APEX III software package or an IMS microsource with MoKα radiation (λ = 0.71073 Å) or CuKα radiation (λ = 1.54184 Å) and a Helios mirror optic by using the APEX III software package.[S9] The measurement was performed on single crystals coated with perfluorinated ether. The crystal was fixed on the top of a microsampler, transferred to the diffractometer and frozen under a stream of cold nitrogen (100K). A matrix scan was used to determine the initial lattice parameters. Reflections were merged and corrected for Lorenz and polarization effects, scan speed, and background using SAINT.[S10] Absorption corrections, including odd and even ordered spherical harmonics were performed using SADABS.[S10] Space group assignments were based upon systematic absences, E statistics, and successful refinement of the structures. Structures were solved by direct methods with the aid of successive difference Fourier maps, and were refined against all data using the APEX III software[S9] in conjunction with SHELXL-2014[S11] and SHELXLE.[S12] Methyl hydrogen atoms were refined as part of rigid rotating groups, with a C–H distance of 0.98 Å and Uiso(H) = 1.5·Ueq(C). Other H atoms were placed in calculated positions and refined using a riding model, with methylene and aromatic C–H distances of 0.99 and 0.95 Å, respectively, and Uiso(H) = 1.2·Ueq(C). If not mentioned otherwise, non-hydrogen atoms were refined with anisotropic displacement parameters. Full-matrix least-squares refinements were carried out by minimizing $\Delta w(Fo^2-Fc^2)^2$ with SHELXL-97[S13] weighting scheme. Neutral atom scattering factors for all atoms and anomalous dispersion corrections for the non-hydrogen atoms were taken from International Tables for Crystallography.[S14] Images of the crystal structures were generated by Platon and Mercury.[S15] The CCDC numbers 2215503-2215507 contain the supplementary crystallographic data for the structures **2-Te**, **3-Se**, **3-Te**, **5-Te**, **6-Te**. These data can be obtained free of charge from the Cambridge Crystallographic Data Centre via https://www.ccdc.cam.ac.uk/structures/.

2.2 SC-XRD Analysis

2.2.1 Crystal Structure of [*i*PrAl(Tipp)-*μ*-Te]$_2$ (2-Te)

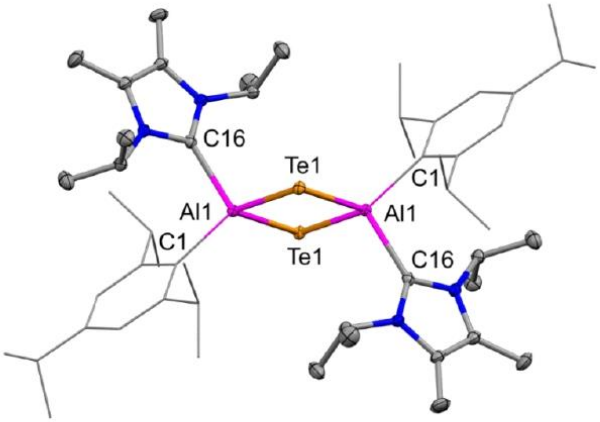

Figure S20. Molecular structure of compound **2-Te** in the solid state. Ellipsoids are set at the 50% probability level; hydrogen atoms and co-crystallized solvent molecules are omitted for clarity and Tipp ligands are depicted in wireframe for simplicity. Selected bond lengths (Å) and angles (°): Al1–Te1 2.6051(5), 2.6363(5), Al1–C1 2.022(1), Al1–C16 2.099(2), Al1–Te1–Al1 81.62(1), Te1–Al1–Te1 98.38(2), C1–Al1–C16 101.55(6). (X-ray quality colorless crystal of compound **2-Te** were grown from pentane solution at -30 °C.

2.2.2 Crystal Structure of [IMe$_4$Al(Tipp)-μ-Te]$_2$ (3-Te)

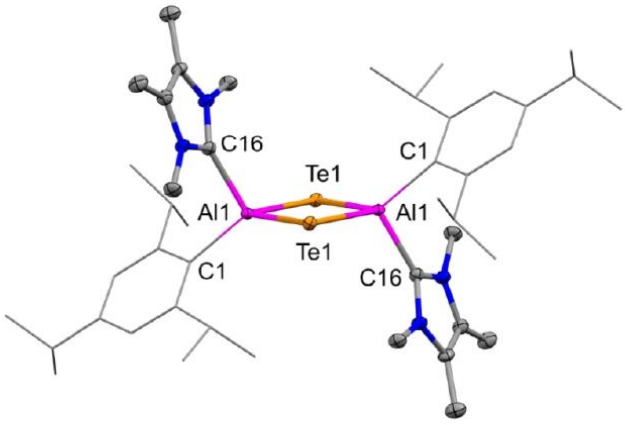

Figure S21. Molecular structure of compound **3-Te** in the solid state. Ellipsoids are set at the 50% probability level; hydrogen atoms and co-crystallized solvent molecules are omitted for clarity and Tipp ligands are depicted in wireframe for simplicity. Selected bond lengths (Å) and angles (°): Al1–Te1 2.5974(9), 2.626(1), Al1–C1 2.014(3), Al1–C16 2.062(3), Al1–Te1–Al1 82.31(3), Te1–Al1–Te1 97.69(3), C1–Al1–C16 102.8(1). (X-ray quality colorless crystal of compound **3-Te** was grown from a saturated THF solution with pentane diffusion.)

2.2.3 Crystal Structure of (IMe$_4$)$_2$Al(Tipp)=Te (5-Te)

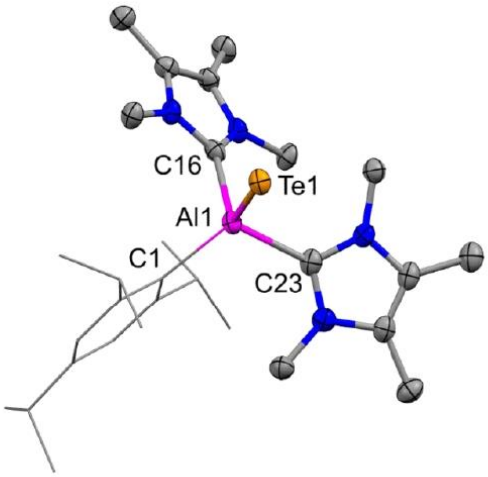

Figure S22. Molecular structure of compound **5-Te** in the solid state. Ellipsoids are set at the 50% probability level; hydrogen atoms and co-crystallized solvent molecules are omitted for clarity and Tipp ligands are depicted in wireframe for simplicity. Selected bond lengths (Å) and angles (°): Al1–Te1 2.534(1), Al1–C1 2.047(4), Al1–C23 2.061(5), Al1–C16 2.082(5), Te1–Al1–C1 127.2(1), Te1–Al1–C16 108.2(1), Te1–Al1–C23 99.9(1). (X-ray quality yellow crystal of compound **5-Te** was grown from saturated THF solution at -30 °C.)

2.2.4 Crystal Structure of [IMe$_4$Al(Tipp)-μ-Se]$_2$ (3-Se)

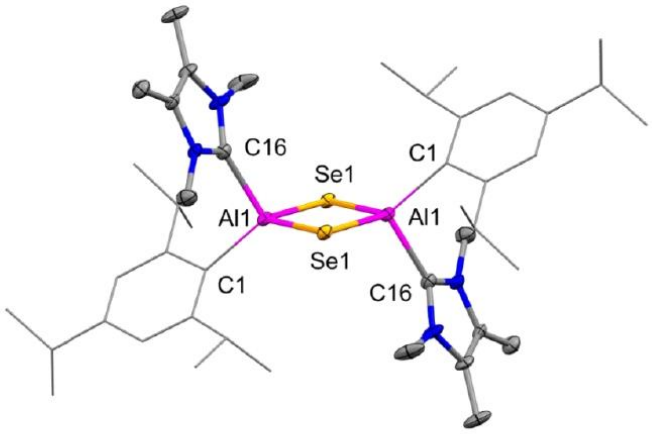

Figure S23. Molecular structure of compound **3-Se** in the solid state. Ellipsoids are set at the 50% probability level; hydrogen atoms and co-crystallized solvent molecules are omitted for clarity and Tipp ligands are depicted in wireframe for simplicity. Selected bond lengths (Å) and angles (°):Al1–Se1 2.386(1), 2.402(2), Al1–C1 2.019(9), Al1–C16 2.078(5), Al1–Se1–Al1 80.56(5), Se1–Al1–Se1 99.44(5), C1–Al1–C16 102.8(4). (X-ray quality colorless crystal of compound **3-Se** was grown from a saturated THF solution with pentane diffusion.)

2.2.5 Crystal Structure of (IMe$_4$CO$_2$)$_2$Al(Tipp)-μ-O$_2$C=Te (6-Te)

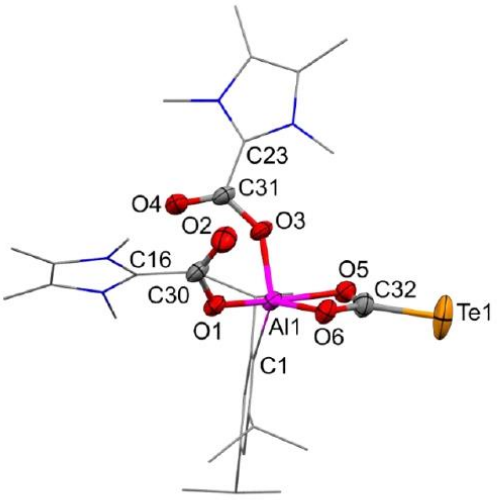

Figure S24. Molecular structure of compound **6-Te** in the solid state. Ellipsoids are set at the 50% probability level; hydrogen atoms and co-crystallized solvent molecules are omitted for clarity and Tipp ligand is depicted in wireframe for simplicity. Selected bond lengths (Å) and angles (°): C32–Te1 2.088(5), Al1–O5 2.028(4), Al1–O6 1.871(4), Al1–O3 1.824(3), Al1–O1 1.865(4), Al1–C1 1.992(5), C32–O5 1.268(7), C32–O6 1.317(7), C31–C23 1.474(7), C31–O3 1.294(6), C31–O4 1.211(6), C30–O1 1.288(6), C30–O2 1.221(7), C30–C16 1.546(16), Te1–C32–O5 123.8(4), O5–C32–O6 113.4(4), O5–Al1–O6 67.16(15), O5–Al1–O3 87.14(15), O6–Al1–O1 97.71(16), O3–Al1–O1 94.16(16), C23–C31–O4 121.6(5), O1–C30–C16 111.6(6), O1–C30–O2 126.4(5), C31–O3–Al1 139.5(3), C30–O1–Al1 129.7(3), O5–Al1–C1 92.91(18), O1–Al1–C1 99.51(19), O3–Al1–C1 124.27(17), O6–Al1–C1 118.78(17). (X-ray quality colorless crystal of compound **6-Te** was grown from a saturated toluene/1,2-difluorobenzene (5:1) solution at -30 °C.)

2.3 Crystal data and structure refinement

Table S2. Crystal data and structure refinement.

Compound #	2-Te	3-Te	3-Se	5-Te	6-Te
CCDC-Number	2215503	2215505	2215504	2215506	2215507
Chemical formula	$C_{52}H_{86}Al_2N_4Te_2$	$C_{44}H_{70}Al_2N_4Te_2$ ($C_{10}H_{24}$)	$C_{44}H_{70}Al_2N_4Se_2$	$C_{29}H_{47}AlN_4Te$ (C_4H_7O)	$C_{32}H_{47}AlN_4O_6Te$ ($C_{35}H_{40}$)
Formula weight	1076.41 g/mol	1108.41 g/mol	866.92 g/mol	678.39 g/mol	1198.99 g/mol
Temperature	100 K	100 K	100 K	100 K	100 K
Wavelength	0.71073 Å	0.71073 Å	0.71073 Å	1.54178 Å	0.71073 Å
Crystal size	0.346 x 0.150 x 0.115 mm	0.164 x 0.300 x 0.424 mm	0.080 x 0.117 x 0.248 mm	0.079 x 0.083 x 0.251 mm	1.000 x 0.800 x 0.600 mm
Crystal habit	clear colorless needle	clear colorless fragment	clear colorless fragment	clear yellow fragment	clear colorless fragment
Crystal system	triclinic	triclinic	monoclinic	orthorhombic	monoclinic
Space group	P -1	P-1	C2/c	Pbca	P21/c
Unit cell dimensions	a = 9.6841(3) Å; α = 102.161(1)°	a = 10.3675(9)Å; α = 93.606(2)°	a = 28.047(3)Å; α = 90°	a = 15.9506(5)Å; α = 90°	a = 16.3998(19)Å; α = 90°
	b = 9.9384(4) Å; β = 92.218(1)°	b = 15.9930(13)Å; β = 90.327(2)°	b = 10.0704(9)Å; β = 103.119(2)°	b = 16.4527(6)Å; β = 90°	b = 21.902(2)Å; β = 108.796(4)°
	c = 14.2476(5) Å; γ = 91.835(1)°	c = 17.5663(15)Å; γ = 108.538(2)°	c = 17.7757(16) Å; γ = 90°	c = 27.1253(9)Å; γ = 90°	c = 18.323(2)Å; γ = 90°
Volume	1338.34(8) Å³	2755.0(4) Å³	4889.6(8) Å³	7118.5(4) Å³	6230.4(12)Å³
Z	1	2	4	8	4
Density (calculated)	1.336 g/cm³	1.336 g/cm³	1.178 g/cm³	1.266 g/cm³	1.278 g/cm³
Radiation source	IMS microsource (Mo)	IMS microsource (Mo)	IMS microsource (Mo)	IMS microsource (Mo)	IMS microsource (Cu)
Theta range for data collection	2.10 to 25.35°	2.07 to 25.35°	2.15 to 25.35°	3.26 to 68.33°	1.860 to 25.824°
Index ranges	-11<=h<=11, -11<=k<=11, -17<=l<=17	-12<=h<=12, -19<=k<=19, -21<=l<=21	-33<=h<=33, -12<=k<=12, -21<=l<=21	-18<=h<=19, -19<=k<=19, -32<=l<=32	-20<=h<=20, -26<=k<=26, -22<=l<=22
Reflections collected	74361	77501	39397	110283	264488
Independent reflections	4894	10097	4474	6513	11913
Completeness	0.999	0.999	1.000	0.999	0.991
Absorption correction	Multi-Scan	Multi-Scan	Multi-Scan	Multi-Scan	Multi-Scan
Max. and min. transmission	0.7452 and 0.6956	0.7452 and 0.6334	0.7452 and 0.5598	0.7531 and 0.5240	0.7453 and 0.6910
Refinement method	Full-matrix least-squares on F^2	Full-matrix least-squares on F^2	Full-matrix least-squares on F^2	Full-matrix least-squares on F^2	Full-matrix least-squares on F^2
Function minimized	$\Sigma w(F_o^2 - F_c^2)^2$	$\Sigma w(F_o^2 - F_c^2)^2$	$\Sigma w(F_o^2 - F_c^2)^2$	$\Sigma w(F_o^2 - F_c^2)^2$	$\Sigma w(F_o^2 - F_c^2)^2$
Data / restraints / parameters	4894/0/283	10097/0/580	4474/480/388	6513/0/375	11913/1098/988
Goodness-of-fit on F^2	1.097	1.163	1.115	1.058	0.859
Final R indices [I>2sigma(I)]	R1 = 0.0142, wR2 = 0.0339	R1 =0.0251, wR2 = 0.0526	R1= 0.0648, wR2 = 0.1547	R1 =0.0418, wR2 = 0.1085	R1 =0.0956, wR2 = 0.2617
R indices (all data)	R1 = 0.0148, wR2 = 0.0342	R1 =0.0279, wR2 = 0.0544	R1 =0.0759, wR2 = 0.1605	R1 =0.0645, wR2 = 0.1318	R1 =0.1201, wR2 = 0.2880
Largest diff. peak and hole	0.321 and -0.311 eÅ^{-3}	0.533 and -0.549 eÅ^{-3}	2.401 and -1.159 eÅ^{-3}	1.376 and -1.013 eÅ^{-3}	2.158 and -1.637eÅ^{-3}

3 Spectra

3.1 NMR spectra of $IMe_4Al(Tipp)H_2$ (1-IMe_4)

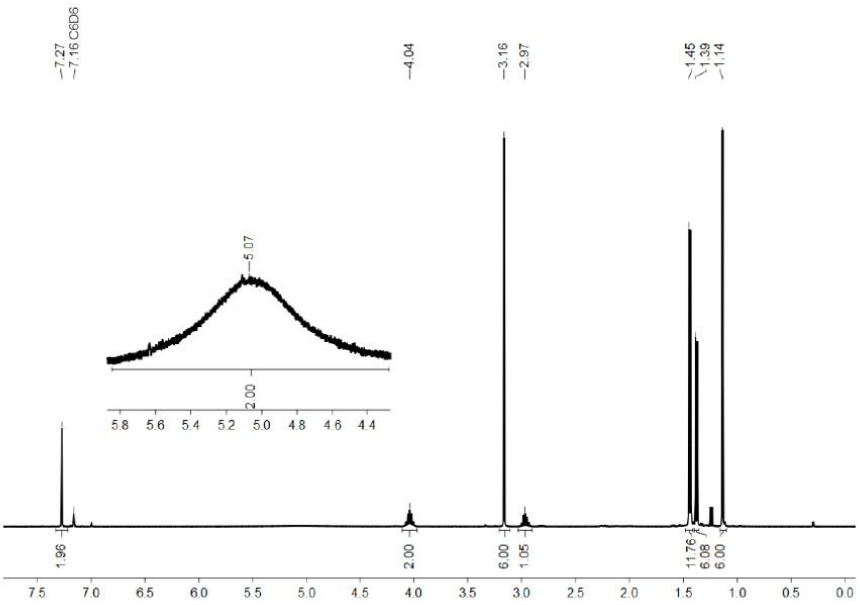

Figure S25. ^1H NMR spectrum (400 MHz) of compound **1-IMe_4** in C_6D_6 at 300 K. [δ (silicone grease) = 0.295 ppm]

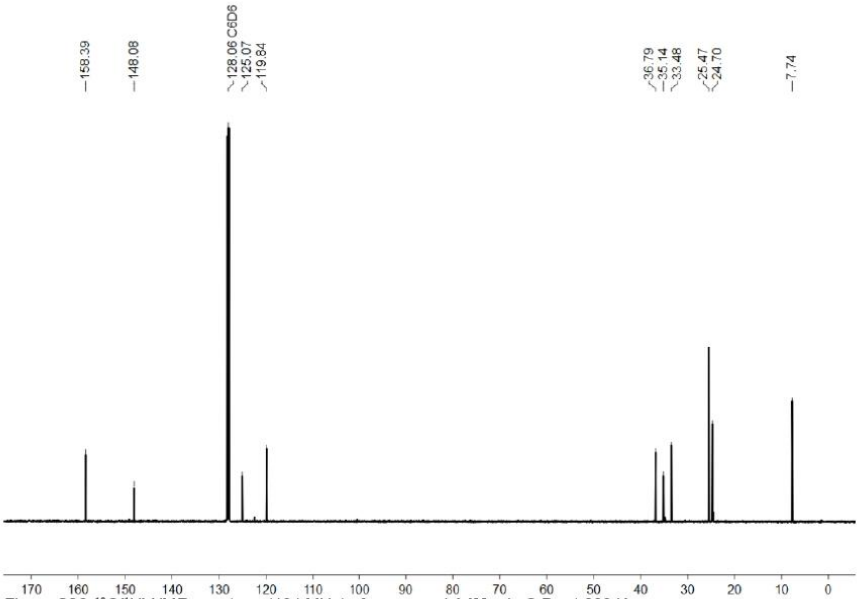

Figure S26. $^{13}C\{^1H\}$ NMR spectrum (101 MHz) of compound **1-IMe_4** in C_6D_6 at 300 K.

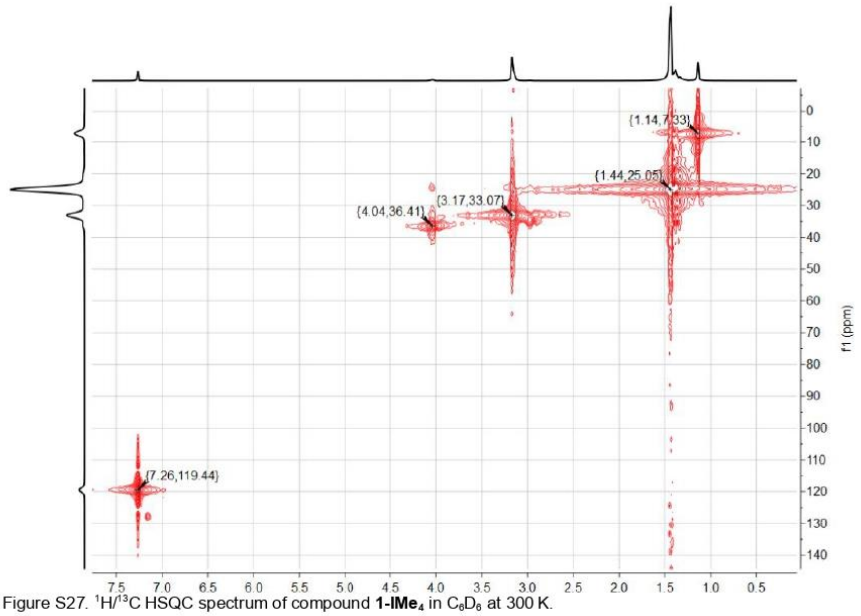

Figure S27. $^{1}H/^{13}C$ HSQC spectrum of compound **1-IMe$_4$** in C_6D_6 at 300 K.

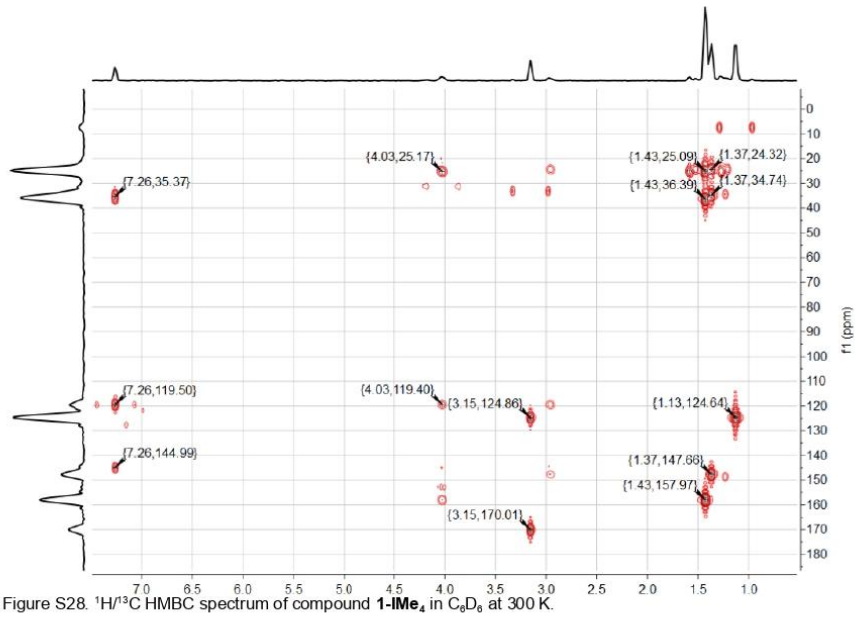

Figure S28. $^{1}H/^{13}C$ HMBC spectrum of compound **1-IMe$_4$** in C_6D_6 at 300 K.

3.2 Spectra of [*i*PrAl(Tipp)-*μ*-Te]$_2$ (2-Te)

3.2.1 NMR spectra

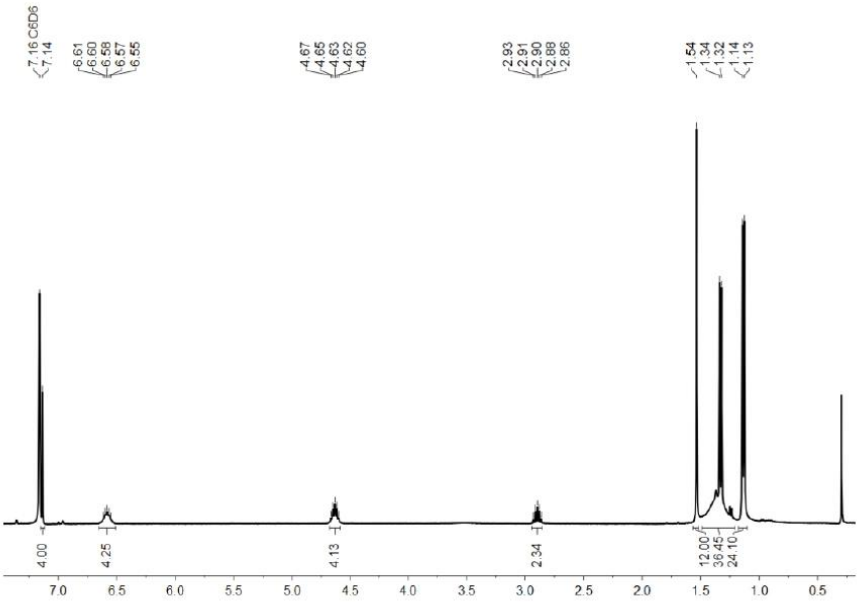

Figure S29. ^{1}H NMR spectrum (400 MHz) of compound **2-Te** in C_6D_6 at 300 K. [δ (silicone grease) = 0.297 ppm]

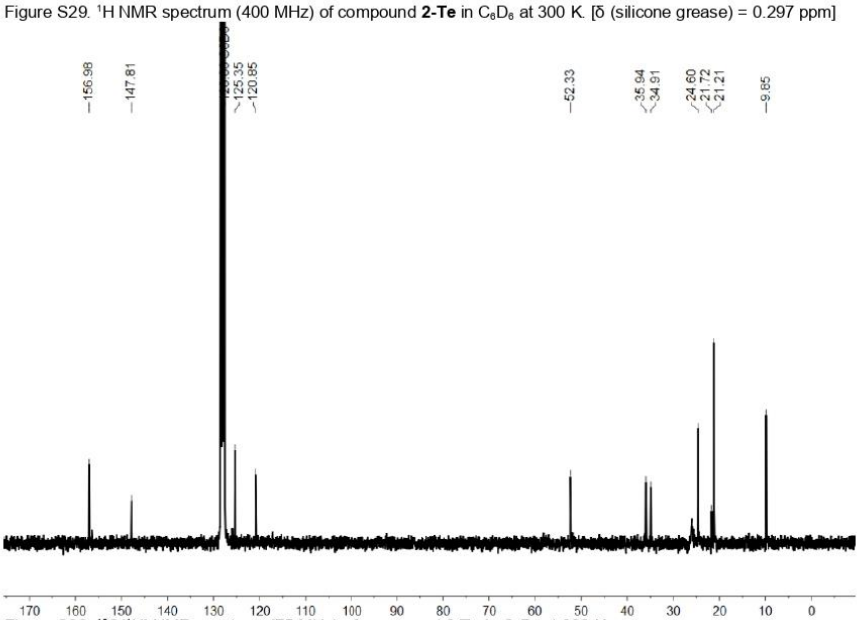

Figure S30. ^{13}C{^{1}H} NMR spectrum (75 MHz) of compound **2-Te** in C_6D_6 at 300 K.

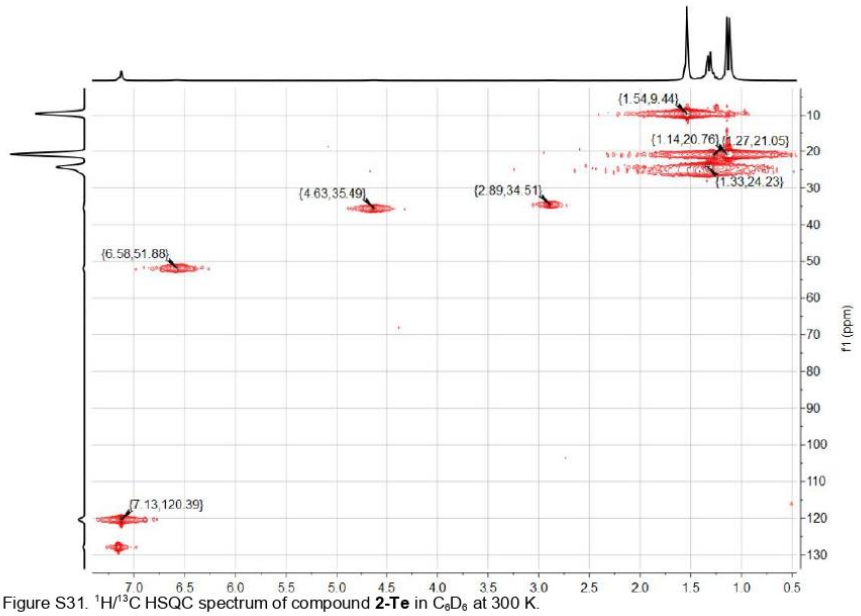

Figure S31. $^{1}H/^{13}C$ HSQC spectrum of compound **2-Te** in C_6D_6 at 300 K.

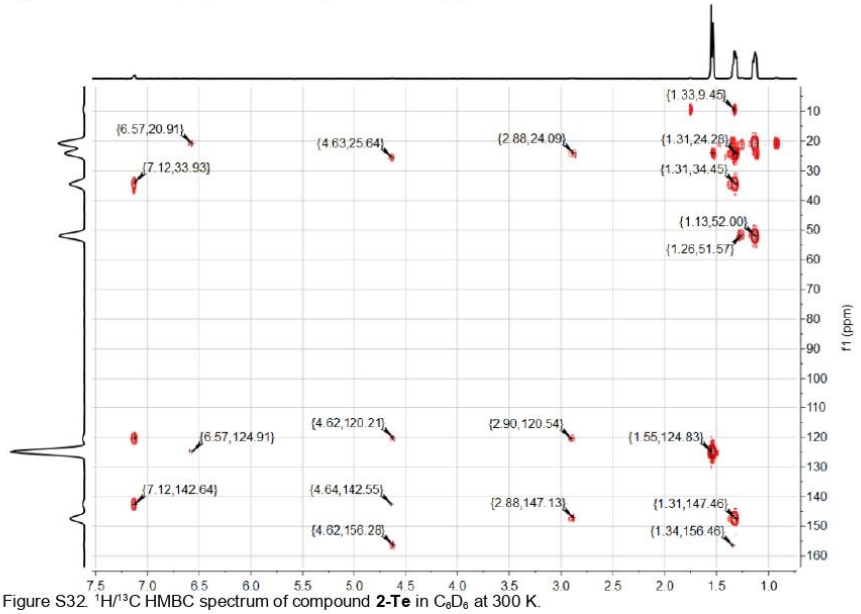

Figure S32. $^{1}H/^{13}C$ HMBC spectrum of compound **2-Te** in C_6D_6 at 300 K.

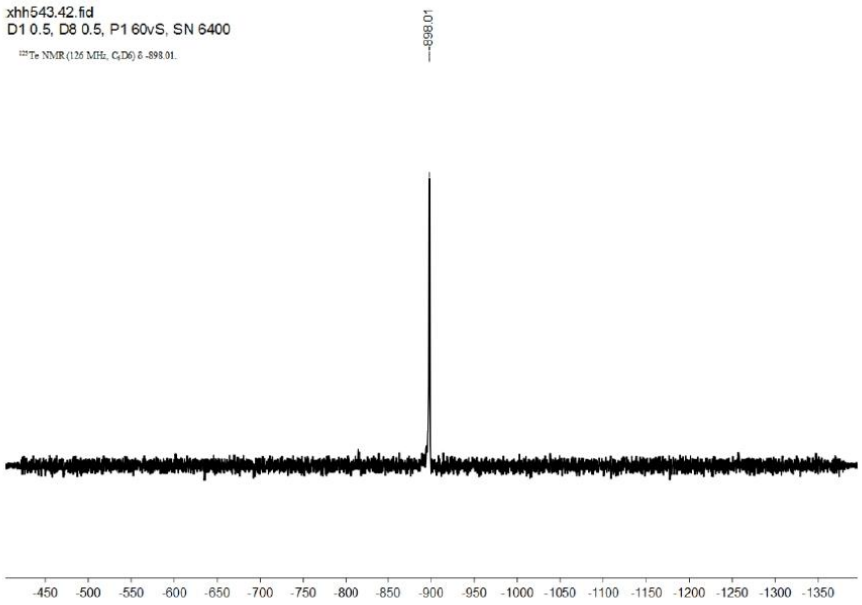

Figure S33. ^{125}Te NMR spectrum (126 Hz) of compound **2-Te** in C_6D_6 at 300 K.

3.2.2 Mass spectra

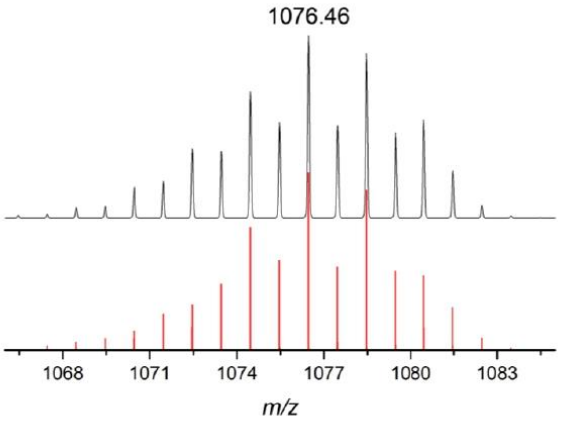

Figure S34. LIFDI-MS spectrometry (detail view with isotope pattern) of [I*i*PrAl(Tipp)-μ-Te]$_2$ (**2-Te**) (Measured spectrum: top; Simulated spectrum: bottom).

3.3 Spectra of [IMe$_4$Al(Tipp)-μ-Te]$_2$ (3-Te)

3.3.1 NMR spectra

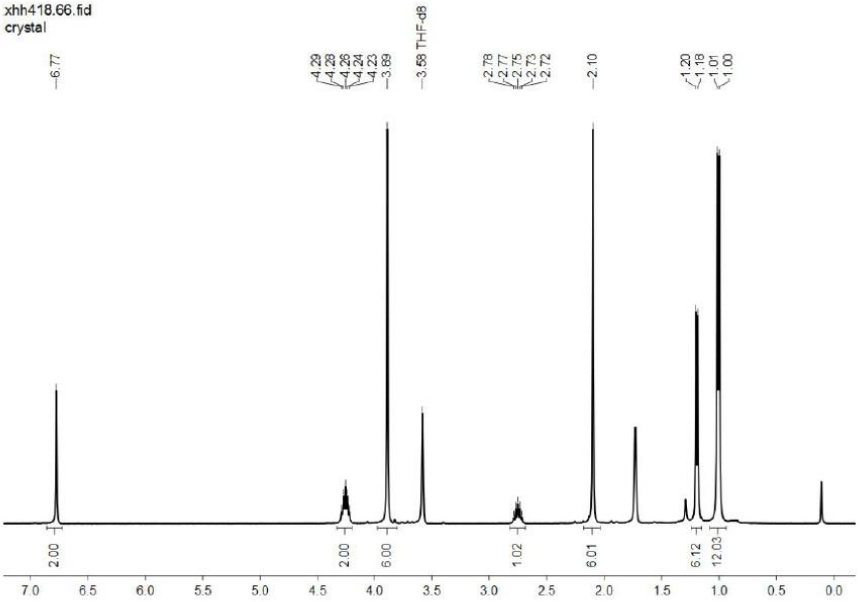

Figure S35. ^{1}H NMR spectrum (400 MHz) of compound **3-Te** in THF-d$_8$ at 300 K. [δ (silicone grease) = 0.108 ppm]

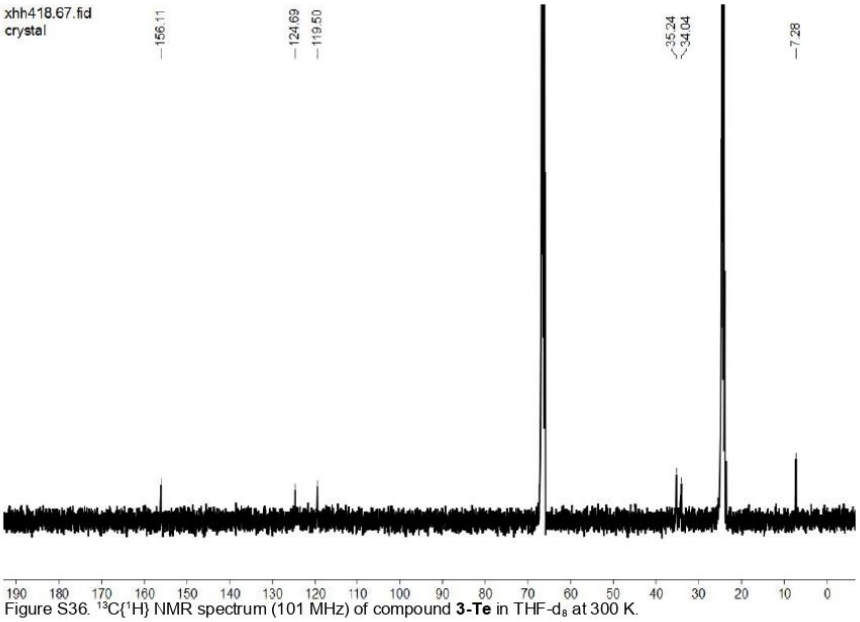

Figure S36. ^{13}C{^{1}H} NMR spectrum (101 MHz) of compound **3-Te** in THF-d$_8$ at 300 K.

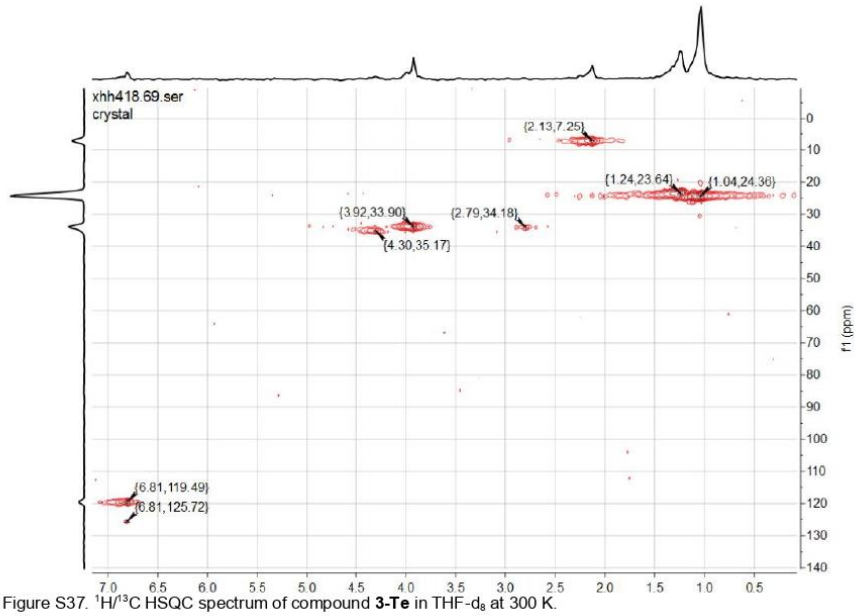

Figure S37. $^{1}H/^{13}C$ HSQC spectrum of compound **3-Te** in THF-d_8 at 300 K.

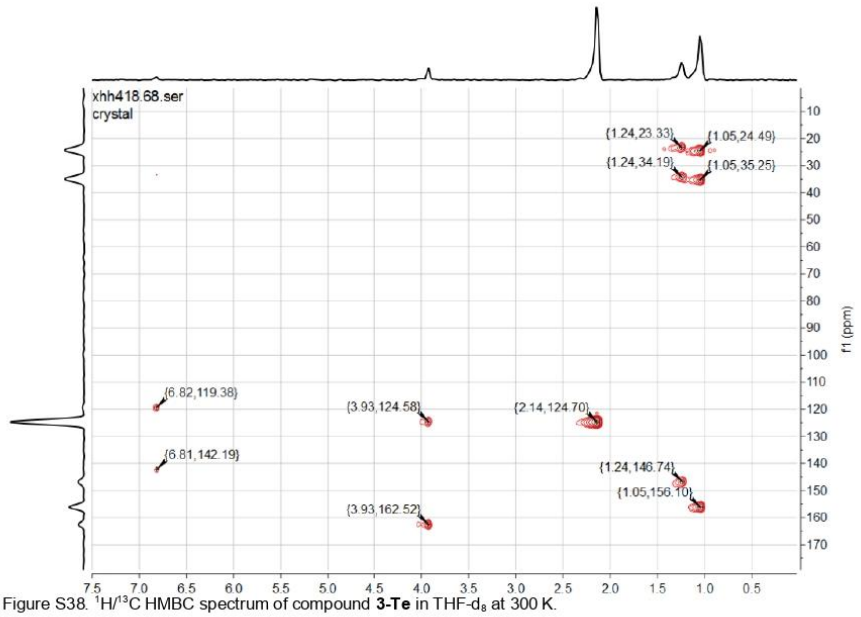

Figure S38. $^{1}H/^{13}C$ HMBC spectrum of compound **3-Te** in THF-d_8 at 300 K.

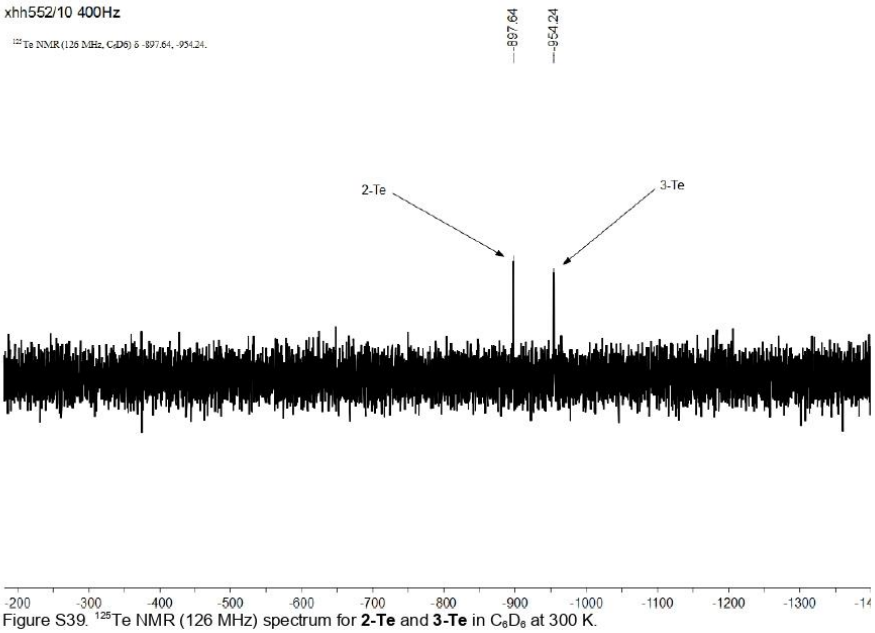

Figure S39. ^{125}Te NMR (126 MHz) spectrum for **2-Te** and **3-Te** in C_6D_6 at 300 K.

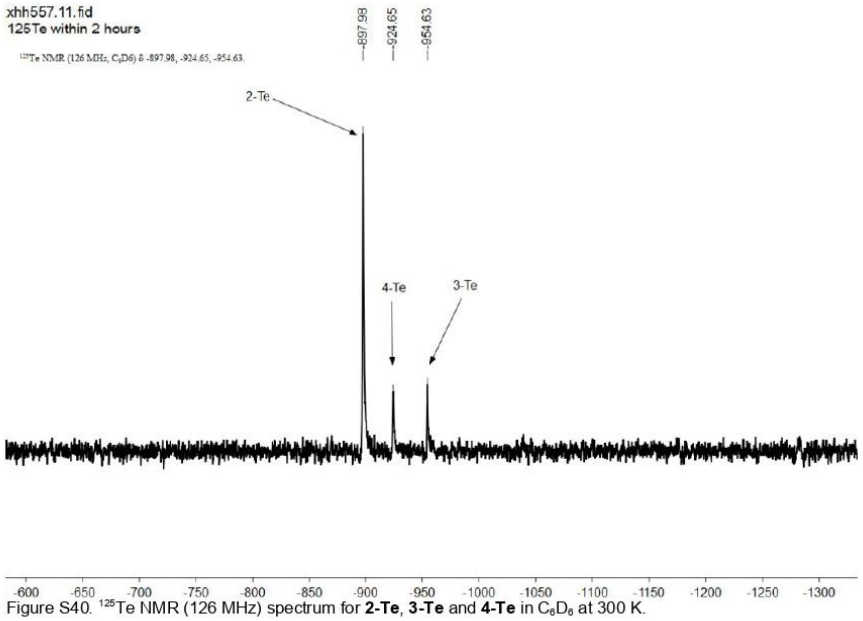

Figure S40. ^{125}Te NMR (126 MHz) spectrum for **2-Te**, **3-Te** and **4-Te** in C_6D_6 at 300 K.

3.3.2 Mass spectra

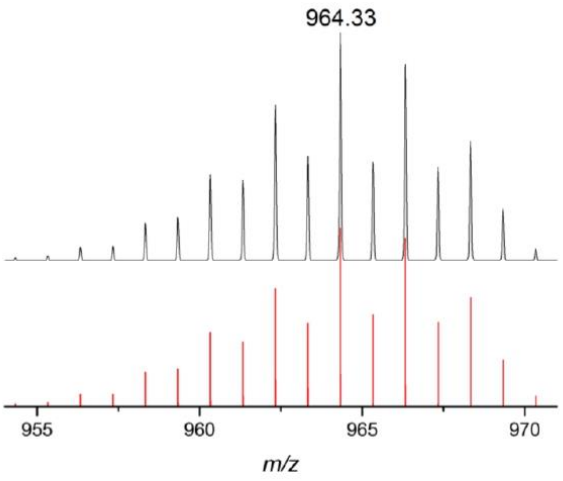

Figure S41. LIFDI-MS spectrometry (detail view with isotope pattern) of [IMe$_4$Al(Tipp)-μ-Te]$_2$ (**3-Te**) (Measured spectrum: top; Simulated spectrum: bottom).

3.4 Spectra of (IMe$_4$)$_2$Al(Tipp)=Te (5-Te)

3.4.1 NMR spectra

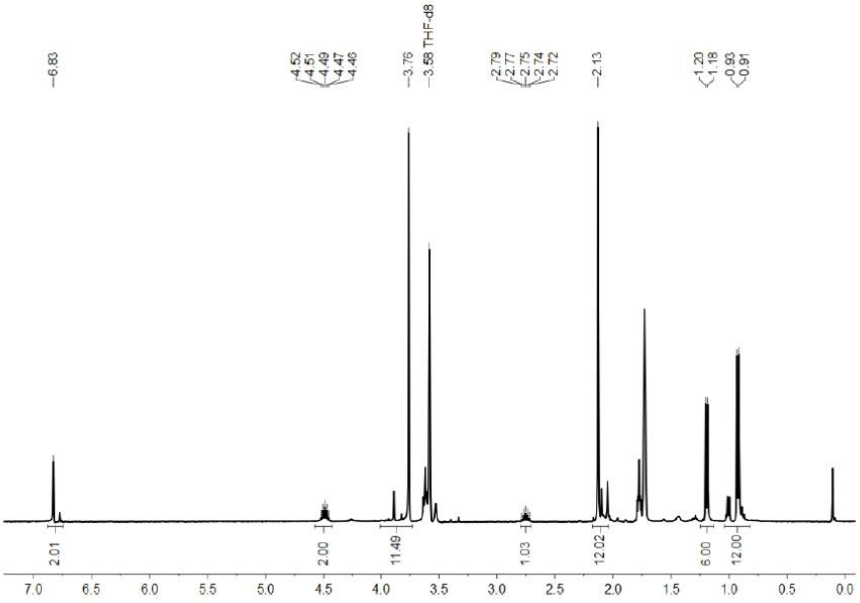

Figure S42. ^{1}H NMR spectrum (400 MHz) of compound **5-Te** in THF-d$_8$ at 300 K. [δ (silicone grease) = 0.108 ppm]

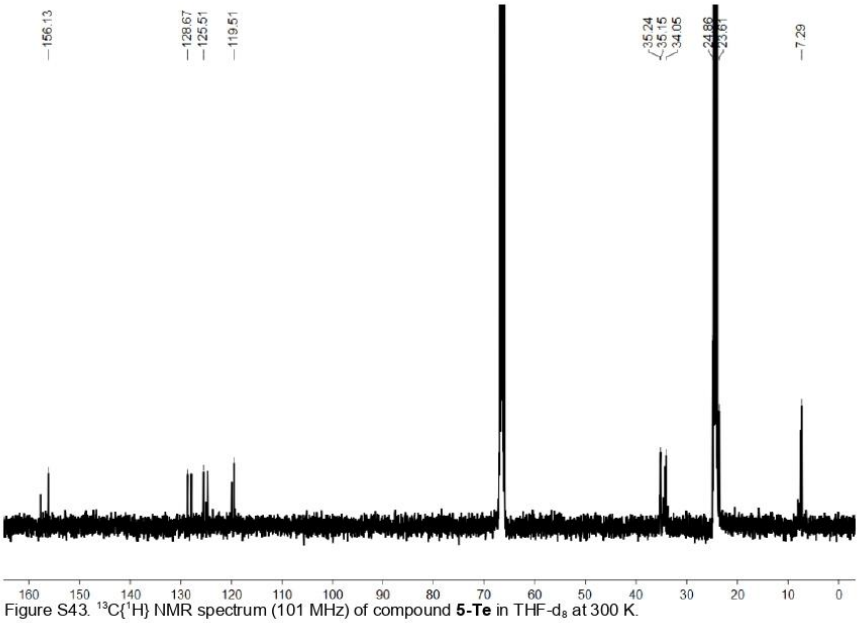

Figure S43. $^{13}C\{^{1}H\}$ NMR spectrum (101 MHz) of compound **5-Te** in THF-d_8 at 300 K.

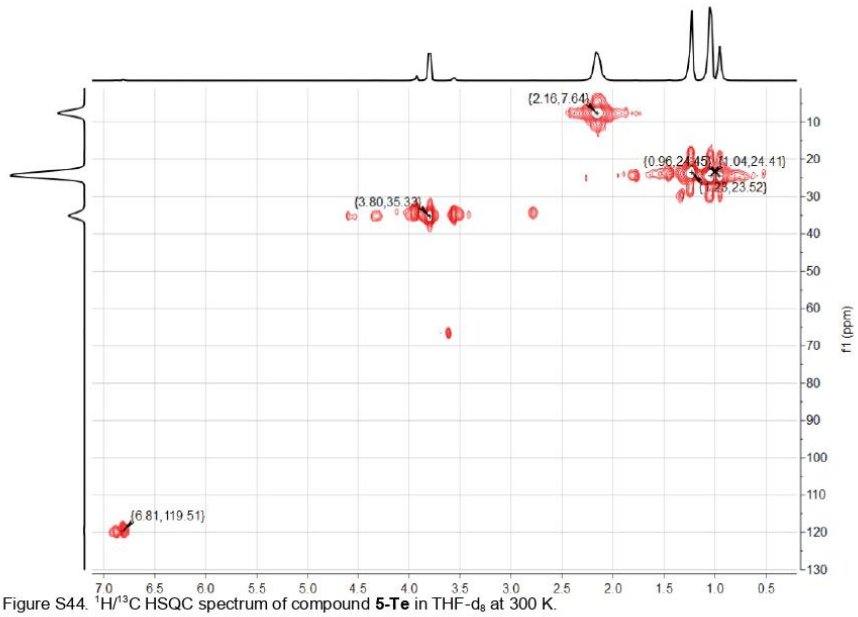

Figure S44. $^{1}H/^{13}C$ HSQC spectrum of compound **5-Te** in THF-d_8 at 300 K.

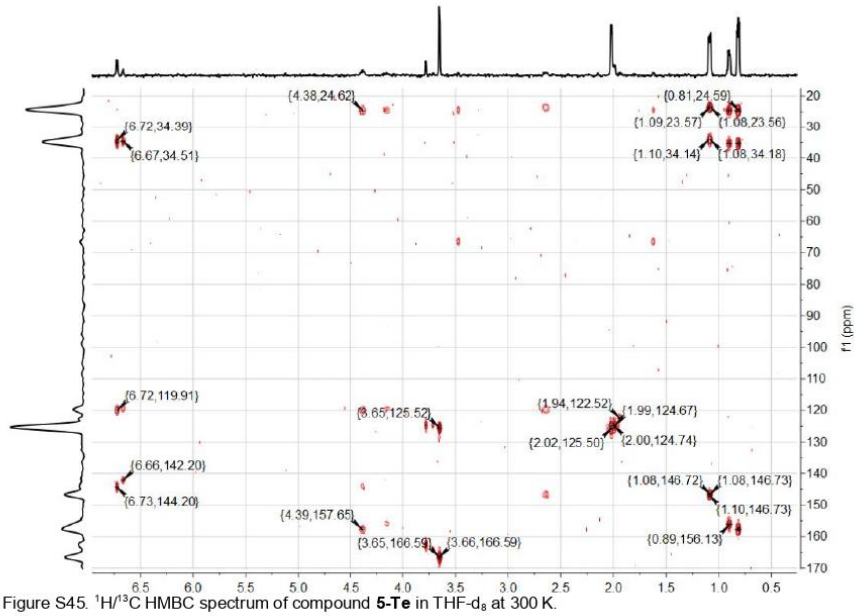

Figure S45. $^{1}H/^{13}C$ HMBC spectrum of compound **5-Te** in THF-d_8 at 300 K.

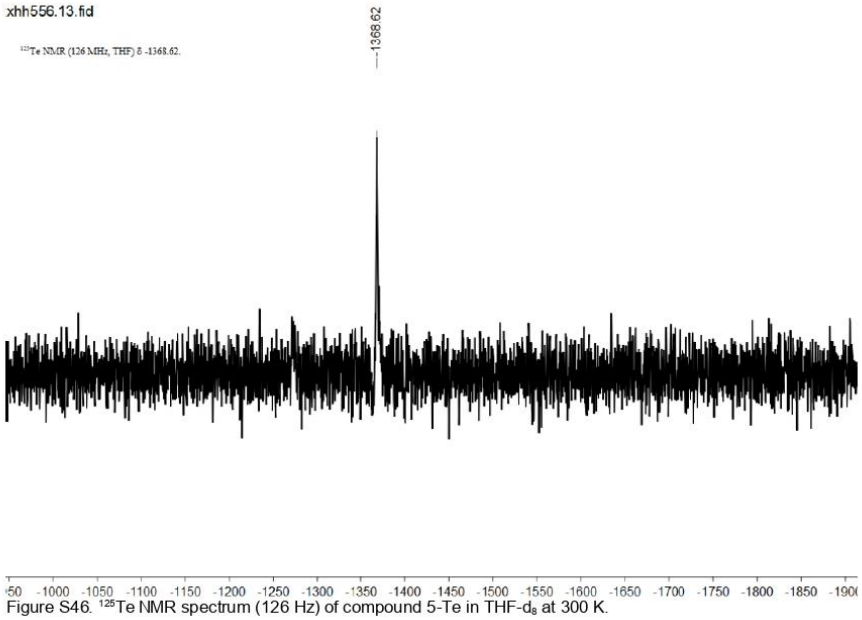

Figure S46. ^{125}Te NMR spectrum (126 Hz) of compound 5-Te in THF-d_8 at 300 K.

3.4.2 Mass spectra

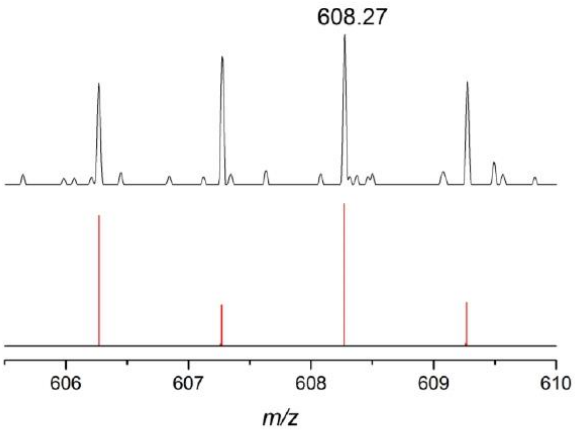

Figure S47. LIFDI-MS spectrometry (detail view with isotope pattern) of $(IMe_4)_2Al(Tipp)=Te$ (**5-Te**) (Measured spectrum: top; Simulated spectrum: bottom).

3.4.3 IR spectrum

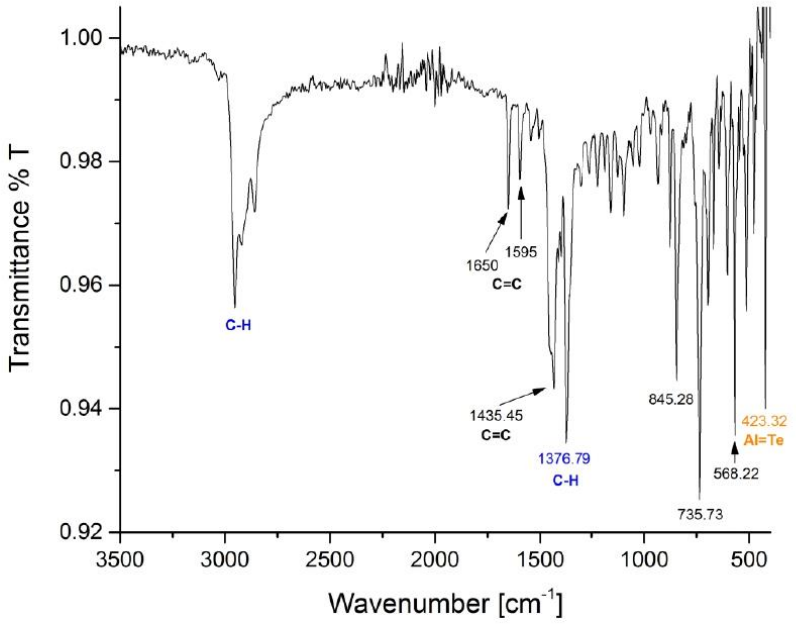

Figure S48. Solid-state FT-IR spectrum of $(IMe_4)_2Al(Tipp)=Te$ (**5-Te**)

3.5 Spectra of [*i*PrAl(Tipp)-*μ*-Se]$_2$ (2-Se)

3.5.1 NMR spectra

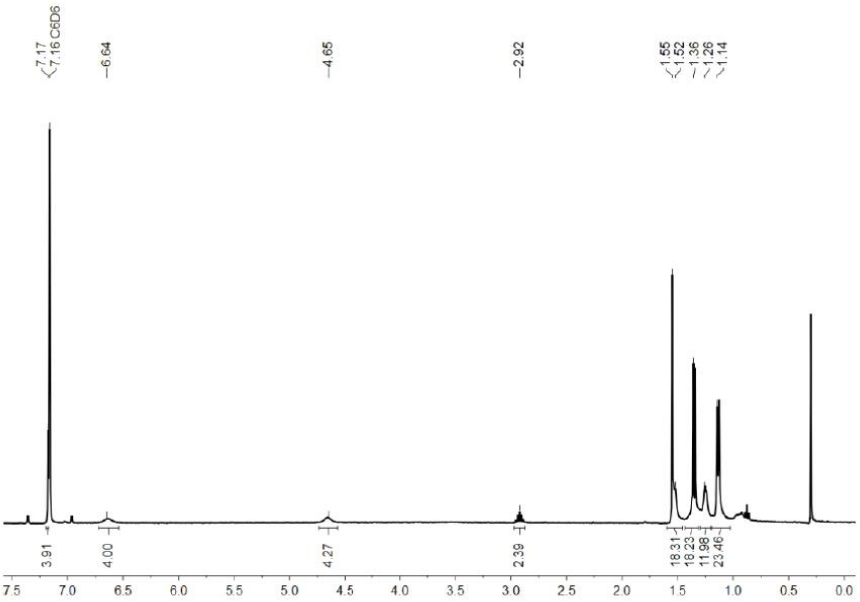

Figure S49. ^{1}H NMR spectrum (400 MHz) of compound **2-Se** in C_6D_6 at 300 K. [δ (silicone grease) = 0.299 ppm]

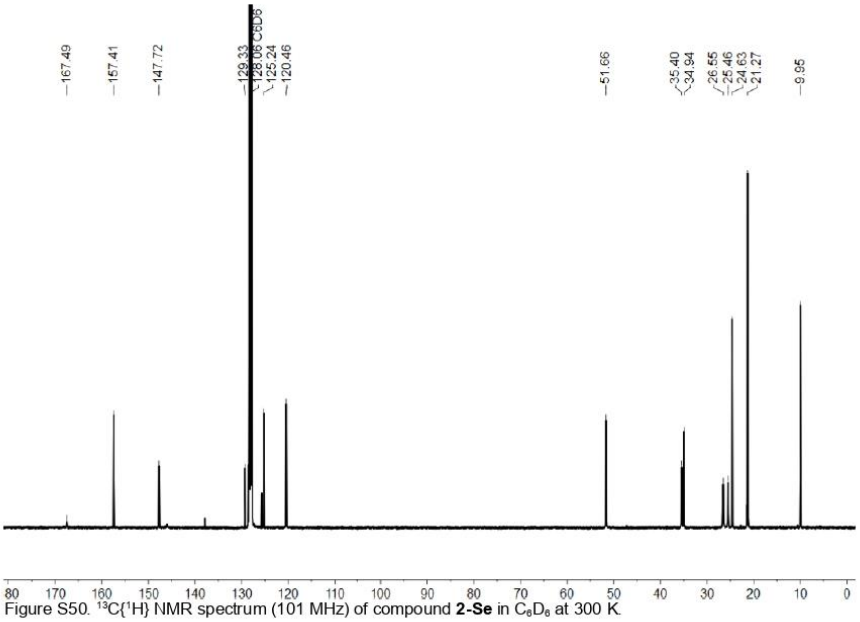

Figure S50. ^{13}C{^{1}H} NMR spectrum (101 MHz) of compound **2-Se** in C_6D_6 at 300 K.

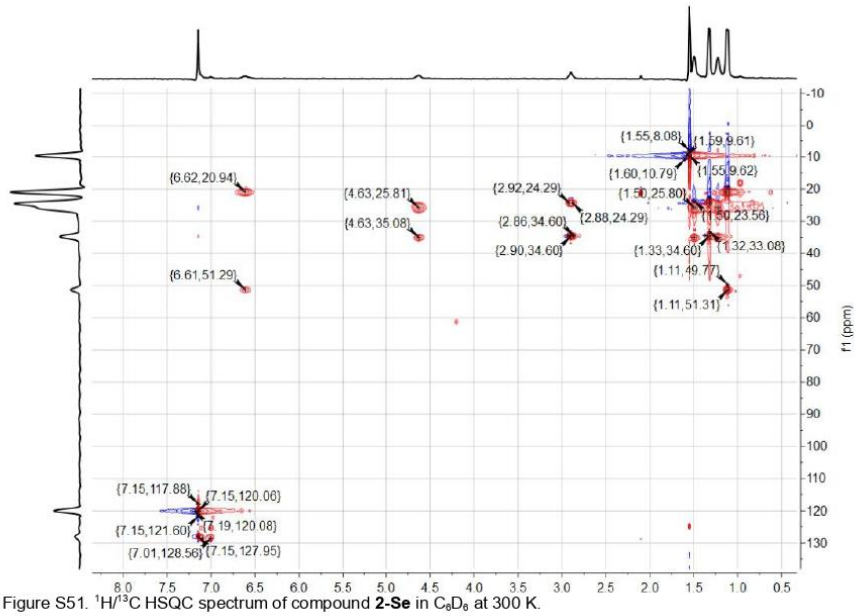

Figure S51. $^{1}H/^{13}C$ HSQC spectrum of compound **2-Se** in C_6D_6 at 300 K.

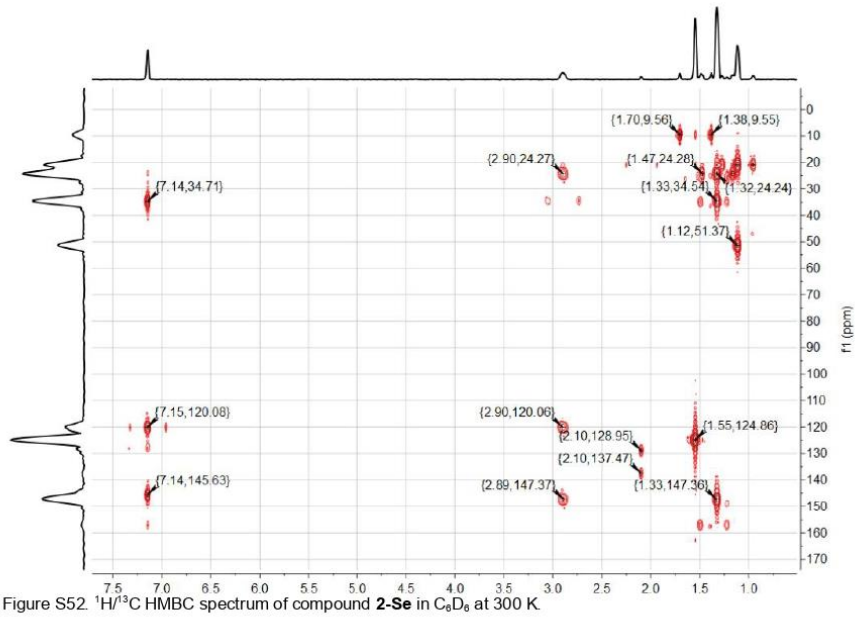

Figure S52. $^{1}H/^{13}C$ HMBC spectrum of compound **2-Se** in C_6D_6 at 300 K.

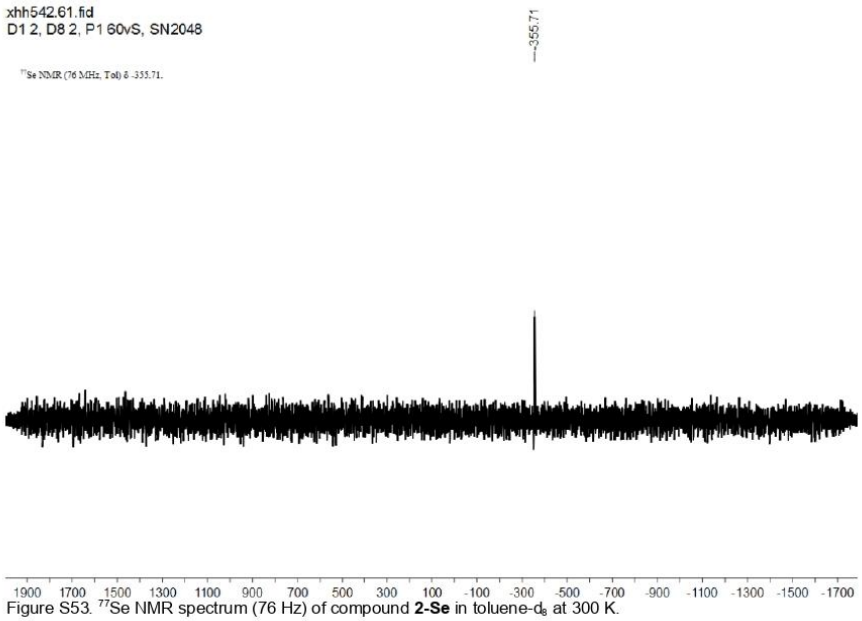

Figure S53. ^{77}Se NMR spectrum (76 Hz) of compound **2-Se** in toluene-d_8 at 300 K.

3.5.2 Mass spectra

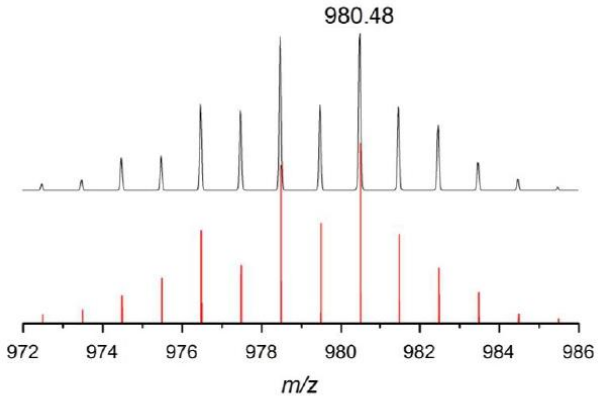

Figure S54. LIFDI-MS spectrometry (detail view with isotope pattern) of [I*i*PrAl(Tipp)-μ-Se]$_2$ (**2-Se**) (Measured spectrum: top; Simulated spectrum: bottom).

3.6 Spectra of [IMe$_4$Al(Tipp)-μ-Se]$_2$ (3-Se)

3.6.1 NMR spectra

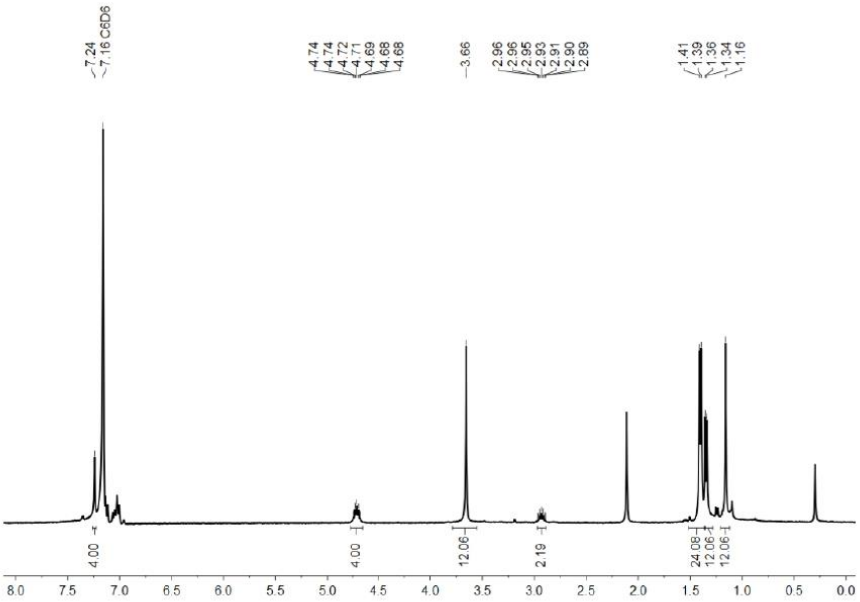

Figure S55. ^{1}H NMR spectrum (400 MHz) of compound **3-Se** in C_6D_6 at 300 K. [δ (silicone grease) = 0.297 ppm]
xhh226.71.fid

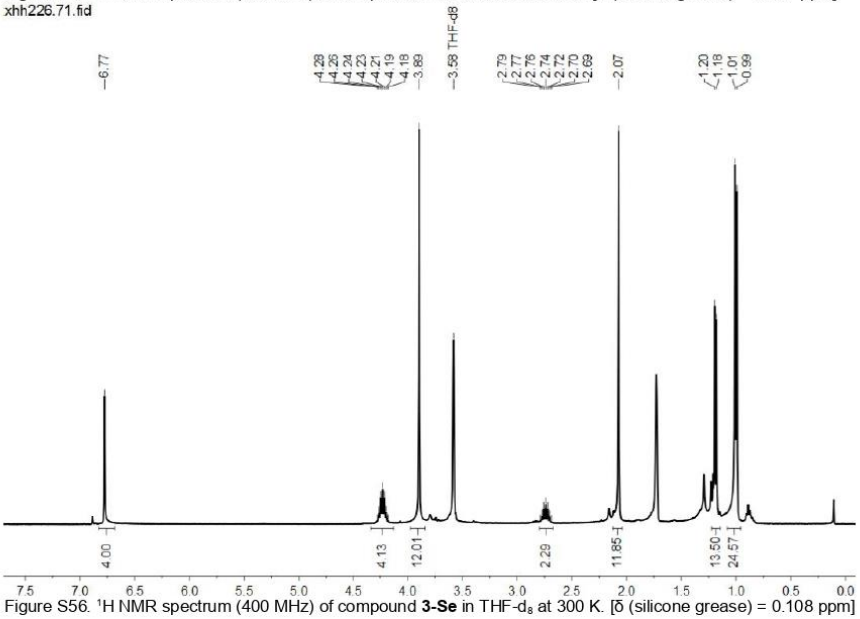

Figure S56. ^{1}H NMR spectrum (400 MHz) of compound **3-Se** in THF-d_8 at 300 K. [δ (silicone grease) = 0.108 ppm]

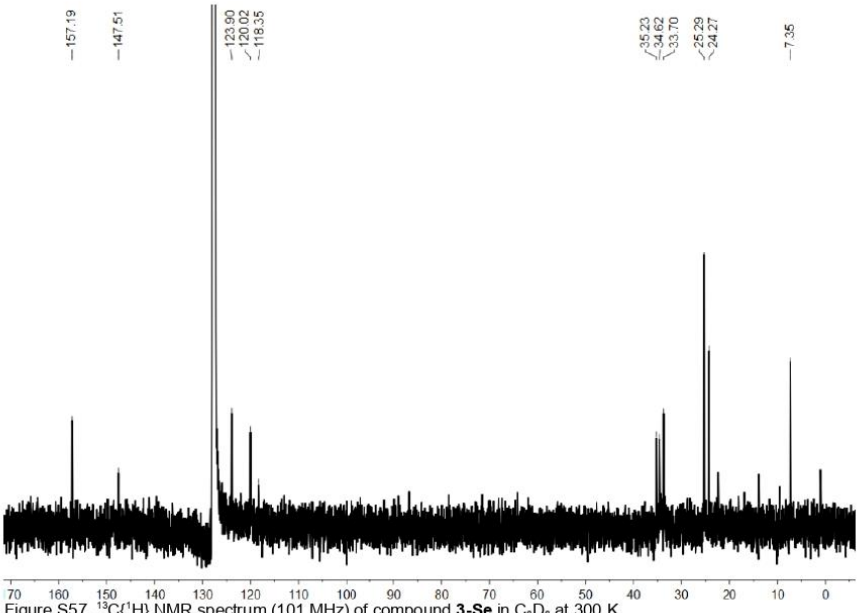

Figure S57. $^{13}C\{^{1}H\}$ NMR spectrum (101 MHz) of compound **3-Se** in C_6D_6 at 300 K.

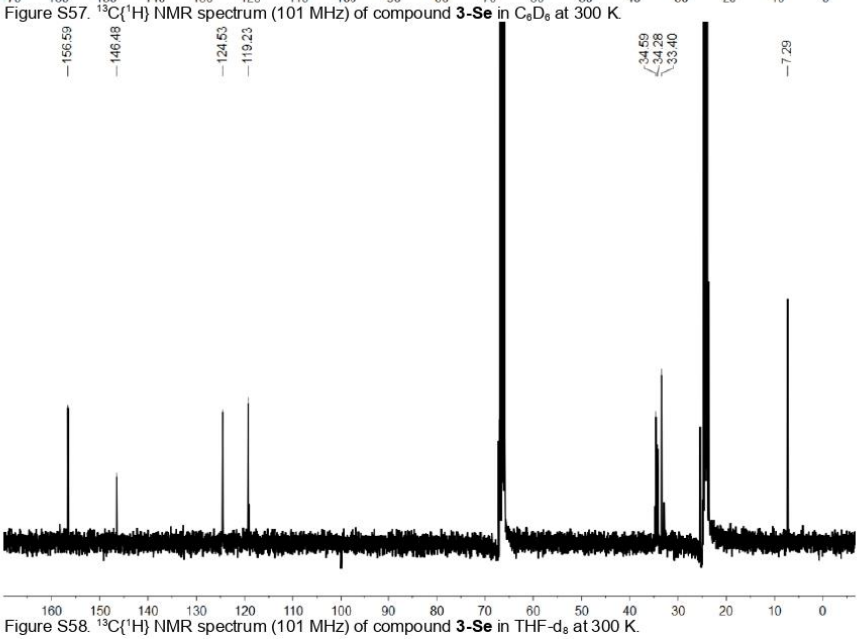

Figure S58. $^{13}C\{^{1}H\}$ NMR spectrum (101 MHz) of compound **3-Se** in THF-d_8 at 300 K.

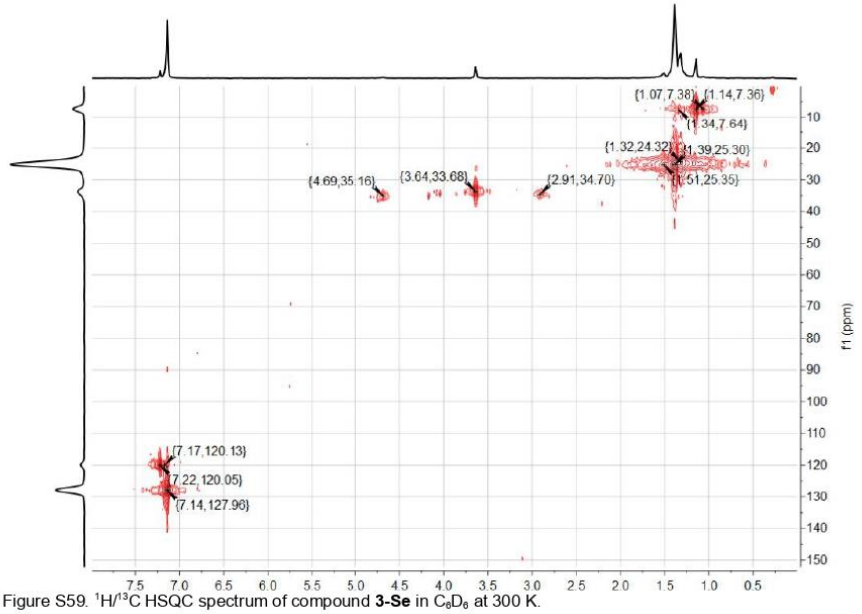

Figure S59. $^{1}H/^{13}C$ HSQC spectrum of compound **3-Se** in C_6D_6 at 300 K.

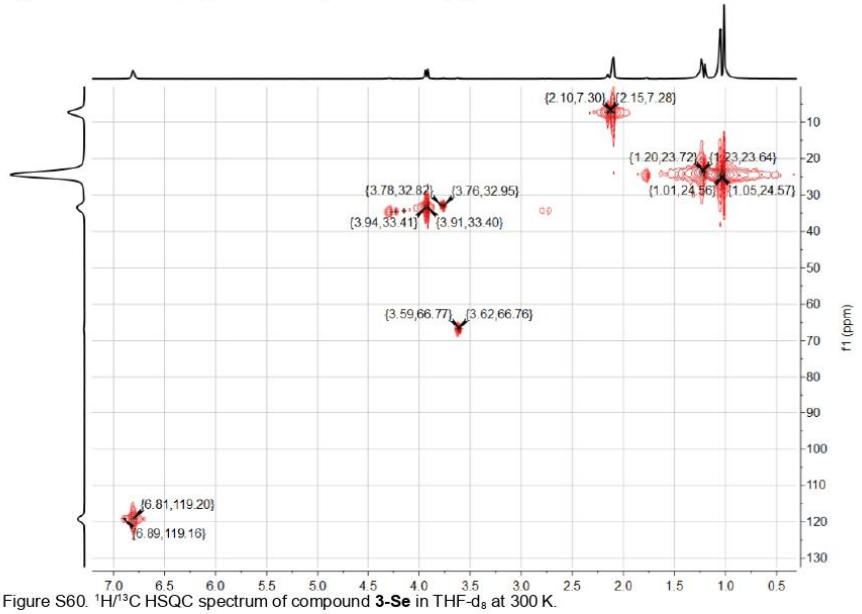

Figure S60. $^{1}H/^{13}C$ HSQC spectrum of compound **3-Se** in THF-d_8 at 300 K.

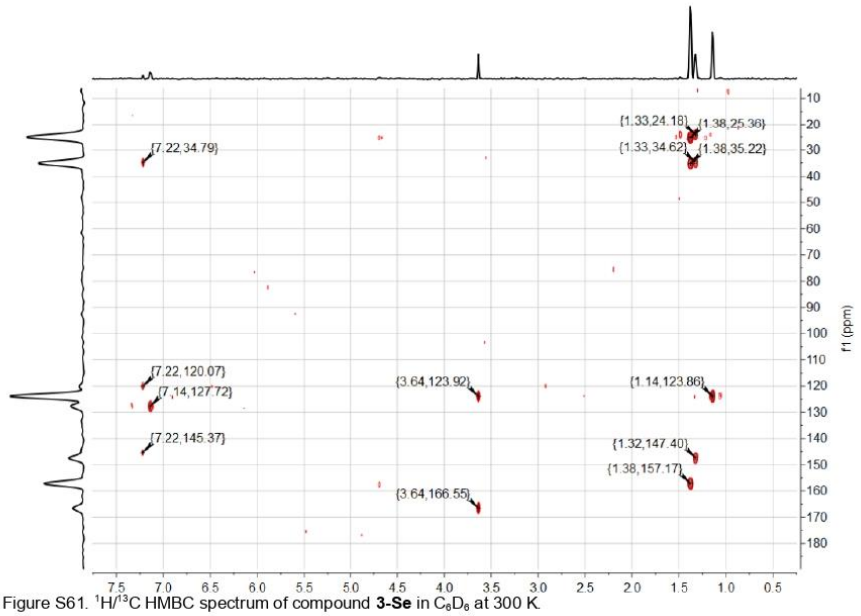

Figure S61. $^{1}H/^{13}C$ HMBC spectrum of compound **3-Se** in C_6D_6 at 300 K.

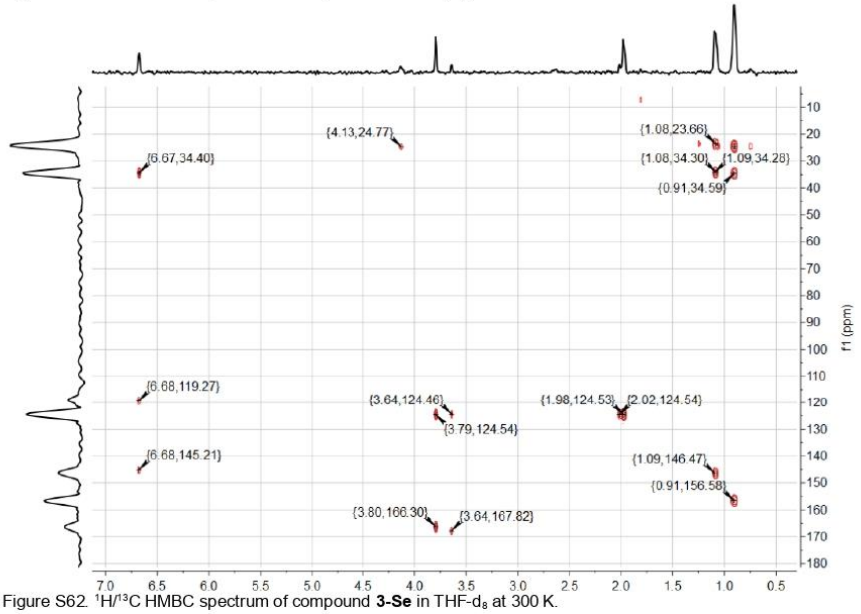

Figure S62. $^{1}H/^{13}C$ HMBC spectrum of compound **3-Se** in THF-d_8 at 300 K.

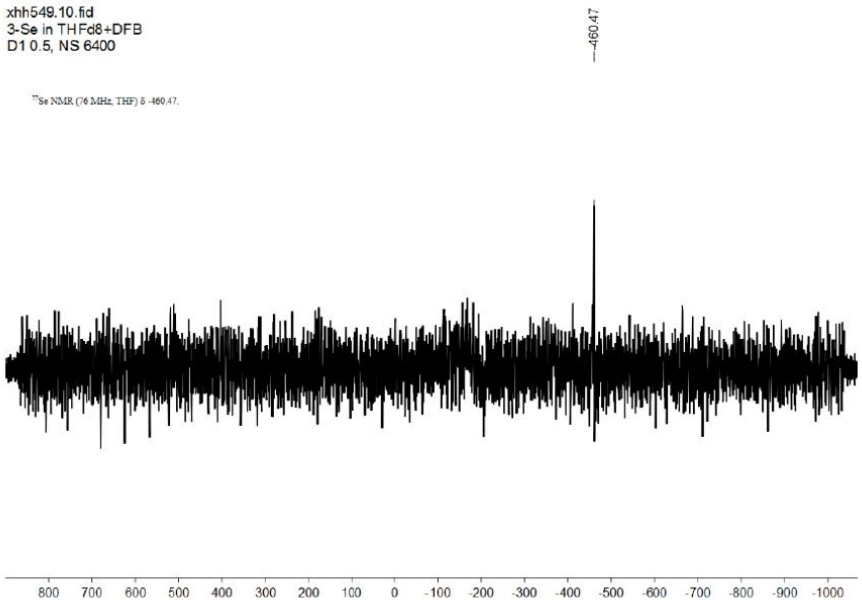

Figure S63. ^{77}Se NMR spectrum (76 Hz) of compound **3-Se** in THF-d_8 at 300 K.

3.6.2 Mass spectra

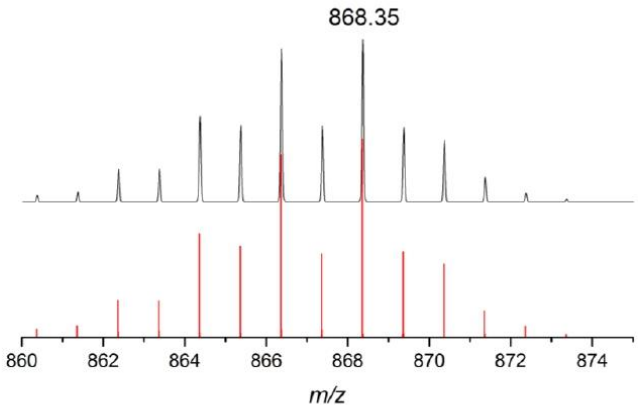

Figure S64. LIFDI-MS spectrometry (detail view with isotope pattern) of [IMe$_4$Al(Tipp)-μ-Se]$_2$ (**3-Se**) (Measured spectrum: top; Simulated spectrum: bottom).

3.7 Spectra of $(IMe_4CO_2)_2Al(Tipp)$-μ-O_2C=Te (6-Te)

3.7.1 NMR spectra

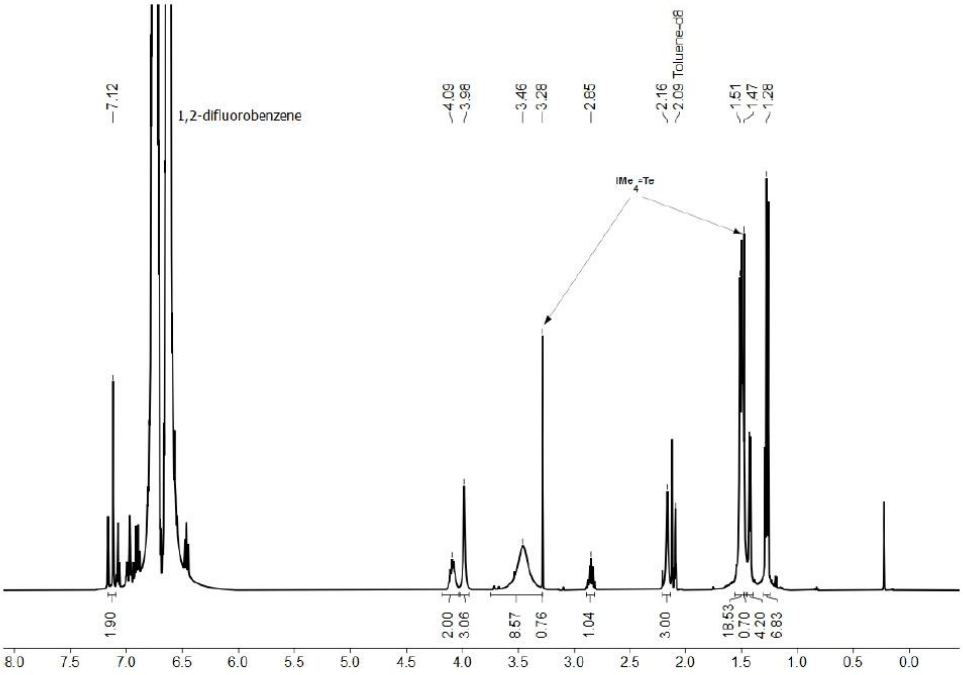

Figure S65. ^{1}H NMR spectrum (500 MHz) of compound **6-Te** (with 13% IMe_4=Te) in Toluene-d_8/1,2-Difluorobenzene (5:1) at 300 K. [δ (silicone grease) = 0.227 ppm]

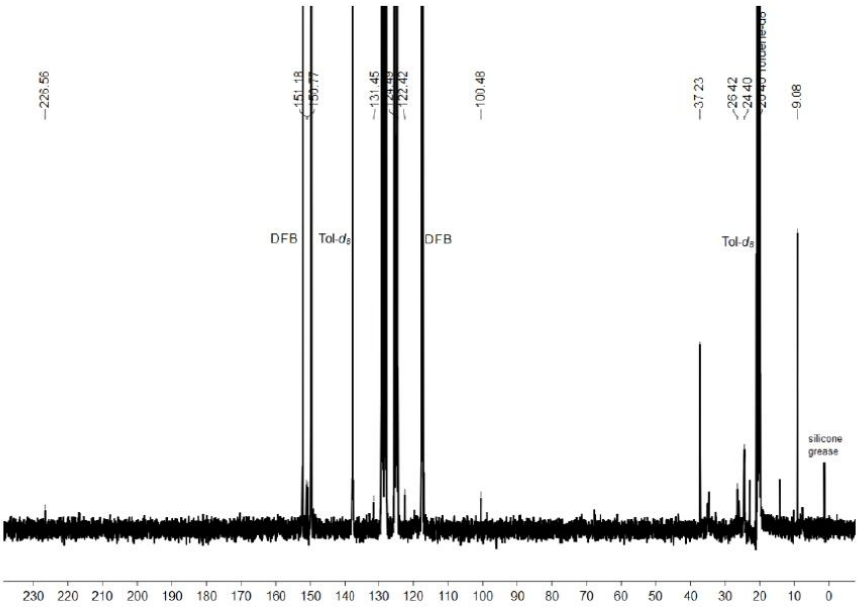

Figure S66. $^{13}C\{^1H\}$ NMR spectrum (101 MHz) of compound **6-Te** in Toluene-d_8/1,2-Difluorobenzene (5:1) at 300 K.

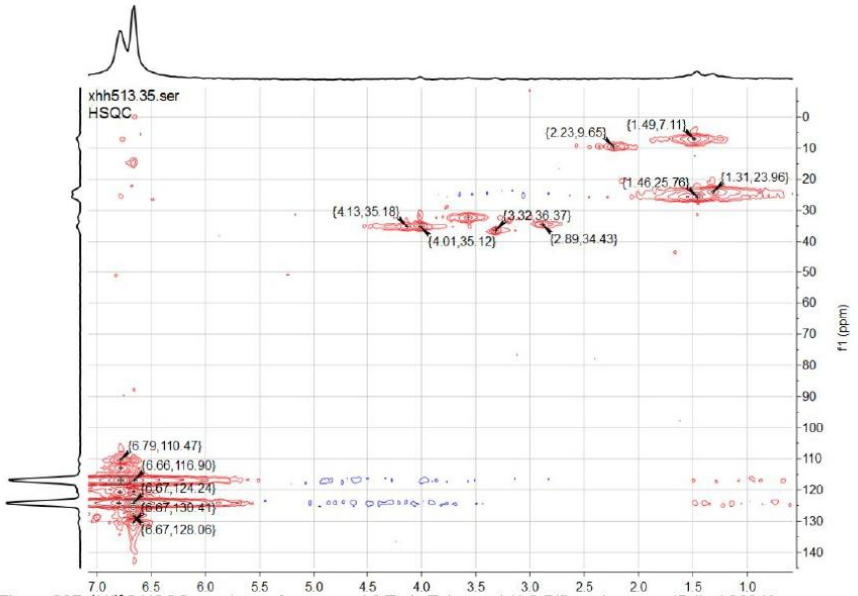

Figure S67. $^{1}H/^{13}C$ HSQC spectrum of compound **6-Te** in Toluene-d_8/1,2-Difluorobenzene (5:1) at 300 K.

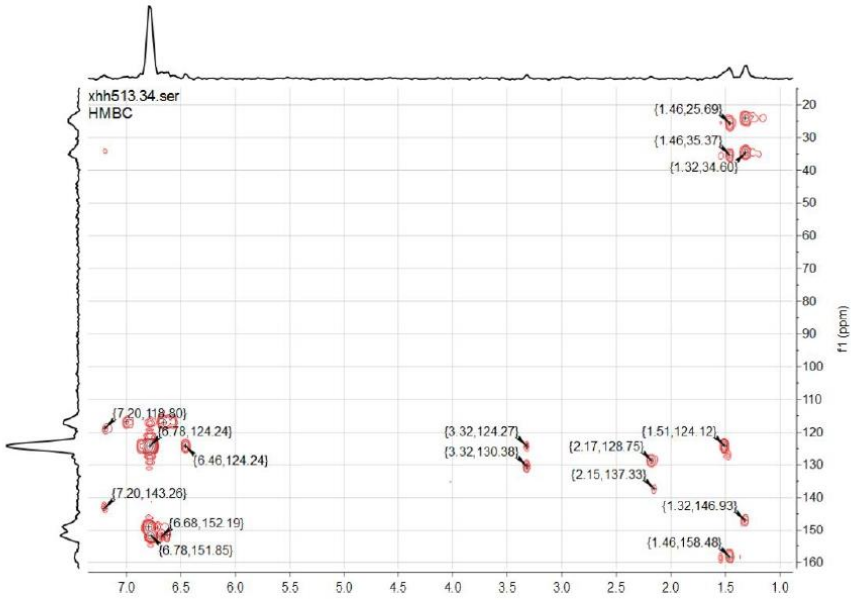

Figure S68. $^{1}H/^{13}C$ HMBC spectrum of compound **6-Te** in Toluene-d_8/1,2-Difluorobenzene (5:1) at 300 K.

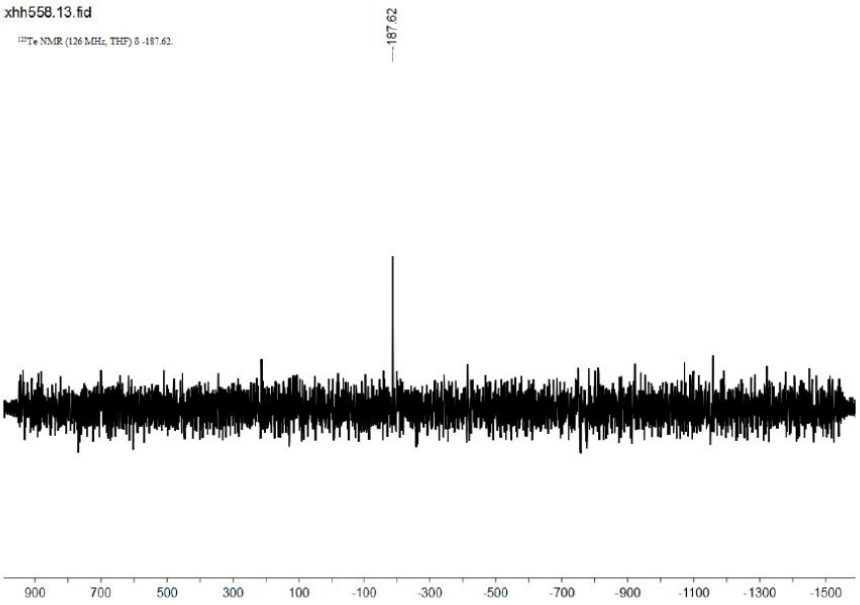

Figure S69. ^{125}Te NMR spectrum (126 MHz) of compound **6-Te** in THF-d_8/1,2-difluorobenzene (5:1) at 300 K

3.7.2 Mass spectra

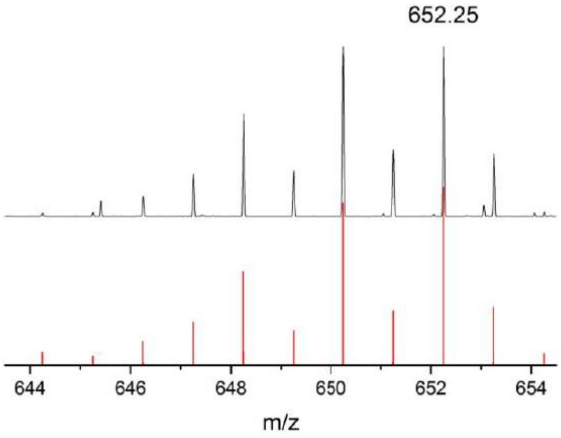

Figure S70. LIFDI-MS spectrometry (detail view with isotope pattern) of the fresh-prepared crystalline **6-Te** (**[6-Te – 2(CO_2)]**, *m/z* calcd: 652.24) (Measured spectrum: top; Simulated spectrum: bottom).

3.7.3 IR spectrum

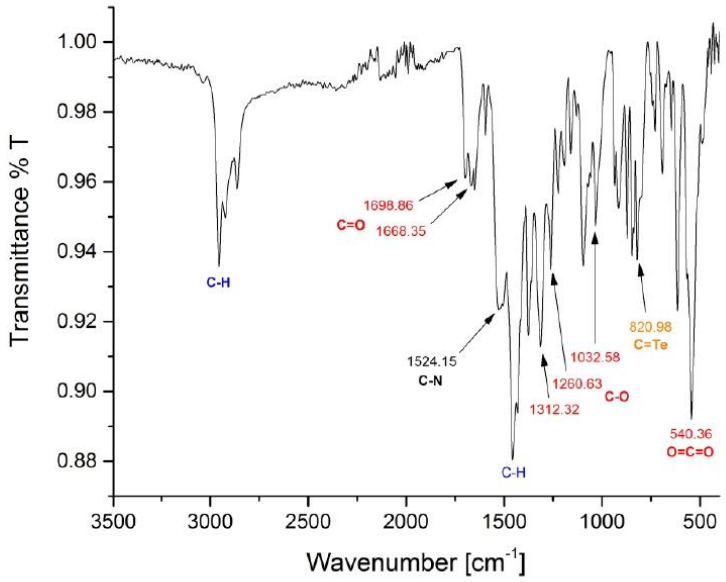

Figure S71. Solid-state FT-IR spectrum of **6-Te**

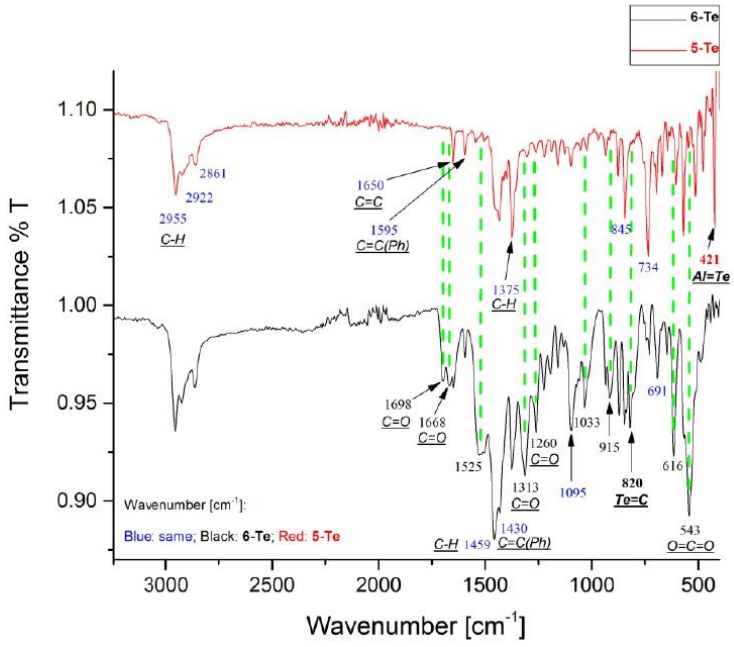

Figure S72. Stacked solid-state FT-IR spectra of **5-Te** (red) and **6-Te** (black).

4 Computational Section

4.1 Computational details

Calculations were carried out using ORCA 5.0.3 [S16]. The geometries of all compounds were optimized at the r^{2}SCAN-3c level of theory[S17] with def2-ECP for Te, utilizing the geometrical counter-poise correction scheme (gCP) and, where applicable, conductor-like polarizable continuum model (CPCM) to account for the solvation effect of THF.[S18] The optimized geometries were verified as minima by analytical frequency calculations and the absence of imaginary frequencies. The calculations were accelerated by resolution-of-identity (RI) approximation with the def2-mTZVPP/J auxiliary basis sets. The reported Gibbs energies are at the r^{2}SCAN-3c(CPCM=THF)//r^{2}SCAN-3c(CPCM=THF) level of theory (Table S3). Properties and NBO analysis are reported at the PBE0[S19]-D3BJ[S20]/def2-TZVP[S21]//r^{2}SCAN-3c level of theory with def2-ECP for Te and def2/J auxiliary basis sets.[S22] NBO 7 software was used for NBO analysis.[S23]

4.2 Calculated energies of compounds

Table S3. Energies (E_h) (E – electronic energy; H – total enthalpy; G – Gibbs energy) of the calculated compounds at the r^{2}SCAN-3c(CPCM=THF)//r^{2}SCAN-3c(CPCM=THF) level of theory. Thermochemistry at 298.15 K, 1 atm.

	Compound	E	H	G
01	**2-Te**	-3273.13293	-3271.778898	-3271.952407
02	**2-Se**	-7539.979126	-7538.624348	-7538.795978
03	**3-Te**	-2958.714133	-2957.595982	-2957.753474
04	**3-Se**	-7225.56296	-7224.444319	-7224.601446
05	**4-Te**	-2019.919192	-2019.047693	-2019.169098
06	**4-Se**	-4153.335552	-4152.463977	-4152.584633
07	**5-Te**	-1862.712211	-1861.958406	-1862.071126
08	**5-Se**	-3996.12807	-3995.374208	-3995.486014
09	**6-Te**	-2428.511551	-2427.707173	-2427.839877
10	**6-Te'**	-2428.503574	-2427.699629	-2427.831627
11	**IMe$_4$**	-383.3344038	-383.1423674	-383.1880788
12	**I*i*Pr**	-540.5468942	-540.2376716	-540.2946038
13	**7-Te**	-2051.321448	-2050.550331	-2050.669807
14	**7-Te'**	-2051.299416	-2050.529649	-2050.647923
15	**8-Te**	-2239.92042	-2239.13157	-2239.257466
16	**8-Te'**	-2239.904838	-2239.11778	-2239.244345
17	**CO$_2$**	-188.5723039	-188.5582943	-188.5771798

4.3 Electronic Structure of 2-Te, 2-Se, 3-Te, 3-Se

NBO analysis shows that each tellurium centre possesses a σ- (NBOs 85, 89) and a π-type (NBOs 86, 90) in **2-Te** (Figure S73, A). Each of the π-type lone pairs with occupancy of 1.82 el., according to the second order perturbation theory, shows donor-acceptor interactions with low-vacancy sp$^{13.49}$ orbitals of the Al centres with stabilization energy of 10.2 and 9.2 kcal mol^{-1}. Each of the aluminum centres shows two bonding interactions with the two tellurium atoms Figure S73, B, NBOs 93, 94, 96, 173). The four Al-Te bonds are polarized toward Te and show essentially identical composition. NBOs 88, 92 (Figure S73, C) with occupancy of 1.67 el. correspond to the lone pairs of the carbenes show donor-acceptor interactions mainly with the lone-vacancy sp$^{13.49}$ orbitals of Al with stabilization energy of 120.7 kcal·mol^{-1}. NBOs 95, 175 correspond to the polarized σ bonds between the Al centres and the ipso-carbons of the Tipp substituent (Figure S73, D).

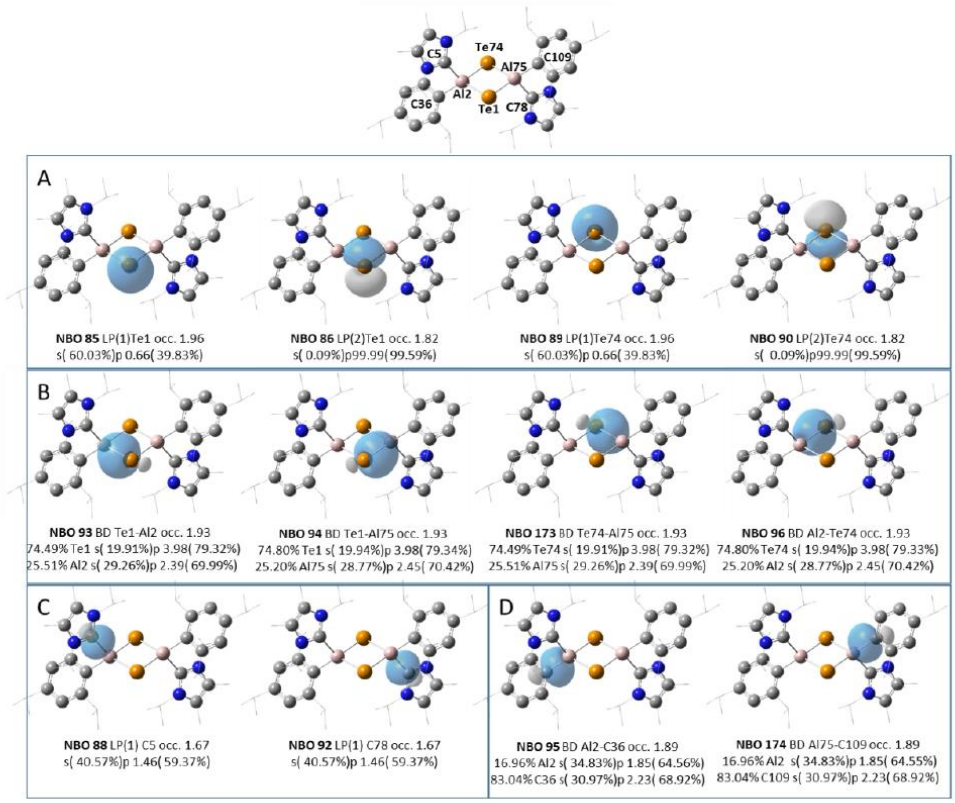

Figure S73. Selected NBOs of **2-Te**.

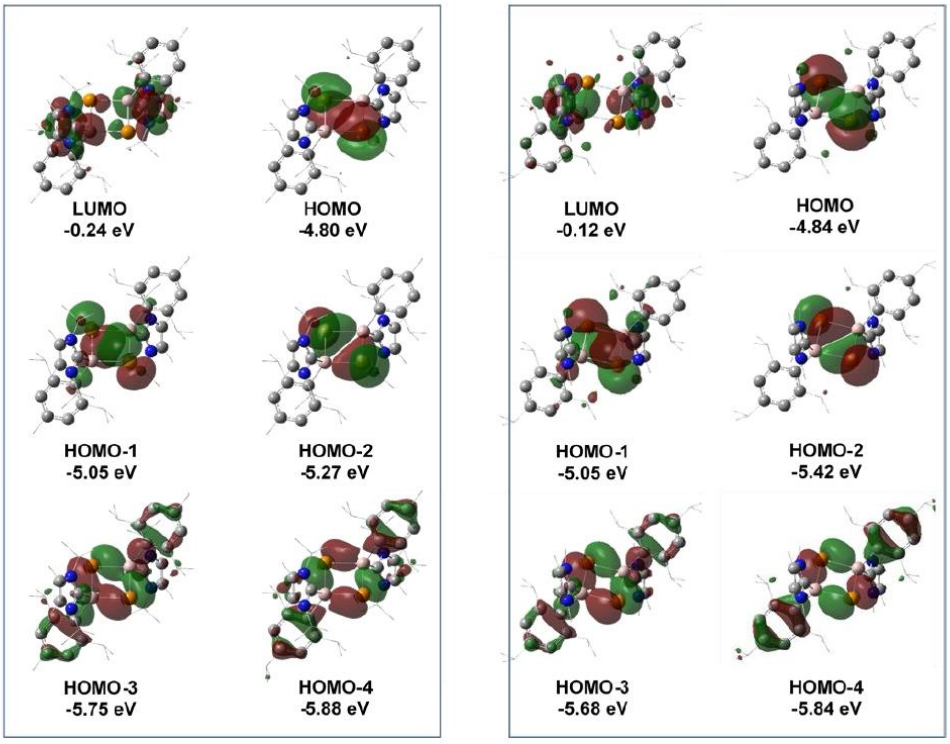

Figure S74. Selected molecular orbitals of **2-Te** (left) and **3-Te** (right), at the PBE0-D3BJ/def2-TZVP//r^{2}SCAN-3c level of theory. For clarity, hydrogens are omitted, and methyl and iso-propyl substituents are shown as wireframes.

Selected molecular orbitals of **2-Te** and **3-Te** are presented in Figure S74. Selected molecular orbitals of **2-Se** and **3-Se** are presented in Figure S75. All complexes show essentially similar electronic structure. In order to understand nature of the frontier molecular orbitals we analysed the MOs of **2-Te** in the NBO basis (Table S4).

Table S4. Frontier molecular orbitals of **2-Te** in NBO basis. Only coefficients |c|>0.1 are shown.

MO251	336	258	91	87	254	256	192	114	253	333						
LUMO	-0.5020	0.5017	-0.2390	0.2389	0.1761	-0.1761	-0.1451	0.1450	0.1202	-0.1202						
MO250	90	86														
HOMO	0.6827	0.6826														
MO249	86	90	85	89	96	94	95	174	255	88	334	92	252	251	173	93
HOMO-1	-0.5523	0.5522	0.2192	-0.2192	0.1655	-0.1655	-0.1332	0.1331	0.1232	0.1232	-0.1232	-0.1232	0.1208	-0.1208	0.1161	-0.1161
MO248	89	85	94	96	173	93	90	86								
HOMO-2	-0.43	0.43	-0.3235	0.3235	0.2945	-0.2944	-0.2751	0.275								
MO247	173	93	94	96	95	174	212	134	88	92	220	142	296	374	192	114
HOMO-3	0.3693	-0.3693	0.3141	-0.3141	0.2765	-0.2765	0.1775	-0.1775	0.1462	-0.1462	0.1341	-0.134	0.1244	-0.1244	0.1114	-0.1114
MO246	96	94	93	173	134	212	142	220	296	374	114	192	174	95		
HOMO-4	-0.3775	-0.3775	0.3521	0.3521	-0.2554	-0.2553	-0.2049	-0.2049	0.1595	0.1594	0.1411	0.1411	0.1255	0.1255		

NBO 85. LP (1) Te 1
NBO 86. LP (2) Te 1
NBO 87. LP (1) N 4
NBO 89. LP (1) Te 74
NBO 90. LP (2) Te 74
NBO 91. LP (1) N 77
NBO 93. BD (1) Te1-Al2
NBO 94. BD (1) Te1-Al75
NBO 95. BD (1) Al2-C36
NBO 96. BD (1) Al2-Te74
NBO 134. BD (2) C36-C53
NBO 142. BD (2) C40-C51
NBO 173. BD (1) Te74-Al75
NBO 174. BD (1) Al75-C109
NBO 212. BD (2) C109-C126
NBO 258. BD*(2) N3-C5
NBO 336. BD*(2) N76-C78

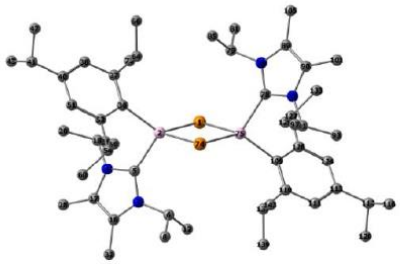

The LUMO mainly corresponds to the π*(C-N) orbitals of the carbene moieties. The HOMO corresponds to the π-type lone pairs of the Te atoms. The HOMO-1 mainly corresponds to the π-type and the σ-type lone pairs of the Te atoms. The HOMO-2 consists of the contributions from the σ-type lone pairs of the Te atoms and the σ(Al-Te) bonds. The HOMO-3 mainly corresponds the σ(Al-Te) bonds, with contributions from the Al-CT^{ipp} σ-bonds. The HOMO-4 mainly corresponds the σ(Al-Te) bonds, delocalized to π bonds of the Tipp substituent.

The Al and Te atoms in 2-Te are connected by single bonds with Wiberg bond indexes (WBI) of 0.83 and 0.81 and Mayer bond orders (MBO) of 1.02 and 0.97. According to NBO analysis these bonds are considerably polarized toward the Te center (75.5% Te (sp4.0), 25.5% Al (sp2.4); 74.8% Te (sp4.0), 25.2% Al (sp2.5)). The polarization is also reflected in NPA charges with -0.70 el. on Te and +1.08 el. on Al atoms.

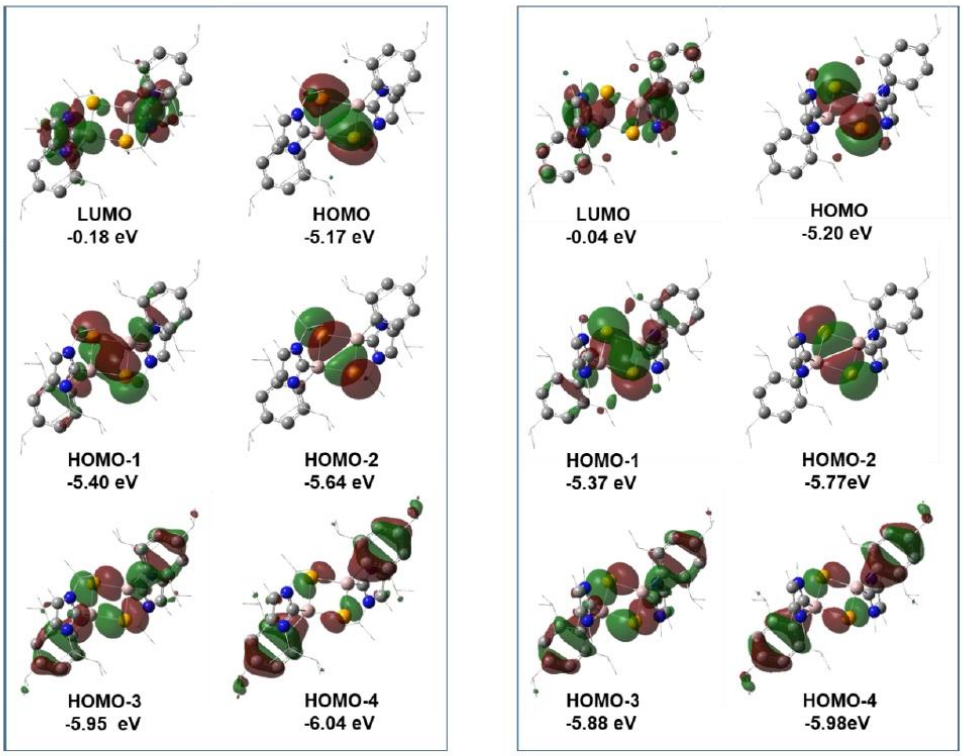

Figure S75. Selected molecular orbitals of **2-Se** (left) and **3-Se** (right), at the PBE0-D3BJ/def2-TZVP//r^{2}SCAN-3c level of theory. For clarity, hydrogens are omitted, and methyl and iso-propyl substituents are shown as wireframes.

Table S5. Al–Ch bonding interactions in **2-Te**, **2-Se**, **3-Te**, **2-Se**,

Complex	NBO BD(Al–Ch)	Occupancy	WBI	MBO	NPA Charge Ch	NPA Charge Al
2-Te	75.5% Te ($sp^{4.0}$), 25.5% Al ($sp^{2.4}$)	1.93	0.83	1.02	-0.70	+1.08
	74.8% Te ($sp^{4.0}$), 25.2% Al ($sp^{2.5}$)	1.93	0.81	0.97		
3-Te	74.6% Te ($sp^{4.1}$), 25.4% Al ($sp^{2.2}$)	1.93	0.84	0.96	-0.69	+1.08
	75.1% Te ($sp^{4.6}$), 24.9% Al ($sp^{2.6}$)	1.92	0.79	0.97		
2-Se	79.9% Se ($sp^{3.0}$), 20.1% Al ($sp^{2.3}$)	1.94	0.74	0.98	-0.92	+1.28
	80.0% Se ($sp^{3.1}$), 20.0% Al ($sp^{2.4}$)	1.94	0.72	0.96		
3-Se	79.6% Se ($sp^{3.1}$), 20.4% Al ($sp^{2.2}$)	1.94	0.75	0.95	-0.91	+1.27
	80.1% Se ($sp^{3.5}$), 19.9% Al ($sp^{2.6}$)	1.93	0.70	0.96		

4.4 NBO/NLMO steric analysis of 2-Te, 2-Se, 3-Te, 2-Se

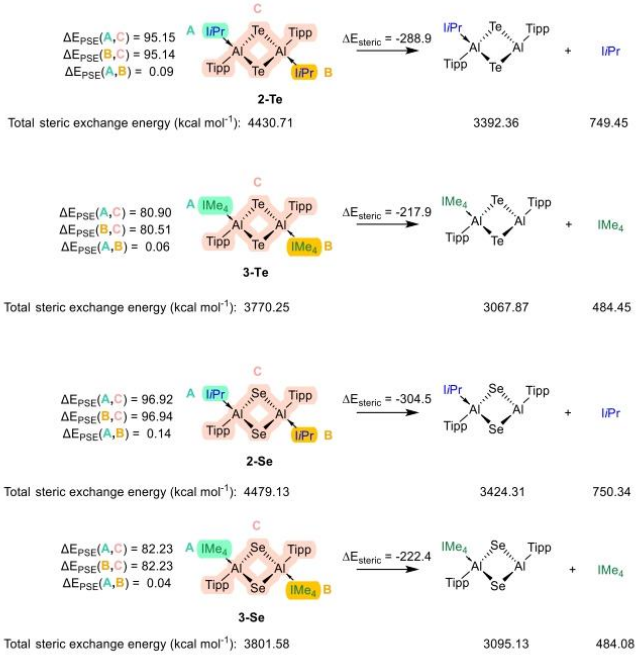

Figure S76.NBO/NLMO steric analysis of **2-Te**, **2-Se**, **3-Te**, **2-Se** at the PBE0-D3BJ/def2-TZVP//r²SCAN-3c level of theory.

Steric analysis (Figure S76) shows that the total steric interaction energy (ΔE_{steric}) for the I*i*-Pr ligand in **2-Te** is 288.9 kcal mol^{-1}, which is by 71.0 kcal mol^{-1} higher than that of IMe_4 in **3-Te** (217.9 kcal mol^{-1}). The pairwise steric exchange energies (ΔE_{PSE}) for disjoint interactions between the corresponding NLMOs for the I*i*-Pr ligands in **2-Te** are ≈ 95 kcal mol^{-1}, ≈ 14 kcal mol^{-1} higher than the values of ≈ 81 kcal mol^{-1} calculated for IMe_4 ligands in **3-Te**. Similar results were obtained for the selenium analogues **2-Se** and **3-Se**. The total steric interaction energy for the I*i*-Pr ligand in **2-Se** of 304.5 kcal mol^{-1} is by 82.1 kcal mol^{-1} higher than the ΔE_{steric} for IMe_4 in **3-Se** (222.4 kcal mol^{-1}). Pairwise steric exchange energies for the I*i*-Pr ligands in **2-Te** are ≈ 97 kcal mol^{-1}, ≈15 kcal mol^{-1} higher those of IMe_4 ligands in **3-Se** (≈ 81 kcal mol^{-1}).These results suggest that although IMe_4 ligands are weaker donors than I*i*-Pr, their binding to the aluminum chalcogenide dimers is stronger due to the steric effects.

4.5 Electronic structure of 5-Te

NBO analysis of **5-Te** (Figure S77) shows a polarized bonding interaction between Al and Te centres (NBO 55), and an even more polarized bonding interaction between aluminum and the *ipso*-carbon of the Tipp substituent (NBO 56). Additionally, Al possess two lone-vacancy orbitals with high occupancy (NBO 144,145). The Te centre has one σ-type lone pair (NBO 48) with high occupancy and two π-type lone pairs, NBOs 49-50, with occupancies of only 1.83 and 1.79 el., respectively. One π-type lone pairs (NBO 49) exhibits DAI with the lone-vacancy orbital of Al (NBO 144) of 13.0 kcal mol^{-1}. Additional DAI of NBO 49 with Al sum up to 6.4 kcal mol^{-1}. The second π-type lone pair of Te (NBO 50) exhibits DAI with the lone-vacancy orbital of Al (NBO 145) of 25.3 kcal mol^{-1}, and a minor interaction with NBO 144 of 1.1 kcal mol^{-1}. Additional DAIs between the Al and Te centres sum up to 13.9 kcal mol^{-1}. Thus, the sum of all DAIs between Al and Te is 58.6 kcal mol^{-1}, which results in the Al–Te interaction with a double bond character.
The carbons of the carbene ligands (C16 and 23) possess σ-type lone pairs (NBO 53, 54) with low occupancy of 1.68 and 1.67 el., respectively. The lone pairs are donated to the lone-vacancy orbitals of the Al. The respective DAI energies for the interaction of NBO 53 with NBO 144 and NBO 145 are 86.6 and 48.5 kcal mol^{-1}. The respective DAI energies for the interaction of NBO 54 with NBO 144 and NBO 145 are 85.3 and 54.1 kcal mol^{-1}.

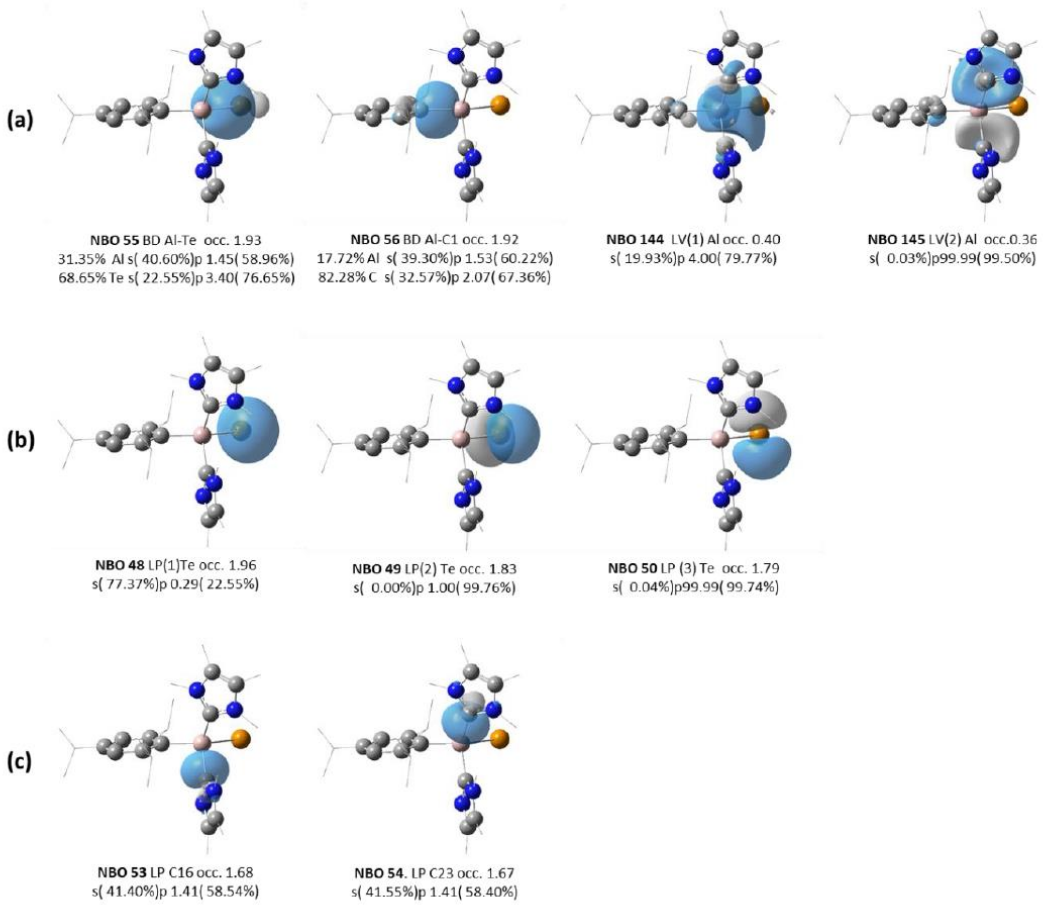

Figure S77. Selected NBOs of **5-Te** at the PBE0-D3BJ/def2-TZVP//r^{2}SCAN-3c level of theory. For clarity, hydrogens are omitted, and methyl and iso-propyl substituents are shown as wireframes.

4.6 Routes of formation of 6-Te

Possible routes of formation of **6-Te** from **5-Te** and 3 equivalents of CO_2 were considered. The most likely scenario for this transformation is via the green path (Figure S78), as the intermediates **7-Te** and **8-Te** are lower in energy than the corresponding **7-Te'** and **8-Te'** intermediates on the red path. The first CO_2 addition should proceed across the Al-C^{NHC} bond as the resulting intermediate **7-Te** is by 13.7 kcal mol^{-1} more favorable than **7-Te'** that would form via CO_2 insertion across the Al-Te bond. Calculations show that the reaction with the second equivalent of CO_2, which would results in either intermediate **8-Te**, as a result of addition across the Al-C^{NHC} bond, or intermediate **8-Te'**, as a result of addition across Al-Te bond, is most likely to proceed via the former route as **8-Te** is energetically more favored than **8-Te'** by 8.3 kcal mol^{-1}.

According to a request of one of the referees, we also calculated the energies for the reaction paths at the PBE0-D3BJ(CPCM=THF)/def2-TZVP//PBE0-D3BJ(CPCM=THF))/def2-TZVP level of theory. The results are presented in the Figure S78 below in blue. The PBE0 and r2SCAN-3c are in a food agreement with each other.

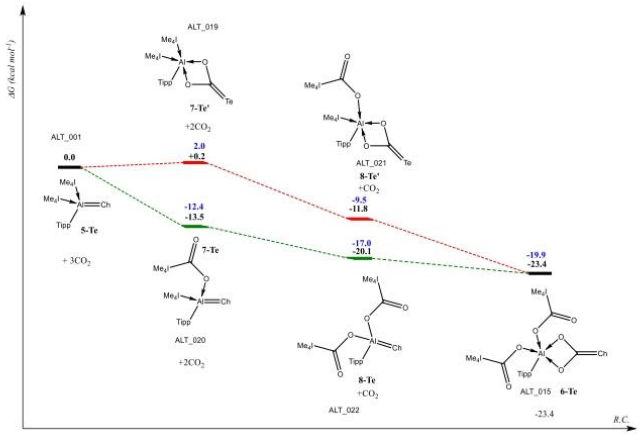

Figure S78. Calculated energies of intermediates in the formation of **6-Te** from **5-Te** in the presence of 3 equivalents of CO_2, at the r²SCAN-3c(CPM=THF)//r²SCAN-3c(CPM=THF) level of theory (black) at the PBE0-D3BJ(CPCM=THF)/def2-TZVP//PBE0-D3BJ(CPCM=THF))/def2-TZVP level of theory (blue).

4.7 Electronic structure of 6-Te

The NBO analysis of the bonding situation around the Al centre in 6-Te shows Al having four partially occupied lone-vacancy NBOs (NBO 177-180, Figure S79 (a)). The oxygen atoms NHC–CO_2 moieties closest to the Al centre, i.e. O2 and O3, possess three lone pairs (NBOs 63-65 and NBOs 71-73, Figure S79 (b) and (c)). Similarly, each of the oxygen atoms of the tellurocarbonate moiety possesses three lone pairs (NBOs 68-70 and NBOs 60-62, Figure S79 (d) and (e)). The Al lone-vacancy orbitals act as acceptors to the lone pairs of the coordinating oxygen atoms of the two NHC–CO_2 moieties and the $[CO_2Te]^{2-}$ moiety. The oxygen aluminum donor-acceptor interactions are summarized in Table S6.
Additionally, the Al–C^{Tipp} bonding is depicted as a donor acceptor interaction between a lone-pair of C1 (NBO 78, Figure S80) and the lone-vacancy orbital of Al NBO177. In this case, however the high occupancy of NBO 177 (0.44 el.), the low occupancy of the LP (1.63), the high donor-acceptor interaction energy between two orbitals 181.4 kcal mol^{-1}, and the relatively high WBI (0.50) and MBO (1.01), are reflective of a polarized Al–C single bond rather than a dative bond. The corresponding NLMO (80.2% C1, 16.7 % Al) and its composition are presented in Figure S80.

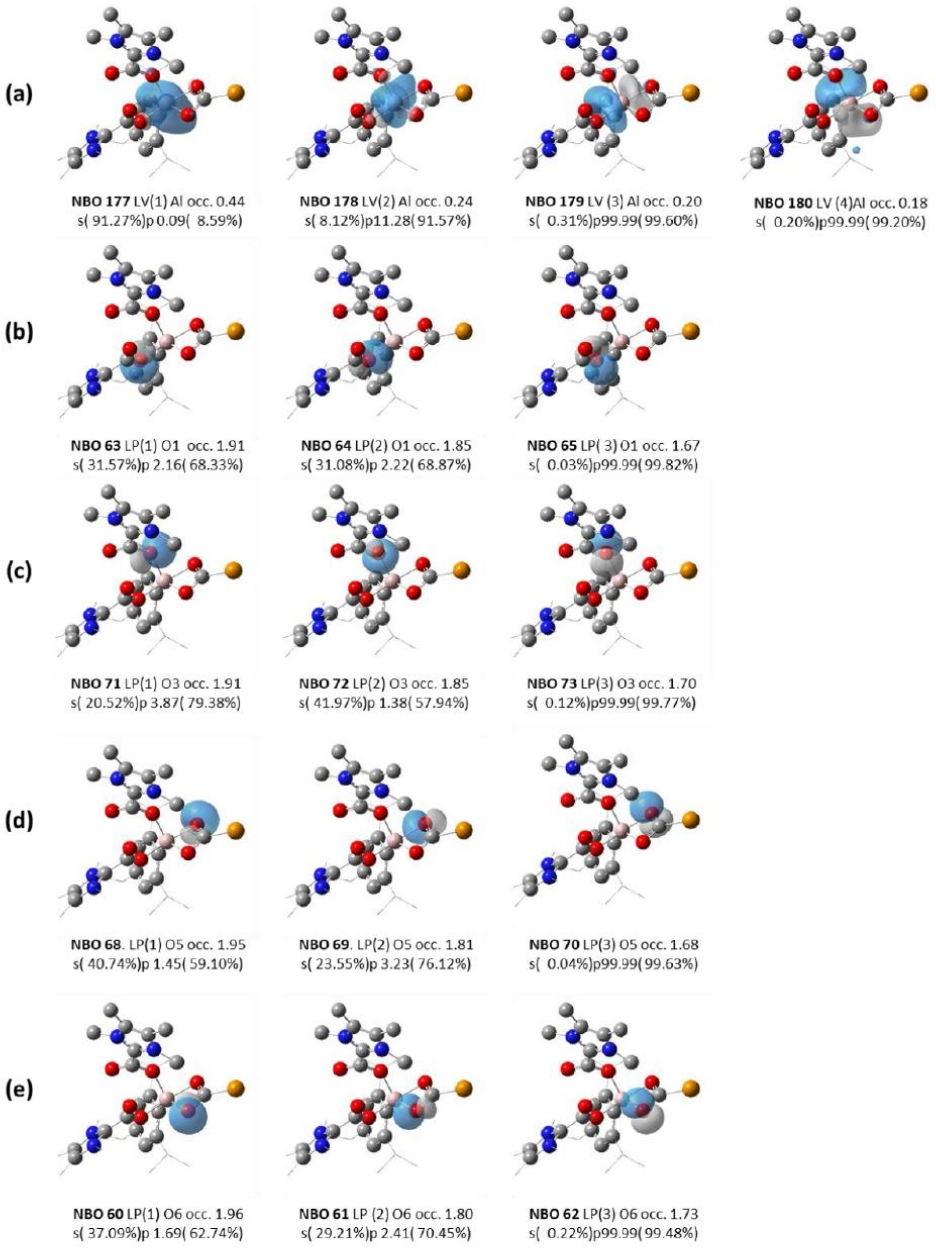

Figure S79. Selected NBOs of **6-Te** at the PBE0-D3BJ/def2-TZVP//r^{2}SCAN-3c level of theory. For clarity, hydrogens are omitted, and methyl and iso-propyl substituents are shown as wireframes.

Table S6. Summary of the donor acceptor interaction between the lone pairs O1, O3, O5, O6 and the low-vacancy orbitals of Al.

	Donor	Acceptor	Energy (kcal mol^{-1})
O1→Al	NBO 64	NBO 179	46.23
	NBO 64	NBO 177	26.16
	NBO 63	NBO 179	18.73
	NBO 63	NBO 177	6.43
	Sum of additional DAEs between O1 LPs and LVs of Al		17.3
	Sum of all DAEs between O1 LPs and LVs of Al		114.81
O3→Al	NBO 72	NBO 180	49.02
	NBO 72	NBO 177	23.08
	NBO 72	NBO 178	13.51
	NBO 71	NBO 178	12.35
	Sum of additional DAEs between O3 LPs and LVs of Al		28.16
	Sum of all DAEs between O1 LPs and LVs of Al		126.12
O5→Al	NBO 69	NBO 179	44.60
	NBO 69	NBO 177	32.77
	NBO 68	NBO 179	10.02
	Sum of additional DAEs between O5 LPs and LVs of Al		18.99
	Sum of all DAEs between O5 LPs and LVs of Al		106.38
O6→Al	NBO 61	NBO 178	41.68
	NBO 61	NBO 180	28.44
	NBO 61	NBO 177	25.91
	Sum of additional DAEs between O6 LPs and LVs of Al		22.05
	Sum of all DAEs between O6 LPs and LVs of Al		118.08

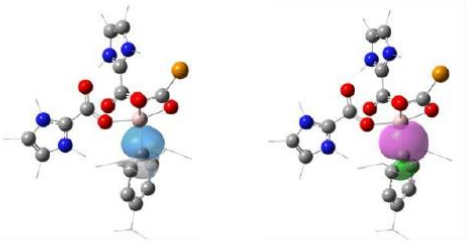

NBO 78 LP(1) C1 occ. 1.63
s(24.94%)p 3.00(74.89%)

NLMO 78 LP(1) C1 80.18%
80.203% C1 s(26.20%)p 2.81(73.64%)
16.698% Al s(58.01%)p 0.72(41.55%)

Figure S80. NBO and NLMO corresponding to LP of C1 in **6-Te** at PBE0-D3BJ/def2-TZVP//r^{2}SCAN-3c level of theory. For clarity, hydrogens are omitted, and methyl and iso-propyl substituents are shown as wireframes.

Calculations show that the charge distribution and bonding within the tellurocarbonate moiety in **6-Te** significantly differs from that of the hypothetical free $[CO_2Te]^{2-}$ (Figure S81). The $[CO_2Te]^{2-}$ moiety undergoes substantial geometrical and electronic changes upon its coordination to the Al center. The deformation energy of $[CO_2Te]^{2-}$ in **6-Te**, as the difference between the energy of a fragment in the geometry it has in a complex and the energy of its optimized geometry, is 19.8 kcal mol^{-1}. The magnitude of the negative charge of on the tellurium center is much higher in the optimized structure of free $[CO_2Te]^{2-}$ in comparison to the tellurocarbonate moiety in **6-Te** , while the magnitude of the negative charges on the oxygen atoms is slightly lower. The lone pair of the oxygen atoms that are involved in coordination to the Al center in **6-Te**, are delocalized to the carbon center in the free $[CO_2Te]^{2-}$. This diminishes the delocalization of the Te lone pairs to the carbon center, which results in shortening of the C-O bonds, a higher negative charge on Te and a weaker and longer C-Te bond.

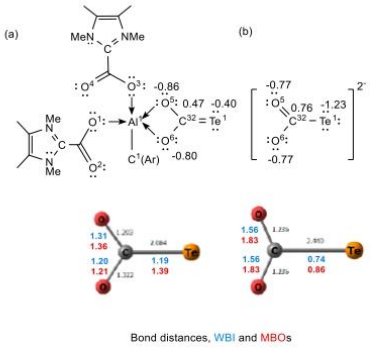

Figure S81. Comparison between the tellurocarbonate moiety in **6-Te** (a) and the the optimized structure of free $[CO_2Te]^{2-}$ (b).

4.8 Optimized geometries

Cartesian coordinates of the optimized geometries at the r²SCAN-3c(CPM=THF) level of theory

2_Te

Te	2.945723	5.752979	0.588024
Al	4.339424	5.473663	-1.637616
N	5.705161	8.260067	-2.091382
N	3.830564	8.099862	-3.144039
C	4.636560	7.443122	-2.266729
C	6.686245	8.033559	-1.008086
H	6.456004	7.023922	-0.647415
C	8.129854	8.014644	-1.494812
H	8.514729	9.012467	-1.719739
H	8.751759	7.585620	-0.702147
H	8.232198	7.382740	-2.383258
C	6.428297	9.012562	0.133264
H	5.392406	8.930557	0.477920
H	7.088867	8.769259	0.967347
H	6.622611	10.049244	-0.155328
C	5.589604	9.408313	-2.869331
C	4.398830	9.308719	-3.533220
C	2.458547	7.638017	-3.446968
H	2.433462	6.625650	-3.038298
C	2.174944	7.516025	-4.939782
H	2.995299	7.000274	-5.447331
H	1.271698	6.910564	-5.065330
H	1.999721	8.484234	-5.414803
C	1.430725	8.481694	-2.696814
H	1.411222	9.516227	-3.050399
H	0.435375	8.054624	-2.855445
H	1.641921	8.480255	-1.622456
C	3.827850	10.235105	-4.549410
H	3.897850	9.813281	-5.558229
H	2.778659	10.472333	-4.358516
H	4.384415	11.173995	-4.541796
C	6.637311	10.456991	-3.007890
H	6.238863	11.296717	-3.579844
H	6.980506	10.844467	-2.045934
H	7.511455	10.072627	-3.545194
C	3.740864	4.618429	-3.376144
C	2.478722	4.027441	-3.647622
C	2.105834	3.715127	-4.956972
H	1.119374	3.297349	-5.143420
C	2.964670	3.910704	-6.037345
C	2.532624	3.588941	-7.453817
H	3.395453	3.780454	-8.107228
C	1.388683	4.510509	-7.900414
H	1.673386	5.564156	-7.805728
H	1.120770	4.316731	-8.945414
H	0.495857	4.344787	-7.286133
C	2.137536	2.115295	-7.613953
H	1.258562	1.876668	-7.004241
H	1.890056	1.895937	-8.658806
H	2.953709	1.453111	-7.306042
C	4.231560	4.413745	-5.770688
H	4.929698	4.535194	-6.597838
C	4.621206	4.776592	-4.476159
C	6.044112	5.296574	-4.309459
H	6.183491	5.602742	-3.264033
C	7.066956	4.181959	-4.570533
H	7.022886	3.849150	-5.614125
H	8.083852	4.540157	-4.370173
H	6.874038	3.318212	-3.925606
C	6.342891	6.521378	-5.182908
H	5.607442	7.315807	-5.021086
H	7.336906	6.920081	-4.948329
H	6.331680	6.261454	-6.247348
C	1.481909	3.705023	-2.537168
H	2.052037	3.646398	-1.599382
C	0.776171	2.357768	-2.753973
H	0.028322	2.420412	-3.552277
H	1.484882	1.566945	-3.021701
H	0.247973	2.060251	-1.840914
C	0.420874	4.800391	-2.362007
H	-0.319812	4.495138	-1.612982
H	0.860802	5.739923	-2.017609
H	-0.102452	4.983677	-3.308782
Te	6.420175	4.179632	-0.588261
Al	5.026617	4.459114	1.637457
N	3.660766	1.672961	2.091887
N	5.535393	1.833090	3.144516
C	4.729465	2.489817	2.267112
C	2.679763	1.899341	1.008509
H	2.910075	2.908895	0.647653
C	1.236117	1.918408	1.495119
H	0.851200	0.920633	1.720191
H	0.614313	2.347299	0.702300
H	1.133682	2.550469	2.383443
C	2.937677	0.920139	-0.132674
H	3.973625	1.001872	-0.477228
H	2.277248	1.163542	-0.966831
H	2.743101	-0.116477	0.155984
C	3.776160	0.524848	2.870036
C	4.966931	0.624407	3.533934
C	6.907434	2.294844	3.447514
H	6.932580	3.307245	3.038940
C	7.191034	2.416743	4.940341
H	6.370873	2.932804	5.447884
H	8.094522	3.021845	5.065882

H	7.365904	1.448490	5.415405
C	7.935219	1.451117	2.697372
H	7.954631	0.416581	3.050957
H	8.930596	1.878114	2.856019
H	7.724046	1.452566	1.623010
C	5.537852	-0.301980	4.550155
H	5.467799	0.119816	5.558982
H	6.587051	-0.539192	4.359298
H	4.981293	-1.240873	4.542496
C	2.728361	-0.523723	3.008711
H	3.126810	-1.363533	3.580543
H	2.384958	-0.911095	2.046789
H	1.854345	-0.139293	3.546181
C	5.625207	5.314751	3.375750
C	6.887322	5.905816	3.647224
C	7.259909	6.218788	4.956499
H	8.246313	6.636667	5.142988
C	6.400875	6.023626	6.036803
C	6.832657	6.345978	7.453220
H	5.969734	6.154642	8.106562
C	7.976584	5.424653	7.900349
H	7.691959	4.370954	7.805976
H	8.244293	5.618812	8.945330
H	8.869513	5.590211	7.286173
C	7.227605	7.819716	7.612853
H	8.106642	8.058176	7.003167
H	7.474928	8.039489	8.657655
H	6.411421	8.481718	7.304577
C	5.134074	5.520389	5.770127
H	4.435791	5.399229	6.597197
C	4.744665	5.157055	4.475659
C	3.321776	4.637023	4.308902
H	3.182474	4.330781	3.263485
C	2.298890	5.751650	4.569782
H	2.342824	6.084551	5.613349
H	1.282021	5.393428	4.369323
H	2.491885	6.615337	3.924799
C	3.022938	3.412270	5.182398
H	3.758341	2.617790	5.020614
H	2.028902	3.013611	4.947834
H	3.034158	3.672237	6.246827
C	7.884504	6.227367	2.536847
H	7.314588	6.285798	1.598924
C	8.590838	7.574396	2.753116
H	9.338702	7.511769	3.551409
H	7.882484	8.365649	3.020526
H	9.119118	7.871325	1.839914
C	8.945099	5.131445	2.362413
H	9.686298	5.436204	1.613697
H	8.504921	4.192052	2.017964
H	9.467848	4.948095	3.309492

2_Se

Se	3.066803	5.605924	0.536257
Al	4.354863	5.433708	-1.492069
N	5.692959	8.228753	-1.972938
N	3.825855	8.054282	-3.033113
C	4.625349	7.408933	-2.141148
C	6.672735	8.014230	-0.887116
H	6.448116	7.005516	-0.522397
C	8.116702	7.999932	-1.375032
H	8.502774	8.999413	-1.590149
H	8.739962	7.561061	-0.589356
H	8.216496	7.377526	-2.270410
C	6.402994	9.001067	0.245190
H	5.374993	8.891262	0.605668
H	7.082656	8.795101	1.073754
H	6.558064	10.038821	-0.062637
C	5.582545	9.366815	-2.765670
C	4.395246	9.258440	-3.434185
C	2.457712	7.587489	-3.342870
H	2.436352	6.573676	-2.939275
C	2.179730	7.469933	-4.837295
H	3.007937	6.967584	-5.345619
H	1.285269	6.852914	-4.968321
H	1.992539	8.437649	-5.308567
C	1.424524	8.424895	-2.593414
H	1.408637	9.462528	-2.938585
H	0.430106	7.999683	-2.761913
H	1.628793	8.414540	-1.517795
C	3.826564	10.176597	-4.459109
H	3.900018	9.748541	-5.464990
H	2.776484	10.413569	-4.272475
H	4.381816	11.116327	-4.455826
C	6.630207	10.414732	-2.911560
H	6.232604	11.248986	-3.492104
H	6.971483	10.811380	-1.952597
H	7.505785	10.026158	-3.443510
C	3.751162	4.578651	-3.230618
C	2.483269	4.004204	-3.517768
C	2.122309	3.696633	-4.831639
H	1.134067	3.289947	-5.031055
C	2.996358	3.879064	-5.902311
C	2.577418	3.557259	-7.322699
H	3.450064	3.736766	-7.966444
C	1.449244	4.489629	-7.786595
H	1.744653	5.540405	-7.693240
H	1.191154	4.294153	-8.833759
H	0.547592	4.336729	-7.181986
C	2.167745	2.087526	-7.482467
H	1.278485	1.861239	-6.883020
H	1.930931	1.866845	-8.529524
H	2.972338	1.417335	-7.161663
C	4.264695	4.369246	-5.621964
H	4.973460	4.482648	-6.441150
C	4.642197	4.730054	-4.322946
C	6.065543	5.245879	-4.144146
H	6.193385	5.569324	-3.103337
C	7.086585	4.122489	-4.371313
H	7.049989	3.765524	-5.407275
H	8.103139	4.481395	-4.170431
H	6.884374	3.275521	-3.707444
C	6.380977	6.455461	-5.033197
H	5.642859	7.252684	-4.897854
H	7.370608	6.858061	-4.786990
H	6.389455	6.179017	-6.093446
C	1.467975	3.693085	-2.418905
H	2.036083	3.565671	-1.487876
C	0.680348	2.401867	-2.690464
H	-0.081060	2.553260	-3.463886
H	1.331199	1.585396	-3.020582
H	0.154644	2.084516	-1.783012
C	0.469191	4.836522	-2.185865
H	-0.299824	4.524493	-1.468745
H	0.954994	5.723013	-1.771127
H	-0.028060	5.111643	-3.124394
Se	6.298969	4.327569	-0.535857
Al	5.010948	4.499784	1.492463
N	3.674279	1.704041	1.971805
N	5.540446	1.879082	3.033559
C	4.741223	2.524451	2.141361
C	2.695163	1.918458	0.885350
H	2.919360	2.927508	0.521310
C	1.250857	1.931650	1.372304
H	0.865047	0.931832	1.586332
H	0.627883	2.370949	0.586639
H	1.150291	2.553280	2.268137
C	2.966473	0.932455	-0.247312
H	3.994368	1.044039	-0.607566
H	2.286646	1.137684	-1.075912
H	2.813004	-0.105627	0.060158
C	3.784473	0.565899	2.764466
C	4.971203	0.674614	3.433932
C	6.908277	2.346215	3.344273

H	6.929448	3.360310	2.941380
C	7.185607	2.463067	4.838883
H	6.357266	2.965256	5.347151
H	8.080114	3.079907	4.970495
H	7.372579	1.495163	5.309847
C	7.942066	1.509475	2.594907
H	7.957979	0.471681	2.939606
H	8.936317	1.934814	2.764049
H	7.738279	1.520275	1.519199
C	5.539516	-0.243668	4.458954
H	5.465512	0.184146	5.464888
H	6.589721	-0.480481	4.272770
H	4.984387	-1.183465	4.455187
C	2.737104	-0.482463	2.909317
H	3.134496	-1.316562	3.490226
H	2.396908	-0.879225	1.950019
H	1.860861	-0.094273	3.440440
C	5.614017	5.355130	3.230995
C	6.881703	5.929928	3.518311
C	7.242359	6.237755	4.832205
H	8.230456	6.644714	5.031772
C	6.368196	6.055079	5.902747
C	6.786839	6.377026	7.323188
H	5.914091	6.197489	7.966787
C	7.914978	5.444731	7.787335
H	7.619649	4.393941	7.693849
H	8.172787	5.640172	8.834574
H	8.816765	5.597710	7.182949
C	7.196383	7.846789	7.482975
H	8.085662	8.073163	6.883593
H	7.433118	8.067482	8.530047
H	6.391750	8.516915	7.162134
C	5.100088	5.564401	5.622257
H	4.391267	5.450753	6.441361
C	4.722851	5.203467	4.323195
C	3.299657	4.687287	4.144270
H	3.171853	4.364100	3.103384
C	2.278308	5.810325	4.371801
H	2.314884	6.167002	5.407867
H	1.261845	5.451167	4.170901
H	2.480202	6.657537	3.708164
C	2.984518	3.477373	5.032979
H	3.722843	2.680364	4.897491
H	1.995020	3.074586	4.786553
H	2.975871	3.753546	6.093297
C	7.897286	6.240573	2.419606
H	7.329397	6.368272	1.488478
C	8.685670	7.531307	2.691234
H	9.446844	7.379453	3.464800
H	8.035276	8.348219	3.021164
H	9.211736	7.848218	1.783844
C	8.895389	5.096508	2.186678
H	9.664702	5.408072	1.469676
H	8.409048	4.210370	1.771815
H	9.392301	4.821010	3.125277

3_Te

Te	3.732173	7.146590	7.078136
Al	1.938710	5.558637	8.150188
N	-0.574586	6.314079	6.421465
N	-0.993118	4.884187	7.961459
C	2.439944	3.613893	7.990157
C	2.155057	2.960849	6.762241
C	2.273031	1.575220	6.640100
H	2.039170	1.103148	5.687372
C	2.696195	0.782066	7.706286
C	3.053963	1.423720	8.887732
H	3.431785	0.821885	9.713291
C	2.948841	2.812112	9.036074
C	1.784539	3.743835	5.508806
H	1.747414	4.809412	5.771644
C	2.875503	3.610218	4.436581
H	3.849865	3.913677	4.834642
H	2.642786	4.244268	3.572923
H	2.958013	2.575391	4.085329
C	0.412862	3.352948	4.946147
H	-0.366157	3.421911	5.712941
H	0.424353	2.323391	4.570619
H	0.135983	4.009369	4.112514
C	2.801771	-0.724084	7.572056
H	3.132899	-1.113512	8.544992
C	3.849789	-1.122845	6.523731
H	3.955833	-2.212864	6.480704
H	4.827395	-0.689594	6.760459
H	3.556300	-0.772932	5.527311
C	1.441750	-1.356840	7.248399
H	0.693002	-1.086236	8.000532
H	1.522797	-2.449394	7.218978
H	1.077293	-1.020243	6.270871
C	3.446010	3.421676	10.337529
H	3.320364	4.509179	10.260571
C	4.942158	3.143832	10.540815
H	5.298383	3.625565	11.458368
H	5.528915	3.529178	9.699394
H	5.140952	2.069869	10.630777
C	2.632908	2.955812	11.550328
H	2.973646	3.465782	12.459590
H	2.739244	1.876019	11.707579
H	1.568291	3.178422	11.416770
C	0.015920	5.610848	7.417497
C	-1.933860	6.033576	6.335568
C	-2.201663	5.129268	7.321008
C	0.116832	7.180742	5.473653
H	1.124707	7.380983	5.846052
H	-0.425354	8.123750	5.370014
H	0.180542	6.692344	4.494518
C	-2.813395	6.656749	5.314707
H	-2.860608	7.745540	5.434362
H	-3.827240	6.262103	5.403274
H	-2.454946	6.448770	4.299827
C	-3.467682	4.466936	7.724534
H	-3.702084	4.660780	8.777470
H	-3.412974	3.380245	7.590312
H	-4.294622	4.841591	7.118525
C	-0.863734	3.976710	9.097188
H	-1.339006	4.407331	9.984806
H	0.193612	3.801704	9.300513
H	-1.335463	3.019282	8.857939
Te	1.452124	6.816019	10.448435
Al	3.244670	8.404541	9.375954
N	5.759495	7.650994	11.102651
N	6.175869	9.082705	9.563756
C	2.742349	10.348973	9.535540
C	3.027876	11.002575	10.763000
C	2.909786	12.388225	10.884622
H	3.144009	12.860729	11.837046
C	2.485990	13.180881	9.818275
C	2.127464	12.538624	8.637384
H	1.748887	13.140016	7.811840
C	2.232621	11.150173	8.489649
C	3.398958	10.220101	12.016638
H	3.437205	9.154499	11.753977
C	2.307557	10.352866	13.088524
H	1.333580	10.048572	12.690153
H	2.540523	9.719101	13.952317
H	2.224086	11.387679	13.439602
C	4.770067	10.612414	12.579666
H	5.549496	10.543592	11.813286
H	4.757634	11.642186	12.954565
H	5.047083	9.956755	13.413851
C	2.380630	14.687108	9.951777
H	2.049149	15.076062	8.978773
C	1.333010	15.086556	11.000269
H	1.227169	16.176613	11.042838

H	0.355249	14.653384	10.764044
H	1.626747	14.737036	11.996755
C	3.740835	15.319828	10.274625
H	4.489254	15.048852	9.522300
H	3.659899	16.412402	10.303640
H	4.105639	14.983576	11.252138
C	1.734318	10.539785	7.188999
H	1.861089	9.452401	7.266136
C	0.237603	10.816178	6.988002
H	-0.119305	10.335502	6.070170
H	-0.347623	10.428854	7.829587
H	0.037467	11.890061	6.900021
C	2.545169	11.006019	5.974853
H	2.204002	10.494906	5.066396
H	2.437073	12.085539	5.816906
H	3.610285	10.785092	6.107216
C	5.167852	8.354499	10.107488
C	7.118426	7.933095	11.188472
C	7.384860	8.838641	10.203804
C	5.069248	6.782543	12.049677
H	4.062082	6.580290	11.676455
H	5.613411	5.840689	12.153441
H	5.003642	7.270477	13.028927
C	7.999068	7.310149	12.208517
H	8.048102	6.221578	12.087591
H	9.012261	7.706542	12.120247
H	7.640407	7.516358	13.223679
C	8.649846	9.503109	9.800615
H	8.885326	9.309054	8.747949
H	8.592853	10.589772	9.934086
H	9.477137	9.130507	10.407406
C	6.045288	9.991224	8.429006
H	6.525639	9.564314	7.542337
H	4.987746	10.160984	8.222472
H	6.511411	10.950749	8.670990

3_Se

N	6.049775	-0.529032	6.444896
N	6.969876	-1.030637	8.313681
Al	6.393245	1.929038	8.371621
Se	5.133761	3.514247	7.098753
C	8.326491	2.420263	8.658307
C	8.848687	2.965818	9.855709
C	10.227458	3.050275	10.066305
H	10.597666	3.460738	11.004110
C	11.142853	2.641710	9.097482
C	10.639097	2.192368	7.880246
H	11.341755	1.927587	7.090960
C	9.263225	2.090972	7.647870
C	7.935529	3.548497	10.923937
H	6.903417	3.433674	10.570728
C	8.200582	5.050710	11.101790
H	8.078568	5.583699	10.152212
H	9.217752	5.236221	11.465596
H	7.505063	5.482749	11.830239
C	8.044107	2.807645	12.260474
H	7.830192	1.740621	12.132581
H	7.326697	3.212731	12.984756
H	9.048392	2.906426	12.689675
C	12.636741	2.729879	9.339349
H	13.134605	2.333524	8.443234
C	13.089457	4.184694	9.524367
H	12.801651	4.798941	8.664458
H	14.178344	4.237939	9.637976
H	12.635209	4.622167	10.420974
C	13.065489	1.872201	10.537314
H	12.754186	0.830158	10.407631
H	12.617203	2.247140	11.464612
H	14.154680	1.895129	10.657132
C	8.816620	1.700233	6.245390
H	7.719697	1.679529	6.236685
C	9.229853	2.767696	5.221552
H	10.320624	2.833563	5.139417
H	8.849200	3.752745	5.512381
H	8.829543	2.521299	4.230953
C	9.318110	0.314637	5.822048
H	8.890781	0.029547	4.853193
H	9.045320	-0.449537	6.557724
H	10.409175	0.309366	5.720210
C	6.471356	0.016948	7.611545
C	6.281176	-1.899788	6.411145
C	6.860226	-2.220567	7.604117
C	5.545683	0.218791	5.297423
H	6.323299	0.295033	4.528540
H	5.255910	1.219701	5.626152
H	4.677306	-0.291383	4.874464
C	5.925718	-2.738454	5.238684
H	4.847004	-2.719022	5.043310
H	6.218569	-3.774786	5.416750
H	6.434476	-2.392154	4.331486
C	7.327090	-3.521020	8.147818
H	7.102480	-4.323487	7.442785
H	6.836325	-3.755841	9.099296
H	8.409310	-3.516769	8.323335
C	7.541194	-0.947992	9.654765
H	7.735134	0.097368	9.899987
H	8.487025	-1.495964	9.683503
H	6.850138	-1.370084	10.391595
N	3.939369	5.563705	10.866681
N	3.019367	6.065588	8.997921
Al	3.595691	3.105828	8.939867
Se	4.855103	1.520503	10.212667
C	1.662390	2.614731	8.653366
C	1.139925	2.069469	7.455926
C	-0.238886	1.985130	7.245581
H	-0.609300	1.574872	6.307761
C	-1.154040	2.393616	8.214655
C	-0.650021	2.842769	9.431872
H	-1.352510	3.107482	10.221330
C	0.725895	2.944024	9.664031
C	2.052866	1.487105	6.387328
H	3.085048	1.601738	6.740386
C	1.787694	-0.015012	6.208968
H	1.909821	-0.548323	7.158342
H	0.770427	-0.200276	5.845292
H	2.483034	-0.446886	5.480252
C	1.943989	2.228463	5.051112
H	2.158016	3.295417	5.179391
H	2.661215	1.823610	4.326509
H	0.939604	2.129944	4.622061
C	-2.647987	2.305619	7.973099
H	-3.145609	2.701942	8.869364
C	-3.100907	0.850873	7.788068
H	-2.812976	0.236531	8.647867
H	-4.189826	0.797766	7.674701
H	-2.646914	0.413405	6.891324
C	-3.076912	3.163441	6.775300
H	-2.765476	4.205439	6.905008
H	-2.628861	2.788533	5.847876
H	-4.166129	3.140631	6.655717
C	1.172827	3.334787	11.066368
H	2.269753	3.355604	11.074784
C	0.759958	2.267259	12.090285
H	-0.330785	2.201323	12.172740
H	1.140583	1.282236	11.799326
H	1.160542	2.513645	13.080782
C	0.671325	4.720341	11.489848
H	1.098895	5.005439	12.458584
H	0.943848	5.484561	10.754107
H	-0.419708	4.725523	11.591976
C	3.517768	5.017883	9.699980
C	3.708246	6.934494	10.900540
C	3.129228	7.255439	9.707597
C	4.443373	4.815633	12.014059

H	3.665798	4.739474	12.782976
H	4.732924	3.814701	11.685203
H	5.311886	5.325552	12.437008
C	4.063954	7.773029	12.073006
H	5.142662	7.753318	12.268367
H	3.771372	8.809438	11.894952
H	3.555114	7.426844	12.980207
C	2.662703	8.556048	9.163951
H	2.887481	9.358431	9.869024
H	3.153547	8.790796	8.212498
H	1.580487	8.552057	8.988409
C	2.448046	5.983240	7.656845
H	2.253717	4.937996	7.411485
H	1.502405	6.531546	7.628168
H	3.139257	6.405184	6.920078

4_Te

Te	-1.510823	0.186334	-2.795097
Al	-0.435744	0.312731	-0.443288
N	-1.342157	2.887281	1.051166
N	-3.040342	1.664686	0.585927
N	-1.210867	-2.315486	1.202057
N	0.319762	-2.606301	-0.295278
C	1.518522	0.798940	-0.042164
C	2.413709	1.339964	-1.003348
C	3.774806	1.493906	-0.725195
H	4.426814	1.901128	-1.495809
C	4.317862	1.150716	0.509194
C	3.444960	0.672272	1.479308
H	3.847018	0.423418	2.460238
C	2.079370	0.498633	1.228048
C	1.941184	1.818539	-2.365208
H	0.867020	1.613853	-2.433463
C	2.131783	3.333036	-2.522897
H	1.638817	3.875952	-1.708476
H	1.699085	3.673572	-3.471204
H	3.193321	3.608616	-2.518308
C	2.611535	1.060348	-3.516821
H	3.691544	1.247336	-3.550608
H	2.184573	1.372879	-4.477204
H	2.456060	-0.019965	-3.415699
C	5.799835	1.292151	0.791460
H	5.960426	0.992064	1.836594
C	6.275495	2.742955	0.637349
H	6.164178	3.082501	-0.398728
H	7.333992	2.830945	0.907412
H	5.698165	3.417123	1.278937
C	6.622245	0.352471	-0.101438
H	7.686591	0.409622	0.153963
H	6.512754	0.626651	-1.157138
H	6.294092	-0.686286	0.014107
C	1.245424	-0.005396	2.400516
H	0.198821	-0.046384	2.074104
C	1.677494	-1.415329	2.830400
H	1.056518	-1.788788	3.652432
H	2.714960	-1.403523	3.182525
H	1.612505	-2.127106	2.002315
C	1.299210	0.949219	3.603323
H	2.311093	1.004372	4.019176
H	0.631483	0.597366	4.398707
H	0.993474	1.961867	3.324671
C	-1.677949	1.667927	0.540646
C	-2.465070	3.626298	1.400357
C	-3.543782	2.845998	1.109258
C	-0.005247	3.471127	1.115578
H	0.077672	4.280770	0.382394
H	0.734470	2.704964	0.888533
H	0.175621	3.875900	2.115068
C	-2.379510	4.995973	1.967374
H	-1.864850	5.681245	1.284181
H	-1.836767	5.005809	2.919673
H	-3.382887	5.386819	2.145740
C	-4.999095	3.093690	1.268685
H	-5.164674	4.077841	1.710650
H	-5.464187	2.345045	1.920545
H	-5.518641	3.062517	0.304167
C	-3.922246	0.622186	0.073567
H	-4.557429	1.038263	-0.714565
H	-4.551402	0.233470	0.879286
H	-3.323992	-0.170744	-0.375786
C	-0.495531	-1.659425	0.247081
C	-0.846828	-3.659325	1.260010
C	0.122261	-3.840522	0.314469
C	-2.285715	-1.664788	1.987005
H	-2.309029	-0.645108	1.593789
C	-1.446037	-4.693364	2.149807
H	-2.386844	-5.084185	1.745868
H	-1.640372	-4.322089	3.156902
H	-0.756536	-5.535569	2.240575
C	0.810328	-5.109867	-0.051188
H	1.872943	-4.965801	-0.252929
H	0.359584	-5.572577	-0.936180
H	0.723892	-5.821710	0.772523
C	1.263718	-2.319448	-1.405418
H	1.008229	-1.299106	-1.715908
C	-3.635580	-2.329180	1.723581
H	-3.826567	-2.425943	0.650550
H	-3.692550	-3.318451	2.183015
H	-4.426844	-1.717056	2.165991
C	-1.984217	-1.554212	3.480250
H	-1.018769	-1.079476	3.660312
H	-2.759175	-0.928995	3.935352
H	-2.001357	-2.520955	3.988197
C	2.718844	-2.327816	-0.948730
H	3.063590	-3.326577	-0.666172
H	3.341920	-1.983386	-1.780931
H	2.867809	-1.643173	-0.109842
C	1.011159	-3.214442	-2.615510
H	1.523833	-2.774350	-3.476770
H	1.399460	-4.226213	-2.476951
H	-0.056760	-3.262717	-2.848053

4_Se

Se	-1.359487	0.308943	-2.894104
Al	-0.621554	0.242243	-0.680165
N	-1.950593	2.506552	1.009853
N	-3.436899	1.158059	0.259848
N	-1.108389	-2.629855	0.656931
N	0.583268	-2.527499	-0.678180
C	1.210921	0.879625	-0.004203
C	2.121263	1.622391	-0.802783
C	3.427180	1.874446	-0.373397
H	4.098562	2.431437	-1.024557
C	3.890639	1.443569	0.866493
C	2.991194	0.772204	1.687123
H	3.327298	0.458032	2.674351
C	1.682574	0.490653	1.277922
C	1.719540	2.218525	-2.143928
H	0.673930	1.948274	-2.330118
C	1.807630	3.751457	-2.123359
H	1.215763	4.169124	-1.301033
H	1.425641	4.166485	-3.063722
H	2.842146	4.094037	-2.001008
C	2.542787	1.646935	-3.305110
H	3.606087	1.896906	-3.205395
H	2.188683	2.053069	-4.260095
H	2.452521	0.555758	-3.350819
C	5.317339	1.696164	1.310001
H	5.419001	1.288823	2.325949
C	5.640934	3.194619	1.370072
H	5.579921	3.649086	0.374591
H	6.656676	3.353910	1.749769
H	4.940672	3.722150	2.026588
C	6.314758	0.959357	0.404816

H	7.339420	1.090244	0.771273
H	6.269737	1.347919	-0.619187
H	6.094011	-0.113120	0.369205
C	0.801026	-0.222712	2.297204
H	-0.183841	-0.379746	1.841955
C	1.377609	-1.594029	2.678298
H	0.688060	-2.145052	3.327985
H	2.321083	-1.476952	3.222833
H	1.573916	-2.204065	1.792086
C	0.573615	0.619125	3.561610
H	-0.105978	0.097037	4.246112
H	0.133655	1.591271	3.321783
H	1.514811	0.796099	4.093948
C	-2.087784	1.326461	0.340414
C	-3.182730	3.058583	1.338430
C	-4.127239	2.197010	0.866446
C	-0.709322	3.245112	1.226731
H	0.137004	2.604287	0.983133
H	-0.643469	3.567878	2.269274
H	-0.690392	4.128440	0.578883
C	-3.315282	4.350412	2.058630
H	-2.843700	4.311272	3.047359
H	-4.370516	4.593360	2.196420
H	-2.848812	5.170171	1.500237
C	-5.610210	2.246102	0.923002
H	-5.934225	3.128045	1.478388
H	-6.021090	1.360075	1.420476
H	-6.049523	2.297164	-0.079989
C	-4.126035	0.093635	-0.460324
H	-4.727006	-0.505550	0.229579
H	-3.388365	-0.519000	-0.981091
H	-4.781369	0.534645	-1.217984
C	-0.453415	-1.792495	-0.190992
C	-0.484502	-3.874109	0.713103
C	0.587294	-3.807992	-0.131389
C	-2.394209	-2.266597	1.291426
H	-2.509361	-1.204768	1.055160
C	-0.860301	-4.992118	1.622727
H	-1.929520	-5.212609	1.612242
H	-0.572878	-4.775389	2.658198
H	-0.335679	-5.899976	1.318973
C	1.639706	-4.839372	-0.349143
H	1.269490	-5.813952	-0.024977
H	2.541033	-4.617374	0.234114
H	1.932671	-4.930607	-1.395825
C	1.512911	-2.013108	-1.714170
H	1.184914	-0.981010	-1.881728
C	-3.543119	-3.041311	0.647117
H	-3.545071	-2.907203	-0.438663
H	-3.480634	-4.110454	0.863591
H	-4.494880	-2.679800	1.047348
C	-2.384495	-2.390265	2.812663
H	-2.377046	-3.429837	3.147015
H	-1.527654	-1.869293	3.246767
H	-3.296230	-1.922521	3.197284
C	2.957162	-1.973235	-1.228616
H	3.027503	-1.439737	-0.275746
H	3.388413	-2.971629	-1.119951
H	3.555617	-1.429266	-1.966631
C	1.332915	-2.743451	-3.042717
H	1.733266	-3.760145	-3.025658
H	0.275833	-2.775452	-3.321302
H	1.870032	-2.186377	-3.817198

5_Te

Te	10.562521	11.915126	13.481337
Al	8.904616	12.149805	11.513873
N	8.357178	9.218664	11.225424
N	6.481844	10.096665	11.775823
N	7.098984	13.928947	13.272960
N	7.755545	15.020472	11.547774
C	9.363068	12.293283	9.522515
C	10.675221	12.430766	9.004609
C	10.914340	12.433709	7.624518
H	11.935136	12.543223	7.260702
C	9.887897	12.307187	6.696732
C	8.589554	12.193915	7.189078
H	7.763079	12.107884	6.485978
C	8.319829	12.193638	8.559415
C	11.881625	12.618711	9.907435
H	11.531121	12.545318	10.942812
C	12.936606	11.522752	9.714720
H	13.393185	11.568172	8.718857
H	12.495125	10.527425	9.840450
H	13.736874	11.633966	10.456059
C	12.500813	14.011608	9.733132
H	12.912320	14.143502	8.725036
H	13.315142	14.159777	10.452521
H	11.752827	14.795450	9.899048
C	10.171631	12.303762	5.207994
H	11.257886	12.417178	5.086001
C	9.491574	13.484029	4.501132
H	9.759368	13.501889	3.438537
H	9.792076	14.437252	4.949018
H	8.400573	13.405063	4.571629
C	9.759859	10.973464	4.562493
H	10.026990	10.962111	3.499658
H	8.676764	10.822686	4.639403
H	10.255230	10.128588	5.052537
C	6.852691	12.096676	8.956952
H	6.795638	12.187033	10.046535
C	6.007371	13.242942	8.384039
H	5.958910	13.196244	7.290625
H	6.421540	14.217246	8.662034
H	4.981786	13.184371	8.767334
C	6.255719	10.739036	8.560763
H	6.219986	10.639691	7.469893
H	5.231711	10.633923	8.939130
H	6.855099	9.910664	8.953148
C	7.780546	10.409390	11.532496
C	7.439257	8.176950	11.267606
C	6.246305	8.734295	11.622891
C	9.745755	9.057054	10.800533
H	10.125780	8.094976	11.150818
H	10.348899	9.852245	11.250485
H	9.816743	9.106246	9.708462
C	7.803739	6.770744	10.959240
H	8.241117	6.683590	9.958204
H	6.914836	6.138315	10.997107
H	8.531485	6.375306	11.677388
C	4.906034	8.129638	11.829609
H	4.171737	8.524515	11.117263
H	4.529543	8.327054	12.839919
H	4.959471	7.047978	11.694307
C	5.408928	11.043042	12.055751
H	5.801965	12.057572	12.008527
H	4.986175	10.860976	13.048406
H	4.618589	10.937983	11.306166
C	7.782039	13.780018	12.105276
C	6.656290	15.232919	13.445720
C	7.078009	15.929122	12.351335
C	6.923902	12.905912	14.298640
H	5.859447	12.742365	14.491909
H	7.416908	13.226560	15.221611
H	7.402451	11.981656	13.973185
C	5.881961	15.660372	14.638163
H	5.628379	16.719069	14.559885
H	6.455870	15.515302	15.560625
H	4.949213	15.092728	14.734135
C	6.915750	17.357956	11.981398
H	7.886497	17.849597	11.850474
H	6.372309	17.886797	12.766509
H	6.356160	17.471166	11.045559
C	8.463690	15.430299	10.337958

H	8.827166	14.542309	9.819990
H	9.313464	16.067709	10.605181
H	7.790637	15.987861	9.681104

5_Se

Se	10.478168	11.821708	13.194803
Al	8.913851	12.137266	11.488996
N	8.290775	9.213444	11.178961
N	6.444291	10.135823	11.749967
N	7.189721	13.886186	13.345905
N	7.739687	15.009785	11.605858
C	9.352941	12.329106	9.497045
C	10.665886	12.516449	8.996270
C	10.931641	12.469919	7.621714
H	11.953220	12.610282	7.270395
C	9.929446	12.258604	6.682749
C	8.625583	12.123139	7.155336
H	7.815596	11.987552	6.440749
C	8.331365	12.165685	8.520072
C	11.840318	12.822810	9.910997
H	11.464954	12.824428	10.940577
C	12.929096	11.745401	9.837962
H	13.385656	11.701153	8.841864
H	12.513993	10.757193	10.066806
H	13.723420	11.954477	10.564434
C	12.426446	14.212382	9.625645
H	12.878520	14.262848	8.627757
H	13.204374	14.454405	10.359584
H	11.650605	14.984568	9.683385
C	10.242912	12.202011	5.200990
H	11.328781	12.334430	5.095569
C	9.552980	13.338886	4.434756
H	9.839964	13.320137	3.377146
H	9.826158	14.315111	4.849427
H	8.462632	13.240474	4.489489
C	9.872398	10.838979	4.600698
H	10.163807	10.790458	3.545254
H	8.791096	10.668590	4.659770
H	10.373121	10.024746	5.135240
C	6.859227	12.064693	8.898883
H	6.788191	12.183196	9.985315
C	6.019792	13.193986	8.283751
H	5.990516	13.119006	7.191135
H	6.426867	14.176302	8.543057
H	4.987908	13.142156	8.651075
C	6.268842	10.698095	8.525211
H	6.236204	10.579745	7.436080
H	5.244021	10.596062	8.902565
H	6.869055	9.878255	8.933112
C	7.746530	10.418249	11.489839
C	7.348760	8.193635	11.232868
C	6.173606	8.779538	11.600955
C	9.668676	9.019276	10.732883
H	10.039689	8.058254	11.095924
H	10.289554	9.815573	11.155164
H	9.719788	9.042879	9.638659
C	7.676401	6.778830	10.922489
H	8.093179	6.678242	9.913846
H	6.774627	6.166216	10.979321
H	8.408525	6.369573	11.628343
C	4.820917	8.208507	11.821802
H	4.087824	8.630694	11.123981
H	4.463713	8.405540	12.839233
H	4.842780	7.127191	11.674894
C	5.399637	11.111046	12.036853
H	5.829691	12.111600	12.021725
H	4.954954	10.919410	13.018057
H	4.618236	11.051992	11.272487
C	7.806356	13.761245	12.139744
C	6.746258	15.182624	13.565123
C	7.100965	15.900184	12.460422
C	7.056175	12.831623	14.345669
H	5.999556	12.649314	14.564274
H	7.570482	13.130124	15.264309
H	7.536019	11.925206	13.974130
C	6.037264	15.583432	14.806571
H	5.770045	16.640720	14.761026
H	6.663981	15.429261	15.692603
H	5.116739	15.004977	14.946246
C	6.907839	17.333353	12.123335
H	7.866206	17.836033	11.949740
H	6.401815	17.844767	12.944195
H	6.299335	17.456488	11.219890
C	8.359744	15.437063	10.354802
H	8.718926	14.556759	9.819953
H	9.204409	16.101314	10.566981
H	7.630676	15.970737	9.738809

6_Te

Te	-1.214109	13.616679	9.370590
Al	2.704053	15.199359	8.000168
O	1.726242	13.767593	8.730309
O	4.298558	14.200750	7.816840
O	3.998047	12.583129	6.265599
O	0.749710	15.652783	8.301811
O	2.360802	15.237633	6.197085
O	4.267391	15.532893	5.020398
N	7.076544	14.241327	6.988262
N	6.863346	12.136092	6.496942
N	1.399480	13.590973	4.089757
N	2.777475	14.566804	2.717724
C	4.688254	13.327318	6.963111
C	8.346304	13.756784	6.733647
C	9.549046	14.622304	6.797549
C	8.213186	12.425124	6.430148
C	9.237458	11.406282	6.093087
C	6.294942	10.802259	6.274414
C	6.817751	15.654607	7.289981
C	3.599716	18.022203	8.474200
C	3.652922	18.909064	6.099213
C	1.713195	19.468288	7.621655
C	4.371458	19.011595	9.089590
C	5.129872	18.741043	10.227874
C	5.662346	14.432871	10.938950
C	3.610041	15.175322	12.214709
C	5.979844	19.814766	10.878473
C	7.086242	20.300227	9.931655
C	5.128357	20.994353	11.366536
C	3.113369	15.135458	5.153103
C	2.432696	14.455780	4.016108
C	-0.000891	12.172140	2.550014
C	1.956898	13.763018	1.953850
C	2.074800	13.665641	0.477788
C	0.726050	13.139016	5.317371
C	1.087991	13.143276	2.821687
C	3.830074	15.430529	2.171861
C	6.178880	13.246149	6.836393
C	4.316554	16.444401	10.153063
C	5.076150	17.453177	10.755670
C	4.276596	15.081978	10.834011
C	2.773899	18.419971	7.258564
C	0.612732	14.458048	8.732165
C	3.577163	16.700375	8.975633
H	5.640283	17.238631	11.662765
H	4.380175	20.017490	8.673242
H	9.507047	15.416107	6.043010
H	9.640601	15.098347	7.779863
H	10.447131	14.029464	6.619664
H	9.299600	10.629727	6.863933
H	9.013224	10.918691	5.138375
H	10.216715	11.879870	6.011796
H	6.027226	10.682421	5.221213
H	7.043037	10.059209	6.553100
H	5.405035	10.677971	6.888504

H	7.304307	15.912094	8.235386
H	7.234375	16.265520	6.485134
H	5.748082	15.822292	7.374840
H	4.166520	19.841742	6.359859
H	4.409276	18.159809	5.842982
H	3.042733	19.099522	5.208193
H	1.072770	19.111105	8.435294
H	2.180628	20.406041	7.943724
H	1.078781	19.688276	6.755052
H	6.335773	15.032700	11.561691
H	5.585185	13.437186	11.391369
H	6.116258	14.323707	9.948190
H	3.509866	14.178545	12.659596
H	4.203154	15.793471	12.898263
H	2.611297	15.618376	12.135958
H	6.461736	19.360447	11.755625
H	7.704576	19.464084	9.587193
H	6.656308	20.789739	9.049999
H	7.735123	21.025358	10.436244
H	4.642382	21.499157	10.523853
H	4.347027	20.657502	12.056016
H	5.752989	21.730899	11.884911
H	0.210037	11.196898	3.002875
H	-0.958074	12.529969	2.943368
H	-0.108982	12.029194	1.474213
H	1.822014	14.615091	-0.007947
H	3.092017	13.391202	0.179152
H	1.392893	12.902604	0.100841
H	1.475794	12.868584	6.061228
H	0.088922	13.934778	5.709447
H	0.120253	12.268265	5.070830
H	3.888681	16.347024	2.756168
H	4.793249	14.915041	2.212421
H	3.578470	15.664991	1.137384
H	3.650162	14.414624	10.229730
H	2.238212	17.530151	6.909295

6_Te'

Te	1.378765	12.896542	9.408814
Al	2.653051	14.969537	8.202486
O	0.834540	15.578237	8.483097
O	4.315883	14.035432	7.912585
O	4.087470	12.479182	6.280759
O	-1.085763	14.766323	9.332884
O	2.278415	14.975082	6.379978
O	4.174279	15.538494	5.280572
N	7.124071	14.115418	7.104918
N	6.935205	11.981783	6.756602
N	1.460999	13.572209	4.028196
N	2.695985	14.918222	2.850073
C	4.736422	13.197563	7.044933
C	8.406265	13.620773	6.934704
C	9.602278	14.496348	6.984000
C	8.288248	12.271341	6.725076
C	9.322446	11.228588	6.515686
C	6.380629	10.632728	6.613027
C	6.837677	15.543733	7.281249
C	3.532323	17.838921	8.453922
C	3.222961	18.793667	6.109926
C	1.428536	19.084356	7.862616
C	4.328082	18.884692	8.932897
C	5.216804	18.703371	9.991067
C	5.998591	14.488354	10.932352
C	3.992330	15.207737	12.287209
C	6.086085	19.839807	10.493696
C	7.074341	20.305043	9.415348
C	5.243166	21.017250	11.001808
C	3.042296	15.064398	5.347232
C	2.405642	14.529801	4.107355
C	0.140454	12.345315	2.270733
C	1.925003	14.199828	1.957143
C	1.998765	14.398775	0.488492
C	0.868033	12.842025	5.157009
C	1.146801	13.346931	2.702075
C	3.643767	15.969874	2.466204
C	6.236360	13.108860	6.987726
C	4.491059	16.379013	10.115636
C	5.271149	17.443925	10.580942
C	4.578157	15.062283	10.875094
C	2.546756	18.170629	7.339202
C	0.092330	14.680765	9.044767
C	3.613480	16.540993	9.016969
H	5.936000	17.295556	11.431348
H	4.246956	19.868768	8.474501
H	9.556573	15.273088	6.212486
H	9.688657	14.994330	7.956205
H	10.504807	13.905635	6.821544
H	9.347771	10.518787	7.350481
H	9.135909	10.662548	5.596812
H	10.306490	11.693051	6.437589
H	6.285737	10.380984	5.552916
H	7.054100	9.926070	7.101071
H	5.399782	10.592223	7.082278
H	7.404603	15.913676	8.139634
H	7.144057	16.081353	6.379460
H	5.773986	15.682589	7.457970
H	3.625063	19.788192	6.334606
H	4.043452	18.162735	5.753410
H	2.497998	18.906930	5.294553
H	0.924916	18.629430	8.721818
H	1.833707	20.053500	8.177396
H	0.679960	19.266613	7.082128
H	6.678791	15.150090	11.480979
H	5.995922	13.517417	11.442023
H	6.402913	14.342136	9.925184
H	3.983021	14.238912	12.800772
H	4.583483	15.906851	12.890503
H	2.963535	15.582009	12.243628
H	6.668314	19.451581	11.341375
H	7.691305	19.471503	9.061951
H	6.539009	20.718799	8.552979
H	7.737812	21.084590	9.807347
H	4.663854	21.463427	10.185326
H	4.540370	20.691949	11.776165
H	5.885790	21.798351	11.424214
H	0.455413	11.326374	2.522618
H	-0.828808	12.527880	2.746633
H	0.004684	12.399839	1.189773
H	1.652328	15.398237	0.201568
H	3.023773	14.276638	0.122770
H	1.367791	13.665608	-0.015555
H	1.632878	12.653484	5.909393
H	0.061306	13.432931	5.599004
H	0.473679	11.897772	4.781679
H	3.646793	16.750863	3.224713
H	4.649496	15.551120	2.376197
H	3.327009	16.383927	1.508716
H	3.950840	14.332254	10.351150
H	2.072922	17.240344	7.013712

IMe4

C	-2.895696	1.252685	1.304140
N	-3.593845	0.334292	2.034273
N	-3.768423	2.301588	1.258534
C	-4.852225	0.788287	2.431101
C	-3.076252	-0.984990	2.364490
C	-4.964168	2.052380	1.932946
C	-3.478625	3.553672	0.575864
H	-2.076297	-1.070642	1.936598
H	-3.715859	-1.771088	1.947570
H	-3.016853	-1.120320	3.450214
H	-2.483463	3.474151	0.135944
H	-3.496690	4.394393	1.278449
H	-4.210077	3.743822	-0.217572

C	-5.793680	-0.036001	3.233980
H	-5.358124	-0.321644	4.199171
H	-6.711580	0.522351	3.431694
H	-6.067480	-0.960710	2.711426
C	-6.065336	3.047421	2.022220
H	-5.736180	3.970495	2.514825
H	-6.443177	3.322029	1.029876
H	-6.899323	2.638942	2.597624

liPr

C	-0.000287	-0.936655	-0.000685
N	-1.056833	-0.083371	0.106697
N	1.056620	-0.083817	-0.108021
C	-0.678766	1.261998	0.061274
C	-2.458342	-0.537944	0.149592
C	0.679133	1.261710	-0.062256
C	2.458048	-0.538663	-0.150313
H	-3.050929	0.327746	0.467119
H	3.050568	0.326013	-0.470755
C	-1.639306	2.396828	0.137584
H	-2.183638	2.410103	1.089731
H	-1.104231	3.345042	0.048191
H	-2.382732	2.356427	-0.667690
C	1.640210	2.396090	-0.138458
H	2.383905	2.354977	0.666534
H	2.184217	2.409463	-1.090792
H	1.105652	3.344541	-0.048503
C	-2.647660	-1.648470	1.176863
H	-2.308989	-1.327200	2.166825
H	-3.709484	-1.908932	1.238015
H	-2.083636	-2.540024	0.890554
C	2.918237	-0.957906	1.245126
H	3.979074	-1.228953	1.228284
H	2.778369	-0.143997	1.964304
H	2.340036	-1.824223	1.583469
C	2.646930	-1.652281	-1.174283
H	2.307445	-1.334201	-2.164990
H	3.708819	-1.912495	-1.235344
H	2.083487	-2.543182	-0.884868
C	-2.917977	-0.961362	-1.244746
H	-2.339816	-1.828804	-1.580244
H	-3.978868	-1.232172	-1.227481
H	-2.777697	-0.149670	-1.966342

7_Te

Te	1.284735	12.983712	8.925054
Al	3.240830	14.371493	8.099358
O	2.987728	14.643920	6.273663
O	3.939892	12.941723	5.119115
N	6.149187	14.105491	7.289559
N	5.637578	12.384523	8.457012
N	1.303863	14.961800	3.921064
N	3.115543	14.601381	2.783197
C	7.290365	13.313700	7.333633
C	8.559432	13.694498	6.663007
C	6.965764	12.221103	8.083758
C	7.769629	11.044165	8.499768
C	4.934753	11.445602	9.325864
C	6.080744	15.374197	6.571732
C	3.117846	17.408772	8.320332
C	2.647404	17.854888	5.867271
C	0.854959	18.287162	7.590237
C	3.588535	18.639346	8.785121
C	4.487370	18.725172	9.848633
C	6.349270	14.854949	10.860720
C	4.234082	15.101265	12.222908
C	5.001278	20.064235	10.339676
C	5.811250	20.786540	9.254467
C	3.861566	20.956344	10.850075
C	3.237645	13.942676	5.224391
C	2.560764	14.491091	4.003081
C	-0.261439	15.932512	2.214700
C	2.201160	15.164828	1.908870
C	2.532816	15.439187	0.489847
C	0.288722	14.947717	4.979555
C	1.053198	15.383340	2.625735
C	4.489261	14.253221	2.413460
C	5.121968	13.537520	7.971544
C	4.427425	16.295227	10.012087
C	4.873043	17.540179	10.469430
C	4.831268	15.061436	10.809146
C	2.065370	17.419548	7.217955
C	3.576319	16.193364	8.886387
H	5.530980	17.595518	11.336157
H	3.237154	19.556532	8.315579
H	8.409521	13.868658	5.591376
H	8.985349	14.608652	7.093345
H	9.294549	12.895507	6.776295
H	7.835756	10.973195	9.591768
H	7.331696	10.108820	8.132614
H	8.783677	11.122361	8.103341
H	4.981194	10.438126	8.901866
H	5.395069	11.440593	10.319792
H	3.888665	11.756096	9.403442
H	7.008831	15.930254	6.725255
H	5.937641	15.203717	5.498614
H	5.250852	15.963749	6.964852
H	3.021160	18.884682	5.921378
H	3.475644	17.204591	5.566708
H	1.880901	17.817801	5.082133
H	0.440988	17.984188	8.557937
H	1.119449	19.348710	7.650121
H	0.068860	18.182830	6.832557
H	6.833670	15.661028	11.423577
H	6.593374	13.907328	11.355769
H	6.781915	14.838888	9.854471
H	4.456778	14.171256	12.759066
H	4.648847	15.934292	12.801679
H	3.146300	15.221844	12.180381
H	5.674173	19.861883	11.184823
H	6.638067	20.162187	8.898991
H	5.177310	21.031291	8.394272
H	6.228113	21.722934	9.642807
H	3.176312	21.219197	10.035959
H	3.282917	20.447884	11.628534
H	4.259659	21.888071	11.268075
H	-1.052261	15.178776	2.302893
H	-0.543554	16.789077	2.836726
H	-0.220153	16.262226	1.175619
H	3.326971	16.189759	0.405047
H	2.872610	14.530699	-0.019281
H	1.652258	15.815409	-0.032532
H	0.664062	14.404853	5.847257
H	0.047485	15.975229	5.266940
H	-0.608349	14.454422	4.597637
H	5.057718	14.025576	3.312899
H	4.479928	13.376171	1.759946
H	4.940201	15.098127	1.887928
H	4.389580	14.183709	10.316725
H	1.696320	16.394592	7.114097

7_Te'

Te	0.051285	13.478407	10.673796
Al	3.331885	15.001214	8.010285
O	2.657790	13.717478	9.195590
O	1.331464	15.361926	8.689980
N	6.361965	14.267322	7.325971
N	5.042944	12.600836	7.077767
N	1.520965	14.148839	5.597650
N	3.290246	15.177150	4.964054
C	7.133258	13.234019	6.806792
C	8.585816	13.379463	6.534313
C	6.292316	12.172571	6.647294
C	6.543174	10.798142	6.143726

C	3.852002	11.757889	6.999173
C	6.914717	15.596696	7.563898
C	3.568796	18.008616	8.286005
C	3.249891	19.032569	5.972251
C	1.268452	18.637733	7.480003
C	3.973547	19.193691	8.906578
C	4.736303	19.185811	10.071953
C	6.497086	15.398317	11.247588
C	4.068758	15.192409	11.862244
C	5.165997	20.477550	10.738643
C	6.099591	21.291594	9.831793
C	3.957681	21.320188	11.168473
C	2.628113	14.769758	6.076356
C	0.376394	13.586278	3.412695
C	2.612774	14.829922	3.804800
C	3.120205	15.165562	2.450067
C	0.467604	13.537926	6.409804
C	1.483404	14.176983	4.207472
C	4.571861	15.872474	4.966660
C	5.064744	13.895361	7.494425
C	4.701440	16.749107	10.004680
C	5.080167	17.949957	10.613194
C	5.058495	15.449246	10.715551
C	2.661447	18.135942	7.071073
C	1.493705	14.310028	9.373354
C	3.945995	16.745885	8.804107
H	5.649372	17.929787	11.540795
H	3.671855	20.147900	8.478852
H	8.784359	14.203902	5.839950
H	9.149491	13.576908	7.453712
H	8.976883	12.462052	6.090441
H	6.377558	10.046607	6.924633
H	5.886323	10.553581	5.301373
H	7.576910	10.709017	5.804679
H	3.471940	11.732675	5.971396
H	4.101798	10.742024	7.313999
H	3.090379	12.151603	7.669990
H	7.797244	15.523073	8.204788
H	7.208114	16.055864	6.613009
H	6.161720	16.215267	8.052442
H	3.253639	20.084024	6.280473
H	4.280540	18.751868	5.731955
H	2.648865	18.958955	5.058262
H	0.827587	17.985333	8.239433
H	1.329950	19.652623	7.890133
H	0.598393	18.663342	6.612210
H	6.635146	16.076991	12.096112
H	6.728587	14.386454	11.598545
H	7.226325	15.669703	10.478116
H	4.261542	14.220659	12.332146
H	4.171191	15.971246	12.627689
H	3.033955	15.198621	11.506767
H	5.726431	20.205118	11.643919
H	6.976298	20.703902	9.539011
H	5.579020	21.602327	8.918529
H	6.445073	22.194918	10.347333
H	3.375774	21.641953	10.297136
H	3.294033	20.750459	11.827446
H	4.287542	22.218424	11.702785
H	0.315444	12.499953	3.545719
H	-0.592136	14.013714	3.694978
H	0.536900	13.785311	2.351547
H	3.170561	16.250084	2.297332
H	4.124521	14.758399	2.286698
H	2.458248	14.749092	1.688922
H	0.898514	13.081720	7.300299
H	-0.267010	14.288290	6.714374
H	-0.024167	12.759036	5.825675
H	4.738791	16.314725	5.950045
H	5.386336	15.177674	4.733125
H	4.557343	16.675063	4.225827
H	4.951408	14.627191	9.994970
H	2.525653	17.133279	6.648297

8_Te

Te	0.841874	13.628915	9.356726
Al	2.791650	14.815888	8.282859
O	4.364476	13.827096	8.132948
O	4.038020	12.288347	6.507683
O	2.453423	14.961370	6.455228
O	4.450034	15.279159	5.434832
N	7.145010	13.864421	7.209078
N	6.888127	11.751235	6.777713
N	1.535961	13.806137	4.000363
N	2.942703	15.075997	2.936589
C	4.740715	12.986715	7.234542
C	8.401289	13.353249	6.935452
C	9.618089	14.200906	6.947729
C	8.240818	12.016403	6.672996
C	9.239545	10.968625	6.348491
C	6.293785	10.421609	6.606496
C	6.907375	15.291933	7.454029
C	3.363136	17.784335	8.422638
C	2.799577	18.484054	6.042455
C	1.209858	18.998048	7.936569
C	4.132653	18.884086	8.812097
C	5.094580	18.780950	9.816775
C	6.006140	14.619540	11.041828
C	4.008419	15.444568	12.344550
C	5.940693	19.973007	10.219034
C	6.826724	20.446474	9.058614
C	5.078039	21.126612	10.748838
C	3.253331	14.995649	5.444729
C	2.582746	14.639386	4.159654
C	0.120207	12.862584	2.146352
C	2.111656	14.517045	1.985813
C	2.242935	14.810998	0.537633
C	0.849199	13.065387	5.067226
C	1.224711	13.710940	2.658058
C	4.019919	16.021884	2.629878
C	6.229722	12.880283	7.102829
C	4.473104	16.440145	10.091692
C	5.228637	17.556281	10.467024
C	4.584463	15.181613	10.944359
C	2.259559	18.014387	7.398719
C	3.560437	16.514140	9.012439
H	5.931997	17.480845	11.295717
H	3.970164	19.846714	8.329819
H	9.533855	15.025057	6.230742
H	9.787944	14.635147	7.939317
H	10.491814	13.604254	6.682304
H	9.308092	10.221037	7.147032
H	8.982733	10.448961	5.419266
H	10.224198	11.421808	6.225724
H	6.054964	10.254150	5.552702
H	7.013657	9.675496	6.945778
H	5.383193	10.350426	7.198220
H	7.549701	15.620793	8.274951
H	7.151396	15.852662	6.547731
H	5.864848	15.449442	7.716218
H	3.238453	19.485811	6.120801
H	3.574673	17.805449	5.672310
H	1.993803	18.529134	5.299686
H	0.807107	18.651428	8.894367
H	1.641980	19.993626	8.089550
H	0.378486	19.095840	7.228489
H	6.690270	15.340272	11.504330
H	6.013574	13.711515	11.656092
H	6.395986	14.361365	10.052751
H	3.998939	14.520728	12.934809
H	4.608861	16.187398	12.882749
H	2.981343	15.819129	12.276614
H	6.600197	19.643083	11.034096
H	7.452896	19.629494	8.683715

H	6.214587	20.813481	8.226491
H	7.481923	21.264183	9.380602
H	4.424120	21.517367	9.960829
H	4.446153	20.794994	11.579556
H	5.709196	21.950272	11.101907
H	0.318013	11.799049	2.321210
H	-0.828959	13.115081	2.630469
H	0.004977	13.012781	1.072125
H	2.012777	15.860239	0.319992
H	3.258837	14.606576	0.183281
H	1.551612	14.188689	-0.031891
H	1.574574	12.747132	5.814966
H	0.102116	13.704519	5.544745
H	0.367028	12.194954	4.622694
H	4.189940	16.670282	3.486624
H	4.939461	15.475295	2.402178
H	3.721156	16.618370	1.766710
H	3.950911	14.406514	10.492793
H	1.745472	17.059214	7.243689

8_Te'

Te	-0.808214	13.672194	9.591824
Al	3.083769	15.183659	7.927218
O	2.092518	13.892682	8.839423
O	1.012938	15.689714	8.262818
O	2.550603	15.127356	6.167305
O	4.319793	15.505526	4.816658
N	6.080904	14.507940	7.528774
N	4.970615	12.688380	7.725686
N	1.211158	13.822926	4.058652
N	2.700196	14.528191	2.634556
C	7.017671	13.483492	7.563461
C	8.478458	13.732816	7.469486
C	6.311328	12.323685	7.690885
C	6.760703	10.910899	7.780168
C	3.894127	11.704106	7.812139
C	6.461528	15.902720	7.326592
C	3.667263	18.093668	8.431099
C	3.760840	19.066842	6.086002
C	1.648458	19.254656	7.458414
C	4.255731	19.161550	9.112657
C	4.965066	18.966371	10.297643
C	5.998125	14.824593	11.200998
C	3.604488	15.114733	11.965176
C	5.606384	20.128449	11.030318
C	6.661235	20.828954	10.163357
C	4.554362	21.131904	11.522654
C	3.185144	15.098131	5.043995
C	2.375172	14.502234	3.944496
C	-0.444668	12.635223	2.574397
C	1.739631	13.857909	1.908383
C	1.798341	13.703105	0.433512
C	0.477449	13.533469	5.301775
C	0.799080	13.410921	2.808485
C	3.875923	15.183034	2.047115
C	4.812703	14.035336	7.643833
C	4.483689	16.583357	10.127445
C	5.055865	17.669889	10.797779
C	4.575113	15.209784	10.779131
C	2.888952	18.401071	7.159261
C	0.953525	14.552532	8.806698
C	3.784841	16.769894	8.913216
H	5.584137	17.510965	11.736730
H	4.157639	20.169800	8.713759
H	8.749778	14.184292	6.507952
H	8.818667	14.410101	8.261413
H	9.025590	12.793290	7.566949
H	6.373603	10.425569	8.683210
H	6.424674	10.323697	6.917346
H	7.851059	10.867022	7.812542
H	4.070637	10.909288	7.082135
H	3.852430	11.268506	8.815845
H	2.945078	12.191804	7.602326
H	6.995558	16.283189	8.203931
H	7.103617	15.979453	6.444351
H	5.565888	16.499038	7.171923
H	4.102255	20.056191	6.411257
H	4.645154	18.460583	5.860845
H	3.191219	19.197653	5.158284
H	1.016170	18.771811	8.210538
H	1.934497	20.243040	7.836785
H	1.053249	19.400833	6.549329
H	6.368195	15.465087	12.009072
H	6.016375	13.790822	11.564844
H	6.695625	14.903342	10.359492
H	3.619116	14.107787	12.398544
H	3.882238	15.829606	12.748798
H	2.579833	15.337237	11.647368
H	6.115750	19.714046	11.911673
H	7.420129	20.119417	9.816527
H	6.199295	21.289170	9.282246
H	7.162635	21.620758	10.731623
H	4.033803	21.595978	10.677070
H	3.805612	20.639082	12.151771
H	5.026359	21.929976	12.107160
H	-0.416223	11.668308	3.088387
H	-1.326654	13.181774	2.924939
H	-0.566415	12.446852	1.507219
H	1.733163	14.671963	-0.074036
H	2.728013	13.215813	0.121070
H	0.964006	13.088949	0.093268
H	1.126858	13.009695	6.004335
H	0.132611	14.461548	5.759395
H	-0.373742	12.902552	5.052456
H	3.977146	16.188040	2.455186
H	4.776010	14.609864	2.278959
H	3.732881	15.231524	0.968491
H	4.250500	14.461925	10.044934
H	2.532616	17.449776	6.747927

CO_2

C	-6.023302	2.861901	0.000000
O	-7.184459	2.795923	-0.000000
O	-4.862129	2.927617	-0.000000

Cartesian coordinates (Å) of the optimized geometries at the r^{2}SCAN-3c level of theory

2_Te

Te	2.919373	5.775402	0.563621
Al	4.348655	5.391355	-1.609168
N	5.711551	8.190381	-2.073488
N	3.841363	8.023918	-3.130985
C	4.650808	7.365481	-2.258024
C	6.672291	7.975307	-0.970698
H	6.472811	6.948623	-0.638922
C	8.128034	8.011871	-1.417977
H	8.501174	9.024703	-1.592075
H	8.737645	7.558922	-0.629801
H	8.268435	7.413632	-2.323835
C	6.337551	8.917528	0.181134
H	5.310940	8.743677	0.519033
H	7.009772	8.720582	1.017899
H	6.447433	9.970689	-0.095751
C	5.585665	9.346162	-2.838785
C	4.400054	9.241567	-3.507354
C	2.467613	7.563656	-3.423357
H	2.446864	6.549558	-3.020140
C	2.170852	7.445722	-4.914060
H	2.995093	6.947879	-5.433085
H	1.282749	6.818351	-5.037587
H	1.968040	8.412508	-5.382913

C	1.448800	8.401971	-2.655118
H	1.427259	9.441693	-2.995003
H	0.450279	7.980702	-2.808600
H	1.669246	8.385724	-1.582921
C	3.824686	10.165827	-4.523088
H	3.885093	9.742626	-5.532032
H	2.777265	10.406804	-4.325591
H	4.381523	11.104815	-4.523526
C	6.623650	10.407096	-2.956818
H	6.227624	11.246041	-3.532203
H	6.943598	10.795435	-1.986620
H	7.513487	10.037370	-3.478444
C	3.742281	4.570417	-3.364398
C	2.472539	4.003354	-3.644288
C	2.089718	3.724705	-4.957610
H	1.097625	3.321605	-5.147117
C	2.947243	3.926973	-6.036183
C	2.508398	3.633999	-7.456548
H	3.373412	3.823214	-8.108255
C	1.378568	4.578231	-7.890067
H	1.679035	5.625536	-7.779745
H	1.103767	4.404794	-8.936874
H	0.483747	4.420160	-7.277027
C	2.095544	2.168339	-7.639082
H	1.212659	1.930376	-7.035290
H	1.848220	1.963034	-8.686865
H	2.901356	1.493320	-7.334098
C	4.221595	4.404307	-5.762940
H	4.920479	4.525913	-6.589364
C	4.620586	4.735650	-4.463699
C	6.054377	5.220023	-4.287871
H	6.194654	5.520846	-3.241388
C	7.045803	4.075704	-4.537154
H	6.994855	3.732630	-5.577053
H	8.072200	4.403485	-4.334318
H	6.823534	3.226265	-3.884111
C	6.389873	6.438132	-5.156835
H	5.672751	7.250466	-4.998937
H	7.391576	6.813754	-4.916028
H	6.382687	6.185214	-6.222895
C	1.477389	3.667088	-2.536752
H	2.049972	3.600877	-1.601537
C	0.778570	2.319636	-2.773565
H	0.025497	2.390398	-3.566287
H	1.490461	1.539512	-3.062181
H	0.252052	1.999107	-1.866939
C	0.415144	4.756945	-2.341577
H	-0.330354	4.438345	-1.603345
H	0.855024	5.683941	-1.965507
H	-0.102522	4.964583	-3.286704
Te	6.446566	4.157563	-0.563789
Al	5.017369	4.541672	1.609112
N	3.654161	1.742821	2.073732
N	5.524428	1.909065	3.131123
C	4.715056	2.567579	2.258158
C	2.693413	1.957845	0.970926
H	2.893157	2.984376	0.638833
C	1.237696	1.921839	1.418319
H	0.864305	0.909174	1.592845
H	0.628133	2.374643	0.630023
H	1.097532	2.520474	2.323953
C	3.027780	1.015197	-0.180664
H	4.054508	1.188439	-0.518489
H	2.355777	1.212393	-1.017555
H	2.917256	-0.037853	0.096377
C	3.779879	0.587108	2.839161
C	4.965526	0.691576	3.507687
C	6.898171	2.369253	3.423622
H	6.918838	3.383533	3.020871
C	7.194932	2.486541	4.914394
H	6.370762	2.984277	5.433636
H	8.083119	3.113748	5.038203
H	7.397621	1.519538	5.382860
C	7.917052	1.531389	2.654958
H	7.938725	0.491515	2.994343
H	8.915538	1.952689	2.808581
H	7.696558	1.548097	1.582776
C	5.540673	-0.232612	4.523621
H	5.479899	0.190562	5.532560
H	6.588178	-0.473451	4.326460
H	4.983966	-1.171679	4.523860
C	2.741662	-0.473568	2.957470
H	3.137504	-1.312450	3.533073
H	2.421602	-0.862082	1.987378
H	1.851926	-0.103506	3.479028
C	5.623885	5.362553	3.364217
C	6.893732	5.929427	3.644128
C	7.276565	6.207882	4.957464
H	8.268665	6.610945	5.147041
C	6.418979	6.005716	6.036001
C	6.857834	6.299085	7.456258
H	5.993458	6.108091	8.108292
C	7.989689	5.357078	7.889227
H	7.691317	4.309180	7.778730
H	8.264362	5.530817	8.936012
H	8.884104	5.517045	7.276091
C	7.267826	7.765592	7.638697
H	8.149567	8.005409	7.033954
H	7.515795	7.971252	8.686261
H	6.460311	8.438983	7.334616
C	5.144508	5.528744	5.762731
H	4.445595	5.407223	6.589143
C	4.745499	5.197520	4.463465
C	3.311625	4.713425	4.287548
H	3.171344	4.412622	3.241060
C	2.320420	5.857955	4.536736
H	2.371306	6.201011	5.576643
H	1.293973	5.530399	4.333781
H	2.542955	6.707356	3.883716
C	2.975819	3.495390	5.156501
H	3.692713	2.682862	4.998589
H	1.974015	3.120039	4.915689
H	2.983094	3.748312	6.222560
C	7.888862	6.266060	2.536696
H	7.316239	6.333083	1.601563
C	8.588207	7.613080	2.774386
H	9.341412	7.541436	3.566911
H	7.876673	8.393255	3.063730
H	9.114677	7.934084	1.867903
C	8.950753	5.175995	2.340685
H	9.696468	5.495021	1.602859
H	8.510600	4.249510	1.963684
H	9.468194	4.967301	3.285702

2_Se

Se	3.045888	5.621538	0.514159
Al	4.364778	5.366096	-1.469577
N	5.696966	8.173418	-1.964767
N	3.837812	7.990645	-3.035083
C	4.638676	7.344678	-2.145192
C	6.656063	7.965803	-0.860293
H	6.462644	6.937505	-0.531715
C	8.112285	8.011910	-1.307205
H	8.483950	9.027665	-1.466878
H	8.723889	7.548795	-0.527015
H	8.252476	7.427546	-2.222027
C	6.310483	8.908584	0.288495
H	5.289181	8.717270	0.632877
H	6.990534	8.733801	1.123677
H	6.395696	9.961510	0.001930
C	5.576854	9.319754	-2.744112
C	4.396812	9.205064	-3.420847
C	2.468603	7.524606	-3.336939
H	2.454412	6.504367	-2.950721
C	2.174266	7.425524	-4.829901
H	3.006135	6.948823	-5.356809
H	1.296654	6.785656	-4.963183
H	1.955056	8.395092	-5.285108
C	1.445793	8.347586	-2.557867
H	1.432773	9.395588	-2.872674
H	0.446597	7.934811	-2.728112
H	1.659167	8.304082	-1.484943
C	3.822888	10.124044	-4.442206
H	3.884523	9.697625	-5.449566

H	2.775013	10.365108	-4.246285
H	4.379253	11.063343	-4.445178
C	6.612307	10.383149	-2.863152
H	6.217405	11.216580	-3.447316
H	6.924324	10.779633	-1.893580
H	7.507020	10.013101	-3.376082
C	3.750123	4.538872	-3.218903
C	2.475445	3.986799	-3.512248
C	2.104979	3.708489	-4.829387
H	1.111511	3.315178	-5.030612
C	2.977208	3.896500	-5.898973
C	2.551925	3.597955	-7.322308
H	3.424665	3.779395	-7.965884
C	1.430962	4.544125	-7.774030
H	1.735237	5.590809	-7.668496
H	1.165800	4.364258	-8.822256
H	0.529253	4.394826	-7.168969
C	2.134508	2.132929	-7.500410
H	1.244589	1.902657	-6.903949
H	1.896823	1.922217	-8.549376
H	2.934251	1.456358	-7.183105
C	4.252241	4.363690	-5.613788
H	4.961087	4.476294	-6.432904
C	4.638975	4.695597	-4.310794
C	6.073076	5.174572	-4.121371
H	6.198205	5.505669	-3.083001
C	7.058797	4.015163	-4.315911
H	7.013348	3.630241	-5.341489
H	8.085654	4.344101	-4.117389
H	6.824457	3.197271	-3.628093
C	6.434618	6.365516	-5.017603
H	5.718149	7.185602	-4.899252
H	7.432134	6.743495	-4.763463
H	6.452361	6.084345	-6.076358
C	1.460226	3.668163	-2.415859
H	2.028341	3.539416	-1.485763
C	0.680008	2.374755	-2.699200
H	-0.089996	2.529970	-3.463366
H	1.333704	1.569314	-3.049435
H	0.159761	2.037056	-1.795555
C	0.459477	4.806999	-2.173015
H	-0.315776	4.488451	-1.465852
H	0.943582	5.682921	-1.735125
H	-0.031340	5.095627	-3.111321
Se	6.319879	4.313703	-0.513176
Al	5.000549	4.568495	1.470401
N	3.669739	1.760083	1.963716
N	5.529488	1.942938	3.032962
C	4.727545	2.589370	2.144419
C	2.709549	1.968538	0.860362
H	2.901499	2.997668	0.533492
C	1.253668	1.919670	1.308164
H	0.883142	0.903055	1.464973
H	0.641061	2.384501	0.529790
H	1.113432	2.501051	2.224872
C	3.055508	1.028222	-0.290362
H	4.076124	1.221852	-0.635500
H	2.374225	1.203043	-1.124534
H	2.972545	-0.025278	-0.005228
C	3.791293	0.612846	2.741509
C	4.971701	0.727599	3.417592
C	6.898342	2.410005	3.334821
H	6.911414	3.430598	2.949456
C	7.192882	2.508046	4.827807
H	6.360579	2.983357	5.355295
H	8.069843	3.148709	4.961569
H	7.413153	1.538268	5.282068
C	7.921792	1.588830	2.554688
H	7.936035	0.540521	2.868420
H	8.920595	2.002498	2.725094
H	7.708098	1.633213	1.481862
C	5.547014	-0.192177	4.437457
H	5.485219	0.232764	5.445437
H	6.595102	-0.431718	4.240856
H	4.991728	-1.132120	4.439301
C	2.756828	-0.451604	2.859688
H	3.152763	-1.285512	3.442470
H	2.444639	-0.846980	1.889714
H	1.862052	-0.083039	3.373571
C	5.614540	5.394775	3.220373
C	6.888857	5.947455	3.514033
C	7.259386	6.224770	4.831357
H	8.252648	6.618501	5.032771
C	6.387439	6.035245	5.900898
C	6.812747	6.332749	7.324450
H	5.940074	6.150646	7.967933
C	7.933892	5.386390	7.775338
H	7.629731	4.339748	7.669078
H	8.199181	5.565523	8.823656
H	8.835490	5.536241	7.170246
C	7.229930	7.797690	7.503750
H	8.119897	8.028592	6.907603
H	7.467452	8.007600	8.552914
H	6.430123	8.474396	7.186894
C	5.112632	5.567572	5.615469
H	4.403952	5.453920	6.434585
C	4.725903	5.236577	4.312243
C	3.291998	4.757078	4.122573
H	3.166808	4.427209	3.083811
C	2.305720	5.915761	4.318636
H	2.351182	6.299616	5.344612
H	1.278986	5.586508	4.119997
H	2.539493	6.734521	3.631655
C	2.931384	3.564942	5.017558
H	3.648143	2.745308	4.897869
H	1.933864	3.186865	4.763599
H	2.914165	3.844915	6.076635
C	7.903570	6.268028	2.417737
H	7.335244	6.396169	1.487673
C	8.681504	7.562701	2.701547
H	9.451152	7.408860	3.466340
H	8.026141	8.367059	3.051156
H	9.201938	7.901138	1.798274
C	8.906193	5.130907	2.174654
H	9.681205	5.450992	1.467921
H	8.423595	4.254436	1.736186
H	9.397174	4.842586	3.112960

3_Te

Te	3.736394	7.192414	7.061545
Al	2.044019	5.553107	8.190989
N	-0.515302	6.322604	6.509742
N	-0.885971	4.820071	7.989832
C	2.511543	3.603392	8.018786
C	2.230325	2.967958	6.782516
C	2.300715	1.580809	6.655278
H	2.077006	1.122408	5.693436
C	2.664940	0.767639	7.726450
C	3.012690	1.388880	8.920039
H	3.341234	0.768093	9.752543
C	2.959850	2.778358	9.072985
C	1.930203	3.773681	5.524498
H	1.884025	4.835341	5.801508
C	3.084281	3.651355	4.519813
H	4.028281	3.952399	4.984448
H	2.908421	4.294340	3.649348
H	3.191561	2.619746	4.165714
C	0.590889	3.404110	4.876340
H	-0.235564	3.492201	5.589919
H	0.600675	2.373851	4.503553
H	0.382059	4.058811	4.021351
C	2.722815	-0.740181	7.585566
H	3.012164	-1.145871	8.565526
C	3.788314	-1.168375	6.567574
H	3.867728	-2.260670	6.523366
H	4.768568	-0.758880	6.831028
H	3.535229	-0.809413	5.563626
C	1.353164	-1.327183	7.221603
H	0.593990	-1.034033	7.953882
H	1.396428	-2.421790	7.186330
H	1.024281	-0.973713	6.237759
C	3.433130	3.362716	10.395197
H	3.381626	4.455198	10.306770
C	4.895024	2.988228	10.673704

H	5.235293	3.446572	11.610173
H	5.545124	3.327674	9.860239
H	5.022602	1.905018	10.777309
C	2.530518	2.963090	11.567051
H	2.867722	3.439734	12.495171
H	2.532910	1.877460	11.720233
H	1.498353	3.283014	11.390368
C	0.106686	5.578457	7.456170
C	-1.877084	6.046447	6.454219
C	-2.114443	5.097641	7.402461
C	0.144587	7.243366	5.593931
H	1.178166	7.393878	5.921438
H	-0.375830	8.205085	5.594718
H	0.144085	6.832460	4.577632
C	-2.788507	6.723155	5.496856
H	-2.830544	7.804662	5.672623
H	-3.801661	6.329454	5.598409
H	-2.472029	6.567505	4.458847
C	-3.373685	4.424912	7.812876
H	-3.571190	4.557629	8.882654
H	-3.346984	3.347896	7.608447
H	-4.218306	4.845495	7.263683
C	-0.714541	3.901776	9.110276
H	-0.907922	4.418003	10.057796
H	0.309060	3.520589	9.106704
H	-1.399971	3.058512	8.997845
Te	1.468907	6.764155	10.475918
Al	3.153619	8.406410	9.342236
N	5.733742	7.649256	10.992427
N	6.075739	9.175640	9.529955
C	2.670412	10.350999	9.519260
C	2.961012	10.990915	10.750936
C	2.882248	12.377811	10.875481
H	3.113710	12.840378	11.833497
C	2.499577	13.185531	9.806444
C	2.140443	12.558791	8.619021
H	1.796097	13.175028	7.789509
C	2.201543	11.169294	8.469237
C	3.278371	10.189054	12.007190
H	3.330598	9.127429	11.730796
C	2.131159	10.303830	13.020638
H	1.185880	9.995519	12.563413
H	2.318231	9.663093	13.890417
H	2.019054	11.335045	13.374436
C	4.619814	10.569241	12.644590
H	5.440914	10.488733	11.924021
H	4.604522	11.598965	13.018745
H	4.841449	9.915000	13.496700
C	2.433340	14.693289	9.944142
H	2.130812	15.094531	8.966328
C	1.375860	15.117114	10.972298
H	1.290779	16.209020	11.015700
H	0.395282	14.701836	10.719263
H	1.640905	14.760995	11.974166
C	3.802890	15.290238	10.291871
H	4.556063	15.000042	9.552240
H	3.752826	16.384632	10.324618
H	4.144795	14.941732	11.273068
C	1.712399	10.575807	7.156923
H	1.775996	9.483978	7.248217
C	0.242067	10.935525	6.904106
H	-0.111707	10.472563	5.975013
H	-0.389399	10.591310	7.730041
H	0.102960	12.017365	6.801106
C	2.591017	10.980113	5.968717
H	2.242644	10.497494	5.047745
H	2.575775	12.065123	5.811999
H	3.628967	10.670282	6.129055
C	5.096119	8.398609	10.061054
C	7.092842	7.939738	11.041008
C	7.311882	8.904065	10.104148
C	5.092754	6.698270	11.890448
H	4.053666	6.555930	11.576966
H	5.614602	5.738002	11.848817
H	5.110893	7.076265	12.919184
C	8.019188	7.260218	11.981885
H	8.070018	6.181420	11.792473
H	9.027577	7.664955	11.876326
H	7.710496	7.399960	13.024486
C	8.559717	9.598035	9.694348
H	8.751805	9.481882	8.621652
H	8.520505	10.671869	9.913038
H	9.413266	9.181236	10.232524
C	5.887076	10.103436	8.420218
H	6.090447	9.601697	7.466993
H	4.856652	10.465455	8.427751
H	6.556636	10.958167	8.542007

3_Se

N	6.078284	-0.487166	6.535789
N	7.091493	-0.904323	8.375495
Al	6.400593	2.039928	8.396128
Se	5.070432	3.495666	7.067802
C	8.335826	2.513900	8.667192
C	8.880185	2.992911	9.881084
C	10.260168	3.008015	10.091752
H	10.649042	3.360689	11.045460
C	11.155240	2.596510	9.107220
C	10.632366	2.217256	7.875459
H	11.323769	1.954563	7.075719
C	9.254610	2.181165	7.643936
C	7.988361	3.561351	10.975282
H	6.956491	3.522225	10.605231
C	8.331088	5.033197	11.243664
H	8.230033	5.627661	10.329618
H	9.357912	5.148312	11.608402
H	7.666426	5.454169	12.008019
C	8.041076	2.734210	12.263115
H	7.747575	1.697746	12.068339
H	7.350167	3.137496	13.013739
H	9.048459	2.734380	12.696248
C	12.651163	2.604879	9.350272
H	13.130305	2.225049	8.436501
C	13.173098	4.026796	9.595523
H	12.905482	4.690234	8.767061
H	14.263873	4.027768	9.703625
H	12.744899	4.447546	10.512422
C	13.039189	1.673771	10.506139
H	12.679111	0.655501	10.327145
H	12.604998	2.020940	11.450471
H	14.127650	1.640130	10.630218
C	8.783436	1.870096	6.229507
H	7.686032	1.842900	6.238710
C	9.169082	3.008434	5.274322
H	10.257922	3.104392	5.195451
H	8.767522	3.960462	5.634622
H	8.769520	2.822577	4.270257
C	9.284720	0.518246	5.708547
H	8.849445	0.295248	4.726554
H	9.025144	-0.295280	6.394513
H	10.373699	0.518386	5.588764
C	6.539226	0.108640	7.662002
C	6.329042	-1.855057	6.542475
C	6.965036	-2.122091	7.717917
C	5.496931	0.211404	5.395630
H	6.211013	0.236192	4.563957
H	5.249206	1.234814	5.694781
H	4.585872	-0.298782	5.071994
C	5.930529	-2.743444	5.421246
H	4.842956	-2.756332	5.281382
H	6.253045	-3.767496	5.619079
H	6.383667	-2.427512	4.474234
C	7.465534	-3.400365	8.285520
H	7.199557	-4.231229	7.629091
H	7.030997	-3.600889	9.271474
H	8.556638	-3.398944	8.394816
C	7.677348	-0.749301	9.703311
H	8.082031	0.261277	9.798215
H	8.494481	-1.464114	9.826193
H	6.917006	-0.907844	10.475831
N	3.910483	5.523456	10.775822
N	2.896489	5.939715	8.936349
Al	3.588594	2.995823	8.916061
Se	4.918825	1.540305	10.244543

C	1.653508	2.521382	8.644889
C	1.109462	2.041968	7.431061
C	-0.270495	2.026413	7.220197
H	-0.659134	1.673455	6.266506
C	-1.165836	2.437826	8.204528
C	-0.643230	2.817514	9.436262
H	-1.334813	3.080214	10.235845
C	0.734495	2.854103	9.667927
C	2.001645	1.473590	6.337131
H	3.033406	1.512927	6.707461
C	1.659289	0.001633	6.068709
H	1.760178	-0.592796	6.982806
H	0.632627	-0.113749	5.703624
H	2.324306	-0.419217	5.304590
C	1.949214	2.300677	5.049251
H	2.242620	3.337172	5.244019
H	2.640328	1.897391	4.298818
H	0.941934	2.300414	4.615908
C	-2.661728	2.428881	7.961285
H	-3.141121	2.808841	8.874867
C	-3.183133	1.006703	7.716422
H	-2.915456	0.343638	8.545165
H	-4.273886	1.005322	7.608105
H	-2.754609	0.585784	6.799756
C	-3.049924	3.359485	6.805068
H	-2.690188	4.377929	6.983760
H	-2.615529	3.012144	5.860897
H	-4.138383	3.392741	6.680862
C	1.205401	3.165785	11.082325
H	2.302804	3.193195	11.073289
C	0.819843	2.027755	12.037904
H	-0.268992	1.931611	12.116635
H	1.221660	1.075669	11.678050
H	1.219203	2.214096	13.041957
C	0.703757	4.517738	11.602680
H	1.138911	4.741241	12.584611
H	0.963204	5.331027	10.916388
H	-0.385232	4.517392	11.722381
C	3.449442	4.927159	9.649892
C	3.659044	6.891231	10.768892
C	3.022625	7.157699	9.593561
C	4.492843	4.825569	11.915866
H	3.779446	4.801244	12.748147
H	4.740341	3.801997	11.617085
H	5.404171	5.335944	12.238470
C	4.057576	7.780080	11.889754
H	5.145164	7.793258	12.029409
H	3.734784	8.803999	11.691676
H	3.604697	7.464323	12.836949
C	2.521486	8.435633	9.025756
H	2.787379	9.266768	9.681876
H	2.955630	8.636061	8.039609
H	1.430347	8.433782	8.916814
C	2.310194	5.784042	7.608784
H	1.905621	4.773350	7.514505
H	1.492899	6.498659	7.485868
H	3.070217	5.942348	6.835903

5_Te

Te	10.439578	11.831804	13.434719
Al	8.897018	12.105736	11.461869
N	8.300908	9.186233	11.213258
N	6.437192	10.087249	11.769675
N	7.131609	13.934999	13.223747
N	7.763637	14.998601	11.471821
C	9.333562	12.233827	9.464212
C	10.661317	12.333759	8.968788
C	10.913021	12.361816	7.593872
H	11.937744	12.441657	7.239045
C	9.892660	12.288568	6.652016
C	8.588255	12.187651	7.121959
H	7.770625	12.125932	6.405821
C	8.303837	12.164997	8.489552
C	11.836889	12.469433	9.921350
H	11.587061	11.917557	10.838393
C	13.159313	11.907140	9.394543
H	13.596033	12.531591	8.605646
H	13.037439	10.893078	8.997551
H	13.884600	11.865747	10.214010
C	12.011512	13.935385	10.340460
H	12.189143	14.572220	9.463645
H	12.854478	14.037185	11.032807
H	11.121737	14.294250	10.868113
C	10.198468	12.316736	5.168100
H	11.287722	12.421687	5.065410
C	9.543710	13.520971	4.478934
H	9.828492	13.565933	3.421493
H	9.844099	14.458014	4.958608
H	8.450863	13.453904	4.528338
C	9.786674	11.006288	4.484101
H	10.072322	11.013354	3.425959
H	8.701448	10.862060	4.537657
H	10.262839	10.146595	4.966106
C	6.832537	12.058909	8.873557
H	6.770243	12.167936	9.961374
C	5.970661	13.176415	8.270289
H	5.918498	13.102479	7.178917
H	6.372967	14.163657	8.516372
H	4.944814	13.119249	8.654383
C	6.261868	10.684232	8.497868
H	6.253172	10.556778	7.409542
H	5.229217	10.570359	8.852366
H	6.865157	9.875185	8.921478
C	7.731346	10.390808	11.478563
C	7.389262	8.146285	11.344795
C	6.202896	8.716972	11.696665
C	9.710217	9.031249	10.855450
H	9.973477	7.972949	10.864759
H	10.318388	9.574415	11.596312
H	9.893419	9.450770	9.860184
C	7.744421	6.720310	11.126644
H	8.135350	6.550394	10.116919
H	6.859642	6.092620	11.250432
H	8.499623	6.375871	11.842479
C	4.869936	8.120902	11.969065
H	4.106090	8.493327	11.275449
H	4.527756	8.337266	12.988269
H	4.913700	7.035689	11.859738
C	5.380023	11.056893	11.999298
H	5.807875	12.058946	11.972410
H	4.907477	10.892436	12.973626
H	4.616518	10.980554	11.216642
C	7.757815	13.753499	12.025805
C	6.780590	15.262622	13.424819
C	7.183696	15.940419	12.314677
C	6.987416	12.921274	14.261649
H	5.927921	12.768119	14.499102
H	7.529542	13.236851	15.158401
H	7.466135	11.995944	13.931455
C	6.112135	15.732061	14.665057
H	5.897024	16.800149	14.596608
H	6.743706	15.573191	15.546840
H	5.163979	15.209892	14.839025
C	7.088786	17.379667	11.960089
H	8.077426	17.813550	11.771242
H	6.631606	17.939133	12.778444
H	6.479290	17.541379	11.062928
C	8.404051	15.366031	10.214209
H	8.716573	14.459454	9.693142
H	9.287648	15.983949	10.408476
H	7.706209	15.928404	9.586111

6_Te

Te	-1.319476	13.300260	8.643330
Al	2.505935	15.250180	7.898800
O	1.660957	13.693810	8.457982
O	4.169057	14.311899	7.577245
O	4.089134	12.775363	5.904024
O	0.614770	15.564939	8.145118
O	2.290234	15.455580	6.060573
O	4.128589	15.723903	4.767169
N	6.926809	14.600232	7.016754
N	6.975104	12.457355	6.682717
N	1.259477	13.667327	4.097729

N	2.656071	14.482623	2.639126
C	4.647057	13.509506	6.719080
C	8.255219	14.211428	7.092213
C	9.353327	15.174995	7.356498
C	8.286826	12.857501	6.889308
C	9.417352	11.895462	6.877841
C	6.545982	11.070502	6.500573
C	6.449984	15.986389	7.159236
C	3.583769	17.972952	8.474746
C	3.351012	18.942226	6.139281
C	1.761227	19.638365	7.981233
C	4.535593	18.848839	9.004738
C	5.390408	18.456758	10.032709
C	5.535343	14.128728	10.689792
C	3.594699	15.002360	12.051575
C	6.447233	19.395820	10.579470
C	7.528575	19.675040	9.525760
C	5.847115	20.705764	11.103942
C	2.997242	15.300102	5.005630
C	2.301930	14.508031	3.944176
C	-0.150639	12.115653	2.701042
C	1.828496	13.611085	1.956921
C	1.947222	13.356919	0.497792
C	0.570340	13.343638	5.362496
C	0.950840	13.096841	2.878154
C	3.735684	15.260795	2.029176
C	6.159568	13.522686	6.779415
C	4.325099	16.266104	10.007120
C	5.247304	17.169237	10.545276
C	4.204474	14.890112	10.646860
C	2.625548	18.502635	7.417006
C	0.491443	14.308446	8.424353
C	3.494222	16.640494	8.928225
H	5.876060	16.870597	11.383698
H	4.603052	19.863125	8.614736
H	9.485191	15.880165	6.527879
H	9.158397	15.755835	8.264277
H	10.295315	14.641071	7.492744
H	9.280610	11.104745	7.624196
H	9.531418	11.414969	5.899235
H	10.351488	12.410973	7.105630
H	7.123410	10.616501	5.690876
H	6.708297	10.507690	7.425094
H	5.487853	11.071071	6.239202
H	6.184946	16.191534	8.201816
H	7.247420	16.655215	6.830749
H	5.569092	16.129215	6.532984
H	4.015673	19.792349	6.334793
H	3.950078	18.123165	5.728280
H	2.628461	19.254732	5.375541
H	1.229237	19.307653	8.878314
H	2.371735	20.508850	8.248361
H	1.019844	19.960005	7.240930
H	6.268673	14.632975	11.329861
H	5.385175	13.119074	11.089538
H	5.963763	14.037709	9.684879
H	3.437769	14.008176	12.485142
H	4.250794	15.569774	12.722196
H	2.628346	15.513950	12.010382
H	6.928590	18.885018	11.425910
H	7.974730	18.739404	9.169251
H	7.100508	20.192749	8.659657
H	8.326786	20.304802	9.936077
H	5.391277	21.283296	10.292294
H	5.071298	20.508450	11.849998
H	6.621288	21.330782	11.563711
H	0.028605	11.200149	3.275045
H	-1.111519	12.530299	3.023215
H	-0.239986	11.840851	1.648857
H	1.729493	14.253793	-0.093893
H	2.949757	13.007152	0.227668
H	1.236436	12.585509	0.198346
H	1.299225	13.018608	6.107039
H	0.032325	14.214848	5.742556
H	-0.137879	12.539554	5.174922
H	3.728869	16.275838	2.424831
H	4.703712	14.810512	2.262670
H	3.578638	15.278183	0.949847
H	3.505244	14.292697	10.049243
H	1.938650	17.690807	7.150624

5 References

[S1] M. Muhr, P. Heiß, M. Schütz, R. Bühler, C. Gemel, M. H. Linden, H. B. Linden, R. A. Fischer, *Dalton Trans.* **2021**, *50*, 9031-9036.

[S2] D. Franz, T. Szilvasi, E. Irran, S. Inoue, *Nat. Commun.* **2015**, *6*, 10037.

[S3] N. Kuhn, T. Kratz, *Synthesis*, **1993**, 561-562.

[S4] C. Weetman, A. Porzelt, P. Bag, F. Hanusch, S. Inoue, *Chem. Sci.* **2020**, *11*, 4817-4827.

[S5] V. Lavallo, Y. Canac, C. Präsang, B. Donnadieu, G. Bertrand, *Angew. Chem. Int. Ed.* **2005**, *44*, 5705-5709.

[S6] L. Jafarpour, E. D. Stevens, S. P. Nolan, *J. Organomet. Chem.* **2000**, *606*, 49-54.

[S7] S. Yao, Y. Xiong, M. Driess, *Chem. Eur. J.* **2010**, *16*, 1281-1288.

[S8] B. R. Van Ausdall, J. L. Glass, K. M. Wiggins, A. M. Aarif, and J. Louie, *J. Org. Chem.* **2009**, *74*, 7935–7942.

[S9] APEX suite of crystallographic software, APEX 3 version 2015.5-2; Bruker AXS Inc.: Madison, Wisconsin, USA, **2015**.

[S10] SAINT, Version 7.56a and SADABS Version 2008/1; Bruker AXS Inc.: Madison, Wisconsin, USA, **2008**.

[S11] G. M. Sheldrick, SHELXL-2014, University of Göttingen, Göttingen, Germany, **2014**.

[S12] C. B. Hübschle, G. M. Sheldrick, B. Dittrich, *J. Appl. Cryst.* **2011**, *44*, 1281-1284.

[S13] G. M. Sheldrick, SHELXL-97, University of Göttingen, Göttingen, Germany, **1998**.

[S14] Wilson, A. J. C. International Tables for Crystallography, Vol. C, Tables 6.1.1.4 (pp. 500-502), 4.2.6.8 (pp. 219-222), and 4.2.4.2 (pp. 193-199); Kluwer Academic Publishers: Dordrecht, The Netherlands, **1992**.

[S15] C. F. Macrae, I. J. Bruno, J. A. Chisholm, P. R. Edgington, P. McCabe, E. Pidcock, L. Rodriguez-Monge, R. Taylor, J. van de Streek, P. A. Wood, *J. Appl. Cryst.* **2008**, *41*, 466-470.

[S16] Neese, F.; Wennmohs, F.; Becker, U.; Riplinger, C., The ORCA quantum chemistry program package. The Journal of Chemical Physics **2020**, 152, 224108.

[S17] S. Grimme, A. Hansen, S. Ehlert, and J.-M. Mewes, *J. Chem. Phys.* **2021**,154, 064103. DOI: 10.1063/5.0040021.

[S18] (a) Furness, J. W.; Kaplan, A. D.; Ning, J.; Perdew, J. P.; Sun, J., The Journal of Physical Chemistry Letters **2020**, 11, 8208-8215. (b) Furness, J. W.; Kaplan, A. D.; Ning, J.; Perdew, J. P.; Sun, J., The Journal of Physical Chemistry Letters **2020**, 11, 9248-9248. (c) Grimme, S.; Hansen, A.; Ehlert, S.; Mewes, J.-M., The Journal of Chemical Physics **2021**, 154, 064103. (d) Kruse, H.; Grimme, S., The Journal of Chemical Physics **2012**, 136, 154101. (e) Caldeweyher, E.; Bannwarth, C.; Grimme, S., The Journal of Chemical Physics 2017, 147, 034112.

[S19] Adamo, C.; Barone, V. J. Chem. Phys. **1999**, 110, 6158-6169.

[S20] (a) Grimme, S.; Ehrlich, S.; Goerigk, L. J. Comput. Chem. **2011**, 32, 1456-1465; (b) Grimme, S.; Antony, J.; Ehrlich, S.; Krieg, H. J. Chem. Phys., **2010** ,132, 154104.

[S21] Weigend, F.; Ahlrichs, R. Phys. Chem. Chem. Phys. **2005**, 7, 3297-3305.

[S22] Weigend, F. Phys. Chem. Chem. Phys. **2006**, 8, 1057-1065.

[S23] Glendening, E. D.; Badenhoop, J. K.; Reed, A. E.; Carpenter, J. E.; Bohmann, J. A.; Morales, C. M.; Karafiloglou, P.; Landis, C. R.; Weinhold, F. NBO 7.0, Theoretical Chemistry Institute, University of Winsconsin: Madison, **2018**.

9.3. Supporting Information for Chapter 6

Supporting Information

Dialumene-Mediated Production of Tertiary Phosphines through P_4 Reduction

H. Xu, M. M. D. Roy, A. Kostenko, S. Fujimori, S. Inoue*

Table of Contents

1. General considerations

All manipulations were carried out using standard Schlenk line or dry-box techniques under an atmosphere of argon. Glassware was heated under vacuum prior to use. Ground glass joints were coated with the PTFE-based grease Merkel Triboflon III. Benzene was distilled from potassium mirror and degassed prior to use. All other solvents were refluxed over sodium/benzophenone, distilled and degassed prior to use. Deuterated benzene (C_6D_6) and toluene (Tol-d_8) were purchased from Sigma Aldridge and stored over 4 Å molecular sieves prior to use. Acetyl chloride was purchased from Sigma Aldridge, distilled from PCl_5 and degassed prior to use. Me_3SiCl, Me_3SiI and Ph_3P were purchased from Sigma Aldridge and used as received. ($I^iPr_2Me_2$)AlH_3,[1] Na*Si*^{t}Bu_2Me,[2] [($I^iPr_2Me_2$)Al(Si^tBu_2Me)]$_2$,[3] [($I^iPr_2Me_2$)Al(Tipp)]$_2$[4] and P_4[5] were synthesized according to literature procedures. NMR samples were prepared under argon in NMR tubes fitted with J. Young Teflon valves. NMR spectra were recorded on Bruker AV400US, DRX4 or AV500cr at ambient temperature unless otherwise stated and referenced internally to residual protio-solvent (^{1}H) or solvent (^{13}C{^{1}H}) resonances and are reported relative to tetramethylsilane (δ = 0 ppm). ^{31}P{^{1}H} NMR spectra were referenced externally to an 85% solution of H_3PO_4 in H_2O (δ = 0 ppm). Elemental analyses were conducted with a EURO EA (HEKA tech) instrument equipped with a CHNS combustion analyzer.

2. Synthesis of novel compounds

2.1 Compound 3-Trans

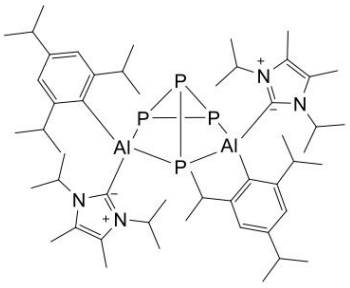

$C_{52}H_{86}Al_2N_4P_4$
945.15

Under exclusion of light, [(I*i*Pr$_2$Me$_2$)Al(Tipp)]$_2$ (0.2 g, 0.244 mmol) in 10 ml of toluene was added via dropping funnel over a period of 15 minutes to a THF and Toluene (1:1, 10 ml) solution of P_4 (0.036 g, 0.292 mmol, 1.2 eqv.) at -30 ^{o}C. The solution became brown immediately from black and the reaction was slowly warmed to room temperature over 2 hours. After that, volatiles were removed under reduced pressure and the obtained rude product was washed with mixing solvent of pentane and hexane (5:2, 10 ml X 3). After dried under reduced pressure, brown powders were obtained in high yields (0.150 g, 65%).

^{1}H NMR (400 MHz, C_6D_6) δ 7.26 (s, 2H, Tipp-H), 7.04 (s, 1H, Tipp-H), 6.96 (s, 1H, Tipp-H), 6.75 (m, *J* = 6.5 Hz, 1H, IM$_4$-N-C<u>H</u>), 5.96 – 5.64 (m, 1H, IM$_4$-N-C<u>H</u>), 4.93 (m, *J* = 6.7 Hz, 1H, Tipp-iso-C<u>H</u>), 4.69 (m, *J* = 6.6 Hz, 1H, IM$_4$-N-C<u>H</u>), 4.22 (s, 1H, IM$_4$-N-C<u>H</u>), 3.46 (m, *J* = 6.7 Hz, 1H, Tipp-iso-C<u>H</u>), 2.95 (m, *J* = 7.0 Hz, 2H, Tipp-iso-C<u>H</u>), 2.81 (m, *J* = 6.9 Hz, 2H, Tipp-iso-C<u>H</u>), 1.63 (d, *J* = 6.7 Hz, 3H, IM$_4$-C-C<u>H</u>$_3$), 1.61 (s, 3H, IM$_4$-C-C<u>H</u>$_3$), 1.57 (d, *J* = 6.7 Hz, 6H, Tipp-iso-C<u>H</u>$_3$), 1.47 (s, 6H, IM$_4$-C-C<u>H</u>$_3$), 1.43 (d, *J* = 6.6 Hz, 9H, IM$_4$-iso-C<u>H</u>$_3$), 1.36 (d, *J* = 6.9 Hz, 9H, Tipp-iso-C<u>H</u>$_3$), 1.34 – 1.28 (m, 12H, Tipp-iso-C<u>H</u>$_3$ and IMe$_4$-N-iso-C<u>H</u>$_3$), 1.26 (dd, *J* = 6.8, 3.9 Hz, 9H, Tipp-iso-C<u>H</u>$_3$), 1.14 (dd, *J* = 11.5, 6.8 Hz, 9H, Tipp-iso-C<u>H</u>$_3$), 1.01 (d, *J* = 6.9 Hz, 6H, IMe$_4$-N-iso-C<u>H</u>$_3$), 0.95 (d, *J* = 6.7 Hz, 3H, IMe$_4$-N-iso-C<u>H</u>$_3$), 0.90 (d, *J* = 6.6 Hz, 3H, Tipp-iso-C<u>H</u>$_3$), 0.79 (d, *J* = 6.6 Hz, 3H, Tipp-iso-C<u>H</u>$_3$).

$^{13}C\{^1H\}$ NMR (101 MHz, C_6D_6) δ 160.41 (IMe_4-C: according to HMBC), 158.12 (IMe_4-C:), 157.22 (Tipp-C-Al), 156.62 (Tipp-C-Al), 148.21 (Tipp-C), 147.66 (Tipp-C), 126.16 (IMe_4-C-CH_3), 125.75 (IMe_4-C-CH_3), 121.04 (Tipp-C), 120.64 (Tipp-C), 120.31 (Tipp-C), 53.17 (IMe_4-N-C-CH_3), 52.66 (IMe_4-N-C-CH_3), 37.79 (Tipp-iso-CH), 35.98 (Tipp-iso-CH), 34.99 (Tipp-iso-CH), 34.86 (Tipp-iso-CH), 27.70 (IMe_4-iso-CH_3), 26.58 (IMe_4-iso-CH_3), 26.49 (IMe_4-iso-CH_3), 25.56 (Tipp-iso-CH-CH_3), 25.46 (Tipp-iso-CH-CH_3), 24.74 (Tipp-iso-CH-CH_3), 24.65 (Tipp-iso-CH-CH_3), 24.59 (Tipp-iso-CH-CH_3), 24.56 (Tipp-iso-CH-CH_3), 24.43 (Tipp-iso-CH-CH_3), 21.98 (IMe_4-iso-CH_3), 21.78 (IMe_4-iso-CH_3), 21.35 (IMe_4-iso-CH_3), 21.21, 10.37 (IMe_4-C-CH_3), 9.89 (IMe_4-C-CH_3).

$^{31}P\{^1H\}$ NMR (162 MHz, Benzene-d_6) δ -52.69 (d, *J* = 101.7 Hz, P1), -128.78 (dd, *J* = 294.3, 169.5 Hz, P2), -138.74 (dd, *J* = 293.3, 162.9 Hz, P3), -147.82 (td, *J* = 165.9, 164.6, 101.4 Hz, P4).

$^{31}P\{^1H\}$ NMR (162 MHz, THF-d_8) δ -52.56 (d, J = 100.2 Hz, P1), -128.63 (dd, J = 294.3, 169.4 Hz, P2), -140.93 (dd, J = 294.4, 162.7 Hz, P3), -145.92 – -158.43 (m, P4).

2.2 Compound 3-Cis

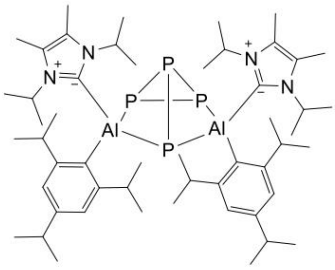

$C_{52}H_{86}Al_2N_4P_4$
944.54

Under exclusion of light, $[(I\textit{i}Pr)Al(Tipp)]_2$ (0.2 g, 0.244 mmol) in toluene (10 ml) was dropwisely added to a THF (5 ml) and Toluene (5 ml) solution of P_4 (0.036 g, 0.292 mmol, 1.2 eqv.) at -30 °C. The solution became brown immediately from black and was stirred over 2 hours at room temperature and then over further 2 hours at 80 °C. After that, volatiles were removed under

reduced pressure. The product was washed by pentane (3 X 10 ml) and then dried under reduced pressure. Finally, pale brown solids were obtained in high yields (0.150 g, 65%). X-ray quality crystals were obtained by the slow evaporation of a THF solution.

^{1}H NMR (500 MHz, Benzene-d_6) δ 7.02 (s, 2H, Tipp-*H*), 7.01 (s, 2H, Tipp-*H*), 6.82 – 6.65 (m, 4H, NHC-N-C*H*), 4.68 (hept, *J* = 6.1 Hz, 2H, Tipp-*o*-isopropyl-C*H*(CH_3)$_2$), 3.49 (hept, *J* = 6.5 Hz, 2H, Tipp-*o*-isopropyl-C*H*(CH_3)$_2$), 2.81 (hept, *J* = 6.9 Hz, 2H, Tipp-*p*-isopropyl-C*H*(CH_3)$_2$), 1.58 (s, 12H, HNC-CC*H*$_3$), 1.54 (d, *J* = 6.7 Hz, 6H, Tipp-*o*-isopropyl-CH(C*H*$_3$)$_2$), 1.33 (d, *J* = 6.7 Hz, 6H, Tipp-*o*-isopropyl-CH(C*H*$_3$)$_2$), 1.30 (d, *J* = 7.0 Hz, 12H, NHC-N-CC*H*$_3$), 1.28 – 1.22 (m, 24H, Tipp-*p*-isopropyl-CH(C*H*$_3$)$_2$ and NHC-N-CC*H*$_3$), 1.04 (dd, *J* = 13.2, 6.6 Hz, 12H, Tipp-*o*-isopropyl-CH(C*H*$_3$)$_2$).

^{1}H NMR (300 MHz, THF-d_8) δ 6.71 (s, 4H), 6.57 – 6.30 (m, 4H), 4.26 (hept, *J* = 6.5 Hz, 2H), 3.09 (hept, *J* = 5.7, 5.0 Hz, 2H), 2.66 (hept, *J* = 6.8 Hz, 2H), 2.30 (s, 12H), 1.42 – 1.30 (m, 24H), 1.08 (dd, *J* = 12.0, 5.9 Hz, 24H), 0.73 (d, *J* = 6.6 Hz, 6H), 0.54 (d, *J* = 6.6 Hz, 6H).

^{13}C{^{1}H} NMR (101 MHz, C_6D6) δ 172.37 (NHC-*C*:, according to the HMBC), 157.25 (Tipp-*C*-Al), 156.63 (Tipp-*C*-Al), 148.16 (Tipp-*p*-*C*-isopropyl), 126.04 (NHC-*C*-CH_3), 120.62 (Tipp-*m*-C), 120.31 (Tipp-*m*-C), 53.27 (NHC-N-*C*-CH_3), 35.99 (Tipp-*o*-*iso*-*C*(CH_3)$_2$), 35.73 (Tipp-*o*-*iso*-*C*(CH_3)$_2$), 34.90 (Tipp-*p*-*iso*-C(CH_3)$_2$), 27.17 (Tipp-*o*-*iso*-C(*C*H_3)$_2$), 25.54 (Tipp-*o*-*iso*-C(*C*H_3)$_2$), 25.35 (Tipp-*o*-*iso*-C(*C*H_3)$_2$), 25.13 (Tipp-*o*-*iso*-C(*C*H_3)$_2$), 24.53 (Tipp-*p*-*iso*-C(*C*H_3)$_2$), 24.49 (Tipp-*p*-*iso*-C(*C*H_3)$_2$), 21.92 (NHC-N-C-*C*H_3), 21.76 (NHC-N-C-*C*H_3), 10.23 (NHC-C-*C*H_3).

^{31}P{^{1}H} NMR (121 MHz, Benzene-d_6) δ -55.06 (d, *J* = 105.0 Hz), -138.25 (d, *J* = 163.3 Hz), -159.36 (ddd, *J* = 169.8, 159.6, 105.1 Hz).

$^{31}P\{^{1}H\}$ NMR (121 MHz, THF-d_8) δ -55.48 (d, *J* = 103.9 Hz), -140.08 (d, *J* = 163.1 Hz), -160.05 (ddd, *J* = 170.1, 159.4, 103.8 Hz).

MS (ESI^+) *m/z* calcd: 944.54; m/z found: 899.67. (**3-(CH_3)$_3$**)

2.3 Compound 4

To a Schlenk flask containing [(I^{i}Pr$_2$Me$_2$)Al(Si^{t}Bu$_2$Me)]$_2$ (0.083 g, 0.114 mmol) and P_4 (0.014 g, 0.113 mmol) was added 5 mL benzene. The resulting pale orange solution was stirred for two hours and then the solvent was removed *in vacuo*. The oily residue was washed with 3×2 mL pentane and the resulting solid was dried *in vacuo* yielding **4** as a pale orange powder (0.040 g, 41%). X-ray quality crystals of **4-Trans** were obtained by the slow evaporation of a THF solution of **4**.

^{1}H NMR (400 MHz, C_6D_6, 298 K): δ = 6.90 (sept, $^3J_{HH}$ = 6.5 Hz, 1H, C$\underline{H}$(CH$_3$)$_2$), 5.88 (sept, $^3J_{HH}$ = 6.6 Hz, 1H, C$\underline{H}$(CH$_3$)$_2$), 5.84–5.75 (br. m, 1H, C$\underline{H}$(CH$_3$)$_2$), 5.25 (sept, $^3J_{HH}$ = 6.5 Hz, 1H, C$\underline{H}$(CH$_3$)$_2$), 1.76 (d, $^3J_{HH}$ = 6.5 Hz, 3H, CH(C$\underline{H}_3$)$_2$), 1.74 (s, 9H, Si-C(C$\underline{H}_3$)$_3$), 1.67 (d, 3H, CH(C$\underline{H}_3$)$_2$), 1.63 (s, 9H, Si-C(C$\underline{H}_3$)$_3$), 1.67 (d, 3H, CH(C$\underline{H}_3$)$_2$), 1.56 (d, 3H, I*i*Pr-C$\underline{H}_3$), 1.54–1.50 (m, 6H, CH(C$\underline{H}_3$)$_2$, I*i*Pr-C$\underline{H}_3$), 1.40 (d, 3H, I*i*Pr-C$\underline{H}_3$), 1.33 (br. d $^3J_{HH}$ = 6.5 Hz, 6H, CH(C$\underline{H}_3$)$_2$), 1.25 (s, 9H, Si-C(CH_3)$_3$), 1.21 (d, $^3J_{HH}$ = 6.5 Hz, 6H, CH(C$\underline{H}_3$)$_2$, I*i*Pr-C$\underline{H}_3$), 1.17 (d, $^3J_{HH}$ = 6.5 Hz, 3H, CH(C$\underline{H}_3$)$_2$), 1.05 (s, 9H, Si-C(CH_3)$_3$), 0.34 (s, 3H, Si-CH_3), -0.04 (s, 3H, Si-CH_3).

$^{13}C\{^{1}H\}$ NMR (400 MHz, C_6D_6, 298 K): 153.8 (N*C*N), 128.0 (H$_3$C-*C*=*C*-CH$_3$), 54.3, 54.0, 53.0, 52.8, 52.4, 52.3 (*C*H(CH$_3$)$_2$), 31.3, 30.9, 30.7 (Si-C(*C*H$_3$)$_3$), 24.0, 22.6, 22.2 (CH(*C*H$_3$)$_2$), 21.6 (CH(*C*H$_3$)$_2$), 22.1, 21.4 (Si-*C*(CH$_3$)$_3$), 10.1, 9.9, 9.4 (H$_3$*C*-C=C-*C*H$_3$), -3.3, -5.7 (Si-*C*H$_3$).

$^{31}P\{^{1}H\}$ NMR (162 MHz, C_6D_6) δ -70.27 (d, *J* = 115.5 Hz), -124.23 (d, *J* = 289.4 Hz), -160.56 (d, *J* = 465.0 Hz).

$^{31}P\{^{1}H\}$ NMR (162 MHz, C_6D_6) δ -70.30 (d, *J* = 48.4 Hz), -120.49 – -127.47 (m), -160.49 (d, *J* = 48.4 Hz).

2.4 Compound 4-Trans

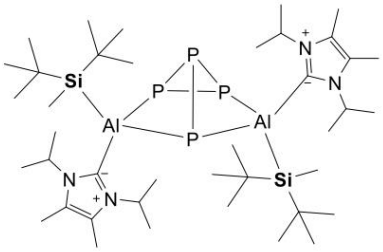

$C_{40}H_{82}Al_2N_4P_4Si_2$
853.15

The pale brown crystals were obtained from the saturated toluene solution of the mixture of **4** at -30 °C. The NMR data bellow were only observed at < 0 °C.

^{1}H NMR (400 MHz, Tol-d_8) δ 6.93 (d, *J* = 6.3 Hz, 1H), 5.79 (s, 1H), 5.62 – 5.39 (m, 1H), 5.37 – 5.15 (m, 1H), 2.09 (dd, *J* = 4.6, 2.4 Hz, 6H), 1.83 (s, 12H), 1.77 (d, *J* = 6.7 Hz, 3H), 1.70 (s, 11H), 1.65 (d, *J* = 6.9 Hz, 3H), 1.58 – 1.45 (m, 18H), 1.40 (d, *J* = 17.9 Hz, 9H), 1.29 (s, 18H), 1.22 (dd, *J* = 10.1, 6.9 Hz, 8H), 1.14 (d, *J* = 6.8 Hz, 3H), 1.08 (s, 9H), 0.29 (s, 4H), 0.05 (s, 3H).

$^{31}P\{^{1}H\}$ NMR (162 MHz, Tol-d_8) δ -72.62 (d, *J* = 119.6 Hz), -119.05 (m, *J* = 167.5 Hz), -124.46 (dd, J = 308.1, 171.0 Hz), -160.06 (dd, *J* = 307.01, 159.7 Hz).

2.5 Compound 5 and 6

Compound 5b

To a Schlenk flask containing a 5 mL solution of (I*i*Pr$_2$Me$_2$)AlH$_3$ (0.200 g, 0.951 mmol) in toluene was added TMSCl (0.4 mL, 3.2 mmol). The resulting solution was stirred for two hours, after which a 5 mL solution of NaSi^{t}Bu$_2$Me (0.177 g, 0.981) in pentane, rapidly forming a colorless precipitate. The slurry was stirred overnight, and the solvent was reduced to approximately half its original volume *in vacuo* (to remove the pentane). The slurry was then filtered and the remaining precipitate was extracted with 5 mL toluene. The filtrate was reduced to a volume of 2 mL *in vacuo*, layered with 2 mL of pentane, and stored in a −30 °C freezer overnight. Decantation of the mother liquor and removal of the volatiles *in vacuo* yielded **5** as a colorless, crystalline solid (0.073 g, 18%). Crystals suitable for X-ray crystallographic analysis were obtained by storing a saturated toluene solution in a -30 °C freezer overnight.

^{1}H NMR (400 MHz, C$_6$D$_6$, 298 K): δ = 5.66 (sept, $^3J_{HH}$ = 6.8 Hz, 2H, C*H*(CH$_3$)$_2$), 1.43 (s, 6H, *H*$_3$C-C=C-C*H*$_3$), 1.36 (s, 18H, Si-C(C*H*$_3$)$_3$), 1.14 (d, $^3J_{HH}$ = 6.5 Hz, 12H, CH(C*H*$_3$)$_2$), 0.33 (s, 3H, Si-C*H*$_3$).

^{13}C{^{1}H} NMR (400 MHz, C$_6$D$_6$, 298 K): 128.0 (H$_3$C-*C*=*C*-CH$_3$), 52.1 (*C*H(CH$_3$)$_2$), 30.3 (Si-C(*C*H$_3$)$_3$), 21.5 (Si-*C*(CH$_3$)$_3$), 9.7 (H$_3$*C*-C=C-*C*H$_3$), −6.4 (Si-*C*H$_3$). *An NCN resonance was not observed due to the relatively poor solubility in benzene.*

Compound 5a

^{1}H NMR (400 MHz, C$_6$D$_6$) δ 7.09 (s, 2H), 5.79 (hept, *J* = 6.8 Hz, 2H), 4.11 (hept, *J* = 6.6 Hz, 2H), 2.84 (hept, *J* = 7.0 Hz, 1H), 1.42 (s, 6H), 1.29 (dd, *J* = 6.8, 3.1 Hz, 17H), 1.00 (d, *J* = 7.1 Hz, 11H).

The compound **6a**, **6b** was consistent with reported data.[3, 4]

2.6 P_4 Functionalization: General Procedure

To a J-Young NMR tube containing $[(I^iPr_2Me_2)Al(Si^tBu_2Me)]_2$ (0.006 g, 0.008 mmol) and P_4 (0.001 g, 0.008 mmol) was added a sealed capillary tube containing a Ph_3P standard (0.003 g, 0.011 mmol) in toluene-d_8. Benzene-d_6 was then added to the NMR tube until the solvent level matched that of the capillary solvent level. The tube was then sealed, removed from the glovebox and sonicated until all of the purple dialumene was consumed (ca. 30 seconds), forming a pale orange solution. The quantitative formation of **1** was confirmed by ^1H and ^{31}P NMR spectroscopy. At this point, an excess of the electrophile in question was added (ca. 1 drop) and the reaction monitored by ^{31}P NMR spectroscopy. Yields were determined by comparison to the internal Ph_3P standard using ^{31}P NMR spectroscopy.

Table S1: Reactions of different electrophiles with compound 4

Electrophile	*t* [h]	T [°C]	Yield vs. P [%]	Product
Me_3SiCl	9	r.t.	3.5	$P(SiMe_3)_3$
Me_3SiI	4	r.t.	6	$P(SiMe_3)_3$
4M HCl in dioxane	1	r.t.	quantitative	PH_3
CH_3COCl	0.25	r.t.	quantitative	$P(OCCH_3)_3$

Table S2: Reactions of different electrophiles with compound 3-Trans

Electrophile	*t* [h]	T [°C]	Yield vs. P [%]	Product
Me_3SiCl	2	50	2	$P(SiMe_3)_3$
Me_3SiI	12	r.t.	1	$P(SiMe_3)_3$
4M HCl in dioxane	0.25	r.t.	8	PH_3
CH_3COCl	0.25	r.t.	quantitative	$P(OCCH_3)_3$

Table S3: Reactions of different electrophiles with compound 3-Cis

Electrophile	*t* [h]	T [°C]	Yield vs. P [%]	Product
Me_3SiCl	2	65	5	$P(SiMe_3)_3$
Me_3SiI	12	50	2	$P(SiMe_3)_3$
4M HCl in dioxane	0.25	r.t.	12	PH_3
CH_3COCl	0.25	r.t.	quantitative	$P(OCCH_3)_3$

3. NMR Spectra

3.1 Compound 3-Trans

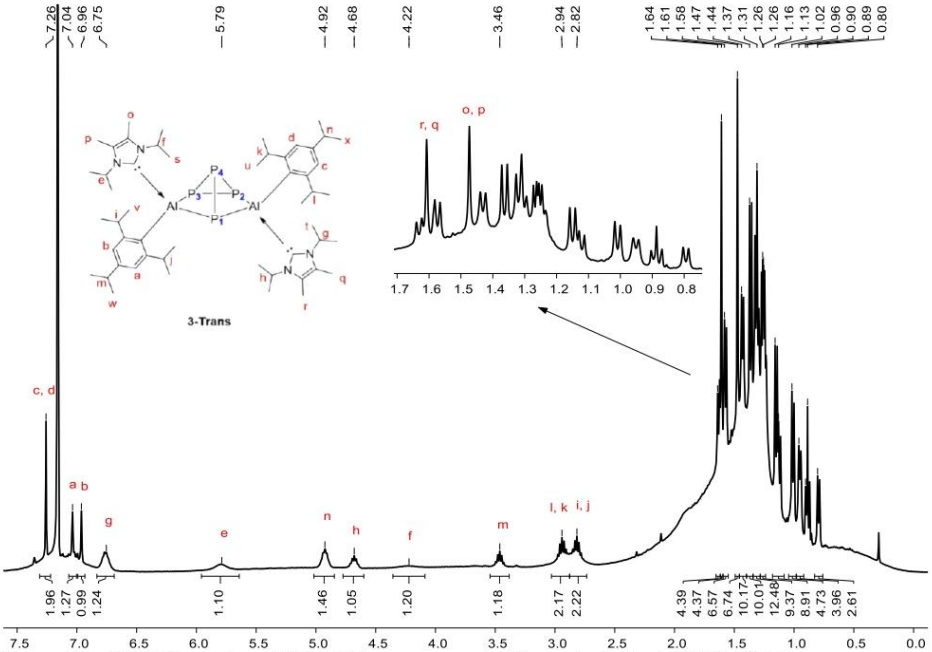

Figure S1. ^{1}H NMR spectrum (400 MHz) of compound **3-Trans** in C_6D_6 at 300 K. [δ (silicone grease) = 0.295 ppm]

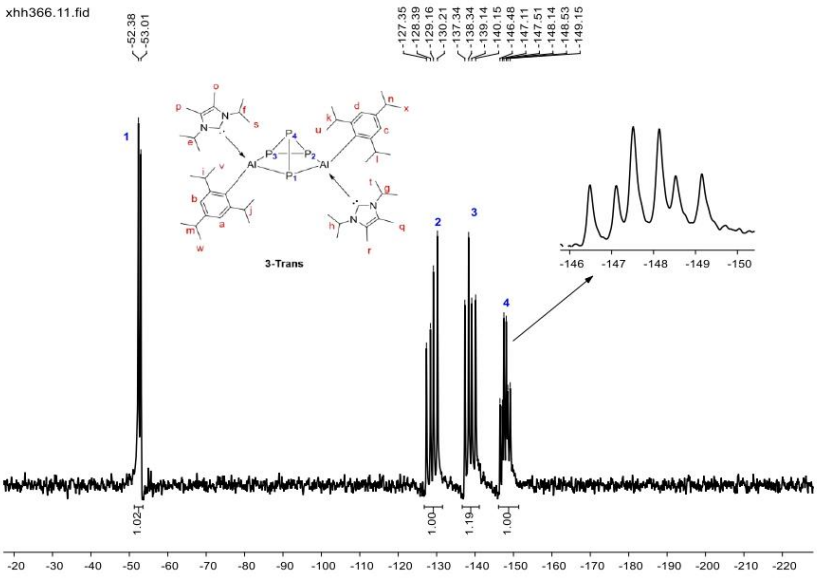

Figure S2. $^{31}P\{^{1}H\}$ NMR spectrum (170 MHz) of compound **3-Trans** in C_6D_6 at 300 K.

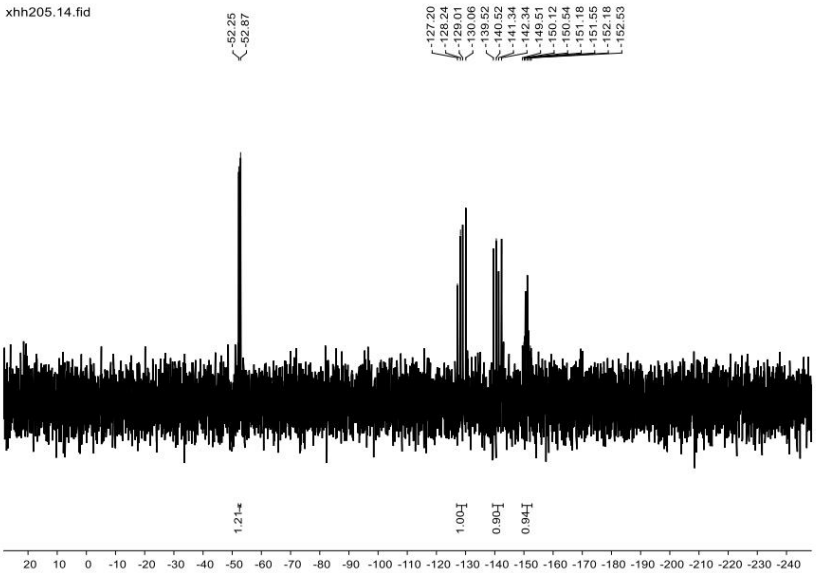

Figure S3. $^{31}P\{^{1}H\}$ NMR spectrum (170 MHz) of compound **3-Trans** in THF-d_8 at 300 K.

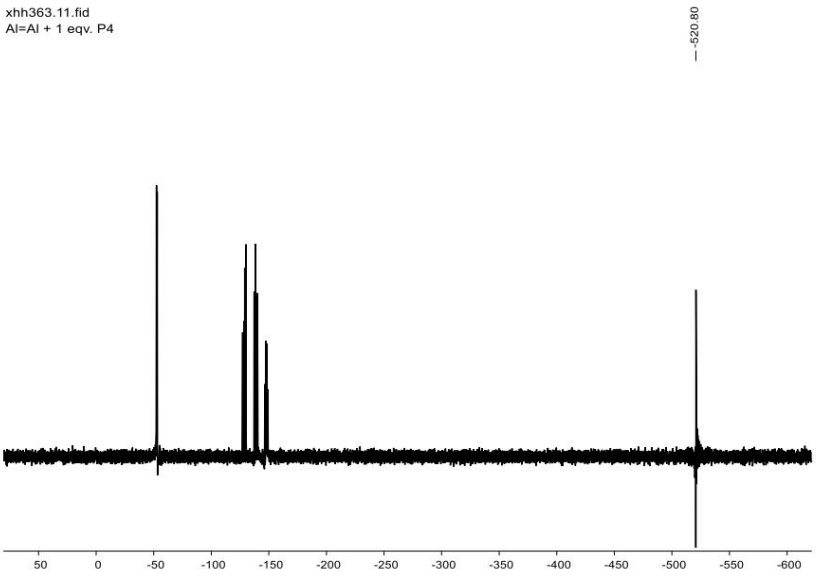

Figure S4. $^{31}P\{^{1}H\}$ NMR spectrum (170 MHz) of compound **3-Trans** in C_6D_6 at 300 K.

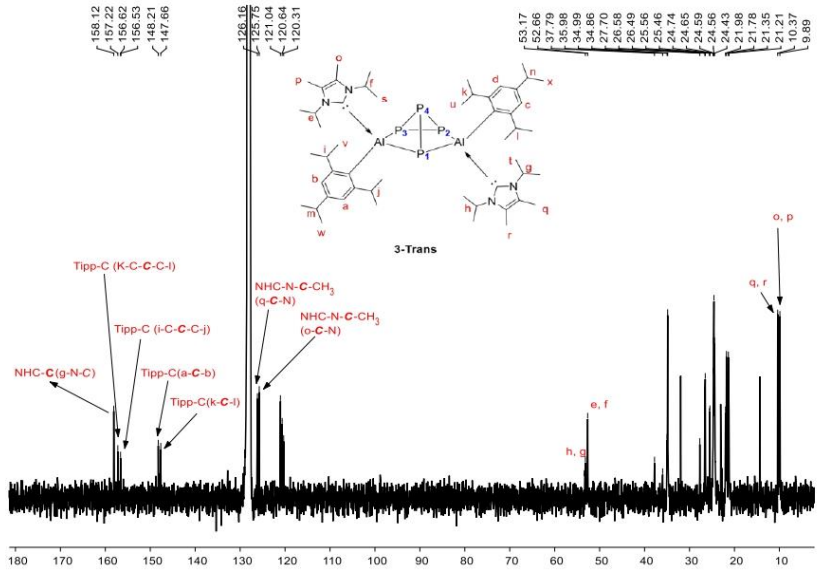

Figure S5. $^{13}C\{^{1}H\}$ NMR spectrum (101 MHz) of compound **3-Trans** in C_6D_6 at 300 K.

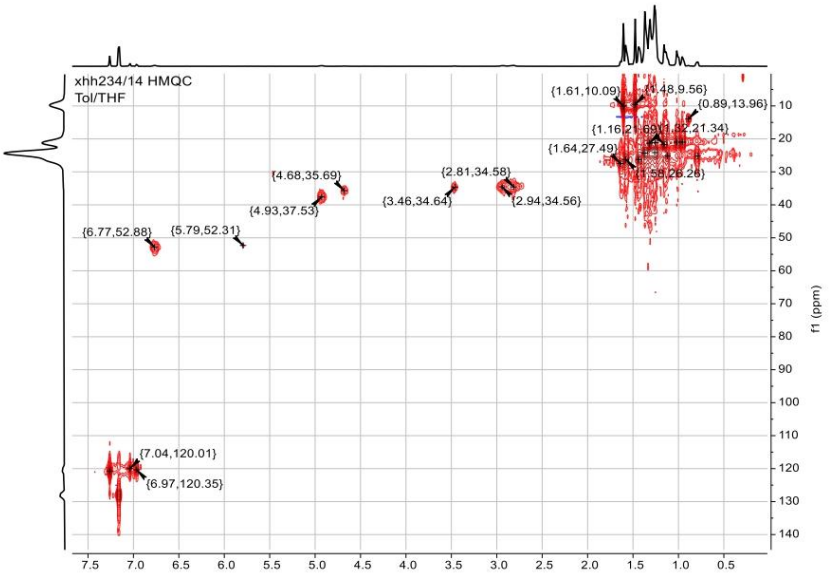

Figure S6. $^{1}H/^{13}C$ HSQC spectrum of compound **3-Trans** in C_6D_6 at 300 K.

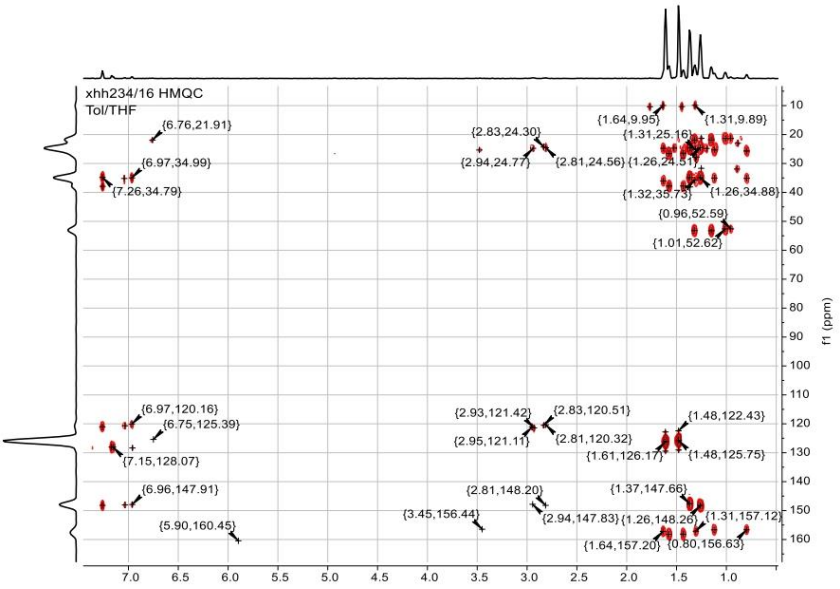

Figure S7. $^{1}H/^{13}C$ HMBC spectrum of compound **3-Trans** in C_6D_6 at 300 K.

3.2 Compound 3-Cis

3.2.1 NMR spectra

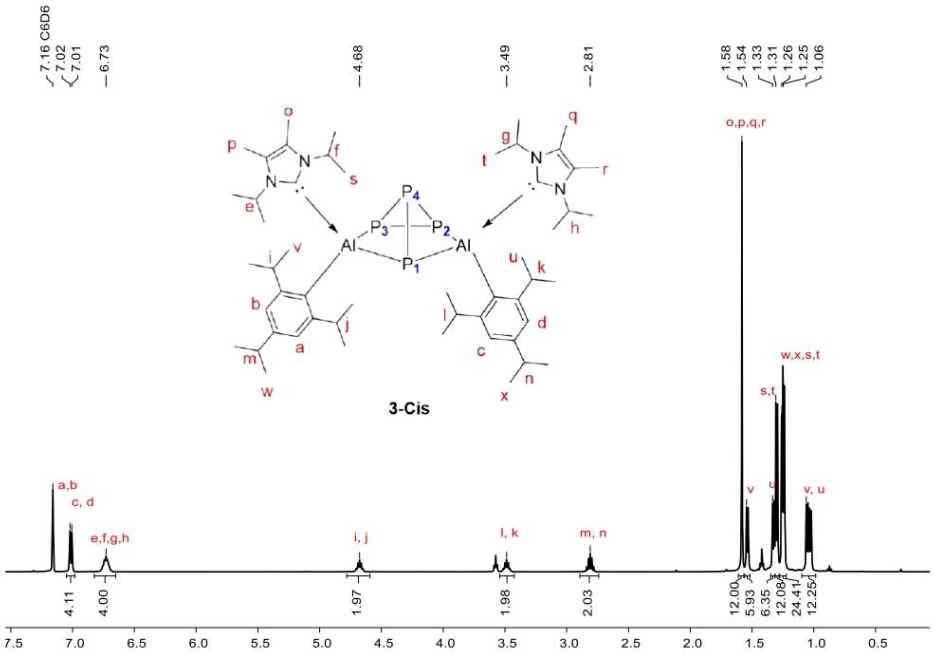

Figure S8. ^{1}H NMR spectrum (500 MHz) of compound **3-Cis** in C_6D_6 at 300 K. [δ (silicone grease) = 0.295 ppm]

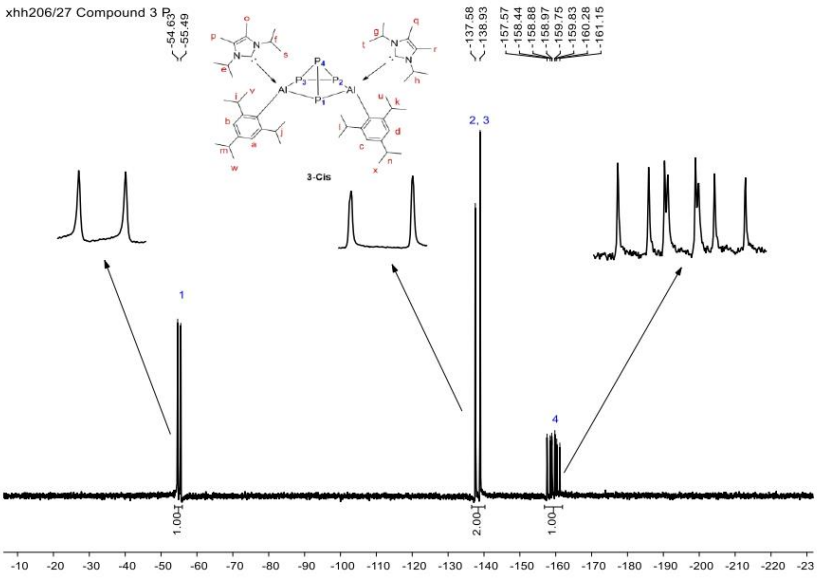

Figure S9. $^{31}P\{^{1}H\}$ NMR spectrum (125 MHz) of compound **3-Cis** in C_6D_6 at 300 K.

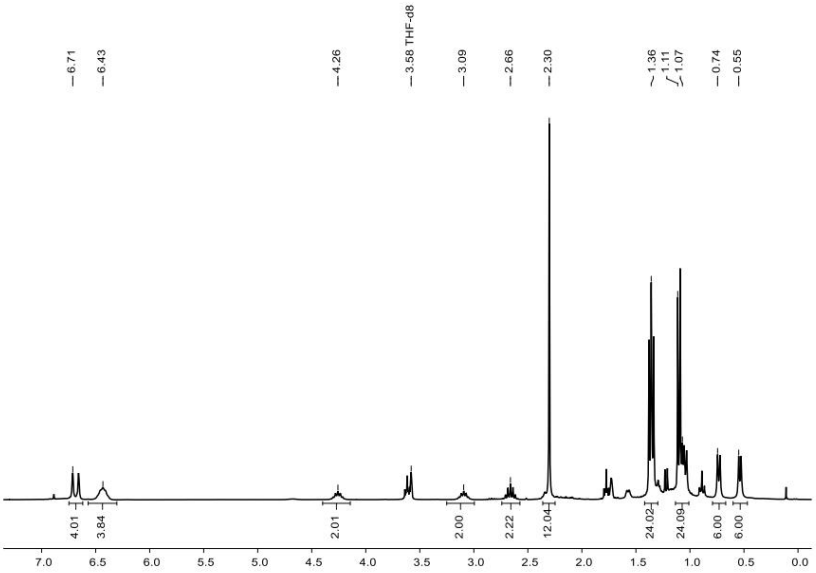

Figure S10. ^{1}H NMR spectrum (300 MHz) of compound **3-Cis** in THF-d_8 at 300 K. [δ (silicone grease) = 0.110 ppm]

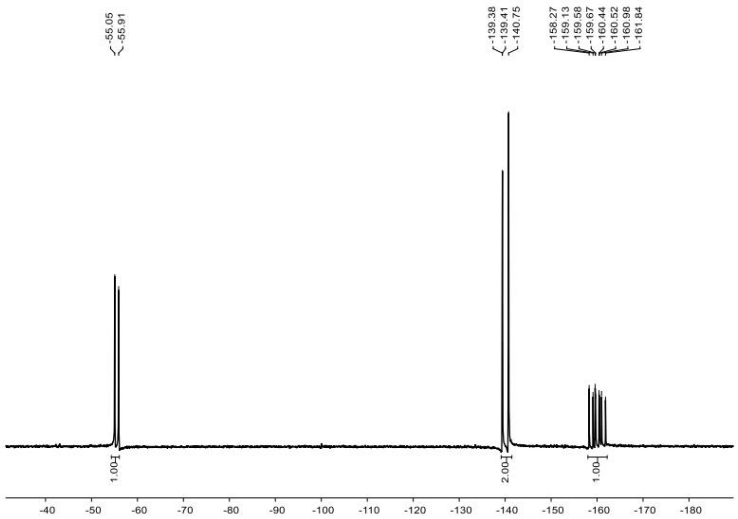

Figure S11. $^{31}P\{^{1}H\}$ NMR spectrum (125 MHz) of compound **3-Cis** in THF-d_8 at 300 K.

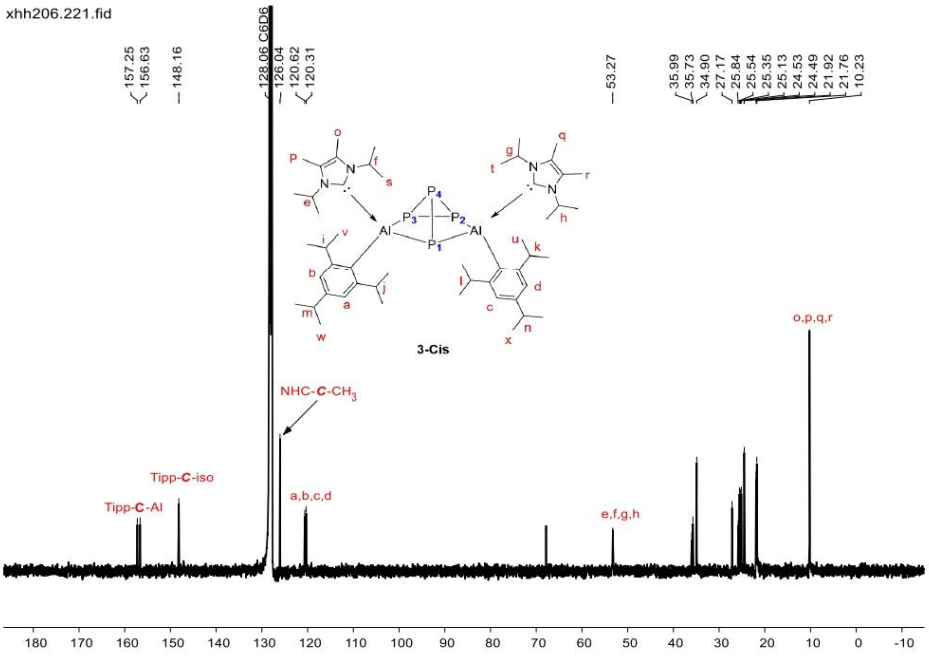

Figure S12. $^{13}C\{^{1}H\}$ NMR spectrum (101 MHz) of compound **3-Cis** in C_6D_6 at 300 K.

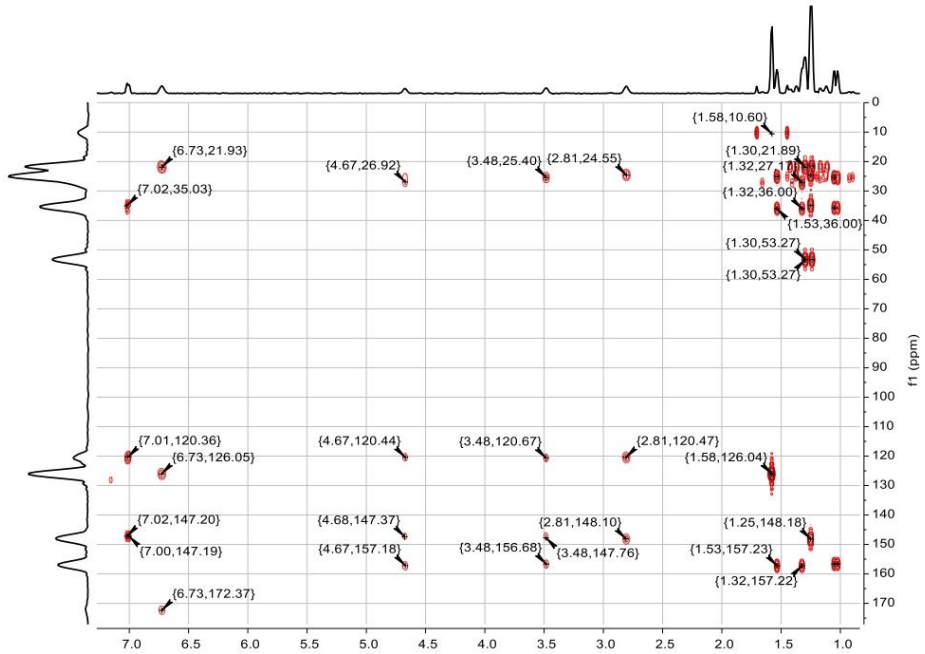

Figure S13. $^{1}H/^{13}C$ HMBC spectrum of compound **3-Cis** in C_6D_6 at 300 K.

3.2.2 Mass of Compound 3-Cis

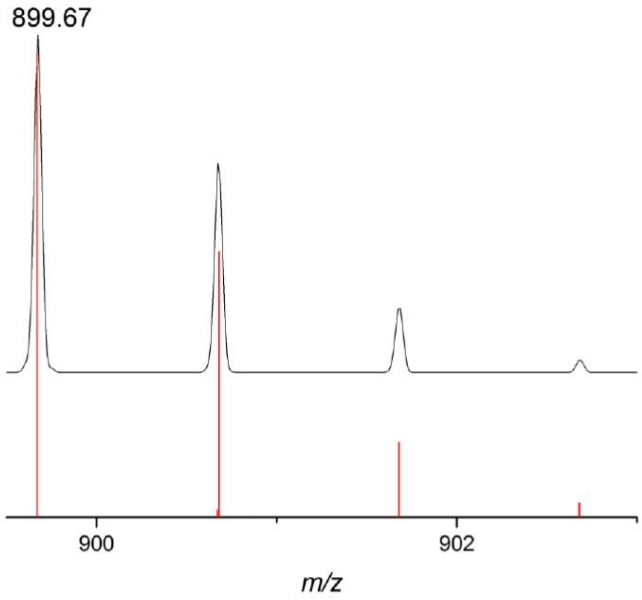

Figure S14. LIFDI-MS spectrometry (detail view with isotope pattern) of **3-Trans** or **3-Cis** (Measured spectrum: top; Simulated spectrum: bottom).

3.3 Compound 4-Trans

3.3.1 NMR spectra

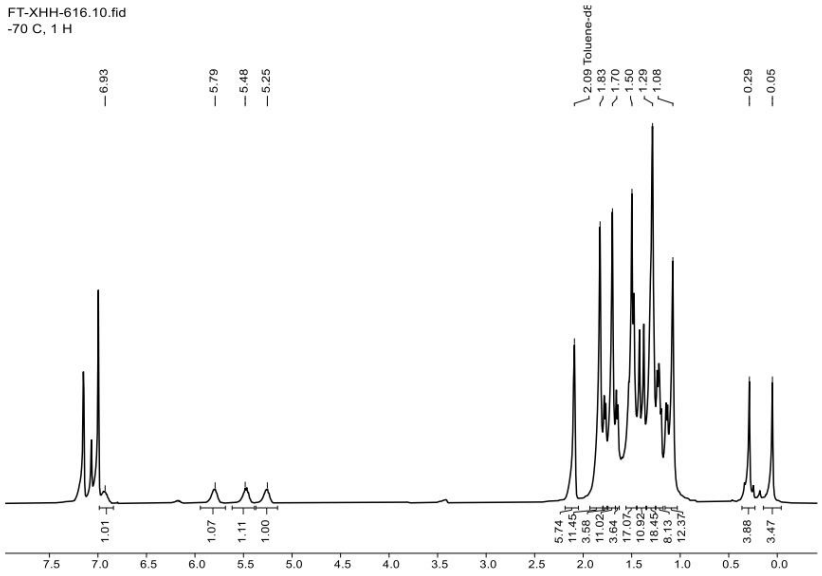

Figure S15. ^{1}H NMR spectrum (400 MHz) of compound **4-Trans** in $Told_8$ at 203.2 K. (Low-temperature NMR)

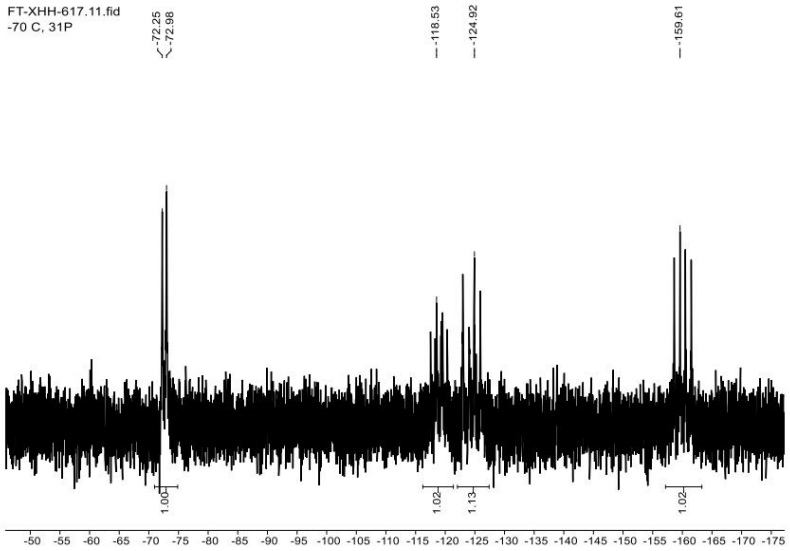

Figure S16. $^{31}P\{^{1}H\}$ NMR spectrum (162 MHz) of compound **4-Trans** in $Told_8$ at 203.2 K. (Low-temperature NMR)

3.3.2 Mass of Compound 4-Trans

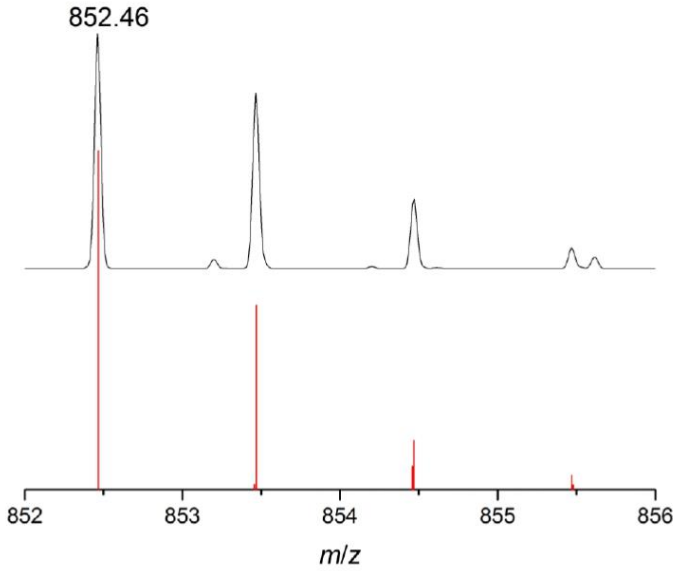

Figure S17. LIFDI-MS spectrometry (detail view with isotope pattern) of **4-Trans** (Measured spectrum: top; Simulated spectrum: bottom).

3.4 Compound 4

3.4.1 NMR spectra

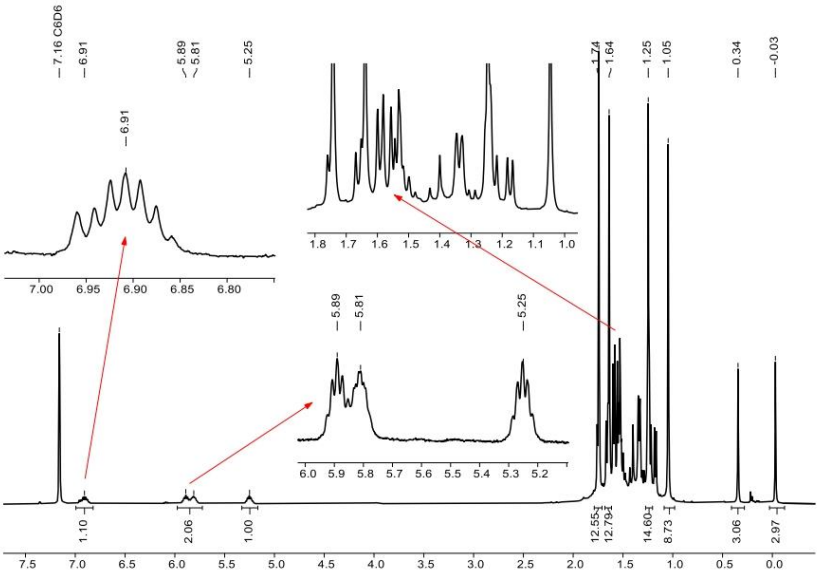

Figure S18. ^{1}H NMR spectrum (400 MHz) of compound **4** in C_6D_6 at 300 K. [δ (silicone grease) = 0.295 ppm]

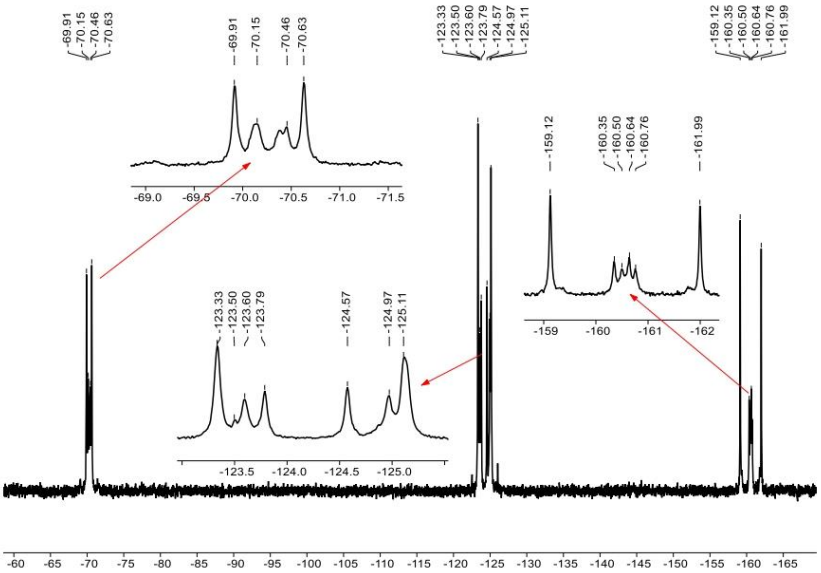

Figure S19. $^{31}P\{^{1}H\}$ NMR spectrum (165 MHz) of compound **4** in C_6D_6 at 300 K.

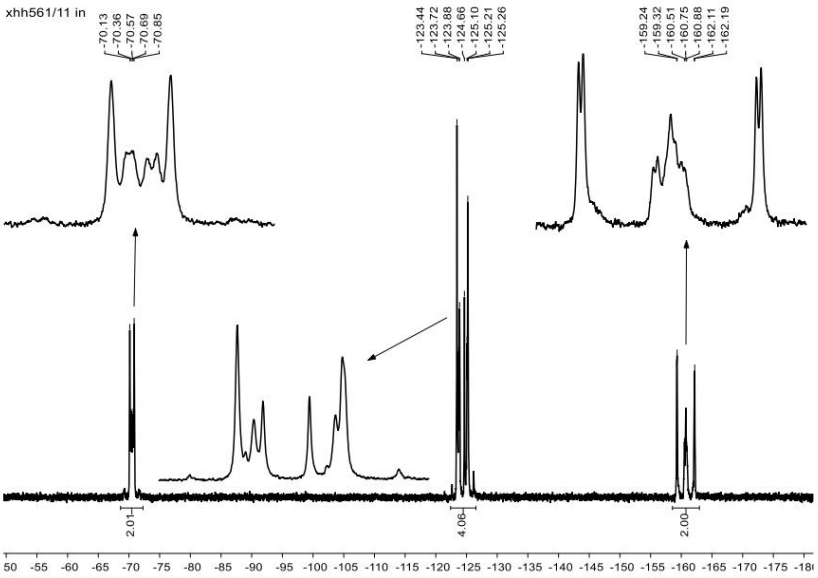

Figure S20. $^{31}P\{^{1}H\}$ NMR spectrum (162 MHz) of compound **4** in C_6D_6 at 300 K.

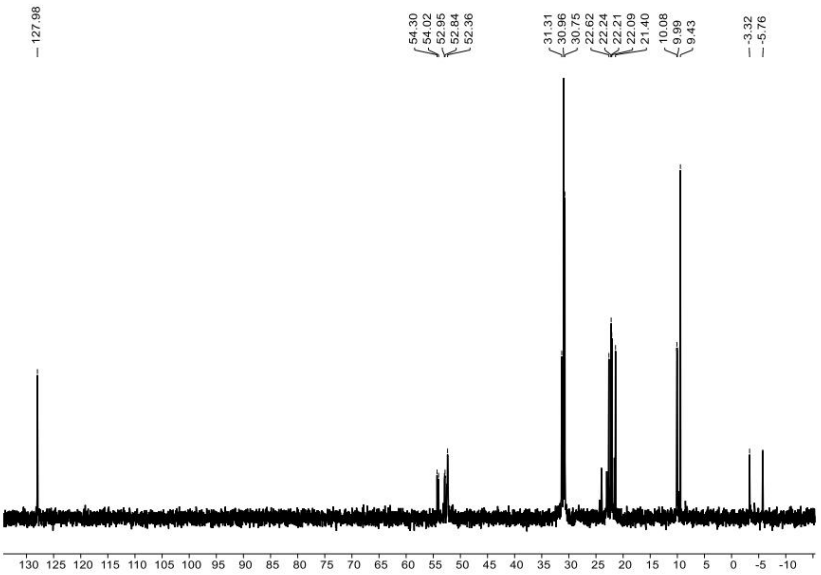

Figure S21. $^{13}C\{^{1}H\}$ NMR spectrum (101 MHz) of compound **4** in C_6D_6 at 300 K.

3.4.2 Thermal stability of compound 4

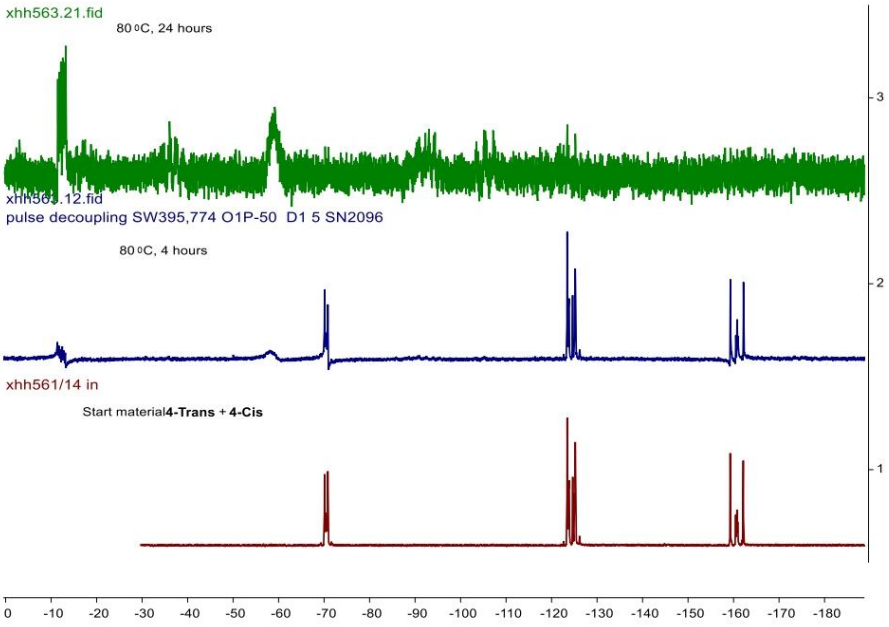

Figure S22. Stacked $^{31}P\{^{1}H\}$ NMR (170 MHz) spectra for **Compound 4** (under different conditions) in C_6D_6 at 300 K.

3.5 Variable-temperature NMR

3.5.1 Variable-temperature NMR of 4-Trans

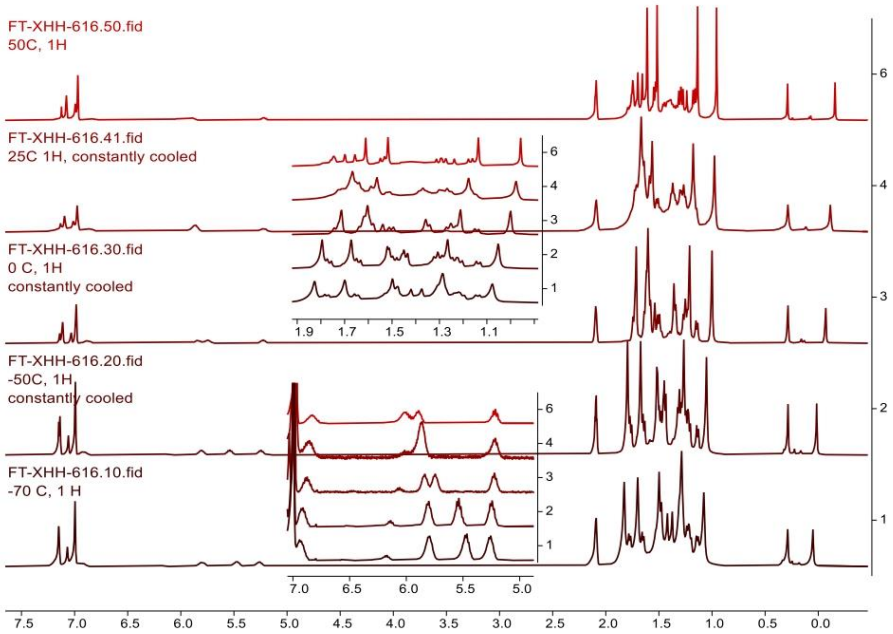

Figure S23. Stacked ^{1}H NMR (401 MHz) spectra for **Compound 4-Trans** in Tol-d_8 at 203.2 K, 223.2 K, 273.2 K, 298.2 K, 323.2 K. (from 203.2 K to 323.2 K)

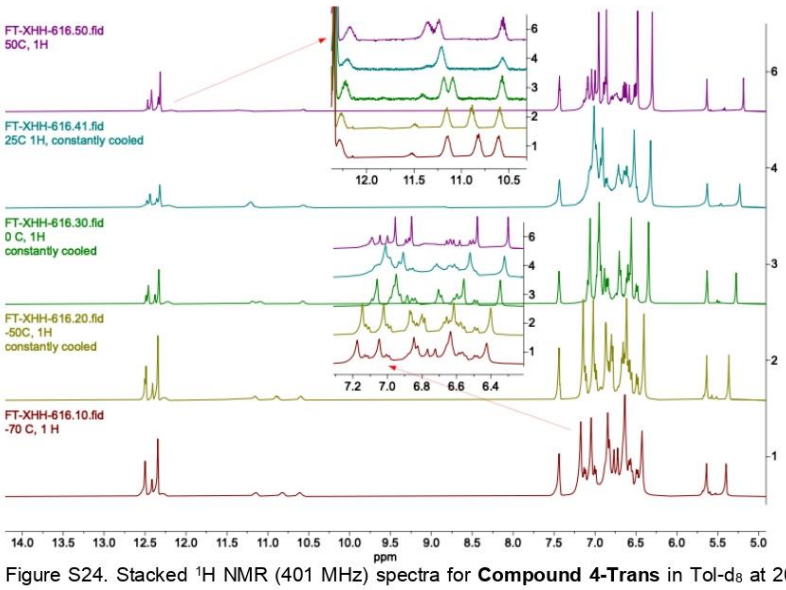

Figure S24. Stacked ^{1}H NMR (401 MHz) spectra for **Compound 4-Trans** in Tol-d_8 at 203.2 K, 223.2 K, 273.2 K, 298.2 K, 323.2 K. [crude data]

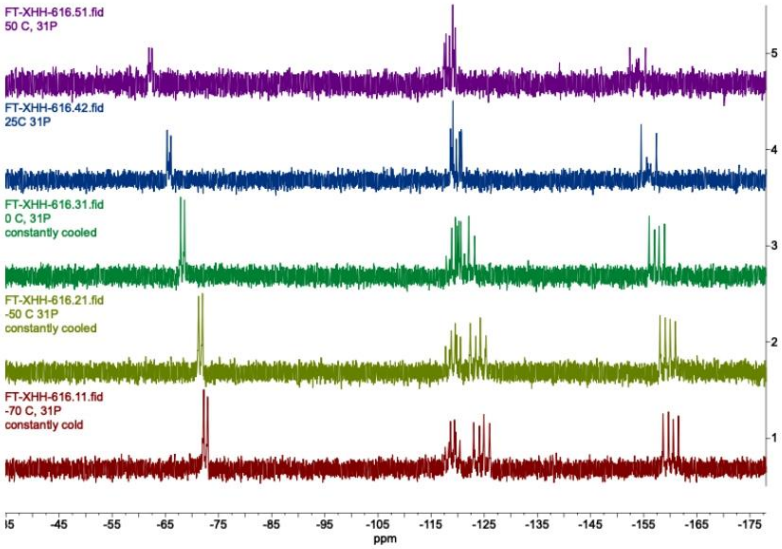

Figure S25. Stacked $^{31}P\{^{1}H\}$ NMR (162 MHz) spectra for **Compound 4-Trans** in Tol-d_8 at 203.2 K, 223.2 K, 273.2 K, 298.2 K, 323.2 K. (from 203.2 K to 323.2 K)

3.5.2 Variable-temperature NMR of 4

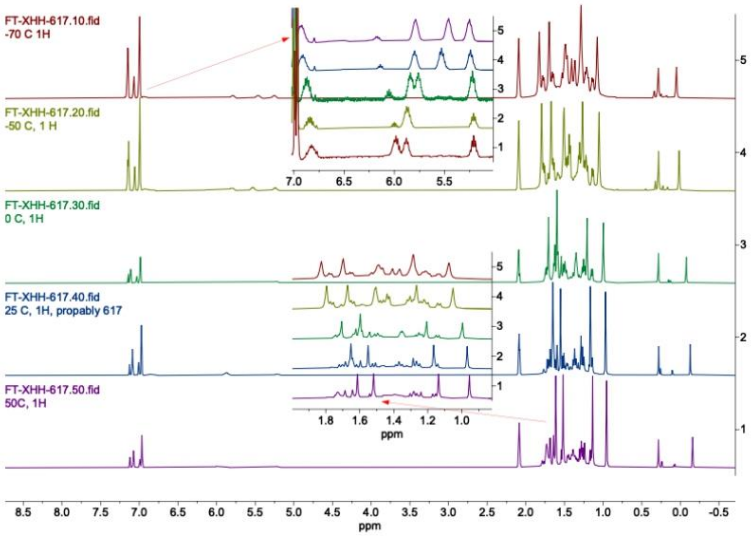

Figure S26. Stacked ^{1}H NMR (401 MHz) spectra for **Compound 4** in Tol-d_8 at 323.2 K, 298.2 K, 273.2 K, 223.2 K, 203.2 K. (from 323.2 K to 203.2 K)

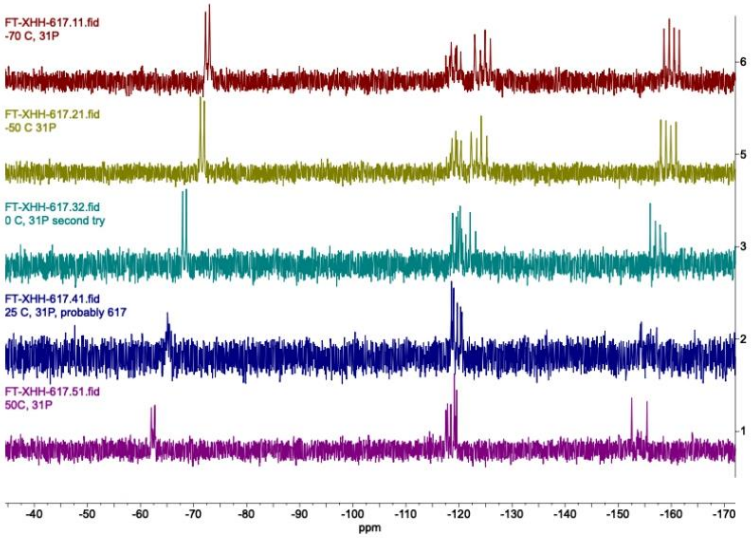

Figure S27. Stacked ^{31}P{^{1}H} NMR (162 MHz) spectra for **Compound 4** in Tol-d_8 at 323.2 K, 298.2 K, 273.2 K, 223.2 K, 203.2 K. (from 323.2 K to 203.2 K)

3.6 Compound 5b

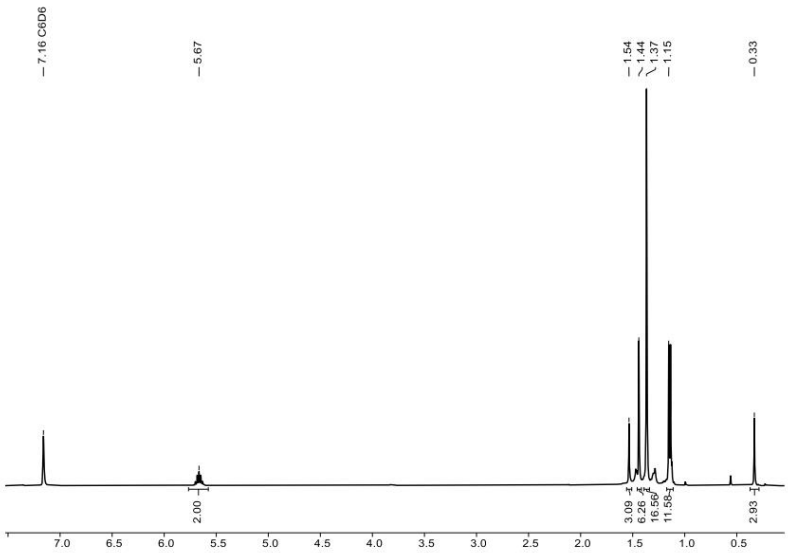

Figure S28. ^{1}H NMR spectrum (400 MHz) of compound **5b** in C_6D_6 at 300 K. [δ (silicone grease) = 0.295 ppm]

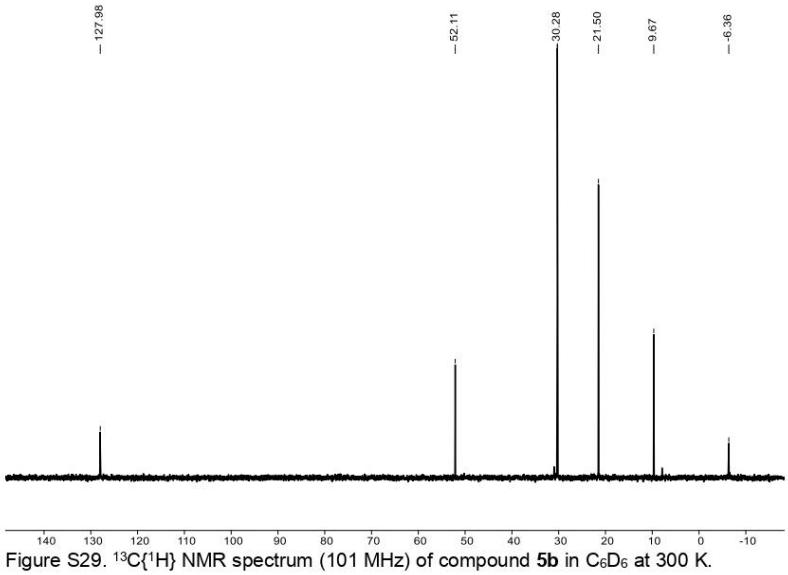

Figure S29. $^{13}C\{^{1}H\}$ NMR spectrum (101 MHz) of compound **5b** in C_6D_6 at 300 K.

3.7 Phosphines

3.7.1 $PTMS_3$

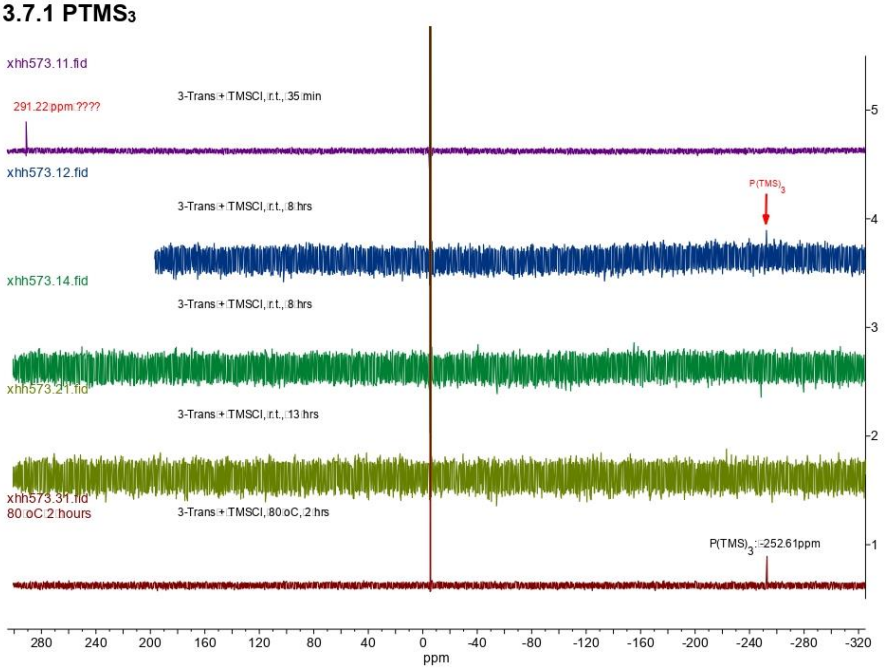

Figure S30. Stacked $^{31}P\{^{1}H\}$ NMR (170 MHz) spectra for the reaction products of **Compound 3-Trans** and **TMSCl** (under different conditions) in C_6D_6 at 300 K.

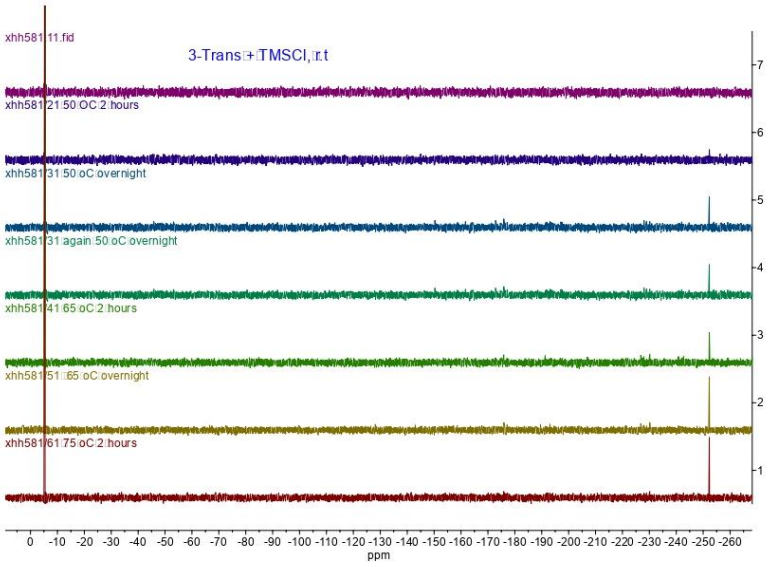

Figure S31. Stacked $^{31}P\{^{1}H\}$ NMR (170 MHz) spectra for the reaction products of **Compound 3-Trans** and **TMSCl** (under different conditions) in C_6D_6 at 300 K.

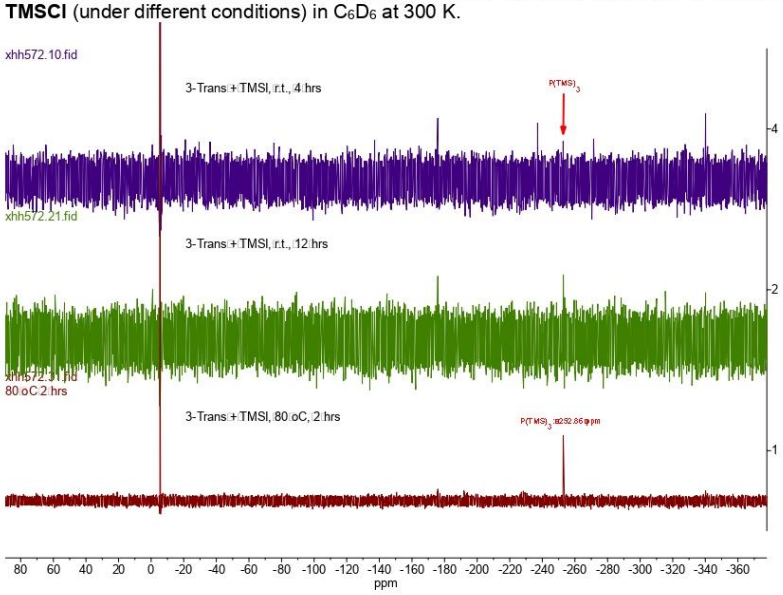

Figure S32. Stacked $^{31}P\{^{1}H\}$ NMR (170 MHz) spectra for the reaction products of **Compound 3-Trans** and **TMSI** (under different conditions) in C_6D_6 at 300 K.

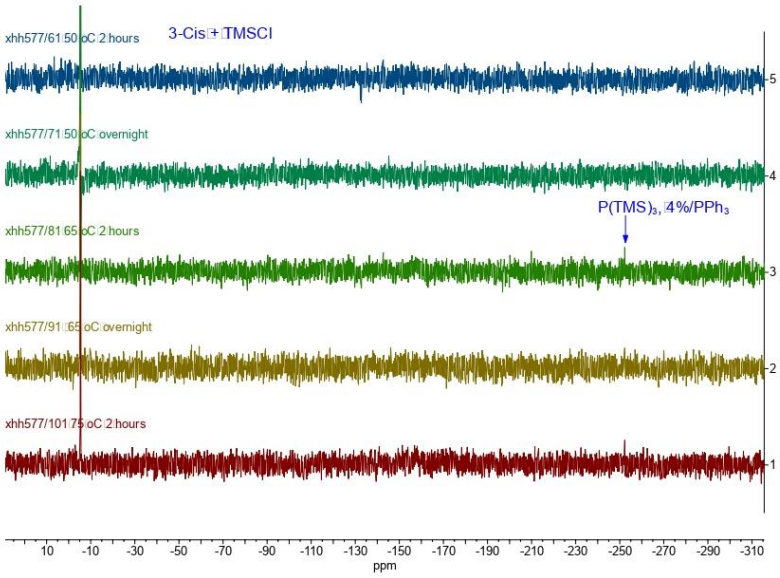

Figure S33. Stacked $^{31}P\{^{1}H\}$ NMR (170 MHz) spectra for the reaction products of **Compound 3-Cis** and **TMSCl** (under different conditions) in C_6D_6 at 300 K.

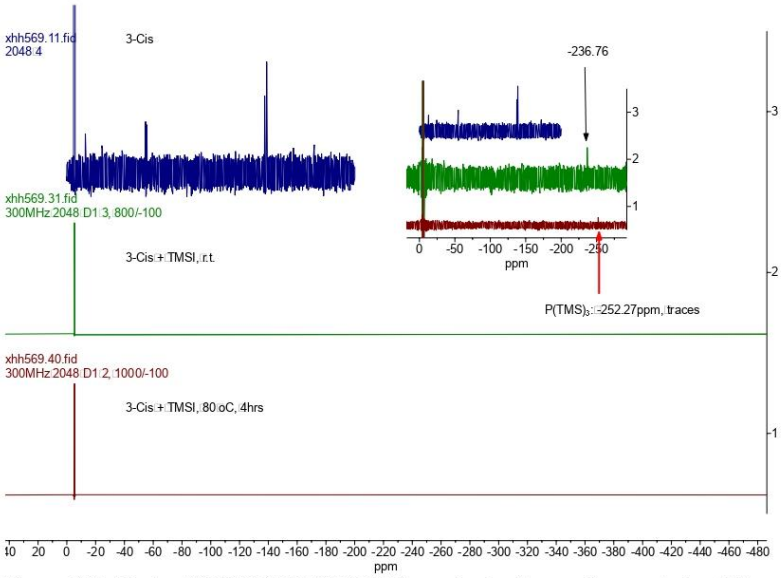

Figure S34. Stacked $^{31}P\{^{1}H\}$ NMR (170 MHz) spectra for the reaction products of **Compound 3-Cis** and **TMSI** (under different conditions) in C_6D_6 at 300 K.

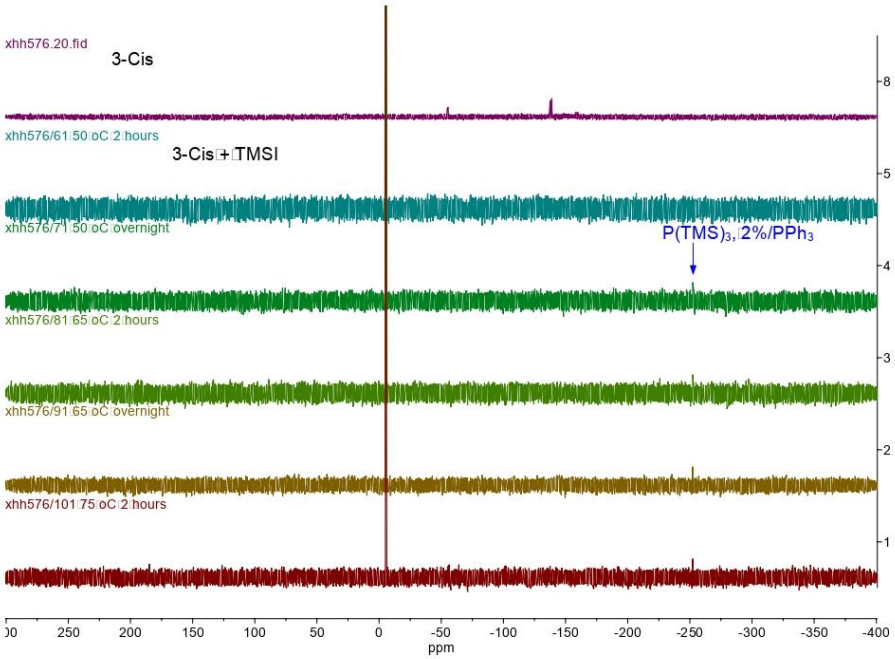

Figure S35. Stacked $^{31}P\{^{1}H\}$ NMR (170 MHz) spectra for the reaction products of **Compound 3-Cis** and **TMSI** (under different conditions) in C_6D_6 at 300 K.

3.7.2 PH_3

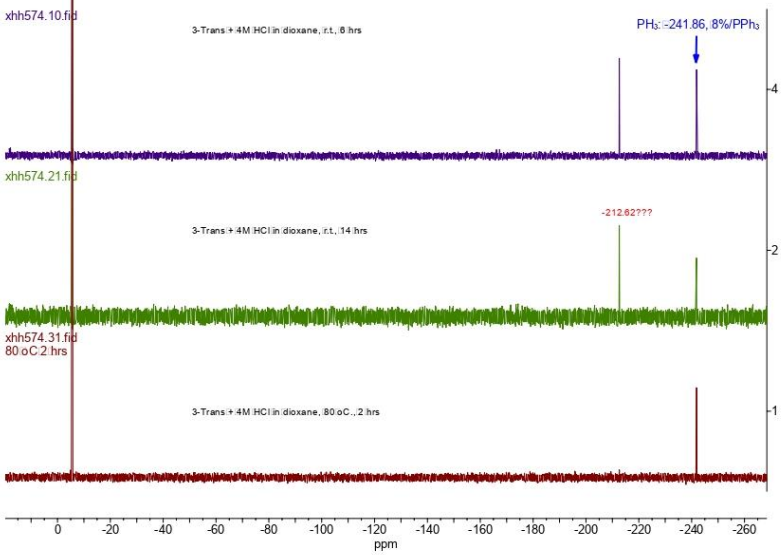

Figure S36. Stacked $^{31}P\{^{1}H\}$ NMR (170 MHz) spectra for the reaction products of **Compound 3-Trans** and **HCl** (under different conditions) in C_6D_6 at 300 K.

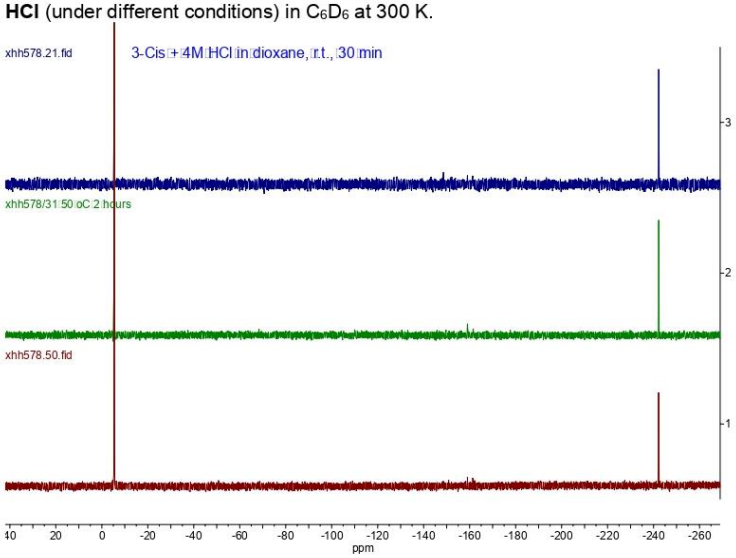

Figure S37. Stacked 31P{1H} NMR (170 MHz) spectra for the reaction products of Compound 3-Cis and HCl (under different conditions) in C6D6 at 300 K.

3.7.3 $P(OCCH_3)_3$

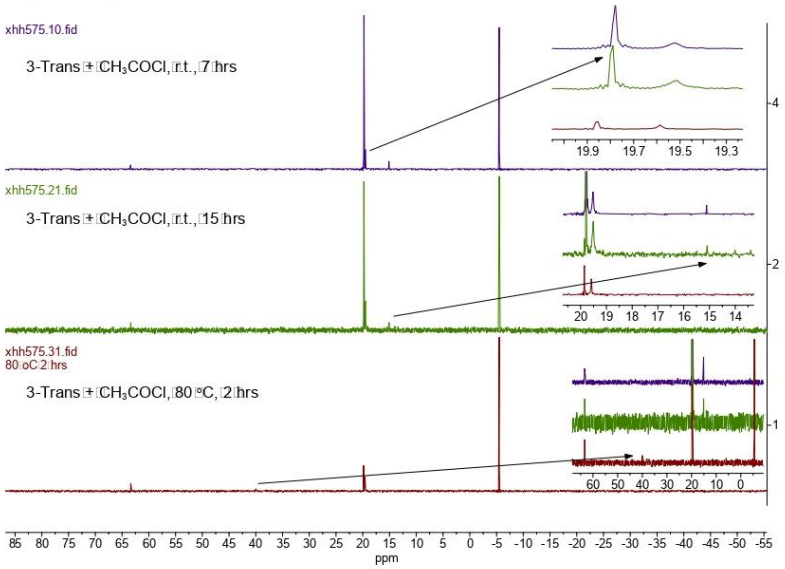

Figure S38. Stacked $^{31}P\{^1H\}$ NMR (170 MHz) spectra for the reaction products of **Compound 3-Trans** and **MeCOCl** (under different conditions) in C_6D_6 at 300 K.

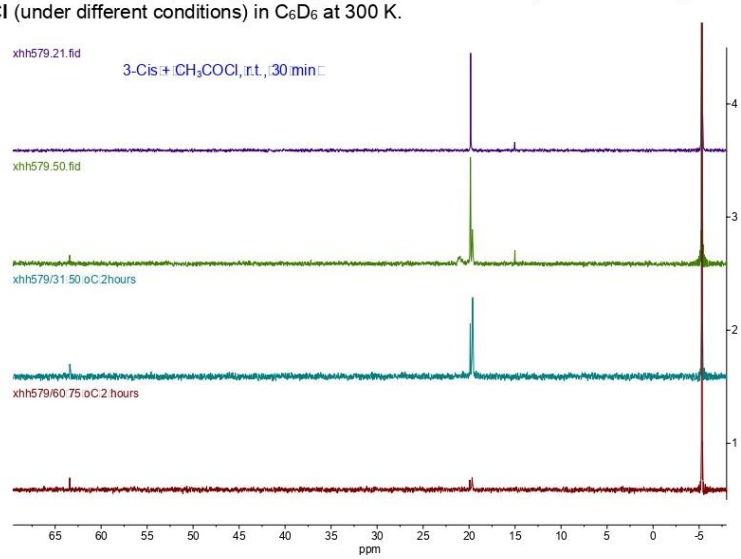

Figure S39. Stacked $^{31}P\{^1H\}$ NMR (170 MHz) spectra for the reaction products of **Compound 3-Cis** and **MeCOCl** (under different conditions) in C_6D_6 at 300 K.

4. X-ray Crystallographic Details

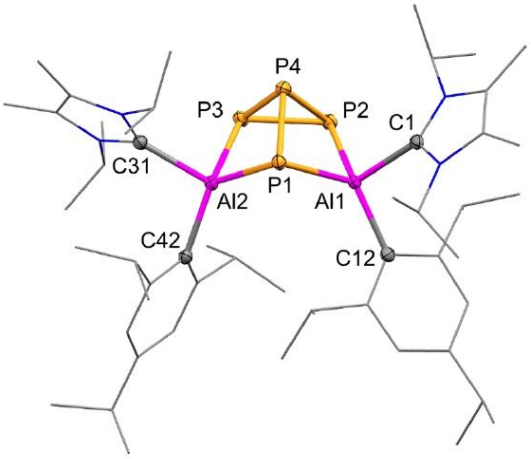

Figure S40. Molecular structures of **3-Cis** in the solid state. Ellipsoids are set at the 50% probability level; hydrogen atoms and co-crystallized solvent molecules are omitted for clarity and NHC, Tipp, and silyl ligands are depicted in wireframe for simplicity. Selected bond lengths (Å) and angles (°): **3-Cis**: Al1-C1 (NHC) 2.1288, Al2-C31 (NHC) 2.0781, Al1-C12 (Tipp) 2.0187, Al2-C42 (Tipp) 2.0116, Al1-P1 2.3515, Al2-P1 2.3539, Al1-P2 2.3998, Al2-P3 2.3842, P1-P4 2.2844, P2-P4 2.2462, P3-P4 2.2189, P2-P3 2.1934, Al1-P1-Al2 79.86, P1-Al2-P3 93.84, P1-Al1-P2 94.12, Al1-P1-P4 78.56, P1-P4-P3 100.43.

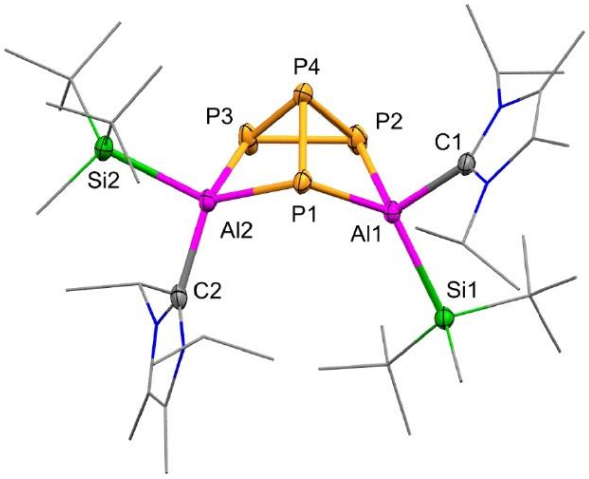

Figure S41. Molecular structures of **4-Trans** in the solid state. Ellipsoids are set at the 50% probability level; hydrogen atoms and co-crystallized solvent molecules are omitted for clarity and NHC, Tipp, and silyl ligands are depicted in wireframe for simplicity. Selected bond lengths (Å) and angles (°): **4-Trans**: Al1-C1 (NHC) 2.103(3), Al2-C2 (NHC) 2.066(3), Al1-Si1 2.520(1), Al2-Si2 2.500(1), Al1-P1 2.366(1), Al2-P1 2.342(1), Al1-P2 2.401(1), Al2-P3 2.391(1), P1-P4 2.291(1), P2-P4 2.226(1), P3-P4 2.232(1), P2-P3 2.198(1), Al1-P1-Al2 105.08(4), P1-Al2-P3 93.84(4), P1-Al1-P2 92.83(4), Al1-P1-P4 79.79(4), P1-P4-P3 99.70(4).

Table S4. Crystal data and structure refinement for compound 3-Cis and 4-Trans.

Compound #	3-Cis (XuHui29 or XuHui18)	4-Trans (RoyMa26)
CCDC-Number		
Empirical formula		$C_{40}H_{82}N_4P_6Si_2$
Formula weight	951.80	861.09
Temperature/K	100.00	100.00
Crystal system	monoclinic	monoclinic
Space group	C 1 2/c 1	$P2_1/n$
a/Å	45.950(5)	14.6085(16)
b/Å	17.5842(19)	18.259(2)
c/Å	18.109(2)	19.449(2)
α/°	90	90
β/°	106.025(4)	104.856(4)
γ/°	90	90
Volume/Å3	14064(3)	5014.5(10)
Z	8	4
ρcalcg/cm3	0.899	1.141
μ/mm 1	0.161	0.293
F(000)	4103	1872.0
Crystal size/mm3	0.185 x 0.173 x 0.067	0.04 × 0.02 × 0.01
Radiation	MoKα (λ = 0.71073)	MoKα (λ = 0.71073)
2Θ range for data collection/°		3.846 to 53.064
Index ranges		-18 ≤ h ≤ 18, -22 ≤ k ≤ 22, -24 ≤ l ≤ 24
Reflections collected		286751
Independent reflections		10370 [R_{int} = 0.2156, R_{sigma} = 0.0528]
Data/restraints/parameters		10370/0/495
Goodness-of-fit on F2		1.044
Final R indexes [I>=2σ (I)]		R_1 = 0.0628, wR_2 = 0.1462
Final R indexes [all data]		R_1 = 0.0866, wR_2 = 0.1629
Largest diff. peak/hole / e Å-3		0.54/-0.82

5. Computational Details

Quantum chemical calculations at the SMD(Benzene)-DLPNO-CCSD(T)/def2-TZVP//r^{2}SCAN-3c level of theory show that the formation of **3-Cis** form **1** and P_4 is expected to be exergonic by 84.5 kcal mol^{-1}. We propose that the formation of **3-Cis** takes place via the initial formation of **3-Trans** that we observe by NMR spectroscopy, which later isomerized to the energetically more favoured isomer **3-Cis**.

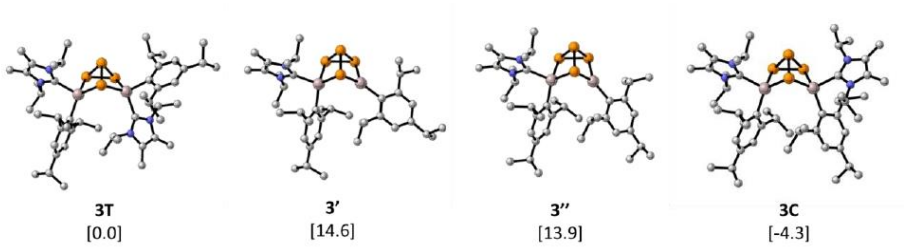

Figure S42. r^{2}SCAN-3c optimized geometries of **3-Trans**, **3'**, **3''** and **3-Cis**. Relative Gibbs energies are shown in brackets. (Relative energies shown below **3'** and **3''** include the G of the NHC).

Relaxed surface scans show that the NHC dissociation from **3-Trans** and **3-Cis**, which are barrierless, result in essentially similar intermediates **3'** and **3''**. We propose that the **3-Trans** → **3-Cis** isomerization proceeds via the NHC dissociation from **3-Trans** to form **3'**, which is only endergonic by 14.6 kcal mol^{-1}. **3'** isomerizes to **3''** at 13.9 kcal mol^{-1}, followed by re-association of the NHC at Al1. **3-Cis** is calculated to be by 4.3 kcal mol^{-1} energetically more favourable, therefore although the low NHC dissociation energies are expected to allow **3-Trans** and **3-Cis** to exist in thermodynamic equilibrium in ambient conditions, only **3-Cis** can be observed when the equilibrium is reached. In the case of **4-**

Trans and **4-Cis**, it is actually the trans isomer that is favoured by 4.1 kcal mol^{-1}. The formation of **4-Trans** from **2** and P_4 is exergonic by 73.8 kcal mol^{-1}.

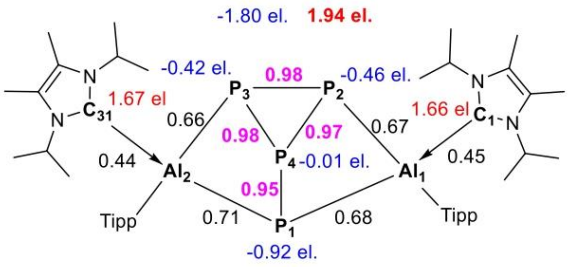

3-Cis

Figure S43. NPA charges (blue) and NBO analysis (WBI (P-P) in purple and WBI (Al-P) in black; occupancy in red) of **3-Cis**

Examination of the NPA charges in **3-Cis** shows that P1 is the phosphorus centre which possesses the highest negative charge of -0.92 el., followed by P2 (-0.46 el.), P3 (-0.42 el.) and P4(-0.01 el). Thus, the sum of NPA charges of the P_4 moiety in **3-Cis** is -1.80 el., indicating that P_4 formally undergoes an almost two electron reduction by the dialumene **1**. Similar situation is observed in **4-Trans**, in which the sum of NPA charges in the P_4 moiety is -1.75 el.

NBO analysis shows that each of the phosphorus centres possesses a σ-type lone pair (Figure S44, A). The P atoms of the P_4 moiety are bound by single bonds between the phosphorus atoms in **3-Cis**, with Wiberg Bond Indexes (WBIs) of WBI(P1-P4) = 0.95 ; WBI(P2-P3) = 0.98 ; WBI(P2-P4) = 0.97 ; WBI(P3-P4) = 0.98. The NBOs corresponding to these bonding interactions retain high occupancy of 1.94 el. (Figure S44, B). According to the NBO analysis P-Al bonds (Figure S44, C) in **3-Cis** are rather polarized, with ≈ 78%

electron density of P and ≈ 22% on Al, and weak WBI(Al1-P1) = 0.68; WBI(Al1-P2) = 0.67; WBI(Al2-P1) = 0.71; WBI(Al2-P3) = 0.66. The bonding between the NHC and the Al centres in **3-Cis** is essentially dative with WBI(Al1-C1) = 0.45 and WBI(Al2-C31) = 0.44. NBO analysis shows a lone pair on C1 with occupancy of only 1.66 el. engaged in donor-acceptor interaction with low-vacancy orbitals of $sp^{2.92}$ and p orbitals of Al1, with E(2) of 72.9 and 51.5 kcal mol^{-1} respectively (Figure S44, D). Similarly, C31 interacts with low-vacancy $sp^{2.93}$ and p orbitals of Al2, with the respective donor acceptor interaction energies of 65.4 and 58.6 kcal mol^{-1}.

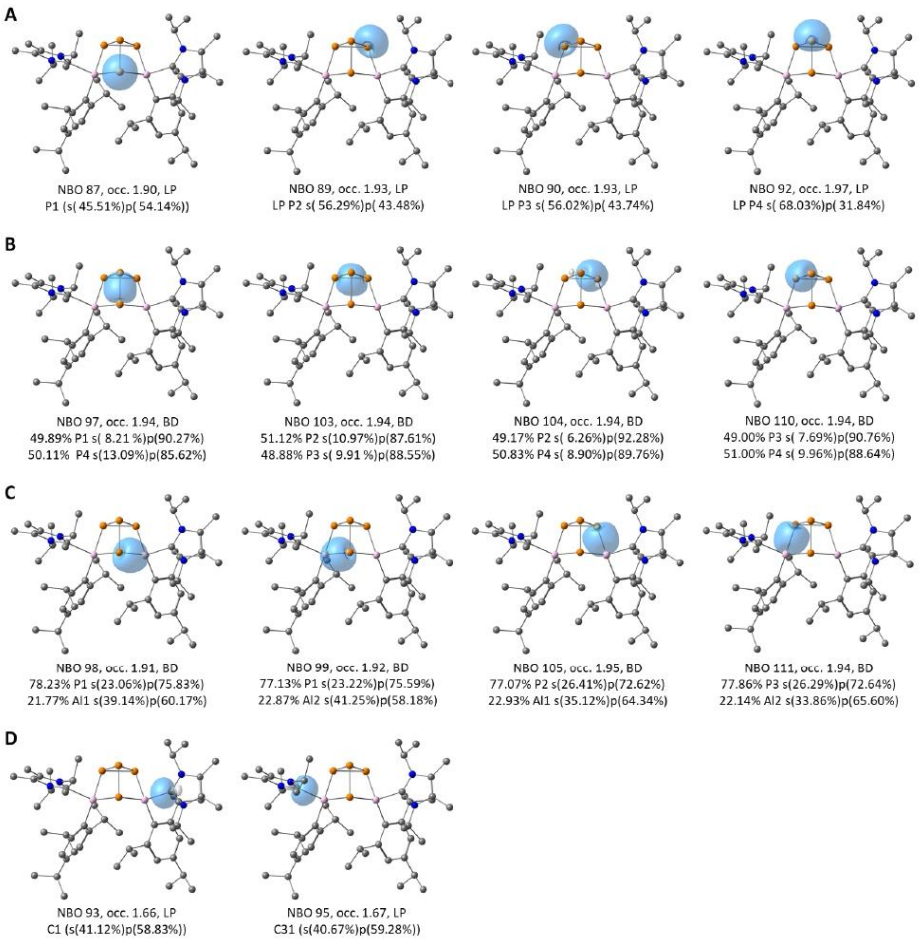

Figure S44. Selected NBOs of **3-Cis**.

In order to support the formation of intermediate **3-Trans** for which single crystals could not be obtained we calculated its ^{31}P NMR chemical shifts and coupling constants and compared the results to the experimental ^{31}P NMR spectrum, as well as to the

experimental and simulated spectra of **4-Trans**, which was characterized by NMR and XRD.

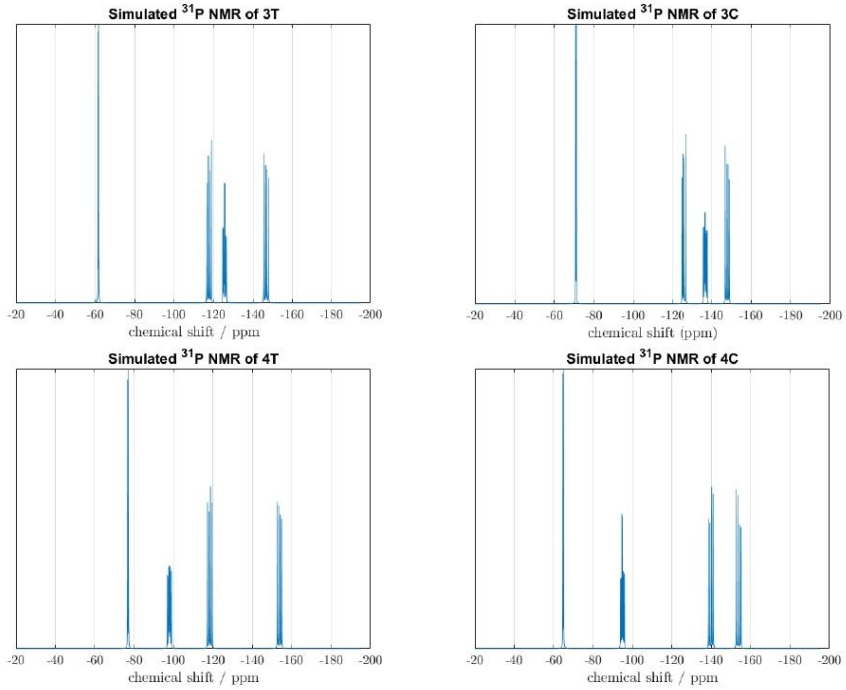

Figure S45. Simulated ^{31}P NMR spectra of **3-Trans**, **3-Cis**, **4-Trans**, **4-Cis**. Chemical shifts and coupling constants calculated at the GIAO PBE0/6-311G(2d,2p)//r^{2}SCAN-3c level of theory.

The simulated spectrum of **4-Trans** reproduces well the experiment. The simulated spectrum of the proposed intermediate **3-Ttrans** reproduces the experimentally observed pattern as well.

6. References

1. H. Schneider, A. Hock, R. Bertermann, U. Radius *Chem. Eur. J.* **2017**, *23*, 12387.
2. B. L. L. Réant, V. E. J. Berryman, A. R. Basford, L. E. Nodaraki, A. J. Wooles, F. Tuna, N. Kaltsoyannis, D. P. Mills, S. T. Liddle *J. Am. Chem. Soc.* **2021**, *143*, 9813.
3. P. Bag, A. Porzelt, P. J. Altmann, S. Inoue *J. Am. Chem. Soc.* **2017**, *139*, 14384.
4. C. Weetman, A. Porzelt, P. Bag, F. Hanusch, S. Inoue, *Chem. Sci.* **2020**, *11*, 4817.
5. C.-W. Hsu, Y.-C. Tsai, B. M. Cossairt, C. Camp, J. Arnold, C. C. Cummins, in *Inorganic Syntheses, Volume 37* (Ed. P. P. Power), John Wiley & Sons, **2018**, Chapter Six.

9.4. Licenses for Copyrighted Content

9.4.1. License for Chapter 4

JOHN WILEY AND SONS LICENSE
TERMS AND CONDITIONS

Feb 28, 2023

This Agreement between Professur für Siliciumchemie, TUM School of Natural Sciences, Technische Universität München -- Huihui Xu ("You") and John Wiley and Sons ("John Wiley and Sons") consists of your license details and the terms and conditions provided by John Wiley and Sons and Copyright Clearance Center.

License Number	5497590320146
License date	Feb 28, 2023
Licensed Content Publisher	John Wiley and Sons
Licensed Content Publication	Chemistry - A European Journal
Licensed Content Title	Isolation of Cyclic Aluminium Polysulfides by Stepwise Sulfurization
Licensed Content Author	Shigeyoshi Inoue, Franziska Hanusch, Catherine Weetman, et al
Licensed Content Date	Dec 21, 2021
Licensed Content Volume	28
Licensed Content Issue	8
Licensed Content Pages	6
Type of Use	Dissertation/Thesis
Requestor type	Author of this Wiley article
Format	Print and electronic
Portion	Full article
Will you be translating?	No
Title	Isolation of Cyclic Aluminium Polysulfides by Stepwise Sulfurization
Institution name	Technische Universität München
Expected presentation date	Feb 2023
Requestor Location	Technische Universität München Lichtenbergstraße 4 Garching, 85748 Germany Attn: Technische Universität München
Publisher Tax ID	EU826007151
Total	**0.00 USD**
Terms and Conditions	

TERMS AND CONDITIONS

This copyrighted material is owned by or exclusively licensed to John Wiley & Sons, Inc. or one of its group companies (each a"Wiley Company") or handled on behalf of a society with which a Wiley Company has exclusive publishing rights in relation to a particular work (collectively "WILEY"). By clicking "accept" in connection with completing this licensing transaction, you agree that the following terms and conditions apply to this transaction (along with the billing and payment terms and conditions established by the Copyright Clearance Center Inc., ("CCC's Billing and Payment terms and conditions"), at the time that you opened your RightsLink account (these are available at any time at http://myaccount.copyright.com).

Terms and Conditions

- The materials you have requested permission to reproduce or reuse (the "Wiley Materials") are protected by copyright.

- You are hereby granted a personal, non-exclusive, non-sub licensable (on a stand-alone basis), non-transferable, worldwide, limited license to reproduce the Wiley Materials for the purpose specified in the licensing process. This license, **and any CONTENT (PDF or image file) purchased as part of your order,** is for a one-time use only and limited to any maximum distribution number specified in the license. The first instance of republication or reuse granted by this license must be completed within two years of the date of the grant of this license (although copies prepared before the end date may be distributed thereafter). The Wiley Materials shall not be used in any other manner or for any other purpose, beyond what is granted in the license. Permission is granted subject to an appropriate acknowledgement given to the author, title of the material/book/journal and the publisher. You shall also duplicate the copyright notice that appears in the Wiley publication in your use of the Wiley Material. Permission is also granted on the understanding that nowhere in the text is a previously published source acknowledged for all or part of this Wiley Material. Any third party content is expressly excluded from this permission.

- With respect to the Wiley Materials, all rights are reserved. Except as expressly granted by the terms of the license, no part of the Wiley Materials may be copied, modified, adapted (except for minor reformatting required by the new Publication), translated, reproduced, transferred or distributed, in any form or by any means, and no derivative works may be made based on the Wiley Materials without the prior permission of the respective copyright owner.**For STM Signatory Publishers clearing permission under the terms of the STM Permissions Guidelines only, the terms of the license are extended to include subsequent editions and for editions in other languages, provided such editions are for the work as a whole in situ and does not involve the separate exploitation of the permitted figures or extracts,** You may not alter, remove or suppress in any manner any copyright, trademark or other notices displayed by the Wiley Materials. You may not license, rent, sell, loan, lease, pledge, offer as security, transfer or assign the Wiley Materials on a stand-alone basis, or any of the rights granted to you hereunder to any other person.

- The Wiley Materials and all of the intellectual property rights therein shall at all times remain the exclusive property of John Wiley & Sons Inc, the Wiley Companies, or their respective licensors, and your interest therein is only that of having possession of and the right to reproduce the Wiley Materials pursuant to Section 2 herein during the continuance of this Agreement. You agree that you own no right, title or interest in or to the Wiley Materials or any of the intellectual property rights therein. You shall have no rights hereunder other than the license as provided for above in Section 2. No right, license or interest to any trademark, trade name, service mark or other branding ("Marks") of WILEY or its licensors is granted hereunder, and you agree that you shall not assert any such right, license or interest with respect thereto

- NEITHER WILEY NOR ITS LICENSORS MAKES ANY WARRANTY OR REPRESENTATION OF ANY KIND TO YOU OR ANY THIRD PARTY, EXPRESS, IMPLIED OR STATUTORY, WITH RESPECT TO THE MATERIALS OR THE ACCURACY OF ANY INFORMATION CONTAINED IN THE MATERIALS, INCLUDING, WITHOUT LIMITATION, ANY IMPLIED WARRANTY OF MERCHANTABILITY, ACCURACY, SATISFACTORY QUALITY, FITNESS FOR A PARTICULAR PURPOSE, USABILITY, INTEGRATION OR NON-INFRINGEMENT AND ALL SUCH WARRANTIES ARE HEREBY EXCLUDED BY WILEY AND ITS LICENSORS AND WAIVED BY YOU.

- WILEY shall have the right to terminate this Agreement immediately upon breach of this Agreement by you.

- You shall indemnify, defend and hold harmless WILEY, its Licensors and their respective directors, officers, agents and employees, from and against any actual or threatened claims, demands, causes of action or proceedings arising from any breach of this Agreement by you.

- IN NO EVENT SHALL WILEY OR ITS LICENSORS BE LIABLE TO YOU OR ANY OTHER PARTY OR ANY OTHER PERSON OR ENTITY FOR ANY SPECIAL, CONSEQUENTIAL, INCIDENTAL, INDIRECT, EXEMPLARY OR PUNITIVE DAMAGES, HOWEVER CAUSED, ARISING OUT OF OR IN CONNECTION WITH THE DOWNLOADING, PROVISIONING, VIEWING OR USE OF THE MATERIALS REGARDLESS OF THE FORM OF ACTION, WHETHER FOR BREACH OF CONTRACT, BREACH OF WARRANTY, TORT, NEGLIGENCE, INFRINGEMENT OR OTHERWISE (INCLUDING, WITHOUT LIMITATION, DAMAGES BASED ON LOSS OF PROFITS, DATA, FILES, USE, BUSINESS OPPORTUNITY OR CLAIMS OF THIRD PARTIES), AND WHETHER OR NOT THE PARTY HAS BEEN ADVISED OF THE POSSIBILITY OF SUCH DAMAGES. THIS LIMITATION SHALL APPLY NOTWITHSTANDING ANY FAILURE OF ESSENTIAL PURPOSE OF ANY LIMITED REMEDY PROVIDED HEREIN.

- Should any provision of this Agreement be held by a court of competent jurisdiction to be illegal, invalid, or unenforceable, that provision shall be deemed amended to achieve as nearly as possible the same economic effect as the original provision, and the legality, validity and enforceability of the remaining provisions of this Agreement shall not be affected or impaired thereby.

- The failure of either party to enforce any term or condition of this Agreement shall not constitute a waiver of either party's right to enforce each and every term and condition of this Agreement. No breach under this agreement shall be deemed waived or

excused by either party unless such waiver or consent is in writing signed by the party granting such waiver or consent. The waiver by or consent of a party to a breach of any provision of this Agreement shall not operate or be construed as a waiver of or consent to any other or subsequent breach by such other party.

- This Agreement may not be assigned (including by operation of law or otherwise) by you without WILEY's prior written consent.
- Any fee required for this permission shall be non-refundable after thirty (30) days from receipt by the CCC.
- These terms and conditions together with CCC's Billing and Payment terms and conditions (which are incorporated herein) form the entire agreement between you and WILEY concerning this licensing transaction and (in the absence of fraud) supersedes all prior agreements and representations of the parties, oral or written. This Agreement may not be amended except in writing signed by both parties. This Agreement shall be binding upon and inure to the benefit of the parties' successors, legal representatives, and authorized assigns.
- In the event of any conflict between your obligations established by these terms and conditions and those established by CCC's Billing and Payment terms and conditions, these terms and conditions shall prevail.
- WILEY expressly reserves all rights not specifically granted in the combination of (i) the license details provided by you and accepted in the course of this licensing transaction, (ii) these terms and conditions and (iii) CCC's Billing and Payment terms and conditions.
- This Agreement will be void if the Type of Use, Format, Circulation, or Requestor Type was misrepresented during the licensing process.
- This Agreement shall be governed by and construed in accordance with the laws of the State of New York, USA, without regards to such state's conflict of law rules. Any legal action, suit or proceeding arising out of or relating to these Terms and Conditions or the breach thereof shall be instituted in a court of competent jurisdiction in New York County in the State of New York in the United States of America and each party hereby consents and submits to the personal jurisdiction of such court, waives any objection to venue in such court and consents to service of process by registered or certified mail, return receipt requested, at the last known address of such party.

WILEY OPEN ACCESS TERMS AND CONDITIONS

Wiley Publishes Open Access Articles in fully Open Access Journals and in Subscription journals offering Online Open. Although most of the fully Open Access journals publish open access articles under the terms of the Creative Commons Attribution (CC BY) License only, the subscription journals and a few of the Open Access Journals offer a choice of Creative Commons Licenses. The license type is clearly identified on the article.

The Creative Commons Attribution License

The Creative Commons Attribution License (CC-BY) allows users to copy, distribute and transmit an article, adapt the article and make commercial use of the article. The CC-BY license permits commercial and non-

Creative Commons Attribution Non-Commercial License

The Creative Commons Attribution Non-Commercial (CC-BY-NC)License permits use, distribution and reproduction in any medium, provided the original work is properly cited and is not used for commercial purposes.(see below)

Creative Commons Attribution-Non-Commercial-NoDerivs License

The Creative Commons Attribution Non-Commercial-NoDerivs License (CC-BY-NC-ND) permits use, distribution and reproduction in any medium, provided the original work is properly cited, is not used for commercial purposes and no modifications or adaptations are made. (see below)

Use by commercial "for-profit" organizations

Use of Wiley Open Access articles for commercial, promotional, or marketing purposes requires further explicit permission from Wiley and will be subject to a fee.

Further details can be found on Wiley Online Library http://olabout.wiley.com/WileyCDA/Section/id-410895.html

Other Terms and Conditions:

v1.10 Last updated September 2015

Questions? E-mail us at customercare@copyright.com.

9.4.2. License for Chapter 5

JOHN WILEY AND SONS LICENSE
TERMS AND CONDITIONS

Feb 28, 2023

This Agreement between Professur für Siliciumchemie, TUM School of Natural Sciences, Technische Universität München -- Huihui Xu ("You") and John Wiley and Sons ("John Wiley and Sons") consists of your license details and the terms and conditions provided by John Wiley and Sons and Copyright Clearance Center.

License Number	5497581471312
License date	Feb 28, 2023
Licensed Content Publisher	John Wiley and Sons
Licensed Content Publication	Angewandte Chemie International Edition
Licensed Content Title	An Aluminum Telluride with a Terminal Al=Te Bond and its Conversion to an Aluminum Tellurocarbonate by CO2 Reduction
Licensed Content Author	Huihui Xu, Arseni Kostenko, Catherine Weetman, et al
Licensed Content Date	Feb 6, 2023
Licensed Content Volume	0
Licensed Content Issue	0
Licensed Content Pages	9
Type of Use	Dissertation/Thesis
Requestor type	Author of this Wiley article
Format	Print and electronic
Portion	Full article
Will you be translating?	No
Title	An Aluminum Telluride with a Terminal Al=Te Bond and its Conversion to an Aluminum Tellurocarbonate by CO2 Reduction
Institution name	Technische Universität München
Expected presentation date	Feb 2023
Requestor Location	Technische Universität München Lichtenbergstraße 4 Garching, 85748 Germany Attn: Technische Universität München
Publisher Tax ID	EU826007151
Total	**0.00 USD**
Terms and Conditions	

TERMS AND CONDITIONS

This copyrighted material is owned by or exclusively licensed to John Wiley & Sons, Inc. or one of its group companies (each a"Wiley Company") or handled on behalf of a society with which a Wiley Company has exclusive publishing rights in relation to a particular work (collectively "WILEY"). By clicking "accept" in connection with completing this licensing transaction, you agree that the following terms and conditions apply to this transaction (along with the billing and payment terms and conditions established by the Copyright Clearance Center Inc., ("CCC's Billing and Payment terms and conditions"), at the time that you opened your RightsLink account (these are available at any time at http://myaccount.copyright.com).

Terms and Conditions

- The materials you have requested permission to reproduce or reuse (the "Wiley Materials") are protected by copyright.

- You are hereby granted a personal, non-exclusive, non-sub licensable (on a stand-alone basis), non-transferable, worldwide, limited license to reproduce the Wiley Materials for the purpose specified in the licensing process. This license, **and any CONTENT (PDF or image file) purchased as part of your order,** is for a one-time use only and limited to any maximum distribution number specified in the license. The first instance of republication or reuse granted by this license must be completed within two years of the date of the grant of this license (although copies prepared before the end date may be distributed thereafter). The Wiley Materials shall not be used in any other manner or for any other purpose, beyond what is granted in the license. Permission is granted subject to an appropriate acknowledgement given to the author, title of the material/book/journal and the publisher. You shall also duplicate the copyright notice that appears in the Wiley publication in your use of the Wiley Material. Permission is also granted on the understanding that nowhere in the text is a previously published source acknowledged for all or part of this Wiley Material. Any third party content is expressly excluded from this permission.

- With respect to the Wiley Materials, all rights are reserved. Except as expressly granted by the terms of the license, no part of the Wiley Materials may be copied, modified, adapted (except for minor reformatting required by the new Publication), translated, reproduced, transferred or distributed, in any form or by any means, and no derivative works may be made based on the Wiley Materials without the prior permission of the respective copyright owner.**For STM Signatory Publishers clearing permission under the terms of the STM Permissions Guidelines only, the terms of the license are extended to include subsequent editions and for editions in other languages, provided such editions are for the work as a whole in situ and does not involve the separate exploitation of the permitted figures or extracts,** You may not alter, remove or suppress in any manner any copyright, trademark or other notices displayed by the Wiley Materials. You may not license, rent, sell, loan, lease, pledge, offer as security, transfer or assign the Wiley Materials on a stand-alone basis, or any of the rights granted to you hereunder to any other person.

- The Wiley Materials and all of the intellectual property rights therein shall at all times remain the exclusive property of John Wiley & Sons Inc, the Wiley Companies, or their respective licensors, and your interest therein is only that of having possession of and the right to reproduce the Wiley Materials pursuant to Section 2 herein during the continuance of this Agreement. You agree that you own no right, title or interest in or to the Wiley Materials or any of the intellectual property rights therein. You shall have no rights hereunder other than the license as provided for above in Section 2. No right, license or interest to any trademark, trade name, service mark or other branding ("Marks") of WILEY or its licensors is granted hereunder, and you agree that you shall not assert any such right, license or interest with respect thereto

- NEITHER WILEY NOR ITS LICENSORS MAKES ANY WARRANTY OR REPRESENTATION OF ANY KIND TO YOU OR ANY THIRD PARTY, EXPRESS, IMPLIED OR STATUTORY, WITH RESPECT TO THE MATERIALS OR THE ACCURACY OF ANY INFORMATION CONTAINED IN THE MATERIALS, INCLUDING, WITHOUT LIMITATION, ANY IMPLIED WARRANTY OF MERCHANTABILITY, ACCURACY, SATISFACTORY QUALITY, FITNESS FOR A PARTICULAR PURPOSE, USABILITY, INTEGRATION OR NON-INFRINGEMENT AND ALL SUCH WARRANTIES ARE HEREBY EXCLUDED BY WILEY AND ITS LICENSORS AND WAIVED BY YOU.

- WILEY shall have the right to terminate this Agreement immediately upon breach of this Agreement by you.

- You shall indemnify, defend and hold harmless WILEY, its Licensors and their respective directors, officers, agents and employees, from and against any actual or threatened claims, demands, causes of action or proceedings arising from any breach of this Agreement by you.

- IN NO EVENT SHALL WILEY OR ITS LICENSORS BE LIABLE TO YOU OR ANY OTHER PARTY OR ANY OTHER PERSON OR ENTITY FOR ANY SPECIAL, CONSEQUENTIAL, INCIDENTAL, INDIRECT, EXEMPLARY OR PUNITIVE DAMAGES, HOWEVER CAUSED, ARISING OUT OF OR IN CONNECTION WITH THE DOWNLOADING, PROVISIONING, VIEWING OR USE OF THE MATERIALS REGARDLESS OF THE FORM OF ACTION, WHETHER FOR BREACH OF CONTRACT, BREACH OF WARRANTY, TORT, NEGLIGENCE, INFRINGEMENT OR OTHERWISE (INCLUDING, WITHOUT LIMITATION, DAMAGES BASED ON LOSS OF PROFITS, DATA, FILES, USE, BUSINESS OPPORTUNITY OR CLAIMS OF THIRD PARTIES), AND WHETHER OR NOT THE PARTY HAS BEEN ADVISED OF THE POSSIBILITY OF SUCH DAMAGES. THIS LIMITATION SHALL APPLY NOTWITHSTANDING ANY FAILURE OF ESSENTIAL PURPOSE OF ANY LIMITED REMEDY PROVIDED HEREIN.

- Should any provision of this Agreement be held by a court of competent jurisdiction to be illegal, invalid, or unenforceable, that provision shall be deemed amended to achieve as nearly as possible the same economic effect as the original provision, and the legality, validity and enforceability of the remaining provisions of this Agreement shall not be affected or impaired thereby.

- The failure of either party to enforce any term or condition of this Agreement shall not constitute a waiver of either party's right to enforce each and every term and condition of this Agreement. No breach under this agreement shall be deemed waived or

excused by either party unless such waiver or consent is in writing signed by the party granting such waiver or consent. The waiver by or consent of a party to a breach of any provision of this Agreement shall not operate or be construed as a waiver of or consent to any other or subsequent breach by such other party.

- This Agreement may not be assigned (including by operation of law or otherwise) by you without WILEY's prior written consent.
- Any fee required for this permission shall be non-refundable after thirty (30) days from receipt by the CCC.
- These terms and conditions together with CCC's Billing and Payment terms and conditions (which are incorporated herein) form the entire agreement between you and WILEY concerning this licensing transaction and (in the absence of fraud) supersedes all prior agreements and representations of the parties, oral or written. This Agreement may not be amended except in writing signed by both parties. This Agreement shall be binding upon and inure to the benefit of the parties' successors, legal representatives, and authorized assigns.
- In the event of any conflict between your obligations established by these terms and conditions and those established by CCC's Billing and Payment terms and conditions, these terms and conditions shall prevail.
- WILEY expressly reserves all rights not specifically granted in the combination of (i) the license details provided by you and accepted in the course of this licensing transaction, (ii) these terms and conditions and (iii) CCC's Billing and Payment terms and conditions.
- This Agreement will be void if the Type of Use, Format, Circulation, or Requestor Type was misrepresented during the licensing process.
- This Agreement shall be governed by and construed in accordance with the laws of the State of New York, USA, without regards to such state's conflict of law rules. Any legal action, suit or proceeding arising out of or relating to these Terms and Conditions or the breach thereof shall be instituted in a court of competent jurisdiction in New York County in the State of New York in the United States of America and each party hereby consents and submits to the personal jurisdiction of such court, waives any objection to venue in such court and consents to service of process by registered or certified mail, return receipt requested, at the last known address of such party.

WILEY OPEN ACCESS TERMS AND CONDITIONS

Wiley Publishes Open Access Articles in fully Open Access Journals and in Subscription journals offering Online Open. Although most of the fully Open Access journals publish open access articles under the terms of the Creative Commons Attribution (CC BY) License only, the subscription journals and a few of the Open Access Journals offer a choice of Creative Commons Licenses. The license type is clearly identified on the article.

The Creative Commons Attribution License

The Creative Commons Attribution License (CC-BY) allows users to copy, distribute and transmit an article, adapt the article and make commercial use of the article. The CC-BY license permits commercial and non-

Creative Commons Attribution Non-Commercial License

The Creative Commons Attribution Non-Commercial (CC-BY-NC)License permits use, distribution and reproduction in any medium, provided the original work is properly cited and is not used for commercial purposes.(see below)

Creative Commons Attribution-Non-Commercial-NoDerivs License

The Creative Commons Attribution Non-Commercial-NoDerivs License (CC-BY-NC-ND) permits use, distribution and reproduction in any medium, provided the original work is properly cited, is not used for commercial purposes and no modifications or adaptations are made. (see below)

Use by commercial "for-profit" organizations

Use of Wiley Open Access articles for commercial, promotional, or marketing purposes requires further explicit permission from Wiley and will be subject to a fee.

Further details can be found on Wiley Online Library http://olabout.wiley.com/WileyCDA/Section/id-410895.html

Other Terms and Conditions:

v1.10 Last updated September 2015

Questions? E-mail us at customercare@copyright.com.